Advances in Luttinger Liquid Theory: Applications to Lattice Anyons and Finite Spin Chains

Dissertation

Martin Bonkhoff

Dem Fachbereich Physik der Technischen Universität Kaiserslautern zur Erlangung des akademischen Grades „Doktor der Naturwissenschaften“ genehmigte Dissertation

Betreuer: Prof. Dr. Sebastian Eggert
Zweitgutachter: Prof. Dr. Michael Thorwart

Datum der wissenschaftlichen Aussprache: 1.3.2022
D 386

Zusammenfassung

Ziel dieser Arbeit ist die analytische Untersuchung eindimensionaler anyonischer Systeme sowie von Spinketten. Die Methode der Wahl zur Beschreibung solcher Modelle, sind Luttinger Flüssigkeiten. Solche Flüssigkeiten beschreiben auf natürliche Weise die kollektiven Anregungen in einer Raumdimension, die durch starke Quantenfluktuationen gekennzeichnet sind. Diese führen, im Gegensatz zu höheren Raumdimensionen, zu einem Abfall von langreichweitigen Korrelationen, wie bereits beschrieben wurde durch die Arbeiten von Mermin, Wagner und Hohenberg. Ansatt dessen können solche Systeme klassifiziert werden durch den algebraischen Abfall von Korrelationsfunktionen, wobei die dominante Korrelation als Charakteristikum der korrespondierenden Phase angesehen werden kann. Weiterhin bilden solche Luttinger Flüssigkeiten das Rückrad unseres Verständnisses von kritischen Phänomenen in einer Dimension und komplementieren leistungsstarke numerische Methoden wie die Dichtematrix-Renormierungsgruppe.
Der Hauptfokus dieser Arbeit bezieht sich auf die Untersuchung von anyonischen Hubbard Modellen in verschiedenen Varianten, und deren ungewöhnliche suprafluiden Eigenschaften. Wir beginnen mit einer rigorosen Beschreibung dieser Eigenschaften mit Hilfe der exakten Lösung des Modells auf nur zwei Gitterplätzen. Danach erweitern wir dass Modell für eine beliebige Anzahl von Gitterplätzen und beschreiben das Spektrum seiner Bogoliubov Anregungen, sowie verschiedene effektive Theorien die das System für starke Wechselwirkungen, oder sehr kleine Dichten, getreu abbilden. Daraufhin leiten wir einen rigorosen Kontinuumslimes des anyon-Hubbard model her, und beschreiben die Eigenschaften der korrespondierenden Luttinger Flüssigkeit. Abschließend betrachten wir den Einfluss der statistischen Wechselwirkungen auf, durch Symmetrie geschützte, topologische Phasen an Hand des erweiterten anyonischen Hubbard Modells. Hierbei kann ein hohes Maß an Übereinstimmung mit den numerischen Vorhersagen, bezüglich der Eigenschaften der unterschiedlichen Phasen und deren Übergängen, erzielt werden. Hauptaugenmerk ist dabei auf die Symmetrien der effektiven Feldtheorien gerichtet, und deren Einfluss auf die Existenz und Stabilität der topologischen Haldane Phase. Weiterhin könen diese feldtheoretische Überlegungen genutzt werden um eine neuauftretende Dimer Phase, und deren Übergänge, zu beschreiben, deren Existenz ausschliselich durch die Balance von statistischer Abstoßung und attraktiver Wechselwirkung gesichert ist.
Der letzten Teil dieser Arbeit wird der Beschreibung von endlichen Spinketten, mit der Methode der nichlinearen Bosonisierung, gewidmet. Hierbei werden bereits bekannte Resultate, bezüglich des Langzeitverhaltens von Korrelationen, mit expliziten Abschätzungen ihrer Validität komplementiert. Des Weiteren finden wir eine neue Darstellung von chiralen Korrelationsfunktionen mit Hilfe von generalisierten Jacobi-

Anger Funktionen, die eine explizite Berechnung des dynamischen Strukturfaktors ermöglichen. Diese Ergebnisse legen den Grundstein zur weiteren Untersuchung des Einflusses von Krümmungseffekten in Neutronen-Streu Experimenten.

Abstract

This work is concerned with the theoretical description and advanced analytical treatment of one-dimensional anyons and finite-size spin chains. The method of choice for such models is the quantum fluid description in terms of collective variables, i.e. the so called Luttinger liquids, that naturally inherit the peculiar properties of one-dimensional systems. In contrast to higher spatial dimensions, where mean-field approaches are valid approximations, the one-dimensional world is governed by strong quantum fluctuations instead. These fluctuations lead to a destruction of real long-range order in the sense of Mermin, Wagner and Hohenberg, but allow to classify gapless phases in terms of dominant, algebraic decay of correlators. Such quantum fluids, and their extensions, can be used furthermore to describe the critical regions of large class of quantum phase transitions, and are necessary to support the numerical results of the omnipresent Density-Matrix-Renormalization-Group method analytically.

The largest part of this thesis is devoted to the properties of one-dimensional anyons, as described by the anyonic Hubbard model and its variants. Thereby the focus is on the description of their unusual superfluid properties compared to canonical particles, which is investigated here by different methods. At first we describe their coherence properties rigorously for the two-site limit and discuss the exact solution. For larger systems sizes, this is complemented by a Bogoliubov approximation in the weak-coupling limit, and two effective models describing either the realm of strong interactions or small densities. Finally these results are placed on more solid grounds by means of a rigorous continuum limit of the lattice anyons and a subsequent discussion of the corresponding Luttinger model. Afterwards we study the impact of statistical transmutation on bosonic Symmetry-Protected-Topological-Phases, by means of the extended anyonic Hubbard model. In perfect agreement with large-scale numerical investigation, we describe the low-energy signatures of the phases and their transitions by means of the bosonization method. Thereby special emphasis is on the symmetry properties of the underlying field theories and their implication on the existence of an anyonic Haldane insulator and its faith with respect to a change of particle statistics. Furthermore, the method is used to describe a new dimerized phase, arising due to the interplay of statistical repulsion and attractive interactions, and its transition beyond the Landau paradigm.

In the last part of the thesis, we apply non-linear bosonization to the correlation

functions of finite-size XXZ chains. We complement previous results on their long-time decay in the bulk or near the boundary, with explicit estimates on the range of validity. Furthermore we find a new representation of chiral correlators in terms of generalized Jacobi-Anger functions, that allows to determine the finite-size dynamical structure factor in closed form. This paves the way for future numerical investigations of the impact of curvature effects in neutron-scattering experiments beyond the Luttinger paradigm.

Contents

Abstract **ii**

1 Introduction to one-dimensional Anyons on a Lattice **2**
1.1 The Anyon-Hubbard Model 3
1.2 Anyonic Algebra 4
1.3 Jordan-Wigner Duality 6
1.4 Experimental Realization 11

2 Introduction to Bosonization **16**
2.1 Exact Bosonization **à** la Luttinger, Lieb and Mattis 18
2.2 Fermionic Bosonization and it's Field-Theoretical Description 21
2.2.1 Periodic Boundary Conditions 24
2.3 Haldane's Harmonic Fluid Bosonization 26
2.3.1 Equivalence of Bosons and Fermions for low Energies 28
2.4 Correlation Functions 30

3 The Anyon-Hubbard Dimer **34**
3.1 Current Algebra and Duality Transformation 35
3.2 Permutation Symmetry and It's Relation to the Braid Group 38
3.3 Algebraic Bethe Ansatz Solution 41
3.4 Coherent States 45
3.5 Quantum Pendulum Approach 49
3.5.1 Bosonic Pendulum 50
3.5.2 Anyonic Mathieu Functions 52
3.5.3 Simple Pendulum Motion and Number and Phase Uncertainties . 54
3.6 Conclusion 57

4 Bogoliubov Approximation **59**
4.1 Derivation 60
4.2 Stability Analysis and Dispersion Relation 67
4.3 Condensate Energy and Healing Length 70
4.4 Dilute Limit 75

4.5 Conclusion . . . 79

5 Dilute Pseudo-Fermions and Fermions 81
5.1 Two Anyon Scattering Solution . . . 82
5.2 Strong Coupling Effective Hamiltonian . . . 88
5.2.1 Continuum Limit . . . 90
5.2.2 Perturbative Bosonization at Half-Filling . . . 92
5.3 Concluding Remarks . . . 95

6 Continuum Limit of Canonical Anyons 97
6.1 Introductory Remarks . . . 98
6.2 Previous Approaches . . . 101
6.3 Normal Ordered Continuum Limit . . . 104
6.3.1 Comparison of the different Approaches . . . 106
6.4 The Relation to Integrable Models . . . 108
6.4.1 The Kundu Model and Beyond . . . 108
6.4.2 Selected Quantities of the Integrable Limits . . . 109
6.5 Harmonic Fluid Approach . . . 114
6.5.1 Friedel Oscillation . . . 116
6.5.2 Mode Expansion for twisted Boundary Conditions . . . 119
6.5.3 Density-Density Correlation Function . . . 125
6.5.4 Remark on Cut-offs, Prefactors and Luttinger Parameters . . . 126
6.6 Conclusion . . . 128

7 Bosonization of the extended Anyon-Hubbard Model 130
7.1 The Extended and Constrained Anyon Hubbard Model . . . 131
7.2 The Relation to the $S = 1$ Heisenberg chain . . . 132
7.3 The λ-D-Model . . . 134
7.3.1 The large D Phase . . . 136
7.3.2 The Anti-Ferromagnetic Phase . . . 137
7.3.3 The XY Phases . . . 139
7.3.4 The Haldane Phase . . . 140
7.4 Modified Gutzwiller Mean-Field . . . 142
7.4.1 Derivation and Order Parameters . . . 143
7.4.2 Superfluid Phases . . . 146
7.4.3 Mean-Field Phase Diagram . . . 150
7.5 Numerical Investigation of The Phase Diagram . . . 152
7.5.1 Correlations for Gapped Phases . . . 152
7.5.2 Entanglement Entropy and the Area Law Conjecture . . . 153
7.5.3 Fidelity and it's Susceptibility . . . 155
7.5.4 Order Parameters and their Scaling . . . 156

7.5.5 BKT Transitions and Level Spectroscopy . . . 161
7.5.6 Phase Diagram for $\theta \approx 0, \pi$ . . . 163
7.5.7 The Fate of the Haldane Insulator . . . 165
7.5.8 Phase Transitions close to the Bosonic Limit . . . 166
7.5.9 Phase Transitions close to the Pseudo-Fermionic Limit . . . 168
7.6 Bosonization close to the bosonic Limit . . . 170
7.6.1 The Elegance of the Schulz Mapping . . . 173
7.6.2 Some Facts about the Bosonization of Spin Ladders . . . 174
7.6.3 Numerical Tests of the Schulz Mapping in the Pseudo-Fermionic Limit . . . 176
7.6.4 Derivation of the Field Theory . . . 178
7.7 Bosonization close to the pseudo-fermionic Limit . . . 188
7.7.1 Numerical Test of the Symmetrized Mapping . . . 189
7.7.2 The effective Field Theory . . . 192
7.8 Phase Transitions in the bosonic Limit . . . 195
7.8.1 Mott to Haldane Insulator Transition . . . 197
7.8.2 Gapless Phases and their Transitions . . . 200
7.8.3 Charge-Density-Wave to Haldane insulator transition . . . 204
7.9 The Dimer Phase and its Transitions at $\theta \approx \pi$ . . . 205
7.9.1 A Microscopic Theory of the Dimer Phase . . . 206
7.9.2 The Dimer to Mott Transition . . . 212
7.9.3 The Dimer to CDW Transition . . . 214
7.10 Conclusion . . . 214
7.11 Appendix: Strong Coupling Perturbation Theory . . . 217
7.11.1 Appendix: Bosonization of correlated Hopping at $\theta \approx 0$ . . . 218
7.11.2 Appendix: Bosonization of correlated Hopping at $\theta \approx \pi$ . . . 220

8 Spin Correlations in the Finite XXZ-Chain 222
8.1 Preliminaries . . . 223
8.1.1 The Model . . . 223
8.1.2 Phases in the XXZ Chain . . . 225
8.1.3 Finite-Size Bosonization of the Dynamical Structure Factor . . . 226
8.1.4 Non-linear Bosonization . . . 232
8.2 Longitudinal Spin Correlation . . . 235
8.3 Single-Particle Impurity . . . 237
8.3.1 Open Boundary Conditions . . . 238
8.3.2 Periodic Boundary Conditions . . . 239
8.3.3 Relativistic Impurities and the Heat Kernel Regularization of the Delta Function . . . 240
8.4 Chiral Field Correlation Function for Open Boundaries . . . 247

8.5 Chiral Field Correlation Function for Periodic Boundaries 249
8.6 Regularization 250
8.7 Bulk and Boundary Limits of Chiral Correlators 252
8.8 Generalized Jacobi-Anger Expansion 255
8.8.1 Infinite-variable Bessel function 256
8.8.2 Correlation Function for arbitrary Cut-off 258
8.8.3 Correlation Function Asymptotics for a vanishing Cut-off 260
8.9 Dynamical Structure Factor for finite Systems 263
8.10 Conclusion 269
8.11 Appendix: Bare Coupling Constants 271
8.12 Appendix: List of the Field Commutators 273
8.13 Appendix: Mode decomposition for Open Boundaries 274
8.14 Appendix: Mode decomposition for Cyclic Boundaries 275

9 Conclusion and Outlook **277**

Bibliography **280**

10 Acknowledgment **302**

11 Curriculum Vitae **304**

12 Selected Conferences and Schools **305**

13 Publications **306**

Chapter 1

Introduction to one-dimensional Anyons on a Lattice

Since the pioneering work of Wolfgang Pauli [1], who showed that particle statistics and the dimensionality of the particle configuration space are inextricably intertwined, anyons are thought to be exclusively existing in two spatial dimensions [2]. Only in $d = 2$ the fundamental group of the underlying configuration space is given by the braid group [3] enabling fractional statistics, whereas in $d = 3$ it is the symmetric group with its symmetric and anti-symmetric representations describing canonical bosons or fermions, respectively. In one spatial dimension the fundamental group is trivial on the other hand, manifesting the blurred concept of particle statistics, which is one of the major subjects of this thesis. It were Leinaas and Myrheim who showed years later that also in $d = 1$ anyonic statistics may emerge in momentum space, as a consequence of ordinary two-particle interactions in real space. This circumstance is manifest for example in the Lieb-Liniger model, which can be equivalently represented in terms of a free anyonic Hamiltonian [4–6]. Such one-dimensional anyons are, thus, restricted to the phenomenology of the Lieb-Liniger model and can not incorporate a breaking of time-reversal and parity symmetry for bosonic observables, which is an inherent property of their two-dimensional counterparts [2]. Later on, it was Anjan Kundu who generalized the concepts of Leinaas and Myrheim even further, to mimic the deformed commutation relations of two-dimensional anyons formally and to induce the previously mentioned asymmetry with respect to spatial and temporal inversion a priori [7]. A structural property, that both of these constructions share, is that the local anyons can be related to ordinary bosonic particles in terms of a fractional Jordan-Wigner transformation [7–9]. In general, Jordan-Wigner transformations may induce additional interactions depending on the local structure of a given Hamiltonian as well as the local Hilbert space dimension of the parent particles, meaning in that context either fermions or bosons [8]. In the anyon approach of Leinaas and Myrheim, this is expressed by their equivalence to δ-interacting bosons, or the well known relation between free fermions

in one dimension and the bosonic Tonks-Girardeaux gas at infinite coupling [10, 11], whereas the model derived by Kundu contains additional three-body interactions as well as a current-density coupling when represented in terms of bosons. This manifestation of the fact, that in one spatial dimension exchange statistics and interactions can not be treated separately, immediately raises the question in which sense the statistically induced interactions of the Hamiltonian of the parent particles allows for an effective local transmutation between bosonic and fermionic Hilbert spaces? This is a task, which is impossible to achieve solely at the level of commutation relations, as a bosonic commutator basically cannot be transformed locally to an anti-commutator by a Jordan-Wigner transformation, inferable from the in-equivalence of the fundamental particles matrix representations.

As the one-dimensional anyon models of Leinaas, Myrheim or Kundu are defined in the continuum, the resulting statistical interactions are relatively limited in form and partially unclear to implement as even singular interactions appear [7, 12]. This suggests to further transfer the concept of one-dimensional Jordan-Wigner anyons to a discrete space [13], which is not only experimentally more versatile. Additionally, it also allows for the generation of higher-order interactions between the parent particles as the density may be reasonably adjusted to much larger values in comparison to the continuum. The drosophila in this case is the so called anyon-Hubbard model, first introduced in **Ref**. [13], whose variants and respective properties are discussed in the following introductory chapter. The focus is especially on a classification of the different types of anyons together with their respective parent particle Hamiltonians, their interrelation, as well on their symmetry properties. Thereby the Jordan-Wigner transformation between the anyons and their parent particles is derived from quite general considerations. In a later chapter about the continuum limit of the anyon-Hubbard model the historically rooted anyonic models are formally introduced in more detail and compared to the low-density limit of the lattice anyons introduced here. But before we have to clearly define what we mean with the entity anyon, which is solely dependent on the a priori definition of their deformed commutation relations, as well as on the explicit form of their Hamiltonian. With this we avoid giving an introduction to two-dimensional anyons on purpose, as their one-dimensional relatives do share structural similarities via their deformed commutation relations defined in the following. But they do not have the same topological origin nor feature the geometrical interpretation of braiding the particles trajectories.

1.1 The Anyon-Hubbard Model

A large part of this thesis is devoted to the properties of one-dimensional anyons and their differences to canonical particles. The model, that is the main subject of our

investigation, is the so-called anyon-Hubbard model, or various extensions of it, i.e.

$$\begin{aligned}\hat{H}_{AH} &= \hat{H}_0^J + \hat{H}^{\text{int}},\\ \hat{H}_0^J &= -J\sum_j \left(\hat{a}_j^\dagger \hat{a}_{j+1} + \text{h.c.}\right),\\ \hat{H}^{\text{int}} &= \frac{U}{2}\sum_j \hat{n}_j\left(\hat{n}_j - 1\right) + ...\end{aligned} \tag{1.1}$$

The summation index j in **Eq**. (1.1) runs from the site number 1 to site L, whereas additional restrictions on the creation/annihilation operators have to be imposed when specific boundary conditions are considered. For a one-dimensional ring the particles need to be periodic in the index, i.e. $\hat{a}_{j+L} = \hat{a}_j$, whereas they need to vanish exactly at the boundary of an open chain, i.e. $\hat{a}_{j=0,L} = 0$. The most important question is which entity $\hat{a}_j$ should represent, as it is expressed by the algebraic relations between the particles. Finally the choice of particles dictates also what kind of interactions, described as polynomial functions of the number operator

$$\hat{n}_j = \hat{a}_j^\dagger \hat{a}_j, \tag{1.2}$$

may appear in $\hat{H}^{\text{int}}$, as it is emphasized by the ellipsis of **Eq**. (1.1). More precisely, if the particles are subject to a hardcore condition, i.e. $(\hat{a}_j)^p = 0$, then there are only up to $(p-1)$ local particle interactions allowed [8, 14]. For instance, density-density interaction of the form $\sum_{i\neq j}\hat{n}_i\hat{n}_j$ or more complicated between distant sites are in principle allowed, as for example in the Fermi-Hubbard model [15]. Conversely if no such restriction on the particles local occupancy exists, i.e. as for example for canonical bosons $(\hat{a}_j^\dagger)^{p=\infty} \neq 0$, then arbitrary local interactions are allowed, as for example the local two-particle interaction scaled by U in **Eq**. (1.1). Furthermore, the particles are allowed to move forward or backward on the lattice, which is expressed by the hopping operator $\hat{H}_0^J$ scaled by J, hence the (anti)-commutation relations of the particles between distinct lattice sites need to be chosen such that a phase convention with respect to the exchange of particles exists. As the title of this chapter suggests we are seeking a more general phase convention here as the ordinary ± 1 for bosons or fermions, respectively. The fact that we are looking just for a scalar phase to formulate the particle exchange of the $\hat{a}_j$'s, and not to a more general transformation of the wave-function, implies that we are dealing with so called abelian anyons, that will be explicitly defined in the next section [2].

1.2 Anyonic Algebra

In the following we will postulate a type of one-dimensional anyonic algebra in close relation to their two-dimensional counterparts [2, 13, 16], whereas the phase the particles

acquire under exchange depends on the relative position of the anyons on the line. In this framework exchange statistics and the restrictions on the size of the local Hilbert space dimension are a priori disjoint concepts [8], i.e. without referring to a specific Hamiltonian and its ground-state properties. The maximal local occupation is therefore dictated by the choice, whether the anyons should locally commute or anti-commute, therefore we will discuss both choices and their implications in the following. In a later chapter we will also discuss the case of constrained anyons that deviate locally from an ordinary commutator, i.e. $(\hat{a}_i^\dagger)^3 = 0$, and embody a second-quantized version of the Haldanes exclusion principle [8, 14]. The deformed Heisenberg (super)-algebra, that we would like to consider, is the following

$$\begin{aligned} &\hat{a}_i\hat{a}_j^\dagger - ke^{-i\theta\mathrm{sign}(i-j)}\hat{a}_j^\dagger\hat{a}_i = \delta_{i,j}, \\ &\hat{a}_i\hat{a}_j - ke^{i\theta\mathrm{sign}(i-j)}\hat{a}_j\hat{a}_i = 0, \\ &\hat{a}_i^\dagger\hat{a}_j^\dagger - ke^{i\theta\mathrm{sign}(i-j)}\hat{a}_j^\dagger\hat{a}_i^\dagger = 0, \quad k = \pm 1, \end{aligned} \tag{1.3}$$

where $\mathrm{sign}(i-j)$ indicates the sign of the relative index $i-j$ and the choice of k implies either $(\hat{a}_i^\dagger)^2 = 0$ for $k = -1$ or no restriction on the local occupation for $k = 1$. Additionally we postulate that the anyons are, indeed, entities that can be counted locally as implied by the definition of the number operator in **Eq**. (1.2), as well as the following algebraic relations,

$$\begin{aligned} \hat{a}_i^\dagger\hat{n}_j - \hat{n}_j\hat{a}_i^\dagger &= \delta_{i,j}\hat{a}_i^\dagger, \\ \hat{a}_i\hat{n}_j - \hat{n}_j\hat{a}_i &= -\delta_{i,j}\hat{a}_i, \end{aligned} \tag{1.4}$$

that are also obeyed by ordinary bosons or fermions. It should be noted that there are in principle different ways to choose the sign of the statistical parameter θ in **Eq**. (1.3), a detail that will be recapitulated in the next section as it turns out to be irrelevant to the following discussion. **Eq**. (1.3) embodies the circumstance that the anyonic particles acquire a phase under exchange, as we exemplary show for $k = 1$ and $i < j$ [17], i.e.

$$\begin{aligned} |\Psi\rangle = \hat{a}_i^\dagger\hat{a}_j^\dagger|0\rangle &\overset{\text{exchange}}{\longrightarrow} \hat{a}_k^\dagger\hat{a}_j\hat{a}_i^\dagger\hat{a}_j^\dagger|0\rangle = e^{i\theta}\hat{a}_k^\dagger a_i^\dagger\hat{a}_j\hat{\hat{a}}_j^\dagger|0\rangle = e^{i\theta}\hat{a}_k^\dagger a_i^\dagger|0\rangle \\ &\overset{\text{translate}}{\longrightarrow} e^{i\theta}\hat{a}_i^\dagger a_j^\dagger|0\rangle\,. \end{aligned} \tag{1.5}$$

The algebra in **Eq**. (1.3) has quite different properties compared to the un-deformed (fermionic) bosonic Heisenberg (super) algebra at $\theta = 0$, where mathematically not even the prerequisite of a Lie (super)-algebra is fulfilled [18]. Most importantly, the locality relation between the constituents is violated, meaning that even particles that are far

away from each other are in general non-commutative, e.g.

$$\hat{a}_i^\dagger \hat{a}_j^\dagger - k\hat{a}_j^\dagger \hat{a}_i^\dagger = -k\left(1 - e^{i\theta \mathrm{sign}(i-j)}\right)\hat{a}_j^\dagger \hat{a}_i^\dagger. \tag{1.6}$$

The circumstance that the ordinary (anti)-commutators of the anyons, as in **Eq**. (1.6), do not evaluate to $\mathbb{C}$-numbers may have far-reaching consequences. For example, the integrability of even non-interacting, i.e. $\hat{H}^{\mathrm{int}} = 0$ in **Eq**. (1.1), anyonic Hamiltonians is potentially spoiled for arbitrary local Hilbert space dimensions and system sizes, due to the lack of ultra-locality [19–21], which can be interpreted as the absence of a single-particle description for such anyons. This can be rephrased such that the anyons are always intrinsically interacting [8], even without explicit inter-particle interactions $\hat{H}^{\mathrm{int}}$, partially formalizable by means of the algebra of bi-linear combinations of the form $\hat{a}_j^\dagger \hat{a}_i$ [22], i.e.

$$\begin{aligned}\left[\hat{a}_i^\dagger \hat{a}_j, \hat{a}_k^\dagger \hat{a}_l\right]_{k=1} &= \delta_{j,k}\hat{a}_i^\dagger \hat{a}_l - \delta_{i,l}\hat{a}_k^\dagger \hat{a}_j \\ &\quad + k\left(e^{-i\theta \mathrm{sign}(j-k)} - e^{-i\theta(\mathrm{sign}(l-i)-\mathrm{sign}(k-i)-\mathrm{sign}(l-j))}\right)\hat{a}_i^\dagger \hat{a}_j^\dagger \hat{a}_k \hat{a}_l.\end{aligned} \tag{1.7}$$

Unlike the case of canonical particles the successive commutation of anyonic bi-linears as in **Eq**. (1.7), generates higher-order contributions, and is thus not closed in an algebraic sense. Hence, non-extrinsically interacting, number preserving, anyonic Hamiltonians induce a non-linear time evolution on its creation/annihilation operators [22]. This is in strong contrast to canonical particles, where the time evolution of a non-interacting Hamiltonian acts as a passive rotation that maps a single creation/ annihilation operator to a particular linear combination of it, i.e.

$$e^{-\frac{i\hat{H}^0_{\theta=0}}{\hbar}t}\hat{a}_i^{\theta=0}e^{\frac{i\hat{H}^0_{\theta=0}}{\hbar}t} = \sum_{ij} u_{i,j}\hat{a}_j^{\theta=0}. \tag{1.8}$$

The case of number non-conserving anyonic Hamiltonians is explicitly excluded here, as they will correspond later on to non-local Hamiltonians in terms of their canonical parent particles, which are neither easy to implement experimentally nor to investigate theoretically. For ordinary particle species the inclusion of number non-conserving terms does not pose any problem on the other hand, and leads to a time evolution similar to a Bogoliubov rotation that mixes creation and annihilation operators linearly [23].

1.3 Jordan-Wigner Duality

Even if the mathematical structure of such one-dimensional anyons is very appealing by itself, it would be of physical importance to relate the abstract objects to ordinary particles. Thereby, the blurred concept of fractional statistics in one dimension could be probed experimentally in the realm of cold atomic gases, elevating anyonic Hubbard

models beyond purely academical examples. As stated before, all of the historically relevant constructions of one-dimensional anyons are related to ordinary particles by means of a generalized Jordan-Wigner transformation [5, 7, 9]. Analogously, the anyonic algebra in **Eq**. (1.3) can be generated by a set of parent particles, related to the choice of $k = \pm 1$, together with an attached Jordan-Wigner string [8, 13]. In the following the Jordan-Wigner transformation is explicitly derived, instead of postulated. This is achieved by means of bond algebra isomorphisms mediating between anyonic Hamiltonians and those of their parent particles, as well as between a particular bond decomposition. Thereby we generalize the approach pursued in **Ref**. [24] to include anyonic statistics.

We choose $k = 1$ for the construction, meaning that we consider bosonic parent particles for the moment, whereas the fermionic case $k = -1$ can be treated in an analogous manner but is poorer in phenomenology. The starting point of the investigation is the observation that anyonic bi-linears of the kinetic energy in **Eq**. (1.1) obey the same algebraic relations, according to **Eq**. (1.7), as analogous bosonic bonds attached to a density-dependent Peierls phase [13]. The explicit form of the bond duality relation Φ_D reads,

$$\begin{aligned} \hat{a}_j^\dagger \hat{a}_{j+1} &\overset{\Phi_D}{\longrightarrow} \hat{a}_j^{\dagger,D} \hat{a}_{j+1}^D = \hat{b}_j^\dagger \hat{b}_{j+1} e^{i\theta \hat{n}_j}, \\ \hat{a}_{j+1}^\dagger \hat{a}_j &\overset{\Phi_D}{\longrightarrow} \hat{a}_{j+1}^{\dagger,D} \hat{a}_j^D = e^{-i\theta \hat{n}_j} \hat{b}_{j+1}^\dagger \hat{b}_j, \end{aligned} \tag{1.9}$$

for the site index $j \in (1, L-1)$, whereas the boundary bonds at $j = L$ will be fixed at a later stage. We may neglect possible interactions $\hat{H}^{\text{int}}$ between the anyons in **Eq**. (1.1), as the definition of the number operator in **Eq**. (1.2), as well as **Eqs**. (1.3) and (1.4), imply that the anyons can be counted locally in the same way as their parent particles, and if the duality is unitary implementable, i.e.

$$\Phi_D(\hat{n}_j = \hat{a}_j^\dagger \hat{a}_j) = \Phi_D(\hat{a}_j^\dagger)\Phi_D(\hat{a}_j) = \hat{a}_j^{\dagger,\theta=0} \hat{a}_j^{\theta=0}, \tag{1.10}$$

such contributions do not conceptually matter in establishing a duality relation. Furthermore **Eq**. (1.10) shows that the dual anyons have a relatively simple form in terms of the parent particles, which we prove to be a fractional Jordan-Wigner string in the following.

So far we have only shown that there is a duality relation, in the sense of **Ref**. [24],

with respect to the anyonic and bosonic kinetic energies, i.e.

$$\Phi_D\Big(\hat{H}_0^J\Big) = \Phi_D\Big(-J\sum_j\Big(\hat{a}_j^\dagger\hat{a}_{j+1}+\text{h.c.}\Big)\Big) = \hat{H}_<^{D,+} = -J\sum_j\Big(\hat{b}_j^\dagger\hat{b}_{j+1}e^{i\theta\hat{n}_j}+\text{h.c.}\Big), \tag{1.11}$$

and their respective bond algebras generated by **Eq**. (1.9), as well as any finite linear combinations of powers and products of bonds and the identity element [24]. But, without the explicit form of the duality transformation in terms of the fundamental modes, this relation is hardly helpful for the calculation of local observables. Therefore, we may attach a single mode operator $\hat{a}_1^D = \hat{b}_1$ at the boundary to the Hamiltonians bond algebra, whose decomposition can be chosen arbitrarily anyway. With this we observe that one can generate a single dual anyon at site $j \neq 1$ recursively from deformed commutation of $\hat{a}_1^D = \hat{b}_1$ with the bi-linear bonds, i.e.

$$\begin{aligned}\hat{a}_1^D &= \hat{b}_1 \\ \hat{a}_j^D &= \Big[\hat{a}_{j-1}^D, \hat{a}_{j-1}^{\dagger,D}\hat{a}_j^D\Big]_{-\theta} = \hat{a}_{j-1}^D\hat{a}_{j-1}^{\dagger,D}\hat{a}_j^D - e^{-i\theta}\hat{a}_{j-1}^{\dagger,D}\hat{a}_j^D\hat{a}_{j-1}^D.\end{aligned} \tag{1.12}$$

Eq. (1.12) can then be solved iteratively, for example for $\hat{a}_2^D$

$$\hat{a}_2^D = \hat{a}_1^D\hat{a}_1^{\dagger,D}\hat{a}_2^D - e^{-i\theta}\hat{a}_1^{\dagger,D}\hat{a}_2^D\hat{a}_1^D = \hat{b}_1\hat{b}_1^\dagger e^{i\theta\hat{n}_1}\hat{b}_2 - e^{-i\theta}\hat{b}_1^\dagger e^{i\theta\hat{n}_1}\hat{b}_2\hat{b}_1 = \hat{b}_2 e^{i\theta\hat{n}_1}, \tag{1.13}$$

to yield the fractional Jordan-Wigner transformation mediating between bosonic and anyonic species [13]

$$\hat{a}_j \overset{\Phi_D}{\longmapsto} \hat{a}_j^D = \hat{b}_j e^{i\theta\sum_{l<j}\hat{n}_l}. \tag{1.14}$$

In analogy to the ordinary Jordan-Wigner transformation we may conclude that even if the dual variables in **Eq**. (1.14) are necessarily non-local, anyonization is a process local in the bonds according to **Eq**. (3.16) [9, 24]. More precisely, the duality between anyonic bonds of the form $\hat{a}_j^\dagger\hat{a}_{j+k}$ and the corresponding bosonic dual is as local as the range of the anyonic hopping k. In addition the explicit form of **Eq**. (1.14) shows the previously mentioned fact, that number non-conserving anyonic Hamiltonians are indeed necessarily non-local in terms of their parent particles and are thus excluded here.

Now the boundary bonds need to be discussed in order to prove the duality relation for finite sizes. The case of open boundaries does not induce any problem, by simply attaching the missing bonds at $j = L$ in **Eq**. (3.16), together with the additional constraints on the virtual sites $\hat{a}_{L+1,0}^\dagger = 0$. The case of periodic boundary conditions is more involved as the boundary bond connecting the sites L and $L+1$ has to acquire an

additional phase such that the same algebraic relations in **Eq**. (1.7) are fulfilled for the dual bonds

$$\begin{aligned} \hat{a}_L^\dagger \hat{a}_{L+1} &\overbrace{\longrightarrow}^{\Phi_D} \hat{a}_L^{\dagger,D} \hat{a}_1^D = e^{-i\theta\hat{N}} \hat{b}_L^\dagger \hat{b}_1 e^{i\theta\hat{n}_j}, \\ \hat{a}_{L+1}^\dagger \hat{a}_L &\overbrace{\longrightarrow}^{\Phi_D} \hat{a}_{L+1}^{\dagger,D} \hat{a}_L^D = e^{-i\theta\hat{n}_L} \hat{b}_1^\dagger \hat{b}_L e^{i\theta N}. \end{aligned} \tag{1.15}$$

Eq. (1.15) may then be interpreted such that anyons with periodic boundary conditions correspond to dual bosons with twisted boundary conditions. This non-trivial boundary effect is a topological property of such one-dimensional anyons and generalizes the even/odd effect, depending on the total particle number N, known from the fermionization of the cyclic XY-chain [25]. This boundary twist leads to a loss of translational invariance for the bosonic Hamiltonian $\hat{H}_<^{+,D}$, whose implications are discussed in a later chapter concerning its low-energy properties for mesoscopic system sizes [26].

In the ordinary Jordan-Wigner duality there is some arbitrariness in the definition of the string operator, mediating between a hardcore boson and a fermion, i.e.

$$\hat{c}_j = \hat{b}_j e^{\pm i\pi \sum_{l>j \vee l<j} \hat{n}_l}. \tag{1.16}$$

Thereby all combinations of complex conjugations and orientations of the string operator in **Eq**. (1.15) lead to the same result and thus can be chosen arbitrarily. For fractional Jordan-Wigner transformations as in **Eq**. (1.14) the situation is much more complicated as different species of anyons are defined for other conventions. To be more explicit, different choices of the string orientation or complex conjugation in **Eq**. (1.14) lead to alternative anyonic algebras in **Eq**. (1.3), expressing a different phase convention under particle exchange, i.e. $e^{\pm i\theta \mathrm{sign}(i-j)}$. Also the dual bosonic bonds in **Eq**. (3.16) look differently, with a complex conjugated phase and/or an attached Peierls phase at site $j+1$ instead of j, i.e.

$$\begin{aligned} \hat{H}_<^{\pm,D} &= -J \sum_j \left(\hat{b}_j^\dagger \hat{b}_{j+1} e^{\pm i\theta\hat{n}_j} + \text{h.c.} \right) \\ \hat{H}_{>,D}^{\pm} &= -J \sum_j \left(\hat{b}_{j+1}^\dagger \hat{b}_j e^{\pm i\theta\hat{n}_{j+1}} + \text{h.c.} \right) \end{aligned} \tag{1.17}$$

The four different Hamiltonians in **Eq**. (1.17) are all (anti-)unitary equivalent, by single or combined applications of a unitary parity transformation $\hat{P}^\dagger \hat{b}_j \hat{P} = \hat{b}_{L-j+1}$ and an

anti-unitary time reversal operation $\hat{T}^\dagger e^{i\alpha}\hat{b}_j\hat{T} = e^{-i\alpha}\hat{b}_j$, e.g.

$$\begin{aligned}
&\hat{P}^\dagger \hat{H}^{\pm,D}_{<}\hat{P} = \hat{H}^{\pm}_{>}, \\
&\hat{T}^\dagger \hat{H}^{\pm,D}_{<}\hat{T} = \hat{H}^{\mp}_{<}, \\
&\left[\hat{T},\hat{P}\right] = 0.
\end{aligned} \tag{1.18}$$

Equations of the form of **Eq**. (1.17) then imply that the different sign conventions of the anyon species are interrelated by the applications of $\hat{P}$ and $\hat{T}$. Conversely, parity and time reversal are not symmetries of such Hamiltonians as in **Eq**. (1.17), which represents a fundamental feature of the one-dimensional bosonic anyons that are discussed here. The asymmetry of fermionic constructions, i.e. $k = -1$, depends on the other hand on the range of anyonic hopping, as well as on the boundary conditions. For example if the hopping is restricted to nearest neighbors, then the only effect of the fractional statistics is potentially encoded in the boundary twist for periodic boundary conditions, whereas anyonic and fermionic versions are equivalent for open boundary conditions [8,27,28]. In this case the Hamiltonians are statistically invariant [8], whereas a boundary-independent operator content appears for fermionic anyons only for a hopping range larger or equal to two lattice sites [28]. In **Ref**. [29] a combination of $\hat{P}$, $\hat{T}$ with a non-linear gauge transformation was found to be a symmetry for such bosonic Hamiltonians, e.g.

$$\left[\hat{G},\hat{H}^{+,D}_{<}\right] = \left[e^{i\theta/2\sum_j \hat{n}_j(\hat{n}_j-1)}\hat{P}\hat{T},\hat{H}^{+,D}_{<}\right] = 0. \tag{1.19}$$

This has a clearer interpretation in the anyonic language as a parity transformation with an attached gauge phase [26], i.e.

$$\hat{G}^\dagger \hat{a}_j \hat{G} = \hat{a}_{L-j+1}e^{-i\theta N}. \tag{1.20}$$

As the duality in **Eq**. (1.14) is unitary implementable, we may trivially conclude that $\Phi_D^{-1}(\hat{G})$ leaves the Hamiltonian in anyonic language, i.e. $\Phi_D^{-1}(\hat{H}^{+,D}_{<})$, invariant [24], whereas the representation in **Eq**. (1.20) implies furthermore that $\hat{G}$ is a hidden symmetry of it [26]. In this section we have derived the fractional Jordan-Wigner transformation by means of a bond algebraic approach, in the spirit of **Ref**. [24]. Thereby the ambiguities in the definition of the fractional Jordan-Wigner string can be related to the phase conventions of the underlying anyonic statistics, as well as to alternative, dual, boson Hamiltonians that are interrelated by time and parity reversal transformations. Additionally, we find an obvious and a hidden symmetry of the anyonic Hamiltonian, by the inverse duality of $\hat{G}$ found in **Ref**. [29] and the application of **Eq**. (1.20). In the next section a potential realization of such density-dependent Peierls phases in the realm of cold atomic gases is discussed. In particular we take emphasis on the first Floquet driving proposal due to the generality inherent to the approach [30].

1.4 Experimental Realization

As we have discussed so far some intriguing algebraic properties of one-dimensional anyons and their relation to ordinary particles, it is now necessary to recapitulate potential experimental realizations. There exist different proposal for realizations for example in optical wave-guides [31], in Rydberg atomic systems [32], or by other means in the realm of cold atomic gases [13, 30, 33–35]. The historically first proposals in **Refs**. [13, 33] rely both on a Raman-laser coupling scheme of tilted, spin-dependent lattices to engineer the density-dependent Peierls phase, by tuning selected hype-fine states accordingly. These approaches are not discussed here and the interested reader should rather consult the original literature [13,33], as we prefer to introduce a different method. Namely, the next scheme in chronological order, that was designed in **Ref**. [30], uses a Floquet driving instead [36–38], which we believe is the most general and versatile among all and has been variously extended since [34, 35]. Thereby the focus is on obtaining an effective model that should represent the anyon-Hubbard model in **Eq**. (1.1), and not on discussing the routine of how to obtain the tight-binding parameters by experimentally adjusting lattice depths or Feshbach tuning of the interactions [39, 40].

The starting point is the following time-dependent version of a bosonic Hubbard Hamiltonian,

$$\hat{H}(t) = -J' \sum_j \left(\hat{b}_j^\dagger \hat{b}_{j-1} + \text{h.c.}\right) + \frac{U'}{2} \sum_j \hat{n}_j(\hat{n}_j - 1) + \sum_j \mu_j \hat{n}_j + \Delta \sum_j j\hat{n}_j + F(t) \sum_j j\hat{n}_j. \tag{1.21}$$

In **Eq**. (1.21), the tight-binding parameters scale the hopping J' of particles, their two-body interaction U', as well as a spatially varying potential that contains different contributions. Here μ_j denotes an arbitrary local potential whereas the other contributions consist of an off-set Δ, as well as a time-periodic function $F(t+T) = F(t)$. off-sets are multiplied by a linear lattice site dependence j, which induces an explicit parity violation of the Hamiltonian even in the absence of a local potential μ_j. It was shown in **Ref**. [30] that, if the following requirements are fulfilled

$$\begin{gathered} \Delta = \hbar\omega \quad , \quad U' = 2\hbar\omega + U, \\ J', U', \mid \mu_j - \mu_{j-1} \mid \ll \hbar\omega, \end{gathered} \tag{1.22}$$

then **Eq**. 1.21 can be mapped to the following high-frequency model to lowest order

$$\hat{H}_{\text{eff}} = \sum_{j=1}^{L} \left[\hat{b}_j^\dagger J_{\text{eff}}(\nu_{j,j-1}) \hat{b}_{j-1} + \text{h.c.}\right] + \frac{U\hat{n}_j(\hat{n}_j - 1)}{2} + \mu_j \hat{n}_j. \tag{1.23}$$

The procedure basically consists of effectively integrating out the strong onsite contributions $\hat{H}_0$ by a suitable time-dependent unitary transformation $\hat{U}(t)$ [36–38]

$$\begin{aligned} \hat{H}_0 &= \hbar\omega \sum_j \hat{n}_j(\hat{n}_j + j - 1) \\ \hat{U}(t) &= e^{-i\left(\hat{H}_0 t - \chi(t) j \hat{n}_j\right)/\hbar} \end{aligned} \tag{1.24}$$

together with a successive averaging over a single driving period T. Fastly oscillating phase factors are thereby eradicated and the hopping matrix elements $J_{\text{eff}}(\nu_{j,j-1})$ are renormalized by the action of $\hat{H}_0$

$$\begin{aligned} J_{\text{eff}}(\nu) &= J/T \int_0^T dt \exp(i\omega\nu t - i\chi(t)) \\ \chi(t) &= -\frac{1}{\hbar}\int_0^t d\tau F(\tau), \end{aligned} \tag{1.25}$$

with $\nu_{j,j-1}$ being the energy change in $\hat{H}_0$ when a particle moves from j to $j-1$, i.e.

$$\nu_{j,j-1} = 2\left(\hat{n}_j - \hat{n}_{j-1}\right) + 3 = \pm 1, \pm 3, .. \quad . \tag{1.26}$$

The crucial part now is the correct engineering of the driving function $F(t)$, such that the density-dependent Peierls phase of the anyonic hopping, as for example in **Eq**. (1.11), is generated. A pictorial representation of **Ref**. [17] of the most probable hopping processes for low densities and a given Peierls phase according to **Eq**. (1.11) is shown below in **Fig**. 1.1.

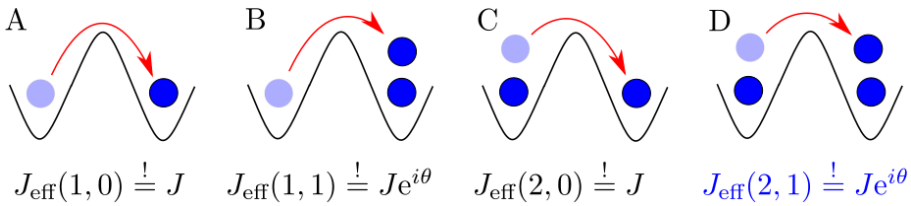

Figure 1.1: *Effective hopping matrix elements as implied by the density-dependent Peierls phase, shown in* **Ref**. *[17] for relatively low densities. In this regime only one-particle process (A) and two particle processes (B,C) are present, whereas three-particle processes (D) and higher order ones become relevant for larger densities.*

A suitable choice of $F(t)$ in the low density regime can be obtained from the following ansatz, i.e.

$$F(t) = -\hbar\dot{\xi}(t) \tag{1.27}$$

with

$$\xi(t) = A\cos(\omega t) + B\cos(2\omega t),$$

under the prerequisite that no three-body processes as (D) in **Fig**.1.1 exist [30]. The amplitudes A, B have then to be chosen such that a given statistical parameter θ in the density-dependent Peierls phase is realized.

Besides the generality that the method possesses, due to the arbitrariness of the function $F(t)$ as well as the possibility to periodically modulate more complicated interactions, we would like to discuss some of it's drawbacks. In the low-density regime the Peierls phase of the anyon-Hubbard model can be faithfully represented by the renormalized hopping of $\hat{H}_{\text{eff}}$, whereas larger densities necessarily include higher order hopping processes that cannot be captured with this choice of driving function $F(t)$, e.g. process (D) in **Fig**. 1.1 and beyond. Furthermore a discrepancy between the Floquet-energy of **Eq**. (1.21) and the ground-state energy of **Eq**. (1.25) has been numerically confirmed in **Ref**. [17], for small system sizes $L = 8$ and increasing densities, see **Fig**. (1.2). This further indicates the necessity of a more general scheme to include such higher order hopping processes, and so investigate the full spectrum of effects that such density-dependent Peierls phases may inherit. Especially important is this in view of potential experimental realization of topological phases for constrained anyons at unit filling, that are theoretically investigated in a later chapter.

Despite such issues, the Floquet engineering of effective models as sketched here [30], is extremely versatile and has been further improved to describe even more complicated correlated hopping models, as for example lattice gauge models [34, 35] or gauge-dressed superfluidity [41]. Hence the formalism should not be viewed only as a possible approach to the dilute anyon-Hubbard model, but more as a general toolbox to engineer non-trivial gauge phases. In the upcoming introductory chapters the impact of the anyonic statistics, discussed here, on various well-known ground-state properties of Bose-Hubbard type models is investigated. Thereby we prefer to recapitulate some known properties of the anyon-Hubbard model, at hand of our own and partially more advanced calculation instead of mechanically reciting the results of the literature [13, 27, 33]. We find generally that the statistical interactions, expressed by the density-dependent Peierls phase, are quite different in nature compared to those occurring as ordinary local interactions, as for example contained in $\hat{H}^{\text{int}}$. These investigations contain in chronological order the integrability of the anyon-Hubbard dimer, which additionally paves the way of rigorously defining anyonic superfluidity through generalized coherent states beyond the two-site system. This is followed by the investigation of the impact of statistical transmutation on the properties of Bogoliubov quasi-particles, whereas we find characteristic but unphysical divergences that are beyond the phenomenology of ordinary inter-particle interactions. In the last introductory chapter the also integrable case of only two

anyons is studied, as well as a strong-coupling perturbative treatment in order to quantify the statistical transmutation by analytical estimates of the universal low-energy parameters. These warm-up chapters are then complemented by an advanced field-theoretical treatment of the anyon-Hubbard model [26], where we explicitly discuss the models low-energy properties as well as its relation to the seminal works of Leinaas, Myrheim and Kundu [4, 7].

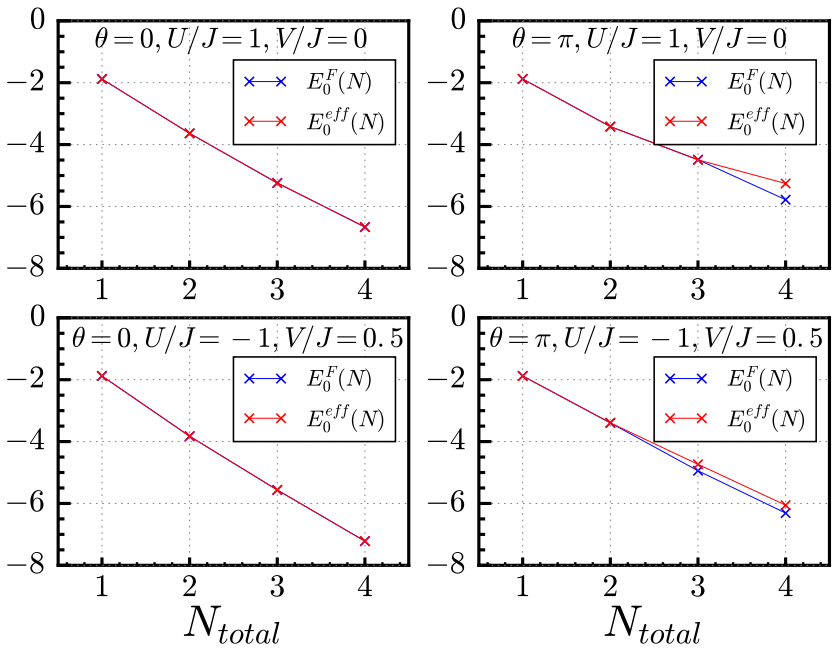

Figure 1.2: *Groundstate energy E_0^F of* **Eq**. *(1.21) compared to E_0^{eff} from $\hat{H}_{\text{eff}}$ that should correspond to the anyon-Hubbard model in* **Ref**. *[17]. The length of the system is $L = 8$, with $\omega = 2 \times 10^5$ and a large Floquet cut-off $N_{Floq.}^{cut} = 200$. Shown are various parameters in the bosonic (left) and pseudo-fermionic (right) limit, where in the bottom two we included extended interactions as well. [17]*

Chapter 2

Introduction to Bosonization

In the following part of the introduction we review the governing principle of one-dimensional gapless quantum fluids, i.e. the Luttinger paradigm. Contrary to our classical understanding of a liquid, to consist of actual particles whether fundamental or composed, those Luttinger liquids may as well represent other degrees of freedom like spins or even more complicated entities, potentially even extended structures [42, 43]. In analogy to other effectively one-dimensional phenomena occurring in nature, as for example traffic jams, traveling wave models of chemo-taxis or pattern formation [44], the motion of such one-dimensional quantum fluids is, indeed, unidirectional and intrinsically collective. This can be understood intuitively already at the classical level, if the particles are postulated to consist of hard-spheres, that cannot pass through each other. Hence their motion is either restricted to individually bounce back and forth around their equilibrium position by scattering off other particles or, alternatively, they perform a collective motion where the initial ordering of the particles remains intact. In higher spatial dimensions the situation changes, as an individual particle has now different possibilities, expressed by the higher connectivity of let's say a crystal lattice, to escape scattering from their direct neighbors and, thus, from the necessity to perform a collective motion. Quantum-mechanically, the Luttinger Hamiltonian is the natural framework to describe collective motion, being a low-energy field-theory that is quadratic in density and phase fluctuations, which represent universal and collective variables of one-dimensional quantum fluids. The field of bosonization is intrinsically rather large with various extensions to incorporate for example the symmetry of non-abelian Lie groups instead of the abelian $U_L(1) \bigotimes U_R(1)$ approach that describes the independent conservation of left and right moving particle species, as explained in the latter. The realm of the abelian Luttinger liquids, as $U_L(1) \bigotimes U_R(1)$ is an abelian group, is then further divided into two branches, in the following sense. The first branch consists of those models that describe the motion of two counter-propagating, linearly dispersing fermion species that are allowed to interact in a more or less specific way following the original ideas of Tomonaga and Luttinger, as well as Lieb and Mattis [25, 45, 46].

The formalization of the second branch was invented by Haldane, who realized first that the Luttinger paradigm was also effectively applicable to systems with non-linear fermion dispersion in the low-energy sector that do not meet the prerequisites of the exact Luttinger liquids [47], and secondly to quite general one-dimensional gapless quantum fluids with the Luttinger model as a universal fix point [48]. The realm of one-dimensional quantum mechanics is tiled with many integrable models, that are so important as they arise also as fix points of more realistic models and provide many powerful analytical techniques as for example the Bethe ansatz. Nevertheless the field theoretical bosonization is omnipresent and represents the method of choice to describe the characteristic decay of correlation functions driven by quantum or thermal fluctuations. As difficult it is to conceptually understand the foundations of the bosonization approach, as useful it is on the other hand as it allows for a straightforward calculation of arbitrary n-point correlation functions by employing the conformal invariance of the underlying field theory at low energies [42, 49–53]. Besides the simple calculation of physical observables, the Luttinger liquid appears also as effective theories at criticality of second order quantum phase transitions that can be used to deduce the universality class of the transition [51]. Successful applications of the method to realistic systems are furthermore extremely broad, for example in the field of carbon nanotubes, scanning tunneling microscopy and quasi one-dimensional spin materials, to name a few historically established examples [42, 43]. More recent applications of Luttinger liquids and its variants concern for example surface currents in topological insulators [54], local representation of non-trivial string orders [55, 56], and Floquet-driven Luttinger liquids. Extensions of the ordinary Luttinger liquid to contain also curvature/high-energy effects, that are related to decay mechanisms of the low-energy excitations, give a more faithful description of energy resolved quantities as for example the dynamical structure factor, and are thus subject of ongoing research [57–59] .

Presenting a self-contained introduction to the field of abelian bosonization, that includes the traditional approach to fermionic systems as well as the harmonic fluid approach for bosons is far beyond the scope of a doctoral thesis [43]. The reader is thus redirected to the literature for a more complete overview and a detailed discussion of the mathematical properties of bosonization [53]. In the following we will thus only shortly review some historical aspects of abelian bosonization as introduced by some of its inventors Luttinger, Lieb and Mattis as well as Haldane [46, 47, 60]. After that the method is exemplary applied to a model of one-dimensional spinless fermions in order to motivate the universality of the method in the spirit of Haldane [47]. Then we will discuss periodic boundary conditions and the meaning of the corresponding selection rule for zero modes. Lastly, the harmonic fluid approach of Haldane is shortly introduced allowing also a long-wavelength representation of an intrinsically bosonic field operator, as well as an extension of ordinary fermionic bosonization to contain higher harmonics beyond $e^{\pm ik_F x}$. Thereby we discuss the non-trivial relation of fermions and bosons in the

harmonic fluid approach and furthermore outline the calculation of arbitrary correlation functions with the help of conformal field theory following Cazalilla [61]. Throughout this chapter we follow the notation of the original publications, such that the attentive reader should not be worried about missing or reappearing Planck constants etc. or an un-uniform notation of operator valued quantities.

2.1 Exact Bosonization à la Luttinger, Lieb and Mattis

In order to appreciate the strength and universality of exact Luttinger liquids in full generality, we recapitulate the duality approach pursued in **Ref**. [24], reformulating Luttingers result in a more rigorous and transparent way. As the fundamental degrees of freedom we take the two-component fermionic spinor $\Psi(x) = (\Psi_L(x), \Psi_R(x))^T$, whose static and dynamical properties are governed by the following Hamiltonian,

$$H_{LL} = \int_0^L dx \;\; \Psi^\dagger(x)\sigma^z\left(-i\partial_x\right)\Psi(x) + \int_0^L \int_0^L dxdy \;\; \Psi_L^\dagger(x)\Psi_L(x)V(x-y)\Psi_R^\dagger(y)\Psi_R(y). \tag{2.1}$$

The actual meaning of the spinor in **Eq**. (2.1) is currently not so relevant, that will be identified later on with left and right moving species relative to the Fermi momentum, i.e. $k_{L,R} = k_F \pm k$. Important is only that both species are linearly dispersing, and counter-propagating as indicated by the diagonal Pauli matrix in **Eq**. (2.1). Furthermore they can interact via a quite arbitrary potential $V(x-y)$ and represent mutually anti-commuting fermionic species. The Hamiltonian in **Eq**. (2.1) conserves each particle number individually, which is formalized by a corresponding product of gauge symmetries, i.e. $U(1)_L \bigotimes U(1)_R$, and can be written in first quantization

$$H_{LL} = \sum_{l=1}^{N_L} p_l - \sum_{r=1}^{N_R} p_r + \sum_{l=1}^{N_L}\sum_{r=1}^{N_R} V(x_l - x_r), \qquad p_j = (-i\partial_{x_j}, x_j). \tag{2.2}$$

In **Eq**. (2.2) we have additionally used a short-hand notation for the particle momenta, and summations are performed over all particle numbers of the (R, L)-species. The Luttinger paradigm for exact models can then be rephrased such that the first quantized Hamiltonian in **Eq**. (2.2) is unitary equivalent to the following Hamiltonian, i.e.

$$H_{LL}^D = \sum_{l=1}^{N_L} p_l^D - \sum_{r=1}^{N_R} p_r^D. \tag{2.3}$$

This bond-duality isomorphism can be proved by defining the new bonds,

$$\begin{aligned} p_l^D \equiv & p_l + \frac{1}{2}\sum_{r=1}^{N_R} V(x_l - x_r) \\ p_r^D \equiv & p_r - \frac{1}{2}\sum_{l=1}^{N_L} V(x_l - x_r), \end{aligned} \tag{2.4}$$

obeying the same algebra as the original entities p_r, p_l, i.e.

$$\left[p_l^D, p_{\tilde{l}}^D\right] = \left[p_r^D, p_{\tilde{r}}^D\right] = \left[p_l^D, p_{\tilde{r}}^D\right] = 0. \tag{2.5}$$

Thus following **Ref**. [24], we have just shown that the Luttinger Hamiltonian **Eq**. (2.2) is dual to **Eq**. (2.3) as both Hamiltonians are related by the duality transformation **Eq**. (2.4) which preserves additionally the algebra of bonds in **Eq**. (2.5). One can prove on general grounds that the duality is unitary implementable, with all the consequences that trivially follow from that [24]. A less trivial statement is that whatever physical interpretation was attached to p_l and p_r, remains attached to the dual operators p_l^D and p_r^D as they fulfill the same algebraic relation. Meaning that even if p_l^D and p_r^D are shifted by the interactions, they still represent the dual particles momenta. Hence for the exact Luttinger liquids, as in **Eq**. (2.1), the renormalization of the kinetic energy by the interactions is independent on the functional form of $V(x_l - x_r)$, which is a quite strong statement that will remain true in a renormalization group sense for the non-exact Luttinger liquids. Luttinger himself constructed such a duality transformation for the special case that the potential averages out over the system length, i.e. $\bar{V} = \int_0^L V(x)dx = 0$ [60], a restriction that was later on relaxed by Lieb and Mattis [46]. The generality of the Luttinger duality in **Eq**. (2.4) is quite mesmerizing in the sense that arbitrary interactions $V(x-y)$ between the two species can be considered, which still lead to a solvable Hamiltonian under the assumption that they are linearly dispersing. Nevertheless, more realistic models are usually not in the form of the Luttinger Hamiltonian in **Eq**. (2.1), hence the concept needed to be adjusted and Luttingers original work was plagued by inconsistencies as his Hamiltonian was not bounded from below and thus did not posses a groundstate [46].

This was achieved by Lieb and Mattis who have further generalized **Eq**. (2.1) to obey more general interactions between the two species and themselves [46]

$$H' = \frac{\lambda}{L}\sum_k V(k)\left[\rho_L(-k) + \rho_R(-k)\right]\left[\rho_L(k) + \rho_R(k)\right] \tag{2.6}$$

with the only premise on the Fourier components of the potential to be absolutely bounded, i.e. $|\lambda V(k)| < \pi \quad \forall k$, such that the full Hamiltonian remains diagonalizable.

The momentum operators of the two species are defined in **Ref**. [46, 60]

$$\begin{aligned}
\Psi^\dagger_{R,L}(x) &= \frac{1}{\sqrt{L}} \sum_{k\in\mathbb{Z}} e^{ikx} c^\dagger_{(R,L),k} \\
\rho_{R,L}(p) &= \sum_{k\in\mathbb{Z}} c^\dagger_{(R,L),k+p} c_{(R,L),k} \\
c_{R,k} &= b_k \text{ if } k \geq 0, \text{ or } c_{R,k} = c^\dagger_k \text{ if } k < 0 \\
c_{L,k} &= b_k \text{ if } k < 0, \text{ or } c_{L,k} = c^\dagger_k \text{ if } k \geq 0,
\end{aligned} \tag{2.7}$$

following the same notation as in Luttingers original publication. The special (anti)-normal ordering prescription in **Eq**. (2.7) is related to exchanging the role of particles and holes, depending on the species momenta relative to the Fermi momentum. In the language of **Eq**. (2.7), the total number of particles then becomes [46],

$$N = \sum_{k\in\mathbb{Z}} \left(b^\dagger_k b_k - c^\dagger_k c_k \right). \tag{2.8}$$

By considering a more mathematically sound treatment of the occurring infinities, that arise through the linearized dispersion and an unbounded set of momenta in **Eq**. (2.7), Lieb and Mattis could correct Luttingers original results leading to the final diagonal form [46], i.e.

$$H_{LL} = \sum_{k\in\mathbb{Z}} |k| \sqrt{1 + \left(\frac{\lambda V(k)}{\pi}\right)^2} \left(b^\dagger_k b_k + c^\dagger_k c_k \right) + \sum_{k>0} k \left(\sqrt{1 + \left(\frac{\lambda V(k)}{\pi}\right)^2} - 1 \right). \tag{2.9}$$

Indeed the results in **Eq**. (2.9) looks like a generalization of the Luttinger duality in **Eq**. (2.4) to more complicated processes in between the two species, where remarkably the dual Hamiltonian is again the sum of two single-particle Hamiltonians as in **Eq**. (2.3). The diagonal form of the Hamiltonian should be interpreted such that the $\hat{b}_k, \hat{c}_k$ operators describe the excitations above the ground state inferred from the positivity of the phonon dispersion. The shift in the ground state energy is given by the constant term in **Eq**. (2.9) that is, indeed, bounded from below in contrast to Luttingers original work [60].

Despite having satisfactorily corrected Luttinger's results and slightly generalized it to incorporate interactions of the form **Eq**. (2.6), the procedure of Lieb and Mattis seems to be of purely academical interest up to now, as the premises of the Luttinger duality seems to be artificial at first sight and not generally fulfilled by realistic models. This gap was closed by Haldane who realized first that also models, that do not precisely obey the form of a Luttinger Hamiltonian, can nevertheless be treated as such, as relativistic invariance is nevertheless granted in a renormalization group sense for low energies [47]. Later on he generalized that observation to include also bosonic degrees

of freedom and thereby generalized also the fermionic description a priori to include higher harmonics then beyond the ordinary $2k_F, 4k_F$ oscillations that will be introduced shortly [47].

2.2 Fermionic Bosonization and it's Field-Theoretical Description

Having experienced the beauty of the exact duality transformation of specifically interacting, counter-propagating and relativisticly dispersing fermionic species to the non-interacting case, it is time to apply the method to more realistic systems. To this end we focus merely on the rough derivation of the Luttinger Liquid for a specific model, motivate the universality of the approach in the sense of Haldane, and subsequently introduce the field-theoretical terminology that naturally embodies the collective variables of density and phase fluctuations. We choose the more applied approach to the bosonization treatment instead of the derivation of exact operator identities in the constructive bosonization [53], as it is conceptually difficult to grasp Haldane harmonic fluid approach for bosons in that framework, whereas the zero-mode approach to bosonization remains straight-forwardly applicable [42, 43, 62]. The model that we exemplary investigate describes spin-polarized fermions on a ring, i.e.

$$\hat{H} = -J\sum_{j=1}^{L}\left(\hat{c}_j^\dagger \hat{c}_{j+1} + \text{h.c.}\right) + V\sum_{j=1}^{L}\hat{n}_j\hat{n}_{j+1}, \quad \hat{c}_{j+L} \equiv \hat{c}_j, \tag{2.10}$$

that are repulsively interacting, i.e. we assume $V > 0$ with their nearest neighbors. For the next step the lattice operators have to be formally projected onto the relevant low-energy degrees of freedom close to the Fermi momentum, i.e.

$$\lim_{a\to 0}\frac{\hat{c}_j}{\sqrt{a}} \approx \hat{\Psi}_R(x)e^{ik_F x} + \hat{\Psi}_L(x)e^{-ik_F x}, \tag{2.11}$$

where a continuum limit is additionally performed in **Eq**. (2.11) [1]. In order to ensure the correct anti-commutation relation for the fermionic operators $\hat{c}_j$, one can conclude that the low-energy projections need to be algebraically independent, e.g

$$\left[\hat{\Psi}_R(x), \hat{\Psi}_L^\dagger(y)\right]_+ = \delta_{R,L}\delta(x-y), \tag{2.12}$$

whereas the left- and right-moving species are defined exactly as in **Eq**. (2.7). Interestingly, only by the inclusion of infinitely many momentum modes the correct anti-commutation relation between the left and right moving species, as well as bi-

[1] The continuum limit in **Eq**. 2.11 interchanges the discrete Kronecker δ in the particle's commutators into discrete δ-functions, according to $\lim_{a\to 0}\delta_{i,j}/a \to \delta(x_i - x_j)$ [15].

linear combinations of them, are preserved, together with the suitable normal ordering description in **Eq**. (2.7) [42, 53]. This so called anomaly should not bother us now conceptually. But it should be noted that once a specific regularization is chosen, that limits the momentum support of the Dirac sea, the commutation relations of the fields are not strictly preserved anymore but correlation functions are therefore free of un-physical divergences. Insertion of the expansion in **Eq**. (2.11) into the Hamiltonian **Eq**. (2.10) and performing a gradient expansion to lowest order, we obtain an interacting model

$$\begin{aligned}\hat{H} \approx \;& v_F \int_0^L dx \left[: \hat{\Psi}_R^\dagger(x)(-i\partial_x)\hat{\Psi}_R(x) : + : \hat{\Psi}_L^\dagger(x)(i\partial_x)\hat{\Psi}_L(x) : \right] \\ &+ \int_0^L dx \left[\frac{g_4}{2} \left(\left(: \hat{\Psi}_R^\dagger(x)\hat{\Psi}_R(x) : \right)^2 + \left(: \hat{\Psi}_L^\dagger(x)\hat{\Psi}_L(x) : \right)^2 \right) \right], \\ &+ \int_0^L dx \left[g_2 : \hat{\Psi}_R^\dagger(x)\hat{\Psi}_R(x) :: \hat{\Psi}_L^\dagger(x)\hat{\Psi}_L(x) : \right],\end{aligned} \tag{2.13}$$

strikingly similar to the extension of Luttingers model by Lieb and Mattis in **Eq**. (2.6). The approximation sign in **Eq**. (2.13) indicates that we have neglected higher order derivatives of the fields in the gradient expansion, as well as higher order interactions between the species that may spoil the integrability of the effective model and are currently assumed to be irrelevant in a renormalization group sense. It should be noted that the form of **Eq**. (2.13) implies that the left and right moving species are separately conserved, indicating an enrichment of the $U(1)$ symmetry of fermionic particle number conservation in **Eq**. (2.10) to a $U(1)_R \bigotimes U(1)_L$ symmetry in the low-energy sector. The beauty of **Eq**. (2.13) should be appreciated with Haldane's approach to non-exact Luttinger liquids in mind [47]. Namely we have effectively derived a Hamiltonian of the form of Lieb and Mattis from a more realistic model that does not obey the prerequisites of the Luttinger duality. Immediately it is clear that the form of **Eq**. (2.13) is universal in the sense that modifications of **Eq**. (2.10), let's say by enlarging the range of hopping to next-nearest neighbors or inclusion of larger range and or higher order interactions, only modifies the constants v_F, g_2 and g_4, that are currently kept arbitrary for that reason. On the other hand the operator content in **Eq**. (2.13) is invariant with respect to such modifications, as long as the symmetry properties of **Eq**. (2.10) are not altered by such perturbations in a renormalization group sense. Thereby it does not matter conceptually if the lattice model is a Bethe integrable model like **Eq**. (2.10) or generally non-integrable, as long as they can be projected onto an effective model of the form of **Eq**. (2.13).

Hence we are allowed to conclude from **Eq**. (2.13) in the spirit of Haldane, that also a realistic fermion model is asymptotically represented by counter propagating relativistic species by the Luttinger duality, if the system is in a compressible state,

i.e. a gapless one. In analogy to the diagonal form that Lieb and Mattis obtained, the Hamiltonian in **Eq**. (2.13) can be brought to a similar form by employing the definitions in **Eq**. (2.7), resulting in the following form for an infinite system

$$\hat{H}_{LL} = \sum_{k\in\mathbb{Z}} \frac{|k|}{2\pi\hbar}\sqrt{[v_F + (g_4 - g_2)][v_F + (g_4 + g_2)]}\left(\hat{b}_k^\dagger \hat{b}_k + \hat{c}_k^\dagger \hat{c}_k\right) + \text{const.}. \tag{2.14}$$

The placeholders g_2 and g_4 in **Eq**. (2.14) are allowed to depend on the momentum k and to be different, which generalizes also the interactions considered by Lieb and Mattis in **Eq**. (2.6), but are generally restricted by the diagonalizability of the underlying Bogoliubov Hamiltonian. Hence any fermionic model that can be projected onto **Eq**. (2.14) in the low-energy regime can be considered a Luttinger liquid in the sense of Haldane [47].

In order to investigate the implications of the Luttinger liquid for correlation functions and connect the excitations to collective variables, it is useful to switch to a terminology that is used more in a field-theoretical context [42,43]. Thereby the left- and right-moving fields are non-regularly represented as vertex operators [51, 63], i.e.

$$\hat{\Psi}_{R,L}^\dagger(x) \propto e^{i(\hat{\phi}(x) \pm \hat{\Theta}(x))}, \tag{2.15}$$

where the proportionality sign in **Eq**. (2.15) indicates neglecting of normal ordering ambiguities. Insertion of **Eq**. (2.15) into **Eq**. (2.13) leads then to the more familiar form of the Tomonaga-Luttinger liquid in terms of bosonic density and phase variables [42], i.e.

$$\hat{H} = u\int_0^L dx \left[K\Big(\partial_x\hat{\phi}(x)\Big)^2 + \frac{1}{K}\Big(\partial_x\hat{\Theta}(x)\Big)^2\right]. \tag{2.16}$$

The gradients of the density and phase variables represent symmetric and anti-symmetric linear combinations of the normal ordered left- and right-moving densities, i.e.

$$\begin{aligned} \partial_x\hat{\phi}(x) &\propto :\hat{\Psi}_R^\dagger(x)\hat{\Psi}_R(x): + :\hat{\Psi}_L^\dagger(x)\hat{\Psi}_L(x):, \\ \partial_x\hat{\Theta}(x) &\propto :\hat{\Psi}_R^\dagger(x)\hat{\Psi}_R(x): - :\hat{\Psi}_L^\dagger(x)\hat{\Psi}_L(x):, \end{aligned} \tag{2.17}$$

that mutually obey dual bosonic commutation relation and are thus easier to interpret then the original fields

$$\Big[\partial_x\hat{\phi}(x), \hat{\Theta}(y)\Big] = \Big[\hat{\phi}(x), \partial_y\hat{\Theta}(y)\Big] = i\delta(x-y). \tag{2.18}$$

The bosonic variables in **Eq**. (2.17) are collective meaning that in order to diagonalize **Eq**. (2.16)), in the form of **Eq**. (2.9), the dual fields have to be decomposed into smaller sets of constituents, the modes, such that the canonical commutation relation **Eq**. (2.18) between the collective variables is conserved. An additional complication of the task is that the properties of the collective fields also depend on the kind of boundary conditions that is chosen for the original model, which then translates immediately to the left and right movers in **Eq**. (2.11) [64–66]. In the following subsection we will discuss those implications for the simple case of periodic boundary conditions.

2.2.1 Periodic Boundary Conditions

In this short subsection we discuss the mode decomposition of the bosonic density and phase fields in terms of their finite momentum components and the independent zero modes. The top-down approach pursued in the following is logically in different order than most of the literature, as we prefer to define the fields from scratch and then deduce their properties successively. For a more detailed discussion and a more coherent derivation of the bosonization approach for finite system sizes the reader is referred to the literature [64–67]. A suitable choice for periodic boundary conditions is the following mode decomposition of the fields [52], i.e.

$$\begin{aligned}\hat{\phi}(x) &= \hat{\phi}_0 - \left(\hat{N} - N_0\right)\frac{\pi x}{L} - \frac{i}{2}\sum_{q\neq 0}\left(\frac{2\pi K}{L|q|}\right)^{1/2}\mathrm{sgn}(q)e^{-iqx}\left[\hat{a}_q^\dagger + \hat{a}_q\right], \\ \hat{\Theta}(x) &= \hat{\Theta}_0 + \hat{J}\frac{\pi x}{L} + \frac{i}{2}\sum_{q\neq 0}\left(\frac{2\pi}{KL|q|}\right)^{1/2}e^{-iqx}\left[\hat{a}_q^\dagger - \hat{a}_q\right], \quad q \equiv q_l = 2\pi l/L\end{aligned} \tag{2.19}$$

Here two independent sets of zero-modes $\left(\hat{\phi}_0, \hat{J}\right)$ and $\left(\hat{\Theta}_0, \hat{N}\right)$ are used, as well as bosonic modes b_q that are quantized according to the boundary conditions. As the definitions in **Eq**. (2.19) are postulated at the moment, let us deduce their properties from the duality relation **Eq**. (2.18). The zero-mode operators ensure the correct commutation relation between the dual field in **Eq**. (2.18) if they obey the following compatibility relation

$$\begin{aligned}\hat{N} &\equiv i\frac{\partial}{\partial\hat{\Theta}_0}, \\ \hat{J} &\equiv i\frac{\partial}{\partial\hat{\phi}_0}.\end{aligned} \tag{2.20}$$

This allows for the interpretation of the zero-mode pairs abstractly, as conjugated position and momentum operators that obey real eigenvalues. But to what they do correspond

physically? Well, the conjugation relation **Eq**. (2.20) implies that exponentials of $\hat{\Theta}_0, \hat{\phi}_0$ obey the following relation

$$\begin{aligned}\left[\hat{N}, e^{-i\hat{\Theta}_0}\right] =& e^{-i\hat{\Theta}_0}, \\ \left[\hat{J}, e^{-i\hat{\phi}_0}\right] =& e^{-i\hat{\phi}_0},\end{aligned} \tag{2.21}$$

meaning that they act as raising and lowering operators on the eigenvalues of $\hat{N}, \hat{J}$. This implies furthermore that exponentials of the zero modes have the effect of raising or lowering the particle number of the fermionic species according to **Eq**. (2.15), a peculiar property that never could be achieved by the finite momentum components $\hat{a}_q$. Inserting the mode expansion of **Eq**. (2.19) into the Luttinger liquid **Eq**. (2.16) one obtains the wanted diagonal form

$$\hat{H} = u \sum_{l \neq 0} \frac{2\pi}{L} |l| \hat{b}_q^\dagger \hat{b}_q + \frac{\pi v_N}{2L} \left(\hat{N} - N_0\right)^2 + \frac{\pi v_J}{2L} \left(\hat{J}\right)^2, \tag{2.22}$$

which is additive in the zero mode as well as the finite momenta part and mutually independent as all parts commute. **Eq**. (2.22) implies then that general states are labeled by the number of excitations $\hat{b}_q^\dagger, \hat{b}_q$, as well as the eigenvalues of $\hat{N}, \hat{J}$ independently, which finally is just a reformulation of the $U(1)_R \bigotimes U(1)_L$ symmetry of the Hamiltonian in **Eq**. (2.13). Hence a generic eigenstate of the Luttinger liquid can be written in the following form

$$|\Psi\rangle_{\mathrm{LL}} \equiv |\{l\}, \{n\}, \{j\}\rangle \propto e^{in\hat{\Theta}_0} e^{ij\hat{\phi}_0} \prod_{l=1}^{\infty} \left(\hat{b}^\dagger_{\frac{2\pi l}{L}}\right)^l |0\rangle\,, \tag{2.23}$$

where the eigenvalues (n, j) are symmetric and anti-symmetric combinations of the particle numbers of the left and right moving species according to **Eq**. (2.17) and **Eq**. (2.19) respectively. Thus one can conclude that the values of (n, j) are not fully independent of each other and are a priori restricted to a set of integers [50].

Besides the labeling of the non-excited states of the Luttinger liquid, one can conclude that the zero-mode operators set the boundary conditions of the dual fields as can be seen from the mode decomposition in **Eq**. (2.19) [42, 51], i.e.

$$\begin{aligned}\hat{\phi}(0) - \hat{\phi}(L) &= \pi \left(\hat{N} - N_0\right), \\ \hat{\Theta}(0) - \hat{\Theta}(L) &= -\pi \hat{J}.\end{aligned} \tag{2.24}$$

Following the definition of the vertex operators **Eq**. (2.15), the zero modes are then also responsible for the boundary conditions of the chiral species and consequently for the

lattice operators, i.e.

$$\frac{\hat{c}_{j+L}}{\sqrt{a}} \propto e^{-i(\phi(x+L)+\Theta(x+L))}e^{ik_F(x+L)} + e^{-i(\phi(x+L)-\Theta(x+L))}e^{-ik_F(x+L)} \tag{2.25}$$

$$\propto \hat{\Psi}_R(x)e^{ik_Fx}e^{-i\pi(\hat{N}-\hat{J})} + \hat{\Psi}_L(x)e^{-ik_Fx}e^{-i\pi(\hat{N}+\hat{J})} \overset{!}{\equiv} \frac{\hat{c}_j}{\sqrt{a}}.$$

Eq. (2.25) is called a selection rule [48], which implies that imposing periodic boundary conditions on the fermionic lattice operators requires the same parity for the integers (n, j) and thus fundamentally fixes a relation between left and right moving species even if they are separately conserved.

Hence we can conclude in total that the zero modes fix the correct boundary conditions for the original fields and create or destroy the fundamental quantum numbers of these intrinsically fermionic degrees of freedom, which would otherwise be impossible to achieve by bosonic excitations $\hat{b}_q$. Furthermore they insure the correct commutation relation between the dual fields and thus engineer the correct anti-commutation relations for the low-energy projections $\hat{\Psi}_{R,L}$ and thus a one to one correspondence between the states of the bosonic and fermionic Fock spaces. In case of many species of fermions the concept of Klein factors has to be introduced as the correct anti-commutation relations as well as creation or annihilation of quantum numbers cannot be achieved in terms of zero modes anymore if there exist more than two species [42, 53].

2.3 Haldane's Harmonic Fluid Bosonization

So far we have seen that the fermionic bosonization approach is extremely powerful, embodying the paradigm for the low-energy properties of gapless fermionic matter in one spatial dimension. Decades after the seminal publications of Luttinger and Tomonaga as well as Lieb and Mattis, it was again Haldane who realized that the concept of collective motion reaches further as originally anticipated and is in fact ubiquitous in one dimension [47, 48]. It turns out that an analogous low-energy projection of the fermionic operators onto independent left- and right-moving species can be obtained also for bosons. For the derivation Haldane considers solely that the overall particle density of one-dimensional bosons can be universally modeled by assuming it to be expressible by slight fluctuations around a classical configuration of particles residing at $\hat{x}_j$ [48, 52, 61], i.e.

$$\hat{\rho}_B(x) = \sum_{j=1}^{N} \delta(x - \hat{x}_j). \tag{2.26}$$

In the next crucial step Haldane introduces a labeling field $\hat{\tilde{\phi}}(x)$ that incorporates effectively the positions of the individual particles by replacing **Eq**. (2.26) with

$$\begin{aligned}\hat{\rho}_B(x) =&\partial_x\hat{\tilde{\phi}}(x)\sum_{j=1}^{N}\delta(\hat{\tilde{\phi}}(x)-j\pi)\\ =&\frac{1}{\pi}\partial_x\hat{\tilde{\phi}}(x)\sum_{m\in\mathbb{Z}}\alpha_m e^{2im\hat{\tilde{\phi}}(x)},\end{aligned} \tag{2.27}$$

where the Poisson summation formula was used in **Eq**. (2.27 [68]). After a redefinition of the field via a local gauge transformation the final form of the bosonized density operator is given by

$$\hat{\rho}_B(x)=\left(\rho_0-\frac{1}{\pi}\partial_x\hat{\phi}(x)\right)\sum_{m\in\mathbb{Z}}\alpha_m e^{2im\left(\pi\rho_0 x-\hat{\phi}(x)\right)}, \tag{2.28}$$

which generalizes the left/right decomposition of fermionic operators **Eq**. (2.11) to higher orders in the lattice harmonics. The corresponding creation operator to **Eq**. (2.11) can be obtained formally by a suitable regularization of the square-root of the delta function arising from another polar decomposition

$$\hat{\Psi}_B^\dagger(x)=\sqrt{\rho_B(x)}e^{-i\hat{\Theta}(x)}=\left(\rho_0-\frac{1}{\pi}\partial_x\hat{\phi}(x)\right)^{1/2}\sum_{m\in\mathbb{Z}}\beta_m e^{2im\left(\pi\rho_0 x-\hat{\phi}(x)\right)}e^{-i\hat{\Theta}(x)}, \tag{2.29}$$

where the density and the phase field are defined as conjugated operators as before in **Eq**. (2.18). The constants α_m and β_m in **Eq**. (2.28) and **Eq**. (2.29), respectively, represent a non-universal feature of the harmonic fluid approach that depends on the short-wavelength structure of the model. In the case of integrable models such constants can sometimes be fixed by the exact solution, otherwise they have to be numerically computed [52, 69].

As the harmonic fluid approach seems to treat bosons analogously to fermions, let us consider a specific bosonic Hamiltonian and study its low-energy projection according to **Eq**. (2.29),

$$\hat{H}=\int_0^L dx\ \left[\partial_x\hat{\Psi}^\dagger(x)\partial_x\hat{\Psi}(x)+c:\hat{\Psi}^\dagger(x)\hat{\Psi}^\dagger(x)\hat{\Psi}(x)\hat{\Psi}(x):\right], \tag{2.30}$$

where we use the Lieb-Liniger model in the following [6]. Insertion of **Eq**. (2.29) into **Eq**. (2.30) and keeping only quadratic terms in the fields fluctuation leads exactly to

the Luttinger Hamiltonian in **Eq**. (2.16), i.e.

$$\hat{H} = u \int_0^L dx \left[K \Big(\partial_x \hat{\phi}(x) \Big)^2 + \frac{1}{K} \Big(\partial_x \hat{\Theta}(x) \Big)^2 \right], \tag{2.31}$$

where of course a redefinition of the universal parameters u and K occurs. In the case of the Lieb-Liniger model the rather uncontrolled derivation of the Luttinger Hamiltonian can be justified rigorously, due to the Bethe integrability of the Hamiltonian [70, 71], and also the linear momentum dependence of low-energy excitation can be shown. The conclusion is that the low-energy projection of a bosonic system has exactly the same operator content as the fermionic low-energy projection discussed before. This instance is usually subsumed under the notion of Bose-Fermi equivalence in one dimension that is more deeply discussed in the next subsection. Due to the asymptotic equivalence of a generic, gapless boson Hamiltonian to **Eq**. (2.10) and from the properties of the Bogoliubov transformation we can conclude that also more general $g_2(k)$ and $g_4(k)$ interacting bosons fall under the Luttinger paradigm. On the other hand, projecting a generic, gapless boson Hamiltonian to the form of **Eq**. (2.13) is a non-trivial task, and usually one has to guess the right operator content of the field theory by symmetry considerations and compute the universal constants numerically.

Eq. (2.29) inherits already an important information that limits the applicability of the harmonic fluid approach, namely that polar decompositions of field operators can include unphysical states and are not well defined if the density fluctuations in the square root are small [72], i.e. $\langle \partial_x \hat{\phi}(x) \rangle \not\ll \rho_0$. Hence we have to be well aware that we have to consider a situation where the density fluctuations $\partial_x \hat{\phi}(x)$ need to be small relative to the average density ρ_0 which might not be always the case. In the same spirit, Didier et al. showed that the inclusion of higher orders in the square root expansion beyond the trivial one in **Eq**. 2.29, i.e. $\Big(\rho_0 - \frac{1}{\pi} \partial_x \hat{\phi}(x) \Big)^{1/2} \approx \sqrt{\rho_0}$, severely improve the short-distance asymptotics of the single-particle density matrix towards numerically exact results [73].

2.3.1 Equivalence of Bosons and Fermions for low Energies

In his seminal publication [48], Haldane used the long-wavelength approximation of the Jordan-Wigner transformation to relate **Eq**. (2.29) to fermionic degrees of freedom, yielding essentially the following form

$$\hat{\Psi}_F^\dagger(x) = \left(\rho_0 - \frac{1}{\pi} \partial_x \hat{\phi}(x) \right)^{1/2} \sum_{m \in \mathbb{Z}} \beta_m e^{i(2m+1)\left(\pi \rho_0 x - \hat{\phi}(x)\right)} e^{-i\hat{\Theta}(x)}. \tag{2.32}$$

But how to understand **Eq**. (2.32), as the Jordan-Wigner transformation cannot change the local statistics from bosonic to fermionic one and thus Haldane's construction would only make sense as an operator identity if the bosons in **Eq**. (2.29) would

represent hardcore particles, i.e. $\left(\hat{\Psi}_B^\dagger(x)\right)^2 = 0$? The spirit of the harmonic fluid approach for bosons is employing one of the principles of one-dimensional systems, as can be seen for example by the Lieb-Liniger model. Namely, that even relatively small interactions quickly overpower the kinetic energy and tune the system to the strong-coupling regime. À la Tonks-Girardeau this implies that the bosons locally behave more and more fermionic as their wave-functions disfavor an overlap for increasing interactions [10, 11]. On the other hand, for free bosons this is clearly not the case and the particles can in principle accumulate on a single point in space. Hence the relation between fermions and bosons that is implied by **Eq**. (2.29) and **Eq**. (2.32) should be understood to hold effectively in the sense of low-energy projections, if and only if the system is sufficiently interacting or sufficiently dilute, such that $\left(\hat{\Psi}_B^\dagger(x)\right)^2 = 0$ is approximately valid. Furthermore, due to the projection to low-energies in terms of non-regular representations of creation and annihilation operators [63], products of operators actually only make sense with a suitable regularization, i.e.

$$\left(\hat{\Psi}_B^\dagger(x)\right)^2 \propto \lim_{a\to 0}\left[\hat{\Psi}_B^\dagger(x)\hat{\Psi}_B^\dagger(x+a) - \langle\hat{\Psi}_B^\dagger(x)\hat{\Psi}_B^\dagger(x+a)\rangle\right]. \tag{2.33}$$

Eq. (2.33) means that a potential hardcore condition appearing when two particles are at the same place in space, is relaxed to a specific region in space determined by the regularization of the modes that sets the resolution of the underlying theory [47, 51].

Anyhow in the absence of interactions we do not expect a hardcore condition for the bosons to be valid, even in the low-energy regime. Thus one concludes that a non-interacting boson system is not a Luttinger liquid, as a vanishing density stiffness implies for a Luttinger Hamiltonian as in **Eq**. (2.16), that there are only phase fluctuations possible, i.e.

$$\lim_{K\to\infty}\hat{H} \equiv \int_0^L dx\ \ v_J\left(\partial_x\hat{\Theta}(x)\right)^2. \tag{2.34}$$

But, does **Eq**. (2.34) mean that in the case of free bosons there exist no density fluctuations $\partial_x\hat{\phi}(x)$ that hinder the system from forming a macroscopically occupied state? Well, from the single-particle density matrix one can conclude that the fate of its long-distance behavior depends on the order in which the following limits are performed

$$\lim_{K\to\infty}\lim_{|x-y|\to\infty}\langle\hat{\Psi}_B^\dagger(x)\hat{\Psi}_B(y)\rangle = 0, \tag{2.35}$$

$$\lim_{|x-y|\to\infty}\lim_{K\to\infty}\langle\hat{\Psi}_B^\dagger(x)\hat{\Psi}_B(y)\rangle \neq 0. \tag{2.36}$$

This indicates either a short-range order according to the Luttinger paradigm, or true long-range order as observed in higher dimensions. Nevertheless, violations of the cluster

decomposition theorem like in **Eq**. (2.36), that explains the spurious loss of quantum mechanical locality in the case of spontaneous symmetry breaking, are not observed for one-dimensional bosons. In the case of interactions the scenario is ruled out by the Mermin-Wagner-Hohenberg theorem and the continuity of the $U(1)$ group of particle number conservation [74, 75]. For free bosonic particles one can explain the absence of a Bose-Einstein condensate in one dimension by a non-vanishing density of states in the thermodynamic limit [40]. This is in contrast to the former bogus argument originating from the rather symbolic exchanging of limits in **Eq**. (2.36) and **Eq**. (2.35). Anyhow, even if non-interacting one-dimensional bosons are intrinsically different from their higher-dimensional counterparts, we can still conclude that the non-interacting limit, i.e. $K \to \infty$, faces some conceptual problems in the harmonic fluid approach. Such subtleties quite often arise for free bosons in one dimension, as for example the absence of an analytical connection between interacting and non-interacting bosons in the Lieb-Liniger model in **Eq**. (2.30) [6, 70, 71], or the breakdown of the Landau argument of superfluidity just to name a few [52].

Let us exclude the pathological case of non-interacting bosons, does this imply that the only effect of the underlying statistics in the framework of bosonization is the slightly different operator content in **Eq**. (2.29) and **Eq**. (2.32)? The answer to this question is quite subtle, as it depends on the given boundary conditions of the original system. In the last subsection we have seen that enforcing boundary conditions on the original particles leads to a so-called selection rule for the zero-modes of the dual fields, as seen in **Eq**. (2.25). For bosonic particles on a ring the selection rule reads $(-1)^{\hat{J}} = 1$, which only requires that the eigenvalues of the current zero modes are even integers, whereas the fermionic one is given by $(-1)^{\hat{J}} = (-1)^{\hat{N}}$. Anyhow the zero-mode contributions in the mode form of the Luttinger liquid as in **Eq**. (2.22) vanish as least of the order of L^{-1}, thus a distinction between bosonic and fermionic entities in terms of zero modes can only be relevant for mesoscopic systems. Another origin of the potential differences between the two fundamental entities in the bosonization approach is hidden in the universal parameters u and K. The precise form of theses parameters are generally related to the compressibility of the fluid and hence depend also on the microscopic interactions that are inextricably intertwined with the underlying statistics, as mentioned by Haldane himself [48].

2.4 Correlation Functions

Besides the universal categorization of one-dimensional quantum fluids with respect to a guiding principle, what does it tell us that the elementary degrees of freedom are free? Well from a practical perspective, free-particle Hamiltonians like the Luttinger liquid one posses eigenstates in product form for which the calculation of observables is drastically simplified, as product states are free of entanglement and classical statistics. But this is

true also for other Hamiltonians for example of the Bogoliubov-De-Gennes type, so why are the correlation functions in bosonization so special? The calculation of arbitrary correlation functions is so simple for the Luttinger liquid, as the building blocks of correlation functions consists of special operators. In order to see this simplification we follow the discussion of Cazalilla [61], where the physical density and phase fields are re-expressed as linear combination of the chiral fields, leading to the equivalent formulation of the Luttinger Hamiltonian in **Eq**. (2.16), which is more useful to discuss the implications of conformal invariance, i.e.

$$\hat{H} = u \int_0^L dx \left[\left(\partial_x \hat{\phi}_R \right)^2 + \left(\partial_x \hat{\phi}_L \right)^2 \right]. \tag{2.37}$$

The first conclusion can be drawn from the algebraic independence of the left and right movers, which implies that the eigenfunctions of **Eq**. (2.37) factorize. Hence an arbitrary vertex operator is expressible in imaginary time $\tau = it$ as

$$\begin{aligned} A_{m,n} =& e^{im\hat{\phi}(x,\tau)} e^{in\hat{\Theta}(x,\tau)} = e^{i\beta(m,-n)\hat{\phi}_L(x,\tau)} e^{i\beta(m,n)\hat{\phi}_R(x,\tau)} \\ \beta(m,n) =& \frac{1}{2}\left(m\sqrt{K} + \frac{n}{\sqrt{K}} \right), \end{aligned} \tag{2.38}$$

that has to be normal ordered in order to isolate and control intrinsic infinities [61]. To use the toolbox of conformal field theory conveniently, it is useful to switch to complex coordinates, i.e. $z = e^{\frac{2\pi/(u\tau+ix)}{L}}$ and $\bar{z} = e^{\frac{2\pi/(u\tau-ix)}{L}}$, and rewrite the mode decomposition in **Eq**. (2.19), as follows

$$\begin{aligned} \hat{\phi}_L(z) &= -\hat{\phi}_{0,L} - i\hat{N}_L \ln(z) + \sum_{m=1}^{\infty} \frac{1}{\sqrt{m}} \left[z^{-m} \hat{b}_{-\frac{2\pi m}{L}} + z^m \hat{b}^\dagger_{-\frac{2\pi m}{L}} \right] \\ \hat{\phi}_R(\bar{z}) &= +\hat{\phi}_{0,R} + iN_R \ln(\bar{z}) + \sum_{m=1}^{\infty} \frac{1}{\sqrt{m}} \left[\bar{z}^{-m} \hat{b}_{-\frac{2\pi m}{L}} + \bar{z}^m \hat{b}^\dagger_{-\frac{2\pi m}{L}} \right]. \end{aligned} \tag{2.39}$$

The mode decomposition in **Eq**. (2.39) manifests the independence of the left- and right-moving species and is used furthermore to define a chiral vertex operator

$$\begin{aligned} :e^{i\beta\hat{\phi}_L(z)}: :=& a^{-\frac{\beta^2}{2}}\left(\frac{2\pi z}{L}\right)^{-\frac{\beta^2}{2}} e^{i\beta\hat{\phi}_L(z)} \\ =& e^{-i\beta\hat{\phi}_{0,L}} e^{+i\beta\hat{N}_L \ln(z)} e^{i\beta\sum_{m=1}^{\infty}\frac{z^m}{\sqrt{m}}\hat{b}^\dagger_{-\frac{2\pi m}{L}}} e^{i\beta\sum_{m=1}^{\infty}\frac{z^{-m}}{\sqrt{m}}\hat{b}_{-\frac{2\pi m}{L}}} \\ :e^{i\beta\hat{\phi}_R(\bar{z})}: :=& a^{-\frac{\beta^2}{2}}\left(\frac{2\pi \bar{z}}{L}\right)^{-\frac{\beta^2}{2}} e^{i\beta\hat{\phi}_L(z)} \\ =& e^{+i\beta\hat{\phi}_{0,R}} e^{-i\beta\hat{N}_R \ln(\bar{z})} e^{i\beta\sum_{m=1}^{\infty}\frac{\bar{z}^m}{\sqrt{m}}\hat{b}^\dagger_{-\frac{2\pi m}{L}}} e^{i\beta\sum_{m=1}^{\infty}\frac{\bar{z}^{-m}}{\sqrt{m}}\hat{b}_{-\frac{2\pi m}{L}}}, \end{aligned} \tag{2.40}$$

where the symbols :: denote normal ordering and a represents an exponential short distance cut-off for the modes in **Eq**. (2.39). The chiral vertex operators in **Eq**. (2.40) have a special property that allows for a maximally simple computation of correlation functions in bosonization, i.e.

$$\begin{aligned} \langle\prod_{i=1}^{p} :e^{i\beta_i\hat{\phi}_L(z_i)}:\rangle &= \prod_{j<k}(z_j - z_k)^{\beta_j\beta_k}, \quad \sum_{i=1}^{p}\beta_i = 0 \\ \langle\prod_{i=1}^{p} :e^{i\beta_i\hat{\phi}_R(\bar{z}_i)}:\rangle &= \prod_{j<k}(\bar{z}_j - \bar{z}_k)^{\beta_j\beta_k}, \quad \sum_{i=1}^{p}\beta_i = 0. \end{aligned} \tag{2.41}$$

The so called neutrality condition in **Eq**. (2.41) is a consequence of the $U_R(1)\bigotimes U_L(1)$ symmetry of the Luttinger liquid in **Eq**. (2.16), with respect to whom the expectation values in **Eq**. (2.41) are defined. Thus the rather formal looking restrictions, that the sum of all powers of vertex operators has to vanish, just means that only expectation values with an equal number of creation and annihilation operators exist for particle number conserving Hamiltonians, unless this symmetry is spontaneously broken in the thermodynamic limit. On the other hand, depending on the boundary conditions of the Luttinger liquid it might be the case that only a single species exists and thus also the neutrality condition is modified accordingly.

So we can conclude that the structure of correlation functions in the bosonization approach is remarkably simple, as the Luttinger liquid decomposes into two independent parts that furthermore conserve the number of particles individually. Arbitrary n-particle correlation functions are represented by products of vertex operators of the form of **Eq**. (2.38) that consist themselves of chiral vertex operators that can be treated then by means of the neutrality condition in **Eq**. (2.41). The functional behavior of expectation values of such vertex operators seems to be predestined to describe algebraic or exponential decay of correlators, whereas the most dominant one is the

equivalent of real long-range order in one-dimensional systems [52]. Furthermore by the use of conformal transformations the correlation functions of a spatially finite system can be mapped elegantly to the correlation functions of an infinite system at finite temperatures [61, 66].

Chapter 3

The Anyon-Hubbard Dimer

In the following chapter the two-site limit of the anyon-Hubbard Hamiltonian is studied, where in particular its integrability, its symmetries, and its relation to the Bose-Hubbard dimer is emphasized [76–80]. The Bose-Hubbard dimer itself can be regarded as the minimal model to investigate tunneling processes between two Bose-Einstein condensates [81], semi-classical limits of strongly correlated bosonic matter [82] [83] as well as the investigation of quantum information-theoretic measures [84] in the realm of cold atomic gases. Hence, the isolated two-site anyon model may serve as well as a valid toy model to investigate the impact of the density-dependent Peierls phase analytically, before we turn the focus on thermodynamic or mesoscopic system sizes. In order to be more explicit, we find a duality according to the definition in **Ref**. [24], mediating between the bosonic and the anyonic dimer and hence prove the integrability of the latter by unitary equivalence to the former integrable model [76–78]. With the aid of the duality transformation, we find an unexpected relation between a permutation symmetry of the Bose dimer at $\mu = 0$ and the Braid group with two strands, whose l-fold application turns out to be a symmetry of the anyonic version for some values of the statistical parameter [3]. We use the algebraic Bethe solution of the Bose dimer to construct the solutions of the dual model in explicit form, which allows then, in principle, for further numerical investigation of form factors for various observables, as for instance the coherence factor of two wells or their particle number fluctuations [81]. For the special case of a vanishing onsite interaction, we discuss yet another exact solution of the anyon dimer in terms of the dual $su(2)$ coherent states [85, 86]. Thereby we find a microscopic interpretation of the superfluid ground state of the anyon dimer, in terms of dual or gauge-dressed bosonic operators [41], that substantially complements the various decoupling mean-field approaches to anyonic superfluidity in the context of the anyon-Hubbard model [13, 87, 88]. Finally the chapter is rounded, by a quantum pendulum approach that allows to treat finite interactions, while partially including quantum effects beyond the mean-field picture.

3.1 Current Algebra and Duality Transformation

In the following we will show a relation between the anyon-Hubbard dimer and its bosonic pendant, via isomorphisms of the Hamiltonians as well as their bond algebras, that generalizes the notion of local unitary equivalence [24]. To this end, it is instructive to investigate the properties of the $su(2)$ current algebras of both models, that determine the particle transport in between the two wells and are directly related to the, experimentally relevant, bosonic quasi-momentum distribution [81, 84]. Studying their connection in detail furthermore paves the way for defining number-conserving group-theoretical coherent states for the anyonic dimer, in full analogy to the bosonic case [85, 86].

The model of interest is given by the following anyonic model on two lattice sites,

$$\hat{H}_{\mathrm{AH}} = -2J\left[\hat{a}_1^\dagger \hat{a}_2 + \mathrm{h.c.}\right] + \frac{U}{2}\sum_{i=1}^{2}\hat{n}_i(\hat{n}_i - 1) - \mu\left(\hat{n}_1 - \hat{n}_2\right), \tag{3.1}$$

which is expressible in bosonic form via the fractional Jordan-Wigner transformation [9, 13]. The anyonic species in **Eq**. (3.1) are defined according to the string orientation

$$\hat{a}_j^\dagger = \hat{b}_j^\dagger e^{i\theta\sum_{l<j}\hat{n}_l}, \tag{3.2}$$

implying the sign convention of their exchange phase, and the density-dependent Peierls phase, used throughout this thesis

$$\hat{H}_{\mathrm{AH}} = -2J\left[\hat{b}_1^\dagger \hat{b}_2 e^{i\theta\hat{n}_1} + \mathrm{h.c.}\right] + \frac{U}{2}\sum_{i=1}^{2}\hat{n}_i(\hat{n}_i - 1) - \mu\left(\hat{n}_1 - \hat{n}_2\right). \tag{3.3}$$

One should remark at this point, that the two-site system is assumed to be tilted, as indicated by the potential off-set scaled by μ that corresponds to an additional local potential for the second well. This choice is rather historically motivated due to being the preferred form of the Hamiltonian for the subsequent discussion of the systems integrability [78, 89, 90]. From the Jordan-Wigner duality in **Eq**. (3.2) we have seen in the introduction, that the L-site Bose-Hubbard model corresponds to the case of a vanishing statistical parameter in the general anyon-Hubbard model. In the following section it is shown that both are connected for general θ if only two lattice sites are considered, i.e. $L = 2$,

$$\hat{H}_{\mathrm{BH}} = -2J\left[\hat{b}_1^\dagger \hat{b}_2 + \mathrm{h.c.}\right] + \frac{U}{2}\sum_{i=1}^{2}\hat{n}_i(\hat{n}_i - 1) - \mu\left(\hat{n}_1 - \hat{n}_2\right). \tag{3.4}$$

Eq. (3.4) can be conveniently represented by Jordan-Schwinger bosons [89, 91],

$$\begin{aligned} \hat{S}^{+} &= \hat{b}_1^{\dagger}\hat{b}_2, \quad \hat{S}^{-} = \hat{b}_2^{\dagger}\hat{b}_1, \\ \hat{S}^{z} &= \frac{1}{2}\left(\hat{n}_1 - \hat{n}_2\right), \qquad \langle \hat{n}_1 + \hat{n}_2 \rangle = N = 2S, \end{aligned} \tag{3.5}$$

which denote the generators of the $su(2)$ algebra in its spin $S = N/2$ representation, i.e.

$$\left[\hat{S}^{\pm}, \hat{S}^{z}\right] = \pm\hat{S}^{\pm} \qquad \left[\hat{S}^{+}, \hat{S}^{-}\right] = 2\hat{S}^{z} \qquad \vec{S}^2 = S(S+1)\hat{1}_{(2S+1)\times(2S+1)}. \tag{3.6}$$

The Jordan-Schwinger bosons in **Eq**. (3.5) build the so called current algebra of the Hamiltonian **Eq**. (3.4) [79–81], which is nothing else than the real form of **Eq**. (3.5), i.e.

$$\begin{aligned} \hat{S}^{x} &= \frac{1}{2}\left(\hat{S}^{+} + \hat{S}^{-}\right), \\ \hat{S}^{y} &= \frac{1}{2i}\left(\hat{S}^{+} - \hat{S}^{-}\right), \\ \hat{S}^{z} &= \hat{S}^{z}. \end{aligned} \tag{3.7}$$

The operators in **Eq**. (3.7) can be derived from the Hamiltonian **Eq**. (3.4) by the Peierls substitution [92] or the equation of motion technique [79], i.e. $\frac{d}{dt}\hat{n}_{1,2} = \pm\hat{S}^{y}$, and additionally demanding closeness with respect to the dynamical $su(2)$ algebra [79]. Whereas dynamical means in this context, that a non-linear Hamiltonian may be represented as a linear combination of the generators of its dynamical group [82, 85, 86]. The x, y, z-components of the spin operators in **Eq**. (3.7) correspond to the coherent, Josephson and imbalance current of the Bose-Hubbard dimer, respectively [79] [80]. For the anyonic dimer in **Eq**. (3.3), the current algebra can be determined analogously, yielding the θ dependent expression

$$\begin{aligned} \hat{s}^{x} &= \frac{1}{2}\left(\hat{b}_1^{\dagger}\hat{b}_2 e^{i\theta(\hat{s}^z+S)} + \text{h.c.}\right) = \frac{1}{2}\left(\hat{s}^{+} + \text{h.c.}\right), \\ \hat{s}^{y} &= \frac{1}{2i}\left(\hat{b}_1^{\dagger}\hat{b}_2 e^{i\theta(\hat{s}^z+S)} - \text{h.c.}\right) = \frac{1}{2i}\left(\hat{s}^{+} - \text{h.c.}\right), \\ \hat{s}^{z} &= \hat{S}^{z}. \end{aligned} \tag{3.8}$$

The crucial point is now that the slightly more complicated definition of generators in **Eq**. (3.8), generalizing the Condon-Shortley phase convention to a state-dependent gauge [93], i.e.

$$\hat{s}^{+} = \hat{b}_1^{\dagger}\hat{b}_2 e^{i\theta(\hat{s}^z+S)}, \qquad \hat{s}^{-} = e^{-i\theta(\hat{s}^z+S)}\hat{b}_2^{\dagger}\hat{b}_1, \qquad \hat{s}^{z} = \hat{S}^{z}, \tag{3.9}$$

fulfills also the $su(2)$ algebra **Eq**. (8.2), as can be shown straight-forwardly

$$\left[\hat{s}^{n=\pm},\hat{s}^{z}\right]=\delta_{n,+}\left[\hat{S}^{+},\hat{S}^{z}\right]e^{i\theta(\hat{s}^{z}+S)}+\delta_{n,-}e^{-i\theta(\hat{s}^{z}+S)}\left[\hat{S}^{-},\hat{S}^{z}\right]=\pm\hat{s}^{\pm}, \tag{3.10}$$

$$\begin{aligned}&\left[\hat{s}^{+},\hat{s}^{-}\right]=\hat{S}^{+}\hat{S}^{-}-e^{-i\theta(\hat{s}^{z}+S)}\hat{S}^{-}\hat{S}^{+}e^{+i\theta(\hat{s}^{z}+S)}\\&=\hat{S}^{+}\hat{S}^{-}-e^{-i\theta(\hat{s}^{z}+S)}\hat{S}^{-}e^{+i\theta(\hat{s}^{z}+S)}e^{-i\theta(\hat{s}^{z}+S)}\hat{S}^{+}e^{+i\theta(\hat{s}^{z}+S)}=2\hat{s}^{z}.\end{aligned} \tag{3.11}$$

As both current algebras in **Eqs**. (3.7) and (3.8) fulfill the same algebraic relations, one can conclude that they are in fact unitary equivalent, with the exact form of the unitary operator given by the following expression [93]

$$\begin{aligned}&\hat{S}^{\pm,z}=\hat{U}^{\dagger}\hat{s}^{\pm,z}\hat{U},\\&\hat{U}=e^{-i\frac{\theta}{2}\hat{S}^{+}\hat{S}^{-}}e^{i\frac{\theta}{2}(2S+1)\hat{S}^{z}}.\end{aligned} \tag{3.12}$$

Following the discussion in **Ref**. [24], we have just shown that the Bose dimer is trivially dual to the anyonic dimer. To be more precise we have related one possible bond algebra of the anyon-Hubbard dimer in **Eq**. (3.3) generated by the bonds

$$\mathcal{A}_{\mathrm{AH}}=\left[\hat{b}_{1}^{\dagger}\hat{b}_{2}e^{i\theta\hat{n}_{1}},e^{-i\theta\hat{n}_{1}}\hat{b}_{2}^{\dagger}\hat{b}_{1},(\hat{n}_{1}-\hat{n}_{2})^{2},\hat{n}_{1}-\hat{n}_{2},\hat{\mathbb{I}}\right]=\left[\hat{s}^{+},\hat{s}^{-},(\hat{s}^{z})^{2},\hat{s}^{z},\hat{\mathbb{I}}\right] \tag{3.13}$$

to one possible bond algebra of the Bose-Hubbard dimer generated by the following bond decomposition

$$\mathcal{A}_{\mathrm{BH}}=\left[\hat{b}_{1}^{\dagger}\hat{b}_{2},\hat{b}_{2}^{\dagger}\hat{b}_{1},(\hat{n}_{1}-\hat{n}_{2})^{2},\hat{n}_{1}-\hat{n}_{2},\hat{\mathbb{I}}\right]=\left[\hat{S}^{+},\hat{S}^{-},(\hat{S}^{z})^{2},\hat{S}^{z},\hat{\mathbb{I}}\right], \tag{3.14}$$

where the explicit duality relation Φ_d between the bonds reads

$$\begin{aligned}&\hat{s}^{+}=\hat{b}_{1}^{\dagger}\hat{b}_{2}e^{i\theta\hat{n}_{1}}\xrightarrow{\Phi_d}\hat{S}^{+}=\hat{b}_{1}^{\dagger}\hat{b}_{2},\\&\hat{s}^{-}=e^{-i\theta\hat{n}_{1}}\hat{b}_{2}^{\dagger}\hat{b}_{1}\xrightarrow{\Phi_d}\hat{S}^{-}=\hat{b}_{2}^{\dagger}\hat{b}_{1},\\&(\hat{s}^{z})^{2}=(\hat{n}_{1}-\hat{n}_{2})^{2}\xrightarrow{\Phi_d}(\hat{S}^{z})^{2}=(\hat{n}_{1}-\hat{n}_{2})^{2},\\&(\hat{s}^{z})=(\hat{n}_{1}-\hat{n}_{2})\xrightarrow{\Phi_d}(\hat{S}^{z})=(\hat{n}_{1}-\hat{n}_{2}).\\&\hat{\mathbb{I}}\xrightarrow{\Phi_d}\hat{\mathbb{I}}.\end{aligned} \tag{3.15}$$

The unitary operator in **Eq**. (3.12) transforms both bond algebras into each other, as well as their corresponding Hamiltonians, meaning their full algebraic structure is preserved, i.e.

$$\begin{aligned}&\Phi_d(\mathcal{A}_{\mathrm{AH}})=\hat{U}^{\dagger}\mathcal{A}_{\mathrm{AH}}\hat{U}=\mathcal{A}_{\mathrm{BH}},\\&\Phi_d(\hat{H}_{\mathrm{AH}})=\hat{U}^{\dagger}\hat{H}_{\mathrm{AH}}\hat{U}=\hat{H}_{\mathrm{BH}}.\end{aligned} \tag{3.16}$$

The duality transformation in **Eq**. (3.12) is necessarily non-local in terms of bosonic operators, whereas this non-locality is rather trivial for a two-site system, but corresponds just to a local $su(2)$ similarity transformation in terms of the Jordan-Schwinger spins [93]. **Eq**. (3.16) implies a stronger connection between the two models as just local unitary equivalence. Consequences of this duality are the equivalence of the spectra, as well as the temporal evolution of observables with respect to their respective Hamiltonians [24]. More importantly the physical interpretation stays attached to the dual bonds as the algebraic structure among them and the Hamiltonian is preserved, which is not true for general local unitary equivalences in terms of fundamental modes.

As the Bose-Hubbard dimer in **Eq**. (3.4) is integrable [76, 78, 89, 90], the same holds also true for the anyonic version, due to the duality relation in **Eq**. (3.16). Nevertheless, before we discuss the exact solution of **Eqs**. (3.3) and (3.4), we investigate the impact of the duality in **Eq**. (3.16) on a particular permutation symmetry of the Bose dimer for a vanishing chemical potential μ [24, 94]. Thereby an unexpected relation to the Braid group is revealed [3], representing itself a cornerstone of two-dimensional anyonic physics as being the fundamental group of the particle configuration space [2, 4].

3.2 Permutation Symmetry and It's Relation to the Braid Group

In the following section a kind of permutation symmetry of the anyon dimer is discussed that can be obtained via the duality in **Eq**. (3.12) to the corresponding permutation symmetry of the Bose dimer [24, 94]. While both symmetries represent the permutation group acting on the two lattice sites, a hidden symmetry for special values of the statistical parameter θ can be obtained by the duality transformation too. This hidden symmetry represents the Braid group acting on the two lattice sites [3], whereas we find the explicit form of its generators as well as their action on the bosonic operators in analogy to the constructions for the permutation group in **Ref**. [95].

The Bose dimer in **Eq**. (3.4) obeys a permutation symmetry for a vanishing chemical potential [79, 95], which is generated by the following transposition

$$\begin{aligned} &\hat{P}_{i,j} = -ie^{i\frac{\pi}{2}\left(\hat{b}_i^\dagger \hat{b}_j + \hat{b}_j^\dagger \hat{b}_i\right)} e^{i\frac{\pi}{2}(1-\hat{n}_i-\hat{n}_j)}, \qquad i,j=1,2 \\ &\hat{P}_{i,j}\hat{b}_j\hat{P}_{i,j}^\dagger = \hat{b}_i. \end{aligned} \tag{3.17}$$

The transposition $\hat{P}_{i,j}$, that exchanges the two well indices, is an element of the symmetric group of two letters S_2 [95]. This symmetry for a vanishing chemical potential implies, that the eigenstates of the Hamiltonian in **Eq**. (3.4) are also eigenstates of the permutation operator in **Eq**. (3.17). Interestingly, the transpositions in **Eq**. (3.17) take exactly the same algebraic form if represented in terms of fermions instead of

bosons [95], whereas their difference is related to the underlying particle statistics via the eigenvalue of $\hat{P}_{i,j}$, which is $+1$ for bosons and -1 for fermions [95].

By taking the inverse duality transform, one concludes that $\Phi_d^{-1}(\hat{P}_{i,j}) = \hat{U}\hat{P_{i,j}}\hat{U}^\dagger$ is a symmetry of the dual model in **Eq**. (3.3) [94] and both share common eigenfunctions. Whereas the initial interpretation of the transformation as a site permutation in **Eq**. (3.17) only applies to the dual operators, i.e.

$$\Phi_d^{-1}(\hat{P}_{i,j})\Phi_d^{-1}(\hat{b}_i)\Phi_d^{-1}(\hat{P}_{i,j}^\dagger) = \Phi_d^{-1}(\hat{b}_j). \tag{3.18}$$

The physical action attached to the dual permutation $\Phi_d^{-1}(\hat{P}_{i,j})$ has then to be interpreted in terms of the ordinary bosons [94]

$$\begin{aligned} \Phi_d^{-1}(\hat{P}_{i,j})\hat{b}_1^\dagger\Phi_d^{-1}(\hat{P}_{i,j}^\dagger) &= \hat{b}_2^\dagger e^{-i\frac{\theta}{2}N}, \\ \Phi_d^{-1}(\hat{P}_{i,j})\hat{b}_2^\dagger\Phi_d^{-1}(\hat{P}_{i,j}^\dagger) &= \hat{b}_1^\dagger e^{i\frac{\theta}{2}N}, \end{aligned} \tag{3.19}$$

which corresponds to a transposition like in **Eq**. (3.17) with an additional phase factor depending on the spatial ordering of the operators. The dual permutation operators in **Eq**. (3.19) have therefore the same eigenvalue $+1$ as an ordinary bosonic permutation in **Eq**. (3.17).
The transformation $\Phi_d^{-1}(\hat{P}_{i,j}) = \hat{U}\hat{P}_{i,j}\hat{U}^\dagger$ should not be confused with $\Phi_d(\hat{P}_{i,j}) = \hat{U}^\dagger\hat{P}_{i,j}\hat{U}$ [94], which is not necessarily a symmetry of the Hamiltonians $\hat{H}_{\mathrm{BH}}, \hat{H}_{\mathrm{AH}}$ but shows some interesting properties when applied to the original bosons, i.e.

$$\begin{aligned} \Phi_d(\hat{P}_{i,j})\hat{b}_1^\dagger\Phi_d(\hat{P}_{i,j}^\dagger) &= \hat{b}_2^\dagger e^{-i\frac{\theta}{2}N}, \\ \Phi_d(\hat{P}_{i,j})\hat{b}_2^\dagger\Phi_d(\hat{P}_{i,j}^\dagger) &= \hat{b}_1^\dagger e^{i\frac{\theta}{2}(N+1)}. \end{aligned} \tag{3.20}$$

In analogy to the inverse dual permutation, $\Phi_d(\hat{P}_{i,j}) = \hat{U}^\dagger\hat{P}_{i,j}\hat{U}$ acts only as an ordinary permutation when applied to the dual operators $\Phi_d(\hat{b}_j) = \hat{U}^\dagger\hat{b}_j\hat{U}$. The difference between the ordinary permutation $\hat{P}_{i,j}$ in **Eq**. (3.17) and the dual $\Phi_d(\hat{P}_{i,j})$ in **Eq**. (3.20) can be investigated in terms of their idempotency properties, i.e.

$$\begin{aligned} &(\hat{P}_{i,j})^n = 1 \quad \text{if} \quad n \quad \text{even}, \\ &(\hat{P}_{i,j})^n = \hat{P}_{i,j} \quad \text{if} \quad n \quad \text{odd}, \\ &(\Phi_d(\hat{P}_{i,j}))^n \neq (\Phi_d(\hat{P}_{i,j}))^m \quad \text{if} \quad n \neq m, \end{aligned} \tag{3.21}$$

that can be interpreted in the $\mathcal{S}_2$ case as either an application of the transposition or the identity element. In the other case one observes that the dual transposition generates the set

$$\mathbb{Z} = \left\{..., (\Phi_d(\hat{P}_{j,i}))^2, (\Phi_d(\hat{P}_{j,i}))^1, 1, (\Phi_d(\hat{P}_{i,j}))^1, (\Phi_d(\hat{P}_{i,j}))^2, ...\right\}, \tag{3.22}$$

which is exactly the defining relation of the infinite cyclic group isomorphic to the Braid group of two strands $\mathbb{Z} \equiv \mathcal{B}_2$ [3]. The eigenvalue of the dual permutation lies on the unit circle, e.g. $\Phi_d(\hat{P}_{i,j})\hat{b}_1^\dagger \hat{b}_2^\dagger |0,0\rangle = e^{i\frac{\theta}{2}}\hat{b}_1^\dagger \hat{b}_2^\dagger |0,0\rangle$, which generalizes the bosonic or fermionic transpositions in **Eq**. (3.17) with eigenvalue ± 1.

As stated before, a single braiding operation in **Eq**. (3.20) is not a symmetry of the anyonic model $\hat{H}_{\mathrm{AH}}^{\mu=0}$ for non-zero θ. Nevertheless, for specific values of the statistical parameter θ, an l-fold braiding, according to **Eq**. (3.22), may trivially emerge as a symmetry, i.e.

$$\Phi_d(\hat{P}_{i,j})^l \hat{H}_{\mathrm{AH}}^{\mu=0} \Phi_d(\hat{P}_{i,j}^\dagger)^l = -2J\left[\hat{a}_1^\dagger \hat{a}_2 e^{-i\frac{\theta}{2}l} + \mathrm{h.c.}\right] + \frac{U}{2}\sum_{i=1}^{2}\hat{n}_i(\hat{n}_i - 1), \tag{3.23}$$

acting as a local gauge transformation on the Hamiltonian. From **Eq**. (3.23) one can then conclude, that the l-braiding operations leave $\hat{H}_{\mathrm{AH}}^{\mu=0}$ invariant if the statistical parameter takes its values in

$$\theta_{\mathcal{B}_2}^{f,l} = \frac{4\pi f}{l} \overset{!}{\in} [0,\pi]\,, \quad f, l \in \mathbb{Z}. \tag{3.24}$$

The invariance of the eigenstates can then be shown explicitly, due to their simple structure in Fock space, which are generically expressible in the form $|\Phi\rangle = \sum_{n,m=0,n+m=N}^{N} c_{n,m}(\hat{b}_1^\dagger)^n(\hat{b}_2^\dagger)^m |0,0\rangle$ [84], i.e.

$$\Phi_d(\hat{P}_{i,j})^l |\Phi\rangle = \sum_{n,m=0,n+m=N}^{N} c_{n,m}(\hat{b}_1^\dagger)^m(\hat{b}_2^\dagger)^n e^{-i\frac{\theta}{2}(m-n)lN} e^{i\frac{\theta}{2}nl} |0,0\rangle \overset{\theta=\theta_{\mathcal{B}_2}^{f,l}, c_{n,m}=c_{m,n}}{=} |\Phi\rangle\,. \tag{3.25}$$

The braids l may represent left/right twisting operations, that can be related via the idempotency property $\Phi_d(\hat{P}_{i,j}^{-1}) = e^{-i\frac{\theta}{2}}\Phi_d(\hat{P}_{i,j})$ that ultimately distinguishes the braid and the symmetric group in **Eqs**. (3.21).

So besides the rather obvious permutation symmetry $\Phi_d^{-1}(\hat{P}_{i,j})$, the anyon-Hubbard dimer may be as well invariant under certain braiding operations for special values of θ according to **Eqs**. (3.23)and (3.24). The exact duality transformation in **Eq**. (3.16), which relates the bosonic version of the dimer to its anyonic relative, also relates the permutation group of two elements to the corresponding Braid group [3], ubiquitously present in the context of two-dimensional anyons and quantum computation [2, 4] but rather trivial in the case of two letters. Therefore, it would be interesting to generalize the generators in **Eq**. (3.20) to the case of the L-stranded Braid group, even if a duality between the anyon and Bose model is not expected beyond $L = 2$ and different methods should be used to find them in explicit form.

3.3 Algebraic Bethe Ansatz Solution

Like its closest relative the L-site Bose-Hubbard model, the anyonic Hubbard Hamiltonian is probably not integrable except for some special cases [96][1]. In principle one would have to check the integrability of the model by means of braided Yang-Baxter relations as explained by Kundu [19, 21] and others [20], as the underlying algebraic structure is not ultra-local [19–21]. This weakened locality condition formalizes the instance that anyonic operators at different places do not commute in contrast to ordinary bosons. Although it seems to be unlikely that the general anyon-Hubbard model is integrable as none of the constructions in [19–21] lead to the anyonic algebra of the model in **Eq**. (3.3) and most of them require some kind of additional hardcore condition on the anyonic operators that is not contained in the anyonic algebra of the anyon-Hubbard model. Nevertheless a potential candidate for an integrable limit is given by the isolated two-site system in accordance to its bosonic pendant [76–78,89,90]. Since quantum integrability is by itself less uniquely defined as in classical mechanics [97], we non-rigorously use a classical argument to motivate the integrability of the dimer system. This is based on the equality of the number of degrees of freedom and the number of conserved quantities which are given by the energy $\hat{H}$ and total particle number $\hat{N}$, respectively. Later on we will see that in the present context, quantum integrability amounts then to the existence of an infinite set of conserved quantities $t(u)$ [97].

The duality in **Eq**. (3.12) and the Jordan map in **Eq**. (3.5) are both unitarily implementable, thus one can conclude that all kinds of solutions to the Bose-Hubbard dimer are also applicable to the anyon-Hubbard model [78, 90]. So now, we will briefly review the algebraic Bethe Ansatz solution of the Bose dimer following **Refs**. [89, 90]. Subsequently, we calculate the eigenvectors of the corresponding anyonic dimer by the application of the duality isomorphism. This finally paves the way of investigating the anyonic model by means of rigorous methods.

As the starting point for the discussion, we have to invert the non-linear $su(2)$ operators *à* la Schwinger and begin with the following Hamiltonian

$$\hat{H} = -2J\left(\hat{b}_1^\dagger \hat{b}_2 + \hat{b}_2^\dagger \hat{b}_1\right) + \frac{U}{8}\left(\hat{n}_1 - \hat{n}_2\right)^2 - \mu\left(\hat{n}_1 - \hat{n}_2\right), \tag{3.26}$$

where we have subtracted a global energy shift due to the conserved total number operator. Integrability can now be shown with the aid of the $su(2)$ invariant R-matrix

[1] In the last introductory chapter yet another integrable sub-case of L-site the anyon-Hubbard model is studied, namely the two-particle case in analogy to the Bose-Hubbard model.

$R(u)$ that depends on the spectral parameter $u \in \mathbb{C}$, i.e.

$$R(u) = \begin{pmatrix} 1 & 0 & 0 & 0 \\ 0 & b(u) & c(u) & 0 \\ 0 & c(u) & b(u) & 0 \\ 0 & 0 & 0 & 1 \\ , & & & \end{pmatrix} \tag{3.27}$$

with $b(u) = u/(u+\eta)$, $c(u) = \eta/(u+\eta)$ and η arbitrary. The matrices $R_{ij}(u)$, as defined in **Eq**. (3.27), satisfy the Yang-Baxter equation [98]

$$R_{12}(u-v)R_{13}(u)R_{23}(v) = R_{23}(v)R_{13}(u)R_{12}(u-v), \tag{3.28}$$

and act only non-trivially on the spaces indicated by i, j. Whereas the Yang-Baxter algebra is defined with the aid of the monodromy matrix $T(u)$, i.e.

$$T(u) = \begin{pmatrix} A(u) & B(u) \\ C(u) & D(u) \\ , & \end{pmatrix} \tag{3.29}$$

fulfilling the following constraint

$$R_{12}(u-v)T_1(u)T_2(v) = T_2(v)T_1(u)R_{12}(u-v). \tag{3.30}$$

For a particular representation Π of $T(u)$, the transfer matrices are defined as

$$t(u) = \Pi(A(u) + D(u)), \tag{3.31}$$

where they commute for arbitrary parameter choices as a consequence of the Yang-Baxter equation in **Eq**. (3.28) and hence embody the set of infinitely many conserved quantities. Now if it exists a pseudo-vacuum $|\chi\rangle$ which satisfies

$$\begin{aligned} &\Pi(A(u))\,|\chi\rangle = a(u)\,|\chi\rangle\,, \qquad \Pi(B(u))\,|\chi\rangle = 0\,|\chi\rangle\,, \\ &\Pi(C(u))\,|\chi\rangle \neq 0\,|\chi\rangle\,, \qquad \Pi(D(u))\,|\chi\rangle = d(u)\,|\chi\rangle\,, \end{aligned} \tag{3.32}$$

then the transfer matrix obeys the following eigenvalue equation

$$\Lambda(u) = a(u)\prod_{k=1}^{M}\frac{u-v_k+\eta}{u-v_k} + d(u)\prod_{k=1}^{M}\frac{u-v_k-\eta}{u-v_k}, \tag{3.33}$$

under the premise that the eigenvalues obey the Bethe-Ansatz equation

$$\frac{a(v_k)}{d(v_k)} = \prod_{j\neq k}^{M} \frac{v_k - v_j - \eta}{v_k - v_j + \eta}, \qquad k = 1, ..., M. \tag{3.34}$$

So far it was shown that the eigenvalues of the transfer matrix in **Eq**. (3.32) can be calculated exactly by the Bethe ansatz equations in **Eq**. (3.34). Now one needs to relate a particular representation of the monodromy matrix to the Bose dimer in order to show its integrability. Therefore, we will choose a representation of the monodromy matrix in terms of the bosonic Lax operators [99] with $i = 1, 2$,

$$\begin{aligned} &\Pi(T(u)) = L_1^b(u+\omega)L_2^b(u-\omega), \\ &L_i^b(u) = \begin{pmatrix} u + \eta N_i & b_i \\ b_i^\dagger & \eta^{-1} \end{pmatrix}. \end{aligned} \tag{3.35}$$

The Lax operators obey the Yang-Baxter algebra in **Eq**. (3.28) with the generators explicitly given by the following expressions

$$\begin{aligned} \Pi(A(u)) &= (u^2 - \omega^2)\hat{I} + \eta u\hat{N} + \eta^2\hat{n}_1\hat{n}_2 - \eta\omega(\hat{n}_1 - \hat{n}_2) + \hat{b}_1^\dagger\hat{b}_2, \\ \Pi(B(u)) &= (u + \omega + \eta\hat{n}_1)\hat{b}_2 + \eta^{-1}\hat{b}_1, \\ \Pi(C(u)) &= \hat{b}_1^\dagger(u - \omega + \eta\hat{n}_2) + \eta^{-1}\hat{b}_2^\dagger, \\ \Pi(D(u)) &= \hat{b}_1^\dagger\hat{b}_2 + \eta^{-2}\hat{I}. \end{aligned} \tag{3.36}$$

They can be used to verify that the Bose-Hubbard Hamiltonian can be expressed solely in terms of the transfer matrix [76, 78, 89], i.e.

$$\hat{H} = -\rho\left[t(u) - \frac{1}{4}(\partial_u t(0))^2 - u\partial_u t(0) - \eta^{-2} + \omega^2 - u^2\right]. \tag{3.37}$$

The coupling constants of the model are related to the parameters of the Yang-Baxter algebra via

$$\frac{U}{8} = \frac{\rho\eta^2}{4}, \qquad \mu = -\rho\eta\omega, \qquad 2J = \rho, \tag{3.38}$$

and the algebraic Bethe Ansatz are applied on the Fock state $|0\rangle$ as the pseudo-vacuum, yielding

$$a(u) = u^2 - \omega^2, \qquad d(u) = \eta^{-2}. \tag{3.39}$$

Hence the Bethe-Ansatz equation take finally the following form

$$\eta^2(v_k^2-\omega^2)=\prod_{j\neq k}^{N}\frac{v_k-v_j-\eta}{v_k-v_j+\eta},\qquad k=1,...,N. \tag{3.40}$$

where the Hamiltonian's energy together with an arbitrary spectral parameter u

$$\begin{aligned}E=&-\rho\left[\eta^{-2}\prod_{j=1}^{N}\left(1+\frac{\eta}{v_i-u}\right)-\frac{\eta^2N^2}{4}-u\eta N-u^2-\eta^{-2}+\omega^2\right]\\&-\rho(u^2-\omega^2)\prod_{j=1}^{N}\left(1-\frac{\eta}{v_i-u}\right),\end{aligned} \tag{3.41}$$

and the corresponding Bethe states [97] according to the definition of the pseudo-vacuum in **Eq**. (3.32)

$$|\Psi\rangle=\prod_{j=1}^{N}C(v_j)\,|0\rangle\,. \tag{3.42}$$

As we have obtained the exact eigenstates of the Bose Dimer and its energy [89, 90], it is time to calculate the anyonic eigenstates. The energies on the other hand are θ independent, due to the unitary relation between the two models. In order to obtain the anyonic eigenstates, we have to express the nonlinear transformation in bosonic language and apply it on the Bethe states of the Bose-Hubbard dimer in **Eq**. (3.42), where the explicit bosonic form of **Eq**. (3.12) reads

$$\hat{U}=e^{-i\frac{\theta}{2}(\hat{n}_1+\hat{n}_1\hat{n}_2)}e^{i\frac{\theta}{4}(N+1)(\hat{n}_1-\hat{n}_2)}. \tag{3.43}$$

So we obtain the following anyonic Bethe states

$$\begin{aligned}|\tilde{\Psi}\rangle&=\hat{U}\prod_{j=1}^{N}C(v_j)\,|0\rangle \qquad (3.44)\\&=\prod_{j=1}^{N}\left[\Phi_d^{-1}(\hat{b}_1^\dagger)(v_j-\omega+\eta\Phi_d^{-1}(\hat{n}_2))+\eta^{-1}\Phi_d^{-1}(\hat{b}_2^\dagger)\right]|0\rangle\,,\\&=\prod_{j=1}^{N}\left[\hat{b}_1^\dagger e^{i\frac{\theta}{4}(N+1)}e^{-i\frac{\theta}{2}(\hat{n}_2+1)}(v_j-\omega+\eta\hat{n}_2)+\eta^{-1}\hat{b}_2^\dagger e^{-i\frac{\theta}{4}(N+1)}e^{i\frac{\theta}{2}\hat{n}_1}\right]|0\rangle\,,\end{aligned}$$

where the set $\{v_j\}_{j=1}^{N}$ contains the solutions of the Bethe equation **Eq**. (3.40). In comparison, **Eq**. (3.44) contains additional operator-valued gauge phases in contrast to the bosonic case [41]. In contrast to that the gauge dressed operators may as well represent independent bosonic creation and annihilation operators due to the unitarity of the duality transformation **Eq**. (3.43) [41].

The anyonic Bethe states may be used to semi-analytically calculate arbitrary observables in closed form. Thus, this approach is more favorable compared, for example, to exact diagonalization, in the sense that it predetermines the structure of correlation functions and eigenvalues and the Bethe roots v_j being the only quantities that have to be determined numerically. This is especially important for large number of particles N, where sophisticated conjectures of the Bethe root structure may provide results but matrix diagonalization becomes unfeasible without choosing a suitable cut-off dimension [76–78]. Despite their closed form, the calculation of observables with respect to the Bethe states in **Eq**. (3.44) is still a numerically demanding task for sufficiently large N and is not the focus of the current chapter. Nevertheless one can immediately conclude that all observables consisting only of the local densities $\hat{n}_{1,2}$, or functions of it, remain the same as for the Bose dimer. Thus we expect the deviations from the bosonic dimer to appear for observables related to the transport between the two wells, as for example the x, y-components of the current algebra in **Eq**. (3.7). In the next section we, therefore, restrict ourselves to the simpler case of a vanishing onsite interaction U, that corresponds exactly to the coherent regime of the Bose dimer whose eigenfunctions are then given by the $su(2)$ coherent states defined by its currents in **Eq**. (3.7) [81, 82, 84]. Additionally we neglect the effect of the lattice tilting μ, for simplicity.

3.4 Coherent States

As we have seen in the last section, the Bethe solutions to the anyon dimer are, indeed, powerful tools, as they allow in principle for the calculation of arbitrary observables without any approximation. The aim of the following section is to provide a simpler picture in the coherent regime without the need of employing extensive numerical evaluations. Especially as the form of the statistical interaction of the anyon model **Eq**. (3.3) already suggests, that deviations from the bosonic behavior should be pronounced deep in the superfluid regime, i.e. for $U \approx 0$. In this case the Bose model is still integrable, though not Bethe-integrable [100], where the ground-state is given by an $su(2)$ coherent state whose properties are briefly reviewed below [82,85,86]. Subsequently, the corresponding states of the anyon dimer can be obtained by their duality relation in **Eq**. (3.16). Interestingly the dual coherent states have already appeared in the context of quantum information theory [93, 101], whereas a microscopic definition of anyonic superfluidity is rather the motivation in our case. This seems to be especially important as previous definitions of anyonic superfluidity in the mean-field framework always rely on a, mathematically non-unique, c-number substitution in the hopping part of the anyon model [13, 87, 88]. In contrast to that, the rigor of group-theoretical coherent states can be used to overcome such issues, and indicates the procedure for future investigations beyond the two site case [85, 86].

For a vanishing onsite interaction U, the exact eigenstates of the Bose-Hubbard dimer in **Eq**. (3.4) are given by the $su(2)$ coherent states [82]

$$|\gamma\rangle_{\mathrm{BH}} = e^{\gamma \hat{S}^{+} - \mathrm{h.c.}} |0\rangle = (1+|\gamma|^2)^{-j} \sum_{m=0}^{2j} \binom{2j}{m}^{1/2} \gamma^m |j, m-j\rangle \,. \tag{3.45}$$

The spin operators in **Eq**. (3.45) are given by the current algebra of the model defined in **Eq**. (3.5) and $\gamma = e^{i\phi}\tan(\Theta/2)$ denotes a complex number that parametrizes the state. The angular quantum number $j = N/2$ in **Eq**. (3.45) describes the average particle number, while the magnetic one $m = (n_1 - n_2)/2$ describes the relative occupation difference in between the wells [82]. In terms of bosonic operators the coherent states have the physically more appealing interpretation as number-conserving macroscopic superpositions of the two modes [82, 83],

$$|\Psi_1, \Psi_2\rangle_{\mathrm{BH}} = \frac{1}{\sqrt{N!}} \left(\frac{1}{\sqrt{2}} \hat{b}_1^{\dagger} + \frac{1}{\sqrt{2}} \hat{b}_2^{\dagger} \right)^N |0,0\rangle \,. \tag{3.46}$$

This corresponds to a large but finite occupation of the lowest momentum *à* la Bose-Einstein, as can be inferred from the definition of the creation/annihilation operators in momentum space, i.e. $\hat{b}_k = \sum_{j=1}^{2} \hat{b}_j e^{-ikj}$. Coherent states, as in **Eq**. (3.45), have a number of quite remarkable properties. For example, they minimize the uncertainty of their generators, they describe the transport in between the wells, and furthermore allow for a geometrical interpretation of their expectation values as coordinates pointing on the surface of a sphere, i.e.

$$\langle \hat{\vec{\mathcal{S}}} \rangle = \begin{pmatrix} \langle \hat{S}^x \rangle \\ \langle \hat{S}^y \rangle \\ \langle \hat{S}^z \rangle \end{pmatrix} = \frac{N}{2} \begin{pmatrix} \sin(\Theta)\cos(\phi) \\ \sin(\Theta)\sin(\phi) \\ \cos(\Theta) \end{pmatrix} . \tag{3.47}$$

Another special property of such coherent states, which is based on the dynamical symmetry group of a given model, is the persistence of coherence if the initial state is a coherent one and the Hamiltonian is linear in the generators of the dynamical group [85, 86]. This means that also the eigenstates of the anyon dimer in **Eq**. (3.1) are given by their corresponding coherent states, whereas the dynamical symmetry group is given by the dual $su(2)$ current algebra in **Eq**. (3.8).

As we have discussed the form and some properties of the coherent states of the Bose dimer, we can now investigate the anyonic ones by their duality. In fact, the generalized coherent states according to the anyonic currents,

$$|\gamma\rangle_{AH} = e^{\gamma \hat{s}^{+} - \mathrm{h.c.}} |0\rangle = (1+|\gamma|^2)^{-j} \sum_{m=0}^{2j} \binom{2j}{m}^{1/2} \gamma^m e^{-i\theta(2jm - m(m+1)/2)} |j, m-j\rangle \,, \tag{3.48}$$

are already known from quantum information theory, but have not been related to a particular particle model so far. These states are known in the context of entangled coherent states [101] and the generation of mutually unbiased bases via $su(2)$ phase operators [93]. Whereas **Eq**. (3.48) differs from **Eq**. (3.45) by an m-dependent phase factor which is, in the special case of $\theta = \pi$, interpretable as a superposition of two ordinary $su(2)$ coherent states with a phase difference of π [101]. A more descriptive representation of the ground state of the non-interacting anyonic dimer can be obtained by applying the duality transformation in **Eq**. (3.12) to **Eq**. (3.46), i.e.

$$\begin{aligned} |\tilde{\Psi}_1, \tilde{\Psi}_2\rangle =& \frac{1}{\sqrt{N!}} \left(\frac{1}{\sqrt{2}} \Phi_d^{-1}(\hat{b}_1^\dagger) + \frac{1}{\sqrt{2}}\ \Phi_d^{-1}(\hat{b}_1^\dagger) \right)^N |0,0\rangle \\ =& \frac{1}{\sqrt{N!}} \left(\frac{1}{\sqrt{2}} \hat{b}_1^\dagger e^{i\frac{\theta}{4}(N+1)} e^{-i\frac{\theta}{2}(\hat{n}_2+1)} + \frac{1}{\sqrt{2}} \hat{b}_2^\dagger e^{-i\frac{\theta}{4}(N+1)} e^{i\frac{\theta}{2}\hat{n}_1} \right)^N |0,0\rangle \,. \end{aligned} \tag{3.49}$$

Eq. (3.46) can then be interpreted formally as a macroscopic occupation of the zero momentum mode of the dual/gauge-dressed operators, i.e. $\Phi_d^{-1}(\hat{b}_k^\dagger) = \sum_{j=1}^2 \Phi_d^{-1}(\hat{b}_j^\dagger) e^{ikj}$, that is of course not related to the momentum of ordinary bosons. In analogy to the bosonic case, the anyonic coherent states in **Eq**. (3.48) minimize the variance of their currents too [85], whereas their expectation values enjoy a particularly nice representation in terms of the bosonic Bloch vector in **Eq**. (3.47), i.e.

$$\begin{pmatrix} \langle \hat{s}^x \rangle_{\mathrm{AH}} \\ \langle \hat{s}^y \rangle_{\mathrm{AH}} \\ \langle \hat{s}^z \rangle_{\mathrm{AH}} \end{pmatrix} = \hat{R}^z[\theta, N] \begin{pmatrix} \langle \hat{S}^x \rangle_{\mathrm{BH}} \\ \langle \hat{S}^y \rangle_{\mathrm{BH}} \\ \langle \hat{S}^z \rangle_{\mathrm{BH}} \end{pmatrix}, \tag{3.50}$$

where the matrix is given by

$$\hat{R}^z[\theta, N] = \begin{pmatrix} \cos[\theta(N-1)] & -\sin[\theta(N-1)] & 0 \\ \sin[\theta(N-1)] & \cos[\theta(N-1)] & 0 \\ 0 & 0 & 1 \end{pmatrix} \tag{3.51}$$

In **Eq**. (3.50), $\hat{R}^z[\theta, N]$ denotes a 3x3 matrix that induces rotations around the $\langle \hat{S}^z \rangle$-axis by the angle $\theta(N-1)$. Thus we may interpret the difference between the currents of the anyon and the Bose dimer, for $U = 0$, geometrically as simple θ and N dependent rotations, that mix the x, y components but leave $\langle \hat{S}^z \rangle$ invariant. This implies that the expectation value of the energy of the non-interacting anyon dimer, which is proportional to $\langle \hat{s}^x \rangle_{\mathrm{AH}}$, consists essentially of the expectation value of the hopping operator of free bosons, proportional to $\langle \hat{S}^x \rangle_{\mathrm{BH}}$, and the bosonic Josephson current $\langle \hat{S}^y \rangle_{\mathrm{BH}}$. The coupling to the Josephson current $\langle \hat{S}^y \rangle_{\mathrm{BH}}$ manifests the breaking of spatio-temporal inversion symmetry as induced by the correlated hopping in **Eq**. (3.3). Additionally, **Eq**. (3.50) shows that the current expectation values are, indeed, periodic functions of the statistical parameter θ, with the periodicity $\theta \to \theta + 2\pi l/(N-1)$, $l \in \mathbb{Z}$, as expected from the

periodicity of the density-dependent Peierls phase in the Hamiltonian in **Eq**. (3.3).

The question that immediately arises is in what sense the kind of superfluidity shown in **Eq**. (3.49), is also present for larger system sizes and how it is related to the rather phenomenological defined broken-symmetry or pair-superfluids in the anyon-Hubbard model, obtained by various c-number substitutions [13, 87, 88]. The ambiguity of the c-number substitution for such correlated hopping models arises from the non-uniqueness of the choice, which decomposition of the hopping operator is expressed as a mean-field plus fluctuations surrounding it[2]. For example, this is visible in the following equivalent bond decompositions of the density-dependent Peierls phase prior to the mean-field approximation, i.e.

$$\hat{b}_j^\dagger e^{i\theta\hat{n}_j} b_{j+1} = \hat{b}_j^\dagger \sum_{q=0}^{\infty} \frac{(i\theta\hat{n}_j)^q}{q!} b_{j+1} = \sum_{q=0}^{\infty}\sum_{m=1}^{q} \frac{(i\theta)^q}{q!} S(q,m) \left(\hat{b}_j^\dagger\right)^{m+1} \left(\hat{b}_j\right)^m b_{j+1}. \quad (3.52)$$

Assuming a product state in the lattice basis $j \in [1, L]$ one would have to decouple any local operator $\hat{x}_j$ in **Eq**. (3.52) into its expectation value $\langle \hat{x}_j \rangle$ plus its fluctuation $\delta\hat{x}_j$, yielding the three a priori different choices,

$$\left(\hat{b}_j^\dagger e^{i\theta\hat{n}_j}, b_{j+1}\right) \Longrightarrow \langle\left(\hat{b}_j^\dagger e^{i\theta\hat{n}_j}, b_{j+1}\right)\rangle + \delta\left(\hat{b}_j^\dagger e^{i\theta\hat{n}_j}, b_{j+1}\right),$$

$$\left(\hat{b}_j^\dagger \hat{n}_j^q, b_{j+1}\right) \Longrightarrow \langle\left(\hat{b}_j^\dagger \hat{n}_j^q, b_{j+1}\right)\rangle + \delta\left(\hat{b}_j^\dagger \hat{n}_j^q, b_{j+1}\right), \quad q \in \mathbb{N} \quad (3.53)$$

$$\left((\hat{b}_j^\dagger)^{m+1}(\hat{b}_j)^m, b_{j+1}\right) \Longrightarrow \langle\left((\hat{b}_j^\dagger)^{m+1}(\hat{b}_j)^m, b_{j+1}\right)\rangle + \delta\left((\hat{b}_j^\dagger)^{m+1}(\hat{b}_j)^m, b_{j+1}\right), \quad m \subseteq q \in \mathbb{N}.$$

It is not clear how to interrelate the different possibilities in **Eq**. (3.53) of having only two or two whole sets of infinitely many variational parameters, unless the precise variational ground-states are known together with their corresponding self-consistency relations. Without such analysis it is impossible to judge how higher order moments are related to lower order ones and, thus, which expectation values are the fundamental and physically reasonable ones, that are identified with the order parameters of potentially different kinds of superfluids[3]. Hence, a rigorous construction of particle non-conserving coherent states based on the anyonic Heisenberg algebra that is contained in **Eq**. (3.1), or particle conserving ones based on the respective deformation of the dynamical symmetry group $su(L > 2)$ [22, 82, 85, 86], would be useful in order to illuminate the microscopic origins

[2]Another source of ambiguities is the spatial resolution of the c-number substitution, that can strictly speaking only be considered as global for translation invariant systems.

[3]In the next chapter, a Bogoliubov decoupling is used that chooses the zero momentum mode $\hat{b}_{k=0}$ as the fundamental order parameter, this fixes the relation between higher and lower order moments with respect to the variational ground-state a priori. Phenomenologically, the approach is only approximately valid for extremely low-densities, as beyond that the model is known to (quasi)-condense at finite momentum [13, 18, 27, 33].

of such anyonic superfluids beyond the two-site system [22]. Furthermore, the anyon-dimer may serve as a platform to investigate experimentally the quantum-information theoretical properties of such special coherent states, described in **Refs**. ([93, 101]).

3.5 Quantum Pendulum Approach

In the last section of this introductory chapter we re-include interactions into the anyonic dimer by means of a quantum pendulum mean-field approach [81, 96, 102]. With this we avoid an extensive analysis of the mean-field limit of **Eq**. (3.3) in terms of its generalized coherent states, by reducing the problem from a spherical to a cylindrical phase-space, while including quantum effects by the Heisenberg uncertainty between effective number and phase operators. Due to the exact solution of the bosonic quantum pendulum in terms of Mathieu functions [103–105], we may treat the anyon dimer analytically by studying the impact of the non-linear gauge transformation in **Eq**. (3.12) on the properties of the pendulum. This rather drastic reduction of complexity to a single-particle problem is only justifiable as long as the population imbalance between the wells is comparably low which allows to treat the vicinity of the center of the sphere according to the Bloch vector in **Eq**. (3.47) as approximately cylindrical. Hence, we consider here the effect of the statistical transmutation on the transport properties and phase information of two macroscopically occupied condensates, that are allowed to interact weakly.

The starting point of the analysis is a naive polar decomposition of the creation/annihilation operators [106, 107], i.e.

$$\begin{aligned} \hat{b}_j^\dagger &= \sqrt{\langle \hat{n}_j \rangle - \hat{n}_j} e^{i\hat{\phi}_j}, \\ \left[\hat{n}_i, \hat{\phi}_j\right] &= i\delta_{i,j}, \quad \hbar = 1 \end{aligned} \tag{3.54}$$

into conjugated phase $\hat{\phi}_j$ and number operators $\hat{n}_j$ in each well $j = 1, 2$. The reader cannot be warned enough about the inconsistencies inherent to the approach [106, 107], that originate from the non-existence of a Taylor series of the square root function around zero and the inclusion of un-physical states of negative occupancy arising due to the repeated application of the non-unitary phase operator $e^{-i\hat{\phi}_j}$ on the vacuum. Nevertheless these well known ambiguities of defining a quantum mechanical phase operator can be neglected as long as the coherence between the two wells is sufficiently high [81]. A premise that is fulfilled deep in the Rabi, i.e. $U/J \ll N^{-2}$, the Josephson, $N^{-2} \ll U/J \ll 1$, but not in the Fock regime $1 \ll U/J$. The role that the interaction plays here, is to reduce the number fluctuations of the condensate until a localization

inside the two wells emerges, which corresponds then to a maximal uncertainty in the condensate phase.

3.5.1 Bosonic Pendulum

Insertion of the mapping **Eq**. (3.54) into the canonical form of the Bose-Hubbard Hamiltonian, while expanding the square root to lowest order around $N/2 = \hat{n}_j$, yields the quantum pendulum Hamiltonian in canonical relative coordinates [81],

$$\begin{aligned} \hat{H}_{\mathrm{BH}} &\approx \frac{U}{2}\hat{n}_- - 2JN\cos(\hat{\phi}_-) \\ \hat{n}_- &= \frac{1}{2}\left(\hat{n}_1 - \hat{n}_2\right), \quad \hat{\phi}_- = \left(\hat{\phi}_1 - \hat{\phi}_2\right). \end{aligned} \tag{3.55}$$

In the phase representation, the quantum pendulum in **Eq**. (3.55) leads to an eigenvalue problem that is known in mathematics as the Mathieu equation [102], i.e.

$$\left(\frac{\partial}{\partial\phi_-}\right)^2 \Psi(r) + \left[p - 2q\cos(2r)\right]\Psi(r) = 0, \tag{3.56}$$

with the identifications $p = 8E/(U)$, $2r = \phi_-$ and $q = 8JN/U$. The periodicity condition of the phase variable $\phi_- + 2\pi = \phi_-$ implies that the solutions of **Eq**. (3.56) have to be invariant under the shift of half a period $r + \pi = r$. This requirement is fulfilled by both the even and the odd Mathieu functions of even order and negative q [4], i.e.

$$\begin{aligned} ce_{2m}(-r,-q) &= (-1)^m ce_{2m}(\pi/2 - r, q), \\ se_{2m+2}(-r,-q) &= (-1)^m se_{2m+2}(\pi/2 - r, q), \quad m \in \mathbb{N}. \end{aligned} \tag{3.57}$$

[4] Note that we are not interested here in non-periodic solutions to the Mathieu equation, as they obviously do not obey the boundary conditions and furthermore can become unbounded. Conversely, such solutions are unacceptable in view of an interpretation of ϕ_- as a variable of angular character, as well as a probabilistic interpretation of the wavefunction.

The orthonormal basis set of the quantum pendulum in **Eq**. (3.57) can conveniently be expressed in terms of Fourier series [102],

$$\begin{aligned}
\Psi^{e}_{0}(\phi_{-},-q) &= \frac{1}{\sqrt{2\pi}} ce_{0}\Big(\frac{\pi-\phi_{-}}{2},q\Big) = \frac{1}{\sqrt{2\pi}}\sum_{j=0}^{\infty} A^{0}_{2j}\cos\left(j\phi_{-}\right),\\
\Psi^{e}_{2m}(\phi_{-},-q) &= \frac{(-1)^{m}}{\sqrt{\pi}} ce_{2m}\Big(\frac{\pi-\phi_{-}}{2},q\Big) = \frac{1}{\sqrt{\pi}}\sum_{j=0}^{\infty} A^{2m}_{2j}\cos\left(j\phi_{-}\right), \quad m\in\mathbb{N}^{+}\\
\Psi^{o}_{2m}(\phi_{-},-q) &= \frac{(-1)^{m+1}}{\sqrt{\pi}} se_{2m+2}\Big(\frac{\pi-\phi_{-}}{2},q\Big) = \frac{1}{\sqrt{2\pi}}\sum_{j=0}^{\infty} B^{2m+2}_{2j+2}\sin\left[(j+1)\phi_{-}\right],
\end{aligned} \tag{3.58}$$

which enables the derivation of the corresponding anyonic states. This is a task, that is otherwise hindered by the sparse amount of functional identities concerning the Mathieu functions [104]. In **Eq**. (3.58) the superscript (o,e) indicates the parity of the Mathieu functions and the coefficients $A^{0,2m}_{2j}, B^{2m+2}_{2j+2}$ can be found by inserting the Fourier series representation into the Mathieu equation, e.g. for the even states

$$\begin{aligned}
&aA_{0} - qA_{2} = 0,\\
&(a-4)A_{2} - q(A_{4}+2A_{0}) = 0,\\
&(a-j^{2})A_{2j} - q(A_{2j+2}+A_{2j-2}) = 0, \quad 2\leq j.
\end{aligned} \tag{3.59}$$

Nevertheless, it should be noted that finding the solution in **Eq**. (3.59) is non-trivial numerically, as convergence problems may appear for uncertain values of the constants $a_{m}(q), b_{2m+2}(q)$ and sophisticated numerical techniques have to be employed [104].

The energy eigenvalues contain then these characteristic constants, according to

$$\begin{aligned}
E_{2m}(q) &= \frac{U}{8}a_{2m}(q),\\
E_{2m+2}(q) &= \frac{U}{8}b_{2m+2}(q).
\end{aligned} \tag{3.60}$$

They denote the specific values for which the even and odd Mathieu functions are in fact periodic, as for example shown in **Eq**. (3.59) for the even functions. The pendulum's energies can then be approximately depicted as transmuting smoothly between the energy of a free rotor for small q and an effectively harmonic potential for large q [81,102]. Due to the duality relation between the two models in **Eq**. (3.16), the energy of the anyonic dimer is also approximately given by **Eq**. (3.60). Thus in the next subsection the emphasis is on studying the impact of statistical transmutation on the pendulum's eigenfunctions.

3.5.2 Anyonic Mathieu Functions

So far we have only derived a set of approximately exact eigenfunctions for the large N Bose-Hubbard dimer. In order to compute the anyonic ones we need to express the duality transformation in **Eq**. (3.16) first in terms of number and phase variables, i.e.

$$\hat{U} = e^{i\frac{\theta N}{2}\hat{n}_-} e^{i\frac{\theta}{2}\hat{n}_-^2}. \tag{3.61}$$

The transformation in **Eq**. (3.61) acts on the phase operator as a trivial shift by a constant and a non-trivial shift by its conjugated operator $\hat{n}_-$, i.e.

$$\hat{U}^\dagger \hat{\phi}_- \hat{U} = \hat{\phi}_- - \frac{\theta N}{2} + \theta \hat{n}_-. \tag{3.62}$$

Here the latter is slightly reminiscent to a Galilean boost after taking the expectation value with velocity $v = \langle \hat{n}_- \rangle$ and time $t = \theta$. **Eq**. (3.61) enjoys yet a clearer interpretation when applied to the Mathieu functions, as we will show in the following. In ϕ_- representation the unitary operator in **Eq**. (3.61) can be related to a translation operator that shifts the argument of the Mathieu functions by $\theta N/2$, as well as Schrödinger kernel on the circle with time $t = \theta$ and unit mass, i.e.

$$\hat{U} = e^{\frac{\theta N}{2}\frac{\partial}{\partial \phi_-}} e^{-i\frac{\theta}{2}\left(\frac{\partial}{\partial \phi_-}\right)^2}. \tag{3.63}$$

The action on the Schrödinger kernel on the constituents of the eigenfunctions can be calculated by an analytic continuation to imaginary statistical parameters $\tilde{\theta} = -i\theta$ and using the damping properties of the corresponding heat semi-group on the circle [108,109], i.e.

$$e^{\tilde{\theta}\left(\frac{\partial}{\partial \phi_-}\right)^2/2} f(\phi_-) = \int_0^{2\pi} dy f(y + \phi_-) p(y, \tilde{\theta}), \tag{3.64}$$

with the periodic heat kernel

$$p(y, \tilde{\theta}) = \frac{1}{\sqrt{4\pi\tilde{\theta}}} \sum_{k\in\mathbb{Z}} e^{\frac{(y-2\pi k)^2}{4\tilde{\theta}}} = \frac{1}{2\pi} \sum_{m\in\mathbb{Z}} e^{-m^2\tilde{\theta}} e^{imy}. \tag{3.65}$$

Eq. (3.64) has then to be interpreted as a convolution of the pendulum's eigenfunction, i.e. $f(\phi_-) \equiv \Psi(\phi_-, -q)^{e,o}_{0,2m}$, with the periodic heat kernel in **Eq**. (3.65) and a Wick rotated statistical phase $\tilde{\theta}$. In terms of the ordinary statistical parameter θ, this leads

finally to the eigenfunctions of the anyonic dimer in pendulum approximation:

$$\begin{aligned}
\tilde{\Psi}^e_0(\phi_-,-q) &= \frac{1}{\sqrt{2\pi}}\sum_{j=0}^{\infty} A^0_{2j} e^{ij^2\theta/2}\cos\Big(j\phi_- + j\theta N/2\Big),\\
\tilde{\Psi}^e_{2m}(\phi_-,-q) &= \frac{1}{\sqrt{\pi}}\sum_{j=0}^{\infty} A^{2m}_{2j} e^{ij^2\theta/2}\cos\Big(j\phi_- + j\theta N/2\Big), \quad m\in\mathbb{N}^+\\
\tilde{\Psi}^o_{2m}(\phi_-,-q) &= \frac{1}{\sqrt{\pi}}\sum_{j=0}^{\infty} B^{2m+2}_{2j+2} e^{i(j+1)^2\theta/2}\sin\Big[(j+1)\phi_- + (j+1)\theta N/2\Big].
\end{aligned} \tag{3.66}$$

The Fourier coefficients of the Mathieu functions in **Eq**. (3.66) are shifted and acquire a non-linear phase depending on the mode index j by the action of the duality transform. Contrary to the heat kernel, the Schrödinger kernel on a compact space is not smoothing in general [108, 109], which can be seen from **Eq**. (3.66), where the Fourier coefficients of the eigenfunctions are de-phased instead of damped out. **Eq**. (3.66) can be expressed again in the Mathieu basis, as we exemplarily show for the ground-state $\tilde{\Psi}^e_0(\phi_-,-q)$, i.e.

$$\begin{aligned}
\tilde{\Psi}^e_0(\phi_-,-q) =& \sum_n \alpha_n(\theta) ce_{2n}(\phi_-/2,q) + \sum_n \beta_n(\theta) se_{2n+2}(\phi_-/2,q),\\
=& \sqrt{\pi}\sum_n \alpha_n(\theta)(-1)^n \Psi^e_{2n}(\phi_-,q) + \sqrt{\pi}\sum_n \beta_n(\theta)(-1)^{n+1}\Psi^o_{2n}(\phi_-,q).
\end{aligned} \tag{3.67}$$

Following **Eq**. (3.67), the anyonic ground-state corresponds to a superposition of even and odd Mathieu functions of even order with an angle ϕ_- shifted by π with respect to the bosonic case. This is equivalent to a linear combination of the bosonic pendulum's excited eigenstates for negative q, i.e repulsive hopping $J = -|J|$. The expansion coefficients $\alpha_n(\theta), \beta_n(\theta)$ are given by the overlap integral of the anyonic ground-state with the bosonic excited states with definite parity from **Eq**. (3.58), i.e.

$$\begin{aligned}
\alpha_n(\theta) &= \sqrt{2}\left[\left\langle \Psi^e_{2n}||\tilde{\Psi}^e_0\right\rangle - A^0_0 A^{2n}_0\right] = \sum_j A^0_{2j} A^{2n}_{2j} e^{ij^2\theta/2}\cos(j\theta N/2),\\
\beta_n(\theta) &= \sqrt{2}\left\langle \Psi^o_{2n}||\tilde{\Psi}^e_0\right\rangle = \sum_j B^{2n+2}_{2j+2} A^0_{2j+2} e^{i(j+1)^2\theta/2}\sin\left[(j+1)\theta N/2\right].
\end{aligned} \tag{3.68}$$

The role of the statistical parameter can be inferred from these coefficients, which is to change both the weight and the phase of the different frequencies in the overlap. A smaller overlap indicates a qualitative difference between the respective states, whereas they can become even orthogonal for specific values of θ. Hence the statistical parameter can act as a kind of filter that diminishes or enhances particular frequencies in the expansion **Eq**. (3.67), as well as shifts their mutual phase information.
Besides the explicit form and interpretation of anyonic Mathieu functions discussed

here, a direct comparison of bosonic and anyonic Mathieu functions is performed in the next section by comparing selected properties of both pendula.

3.5.3 Simple Pendulum Motion and Number and Phase Uncertainties

Having determined the anyonic eigenfunctions in **Eq**. (3.66) exactly, we need to relate them to the motion of the ordinary bosonic pendulum. Therefore we exemplarily calculate the expectation values of the anyonic pendulums position $\langle\hat{\phi}_-\rangle$, as well as its conjugated momentum $\langle\hat{n}_-\rangle$ in the groundstate or the originally even states,

$$\begin{aligned}\langle\hat{\phi}_-\rangle^e_{0,2r} &\propto \sum_{m,n} A^{0,2r}_{2m} A^{0,2r}_{2n} e^{i(m^2-n^2)\theta/2} \sin\left(\frac{mN\theta}{2}\right)\cos\left(\frac{nN\theta}{2}\right), \\ \langle\hat{n}_-\rangle^e_{0,2r} &= 0,\end{aligned} \tag{3.69}$$

and in the odd states respectively, i.e.

$$\begin{aligned}\langle\hat{\phi}_-\rangle^o_{2r} &= 2\sum_{m,n} B^{2r+2}_{2m+2} B^{2r+2}_{2n+2} e^{i\left[(m+1)^2-(n+1)^2\right]\theta/2} \sin\left[\frac{(m+1)N\theta}{2}\right]\sin\left[\frac{(n-1)N\theta}{2}\right], \\ \langle\hat{n}_-\rangle^o_{0,2r} &= -\sum_m (m+1) B^{2r+2}_{2m+2} B^{2r+2}_{2n+2}.\end{aligned} \tag{3.70}$$

Here the proportionality sign in **Eq**. (3.69) corresponds either to the constant 1 in the ground-state or 2 in the excited ones. **Eqs**. (3.69) and (3.70) can then be interpreted such that in the ground (even) states the pendulum is at rest, i.e. $\langle\hat{n}_-\rangle^e_{0,2r} = 0$, whereas the odd states have a non-zero momentum, which is independent on the statistical parameter, as is indicated by the invariance of the momentum $\hat{n}_-$ with respect to the duality transformation. Furthermore, the pendulum angle is not in the classical equilibrium position, unless the statistical parameter is quantized according to $\theta = 2\pi l/N,\ \ l \in [0, N/2]$. Such special values of the exchange phase correspond to the case where the anyonic and the bosonic Bloch vectors coincide, according to **Eq**. (3.50) in the former section, for a macroscopically large number of particles, i.e. $N-1 \approx N$. In terms of the original model this means that in the ground (even)-states the population imbalance between the two wells is zero, but they are off-phase contrary to the bosonic pendulum where both are synchronized[5]. The odd states on the other hand have in addition a finite momentum and thus allow for particle transport in between the wells, whereas the imbalance current itself is equivalent to the bosonic case.

As we have kept a pinch of quantum behavior in the mean-field discussion, the pendulum is not really at rest in the ground (even)-states, nor has it a definite momentum

[5]Synchronized condensates are strictly defined as $\langle\hat{\phi}_-\rangle = 0$ modulo 2π due to the angular character of the phase $\hat{\phi}_-$.

in the odd states, as the observables are allowed to fluctuate around their mean value. This circumstance is expressed in general by the non-zero variance of the conjugated operators with respect to the respective states. In the case of momentum fluctuations the anyonic ones are generally related to those of the bosonic pendulum for all possible states without any further approximation, i.e.

$$\Delta^{\mathrm{AH},o,e}\hat{n}_- = \langle(\hat{n}_- - \langle\hat{n}_-\rangle)^2\rangle_{\mathrm{AH},o,e} = \Delta^{\mathrm{BH},o,e}\hat{n}_-. \tag{3.71}$$

The circumstance in **Eq**. (3.71) is again caused by the equality of the dual momenta. The expectation value of $\hat{n}_-^2$ for each type of states reads,

$$\begin{aligned}\langle\hat{n}_-^2\rangle_{0,2r}^e &= \Delta^{\mathrm{AH},e}\hat{n}_- \propto \sum_j j^2\left(A_{2j}^{0,2r}\right)^2,\\ \langle\hat{n}_-^2\rangle_{2r}^o &= \sum_j (j+1)^2\left(B_{2j+2}^{2r+2}\right)^2,\end{aligned} \tag{3.72}$$

where the proportionality sign in **Eq**. (3.72) corresponds to a factor 1/2 for the groundstate and to a factor 1 for the even states.

Besides the momentum, the pendulum also fluctuates spatially around its expectation value, as can be inferred from the angle variance $\Delta^{\mathrm{AH},o,e}\hat{\phi}_-$. Therefore, we have to calculate first the expectation values of the squared angles in the even states, i.e.

$$\begin{aligned}\langle\hat{\phi}_-^2\rangle_{0,2r}^e \propto& \pi\sum_{\tilde{j},j} A_{2j}^{0,2m}A_{2\tilde{j}}^{0,2m}e^{i\left(j^2-\tilde{j}^2\right)\frac{\theta}{2}}\left[\frac{\sin\left[(j-\tilde{j})\frac{\theta N}{2}\right]}{j-\tilde{j}}+\frac{\sin\left[(j+\tilde{j})\frac{\theta N}{2}\right]}{j+\tilde{j}}\right]\\ &+\sum_{\tilde{j},j} A_{2j}^{0,2m}A_{2\tilde{j}}^{0,2m}e^{i\left(j^2-\tilde{j}^2\right)\frac{\theta}{2}}\left[\frac{\cos\left[(j-\tilde{j})\frac{\theta N}{2}\right]}{(j-\tilde{j})^2}+\frac{\cos\left[(j+\tilde{j})\frac{\theta N}{2}\right]}{(j+\tilde{j})^2}\right],\end{aligned} \tag{3.73}$$

and in the odd states,

$$\begin{aligned}\langle\hat{\phi}_-^2\rangle_{2r}^o =& 2\pi\sum_{\tilde{j},j} B_{2j+2}^{2r+2}B_{2\tilde{j}+2}^{2r+2}e^{i\left(j^2-\tilde{j}^2\right)\frac{\theta}{2}}\left[\frac{\sin\left[(j-\tilde{j})\frac{\theta N}{2}\right]}{j-\tilde{j}}-\frac{\sin\left[(j+\tilde{j}+2)\frac{\theta N}{2}\right]}{j+\tilde{j}+2}\right]\\ &+2\sum_{\tilde{j},j} B_{2j+2}^{2r+2}B_{2\tilde{j}+2}^{2r+2}e^{i\left(j^2-\tilde{j}^2\right)\frac{\theta}{2}}\left[\frac{\cos\left[(j-\tilde{j})\frac{\theta N}{2}\right]}{(j-\tilde{j})^2}-\frac{\cos\left[(j+\tilde{j}+2)\frac{\theta N}{2}\right]}{(j+\tilde{j}+2)^2}\right],\end{aligned} \tag{3.74}$$

respectively. Here the proportionality sign in **Eq**. (3.73) corresponds to a factor of 1 or 2 in the ground state or excited ones. As the expressions for the phase variances

turn out to be quite complicated, we restrict ourselves to the case of even states and a parametrization of $\theta = 2\pi l/N$, that corresponds exactly to the expectation value of the bosonic pendulum angle. Under the former requirements we obtain the phase variance

$$\Delta^{\mathrm{AH},0,e}\hat{\phi}_- \propto \pi^2 l\left(1+(A_0^{0,2m})^2\right)+\sum_{\tilde{j},j} A_{2j}^{0,2m}A_{2\tilde{j}}^{0,2m}e^{i(j^2-\tilde{j}^2)\frac{\pi l}{N}}\left[\frac{(-1)^{(j-\tilde{j})l}}{(j-\tilde{j})^2}+\frac{(-1)^{(j+\tilde{j})l}}{(j+\tilde{j})^2}\right], \tag{3.75}$$

that can be further simplified by expanding in first order in large N and assume an even integer l,

$$\overset{N\to\infty,l=2\tilde{l}}{\overbrace{\approx}} 2\pi^2\tilde{l}\left(1+(A_0^{0,2m})^2\right)+\Delta^{\mathrm{BH},0,e}\hat{\phi}_-. \tag{3.76}$$

For this special case, where N is large and dividable by 4, **Eq**. (3.76) yields a simple relation between the phase fluctuations of the anyonic and the bosonic pendulum. Thereby the variance of the angle is always larger for the anyonic pendulum and their difference is increasing for increasing statistical parameters. As the momentum variance is equivalent for both models the Heisenberg uncertainty relation in this special case reads

$$\Delta^{\mathrm{AH},0,e}\hat{\phi}_-\Delta^{\mathrm{AH},0,e}\hat{n}_- \overset{N\to\infty,l=2\tilde{l}}{\overbrace{\approx}} \Delta^{\mathrm{BH},0,e}\hat{\phi}_-\Delta^{\mathrm{BH},0,e}\hat{n}_- + 2\tilde{l}\pi^2\left(1+(A_0^{0,2m})^2\right)\Delta^{\mathrm{BH},0,e}\hat{n}_-, \tag{3.77}$$

whereas the anyonic ones always exceeds the uncertainty of the bosonic dimer. So we may conclude that the impact of the statistical transmutation on the phase coherence of the two condensates tends to increase the phase fluctuations even if their phases are synchronized for special values of θ. A relation between both models similar to **Eqs**. (3.76) and (3.77) holds probably also away from this special cases, but of course such assertions should be proven by a deeper numerical investigation of the Fourier components of the Mathieu functions. Nevertheless, it should be noted that **Eq**. (3.76) is independent from the exact form of the Fourier coefficients, even if large N implies relatively weak interactions, and additionally the quantization of θ may become effectively negligible in this limit.

Finally one should remark that the discussion of the expectation values calculated in this subsection, except for **Eqs**. (3.76) and 3.77, holds in principle for arbitrary effective interaction constants q, of the Mathieu equation **Eq**. (3.56). Thus one can conclude that the results presented here are valid as long as the coherence prerequisite of the pendulum approximation is obeyed. If one is interested in a more quantitative discussion of observables, the pendulum approximation allows additionally for a relatively simple calculation of the mean-field properties of the anyonic dimer in comparison to other

methods, e.g. calculating the quite complicated Bethe states in **Eq**. (3.44), or analyzing classical but non-linear equations of motions that appear for $U \neq 0$ in terms of the generalized coherent states in **Eq**. (3.49). Thereby we can pictorially describe the effect of the duality transformation between the bosonic and the anyonic dimer for finite interactions by analogy to a simple pendulum and include quantum effects in the discussion beyond mean-field.

3.6 Conclusion

To summarize again the results obtained in this warm up chapter, we have most importantly proved the intergrability of the anyon-Hubbard dimer by showing it's unitary equivalence to the bosonic dimer, a property which is probably not extendable to larger system sizes [19–21]. The link between the two models can be expressed elegantly in terms of bond algebra isomorphisms [24], where we have found the explicit form of the duality transformation mediating between the two, employing a Jordan-Schwinger representation. Furthermore, this transformation allows for the explicit construction of the models eigenstates in terms of the algebraic Bethe states of the Bose-Hubbard dimer [78], as well as anyonic coherent states based on the dual $su(2)$ algebra. The latter can be seen as a starting point to fundamentally investigate anyonic superfluidity beyond the two-site system, in terms of their generalized coherent states [82] instead of more phenomenological approaches of c-number substitutions [13, 87, 88], which are generically plagued by ambiguities. Whereas we find a clear interpretation of the anyon coherent ground state in terms of gauge-dressed operators and furthermore a geometrical relation between the anyonic and the bosonic Bloch vector describing the dynamics of the respective non-interacting Hamiltonians. The anyonic Bethe states on the other hand may be used for future numerical investigation of the model properties in relation to its bosonic relative. In particular we have tried to motivate in this chapter that especially the coherence properties of the two wells are non-trivially affected by statistical transmutations.

For comparably weak interactions and small population imbalances, we have additionally employed an effective quantum pendulum model, which complements the Bethe ansatz results for macroscopically large number of particles N. This allows for a direct interpretation of the coherence properties of the two wells in terms of a quantum phase operator, whereas we find that the equilibrium value of the phases of the wells are not synchronized in general and may fluctuate substantially stronger as compared to the bosonic case. Furthermore we find yet another illustrative interpretation of the anyonic groundstate in this regime, as a linear combination of excited states of the bosonic pendulum with negative hopping parameter J.

For the mathematically interested, we additionally show that the duality transformation can be used to relate the permutation group of two letters $\mathcal{S}_2$ to the corresponding

braid group $\mathcal{B}_2$ [2, 3]. Thereby we find that the anyon-Hubbard dimer may possess an l-folded braiding symmetry for certain values of the statistical parameter. Due to the connection of the anyonic Josephson junction to the Braid group, and to mutually unbiased bases [93] as well as entangled coherent states [101], it seems fair to say that the dimer discussed here may have interesting applications in the realm of quantum information theory or computing and deserve deeper investigations [22]. Nevertheless, in the upcoming introductory chapters the emphasis is on the many-body properties of the L-site system, whereas we study first the impact of statistical transmutations on the stability of the Bogoliubov modes, and later on we determine the models universal low-energy parameters in the strong-coupling regime.

Chapter 4

Bogoliubov Approximation

In the following chapter the Bogoliubov spectrum [23] of the one-dimensional anyonic hopping operator is derived. This allows to illustrate the effect of statistical transmutations on an otherwise free Bose gas from a mean-field perspective. Despite the notorious disadvantages of one-dimensional mean-field theories, they can nevertheless be useful to investigate the ground-state of the real system and the fluctuations surrounding it, provided one addresses a regime where the ground-state can be reasonably approximated by a product state [110]. Various physical quantities can be calculated in this approach but they have to be critically contrasted with other methods more suitable to reduced dimensions, especially with the bosonization approach pursued in chapter (**6**) [43,61]. A well studied feature of the anyon-Hubbard model is the quasi-condensation of bosonic particles at finite momenta. This phenomenon is generally dependent on the average paticle density, as well as on the statistical parameter, and embodies the breaking of time reversal or parity symmetry inherent to the model [18, 27, 29]. The quasi-momentum distribution $\langle \hat{n}_k \rangle$ is furthermore experimentally accessible in time-of-flight experiments and thus a potential candidate to prove the correct implementation of such one-dimensional anyons in optical lattices [39]. As the system is then expected to be in the weakly coupled regime and thus approximately describable by a product state, the quasi-condensation at finite momenta has been well described qualitatively within the Gutzwiller mean-field framework [18, 27]. Nevertheless the physical interpretation is hidden in the rather abstract variational coefficients of the Gutzwiller wave function, that do not provide a straight-forward interpretation in terms of quasi-particles *à* la Landau. Furthermore, a perturbative treatment of the statistical transmutations was pursued in [29], in order to investigate various quantities including also the quasi-momentum distribution. Despite the good agreement with purely numerical methods, the results in **Ref**. [29] suffer from certain unphysical instabilities, as well as from the generic opaqueness of a perturbative treatment. So a more microscopic illustration of these processes is the aim of the following introductory chapter. We find that analogous instabilities as observed in **Ref**. [29] appear also in the current mean-field framework,

in contrast to ordinary two-body interacting bosons. In the following analysis, we focus mainly on the Bogoliubov dispersion minimum as well as its stability analysis relative to the free boson ground-state, which is non-trivially affected by the statistical transmutation. As none of the instabilities studied in the following, or those in the perturbative treatment in **Ref**. [29], are present in the actual physical system, a detailed discussion seems to be redundant. Nevertheless the breakdown of a perturbative or a mean-field treatment per se reveals a special feature of such statistical interactions, that formally distinguishes them from ordinary n-particle interactions. Further differences to Landau quasi-particles arising from ordinary contact interactions are manifest in the absence of a speed of sound, that also has to be understood as a mean-field artifact due to its incompatibility with the Luttinger paradigm. Another interesting quantity usually related to the speed of sound and its vanishing is the so called healing length [40,111,112], which normally corresponds to the length scale at which the phononic dispersion is changing to a massive one. In our case this length has to be defined as the scale at which a massive quasi-particle excitation exceeds the chemical potential of the condensate fluctuations, whereas for the ordinary Bose gas these two definitions of the healing length coincide. This quantity can be used later on as an analytical estimate for the sound wave momentum cut-off in the bosonization approach [61]. At first sight it might sound rather contradictory to relate the healing length derived from a mean-field theory to the properties of the real one-dimensional system, as the phenomenology is quite different in both cases. Nevertheless one can show that the predictions of the Bogoliubov treatment concerning the excitation spectrum becomes essentially exact in the case of the weakly interacting one-dimensional Bose gas [113]. Furthermore the Bogoliubov dispersion for a one-dimensional Bose gas is inextricably linked to the Tomonaga-Luttinger liquid [52], from which it can be derived without assuming the presence of a condensate. Hence one could be tempted to apply the procedure also to the present model, even if not all structural premises of the standard Bose gas are fulfilled [7, 113–118] .

4.1 Derivation

For the derivation it is convenient to normal order the density-dependent Peierls phase [119] of the anyonic hopping operator in bosonic representation and to consider all resulting orders of interactions therein, a fact that was not fully appreciated in various mean-field treatments before, that leads to the necessity of a redundant order parameter [13, 88, 120]. Hence the starting point of the investigation is the following

Hamiltonian in its bosonic description,

$$\begin{aligned}\hat{H}_\mu &= -\sum_{j=1}^{L}\left[\hat{b}_j^\dagger e^{i\theta\hat{n}_j}\hat{b}_{j+1} + \text{h.c.}\right] - \mu\hat{N} \\ &= -\sum_{j=1}^{L}\sum_{q=0}^{\infty}\sum_{m=1}^{q}\left[\frac{(i\theta)^q}{q!}S(q,m)(\hat{b}_j^\dagger)^{m+1}(\hat{b}_j)^m\hat{b}_{j+1} + \text{h.c.}\right] - \mu\hat{N},\end{aligned} \tag{4.1}$$

where $S(q,m)$ denote the Stirling numbers of second kind [121], and periodic boundary conditions are assumed for **Eq**. (4.1). Those Stirling numbers give the number of possibilities how a set of cardinality q is partitioned into m non-empty subsets, and are deeply related to the moments of a Possonian distributed random variable. Physically this means in this context, that the density-dependent Peierls phase is decomposed into m-particle interactions, where all contributions from the q-th moments are summed over. In the following step we express the bosonic operators in terms of plane waves, i.e.

$$\hat{b}_j^\dagger = \frac{1}{\sqrt{L}}\sum_k \hat{b}_k^\dagger e^{ikj}. \tag{4.2}$$

The Bogoliubov approximation basically consists of decomposing the momentum states in a condensed part $\sqrt{N_0}$, which is replaced by a c-number, plus small fluctuations around the mean value $\delta\hat{b}_0$ and the quasi-particles that are completely treated as operators $\hat{b}_{\tilde{k}}$ [122]

$$\sum_k \hat{b}_k e^{ikj} \to \sqrt{N_0} + \delta\hat{b}_0 + \sum_{\tilde{k}\neq 0}\hat{b}_{\tilde{k}}e^{-i\tilde{k}j}. \tag{4.3}$$

Physically this decomposition corresponds to a macroscopic occupation of the ground-state as well as small fluctuations surrounding it. The non-condensed particles arise through inter-particle interactions and are described by the finite momentum components in **Eq**. (4.3). Here it should be clear from the beginning that the assumption of a macroscopic occupation of the $k \approx 0$ state is, besides the generic inadequacy of the method in one dimension, only approximately fulfilled in the case of the anyon-Hubbard model and requires working in the dilute regime [18, 27, 29], where this premise is approximately fulfilled and the point of the quasi-momentum maximum only slightly deviates from the ordinary bosonic case. One word of caution should be devoted to the density-dependence of interactions in one-dimensional systems in comparison to higher spatial dimensions. Namely, that in one-dimensional systems low densities correspond to strong interactions, whereas high densities correspond to weak ones as in the Lieb-Liniger model [6]. In higher spatial dimensions this behavior is reversed, hence the consideration of the small densities still corresponds to the weak-coupling regime in the mean-field context which becomes essentially exact in infinite dimension.

After the insertion of the approximation **Eq**. (4.3) into the Hamiltonian we obtain the following form

$$\hat{H}_\mu \approx \hat{H}_0 + \hat{H}_1 + \hat{H}_2, \tag{4.4}$$

while keeping only contributions of bi-linear order in the quasi-particles. Bi-linear terms in the condensate fluctuations are neglected as they do not contribute, as a set of measure zero, in the thermodynamic limit [122, 123]. Every bilinear combination of non-condensed creation and annihilation operators can be considered leading to

$$\begin{aligned}\hat{H}_2 \approx &- \sum_k \sum_{q=0}^{\infty} \sum_{m=0}^{q} \frac{(i\theta)^q}{q!} \left(\frac{N_0}{L}\right)^m S(q,m) \left[(m+1)(m+e^{ik})\hat{n}_k + \frac{m(m+1)}{2}\hat{b}_k^\dagger \hat{b}_{-k}^\dagger\right] \\ &- \sum_k \sum_{q=0}^{\infty} \sum_{m=0}^{q} \frac{(i\theta)^q}{q!} \left(\frac{N_0}{L}\right)^m S(q,m) \left(\frac{m(m-1)}{2} + me^{ik}\right) \hat{b}_k \hat{b}_{-k} + \text{h.c.}.\end{aligned} \tag{4.5}$$

Constant contributions and first order fluctuations of the condensate are encoded in $\hat{H}_0, \hat{H}_1$,

$$\hat{H}_0 \equiv E_0 = -N_0 \left[\sum_{q=0}^{\infty} \sum_{m=0}^{q} \frac{(i\theta)^q}{q!} \left(\frac{N_0}{L}\right)^m S(q,m) + \text{h.c.}\right] - \mu N_0, \tag{4.6}$$

$$\begin{aligned}\hat{H}_1 = &- \sqrt{N_0} \left[\sum_{q=0}^{\infty} \sum_{m=0}^{q} \frac{(i\theta)^q}{q!}(m+1) \left(\frac{N_0}{L}\right)^m S(q,m) \left(\delta\hat{b}_0^\dagger + \delta\hat{b}_0\right) + \text{h.c.}\right] \\ &- \mu\sqrt{N_0} \left(\delta\hat{b}_0^\dagger + \delta\hat{b}_0\right),\end{aligned} \tag{4.7}$$

whereas couplings between the condensate fluctuations and the Bogoliubov modes, as well as linear terms in quasi-particle fluctuations, vanish due to momentum conservation [23, 122, 123]. In order to evaluate the sums above, it is necessary to realize that the Stirling numbers of second kind can be generated by the following function

$$\begin{aligned}\sum_{q=0}^{\infty} \sum_{m=0}^{q} \frac{(i\theta)^q}{q!} n_0^m S(q,m) &= \sum_{q=0}^{\infty} \frac{(i\theta)^q}{q!} T_q(n_0) \\ &= e^{(e^{i\theta}-1)n_0} = \langle e^{i\theta\hat{n}} \rangle_{\text{Poisson}} \equiv G(\theta, n_0).\end{aligned} \tag{4.8}$$

In **Eq**. (4.8) $T_q(n_0)$ denotes the Touchard polynomials [121], enjoying the statistical interpretation of being the expectation value of the q-th moment of the Poissonian

distributed random variable $\hat{n}_i$ with an expected value of $n_0 = \frac{N_0}{L}$, i.e.

$$T_q(n_0) = \sum_{m=0}^{q} S(q,m) n_0^m = \langle \hat{n}_i^q \rangle_{\text{Poisson}}. \tag{4.9}$$

Consequently the outer summation in **Eq**. (4.8) over q adds all those moments with their corresponding weight $\frac{(i\theta)^q}{q!}$, where the Poissonian moments additionally satisfy the recurrence relation

$$\langle \hat{n}_i^{q+1} \rangle_{\text{Poisson}} = n_0(1 + \partial_{n_0}) \langle \hat{n}_i^q \rangle_{\text{Poisson}}. \tag{4.10}$$

We see from **Eq**. (4.8) that $G(\theta, n_0)$ exponentially decreases in absolute value with the condensate density n_0. Here the argument $-g = (\cos(\theta) - 1)n_0$ of the absolute value of $G(\theta, n_0)$ can be related to the coupling constant for two-particle interactions in the continuum limit of the anyon-Hubbard model, as derived in a later chapter. The relation becomes exact if the inverse lattice spacing a^{-1} is identified with n_0, in analogy to the bosonization approach where the minimal length scale is given by the inverse density [124]. Thus one can rephrase the former statement such that $G(\theta, n_0)$ exponentially decreases with the effective two-body coupling constants g. Furthermore this behavior should be considered already as a warning sign, in the sense that interactions that exponentially grow with the density might lead to unstable behavior.

Problematic is now that not all parts of the sums in **Eqs**. (4.5) and (4.7) can be straight-forwardly treated in the same way, as some polynomial functions in m reside inside the summands, and a closed forms for such sums are currently unknown to the author. Nevertheless the summation can be approximately performed by a trick similar to Feynmans differentiation under the integral. Essential for the approximation is to assume that n_0 can be treated as continuous and thus we can differentiate a given function with respect to this variable, where this physically implies the consideration of sufficiently large system sizes from now on. As an example we obtain for the lowest power in m from **Eq**. (4.7)

$$\sum_{q=0}^{\infty} \sum_{m=0}^{q} \frac{(i\theta)^q}{q!} m n_0^m S(q,m) = n_0 \partial_{n_0} e^{(e^{i\theta}-1)n_0} \equiv \hat{D}(n_0) G(\theta, n_0). \tag{4.11}$$

Hence we will replace any polynomial in m with its corresponding polynomial in $\hat{D}(n_0) = n_0 \partial_{n_0}$ in the following, which suggests the interpretation of the mean-field interactions of the anyon-Hubbard model in terms of infinitesimal changes of the Poissonian mean value n_0 of the density-dependent Peierls phase $G(\theta, n_0)$. By the properties of a Poissonian process, this can be equivalently interpreted as infinitesimal shifts in the variance of the distribution.

A pathological problem of the Bogoliubov approach is the presence of the number of condensed particles N_0 in the mean-field energy E_0, which is not a good quantum number due to the $U(1)$ symmetry breaking of the Hamiltonian [40, 114]. In order to circumvent this problem, the chemical potential is chosen such that the linearly fluctuating terms in the condensate vanish [122], i.e.

$$\sqrt{N_0}\left(-2\hat{D}(n_0)\mathrm{Re}\left(G(\theta,n_0)\right)-\mu\right)\left(\delta\hat{b}_0^\dagger+\delta\hat{b}_0\right)=0, \tag{4.12}$$

$$\Longrightarrow \mu=-2\hat{D}(n_0)\mathrm{Re}(G(\theta,n_0)).$$

The condensate energy without the fluctuation is then given by the quantity

$$E_0=-2N_0\left(1-\hat{D}(n_0)\right)\mathrm{Re}\left(\langle e^{i\theta\hat{n}}\rangle_{\mathrm{Poisson}}\right), \tag{4.13}$$

which is extensive in the total number of particles with an energy density given by the real part of the expectation value of the Peierls phase with respect to a Poissonian state, minus its scaled derivative. We proceed the derivation by evaluating the appearing sums in **Eqs**. (4.5) and (4.7) analogously, and thus obtain the following fluctuation Hamiltonian

$$\hat{H}\approx-\sum_{k>0}\left(A_k\hat{n}_k+A_{-k}\hat{n}_{-k}\right)+\left[(B_k+B_{-k})\hat{b}_k^\dagger\hat{b}_{-k}^\dagger+\mathrm{h.c.}\right]+E_0. \tag{4.14}$$

The prefactors of the non-diagonal Bogoliubov Hamiltonian **Eq**. (4.14) are given by the following expressions

$$A_k=\left[\left((\hat{D}(n_0))^2+(e^{ik}+1)\hat{D}(n_0)+e^{ik}\right)G(\theta,n_0)+\mathrm{h.c.}\right]+\mu, \tag{4.15}$$

$$B_k=\frac{1}{2}\hat{D}(n_0)\left(\hat{D}(n_0)+1\right)G(\theta,n_0)+\frac{1}{2}\hat{D}(n_0)\left(\hat{D}(n_0)+(2e^{-ik}-1)\right)\bar{G}(\theta,n_0), \tag{4.16}$$

where the overbar denotes complex conjugation. The violation of parity as well as time reversal symmetry of the original Hamiltonian [13, 18, 27, 29] is already indicated by the asymmetry of **Eq**. (4.15) with respect to the reflection of k, as well as the momentum dependence of the off-diagonal coupling **Eq**. (4.16), in contrast to ordinary two-particle interactions in the Bogoliubov framework.

As the Bogoliubov Hamiltonian **Eq**. (4.14) is rather cumbersome to diagonalize, due to the presence of complex and momentum-dependent off-diagonal terms, we transform

the Hamiltonian with a local gauge transformation to eliminate those contributions, i.e.

$$\hat{\tilde{H}} = \left(\prod_k \hat{U}_k^\dagger\right) \hat{H} \left(\prod_k \hat{U}_k\right), \tag{4.17}$$

$$\hat{U}_k = e^{i\Theta(k)\mathrm{Arg}(B_k + B_{-k})\hat{n}_k}, \tag{4.18}$$

where $\Theta(k)$ denotes the Heaviside step function. It should be mentioned that this transformation drastically simplifies the following calculations, but can alter the form of correlation functions non-trivially, by attaching a momentum-dependent phase to the forward propagating quasi-particles, see **Fig**. (4.1). The gauge-transformed Hamiltonian now has real coefficients

$$\hat{\tilde{H}} - E_0 \approx -\sum_{k>0} \left(A_k \hat{n}_k + A_{-k}\hat{n}_{-k}\right) + |B_k + B_{-k}| \left[\hat{b}_k^\dagger \hat{b}_{-k}^\dagger + \text{h.c.}\right]. \tag{4.19}$$

and thus can be solved with the standard Bogoliubov transformation [23]

$$\hat{b}_k = \cosh(\alpha_k)\hat{a}_k - \sinh(\alpha_k)\hat{a}_{-k}^\dagger, \tag{4.20}$$

where we can choose all the appearing parameters to be real. We obtain the following common relation for the Bogoliubov angle

$$\tanh(2\alpha_k) = \frac{|B_k + B_{-k}|}{\left(A_k + A_{-k}\right)}, \tag{4.21}$$

with the final diagonal form of the Hamiltonian

$$\hat{\tilde{H}} - E_0 \approx -\frac{1}{2}\sum_{k\neq 0} \left(\epsilon_k^+ \hat{n}_k + \epsilon_k^- \hat{n}_{-k} + \epsilon_k^{+,-}\right). \tag{4.22}$$

As discussed previously, the spatio-temporal reflection asymmetry leads to the presence of two forward/backward propagating species for a given value of k, where their respective

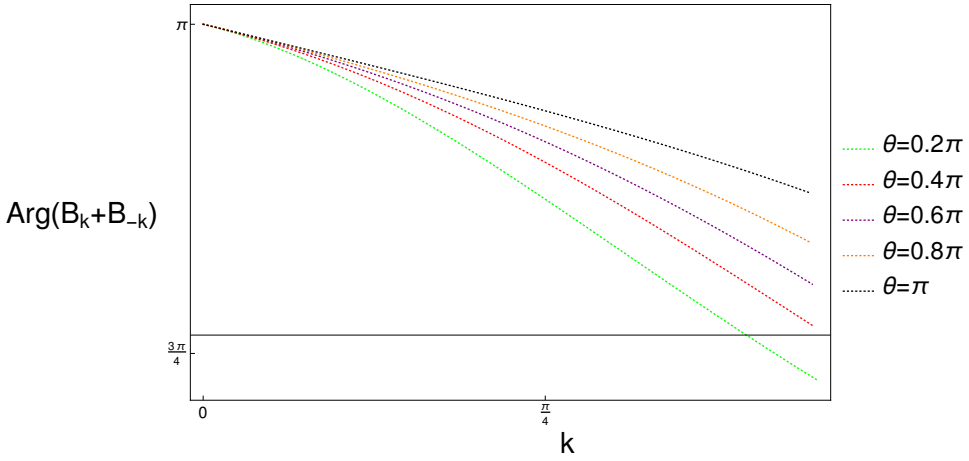

Figure 4.1: *Momentum dependence of the local gauge phase for different values of θ, at a condensate density of $n_0 = 0.01$. Here the phases are evaluated far below to their critical value defined by* **Eq**. *(4.26). The gauge shift decreases as a function of k for a fixed θ, where quasi-particles with larger statistical parameters experience a stronger shift.*

dispersion relations are given by

$$\begin{aligned}\epsilon_k^+ =& A_k \cosh(\alpha_k)^2 + A_{-k} \sinh(\alpha_k)^2 - |B_k + B_{-k}| \sinh(2\alpha_k) \\ =& \frac{A_k \left[1 + \sqrt{1 - \left(\frac{|B_k+B_{-k}|}{(A_k+A_{-k})}\right)^2}\right] - A_{-k} \left[\sqrt{1 - \left(\frac{|B_k+B_{-k}|}{(A_k+A_{-k})}\right)^2} - 1\right] - 2\frac{|B_k+B_{-k}|^2}{(A_k+A_{-k})}}{2\sqrt{1 - \left(\frac{|B_k+B_{-k}|}{(A_k+A_{-k})}\right)^2}},\end{aligned} \tag{4.23}$$

$$\begin{aligned}\epsilon_k^- =& A_k \sinh(\alpha_k)^2 + A_{-k} \cosh(\alpha_k)^2 - |B_k + B_{-k}| \sinh(2\alpha_k) \\ =& \frac{A_{-k} \left[1 + \sqrt{1 - \left(\frac{|B_k+B_{-k}|}{(A_k+A_{-k})}\right)^2}\right] - A_k \left[\sqrt{1 - \left(\frac{|B_k+B_{-k}|}{(A_k+A_{-k})}\right)^2} - 1\right] - 2\frac{|B_k+B_{-k}|^2}{(A_k+A_{-k})}}{2\sqrt{1 - \left(\frac{|B_k+B_{-k}|}{(A_k+A_{-k})}\right)^2}},\end{aligned} \tag{4.24}$$

with $\epsilon_{-k}^- = \epsilon_k^+$. On the other hand, the renormalization of the mean-field energy due to the zero modes of the quasi-particles is given by

$$\begin{aligned}\epsilon_{k,0}^{+,-} =& (A_k + A_{-k}) \sinh(\alpha_k)^2 - |B_k + B_{-k}| \sinh(2\alpha_k) \\ =& \frac{(A_{-k} + A_k) \left[1 - \sqrt{1 - \left(\left(\frac{|B_k+B_{-k}|}{(A_k+A_{-k})}\right)^2\right]} - 2\frac{|B_k+B_{-k}|^2}{(A_k+A_{-k})}\right.}{\sqrt{1 - \left(\frac{|B_k+B_{-k}|}{(A_k+A_{-k})}\right)^2}}.\end{aligned} \tag{4.25}$$

As the Bogoliubov dispersion in **Eqs**. (4.23 and (4.24) is difficult to treat in closed form, we perform a further continuum approximation for the lattice momentum k up

to second order. Thus from here on the lattice dispersion of the bosonic particles is evaluated at the bottom of the band, yielding a free particle kinetic energy. As a last remark, here and in the following the bosonic limit $\theta = 0$ is explicitly excluded as in this case the model is non-interacting and thus the discussion of the Bogoliubov spectrum and its stability redundant.

4.2 Stability Analysis and Dispersion Relation

The form of the Bogoliubov dispersion **Eqs**. (4.23) and (4.24) is algebraically rather unhandy and becomes complex as a function k, θ and n_0, even the Hamiltonian is hermitian. In order to investigate this, we compare in the following different notions of stability for such quadratic bosonic Hamiltonians and apply them to our model, resulting in the stability diagram **Fig**. (4.1). Such instabilities have to be interpreted as boundaries for the range of validity of the current mean-field treatment under certain perspectives e.g. thermodynamic stability of the excitations above the condensate or temporal stability in the evolution of observables with unbounded growth or decay. The presence of such instabilities in the actual physical system is not expected and hence such artificial instabilities are generally considered mean-field artifacts. Nevertheless their evolution with respect to the systems parameters θ and n_0 allows for conclusions concerning the increase of quantum fluctuations and thus the onset of the strongly coupled regime. The existence of such instabilities crucially depends then on the density regime one aims to describe, as it is discussed in more detail in the next section. There we show that the Bogoliubov dispersions are actually smooth up to the order $\mathcal{O}(n_0^2)$, in agreement with the low-density $\leftrightarrow$ weak-coupling correspondence of mean-field systems.

An obvious choice for an indicator of broken stability is that momentum $k^{\pm}_{\text{crit}}$ at which the Bogoliubov dispersion **Eqs**. (4.23-4.24) diverges, i.e

$$\left(\frac{|B_k + B_{-k}|}{(A_k + A_{-k})}\right) = 1, \quad \Longrightarrow k^{\pm}_{\text{crit}} \tag{4.26}$$

This divergence corresponds formally to a Bogoliubov angle of infinite value, which implies infinitely strong interactions in the Bogoliubov treatment of an ordinary Bose gas. The critical momenta can be analytically found from the condition **Eq**.(4.26). This leads to the presence of two possible lower critical momenta related by symmetry ($k^{+}_{\text{crit}} \leftrightarrow -k^{-}_{\text{crit}}$). Nevertheless such quadratic bosonic Hamiltonians are usually only thermodynamically stable provided that the fluctuation Hamiltonian is positive semi-definite [125, 126], thus we have to check how thermodynamic stability is related to the occurring divergence. Here the stability analysis is considered relative to the ground state of free bosons, that was omitted by convention in **Eq**. (4.1).

Thermodynamic instability arises now in the vicinity where the transformed Hamiltonian can not be diagonal anymore, i.e.

$$A_k A_{-k} - |B_k + B_{-k}|^2 = 0, \quad \Longrightarrow k_{\mathrm{td}}^{\pm}, \tag{4.27}$$

originating from the determinant of **Eq**. (4.19) in Bogoliubov-de-Gennes form. This implies additionally that the original Hamiltonian features an unbounded spectrum from below, relative to the free boson ground state. Here the loss of thermodynamic stability implies the absence of a stable quasi-particle vacuum as the ground-state of the Hamiltonian **Eq**. (4.22), see [125, 126]. Thus the effective single-particle description superimposed by the Bogoliubov approximation breaks down and different kind of excitations arise. Also in this case the condition **Eq**. (4.27) can be solved analytically which gives again two lower possible thermodynamically critical momenta related by symmetry ($k_{\mathrm{td}}^{+} \leftrightarrow -k_{\mathrm{td}}^{-}$). Logically we have to compare now the lower divergent k_{crit} value to the lower thermodynamical critical momenta k_{td}, where the lower ones of both serve than consequently as practical indicators of the breakdown of the mean-field treatment.

There exists yet a third independent notion of stability, the so called dynamical stability of effective single-particle Hamiltonians [125–127], to which the last part of our investigation is devoted to. The Heisenberg equations of motion describing the time evolution of all canonical creation/annihilation operators in a given system can host non-real eigenvalues and might be non-diagonalizable for such quadratic bosonic Hamiltonians [125, 126]. The corresponding normal modes can then show oscillatory as well as non-oscillatory dynamics, which consequently leads to unbounded growth or decay of physical observables in time [125, 126]. The matrix which determines the flow of the Nambu array for our system $\hat{\Psi}_k^{\dagger} = (\hat{b}_k^{\dagger}, \hat{b}_k, \hat{b}_{-k}^{\dagger}, \hat{b}_{-k})$ is then given by

$$i\frac{d}{dt}\hat{\Psi}_k^{\dagger} = G_k \hat{\Psi}_k^{\dagger}, \tag{4.28}$$

$$G_k = \frac{1}{2}\begin{bmatrix} A_k & 0 & 0 & |B_k + B_{-k}| \\ 0 & -A_k & -|B_k + B_{-k}| & 0 \\ 0 & -|B_k + B_{-k}| & -A_{-k} & 0 \\ |B_k + B_{-k}| & 0 & 0 & A_{-k} \end{bmatrix} \tag{4.29}$$

and dictates the dynamical stability in terms of its eigenvalues, analogous to the state matrix of ordinary dynamical systems [44]. The effective single-particle is dynamically stable if G is diagonalizable and all of its eigenvalues are real [125, 126]. Again the eigenvalues of G can be calculated in closed form but are rather lengthy and unhandy. Nevertheless the criticality condition whether they cross the imaginary axis or not can

be easily deduced from the four eigenvalues of G

$$k_d^{\pm} = \pm\sqrt{2 - n_0 + n_0 \csc\left[\frac{\theta}{2} + n_0 \sin(\theta)\right] \sin\left[\frac{3\theta}{2} + n_0 \sin(\theta)\right]}, \tag{4.30}$$

where again only the lower ones are shown in **Eq**. (4.30).

As dynamical/thermodynamic stability are independent of each other [125, 126] we would like to investigate their relation, thus also their relation to k_{crit}, and in which part of the parameter space they appear.

By numerically comparing the three criticality indicators **Eqs**. (4.26), (4.27) and (4.30) for sufficiently small densities, we come to the conclusion that thermodynamic stability is always lost before the region of dynamical instability is entered, i.e. $k_{\text{td}} < k_{\text{d}}$, and before the system diverges $k_{\text{td}} < k_{\text{crit}}$. Furthermore, it turns out that the system always diverges before the region of dynamical instability is entered $k_{\text{crit}} < k_{\text{d}}$, which can be interpreted as the general absence of the latter. Here the region separating the two critical lines is generally smaller for low densities and also widens as a function of θ. To summarize the results of the stability analysis we can formulate a "phase"-diagram for the Bogoliubov Hamiltonian **Eq**. (4.22) for each signum of k, displayed below for the positive sector. Generally we observe that the region of thermodynamic stability, which we take as the minimal boundary of a mean-field breakdown, shrinks with increasing condensate density n_0 and θ. The former dependence is again an expression of the large-density $\leftrightarrow$ weak-coupling correspondence of the mean-field method, whereas the latter expresses the repulsive nature of statistical interactions mediated by the Peierls phase [128].

Having completed the stability analysis, the dispersions relation of both species is shown in **Fig**. (4.2) up to their boundary values given by $k_{\text{td}}^{\pm}$. The minima of the respective dispersions relations are shifted away from $k \approx 0$ due to the statistical transmutation, where the shift seems to increase until $\theta \approx \pi/2$, from where on the trend reverses and the minimal value $k \approx 0$ is approached again. Interestingly the minimal k value of the pseudo-fermions coincides with the bosonic one, whereas the pseudo-fermions have a larger energy compared to the bosons, interpretable by the repulsive

momentum range		dispersion $\epsilon_k^{\pm}$	stability of $\hat{H}$
$0 < k < k_{\text{td}}$		$\epsilon_k^{\pm} \in \mathbb{R}$	thermodynamic/dynamical
$k_{\text{td}} < k \leq k_{\text{crit}}$		$\epsilon_{k_{\text{crit}}}^{\pm} \in \mathbb{C}$	dynamical
$k_{\text{crit}} \leq k < k_{\text{d}}$		$\epsilon_{k_{\text{crit}}}^{\pm} \in \mathbb{C}$	none

Table 4.1: *Stability diagram of the Bogoliubov Hamiltonian* **Eq**. *(4.22) for positive momenta, negative momenta are related by symmetry. The point from where on the dispersion relations crosses the imaginary axis first is considered as an unphysical region.*

effect of the statistical interaction [13, 33]. The same behavior is displayed in **Fig**. (4.3) by the zero-mode energy shift of the Bogoliubov dispersion $\epsilon^{\pm}_{k,0}$, which is monotonically increasing with θ. Furthermore the energy shift induced by the zero-mode shows almost no dependence on the momentum, except in the vicinity of the instability where the shifts diverge. This re-occurring behavior of minima of the quasi-particle dispersions is faintly reminiscent to those of the bosonic quasi-momentum distributions in the small density regime, see **Fig**. (4.5). The bosonic quasi-momentum distribution $\langle \hat{n}_k \rangle$, that is defined as the Fourier transform of the pair-correlation function $\langle \hat{b}_i^\dagger \hat{b}_j \rangle$, can be probed by releasing a trapped optical lattice system and observe its coherence in momentum space [39]. In the Gutzwiller mean-field framework, the quasi-momentum distribution is independent on the spatial dimensionality and hence Bose-Einstein condensation is predicted even if the system is one-dimensional. Thus it was shown in **Ref**. [18], that the shifted maxima are approximately described by the corresponding delta function $\langle \hat{n}_k \rangle \approx \delta(k + \Delta\beta)$ in the thermodynamic limit, see **Fig**. (4.4). Here $\Delta\beta$ determines the point of condensation dependent on the amplitudes of the Gutzwiller wave-function [110], which turns out to be a parabolic function of θ in the small density regime. In a later subsection we show that one of the minima of the Bogoliubov dispersion follows the functional form of $\Delta\beta$. We expand the quasi-particle dispersion for small condensate densities to avoid instabilities and to obtain closed form expressions for their minima and effective masses, which we identify with $\Delta\beta$ and the condensate depletion respectively.

4.3 Condensate Energy and Healing Length

Before we investigate the Bogoliubov dispersion in the dilute limit, we briefly discuss the condensate energy and the healing length with special emphasis on the latter. For the derivation of the healing length it is necessary to perform a continuum limit in the momentum k to the free particle dispersion, as the expansion for small momenta consequently corresponds then to the consideration of a long-range length scale in real space, in our case given by the so called healing length ζ.

The condensate energy density per condensed particle **Eq**. (4.13) includes only contributions from the mean-field and is shown in **Figs**. (4.6) and (4.7) as a function of the statistical parameter θ or condensate density n_0 respectively. For a fixed statistical parameter θ an increase in the condensate density n_0 leads to either an increase or decrease in E_0/N_0, depending on if θ is below or above $\pi/2$, see **Figs**. (4.7). Analogously for fixed n_0 in **Figs**. (4.6) the energy density is slightly lowered as a function of θ until $\theta \approx \pi/2$ from where on it increases again. The effect is more pronounced for larger densities. This can be interpreted such that the impact of the density-dependent Peierls phase on the condensate energy as an interaction can be either attractive or repulsive, as long as any fluctuations are neglected. Here the repulsive effect is rather dominant in accordance with previous works [13, 27, 33].

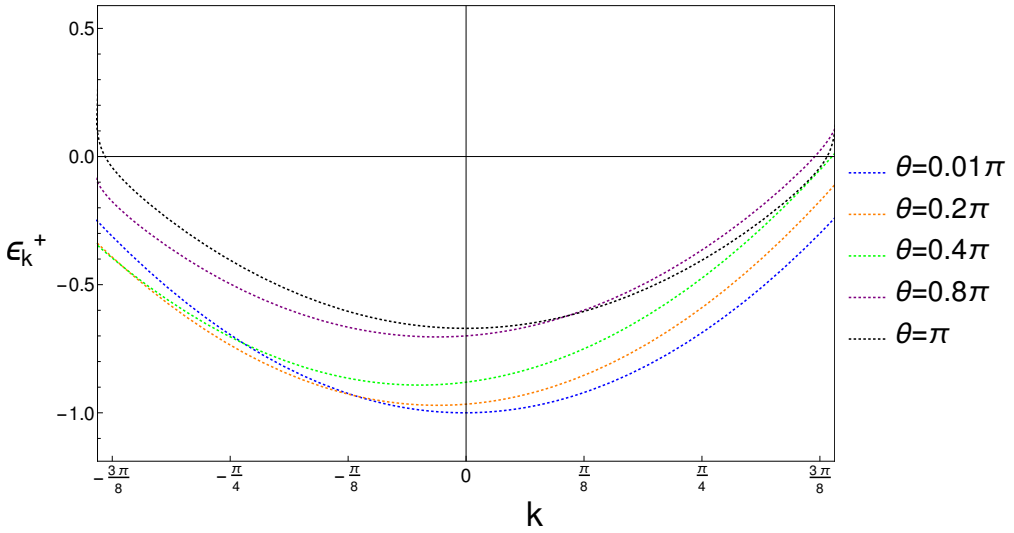

Figure 4.2: *Dispersion relation of ϵ_k^+ sector for a condensate density of $n_0 = 0.04$ and different values of θ, for momenta smaller as k_{td}. In this density regime the respective dispersions are shifted away from $k \approx 0$ for $\theta \in (0, \pi/2)$, from where on the origin is approached again.*

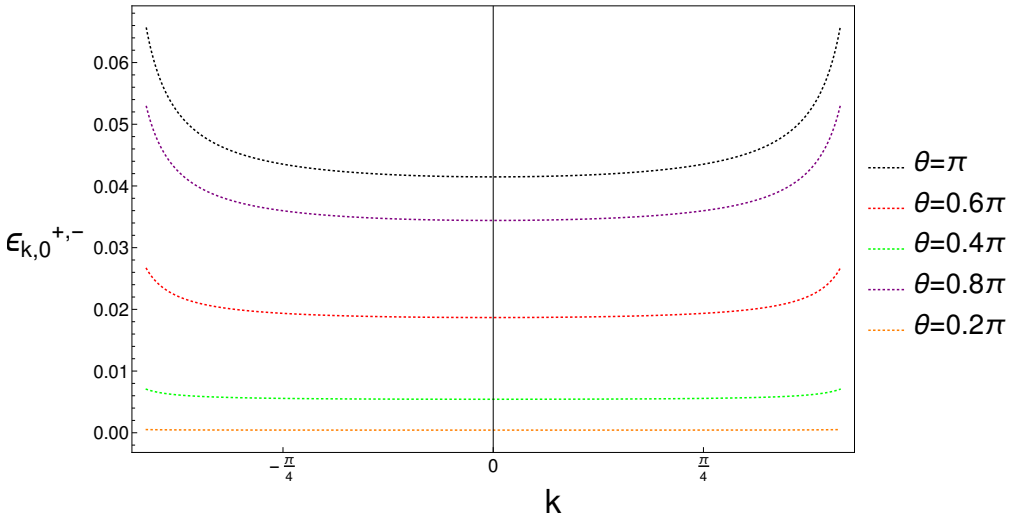

Figure 4.3: *Zero mode $\epsilon_{k,0}^{\pm}$ of the Bogoliubov particles for a condensate density of $n_0 = 0.04$ and different values of θ, as a function of k. The energy shifts $\epsilon_{k,0}^{\pm}$ are almost constant in the momentum k, approaching the instabilities they start to diverge. The zero mode $\epsilon_{k,0}^{\pm}$ is furthermore increasing with θ, related to the repulsive effect of such statistical interactions.*

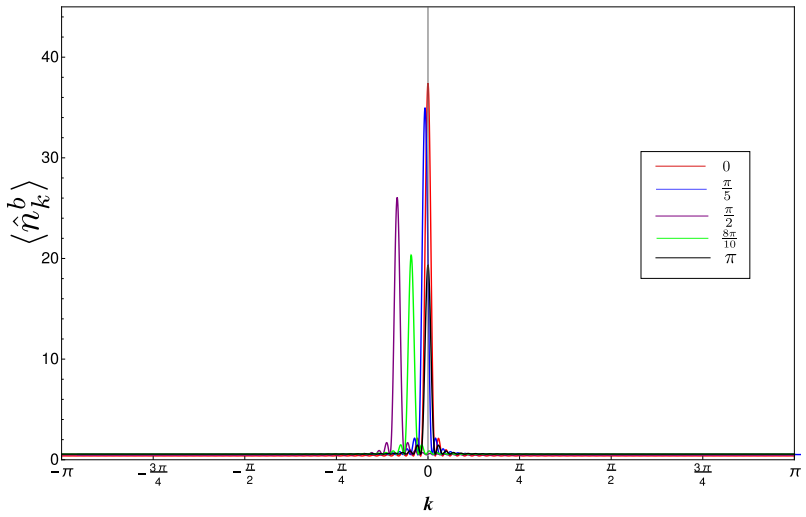

Figure 4.4: *Gutzwiller-data of the bosonic quasi-momentum distribution of the anyon-Hubbard model for a density of $n_0 = 0.75$ and an additional onsite-interaction $U/J = 10$, displayed for different statistical parameters, evaluated in* **Ref**. *[18]. The lattice has a length of $L = 100$ and a maximum of two bosons per site were considered to minimize numerical costs. The shift of maxima of the distribution $\langle \hat{n}_k^b \rangle$ and its returning is reminiscent to the position of energy minima of one of the Bogoliubov sectors in* **Fig**. *(4.2)*

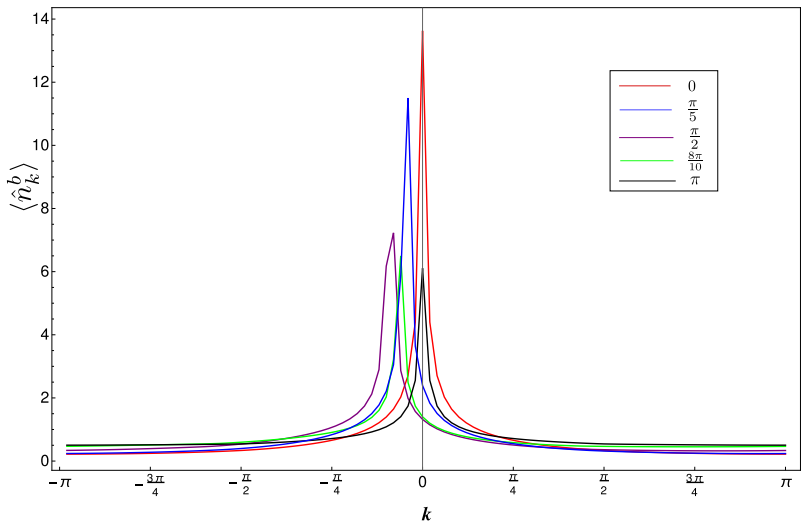

Figure 4.5: *DMRG-data of the bosonic quasi-momentum distribution of the anyon-Hubbard model, corresponding to* **Fig**. *(4.4) with a density of $n_0 = 0.75$, system length $L = 100$ with open boundaries and an additional onsite-interaction $U/J = 10$, displayed for different statistical parameters in* **Ref**. *[18].*

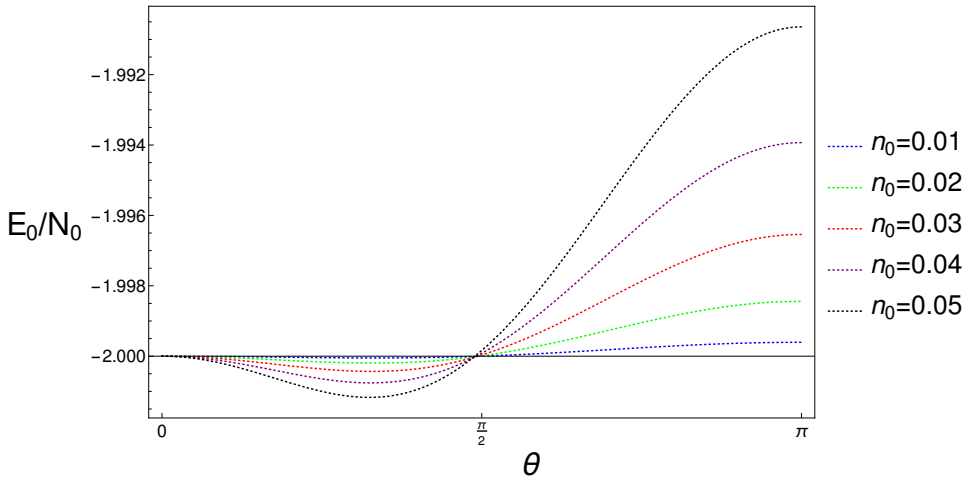

Figure 4.6: *The condensate energy density E_0/N_0 for different condensate densities n_0 as a function of θ. The energy density is decreasing, for fixed n_0, until $\theta \approx 0.5\pi$, which implies an effective attraction induced by the statistical transmutation. After $\theta \approx 0.5\pi$ this trend is reversed and the condensate energy is increasing with θ, where larger densities are stronger affected in accordance to the case $\theta < 0.5\pi$.*

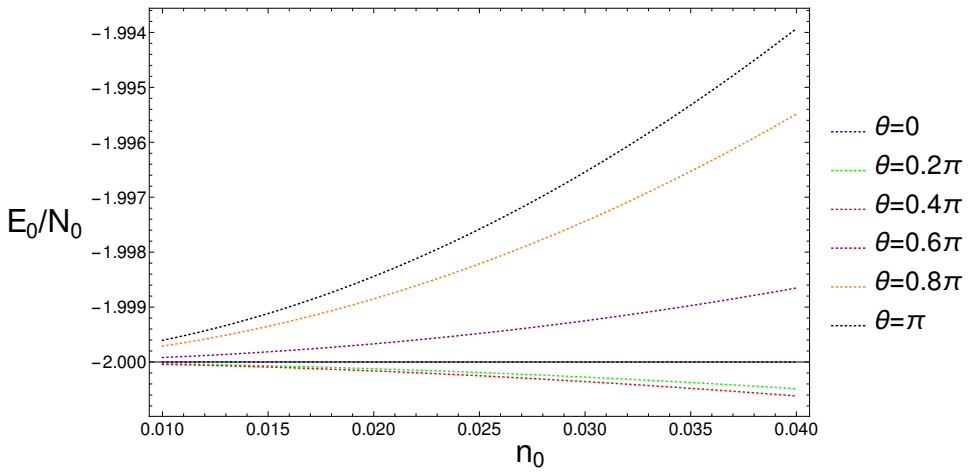

Figure 4.7: *The condensate energy density E_0/N_0 for different statistical parameters θ as a function of n_0. Also here, the condensate energy per particle E_0/N_0 is lowered for θ smaller $\pi/2$, where the effect reverses for larger values of θ*

Now we turn our attention to the derivation of the healing length ζ [40, 111]. In our case we can derive it from **Eq**. (4.15) by expanding $A_{\pm k}$ in **Eq**. (4.14) around $k \approx 0$ and neglecting any pairing of the quasi-particles. Then $\zeta \propto 1/k$ is defined as being the length scale where the kinetic energy of the massive quasi-particles exceeds the chemical potential given by the condensate fluctuation [40, 111] , i.e.

$$\left[(\hat{D}(n_0)+1)G(\theta,n_0)+\text{h.c.}\right]k^2 \stackrel{!}{=} \mu, \tag{4.31}$$

$$\Longrightarrow \zeta = \sqrt{-1-\frac{\text{Re}(G(\theta,n_0))}{\hat{D}(n_0)\text{Re}(G(\theta,n_0))}}.$$

Hence ζ can be used as a measure to quantify if a given system is in the weakly interacting regime and up to what distances correlations can spread across the system. Conversely the length scale corresponds then to a momentum scale for which the particles interact sufficiently weak [40, 111]. For our model the healing length is shown in **Fig**. (4.8), and illustrates how the strong-coupling regime is approached under statistical transmutation for different condensate densities. The weak-coupling regime on the other hand is only approached for small values of θ and very small densities, here ζ diverges near the bosonic limit. An interesting expression for the divergence can be obtained by a Taylor expansion in the condensate density, i.e.

$$\zeta(\theta, n_0 \approx 0) \propto \sqrt{\frac{1}{n_0(1-\cos(\theta))}}. \tag{4.32}$$

Not surprisingly, the bosonic limit leads to the presence of global correlations that correspond to off-diagonal long-range order in the mean-field framework [114]. Anyhow we have to keep in mind that the actual system is defined on a one-dimensional lattice, hence spontaneous symmetry breaking is explicitly ruled out by the Mermin-Wagner-Hohenberg theorem [74, 75, 129]. Instead collective excitations arise, driven by strong quantum fluctuations beyond the mean-field paradigm [43, 124]. As stated before, the healing length obtained in the mean-field approach can be used later as an analytic estimate for the infrared cut-off of these collective excitations, where the procedure even becomes exact in the weak coupling regime of the Lieb-Liniger model [6, 61]. An interesting detail here is the parametric dependence of the divergence of the healing length for small condensate densities n_0, i.e. $\zeta \approx \frac{1}{\sqrt{g}}$. Here g denotes again the effective two-body coupling constant that arises from a continuum limit of the anyonic hopping operator pursued in chapter (**6**), and determining the exponential amplitude decay of effective mean-field interactions $G(\theta, n_0)$ mediated by the density-dependent Peierls phase. The circumstance will be discussed in more depth later where the harmonic fluid approach is introduced.

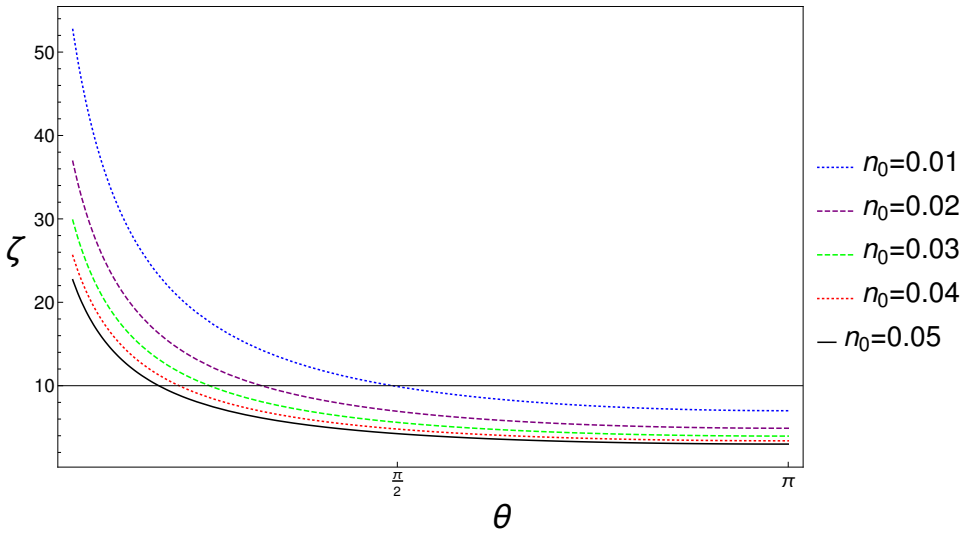

Figure 4.8: *Healing lengths ζ as a function of θ for different condensate densities. The length scale is quickly reduced for increasing densities and exchange phases. The free boson limit is recovered for $\theta \to 0$ implying longer-ranged correlation, whereas the healing length remains small but finite in the strongly coupled regime.*

4.4 Dilute Limit

As discussed previously the mean-field treatment is rather complicated to treat in closed form and features certain instabilities. Hence we expand the Bogoliubov dispersions and energy shifts to low orders in n_0, to address explicitly the weak coupling regime and to avoid the difficulties mentioned above. This facilitates additional insights into the minima of the dispersions as well as the effective masses of the quasi-particles. Thus we obtain the following expression for the quasi-particle dispersion up to the order $\mathcal{O}(n_0^2)$

$$\begin{aligned}\epsilon_k^{\pm} \approx & \frac{1}{4}\left[-4+16n_0-n_0^2-16n_0(1-n_0)\cos(\theta)-15n_0^2\cos(2\theta)\right] \\ & \frac{1}{4}\left[2-4n_0+3n_0^2-2n_0(3n_0-2)\cos(\theta)+3n_0^2\cos(2\theta)\right]k^2 \\ & \frac{1}{4}\left[\mp 24n_0^2\sin(\theta)\pm 12n_0^2\sin(2\theta)\right]k,\end{aligned} \tag{4.33}$$

and analogously for the renormalization of the condensate energy by the fluctuations

$$\epsilon_{k,0}^{\pm} \approx 24\sin^4\left(\frac{\theta}{2}\right)n_0^2. \tag{4.34}$$

Especially interesting in the small density contributions **Eqs**. (4.33 -4.34), is that no divergences occur up to the order $\mathcal{O}(n_0^2)$. The next order in the small density expansion would then lead to a divergence exactly at the lower bound of the critical momenta of a previous section, i.e. $\sup_{n_0}|k_{\mathrm{crit}}| = \sqrt{2} = \sup_{n_0}|k_{\mathrm{td}}|$, which we would like to neglect in the following discussion. On the other hand, if the divergent terms starting from the

order $\mathcal{O}(n_0^3)$ are neglected, then the resulting dispersions **Eq**.(4.33) host a relatively trivial momentum dependence in comparison to the usual Bogoliubov approximation for a two-body interacting Bose gas [23, 122, 123], which ultimately incorporates the interactions present in the original model. To be more precise, up to the order of $\mathcal{O}(n_0)$ the dispersion **Eq**.(4.33) corresponds just to a single free particle with a renormalized mass, whereas the dual quasi-particle appears only in second order in the condensate density. This is yet another manifestation of the fact that such statistical interactions are generally different in nature compared to local inter-particle interactions. The dispersion relations **Eq**. (4.33) can now be used to determine their minimum for small densities and to study the nature of the lowest momentum excitation near $k \approx 0$. Besides the usual k^2-dependence also linear terms in k arise in the dispersion **Eq**. (4.33), which implement the reflection asymmetry for each channel and induce a certain drift on the quasi-particles. Interestingly in both non-anyonic limits $\theta = 0, \pi$ the drift vanishes as a manifestation of a recovered inversion or time reversal symmetry. Furthermore the minima of the dispersion is shifted away from $k \approx 0$ by this linear drift in contrast to the ordinary Bogoliubov dispersion of a Bose gas. Therefore we would like to quantify this in more detail, and thus the extrema of **Eq**. (4.33) are calculated from the following conditions

$$\partial_k \epsilon_k^{+,-} = 0, \tag{4.35}$$

where $k_{\text{min}}^{\pm}$ can be deduced in closed form, i.e.

$$k_{\text{min}}^{\pm} = \frac{2\left[-4n_0 \sin(\theta) + 6n_0^2 \sin(\theta) - 3n_0^2 \sin(2\theta)\right]}{-2 + 4n_0 - 3n_0^2 - 4n_0 \cos(\theta) + 6n_0^2 \cos(\theta) - 3n_0^2 \cos(2\theta)}. \tag{4.36}$$

As discussed previously, the form of quasi-particle dispersions turns out to be rather unusual, see **Fig**. (4.2), in the sense that two species are involved here which are related via parity or time-reversal, i.e. $k \to -k$. This could be interpreted such that the true condensation point of the system, which is given by its macroscopic contribution plus all the excitations surrounding it, is actually shifted away from $k \approx 0$, see for example **Refs**. [18, 27, 29] or **Figs**. (4.4-4.5), where the point of maximal quasi-momentum distribution is qualitatively well described by one of the sectors in **Eq**. (4.36). This minimal k-value rises then roughly until $\theta_{crit} \approx 0.5\pi$, where from here on the condensate momentum $k \approx 0$ is approached again, see **Fig**. (4.9). In order to quantify this reflection asymmetry of the minimal k-values around $\theta \approx 0.5\pi$ in more detail we define the following function

$$\eta^{\pm} = k_{\text{min}}^{\pm}(\theta, n_0) - k_{\text{min}}^{\pm}(\pi - \theta, n_0), \tag{4.37}$$

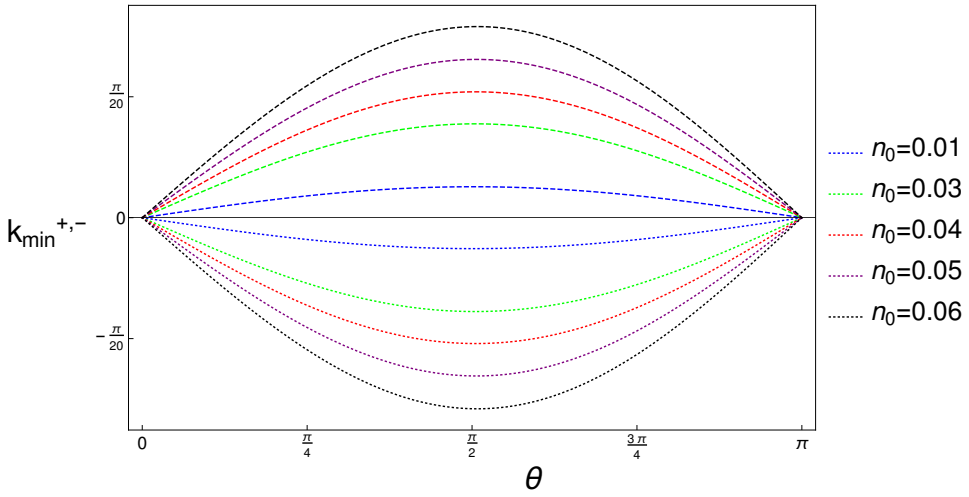

Figure 4.9: *Comparison of minimal k value of* **Eq**. *(4.36) for different values of the condensate density as a function of θ. The condensation point of the excitations is shifted away from $k = 0$ for increasing θ up to $\theta \approx 0.5\pi$ where the critical value decreases towards $k = 0$ for increasing θ afterwards.*

which shows an increase of asymmetry of $k^{\pm}_{\text{min}}$ for larger condensate densities, see **Fig**. (4.10), while $k^{\pm}_{\text{min}}$ is almost symmetric for lower densities. This re-itinerant behavior can be compared to the asymmetry of bosonic quasi-momenta maxima in the anyon-Hubbard model, see **Figs**. (4.4-4.5). In the dilute regime those points of maximal quasi-momentum density show exactly the same re-itinerant behavior, roughly symmetric around $\theta \approx 0.5\pi$, as the minima of the Bogoliubov modes [18, 27]. Hence one could be tempted to relate one of the shifted minima of the quasi-particles with the shifted quasi-condensation point of the actual one-dimensional system, even if in the former case a condensation around $k \approx 0$ is assumed whereas for the latter the concept of macroscopic occupancy breaks down anyway [43, 61]. Another striking similarity is that this re-itinerant behavior is distorted by approaching higher densities, which is in accordance with the trend of $\eta^{\pm}$, until the effect eventually vanishes for larger fillings [18, 27] and the quasi-condensation point is increasingly shifted to the boundary of the Brillouin zone as a function of θ. In order to quantify the interactions between the ordinary particles, we expand the small density dispersion around the minima of the band, i.e.

$$\epsilon_k^{+,-}|_{k^{\pm}_{\text{min}}} \approx \left[1 + \frac{1}{2}(\partial_k)^2 (k^{\pm}_{\text{min}})^2\right] \epsilon^{+,-}_{k^{\pm}_{\text{min}}} - (\partial_k)^2 k^{\pm}_{\text{min}} \epsilon^{+,-}_{k^{\pm}_{\text{min}}} k + \frac{1}{2}(\partial_k)^2 \epsilon^{+,-}_{k^{\pm}_{\text{min}}} k^2. \tag{4.38}$$

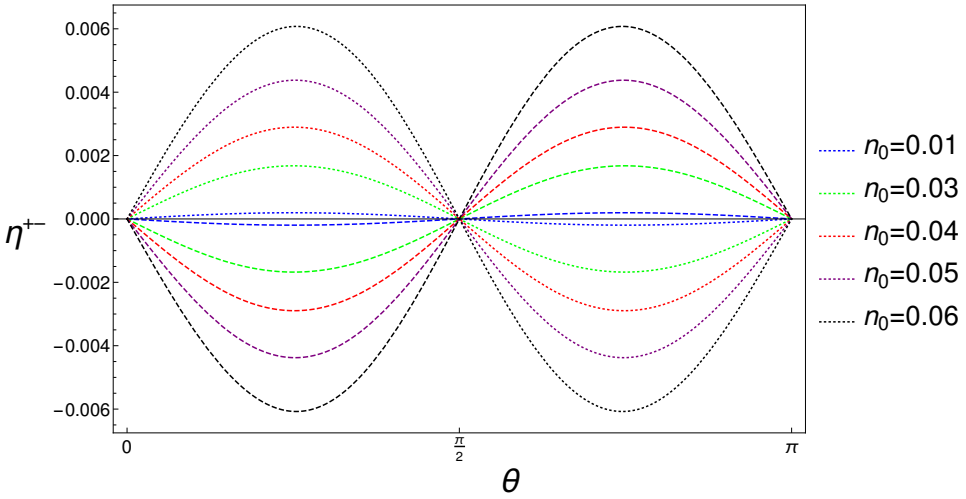

Figure 4.10: *Quantification of the asymmetry of minimal k-value of both species with respect to inversion around $\theta \approx \frac{\pi}{2}$, with the aid of $\eta^{\pm} = k^{\pm}_{min}(\theta, n_0) - k^{\pm}_{min}(\pi - \theta, n_0)$ as a function of θ. The asymmetry is increasing for larger densities, in accordance with the quasi-momentum maxima of the anyon-Hubbard model in the low density regime, see* **Refs**. *[18, 27].*

Physically we can interpret now the second order term in the expansion in terms of the effective band mass of the quasi-particles m_{eff}

$$m^{+}_{\text{eff}} = \left((\partial_k)^2 \epsilon^{+,-}_{k^{\pm}_{\text{min}},0} \right)^{-1} = m^{-}_{\text{eff}} \tag{4.39}$$
$$= \frac{2}{[2 - 4n_0 + 3n_0^2 - 2n_0(-2 + 3n_0)\cos(\theta) + 3n_0^2\cos(2\theta)]}$$

that represents the strength of interactions between the ordinary particles, see **Fig**. (4.11). The repulsive effect of the statistical transmutation is implied by the increase of the band mass for non-zero values of θ, see **Fig**. (4.11), as larger interactions lead to a "clumping" of the quasi-particles and thus to a larger effective mass. Generically an increase of interactions leads to the depletion of condensed particles into the background of the quasi-momentum distribution [6, 40], as for example in the anyon-Hubbard model [13, 27, 29, 128] due to the statistical interaction, see **Fig**. (4.4–4.5). Consequently higher momentum states are populated, whereas states near k_{min} get depopulated. This is consistent with the behavior of the effective mass in **Fig**. (4.11) which shows a monotonous increase with statistical transmutation analogous to the monotonous depopulation of the quasi-condensation maximum in the original model [18, 27, 29]. An interesting interpretation for the pseudo-fermions in this framework follows from the comparison of **Eqs**. (4.9) and (4.11) with their bosonic counterpart, namely as bosonic particles with a mass that increases heavily with the condensate density n_0. An increase in effective mass can be understood as a decreased probability of hopping between adjacent sites in the original lattice model, as $m_{\text{eff}} \propto J^{-1}_{\text{eff}}$, meaning that the kinetic

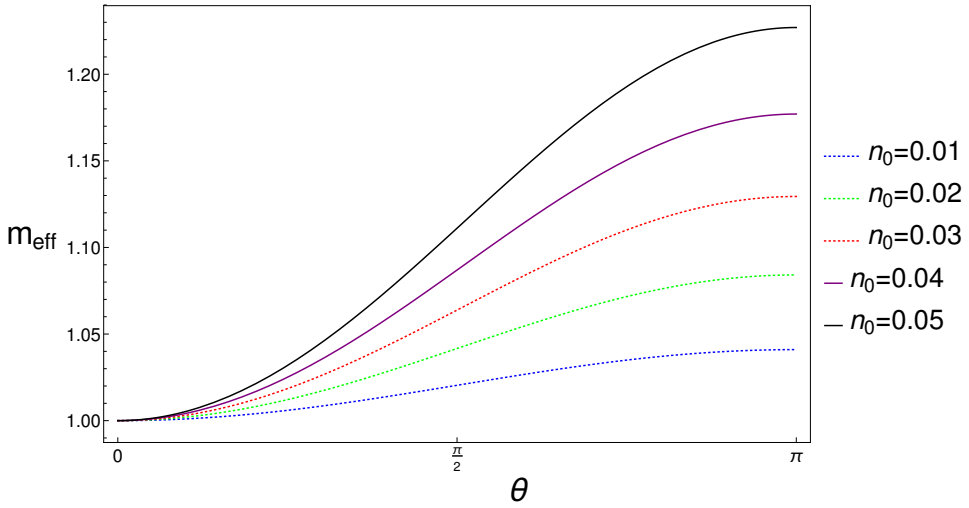

Figure 4.11: *Band mass of both Bogoliubov sectors as a function of θ for different condensate densities n_0. The increase of m_{eff} with respect to the statistical transmutation implies again an increase of interactions for the ordinary particles.*

energy is increasingly reduced during the interaction induced fermionization.

4.5 Conclusion

Finally we would like to close this chapter with a few concluding remarks. Despite the simplicity of the approach in comparison to the numerically demanding Gutzwiller mean-field theory [18, 27], it is nevertheless useful to phenomenologically describe the quasi-momentum distributions in the dilute anyon-Hubbard model [18, 27, 29] with the aid of Bogoliubov quasi-particles. A novelty with respect to other mean-field approaches applied to the anyon-Hubbard model [13, 27], is the inclusion of interactions mediated by the density-dependent Peierls phase to all orders, and thus restoring the crucial topological periodicity in the statistical parameter. Furthermore the treatment reveals how to interpret the statistically induced interaction in the mean-field framework, namely as infinitesimal shifts of the Poissonian mean value or variance n_0 of the moment-generating function $G(\theta, n_0)$. This leads to certain instabilities in the mean-field theory which have no pendant in the actual physical system, which is another manifestation of the fact that such statistical interactions are inherently different from ordinary n-particle interactions. Nevertheless, as such instabilities usually show the onset of new emergent phenomena [123, 125], we relate the shrinking of the region of thermodynamically stable momenta for the quasi-particles as an illustration of the ongoing statistical transmutation on the Bose gas. As stated already in the beginning, many different quantities could be potentially calculated within this approach. Whereas here the focus is more on an analytic illustration of the physical phenomena surrounding the shifted quasi-momentum distribution of the anyon-Hubbard model in order to further support

the mostly numerical investigations in the literature [18, 27, 33]. Here we could roughly identify the point of divergence of the quasi-momentum distribution with the minimal momentum of one of the Bogoliubov particles, as well as their increasing effective mass with a statistical condensate depletion. Later we will use more sophisticated methods to describe those one-dimensional anyons and their ground-state properties, especially with the aid of the bosonization method [43, 52, 61]. Then, we can use the results obtained here for the healing length as an estimate for the weak-coupling momentum cut-off of these chiral fields. An estimate which is not easily analytically accessible in general, for non-integrable models as our one-dimensional anyons [43].

Chapter 5

Dilute Pseudo-Fermions and Fermions

The continuous interpolation of particle statistics from Bose-Einstein to Fermi-Dirac is considered one of the backbones of abelian anyons in two dimensions [2]. Under this perspective, their one-dimensional counterpart seems to be poorer in phenomenology. Namely in this case, only transmutations between fermions and hardcore bosons or between bosons and pseudo-fermions are possible, as implied by the deformed anyonic (anti)-commutators [18,27,88]. Especially interesting is the latter case of pseudo-fermions, as they do obey a strict Pauli principle but still posses an anti-symmetric wavefunction. So it seems that exchange statistics and exclusion principle are two disjoint concepts in the context of such one-dimensional anyons [8]. Nevertheless the anyonic exchange phase in the anyon-Hubbard model is in general non-gaugable as it is inextricably intertwined with the local density of the lattice system. Pseudo-fermions seem to be indistinguishable from ordinary fermions, if the filling in the lattice is sufficiently small [33, 88] and potential boundary effects are neglected [18]. Whereas differences between both entities have been reported for larger densities beyond unit filling, in terms of deformed Fermi-spheres [18, 27] and unconventional superfluid properties [88]. In the following chapter we show the equivalence of pseudo-fermions and canonical fermions for sufficiently low densities in the lattice. The strategy pursued here relies on the derivation of different effective models from the anyon-Hubbard model in the two-particle sector, that are finally related to free fermions in their weak/strong-coupling limit as $\theta \to \pi$ [33]. So we show that the full transmutation of canonical bosons to canonical fermions is indeed possible for the very dilute one-dimensional anyon-Hubbard model. We find from a two-anyon scattering approach that the effective interaction constant, mediated by statistical transmutation, becomes non-renormalizable in the continuum and diverges formally in the limit of a vanishing lattice spacing a. In analogy to the presence of highly singular interactions in related continuum formulations of one-dimensional anyons [7, 12], the lattice description seems to naturally

regularize such contributions by a cut-off of the order of the lattice spacing a. A finding that will be concretized in the next chapter by physically proving the regularization procedure. As such statistical interactions are essentially non-perturbative, we further employ a perturbative treatment of the anyon-Hubbard model including strong onsite interaction U, which also suppresses double occupations [130]. The first approach is then complemented beyond the strict two-particle picture but to the presence of strong interactions, whereas the non-renormalizability of effective interaction does not appear due to the renormalizable scale of the continuum coupling constant of a one-dimensional Bose gas $g = Ua$ [130,131]. With this we obtain two different analytical estimates for the Luttinger parameter K in the strong-coupling regime [130,132], which can be used either for very low densities on the otherwise free anyonic model or for additional strong onsite interactions in an exactly half-filled lattice. Hence we provide analytical insight into the universal behavior of strong-coupling correlation functions of the anyon-Hubbard model, a formidable task that has to be usually pursued by numerical methods due to the model's non-integrability. Furthermore we can calculate the ground-state energy as small deviations of the ideal Tonks-Girardeau gas [10, 11], including additional Hubbard interaction U or for the free anyonic case in the dilute limit.

5.1 Two Anyon Scattering Solution

In order to gain insight into the interactions mediated by the statistical transmutation between bosons and pseudo-fermions we employ a quite simple method, namely a two-anyon scattering Ansatz. If a given physical system is sufficiently diluted the most probable and relevant scattering processes are potentially those in between two particles, thus it is believed that such an Ansatz is adequate to faithfully describe the two-body interactions in a $n > 2$ body system [33,133,134]. To be more precise, a one-dimensional scattering length a_s^{lattice} can be defined by the unitary phase shift that the relative wavefunction of the two particles experiences while crossing the point of a vanishing relative coordinate [135]. As the lattice system lacks the Galilean invariance that its continuum pendant usually possess, the scattering length a_s^{lattice} generically depends on the center-of mass momentum of its constituents [135]. The connection to the continuum scattering length can then be finally made by considering only low-energy scattering between the asymptotically free particles which leads then consequently to Galilean invariance. A delicate issue that may arise here is, that it is a priori unclear if the continuum system corresponding to the lattice anyon model possess Galilean invariance as this might not be the case for anyons directly defined in the continuum [7].

The starting point of the investigation is a general two-anyon wavefunction, i.e.

$$|\Psi\rangle = \sum_{l,m} c_{lm} \hat{a}_l^\dagger \hat{a}_m^\dagger |0\rangle \tag{5.1}$$

on which we apply the free anyonic hopping operator on the infinite line,

$$\hat{H} = -J \sum_{j \in \mathbb{Z}} \left(\hat{a}_j^\dagger \hat{a}_{j+1} + \text{h.c.} \right). \tag{5.2}$$

The resulting time-independent Schrödinger equation

$$\hat{H} \left| \Psi \right\rangle = E \left| \Psi \right\rangle, \tag{5.3}$$

leads to a recurrence relation for the matrix elements c_{lm} which can be severely simplified by the following Ansatz [33, 133]

$$c_{lm} = \tilde{c}_{l-m} e^{-\frac{i\theta}{2}\text{sgn}(l-m)} e^{\frac{i}{2}Q(l+m)}. \tag{5.4}$$

The Ansatz **Eq**. (5.4) decouples the Schrödinger equation **Eq**. (5.3) into relative and center of mass coordinates while respecting the exchange symmetry of the anyonic wave function, i.e.

$$c_{ml} = c_{lm} e^{-i\theta \text{sgn}(m-l)}, \tag{5.5}$$

that is implied by the normalization condition

$$\sum_{\tilde{l},\tilde{m}} \sum_{l,m} \left(\delta_{\tilde{l},l}\delta_{\tilde{m},m} + \delta_{\tilde{m},l}\delta_{\tilde{l},m} e^{-i\theta\text{sgn}(\tilde{l}-l)} \right) c^*_{\tilde{l},\tilde{m}} c_{l,m} = 1. \tag{5.6}$$

Furthermore the bosonic exchange symmetry

$$c_{ml} = c_{lm}, \tag{5.7}$$

is encoded into the coefficients depending on the relative coordinate, i.e.

$$\tilde{c}_{l-m} = \tilde{c}_{m-l}, \tag{5.8}$$

implying an isomorphism between anyonic and bosonic Fock spaces via local gauge transformations [30]. The recurrence relation for the relative coordinate $k = m - l$ can be written in compact form

$$f_-(\theta, Q)\tilde{c}_{k-1} + f_+(\theta, Q)\tilde{c}_{k+1} + \frac{E}{2J}\tilde{c}_k = 0, \tag{5.9}$$

with $k \in \mathbb{Z}$, where the coefficients

$$f_\mp(\theta, Q) = \cos\left(\frac{\theta \left[\text{sgn}(k \mp 1) - \text{sgn}(k) \right] \pm Q}{2} \right), \tag{5.10}$$

parametrically depend on the center of mass momentum $Q = k_1 + k_2$ [135]. We consider two asymptotically free particles with the following energy

$$E = -4J\cos(q)\cos(\frac{Q}{2}), \tag{5.11}$$

and their corresponding scattering states [88, 133, 135]

$$\tilde{c}_k = e^{-iqk} + e^{2i\delta(Q,q)}e^{iqk}, \tag{5.12}$$

with relative momenta $q = \frac{k_1-k_2}{2}$ and the scattering phase shift $\delta(Q,q)$. As a side remark it should be noted that the Ansatz for $\tilde{c}_k$ is by definition bosonic, i.e. is symmetric with respect to $k \leftrightarrow -k$, see [135]. Hence we reduced the anyonic problem via a local gauge transformation to a bosonic one, in analogy to the Jordan-Wigner transformation in the many-body description [9, 13].

The recurrence relation can be further decomposed according to the range of the relative coordinate, i.e.

$$2\tilde{c}_1\cos\left(\frac{\theta-Q}{2}\right) + \frac{E}{2J}\tilde{c}_0 = 0 \quad , \ |k| = 0, \tag{5.13}$$

$$\tilde{c}_0\cos\left(\frac{\theta-Q}{2}\right) + \frac{E}{2J}\tilde{c}_1 + \tilde{c}_2\cos\left(\frac{Q}{2}\right) = 0 \quad , \ |k| = 1, \tag{5.14}$$

$$\cos\left(\frac{Q}{2}\right)(\tilde{c}_{k-1} + \tilde{c}_{k+1}) + \frac{E}{2J}\tilde{c}_k = 0 \quad , \ |k| > 1, \tag{5.15}$$

where the form of the recurrence relation obviously differs from the one obtained by a bosonic two-particle Ansatz in [88]. The scattering phase shift $\delta(Q,q)$ can now be extracted from the first two equations in **Eqs**. (5.13)

$$\delta(Q,q) = \arctan\left(\frac{1 + h(Q,\theta)[\cos(2q) - 2\cos(q)]}{\tan(q)}\right), \tag{5.16}$$

with

$$h(Q,\theta) = \left[\frac{\cos(\frac{Q}{2})}{\cos(\frac{\theta-Q}{2})}\right]^2. \tag{5.17}$$

The one-dimensional scattering length in the lattice can then be defined in the limit of zero relative momentum of the two particles [133, 135], i.e.

$$a_s^{\text{lattice}}(Q) = \lim_{q\to 0}\frac{\cot(\delta(\mathrm{Q},\mathrm{q}))}{q}. \tag{5.18}$$

The continuum pendant of **Eq**. (5.18) is defined in the limit of a vanishing center of mass momentum Q, i.e. for low-energy scattering ($\rightarrow E = -4J$)

$$a_s = \lim_{Q,q\rightarrow 0} \frac{\cot(\delta(\mathrm{Q},\mathrm{q}))}{q}, \tag{5.19}$$

leading naturally to Galilean invariance [135]. For our model we obtain then the following expression,

$$a_s = \frac{a}{1-h(Q,\theta)|_{Q=0}} = -\frac{a\Big(1+\cos(\theta)\Big)}{4\Big(1-\cos(\theta)\Big)}, \tag{5.20}$$

in units of the lattice spacing a. Whereas the dependence on the lattice parameter in **Eq**. (5.20) originates from the physical unit of the relative momentum $q \propto a^{-1}$. The scattering length **Eq**. (5.20) diverges in the bosonic limit and indicates a Tonks-Girardeau gas for $\theta \rightarrow \pi$ [10, 11], if the lattice spacing is assumed to be finite. As can be inferred from the short-distance behavior of the relative wave-function $\Psi_{\mathrm{rel}}(x_2 - x_1)$ between two s-wave scattering particles in a one-dimensional dilute Bose gas [71], i.e.

$$\partial_x \Psi_{\mathrm{rel}}(0^+) - \partial_x \Psi_{\mathrm{rel}}(0^-) = -\frac{1}{a_s}\left[\Psi_{\mathrm{rel}}(0^+) + \Psi_{\mathrm{rel}}(0^-)\right]. \tag{5.21}$$

Hence one could be tempted to conclude that pseudo-fermions and real fermions are equivalent as long as strictly two particles are considered [33].
A peculiar property of these statistically induced two-particle interactions is manifested in **Eq**. (5.20), namely their non-renormalizability in the continuum in contrast to ordinary two-particle interactions. As for example in the Bose-Hubbard model where the onsite interaction U has to be rescaled by the lattice spacing a, in order to sustain a finite coupling constant $c = U/Ja$ in the continuum limit [131]. In **Eq**. (5.20) such a renormalizaton is not possible without breaking the periodicity in the statistical parameter and thus the scattering length formally vanishes in the strict continuum limit which would imply infinitely strong interactions for any $\theta \neq 0$. Nevertheless if the lattice spacing a is understood to remain small but finite in the continuum limit, then such statistical interactions remain in general finite as discussed in more detail in the next chapter. An advantage of the two-particle Ansatz is that the so obtained scattering length can be related to the coupling constant of a bosonic two-body contact potential $V(x,\tilde{x}) = g_2\delta(x-\tilde{x})$ via [134]

$$g_2 = -\frac{2\hbar^2}{m_{eff}a_s}, \tag{5.22}$$

where for our system m_{eff} is given by the effective band mass $\frac{\hbar^2}{2m_{eff}} = Ja^2$. The derived coupling constant g_2 is exactly the same as obtained in [33], via a two-boson

scattering Ansatz for $U = 0$. This circumstance can be explained by the isomorphism between bosonic and anyonic Fock spaces [7, 30, 115] obvious by the effective reduction from $c_{l,m}$ to $\tilde{c}_{l-m}$, and the invariance of the two-body interaction with respect to the Jordan-Wigner transformation. Up to this level of approximation we can identify the non-interacting anyon-Hubbard model with a Lieb-Liniger model with coupling constant g_2 [71], i.e.

$$\mathcal{H}_{\mathrm{LL}} = \frac{\hbar^2}{2m}\int_{-\infty}^{\infty} dx\ \ \partial_x\hat{\Psi}^\dagger(x)\partial_x\hat{\Psi}(x) + \frac{g_2}{2}\int_{-\infty}^{\infty} dx\ \ \hat{\Psi}^\dagger(x)\hat{\Psi}^\dagger(x)\hat{\Psi}(x)\hat{\Psi}(x). \tag{5.23}$$

The effective reduction of the original model to delta-interacting bosons is kind of drastic, in the sense that the symmetry properties with respect to parity and time reversal of the original model are not transferred to the effective model, hence caution is indicated whenever the Lieb-Liniger phenomenology should be related to experimental or numerical data for the anyon-Hubbard model. On the other hand the Lieb-Liniger model allows for the exact calculation of various physical quantities, using the toolbox of Bethe-integrable models [71], that might be approximately applicable to dilute lattice anyons **Eq**. (5.2). The fate of all those physical quantities is only dependent on a single variable the so called Lieb constant [70, 71]

$$\gamma_2 = \frac{m_{\mathrm{eff}} g_2}{\rho} = -\frac{2}{\rho a_s}, \tag{5.24}$$

which in our case essentially consists of the inverse product of the continuum scattering length **Eq**. (5.20) and the continuum density $\rho = \frac{N}{La}$. Remembering that the continuum description should effectively describe the dilute lattice system, we see from **Eq**. (5.24) that the Lieb constant diverges formally with the lattice density that vanishes exactly in that limit, i.e. $\gamma_2 \propto \rho_{Lattice}^{-1}$. Nevertheless in order to numerically compare the actual lattice system with the continuum approximation both densities $\rho_{Lattice} = \rho$ have to be identified anyway, implying that the lattice spacing is set to unity again. Hence the Lieb constant γ_2 in **Eq**. (5.24) should be interpreted as a finite quantity for $\theta \neq \pi$, that is quite abruptly approaching the strong coupling regime ($\gamma_2 \gg 1$) for non-zero statistical parameters. Hence we can formally refine the arguments in [33], showing the equivalence of both entities by a two-boson scattering Ansatz, by the properties of the effective Lieb-Liniger model and assuming a finite regularization in **Eq**. (5.24), by a non-vanishing lattice density in the effective continuum description.

As we have to demand for extremely low densities for the lattice Hamiltonian in order that **Eq**. (5.1) makes sense, we can discuss selected quantities in the strong coupling limit of the Lieb-Liniger model. The restriction to strong interactions in **Eq**. (5.23) allows for a perturbative treatment of the Bethe solution [70, 71], whereas the

ground-state energy was first calculated by Lieb and Liniger [6]

$$E_{\mathrm{gs}}^{\gamma_2\gg1} \approx \langle\hat{N}\rangle \left(\frac{\hbar^2\rho_0^2}{2m}\frac{\pi^3}{3}\right)\left(1-\frac{4}{\gamma_2}+\mathcal{O}(\gamma_2^{-2})\right), \tag{5.25}$$
$$\approx \langle\hat{N}\rangle \left(\frac{\hbar^2\rho_0^2}{2m}\frac{\pi^3}{3}\right)\Big(1+2\rho a_s\Big).$$

Here **Eq**. (5.25) describes deviations from, the ground-state energy of the free fermion gas in descending order in γ_2^{-1}. The corresponding Luttinger parameter and sound velocity in that regime can be approximated to first order in γ_2^{-1} by [71]

$$K_{\gamma_2\gg1} \approx 1+\frac{4}{\gamma_2} = 1-2\rho a_s, \tag{5.26}$$

$$v_{\gamma_2\gg1} \approx 2\pi\rho\left(1-\frac{4}{\gamma_2}\right) = 2\pi\rho\Big(1+2\rho a_s\Big), \tag{5.27}$$

also describing perturbative corrections to the ideal Tonks gas $K_{\gamma_2=\infty}=1$. The analytic estimate of the Luttinger exponent in **Eq**. (5.26) is of exactly the same form as calculated in [132, 136] for a variant of the Bose-Hubbard model, where the Luttinger parameter is related to the compressibility under the premise of an approximately quadratic dispersion. The validity of the two-particle approximation for the anyon-Hubbard model can be tested in principle for sufficiently small densities, by comparing the calculated Luttinger exponents in **Eqs**. (5.26) with the experimentally or numerically measured decay exponents of correlation functions in the strong-coupling regime [43]. Analytically one can estimate up to which statistical angle the two-particle approach is valid by thermodynamic stability of the Luttinger liquid related to the non-negativity of the sound velocity in **Eq**. (5.27) [48, 137], i.e.

$$\theta_{\mathrm{crit.}} = \arccos\Big(\frac{2-a\rho}{2+a\rho}\Big). \tag{5.28}$$

Remarkably **Eq**. (5.28) implies that the Luttinger liquid description remains stable for quite small values of θ as long as the lattice density $\rho^{\mathrm{lattice}} = a\rho$ is sufficiently small. Thus we can expect that the parameters **Eqs**. (5.26-5.27) remain approximately valid while approaching the weak coupling regime. The bosonic limit in **Eq**. (5.28) is only formally stable for a vanishing lattice density, in vague analogy to the absence of adiabatic continuation to free bosons in the interacting Lieb-Liniger model [70]. Nevertheless, whether **Eqs**. (5.26-5.27) are indeed valid approximations for weak interactions or not, has to be compared with the estimates of the next chapter, that are more suited in that regime.

Generally one should be careful about the meaningfulness of the two-particle scattering solution in the case of the dilute anyon-Hubbard model [33], due to the presence of higher order interactions in the density-dependent Peierls phase that cannot be captured in this approach. Furthermore the restoring of parity or time reversal symmetry in **Eq**. (5.23) is in general not acceptable, as it contradicts to the characteristic behavior of correlation functions even in the dilute regime [13, 27, 33]. The restoring of those symmetries is related to the restriction to low-energy scattering in **Eq**. (5.20), leading to Galilean invariance of the underlying field theory. In the case of the non-anyonic Bose-Hubbard model the situation is quite similar. The Galilean invariant Lieb-Liniger model is explicitly recovered by considering only low-energy two-particle scattering in the non-Galilean invariant Bose-Hubbard model [33, 138]. This means that the explicit continuum limit of the Bose-Hubbard model can be alternatively obtained by a two-particle wave-function, where we will explicitly show in a later chapter that this is not the case for the statistical interactions in the dilute anyon-Hubbard model. But before we investigate the explicit continuum limit of the anyon-Hubbard model, we use a perturbative method to approximately describe its dilute regime for strong onsite interactions U as already mentioned in the seminal paper of Haldane concerning similar considerations about the Lieb-Liniger model [48].

5.2 Strong Coupling Effective Hamiltonian

In the following we derive a strong coupling effective Hamiltonian, following the work of Cazalilla [131] on its closest relative the Bose-Hubbard model [40]. In the extremely dilute case the effective Hamiltonian can be mapped onto a Galilean invariant fermionic field theory with weak attractive interactions [131], whereas those interactions exactly vanish in the pseudo-fermionic limit. Hence the equivalence between fermions and pseudo-fermions can be explicitly shown for relatively small densities and strong onsite interactions, complementary to the two-particle approach. Additionally deviations of the ground-state energy with respect to the ideal Tonks gas are calculated for $\theta \neq \pi$ [130], structurally equivalent to **Eq**. (5.25). For a Fermi wavevector of $k_F = \pi/2a$ we furthermore treat the collective excitations in this inherently bosonic system by means of the perturbative bosonization of lattice fermions [42,43]. In analogy to the two-particle scattering approach, another analytical estimate for the Luttinger parameter is derived, whereas the equivalence of both entities can also be approved for this particular case. Potential violations of parity/ time-reversal symmetry away from half-filling, inherent to these anyonic systems even for very small fillings [18], are shortly discussed. In agreement with the effective Lieb-Liniger model of the former section, these findings indicate the necessity of a more refined continuum limit of one-dimensional anyons as it is pursued in the next chapter. Thereby the relation between pseudo-fermions and fermions can be investigated beyond the two-particle picture.

In order to obtain an effective Hamiltonian in the strong-coupling limit, we restrict ourselves to the subspace of up to one particle per site $\langle \hat{n}_j \rangle \leq 1$, generated by large repulsive interaction $U \gg J$. Hence in the following it is essential to add an additional onsite interaction to the otherwise free anyonic gas, i.e.

$$\hat{H}_{\mathrm{AH}} = -J \sum_{j=1}^{L} \left[\hat{b}_j^\dagger \hat{b}_{j+1} e^{i\theta \hat{n}_j} + e^{-i\theta \hat{n}_j} \hat{b}_{j+1}^\dagger \hat{b}_j \right] + \frac{U}{2} \sum_{j=1}^{L} \hat{n}_j (\hat{n}_j - 1). \tag{5.29}$$

We denote $\hat{P}$ as the projector into that subspace and its complement by $\hat{Q}$, where the two satisfy the completeness relation

$$\hat{P} + \hat{Q} = \hat{I}. \tag{5.30}$$

One can derive now an effective Hamiltonian perturbatively in J by the following expansion

$$\hat{H}_{\mathrm{eff}} \approx \hat{P}\hat{H}_{\mathrm{AH}}\hat{P} - \hat{P}\hat{H}_{\mathrm{AH}}\hat{Q}\frac{1}{\hat{Q}\hat{H}_{\mathrm{AH}}\hat{Q}}\hat{Q}\hat{H}_{\mathrm{AH}}\hat{P} + ..., \tag{5.31}$$

see for example [139]. The action of the Hamiltonian on the complement can be approximated by $\hat{Q}\hat{H}_{\mathrm{AH}}\hat{Q} = U/2$ [131], describing the energy gap of the perturbation for adding a single particle. Thus we obtain the following Hamiltonian up to the second order in J

$$\hat{H}_{\mathrm{eff}} = -J \sum_{j=1}^{L} \hat{P} \left[\hat{b}_j^\dagger \hat{b}_{j+1} e^{i\theta \hat{n}_j} + e^{-i\theta \hat{n}_j} \hat{b}_{j+1}^\dagger \hat{b}_j \right] \hat{P} \tag{5.32}$$

$$- \frac{2J^2}{U} \sum_{j=1}^{L} \hat{P} \left[\hat{b}_{j-1}^\dagger e^{i\theta \hat{n}_{j-1}} + \hat{b}_{j+1}^\dagger e^{-i\theta \hat{n}_j} \right] \hat{b}_j \hat{Q}^2 \hat{b}_j^\dagger \left[e^{-i\theta \hat{n}_{j-1}} \hat{b}_{j-1} + e^{i\theta \hat{n}_j} \hat{b}_{j+1} \right] \hat{P}, \tag{5.33}$$

where the projector $\hat{P}$ can be explicitly removed by considering hardcore bosons which are then further related to fermions via the Jordan-Wigner transformation [9], i.e.

$$\hat{P}\hat{b}_j^\dagger \hat{P} = \hat{c}_j^\dagger e^{i\pi \sum_{l<j} \hat{n}_l}. \tag{5.34}$$

Finally the projector into the complement $\hat{Q}$ can be replaced by $\hat{Q} = (\hat{n}_j - 1)$, which leads then to the following Hamiltonian

$$\hat{H}_{\mathrm{eff}} = -J \sum_{j=1}^{L} \hat{b}_j^\dagger \hat{b}_{j+1} + \hat{b}_{j+1}^\dagger \hat{b}_j - \frac{2J^2}{U} \sum_{j=1}^{L} \hat{n}_{j-1}\hat{n}_j + \hat{n}_{j+1}\hat{n}_j \tag{5.35}$$

$$- \frac{2J^2}{U} \sum_{j=1}^{L} \hat{b}_{j-1}^\dagger e^{i\theta} \hat{n}_j \hat{b}_{j+1} + \hat{b}_{j+1}^\dagger e^{-i\theta} \hat{n}_j \hat{b}_{j-1},$$

where the bosonic operators obey now the hardcore constraint $\hat{b}^2 = 0$. Alternatively the Hamiltonian can be written in the fermionic language

$$\begin{aligned}\hat{H}_{\text{eff}} =& -J\sum_{j=1}^{L}\hat{c}_j^\dagger\hat{c}_{j+1} + \hat{c}_{j+1}^\dagger\hat{c}_j - \frac{2J^2}{U}\sum_{j=1}^{L}\hat{n}_{j-1}\hat{n}_j + \hat{n}_{j+1}\hat{n}_j \\ &+ \frac{2J^2}{U}\sum_{j=1}^{L}\hat{c}_{j-1}^\dagger e^{i\theta}\hat{n}_j\hat{c}_{j+1} + \hat{c}_{j+1}^\dagger e^{-i\theta}\hat{n}_j\hat{c}_{j-1},\end{aligned} \tag{5.36}$$

where we suppress any boundary effects coming from the Jordan-Wigner string by assuming periodic boundary conditions for **Eq**. (5.36). Nevertheless it should be noted that the twist in the boundary conditions, originating from the application of the fractional Jordan-Wigner transformation leading to **Eq**. (5.29) and from the ordinary one in **Eq**. (5.34), has to be taken into account for small or mesoscopic systems and embodies a topological property of such one-dimensional anyons. The form of the perturbative Hamiltonian **Eq**. (5.36) is reminiscent of the fermionized form of the one-dimensional XXZ spin-1/2 chain [131] with perturbatively small anisotropy. A deviation with respect to the ordinary spin-chain is the presence of the correlated hopping processes which ultimately reflect the non-integrability of the original model even in the bosonic case [138]. Comparing **Eq**. (5.36) to its bosonic pendant one sees that those correlated hopping processes are altered by a θ dependent phase factor, which leads to an additional breaking of time-reversal symmetry in comparison to the Bose-Hubbard model [13, 27, 33], which should be reflected ultimately in the corresponding low-density/low-energy field theory. Due to the lack of integrability, even for the perturbative Hamiltonian, we apply further approximations on top of the perturbation theory in order to obtain further analytical insights into different density regimes.

5.2.1 Continuum Limit

In the following the effective fermionic Hamiltonian **Eq**. (5.36) is expanded around the bottom of the band $k \approx 0$, in contrast to the usual continuum limit for fermions performed in the next section [43]. The reason for this peculiar continuum limit relies in the fact that we would like to study the low-density regime for the anyon-Hubbard Hamiltonian at strong coupling, which finally is a bosonic system that is only effectively described by fermionic degrees of freedom **Eq**. (5.38). This limiting process in **Eq**. (5.37) is then in accordance with the way the Lieb-Liniger model is derived from the Bose-Hubbard model [52, 131]

$$\lim_{L\to\infty, a\to 0, La=l}\frac{\hat{c}_{j\pm1}}{\sqrt{a}} \approx \hat{\Psi}_F(x) \pm a\partial_x\hat{\Psi}_F(x) + \frac{a^2}{2}(\partial_x)^2\hat{\Psi}_F(x). \tag{5.37}$$

After the neglection of higher orders in the lattice spacing a, we obtain the following Hamiltonian from **Eq**. (5.36)

$$\hat{\mathcal{H}} = \int_0^l dx \ \left(\partial_x \hat{\Psi}_F^\dagger(x)\right)\left(\partial_x \hat{\Psi}_F(x)\right) - c\int_0^l dx \ \partial_x \hat{\Psi}_F^\dagger(x)\partial_x \hat{\Psi}_F(x)\hat{\Psi}_F^\dagger(x)\hat{\Psi}_F(x). \quad (5.38)$$

The attractive and momentum-dependent interaction of the fermions in **Eq**. (5.38) is scaled by the constant c

$$\begin{aligned} c =& \frac{[1+\cos(\theta)]}{\tilde{c}}, \\ \tilde{c} =& \frac{U}{Ja}, \end{aligned} \quad (5.39)$$

where $\tilde{c}$ is the coupling constant arising in the continuum limit of the Bose-Hubbard model [96, 131]. The Hamiltonian **Eq**. (5.38) expresses weak corrections with respect to the free Fermi gas [6, 10, 131]. For $\theta \in [0, \pi)$ the interaction c reduces effectively the ground-state energy of the free fermions, where c can be demagnified either by larger onsite interactions U, or alternatively by reducing the kinetic energy via statistical transmutation. Interestingly, this interaction vanishes for $\theta = \pi$ at any finite value of $\tilde{c}$, which indicates again the equivalence of pseudo-fermions and fermions in the low-density regime where only two-particle processes are relevant, i.e.

$$\hat{\mathcal{H}}|_{\theta=\pi} = \int_0^l dx \ \partial_x \hat{\Psi}_F^\dagger(x)\partial_x \hat{\Psi}_F(x). \quad (5.40)$$

This also illustrates again the non-perturbative nature of such statistical interactions and agrees with the results of the two-anyon scattering Ansatz of the previous section. The problem of the non-renormalizability of such statistical interactions with respect to the lattice constant a is not existent here due to the presence of the renormalizable onsite interaction U in **Eq**. (5.39), in analogy to the continuum limit of the Bose-Hubbard model [131]. Even if the premises of the calculations so far are based on the dominance of the onsite interaction U, the former result can be potentially extrapolated to the case $U = 0$. Hence the equivalence of pseudo-fermions and canonical fermions seems to be valid as long as the lattice Hamiltonian is sufficiently dilute, which substantiates an effective restriction to the subspace where $\langle \hat{n}_j \rangle \leq 1$ is fulfilled.

As the effective Hamiltonian **Eq**. (5.38) has the same structure as in the Bose-Hubbard case [131], except for a re-definition of coupling constants and a phase twist at the boundary that we have neglected, we can use the results of Cazalilla for the ground-state energy correction caused by $\tilde{c}$ relative to the ideal Fermi gas,

$$E_{\mathrm{gs}}^{\gamma \gg 1} \approx \langle \hat{N} \rangle \left(\frac{\hbar^2 \rho_0^2}{2m}\frac{\pi^3}{3}\right)\left(1 - \frac{4(1+\cos(\theta))}{\gamma^{\mathrm{BH}}} + \mathcal{O}(\gamma^{-2})\right). \quad (5.41)$$

The expression **Eq**. (5.41) structurally coincides in leading order with **Eq**. (5.25), a manifestation of the one-dimensional Bose-Fermi duality between hardcore bosons and free fermions [11]. The effective Lieb constant of the two-particle approach of the last section γ_2 is exchanged with $\gamma^{\mathrm{AH}}_{\mathrm{cont.}}$, i.e.

$$\gamma^{\mathrm{AH}}_{\mathrm{cont.}} = \gamma^{\mathrm{BH}}/(1+\cos(\theta)), \qquad \gamma^{\mathrm{BH}} = \tilde{c}/\rho, \tag{5.42}$$

where γ^{BH} denotes the Lieb constant of the low-density limit of the Bose-Hubbard model. **Eq**. (5.41) expresses the fact that the dilute anyon-Hubbard model is effectively described by fermions for strong on-site interaction U. This is not really surprising as formally the limit $U \to \infty$ transmutes any canonical Bose system to the hardcore case and thus locally to fermionic degrees of freedom, see for example [10] [5]. Furthermore one should remark that the continuum limit in terms of the fermionic operators leads also to a restoration of time-reversal symmetry as in the previous section, in contrast to the lattice Hamiltonian **Eq**. (5.36) which is obviously complex. In the next sub-section it is shown that the effective field theory based on a linearization around k_F is in principle capable of sustaining the symmetry properties of **Eq**. (5.36) with respect to spatial inversion and time-reversal, even for very small densities. In analogy to the effective Lieb-Liniger model of the previous section this raises the question how to faithfully describe the continuum limit of these lattice anyons, such that their symmetry properties are at least partially conserved. In addition the equivalence of pseudo-fermions and fermions shown before for low densities, can be extended to the case of half-filling.

5.2.2 Perturbative Bosonization at Half-Filling

In the next part we briefly derive and discuss the Luttinger liquid for the effective fermionic Hamiltonian **Eq**. (5.36). The expansion of the Fermi operators is performed now around the Fermi edge $k \approx \pm k_F$, see [42, 43, 53], instead of at the bottom of the band. Whereas the expansion of the former section corresponds to addressing the low-density regime of the strongly interacting anyon-Hubbard model, the current calculation corresponds to addressing the low-energy regime of the lattice system for strong onsite interactions U. The lattice fermions in **Eq**. (5.36) are projected onto left/right moving excitations relative to the Fermi momentum $k_F = \pi\rho$,

$$\hat{c}_j \approx \hat{\Psi}_R(x)e^{ik_F x} + \hat{\Psi}_L(x)e^{-ik_F x}, \tag{5.43}$$

whereas the presence of a Fermi-sphere for this inherently bosonic system has to be understood in the sense of interaction induced fermionization [10, 11]. These excitations are then further expressed in terms of its vertex operators [42], i.e.

$$\hat{\Psi}_{R,L}(x) \propto : e^{\pm i\sqrt{4\pi}\Phi_{R,L}(x)} :, \tag{5.44}$$

whereas the cut-off implicitly contained in **Eq**. (5.44) is evaluated to the lattice spacing a. This cut-off in **Eq**. (5.44) limits the maximal resolution of the Luttinger liquid in real space and sets the bandwidth of the theory by effectively restricting the momentum support of the fields $\hat{\Psi}_{R,L}(x)$ [43]. Hence for this particular choice of cut-off we do not expect the occurrence of non-renormalizable interactions in the low-energy field theory in the sense of **Eq**. (5.24), even in the absence of an additional scale U that can be renormalized. This originates from the fact that the explicit limit of a vanishing lattice spacing would correspond to an infinite bandwidth of the Luttinger liquid. Thus this particular limit would overclaim the predictive power of the Luttinger liquid, as in this case the starting point of the renormalization procedure would be at infinitely high energies [50]. Now most parts of the Hamiltonian **Eq**. (5.36) can be bosonized straight-forwardly in analogy to the XXZ spin- $1/2$ chain without the consideration of any umklapp processes which are unphysical for the present model [42, 43, 130, 131]. We obtain the following standard expressions for the kinetic energy of the fermions, as well as a renormalization of the density stiffness by the density-density interaction

$$\begin{aligned} &- J \sum_j \hat{c}_j^\dagger \hat{c}_{j+1} + \text{h.c.} \approx Ja \sin(k_F a) \int dx \;\; (\partial_x \phi(x))^2 + (\partial_x \Theta(x))^2 \\ &- \frac{2J^2}{U} \sum_j \hat{n}_j \hat{n}_{j+1} \approx - \frac{8J^2 a}{U\pi} \left(\partial_x \phi(x)\right)^2 . \end{aligned} \tag{5.45}$$

The complex phase in the correlated hopping processes leads to additional operator content in the low-energy field theory as compared to the case of real-valued kinetic energy in **Eq**. (5.45). The terms in **Eq**. (5.46) implement the time-reversal asymmetry of the original model,

$$\begin{aligned} : \left(\hat{c}_{j+1}^\dagger \hat{c}_{j-1} e^{i\theta} + \text{h.c.} \right) :\equiv : Q_{j-1,j+1}(\theta) :\approx & \frac{2\cos(\theta)}{\pi a} \sin\left(2\sqrt{\pi}\phi(x) + 4k_F x\right) \\ & + \frac{2}{\sqrt{\pi}} \Big(\cos(2k_F a)\cos(\theta)\partial_x \phi(x) - \sin(2k_F a)\sin(\theta)\partial_x \Theta(x) \Big) \\ & - 2a \sin(2k_F a)\cos(\theta) \left[\left(\partial_x \phi(x)\right)^2 + \left(\partial_x \Theta(x)\right)^2 \right] , \end{aligned} \tag{5.46}$$

by the un-evenness with respect to reflections of the phase field $\Theta(x) \leftrightarrow -\Theta(x)$, whereas one should remark that the density-dependence of the hopping is temporarily neglected in **Eq**. (5.46). In partial agreement with the previous section, the terms linear in $\partial_x \Theta(x)$ implementing this asymmetry in **Eq**. (5.46) identically vanish for zero filling fractions but are in principle allowed for arbitrary small densities. Hence one could be tempted to conclude that this asymmetry should also be reflected in the continuum limit of lattice anyons contrary to both approaches pursued in this chapter, i.e. **Eqs**. (5.23) and (5.38). As one would expect, in analogy to the Bose-Hubbard model, that the low-energy/low-densities limits commute at least in the very strongly or very weakly

coupled regime.
Time-reversal symmetry is also effectively restored for the case of half-filling $k_F = \pi/2a$, which we choose for simplicity in the following. In order to bosonize such correlated hopping processes carefully we have to use the methods developed in [140, 141], i.e.

$$\left(\hat{c}^{\dagger}_{j-1} e^{i\theta} \hat{n}_j \hat{c}_{j+1} + \hat{c}^{\dagger}_{j+1} e^{-i\theta} \hat{n}_j \hat{c}_{j-1}\right) \equiv Q_{j-1,j+1}(\theta)\hat{n}_j \tag{5.47}$$
$$\approx \left(\langle Q_{j-1,j+1}(\theta)\rangle + : Q_{j-1,j+1}(\theta) :\right)\left(\langle \hat{n}_j\rangle + : \hat{n}_j :\right) \overbrace{\approx}^{k_F=\pi/2a} : Q_{j-1,j+1}(\theta) :: \hat{n}_j : .$$

The procedure in **Eq**. (5.47) amounts basically to decompose such correlated products of operators into their normal ordered contribution as well as their expectation value at different sites, then bosonize each of them individually and finally calculate their operator product expansion [140, 141]. The effect of the correlated hopping processes at this filling fraction in **Eq**.(5.46) is then given by a simple renormalization of the density stiffness as it is usually induced by ordinary two-particle interactions [43], i.e.

$$: Q_{j-1,j+1}(\theta) :: \hat{n}_j :\approx -\frac{8a}{\pi}\cos(\theta)\left(\partial_x \phi(x)\right)^2 , \tag{5.48}$$

formalizing the repulsive effect mediated by the Peierls phase [33]. We show only the result of the calculation here and postpone a more detailed discussion of the technique described in [140,141] to a later chapter where it is excessively used. Collecting all terms leads then to the usual form of a single-component Tomonaga-Luttinger liquid [42, 43]

$$\hat{H}_{\text{eff}} \approx u \int dx \;\; K\left(\partial_x \phi(x)\right)^2 + \frac{1}{K}\left(\partial_x \Theta(x)\right)^2 . \tag{5.49}$$

We have omitted gradients of the density field $\phi(x)$ in **Eq**. (5.49), corresponding just to trivial gauge shifts and are thus not of importance in the current context. As the starting point of this investigation results from a perturbative treatment in J/U we also have to expand the sound velocity and the Luttinger parameter in lowest order, i.e.

$$\begin{aligned} \frac{u}{Ja} &\approx 1 - \frac{4}{\pi}(1+\cos(\theta))\frac{J}{U}, \\ K &\approx 1 + \frac{4}{\pi}(1+\cos(\theta))\frac{J}{U}. \end{aligned} \tag{5.50}$$

In **Eq**. (5.50) the results of Cazalilla in [131] are recovered in the bosonic limit, after a rescaling of the hopping energy $J \to J/2$. Also in this approach the equivalence of canonical fermions and pseudo-fermions is evident by comparing the Luttinger parameter K for $\theta = \pi$ in **Eq**. (5.50) with the known value for free fermions, i.e. $K_{\text{Fermi}} = 1$ [43], whereas one is not restricted to very small densities here but to the presence of additional interactions. In analogy to the Luttinger parameter originating from the two-particle treatment, **Eq**. (5.50) embodies one of the scarce analytic results addressing the strong-

coupling regime of non-integrable models [130, 131].

5.3 Concluding Remarks

Despite the seemingly damning burden of proof for the equivalence of fermions and pseudo-fermions for sufficiently low densities in **Eqs**. (5.24) and (5.40), a few words of caution are indicated. As stated before the density-dependent Peierls phase in the lattice Hamiltonian incorporates processes beyond the two-particle picture which are not captured in the approaches above. One could be tempted to argue that such processes are effectively irrelevant for such small densities, but this would contradict then to elementary constructions of anyonic models in the continuum, like the Kundu model [7] where at least three-particle interactions are naturally present in its bosonic formulation and parity / time-reversal symmetry are strictly broken. Furthermore the continuum description of the anyon-Hubbard model was conjectured to be equivalent to the Kundu model in [13, 88], whereas a clear derivation of that fact was not provided. Based on that premise the equivalence between pseudo-fermions and fermions for low densities would be immediately proven by considering the bosonic gauge equivalent of the Kundu model, namely a Lieb-Liniger model with renormalized coupling constant $c = \frac{\tilde{c}}{cos(\theta/2)}$ [7, 88, 115, 117]. Besides the fact that this construction only works for interacting anyons with $\tilde{c} \neq 0$ [142], we will show in the next chapter that the Kundu model is only a special case of the continuum limit of the anyon-Hubbard model and thus the premise of the statement above turns out to be not fulfilled. Hence the relation between fermions and pseudo-fermions will be investigated again by means of a full continuum limit theory in the next chapter, whereby the symmetry properties of the lattice Hamiltonian are preserved under that procedure. So we can complete the task of showing the relation between pseudo-fermions and fermions on the hand of a microscopic theory and thus provide the conditions under which the full transmutation from canonical bosons to canonical fermions is described by the dilute anyon-Hubbard model. Furthermore we resurrect the occurrence of non-renormalizable two-particle interactions mediated by the underlying particle statistics as in **Eq**. (5.20), where we can prove physically motivated that optical lattices indeed provide natural regularizations to the ill-defined interactions in the continuum formulations of one-dimensional anyons *à* la Kundu and beyond [7, 12].

The strong-coupling Luttinger exponents derived in this chapter **Eqs**. (5.26) and (5.50) have to be contrasted with the weak-coupling result obtained by a crude application of the harmonic fluid approach to the anyon-Hubbard model [33, 128]

$$K_{\mathrm{G}} = \sqrt{\frac{\pi^2}{\theta^2 + \frac{U}{2J\rho_0}}}, \tag{5.51}$$

which suffers from several inconsistencies that will be partially resolved in the upcoming chapter. Obviously **Eq**. (5.51) lacks the characteristic periodicity in the statistical parameter implying a somehow perturbative treatment of the density-dependent Peierls phase, whereas the periodicity is manifest in both **Eqs**. (5.26) and (5.50). A periodic Luttinger parameter implies that the respective low-energy theories are periodic in θ too, a necessity as the original Hamiltonian is periodic in that variable [143] and there is no indication why this symmetry should be spontaneously broken. The Luttinger parameter has to be numerically extracted in general for non-integrable models in the strong coupling regime [52, 61], whereas **Eqs**. (5.26) and (5.50) are considered analytical approximations a priori only reliable in their perturbative regimes. The reason why the Luttinger exponent of the non-integrable anyon-Hubbard model can be estimated by **Eqs**. (5.26) and (5.50) in the strong-coupling regime, is that both approaches effectively relate the model to integrable ones or perturbatively small deviations of them, i.e. the Lieb-Liniger model and free fermions with perturbatively small attractive interactions [48]. Hence the parameters can be calculated directly via the Bethe solution or approximated by the bosonization approach for fermions valid for weak couplings, whereas weak-coupling of the effective model **Eq**. (5.36) corresponds to strong-coupling of the original model. Comparing the Luttinger parameters of both approaches with each other, we see that both results functionally coincide except for a different definition of their effective Lieb constant. In analogy to a one-dimensional bosonic gas that can be tuned to strong coupling either by increasing the interaction $\tilde{c}$ or by lowering the density ρ [6]. The two-particle approach in **Eq**. (5.26) intrinsically favors low densities to achieve the strong-coupling regime, whereas the perturbative approach in **Eq**. (5.50) prefers the first possibility at a finite density. In the next chapter **Eqs**. (5.26) and (5.50) are then complemented in the weak-coupling regime, by the harmonic-fluid approach to the full continuum theory of the anyon-Hubbard model as well as for certain special cases via the relation to other integrable anyon models, whereas the crucial periodicity is always obeyed.

Chapter 6

Continuum Limit of Canonical Anyons

In the following chapter the continuum limit of the kinetic part of the anyon-Hubbard Hamiltonian is explicitly derived. This is achieved by means of a rigorous continuum procedure, that is manifestly normal ordered, with the aim to investigate the low-density limit of the lattice Hamiltonian. We show that the effective continuum theory preserves the crucial periodicity in the statistical parameter, if a careful limiting procedure to the continuum is performed. Thus the dilute anyon-Hubbard model incorporates the topological property of the continuous exchange of abelian anyons into its coupling constants, implying that the time evolution governed by the Hamiltonian obeys this crucial periodicity explicitly [143]. For the historically well known continuum anyons that are also discussed in that chapter, this periodicity is only implicitly contained in the deformed commutation relations but not in the Hamiltonian itself, thus they possess the periodicity constraint on the anyonic wave-function only. We reveal thereby the connection between the lattice anyons as described by the anyon-Hubbard model and those anyonic Hamiltonians that are directly defined in the continuum, who all share structurally similar deformed commutation relations [7, 144]. To be more precise, the dilute lattice Hamiltonian is effectively connected to the historically prevalent definitions of one-dimensional anyons, i.e. *à* la Kundu as well as Leinaas und Myrheim [4, 7]. The ill-defined interactions of the Kundu model of one-dimensional anyons that were harshly criticized as being unphysical [12, 115], are thereby naturally regularized by the ultra-violet cutoff of the lattice spacing a. This renormalization of effective two-particle pseudo-potentials in the continuum limits of lattice models has been shown already for the two-anyon scattering in chapter (**5**). Such a renormalization is further illustrated by numerically investigating the onset of strong-coupling behavior of the Friedel density oscillations via Density-Matrix-Renormalization Group calculations of the hard-wall boundary anyon-Hubbard model [145–148].

We conclude that the optical lattice approach to one-dimensional anyons in the continuum indeed embodies the topological properties of continuous particle exchange in analogy to the original ideas of Wilczek and furthermore elevates the Kundu model and its variants out of the realm of purely academic examples [7, 144, 149]. We can explain various characteristic properties of the anyon-Hubbard model microscopically, via the relation to those integrable limits and the properties of their Bethe-solutions. Furthermore, we can get additional analytical estimates for the universal parameters in the low-energy sector, that complements the strong-coupling approximations of chapter (**5**) to different parameter cases. To study the system away from its integrable limits we derive the Tomonaga-Luttinger liquid corresponding to the effective low-density theory for twisted boundary conditions. The resulting theory reflects the topological properties of those one-dimensional anyons for finite sizes and inherits the space-time asymmetry of the low-density limit by additional operator content with respect to an ordinary Luttinger liquid. The occurrence of non-integrable zero-modes and the relation to one of the rather peculiar effects of Luttinger physics, i.e. persistent currents in the ground state of finite periodic systems, is discussed. Finally selected correlation functions are calculated that naturally reflect the characteristics of anyonic symmetry breaking by inhomogeneously dispersing left/right-moving species relative to the interaction induced effective Fermi-momentum and are accessible observables in cold atom experiments.

6.1 Introductory Remarks

The starting point of our investigation is the formal limit of some Hamiltonian $\hat{H}$ [15], i.e.

$$\lim_{L\to\infty, a\to 0, La=l=\text{const.}} \hat{H}, \tag{6.1}$$

that can be interpreted such that the lattice spacing a is continuously lowered, whereas the number of lattice sites L is increased such that the physical length $l = La$ remains finite, which then subsequently corresponds to a low-density limit for the lattice description [15, 130]. As the replacement of the lattice operators with their continuum pendents is rather symbolic in nature, as we will see soon, we distinguish in the following the continuum limit starting from the anyonic Hamiltonian or the bosonic one, i.e.

$$\begin{aligned} \hat{H}_{\mathrm{A}}^{\mathrm{kin}} &= -J\sum_j \left(\hat{a}_j^\dagger \hat{a}_{j+1} + \text{h.c.}\right), \\ \hat{H}_{\mathrm{B}}^{\mathrm{kin}} &= -J\sum_j \left(\hat{b}_j^\dagger \hat{b}_{j+1} \exp(i\theta\hat{n}_j) + \text{h.c.}\right), \end{aligned} \tag{6.2}$$

and consequently check their relation later on. We focus solely on the kinetic part of the anyon-Hubbard model in our derivation as the onsite-repulsion scaled by U is trivially transformed into its continuum version and can be straight-forwardly included whenever desired [130, 150]. The bosonic field operator in the continuum can be defined as follows [15]

$$\hat{\Psi}_B^\dagger(x) = \lim_{a\to 0} \hat{b}_j^\dagger/\sqrt{a}, \tag{6.3}$$

where the rather mathematically awkward expression preserves symbolically the canonical commutation relations

$$\lim_{a\to 0}\left[\hat{b}_i/\sqrt{a}, \hat{b}_j^\dagger/\sqrt{a}\right] = \lim_{a\to 0}\frac{\delta_{i,j}}{a} = \delta(x-\tilde{x}) = \left[\hat{\Psi}_B(\tilde{x}), \hat{\Psi}_B^\dagger(x)\right]. \tag{6.4}$$

Furthermore **Eq**. (6.3) can be put on a well-defined basis in terms of its unbounded Fourier components

$$\hat{\Psi}_B^\dagger(x) = \lim_{a\to 0} \hat{b}_j^\dagger/\sqrt{a} = \frac{1}{\sqrt{l}}\sum_{k=-\infty}^{\infty} e^{-ikx}\hat{b}_k^\dagger, \tag{6.5}$$

if we restrict ourselves to Fock spaces with ladder operators $\hat{b}_k^\dagger$ [15]. For the anyonic field operators one might be tempted to apply the same procedure

$$\hat{\Psi}_A^\dagger(x) = \lim_{a\to 0} \hat{a}_j^\dagger/\sqrt{a}, \tag{6.6}$$

especially as the deformed commutators are formally preserved

$$\delta(x-\tilde{x}) = \left[\hat{\Psi}_A(\tilde{x}), \hat{\Psi}_A^\dagger(x)\right]_{q_{x,\tilde{x}}} = \hat{\Psi}_A(\tilde{x})\hat{\Psi}_A^\dagger(x) - e^{-i\theta\mathrm{sgn}(x-\tilde{x})}\hat{\Psi}_A^\dagger(x)\hat{\Psi}_A(\tilde{x}). \tag{6.7}$$

On the other hand, even in the case of ordinary fermionic systems naive continuum limits or discretization, as in **Eq**. (6.6), may be incorrect to describe the correct short distance behavior of the many-body wavefunction [151]. This can be already understood at the level of a two-particle scattering of spinfull fermions, whereas the wrong continiuization scheme might fail to reproduce the characteristic discontinuity of the relative wavefunction and/or derivatives at the origin [151]. Hence caution should be indicated when using a simple-minded continuization procedure to operators that in some sense are able to intrinsically change their wavefunction to fermionic behavior. Furthermore, one should be aware that in the case of anyonic operators the formal replacement cannot be related to a Fourier decomposition. The reason for this is that unitary transformations are not necessarily canonical on the level of deformed anyonic commutators as they do not form a Lie-algebraic structure in general [18]. Thus skepticism is indicated in general, concerning the validity of the continuization approach in the case of anyonic lattice operators even if it is used ubiquitously [21, 88].

Ignoring these subtleties for a moment, both kind of field operators can be related via a continuum version of the Jordan-Wigner transformation [7], i.e.

$$\hat{\Psi}^{\dagger}_{A}(x) = \hat{\Psi}^{\dagger}_{B}(x) e^{i\theta \int_0^x dy \ \hat{n}(y)}, \tag{6.8}$$

where the deformed commutation relations are induced by the θ-dependent phase factor. At this point one should clearly highlight the main difference between **Eq**. (6.8) and its lattice pendant, namely the lack of periodicity in θ for the former [59]. One way to see this is to remind ourselves that operator-valued functions have to be understood in terms of functions of the operators eigenvalues with respect to a given state. In the lattice case, the bosonic number operator $\hat{n}_j$ has eigenvalues contained in the natural numbers $\mathbb{N}$ hence the same holds true for $\sum_{l<j} \hat{n}_l$ and thus the Jordan-Wigner string is automatically periodic in θ. In the continuum limit the argument of the unitary transformation $\int_0^x dy \ \hat{n}(y)$ is not necessarily in $\mathbb{N}$ and thus the periodicity of transformation is lost without further refinements [59]. Hence one can conclude by comparing **Eq**. (6.6) and **Eq**. (6.8), that the periodicity is lost in the continuization procedure, a circumstance that will become relevant when comparing the continuum limit with the seminal work of Kundu [7].

The last step in the derivation of the respective low-density effective theories consists of the gradient-expansion of the field operators up to second order in the lattice spacing a,

$$\hat{\Psi}_{A,B}(x+a) = \hat{\Psi}_{A,B}(x) + a\partial_x \hat{\Psi}_{A,B}(x) + \frac{a^2}{2} \Delta \hat{\Psi}_{A,B}(x). \tag{6.9}$$

Here **Eq**. (6.9) assumes that the fields $\hat{\Psi}_{A,B}(x)$ are sufficiently smooth in x, an assumption which is a priori not fulfilled for composite operators like the single anyon field in **Eq**. (6.8). This can be formalized by noting that while a single bosonic field acts trivially with respect to bosonic normal ordering $: \hat{\Psi}_B(x) := \hat{\Psi}_B(x)$ the anyonic field does not $: \hat{\Psi}_A(x) :\neq \hat{\Psi}_A(x)$. Thus the normal ordering procedure produces multiple delta functions in $: \hat{\Psi}_A(x) :$, which are not smooth at all and cannot be safely expanded. Alternatively one could argue that the application of the Jordan-Wigner transformation **Eq**. (6.8) leads to the reformulation of an anyonic wave-function in terms of a bosonic one with a discontinuous phase factor, as it was already pointed out by Kundu in [7]. Hence the prerequisite of the gradient expansion is strictly speaking not fulfilled for the anyons if a regular representation of the underlying canonical commutation relations (CCR) is assumed as usual, a mathematical detail whose neglection led to several incorrect statements in this context [13, 21, 88]. The only extrinsic energy scale J of our

consideration is identified with the effective band mass of the continuum theory via

$$Ja^2 \equiv \frac{1}{2m_{\text{eff}}}, \tag{6.10}$$

where $\hbar = 1$, which itself is set to unity i.e. $2m_{\text{eff}} \equiv 1$, for all the derived theories here.

6.2 Previous Approaches

As we have spent quite some time discussing potential mathematical inconsistencies of the continuization procedure in terms of the anyonic operators, we would like to see which practical consequences arise from a naive application, as it has been done multiple times in that context [21, 88]. Thus we proceed under the assumption that the replacement of lattice operators by continuum ones **Eq**. (6.6) is valid

$$\hat{\mathcal{H}}_A = \lim_{a\to 0} \quad -J \int_0^l dx \ \ \left(\hat{\Psi}_A^\dagger(x)\hat{\Psi}_A(x+a) + \text{h.c.}.\right) \tag{6.11}$$

Contrary to the earlier discussion, we assume that the anyonic fields are sufficiently smooth in space such that we can apply the gradient expansion to second order [21] whereas

$$\hat{\mathcal{H}}_A \approx \lim_{a\to 0} \left[\int_0^l dx \ \ \hat{\mathcal{H}}_A^0(x)\right]. \tag{6.12}$$

Misleadingly, the free anyonic Hamiltonian density is then obtained

$$\hat{\mathcal{H}}_A^0(x) = \ \ \partial_x\hat{\Psi}_A^\dagger(x)\partial_x\hat{\Psi}_A(x), \tag{6.13}$$

up to a global energy shift and the neglection of terms of higher order in the lattice spacing. **Eq**. (6.13) seems to be a very natural result that a "free" theory on the lattice is connected to the "free" theory in the continuum straight-forwardly. Indeed the last statement turns out to be true for ordinary bosons or non-interacting spinless fermions, an equivalence that was falsely implied to apply to anyons by various statements in the relevant literature [13, 21, 88]. Nevertheless as discussed below this conclusion is essentially wrong and is purely based on the correctness of the symbolic limiting procedure in **Eq**. (6.6), as will be proved in the following by requiring physical consistency while trying to avoid mathematical rigor. Thus we will prove in the following that the low-density limit of anyonic creation/annihilation operators on a discrete lattice and continuum field operators, as defined in **Eq**. (6.8), are intrinsically different entities. Therefore we will first calculate the continuum limit of the lattice Hamiltonian in **Eq**. (6.2) in bosonic language.

As the continuization procedure should not depend on the way the Hamiltonian is priorly arranged in the lattice, one could start the limiting process without normal ordering the Peierls phase factor as in [152], i.e.

$$\hat{\mathcal{H}}_N = -J \lim_{a\to 0} \int_0^l dx \ \left(\hat{\Psi}_B^\dagger(x) e^{ia\theta \hat{\Psi}_B^\dagger(x)\hat{\Psi}_B(x)} \hat{\Psi}_B(x+a) + \text{h.c.} \right), \tag{6.14}$$

The presence of the lattice spacing a inside the argument of the Peierls phase suggests an expansion in that small parameter, which then naturally leads to a perturbative dependence of the low-density Hamiltonian on the statistical parameter θ. This dependence on θ obviously spoils the crucial periodicity embedding the topology of abelian braiding into the Hamiltonian's parameters. If we apply now the gradient expansion in **Eq**. (6.9) up to second order but naively discard any term involving orders of $\mathcal{O}(a)$ and beyond with respect to the effective mass definition in **Eq**. (6.10). Then one obtains the following Hamiltonian

$$\hat{\mathcal{H}}_N \approx \lim_{a\to 0} \left[\int_0^l dx \int_0^l d\tilde{x} \ \ \hat{\mathcal{H}}_N(x,\tilde{x}) \delta(x-\tilde{x}) \right], \tag{6.15}$$

up to a global energy shift. The Hamiltonian density $\hat{\mathcal{H}}_N(x,\tilde{x})$, has a rather unusual structure, decomposable into

$$\hat{\mathcal{H}}_N(x,\tilde{x}) = \hat{\mathcal{H}}_N^{\text{r}}(x) + \hat{\mathcal{H}}_N^{\text{s}}(x,\tilde{x}) \tag{6.16}$$

with a regular

$$\hat{\mathcal{H}}_N^{\text{r}}(x) =: \partial_x \hat{\Psi}_B^\dagger(x) \partial_x \hat{\Psi}_B(x) - \theta \hat{\rho}_B(x) \hat{J}_B(x) :$$

$$+\theta^2 : \hat{\Psi}_B^\dagger(x) \hat{\rho}_B^2(x) \hat{\Psi}_B(x) : \tag{6.17}$$

and a singular part arising through explicit normal ordering

$$\hat{\mathcal{H}}_N^{\text{s}}(x,\tilde{x}) = \theta^2 \hat{\Psi}_B^\dagger(x) \hat{\Psi}_B^\dagger(\tilde{x}) \hat{\Psi}_B(x) \hat{\Psi}_B(\tilde{x}) \delta(x-\tilde{x}). \tag{6.18}$$

Here $\hat{\rho}_B(x) = \hat{\Psi}_B^\dagger(x)\hat{\Psi}_B(x)$, $\hat{J}_B(x) = -i\left(\hat{\Psi}^\dagger(x)\partial_x\hat{\Psi}(x) - \text{h.c.}\right)$ denote the density and current operator respectively. The regular part of the Hamiltonian $\hat{\mathcal{H}}_N^{\text{r}}(x)$ in **Eq**. (6.17), contains two unusual terms, i.e. a three-particle interaction as well as a current-density coupling that breaks parity and time reversal symmetry individually [18, 29], both reminiscent of the bosonic formulation of the Kundu model [7], a circumstance that we will further investigate in detail at a later stage.

Mathematically speaking, $\hat{\mathcal{H}}_N^{\text{s}}$ is a priori not defined through the presence of a product

of distributions, a circumstance that was diversely discussed in the context of one-dimensional anyons [7, 12, 116]. As such, singular couplings have to be regularized in general, while a physically motivated regularization scheme is needed which has to be contrasted with, for example, numerical methods in order to physically deduce a unique choice out of mathematically infinitely many possibilities. Thus care should be devoted to finding a physically sensible regularization scheme for such singular interactions, where for example the Shirokov regularization scheme [153–155] states that $\delta^2 \equiv 0$ which would lead to a completely different operator content as in **Eq**. (6.18) and also contradicts to the regularization that is imposed by the presence of the lattice as it is shown in the following. Nevertheless this issue was elegantly bypassed by Kundu who realized that if the inverse of the Jordan-Wigner-transformation in **Eq**. (6.8) is applied, one obtains

$$\hat{\mathcal{H}}_N = \hat{\mathcal{H}}_A \tag{6.19}$$

and the singularity of the two-body potential is formally lifted by the discontinuity of the anyonic wavefunction [7]. Remarkably with this choice of gauge transformation, no such regularization procedure has to be performed. This leads to the seemingly trivial conclusion that the naive continuum limit of the non-interacting anyon-Hubbard model coincides with free theory in the anyonic language up to the order $\mathcal{O}(a^0)$. Nevertheless one should be careful with this derivation of the continuum limit, as formally the Peierls phase leads to infinite-particle interaction in the lattice, as well as dynamical interactions coupled to the field derivatives where the former scale like $\mathcal{O}(a^{n-2})$ as $a \to 0$ and $n \to \infty$. The wording naive stems now from the fact that we have neglected higher orders of the lattice spacing a before explicit normal ordering, meaning that for example a term proportional to

$$\propto a^{n-3} \hat{\Psi}_B^\dagger(x) \left(\hat{\Psi}_B^\dagger(x) \hat{\Psi}_B(x) \right)^n \hat{\Psi}_B(x), \tag{6.20}$$

for $n > 3$, would produce n-body interactions, which vanish in the limit $a \to 0$, as well as higher order singular terms which are neither well defined [12], nor could they be eliminated with a corresponding gauge transformation. Finally the 2π-periodicity in θ of the lattice Hamiltonian seems to be lost in both continuum limits above and with it the topological character of the theory. In the following we provide a refined approach to the continuum limit which restores this symmetry and additionally proves the partial inconsistency of the naive one by direct comparison and reveals how to fix this issue with a particular regularization scheme for products of delta functions.

6.3 Normal Ordered Continuum Limit

For the essential part of our derivation it is important to rewrite the density-dependent Peierls phase of **Eq**. (6.2) in explicit normal ordered form [119]

$$e^{i\theta\hat{n}_j} = \sum_{q=0}^{q=\infty} \frac{(i\theta)^q}{q!}\hat{n}_j^q = \sum_{q=0}^{q=\infty} \frac{(i\theta)^q}{q!} \sum_{m=0}^{m=q} S(q,m)(\hat{b}_j^\dagger)^m(\hat{b}_j)^m, \tag{6.21}$$

where $S(q,m)$ are the Stirling numbers of second kind [156]. Now we can apply the continuum procedure in terms of bosonic operators, where we expand again up to second order in the field gradients. The free part of the dilute theory is obtained now by the $q = 0$ component of the series in **Eq**. (6.21), enjoying the usual interpretation of an energy shift plus the kinetic energy with the usual k^2 continuum dispersion, i.e.

$$\hat{\mathcal{H}}_{\rm kin}(x) = \partial_x\hat{\Psi}_B^\dagger(x)\partial_x\hat{\Psi}_B(x) - \frac{2}{a^2}\hat{\Psi}_B^\dagger(x)\hat{\Psi}_B(x). \tag{6.22}$$

For the interaction part only two/three-body interactions remain as higher orders vanish exactly in the limit $a \to 0$, according to the standard effective mass definition, i.e.

$$\hat{\mathcal{H}}_{\rm int}(x) = \sum_{n=2}^{3} a^{n-3}V_n(\theta)(\hat{\Psi}_B^\dagger(x))^n(\hat{\Psi}_B(x))^n. \tag{6.23}$$

Furthermore in the order of $\mathcal{O}(a^0)$ there exists an additional term coupled to a derivative of the field, i.e.

$$\hat{\mathcal{H}}_{\rm J}(x) = \tilde{V}_2(\theta)(\hat{\Psi}_B^\dagger(x))^2\hat{\Psi}_B(x)\partial_x\hat{\Psi}_B(x) + \text{h.c.}, \tag{6.24}$$

which manifests the breaking of parity as well as time-reversal invariance by reversing the direction of the quantum mechanical probability current. Collecting all terms, we finally obtain a refined continuum limit of the anyonic hopping operator

$$\hat{\mathcal{H}} \approx \lim_{a\to 0}\left[\int_0^l dx\ \ \hat{\mathcal{H}}(x)\right], \tag{6.25}$$

with the Hamiltonian density,

$$\hat{\mathcal{H}}(x) = \partial_x\hat{\Psi}_B^\dagger(x)\partial_x\hat{\Psi}_B(x) + \hat{\mathcal{H}}_{\rm int}(x) + \hat{\mathcal{H}}_{\rm J}(x), \tag{6.26}$$

which is expressible in a more compact form

$$\begin{aligned}\hat{\mathcal{H}}(x) = &: \partial_x\hat{\Psi}_B^\dagger(x)\partial_x\hat{\Psi}_B(x) + V_2(\theta)\hat{\rho}_B^2(x) : \\ &+ V_J(\theta) : \hat{\rho}_B(x)\hat{J}_B(x) : + V_3(\theta) : \hat{\Psi}_B^\dagger(x)\hat{\rho}_B^2(x)\hat{\Psi}_B(x) :,\end{aligned} \tag{6.27}$$

with the following coupling constants

$$\tilde{V}_2(\theta) = (1 - e^{i\theta}), \tag{6.28}$$

$$V_J(\theta) = \mathrm{Im}\left[\tilde{V}_2(\theta)\right] = -\sin(\theta), \tag{6.29}$$

$$V_2(\theta) = \frac{\mathrm{Re}\left[\tilde{V}_2(\theta)\right]}{a} = \frac{2(1-\cos(\theta))}{a}, \tag{6.30}$$

$$V_3(\theta) = -\frac{1}{2}\mathrm{Re}\left[\tilde{V}_2(\theta)^2\right] = -(1 - 2\cos(\theta) + \cos(2\theta)). \tag{6.31}$$

The two-body interaction $V_2(\theta)$ strongly renormalizes with $a \to 0$ if $\theta \neq 0$, which is in fact also the case for the ordinary Bose-Hubbard interaction U [137] or the interaction between fermions with different spin in the Fermi-Hubbard model [15]. In the Bose-Hubbard case this can be resolved by rescaling U with the overall density, leading to a renormalized theory which recovers the so-called Tonks-Girardeau limit with infinitely strong interactions for low densities [10,11]. However the angle cannot simply be rescaled or renormalized without changing the anyonic phase angle, which would violate then the topological character of exchange process manifest in the bosonic form of **Eq**. (6.2).

As stated in the introduction, the lattice model in **Eq**. (6.2) is symmetric with respect to a rather spurious parity/ time reversal transformation in bosonic language [29],

$$\hat{G} = e^{-i\theta/2\sum_j \hat{n}_j(\hat{n}_j-1)}\hat{\mathcal{I}}\hat{\mathcal{T}}, \tag{6.32}$$

that was shown to obey a clearer interpretation as a parity reversal for the anyons combined with a gauge phase, i.e. $\hat{G}^\dagger \hat{a}_j \hat{G} = \hat{a}_{L-j+1} e^{-i\theta N}$. In the continuum limit, the non-linear gauge transformation part of this symmetry $\hat{G}$ reduces to just a global phase, i.e.

$$\lim_{a\to 0} e^{-i\theta/2\int_0^l dx(\ a\hat{\rho}(x)^2 - \hat{\rho}(x))} = e^{i\theta\hat{\mathcal{N}}/2}, \tag{6.33}$$

that acts as the identity to **Eq**. (6.27) due to the conservation of the total particle number, i.e.

$$\left[\hat{\mathcal{H}}, \hat{\mathcal{N}}\right] = 0, \quad \hat{\mathcal{N}} = \int_0^l dx\ \ \hat{\rho}_{\mathrm{B}}(x). \tag{6.34}$$

Hence from **Eq**. (6.33), we can conclude that the continuum model is symmetric with respect to $\hat{\mathcal{I}}\hat{\mathcal{T}}$ only, whereas each individual operation corresponds effectively to reversing the sign of θ. This changes just the current density coupling $V_J(\theta)$, being the only odd function of the statistical parameter, but leaves the others invariant[1]. The existence of

[1]Note that in the continuum of a finite lattice system the parity inversion $j \to L - j + 1$ changes effectively to $x \to l - x$. For an infinite system the replacement $x \to l - x$ is then further reduced to $x \to -x$.

translational invariance requires the Hamiltonian to be defined for periodic (twisted) boundary conditions, which leads then additionally to the conservation of the total momentum

$$\left[\hat{\mathcal{H}}, \hat{\mathcal{P}}\right] = 0, \quad \hat{\mathcal{P}} = i \int_0^l dx \;\; \partial_x \hat{\Psi}_{\mathrm{B}}^{\dagger}(x) \hat{\Psi}_{\mathrm{B}}(x). \tag{6.35}$$

6.3.1 Comparison of the different Approaches

In order to compare both bosonic continuum limits **Eq**. (6.27) and **Eq**. (6.15), we expand the potentials of the normal ordered theory **Eq**. (6.27) to lowest order in θ, i.e.

$$\begin{aligned} V_J(\theta) &\approx -\theta + ..., \\ V_2(\theta) &\approx \frac{\theta^2}{a} + ..., \\ V_3(\theta) &\approx \theta^2 + ... \end{aligned} \tag{6.36}$$

We do so, as the continuum limit in the naive field theory **Eq**. (6.14) effectively corresponds to the respective expansion for small θ, due to the presence of the lattice spacing a inside the Peierls phase. In comparison to the non-normal ordered approach, one sees that the double-delta interaction is exchanged to an also divergent, but mathematically well defined two-body potential. One could interpret this non-rigorously such that the normal ordering procedure regularizes the δ^2 potential, such that the product of distributions is well defined [157, 158]. A possible regularization of the squared δ distribution used in physics, especially in white noise analysis, is the following one [157]

$$\delta^2 \equiv c\delta \;\; , \;\; c \in \mathbb{C}, \tag{6.37}$$

with c arbitrary but finite. Inserting this regularization into the singular part of the naive continuum theory $\hat{\mathcal{H}}_N^{\mathrm{s}}(x)$ yields the two-body potential of the advanced one with the choice $c = 1/a$. This particular choice of regularization leads to the interpretation of the δ^2 potential, as a contact potential with infinite magnitude in the limit of vanishing lattice spacing a, i.e.

$$\delta(x - \tilde{x})^2 \approx \lim_{a \to 0} V(a) \delta(x - \tilde{x}), \tag{6.38}$$

with $\lim_{a\to 0} V(a) = \infty$, as it has been described in the context of anyons [159–161]. The necessity of a finite c in **Eq**. (6.37) is then related to the physical meaning of the limit $\lim_{a\to 0} 1/a$ in the sense of renormalization group. Furthermore for this particular regularization scheme, neglecting terms of the order $\mathcal{O}(a)$ and beyond in the naive

continuum limit in **Eq**. (6.14) cannot be justified. Those terms contribute for $a \to 0$, if we assume that [157]

$$\delta^n \equiv \frac{1}{a^{n-1}}\delta, \tag{6.39}$$

holds in a distributional sense, and we eventually recover the advanced continuum limit and with this the crucial 2π-periodicity if properly included. The requirement of physical equivalence of both bosonic field theories for all θ leads then to a particular regularization scheme for products of delta functions in **Eq**. (6.39). A dual form of the statement above can be obtained by employing again the inverse Jordan-Wigner transformation **Eq**. (6.8) on the lowest order expansion of the normal ordered field theory in **Eq**. (6.27), i.e.

$$\hat{\mathcal{H}}|_{\theta\approx 0}(x,\tilde{x}) = \hat{\mathcal{H}}^0_A(x) + \theta^2\left[\frac{1}{a} - \delta(x-\tilde{x})\right]\delta(x-\tilde{x})(\hat{\Psi}^\dagger_A(\tilde{x}))^2(\hat{\Psi}_A(x))^2, \tag{6.40}$$

implying the equivalence of the advanced continuum theory to free anyons for small θ, with respect to a suitable regularization of the δ^2 potential. Hence we can conclude furthermore that the continuum limit in **Eq**. (6.15) is actually not naive if all orders of interactions are included in the derivation and a specific regularization scheme for the occurring products of delta-functions is chosen. On the other hand the continuization procedure in terms of anyonic operators remains questionable and it is not clear if all higher order corrections to **Eq**. (6.13) would ever recover the refined continuum theory. Finally the regularization of unwanted infinities by the presence of a lattice is actually a subject of a whole field, the lattice quantum field theory [162], even if the procedure is usually done there in reversed order. So the concept of the implicit regularization of the low-density effective field theory of the lattice anyons is rather well known fact, but was up to now not appreciated fully.

By accepting the validity of the lattice regularization scheme and considering subsequent orders in the θ expansion, the refined continuum theory can be interpreted as particular deformation of the free anyonic density in the continuum. For arbitrary densities beyond the dilute limit, the anyon-Hubbard model includes additionally higher order current-density couplings of the form $\hat{\rho}_B\partial_x\hat{J}_B$, $\hat{\rho}^2_B\hat{J}_B$, a unique feature of such lattice anyons in contrast to their continuum pendants. In the following the relation of **Eq**. (6.27) to such anyons *à* la Kundu and its relatives is investigated in more detail. The reasoning behind that is to categorize our low-density field theory relative to the historically established concepts of one-dimensional anyons. Furthermore the relation to those models, that are all integrable, allows to explain various properties of the dilute anyon-Hubbard model by the properties of their Bethe solutions [163].

6.4 The Relation to Integrable Models

The Kundu model, or more precisely a Lieb-Liniger gas consisting of one-dimensional anyons instead of canonical bosons [6], was historically the first seemingly non-trivial extension of one-dimensional anyons in the spirit of Leinaas-Myrheim [4, 7]. Indeed, the bosonic and anyonic Lieb-Liniger model are gauge equivalent as shown by Kundu himself, neglecting minor effects for periodic boundary conditions, a fact that is later on recapitulated in this section. Important is thereby that the two models are linked by their Bethe solutions instead of being related by the Jordan-Wigner duality, a circumstance that is similar in nature to the relation between the bosonic and anyonic dimer discussed in an earlier chapter. In **Ref**. [5] it was additionally shown that Leinaas-Myrheim anyons can be viewed as ordinary Lieb-Liniger bosons with a statistical parameter dependent on the two-body coupling constant of the model. Thereby the effective fermionization of bosons in the Lieb-Liniger model for strong interactions can be understood formally as the emergence of an effective Pauli principle and anti-symmetrized wavefunction for those anyons. In this sense the approaches of Leinnaas/Myrheim and Kundu are indeed equivalent up to a redefinition of coupling constants, as it is already implied in Kundu's seminal paper. By relating the low-density anyon-Hubbard model up to $\mathcal{O}(\theta^2)$ to the Kundu model, we can therefore classify the relation between all those seemingly disjoint concepts of one-dimensional anyons.
Years after the first discovery, Kundu and his coauthors found an integrable extension of his anyon model, in analogy to the derivative δ Bose gas [164], which adds a non-linear, i.e. density dependent, dispersion to the already interacting anyons. This generalization allows for a much richer phenomenology beyond Lieb-Liniger physics, by explicitly breaking spatial and temporal inversion symmetry at the Hamiltonian level. We find that the low-density anyon-Hubbard Hamiltonian corresponds exactly to this model up to the order $\mathcal{O}(\theta^3)$ and to a non-integrable extension for higher orders. This relation further allows us to approximately discuss some characteristic features of our lattice anyons microscopically, that cannot be understood at the level of the Kundu model.

6.4.1 The Kundu Model and Beyond

The Kundu Hamiltonian can be written in second-quantized form as follows [7],

$$\hat{\mathcal{H}}_{\mathrm{K}} = \int_0^l dx \;\; \hat{\mathcal{H}}_A^0(x) + \tilde{c}\int_0^l dx \;\; \hat{\Psi}_A^\dagger(x)\hat{\Psi}_A^\dagger(x)\hat{\Psi}_A(x)\hat{\Psi}_A(x), \tag{6.41}$$

with the two-body coupling constant $\tilde{c}$ and the free anyonic density $\hat{\mathcal{H}}_A^0(x)$ as in **Eq**. (6.13). Comparing the different continuum limits obtained in this chapter with the Kundu model, we conclude that the non-interacting lattice anyon-Hubbard model serves as an experimentally feasible realization of the non-interacting Kundu Hamiltonian in

its low-density regime up to the order $\mathcal{O}(\theta^2)$. The additional two-body potential scaled by $\tilde{c}$, could thereby be straight-forwardly generated by an ordinary bosonic Hubbard interaction in the lattice. The lattice Hamiltonian therefore resolves the problem of well posedeness of the δ^2 potential by a suitable regularization [7, 12, 159, 160, 165, 166].

In the next leading order in the statistical parameter, i.e. $\mathcal{O}(\theta^3)$, our effective continuum theory corresponds to yet another known model of one-dimensional anyons, namely the Batchelor-Guan-Kundu (BGK) model. The BGK model [144] itself is an integrable generalization of the interacting Kundu model in **Eq**. (6.41),

$$\hat{\mathcal{H}}_{\mathrm{BGK}}(x) = \hat{\mathcal{H}}_{\mathrm{K}}(x) + \epsilon \int_0^l dx \;\; : \hat{\rho}_A(x)\hat{J}_A(x) : . \tag{6.42}$$

The generalization with respect to $\hat{\mathcal{H}}_{\mathrm{K}}(x)$ consists of an additional non-linear dispersion scaled by ϵ in analogy to the delta-derivative Bose gas [164]. In our model the anyonic current-density coupling is then exactly given by $\epsilon \equiv \theta^3$, up to this order of approximation. The breaking of spatial and temporal inversion is now manifest by the non-gaugeable dependence of the Hamiltonian on the current $\hat{J}_A(x)$. For general values of the statistical parameter, the continuum theory in **Eq**. (6.27) can be viewed as a generalization of the BGK model, where we leave the realm of integrable models and have to rely on non-exact methods.

Nevertheless, substantial insight into non-integrable models can be gained by investigating the properties of their integrable limits, especially in one-dimension. In our case the non-trivial integrable limits are given by the Kundu model and its generalization the BGK model, which corresponds physically to an expansion in the statistical parameter up to second/third order of our low-density theory. The Bethe solutions to those specific cases allows us to estimate various physical quantities for our generalized model in a perturbative sense, where we have to restrict ourselves to the special case of an additional two-particle interaction shifting the value of $V_2(\theta)$ by U due to the non-perturbative nature of the statistical interactions [117, 118, 144, 167]. In the following only some characteristic results of these Bethe solutions are shown without further derivation, as this is beyond the focus of this thesis and the curious reader should consult the relevant literature [117, 118, 144, 167], and are then consequently related to known properties of the dilute anyon-Hubbard model.

6.4.2 Selected Quantities of the Integrable Limits

It was Kundu himself who solved the one-dimensional anyon gas on a ring exactly [19], by noticing that **Eq**. (6.41) can be related to the Bethe ansatz equations of the ordinary,

N-particle Lieb-Liniger model with twisted boundary conditions

$$e^{ik_j l} = -e^{-i\theta(N-1)} \prod_{l=1}^{N} \frac{k_j - k_l + ic^{'}}{k_j - k_l - ic^{'}}, \tag{6.43}$$

and a redefined coupling constant $c^{'} = c/\cos(\theta/2)$. **Eq**. (6.43) is the determining equation for the Bethe roots k_j in analogy to the algebraic Bethe ansatz used for the anyon-Hubbard dimer in a former chapter. The energy can then be calculated from those roots

$$E = \sum_{j=1}^{N} k_j^2, \tag{6.44}$$

where it is convenient to consider $-\theta(N-1) \equiv \nu \in [-\pi, \pi]$ (mod 2π) for the boundary twist when minimizing the energy in **Eq**. (6.44). Conversely, each momentum k_j shifts to $k_j + \nu/l$ in the ground-state that can be neglected for large enough L^2.

As up to the order of θ^2 we have identified our theory with the Kundu model, we have access to the ground-state energy per particle as perturbatively calculated in the strong-coupling limit, i.e. with a Lieb constant $1 \ll \gamma \equiv c/\rho$ in [118], by means of the Bethe ansatz

$$\frac{E_0^{\text{Strong}}}{N} \approx \frac{\pi^2}{3l^2}\Big(N^2 - 1\Big)\Big(1 - 4\frac{\rho}{\gamma}\cos(\theta/2)\Big) + (\nu/l)^2 + ... \tag{6.45}$$

The energy in **Eq**. (6.45) corresponds to perturbative correction to the ideal Fermi gas as in the Lieb-Liniger model as occurring multiple times in this thesis, where the dynamical coupling constant of the Lieb model is rescaled with a function of the statistical parameter [7]. The result for the ground-state energy in **Eq**. (6.45) is similar to those of the effective strong-coupling theory and the two-particle scattering of a former chapter, expressing the effective fermionization of one-dimensional bosons for strong interactions [10, 11]. Furthermore they have all in common that ordinary interactions of the model are amplified by the gauge constraint of the anyonic wave function, or being created in the otherwise "non-interacting" case.
In the weak-coupling limit on the other hand, i.e. for Lieb constants $\gamma \ll \cos(\theta/2)$ to be more precise, one obtains the following formula perturbatively from the Bethe ansatz solution [118]

$$\frac{E_0^{\text{Weak}}}{N} \approx \frac{\Big(N-1\Big)c^{'}}{l} + (\nu/l)^2 + ..., \tag{6.46}$$

[2]This momentum shift corresponds to performing a local gauge transformation that rotates the boundary twist into the bulk, and is negligible for large system sizes.

in analogy to the ordinary Lieb-Liniger model [7]. Also from **Eq**. (6.46) we see that the statistical transmutation tends to increase the interactions in the system.

The equivalence to the Lieb-Liniger model with an exchanged dynamical coupling constant $c^{'}$ allows also for the analytic determination of the Luttinger exponents in the respective regimes, via **Eqs**. (6.45) and (6.46), which can be used to describe the universal features of the anyon-Hubbard model for small θ and additional onsite interactions, complementing the strong coupling estimates of the former section. The expressions then coincides with those of the Lieb-Liniger model except for a redefinition of the effective Lieb constant $\gamma^{'} = c^{'}/\rho$ [71] [70], i.e.

$$K_{\gamma' \ll 1} = \pi \left(\gamma^{'} - \frac{1}{2\pi} (\gamma^{'})^{3/2} \right)^{-1/2} + ..., \tag{6.47}$$

$$K_{\gamma' \gg 1} = 1 + 4/\gamma^{'} + 4/(\gamma^{'})^2 + ..., \tag{6.48}$$

where the expressions **Eq**. (6.48) and (6.47) embody rare analytical approximations to the universal behavior of non-integrable models like the dilute anyon-Hubbard model and complement the estimates of the former chapter rigorously.

An important quantity of the Bethe ansatz is the cut-off momentum Q that is related to the thermodynamic limit of **Eq**. (6.43), by defining a root density $\rho(k)$ from the discrete distribution $g(k_j - k_{j+1})$ for a vanishing momentum spacing [70, 71]

$$\rho(k) = \lim_{k_j - k_{j+1} \to 0} g(k_j - k_{j+1}) = \lim_{k_j - k_{j+1} \to 0} l^{-1}/(k_j - k_{j+1}). \tag{6.49}$$

The root density is then distributed according to the following integral equation

$$\rho(k) = \frac{1}{2\pi} + \frac{1}{2\pi} \int_{-Q}^{Q} \frac{2c^{'}}{c^{'2} + (k - k^{'})^2} \rho(k^{'}) dk^{'}. \tag{6.50}$$

The integral boundary Q in **Eq**. (6.50) plays the role of an effective Fermi-momentum for the bosonic gas, by only allowing occupied states for $|k| < |Q|$, related to a special kind of Pauli principle of Bethe integrable models, requiring that all the particles momenta are distinct [100]. The value of Q is given by the normalization condition

$$\int_{-Q}^{Q} \rho(k) dk = N/L, \tag{6.51}$$

hence the canonicity of the ensemble implies that a modulation of the cut-off momentum reversely induces a change of distribution of the Bethe roots. In the strong coupling regime the cut-off momentum can be calculated as a perturbative correction to the Tonks gas [117], i.e.

$$Q \approx k_F \left(1 - 2\gamma^{-1} \cos(\theta/2) \right) + ..., \tag{6.52}$$

and is another manifestation of the fermionization of a bosonic system via interactions. It should be stressed that the root distribution $\rho(k)$ should not be mistaken with the bosonic quasi-momentum distribution

$$n_k = \int dx \;\; e^{ikx} \hat{\Psi}^\dagger(x) \hat{\Psi}(0), \tag{6.53}$$

that is actually measurable in time-of-flight measurements [5]. For example in the Tonks-Girardeau limit the cut-off momentum Q coincides with the Fermi momentum k_F showing the root distribution of a Fermi-sphere, anyhow the time-of flight experiments reveal still a quasi-condensation around zero momentum which is a very bosonic feature per se. Now for the anyon-Hubbard model it is known that quasi-condensation occurs at finite momenta as a function of the statistical parameter, where the maximum of n_k is not exactly centered around $k \approx 0$ for $\theta \neq 0, \pi$ in the strongly dilute regime [18,27,29,33]. This motivates the question if this effect is solely explainable with the properties of the Kundu model. Here the answer is negative as the shift of the Bethe roots by ν/L is irrelevant for larger system sizes and furthermore the Kundu model can be formally reduced to the Lieb-Liniger model with a redefined dynamical coupling constant $c^{'}$, hence obeys in principle the same phenomenology as well as symmetries except potential variations of the boundary conditions [7].

Going one order in θ beyond Kundu, we can identify our model with the *BGK* model. The integrability of **Eq**. (6.42) can be shown with its relation to the derivative δ Bose gas [164], with a re-scaled coupling constant $c^{'}$, as in the Kundu model, and an additional rescaling of the non-linear dispersion $\epsilon^{'} = \epsilon/\cos(\theta/2)$ by the statistical parameter. This relation leads then to a set of Bethe equations of the N-particle *BGK*-model that are similar but not fully analogous to **Eq**. (6.43), i.e.

$$e^{ik_j l} = -e^{-i\theta(N-1)} \prod_{l=1}^{N} \frac{k_j - k_l + i(c^{'} - \epsilon^{'}(k_j + k_l))}{k_j - k_l - i\,(c^{'} + \epsilon^{'}(k_j + k_l))}. \tag{6.54}$$

Also in this case we can use the strong/weak-coupling results originating from **Eq**. (6.54) [144], to gain information about the low-density anyon-Hubbard model for small statistical parameters. Similar to **Eq**. (6.46) the weak coupling regime is addressed for $\gamma \ll \cos(\theta/2)$ with the lowest energy per particle given by the expression

$$\frac{E_0^{\text{Weak}}}{N} \approx \frac{(N-1)}{L}(c^{'} - 2\frac{\epsilon^{'}\nu}{l}) + \frac{\nu^2}{l^2} + ..., \tag{6.55}$$

where the non-linear dispersion ϵ induces only a finite-size correction to the ground-state energy of the Kundu model in **Eq**. (6.46), that vanishes in the thermodynamic limit. The same holds true for the strong-coupling regime where the effect of the current-density

coupling ϵ is negligible for large l,

$$\frac{E_0^{\text{Strong}}}{N} \approx \frac{(N^2-1)\pi^2}{3l^2}\left(1+\frac{2N\cos(\theta/2)}{(lc-\epsilon\nu)}\right)^{-2}+\frac{\nu^2}{l^2}+.... \tag{6.56}$$

Eq. (6.56) expresses a perturbation with respect to the ideal Fermi gas in inverse orders of $\gamma^{'}$, similar to **Eq**. (6.45), plus finite size corrections mediated by ϵ.

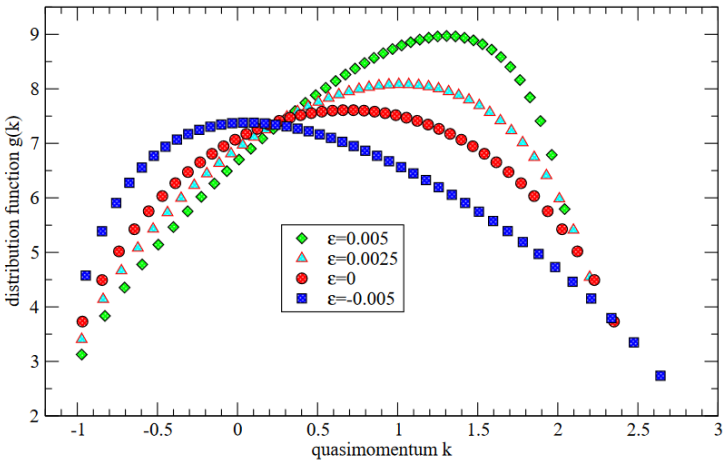

Figure 6.1: *Bethe results from* **Ref**. *[144] showing the deformed distribution function $g(k)$ defined in* **Eq**. *(6.49), for different values of the current-density coupling. The parameters used here are $\theta = 0$, $c = 0.04$ with a system size of $l = 2$ and $N = 45$ particles, which corresponds to the weakly coupled limit of* **Eq**. *(6.42). This result has to be contrasted with the semi-circle law valid for $\rho(k)$ in the weakly coupled Lieb-Liniger model, i.e. $\rho(k) \approx (1-k^2/Q^2)^{1/2}$, that is symmetric with respect to k [70, 71].*

More important is the effect of the nonlinear dispersion on the momentum distribution of the Bethe roots as defined in **Eq**. (6.49). Namely, it induces an asymmetry of the density with respect to the roots, which leads in the weak-coupling regime to a deviation from the semi-circle law [144], see **Fig**. (6.1). This nonlinear dispersion alters thereby the scattering phase by individual pairwise collisions and so shifts and deforms the root-density distribution depending on the sign of ϵ [144]. In the strong-coupling regime, the effect of ϵ is strongly suppressed by interactions as can be seen from the quasi-momenta calculated in **Ref**. [144] for odd particle numbers, i.e.

$$\lambda_j = k_j - \nu/l \approx \left[\frac{2\pi n_j}{l}\left(1-\frac{4\pi n_j\epsilon^{'}}{(lc^{'}-\nu\epsilon^{'})^2}\right)+\frac{2\epsilon^{'}N(N^2-1)\pi^2}{3l(lc^{'}-\nu\epsilon^{'})^2}\right]\left(1+\frac{2N}{(lc^{'}-\nu\epsilon^{'})^2}\right)^{-2}, \tag{6.57}$$

$$n_j \in \Big[-(N-1)/2,(N-1)/2\Big],$$

describing small deviations of the Lieb momenta of the Tonks-Girardeau gas. Nevertheless, **Eq**. (6.57) implies that the flat fermion like distribution according to

Eq. (6.49), that arises from such Lieb momenta, inclines with increasing non-linear dispersion in analogy to the weakly coupled regime, see **Fig**. (6.1) [144].

This polarization of the Lieb quasi-momenta by the current-density coupling ϵ allows to explain the origin of the shift of the actual bosonic quasi-momentum distribution n_k rigorously, by inducing the necessary violation of spatial and temporal inversion that leads finally to $n_{-k} \neq n_k$. Hence we can explain this feature of the dilute anyon-Hubbard model with the aid of the analogy to its integrable small θ approximation the BGK model. These statements about the origin of the shifted quasi-momentum distributions of the anyon-Hubbard model will be complemented and stated more precisely beyond a perturbative treatment in θ, by a hydrodynamic approach of the full non-integrable field theory in the upcoming section. Thereby we confirm additionally that current density couplings do not renormalize the energy in the thermodynamic limit, but imply an imbalanced velocity of counter-propagating species relative to the Fermi-momentum, in analogy to the BGK model.

6.5 Harmonic Fluid Approach

For obtaining the low-energy properties of the non-integrable continuum model non-perturbatively, we follow the harmonic fluid approach invented by Haldane in its seminal work [48, 124]. The creation operator is approximated in terms of fluctuations of a bosonic density field $\phi(x)$ and its dual phase field $\Theta(x)$, by using a polar decomposition

$$\rho_B(x) \approx \left[\rho_0 - \frac{1}{\pi}\partial_x\phi(x)\right] \sum_{m=-\infty}^{\infty} e^{2im[\pi\rho_0 x - \phi(x)]}, \tag{6.58}$$

$$\Psi_B^\dagger(x) \approx \sqrt{\rho_0 - \frac{1}{\pi}\partial_x\phi(x)} \sum_{m=-\infty}^{\infty} e^{2im[\pi\rho_0 x - \phi(x)]} e^{-i\Theta(x)}. \tag{6.59}$$

The density and the derivative of the phase field are conjugate operators [42], whereas a peculiar feature of this approach is their duality relation which makes also the derivative of the density conjugate to the phase operator, i.e.

$$[\phi(x), \partial_y\Theta(y)] = [\partial_x\phi(x), \Theta(y)] = i\delta(x-y). \tag{6.60}$$

Furthermore we see, for example in **Eq**. (6.59), that the dual fields are indeed variables of angular character, with the implication that they are defined according to the compactification radii $r, \tilde{r}$

$$\begin{aligned} \phi(x) &\equiv \phi(x) + 2\pi r, \quad r = 1/2, \\ \Theta(x) &\equiv \Theta(x) + 2\pi\tilde{r}, \quad \tilde{r} = 1. \end{aligned} \tag{6.61}$$

As an interesting side remark, in order to show the consistency of $\hat{\Psi}_B^\dagger \hat{\Psi}_B$ defined in **Eq**. (6.59) with the density operator $\rho(x)$ **Eq**. (6.58), one needs to assume the same regularization of a squared delta function used before, i.e $\delta^2 \propto \delta$ [132]. Yet another example of a physically motivated regularization scheme for mathematically ill-defined products of distributions, that is finally equivalent to our lattice regularization and strongly disagrees with the scheme of Shirokov [153–155]. We neglect furthermore higher orders of the density fluctuations in the square root expansion of the field operators, as well as contributions from higher harmonics, which amounts to only considering small density fluctuations and neglecting lattice effects, respectively [61].

Employing subsequently the bosonization dictionary [61], we obtain for the kinetic part

$$\partial_x \Psi_B^\dagger(x) \partial_x \Psi_B(x) \approx \rho_0 (\partial_x \Theta)^2, \tag{6.62}$$

while the interaction terms can be expressed as

$$: \rho_B(x) J_B(x) : \quad \approx -2\rho_0^2 \, \partial_x \Theta + \frac{4\rho_0}{\pi} \partial_x \Theta \partial_x \phi, \tag{6.63}$$

$$: \rho_B^3(x) : \quad \approx -\rho_0^2 \frac{3}{\pi} \partial_x \phi + \rho_0 \frac{3}{\pi^2} (\partial_x \phi)^2, \tag{6.64}$$

$$: \rho_B^2(x) : \quad \approx -\frac{2}{\pi} \rho_0 \partial_x \phi + \frac{1}{\pi^2} (\partial_x \phi)^2. \tag{6.65}$$

Collecting all terms, the low-energy field theory from **Eq**. (6.27) can be expressed in terms of a generalization of the Tomonaga-Luttinger Hamiltonians to parity/ time-reversal symmetry violating Hamiltonians [43]

$$\mathcal{H}_{\text{cont.}} \approx \frac{u}{2\pi} \int dx \left[\frac{1}{K} (\partial_x \phi)^2 + K (\partial_x \Theta)^2 + \Delta \partial_x \phi \partial_x \Theta + \epsilon_J \partial_x \Theta + \epsilon_N \partial_x \phi \right]. \tag{6.66}$$

The Luttinger parameter K and the sound velocity u take the characteristic form of Galilean invariant systems [43]

$$K = = \sqrt{\frac{v_J}{v_N}} = \sqrt{\frac{\pi^2 \rho_0}{V_2(\theta) + 3\rho_0 V_3(\theta)}}, \tag{6.67}$$

$$u = \sqrt{v_J v_N} = 2\pi\rho_0 / K, \tag{6.68}$$

where the current stiffness equals to the Fermi velocity. It should be stressed that in our case the condition $v_J = \pi\rho_0 = v_F$ expresses only some kind of balance between the systems parameters, which is not sufficient to guarantee Galilean invariance on the operator level. In such parity breaking Luttinger liquids as in **Eq**. (6.66), Galilean invariance is indeed absent, due to the marginal current-density coupling Δ, which can be checked by inserting the transformation behavior of the fields with respect to such transformations into **Eq**. (6.66). A Galilean boost $\hat{U} = e^{imvx\hat{\rho}(x)/\hbar}$ induces a spatially

dependent gauge phase on the original bosonic operators, i.e.

$$\hat{U}^\dagger \Psi_B(x) \hat{U} = \Psi_B(x) e^{imvx/\hbar}, \tag{6.69}$$

that can be solely translated into a gauge shift of the phase field, as can be seen from **Eq**. (6.59) [168], i.e.

$$\pi \partial_x \Theta(x) \Longrightarrow \pi \partial_x \Theta(x) + mv\hbar. \tag{6.70}$$

The interaction Δ originates solely from the current density coupling $V_J(\theta)$ and is related to the momentum density of the bosonic excitations in **Eq**. (6.35) [61], i.e.

$$\Delta = 8\rho_0 V_J(\theta)/u. \tag{6.71}$$

In analogy to the nonlinear dispersion ϵ in the dynamical behavior of the BGK model in **Eq**. (6.42) that neither changes the groundstate energy and thus the Luttinger K in the thermodynamic limit, the current-density coupling Δ does not renormalize the universal parameters of the Luttinger liquid in **Eq**. (6.67) either. Later on we will see explicitly that this term induces an asymmetry of temporal correlation function only.

The linear gradient terms, that are usually neglected for free Luttinger liquids [33], are scaled by the following constants

$$\epsilon_J = -2\rho_0^2 V_J(\theta), \tag{6.72}$$

$$\epsilon_N = -\frac{\rho}{\pi}\Big(2V_2(\theta) + 3\rho V_3(\theta)\Big), \tag{6.73}$$

and lead to gauge shifts of the density $\phi(x)$ and phase field $\Theta(x)$. But in our case especially ϵ_J is important for the description of the shifted quasi-momentum distribution of the low-density anyon-Hubbard model according to **Eq**. (6.53), as it only depends on the current-density coupling $V_J(\theta)$ of the original field theory in **Eq**. (6.27) and furthermore adds a local gauge phase to the $\Theta(x)$ field, i.e. $\Theta(x) \to \Theta(x) + \alpha x$. From **Eq**. (6.59) one can conclude that such local shifts trivially lead to an asymmetry in **Eq**. (6.53), implying the well known quasi-condensation at finite momentum characteristic for the anyon-Hubbard model. Furthermore we see that the functional form of $V_J(\theta)$ perfectly suits to the re-itinerant behavior of the quasi-condensation point for low-enough densities, as we have seen from the Bogoliubov dispersions in chapter (**4**).

6.5.1 Friedel Oscillation

One of the hallmarks of one-dimensional interacting many-body systems, is the presence of characteristic density oscillations in the vicinity of open boundaries, in harmonic traps, or even close to impurities [145, 146, 148, 169]. These so called Friedel oscillations do not

appear in non-interacting bosonic systems, as for example for our low-density anyon theory for a vanishing statistical parameter $\theta \approx 0$. But if the interactions in an arbitrary one-dimensional bosonic system are increasing, the particles behave locally in some sense more and more fermionic, until the hardcore boson limit is reached for infinitely strong interactions *à* la Tonks-Girardeau. As our continuum theory is transmuting the statistics from free bosons to interacting ones, we can use those Friedel oscillations conveniently to determine whether or not our Hamiltonian is strongly interacting for a given statistical parameter or density [30]. Furthermore the non-rescalable two-body interaction $V_2(\theta)$ would imply infinitely strong interactions for any $\theta \neq 0$, if the limit of a vanishing lattice spacing is taken seriously. Nevertheless the principles of renormalization tell us that an effective continuum description might apply already for entities separated from each other by distances much larger than the lattice spacing, which plays also the role of a momentum cut-off. Changing this cut-off further, naturally leads to a stronger renormalization of the coupling constants of the theory as can be formalized by the Lieb constant $\gamma_2 \propto L$ of two-anyon approach of a former chapter. In the following we will numerically illustrate the amplification of interactions in the lattice anyon-Hubbard model **Eq**. (6.2) by the emergence of Friedel oscillations in the dilute regime. The continuum limit is effectively addressed by lowering the lattice density successively, which corresponds formally to an interpolation of a vanishing lattice spacing. Thereby we identify the lattice Hamiltonian for such a low filling fraction with the effective continuum theory derived before **Eq**. (6.27).

As we do not find any evidence for a deviation of Friedel oscillations for the parity-breaking Luttinger liquid **Eq**. (6.66) with the symmetric one, we use the well known formula for ordinary finite-size Luttinger liquids [169]

$$\frac{n_j}{a} \approx \rho_0 + A\cos\left[2\rho_0\pi(ja - l/2)\right]\left(l\sin\frac{\pi ja}{l}\right)^{-K}. \tag{6.74}$$

In **Fig**. (6.2) the Density-Matrix-Renormalization Group calculations for the local particle density of the anyon-Hubbard model $\frac{n_j}{a}$ are compared to the predictions of the ordinary Luttinger liquid, given by **Eq**. (6.74) (solid lines) [170, 171]. Thereby we have used a $DMRG$ code engineered and optimized by Kevin Jägering during his PhD [17, 172]. In the numerical investigation a maximal local occupancy of two particles per lattice site were assumed, as well as up to 500 states in the cut-off procedure. Especially the artificial onsite constraint can lead to deviations for very small statistical parameters θ, related to the generic convergence problems of the $DMRG$ method for gapless ground-states with a large local Hilbert space dimension [173].

In **Fig**. (6.2) *a*) the lattice density is kept constant at $\rho = N/L = 1/10$ and the statistical parameter is varied up to the pseudo-fermionic limit. Hence we can conclude that the two-particle interaction $V_2(\theta)$ remains indeed finite for sufficiently small θ, whereas the strong coupling is approached for larger values of the statistical

parameter. The relatively quick onset of strong oscillations is in perfect agreement with the continuum limit of the Bose-Hubbard model with a Lieb constant of $\gamma_{\mathrm{BH}} = U/\rho$ [130], that formally diverges with a vanishing lattice density $\rho = N/L$ as long as the onsite interaction U is not extremely small. This reflects the general absence of an adiabatic connection between interacting and free bosons in the Lieb-Liniger model and is yet another example of a renormalization of coupling constants with increasing cut-off, i.e. $\gamma_{\mathrm{BH}} \propto L$. Besides the good agreement of the analytics sufficiently far away from the boundaries with the numerical data, one sees how the strong-coupling is quickly approached by statistical transmutations. The appearance of large oscillations signals the onset of the strong coupling regime which is formalized by means of the Luttinger parameter in the inset in **Fig**. (6.2) *a*). The Friedel oscillation for ideal fermions in a one dimensional lattice with open boundaries can be obtained by summing over doubly occupied standing waves [169]

$$\begin{aligned} n_j =& \frac{4}{L+1} \sum_{n=1}^{N/2} \sin\Big(\frac{n\pi}{L+1} x\Big) \\ =& \rho_0 - \frac{\sin(2k_F x)}{(L+1)\sin(\frac{\pi x}{L+1})}, \end{aligned} \tag{6.75}$$

corresponding to the red solid line describing pseudo-fermions in **Fig**. (6.2) *a*), that is valid also close to the boundary. Hence we can conclude that pseudo-fermions and fermions are equal for sufficiently small densities, for this of numerical parametrization [30, 33].

In **Fig**. (6.2) *b*) the statistical parameter is fixed at a given value of $\theta = \pi/2$, whereas the particle number N is subsequently lowered in order to approach the dilute regime and therefore the strong coupling limit. Here the gradual increase of oscillations by lowering the density with otherwise fixed parameters shows how the continuum is effectively reached for the lattice Hamiltonian and is completely coherent with the low-density strong-coupling anomaly of quantum systems in one spatial dimension. This circumstance is again formalized by the inset in **Fig**. (6.2) *b*), which shows the interpolation of the Luttinger parameter for vanishing particles numbers. Both numerical results show how to approach the strong-coupling limit in the already dilute anyon-Hubbard model, namely by fixing an already small density and tuning the statistical parameter to the pseudo-fermionic limit or by fixing a relatively small statistical parameter and lower the density. More importantly, the numerical results illustrate that the effective two-particle interaction potential of the continuum theory $V_2(\theta)$ is indeed renormalized by the inverse density but generally remains finite and approaches the Tonks limit as a function of θ.

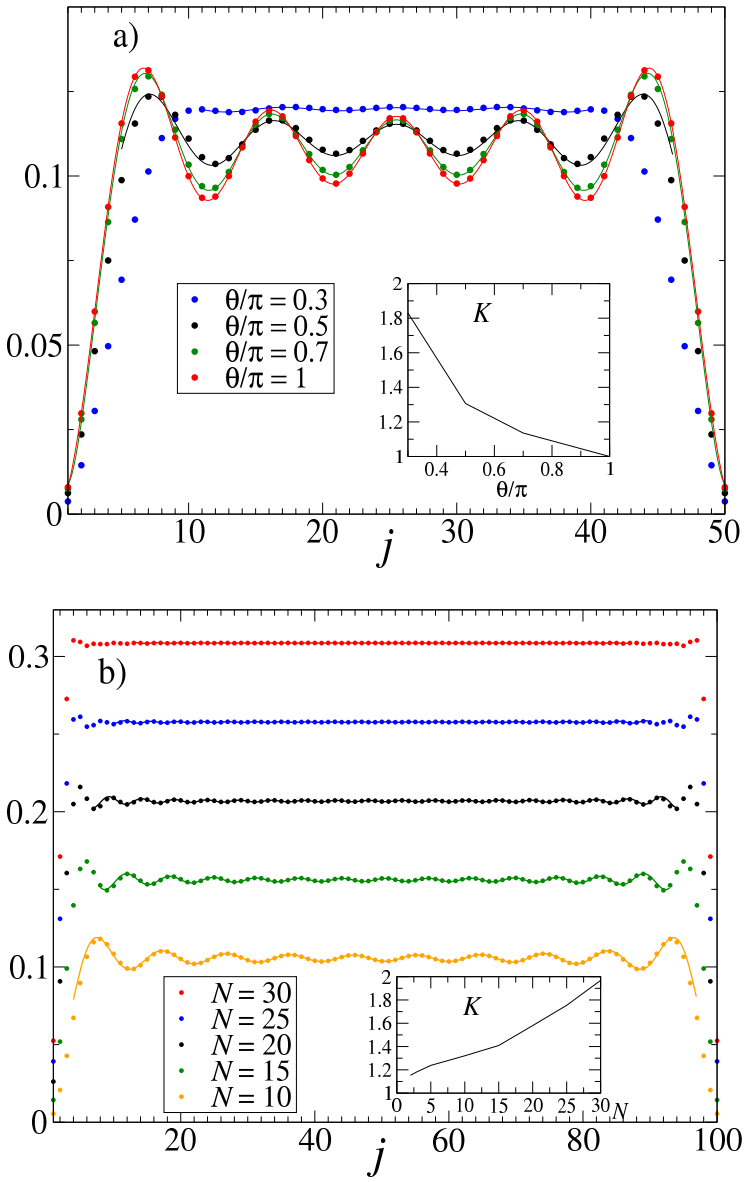

Figure 6.2: *DMRG results for the local particle density n_j/a. a For a chain of $L = 50$ sites with 5 anyons with different θ. b For $\theta = 0.5\pi$ and a chain length $L = 100$ the Friedel oscillations increase with decreasing particle number N. Solid lines are fits to power-law decaying oscillations in* **Eq**. *(6.74). Insets: Luttinger Exponents K from the fits. [26]*

6.5.2 Mode Expansion for twisted Boundary Conditions

For anyonic particles that are defined on a circle, one needs to consider twisted periodic boundary conditions for the bosonic fields, due to counting ambiguities of the Jordan-Wigner string at the boundary [7]

$$\Psi_B(l) = \Psi_B(0)e^{i\theta N}. \tag{6.76}$$

Mathematically this twisted boundary condition is the real topological signature of these anyons, that can only host non-trivial configuration spaces on a one-dimensional circle and thus lead to bosons with topologically non-trivial boundaries [174, 175]. In the Luttinger liquid framework this boundary twist can be easily included by shifting the total current $\hat{J}$ accordingly [61].

$$\delta\hat{J} + \frac{\theta\langle\hat{N}\rangle}{\pi} = J. \tag{6.77}$$

For bosonic systems the topological selection rules related to periodic boundary conditions, imply the evenness of the current zero mode, i.e.

$$(-1)^{\hat{J}} = 1, \quad J = 2j, \tag{6.78}$$

but leave the number zero mode $\hat{N}$ unrestricted, i.e. to odd or even integers, in contrast to fermions [48]. Besides the redefinition of the zero modes the form of the mode decomposition is equivalent to the periodic case

$$\phi(x) = \phi_0 - \frac{\pi\delta\hat{N}x}{l} - \frac{i}{2}\sum_{q\neq 0}\sqrt{\frac{2\pi K}{l|q|}}\frac{q}{|q|}e^{-iqx}\left[\beta_q^\dagger + \beta_{-q}\right], \tag{6.79}$$

$$\Theta(x) = \Theta_0 + \frac{\pi\delta\hat{J}x}{l} + \frac{i}{2}\sum_{q\neq 0}\sqrt{\frac{2\pi}{Kl|q|}}e^{-iqx}\left[\beta_q^\dagger - \beta_{-q}\right], \tag{6.80}$$

where $\beta_q^\dagger$ creates a collective wave with wave-vector $q = \frac{2\pi m}{l}$. The conserved current $\hat{J}$ and particle number $\hat{N}$ can be interpreted as action-angle variables dual to $\hat{\phi}_0, \hat{\Theta}_0$, which are used to discretely label the topological excitations of the system, depending on the type of boundary condition. Those action angle variable incorporate the fact, that the $U(1)$ symmetry of ordinary particle number conservation of **Eq**. (6.27) is additionally enriched to two independent $U(1)_L \bigotimes U(1)_R$ symmetries for the left and right movers separately.

Insertion of the mode decomposition into the Tomonaga-Luttinger liquid in **Eq**. (6.66) leads then to the modified diagonal form

$$\begin{aligned}\mathcal{H}_{\text{cont.}} \approx &\sum_{q\neq 0}\left[u + \Delta sgn(q)/2\right]|q|\beta_q^\dagger\beta_q \\ &+ \frac{\pi^2}{l}\delta\hat{J}\Big(\frac{v_J}{2\pi}\delta\hat{J} + \frac{l}{\pi}\epsilon_J\Big) + \frac{\pi^2}{l}\delta\hat{N}\Big(\frac{v_N}{2\pi}\delta\hat{N} + \frac{l}{\pi}\epsilon_N\Big) + \frac{\Delta}{l}\delta\hat{J}\delta\hat{N}.\end{aligned} \tag{6.81}$$

There are multiple modifications of **Eq**. (6.81) with respect to an ordinary Luttinger liquid. For example, the velocity of finite momentum components is shifted by the current-density interaction Δ, implying an imbalance between the left and right movers, in analogy to the drift in the Bethe roots caused by the non-linear dispersion in the BGK

model, see **Fig**. (6.1). This violation of left/right-symmetry of the finite momentum components, that represent the excitations above the groundstate with energy

$$E_{n_q} = [u + \Delta sgn(q)/2]\,|q| n_q; \quad n_q \in \mathbb{N}, \tag{6.82}$$

leads to a modification of temporal correlators but does not alter static correlation functions of the fluid at zero temperature. This can be seen already by means of the corresponding time-dependent mode decomposition

$$\begin{aligned}\phi(x,t) &= \phi_0(t) - \frac{\pi\delta\hat{N}x}{l} \\ &\quad - \frac{i}{2}\sum_{q\neq 0}\sqrt{\frac{2\pi K}{l|q|}}\frac{q}{|q|}e^{-iqx}\left[\beta_q^\dagger e^{-i|q|\left(u+\frac{\Delta}{2}\mathrm{sgn}(q)\right)\frac{t}{\hbar}} + \beta_{-q}e^{i|q|\left(u-\frac{\Delta}{2}\mathrm{sgn}(q)\right)\frac{t}{\hbar}}\right], \\ \phi_0(t) &= \phi_0 - \left[\frac{\pi v_J}{l}\delta\hat{J} + \frac{\Delta}{l}\delta\hat{N} + \epsilon_J/2\right]t,\end{aligned} \tag{6.83}$$

$$\begin{aligned}\Theta(x,t) &= \Theta_0(t) + \frac{\pi\delta\hat{J}x}{l} \\ &\quad + \frac{i}{2}\sum_{q\neq 0}\sqrt{\frac{2\pi}{Kl|q|}}e^{-iqx}\left[\beta_q^\dagger e^{-i|q|\left(u+\frac{\Delta}{2}\mathrm{sgn}(q)\right)\frac{t}{\hbar}} - \beta_{-q}e^{i|q|\left(u-\frac{\Delta}{2}\mathrm{sgn}(q)\right)\frac{t}{\hbar}}\right], \\ \Theta_0(t) &= \Theta_0 - \left[\frac{\pi v_N}{l}\delta\hat{N} + \frac{\Delta}{l}\delta\hat{J} - \epsilon_N/2\right]t,\end{aligned} \tag{6.84}$$

that additionally show an effective re-definition of the current and charge zero-modes due to the presence of the current-density coupling as well as the chemical potentials ϵ_N, ϵ_J. Following the original arguments of Haldane [48], we can conclude from **Eqs**. (6.83) and (6.84) that this temporal change of the zero modes leads to a variation of the mean current ($\propto \partial_t\phi_0(t)$), as well as the global phase ($\propto \partial_t\Theta_0(t)$) of the fluid.

For finite systems, the parity inversion $\mathcal{I}$ reverses and shifts the density field $\phi(x,t)$, but leaves the phase field $\Theta(x,t)$ invariant, as can be seen from **Eqs**. (6.58) and (6.59), i.e.

$$\begin{aligned}\phi(l-x,t) &= -\phi(x,t) + \pi\rho l, \\ \Theta(l-x,t) &= \Theta(x,t).\end{aligned} \tag{6.85}$$

From **Eqs**. (6.83) and (6.84) it follows that this transformation has the following impact on the constituents of the collective fields [176],

$$\begin{aligned}
&\mathcal{I}^{\dagger}\delta\hat{J}\mathcal{I} = -\delta\hat{J},\\
&\mathcal{I}^{\dagger}\hat{\phi}_0\mathcal{I} = -\hat{\phi}_0 + \pi\rho_0 l + \pi\delta\hat{N} + 2t\left(\frac{\Delta}{l} + \epsilon_J/2\right),\\
&\mathcal{I}^{\dagger}\hat{\Theta}_0\mathcal{I} = \hat{\Theta}_0 - \frac{2\Delta t}{l}\delta\hat{J} - \pi\delta\hat{J},\\
&\mathcal{I}^{\dagger}\hat{\beta}^{\dagger}_{-q}\mathcal{I} = \hat{\beta}^{\dagger}_{q}e^{-i\Delta qt},\\
&\mathcal{I}^{\dagger}\hat{\beta}_{q}\mathcal{I} = \hat{\beta}_{-q}e^{-i\Delta qt},
\end{aligned} \tag{6.86}$$

while the sign of the momentum q needs to be reversed in addition. **Eq**. (6.86) inherits the phase shift of the mode Hamiltonians eigenstates with respect to parity transformations, i.e. via $\hat{\phi}_0$ and $\hat{\Theta}_0$, and the inversion of the current zero mode $\delta\hat{J}$. It implies furthermore that the left movers are transformed into the right movers with an additional temporal phase shift depending explicitly on the current density coupling Δ. In a similar fashion, the impact of time reversal transformation $\mathcal{T}$ on the collective fields[3], i.e.

$$\begin{aligned}
&\phi(x,-t)^{*} = \phi(x,t),\\
&\\
&\Theta(x,-t)^{*} = -\Theta(x,t),
\end{aligned} \tag{6.87}$$

reverses q and yields the corresponding transformation laws om their constituents, fully analogous to **Eq**. (6.86),

$$\begin{aligned}
&\mathcal{T}^{\dagger}\delta\hat{J}\mathcal{T} = -\delta\hat{J},\\
&\mathcal{T}^{\dagger}\hat{\phi}_0\mathcal{T} = \hat{\phi}_0 - 2t\left(\frac{\Delta}{l} + \epsilon_J/2\right),\\
&\mathcal{T}^{\dagger}\hat{\Theta}_0\mathcal{T} = -\hat{\Theta}_0 + \frac{2\Delta t}{l}\delta\hat{J},\\
&\mathcal{T}^{\dagger}\hat{\beta}^{\dagger}_{-q}\mathcal{T} = \hat{\beta}^{\dagger}_{q}e^{-i\Delta qt},\\
&\mathcal{T}^{\dagger}\hat{\beta}_{q}\mathcal{T} = \hat{\beta}_{-q}e^{-i\Delta qt}.
\end{aligned} \tag{6.88}$$

From **Eqs**. (6.86) and (6.88) we see that the mode Hamiltonian in **Eq**. (6.81) breaks both the $\mathcal{I}$ and $\mathcal{T}$ symmetries individually, on the level of its finite mode components $\hat{\beta}_q$, as well as due to the linear dependency on the current zero mode $\delta\hat{J}$. The combination of both leaves **Eq**. (6.81) invariant in accordance with the original continuum model, but induces a phase shift of its eigenstates mediated by $\hat{\phi}_0$ and $\hat{\Theta}_0$.
We can conclude that the bi-quadratic terms in **Eq**. (6.66) incorporate the space-time

[3]In the following equation " $*$ " denotes complex conjugation, arising due to the circumstance that time reversal is represented by an anti-unitary operator.

asymmetry that is superimposed by the anyonic commutation relations. Here the transformation behavior in **Eq**. (6.81) is equivalent to **Eq**. (6.27) in the sense that parity $\mathcal{I}$ or time-reversal $\mathcal{T}$ are not symmetries individually, but the combined operation leaves the Luttinger liquid invariant. The reversal of the probability current with respect to $\mathcal{I}$ and $\mathcal{T}$ but the invariance under $\mathcal{IT}$, reflects the fact that the possible conventions for $1d$ exchange phases $e^{\pm i\theta \mathrm{sgn}(x-y)}$ are naturally invariant under the combined symmetry operations [18].

The zero-mode part of the Hamiltonian **Eq**. (6.81) is non-trivially altered by Δ, which can be seen in the coupling of the current and density zero mode, that is the zero mode part of the fluids momentum density in **Eq**. (6.35) [124]. If there are no particle number fluctuations in the groundstate, i.e. $\langle \delta\hat{N} \rangle = 0$, we find that the zero-mode Hamiltonian is minimized according to the energy

$$E_0 \overbrace{=}^{\langle \delta\hat{N} \rangle = 0} -\frac{l(u\epsilon_J)^2}{8\pi v_J}, \tag{6.89}$$

with a corresponding integer-valued current

$$[J_{\min}] \overbrace{=}^{\langle \delta\hat{N} \rangle = 0} \frac{\theta N}{\pi} - \frac{u\epsilon_J l}{2\pi v_J}, \tag{6.90}$$

where $[x]$ denotes the nearest integer to the *r.h.s.* of **Eq**. (6.90), compatible with the bosonic selection rule in **Eq**. (6.78) [48, 61]. From **Eqs**. (6.89) and (6.90) we see that the ground-state energy contains the chemical potential of phase excitations ϵ_J which creates a current that is additionally shifted by the boundary phase. For a given excitation $k \in \mathbb{Z}$ i.e. $\langle \delta\hat{N} \rangle = k$, the energy and the current are further amplified by the current-density coupling Δ as well as the number stiffness v_N and the chemical potential ϵ_N,

$$\begin{aligned} E_0 &\overbrace{=}^{\langle \delta\hat{N} \rangle = k} \frac{\pi v_N k^2}{2l} - \frac{u\epsilon_N k}{2} - \frac{l}{2\pi v_J}\left(\frac{\Delta k}{l} + \frac{u\epsilon_J}{2}\right)^2, \\ [J_{\text{min.}}] &\overbrace{=}^{\langle \delta\hat{N} \rangle = k} \frac{\theta N_0}{\pi} - \frac{l}{2\pi}\frac{\epsilon_J}{v_J} - \frac{\Delta}{\pi v_J}k. \end{aligned} \tag{6.91}$$

The experimental observation of such characteristic currents could be used to probe the existence of our one-dimensional anyons, but remains a formidable task as one cannot easily separate the zero-modes from the finite momentum components [62, 177–181]. In general we cannot control the fluctuations of $\delta\hat{N}$ or $\delta\hat{J}$ precisely, thus the zero-mode part of the Hamiltonian in **Eq**. (6.81) can be non-diagonal in principle. Therefore the Hamiltonian needs to be rotated by a modular transformation that maps a discrete grid

onto another grid [182], i.e.

$$\begin{bmatrix} a & b \\ c & d \end{bmatrix} \begin{bmatrix} \hat{J} \\ \hat{N} \end{bmatrix} = \begin{bmatrix} \hat{\tilde{J}} \\ \hat{\tilde{N}} \end{bmatrix}, \qquad ad - bc = 1; a, b, c, d \in \mathbb{Z}. \tag{6.92}$$

Eq. (6.92) shows that the zero-mode part of **Eq**. (6.81) is not diagonalizable in general, as the diagonalizing transformation would depend on continuous parameters, i.e. $v_{J,N}$, $\epsilon_{J,N}$ and Δ, but can only host integer solutions due to the selection rule in **Eq**. (6.78) and the integer value of $\hat{N}$. If such a modular transformation exists on the other hand for specific parameter values, then the eigenstates of **Eq**. (6.81) can be expressed via the time evolved modes $\hat{\beta}_q^\dagger(t)$ and the transformed set of temporally dependent zero modes $\tilde{\phi}_0(t)$, $\tilde{\Theta}_0(t)$, i.e.

$$|\tilde{j}, \tilde{n}, n_q, n_{-q}\rangle \propto e^{i\tilde{j}\tilde{\phi}_0} e^{i\tilde{n}\tilde{\Theta}_0} \prod_{q>0} \left(\hat{\beta}_q^{\cdot\dagger}(t)\right)^{n_q} \left(\hat{\beta}_{-q}^{\cdot\dagger}(t)\right)^{n_{-q}} |0,0,0,0\rangle \,. \tag{6.93}$$

In **Eq**. (6.93) the integers $\tilde{j}$ and $\tilde{n}$ denote the eigenvalues of $\tilde{N}$,$\tilde{J}$, and the proportionality sign indicates a, temporal and quantum number dependent, phase factor.

This finding is in stark contrast to finite, parity invariant Luttinger liquids that always have integrable/diagonal zero-modes. This imbalance in the zero modes implies that the topological excitations are coupled. Current excitations relative to the boundary twist depend on the particle number fluctuation relative to the ground-state and conversely any fluctuation in N relative to N_0 is dependent on the value of $\delta\hat{J}$. Hence we conclude that the real topological feature of such anyons is encoded first of all in non-trivial boundary conditions for the respective bosonic degrees of freedom and so in the zero mode structure of the underlying conformal field theory. Finally, such characteristic currents originating from the in general non-separable zero modes, could be hypothetically used to experimentally probe the fractional statistics in the anyon-Hubbard model, as well as other models of parity breaking Luttinger liquids.

Another interesting quantity that is related to the ground-state energy and is affected by statistical transmutations, is the inverse of the macroscopic compressability [43], i.e.

$$\begin{aligned} \kappa^{-1} =& \rho_0^2 l \left[\left(\frac{\partial}{\partial N} \right)^2 E_0(N) \right]_{N=N_0} \\ =& \rho_0^2 \pi v_N = \rho_0^2 \pi \left[V_2(\theta) + 3\rho V_3(\theta) \right]. \end{aligned} \tag{6.94}$$

Eq. (6.94) formalizes the fact that a non-interacting system is infinitely compressible as the energy cost of adding a particle in the ground state vanishes, whereas strong repulsive interactions create such energy gaps that make the fluid less and less compressible [52]. The premise of non-negativity of the compressabillity κ is furthermore related to

thermodynamic stability of the Luttinger liquid and translates into the non-negativity of the density stiffness v_N [137]. From **Eq**. (6.94) we see, that $V_2(\theta)$ is always dominant compared to $3\rho_0 V_3(\theta)$ for sufficiently low-densities. Anyhow the three-body interaction $V_3(\theta)$ becomes attractive for certain values of the statistical parameter and is able to overpower $V_2(\theta)$ if the density rises sufficiently strong. From this we can deduce that in order to properly describe three-body interactions on the level of Luttinger liquids for large densities, one needs to go beyond the weak-coupling analysis used here for low densities. Thus a different bosonization scheme is needed to project the high-density anyon-Hubbard model to a low-energy effective field-theory as in **Eq**. (6.66) and a new set of universal constants that faithfully describe the weak coupling sector [61].

6.5.3 Density-Density Correlation Function

In order to reveal anyonic signatures in the Luttinger liquid theory, we exemplary calculate a time-dependent correlation function for twisted boundary conditions, the density-density correlator related to the dynamical structure factor in Bragg-scattering experiments. For the density-density correlation function we have to evaluate the following expectation values to lowest order,

$$\langle\hat{\rho}(x,t)\hat{\rho}(0,0)\rangle \approx \frac{1}{\pi^2}\langle\partial_x\phi(x,t)\partial_x\phi(0,0)\rangle + \rho^2\sum_{m,\tilde{m}\in\mathbb{Z}}\alpha_m\alpha_{\tilde{m}}e^{2im\pi\rho x}\langle e^{-2im\phi(x,t)}e^{2i\tilde{m}\phi(0,0)}\rangle, \tag{6.95}$$

here the first part in **Eq**. (6.95) corresponds to the long-wavelength part fluctuations whereas the second one includes higher-order harmonics. In order to calculate the expectation values in **Eq**. (6.95), one has to insert the mode decomposition **Eq**. (6.83) of the density field and subsequently normal order the bosonic modes, i.e.

$$\begin{aligned}\langle\rho_B(x,t)\rho_B(0,0)\rangle &= \rho_0^2 - \frac{K}{2(\pi)^2}\left[\frac{1}{d\left(x-u\left(1-\Delta/2\right)t|l\right)^2} + \frac{1}{d(x+u\left(1+\Delta/2\right)t|l)^2}\right] \\ &+ \rho_0^2\sum_{m\neq 0}\alpha_m\frac{\delta_m(x,t)e^{2\pi im\rho_0 x}}{\Big(\rho_0 d(x-u[1-\Delta/2]t|l)d(x+u[1+\Delta/2]t|l)\Big)^{m^2K}}.\end{aligned} \tag{6.96}$$

$$\alpha_m = (b)^{-4m^2K}, \qquad d(x|l) = l|\sin(\pi x/l)|/\pi \tag{6.97}$$

$$\begin{aligned}\delta_m(x,t) = e^{i\frac{2\pi v_J}{l}m^2t}e^{2im\left[\left(\frac{\pi v_J}{l}\langle\delta\hat{J}\rangle+\frac{\Delta}{l}\langle\delta\hat{N}\rangle+\epsilon_J/2\right)t+\frac{\pi x}{l}\langle\delta\hat{N}\rangle\right]} \\ e^{i\frac{2\pi u}{l}m^2t}e^{i\frac{\pi m^2}{2}[\mathrm{sgn}(x+(u+\Delta/2)t)-\mathrm{sgn}(x-(u-\Delta/2)t)]}.\end{aligned}$$

A few preliminary comments are helpful to understand **Eq**. (6.96), for example the meaning of the constants in **Eq**. (6.97). The constant b that appears in the prefactor α_m

originates from adding an exponential cut-off $e^{-b|q|/2}$ to the mode decomposition of the density field **Eq**. (6.83), in order to regularize potentially appearing infinities. This cutoff b effectively sets the bandwidth of the Luttinger theory by restricting its momentum support and thus its minimal spatial resolution. As this cutoff generically varies from the strong to the weak-coupling regime and might depend on the short-range structure of the model, it introduces a non-universal feature into the otherwise universal decay of one-dimensional correlation functions of the form of **Eq**. (6.96), as it is explained later in more detail. The time-dependent phase factor $\delta_m(x,t)$ on the other hand inherits finite-size phase shifts due to zero mode contributions, that lead finally to energy shifts in the dynamical structure factor after Fourier transformation to the frequency domain. Analogously the spatially dependent phase shift leads to a momentum shift after Fourier transformation. Furthermore it includes additional phase shifts depending on the sign of the deformed light-cone coordinates, that arise from the disentangling of vertex operators with the Baker-Campbell-Haussdorf formula in the second part of **Eq**. (6.95) and have to be considered if one is interested in the dynamical structure factor. Leaving out such finite-size details for a moment, **Eq**. (6.96) describes in the limit of $l \to \infty$, the inhomogeneous decay of the density-density fluctuation relative to the mean-value ρ_0 in direction of the Δ-deformed light-cones, as the chord function reduces then to a power-law $d(x|l) \to |x|$. This decay is thereby spatially modulated with the lattice harmonics $e^{2\pi i m \rho_0 x}$, that become less and less relevant for $|m| \gg 1$ and resemble the $\pm 2k_F, \pm 4k_F ...$ oscillations in a one-dimensional fermionic system. The major anyonic signature in the density correlator **Eq**. (6.96) is the inhomogeneity in the light-cone coordinates caused by the presence of the current-density coupling Δ, manifesting the anyonic symmetry violations.

6.5.4 Remark on Cut-offs, Prefactors and Luttinger Parameters

One of the core principles of Haldanes harmonic fluid treatment is that it does provide the universal description of long-range correlation functions, for one-dimensional gapless quantum fluids beyond the Luttinger paradigm [48, 183]. On the other hand it contains non-universal quantities that are dependent on the cut-off, that restricts the momentum support of modes, and the explicit regularization scheme [61]. Non-universal behavior is then expressed by dependencies on the details of the model, such as the short-range structure of correlations [131]. Thus information about these cut-offs and prefactors can, by definition, not be obtained by the bosonization itself and numerical methods or analytical approximations have to be applied.

A remarkable exception to that are the Bethe integrable models, whose excitation structure close to the Fermi-points allows sometimes for an analytical evaluation of the long-range asymptotics of correlation functions, which can then be compared to the results of the harmonic fluid approach as they are structurally equivalent [115].

Also the Luttinger parameters, whether in the strong or weak coupling regime, can be estimated as the ground-state energy per particle is known to arbitrary precision. But, analytically one is always bounded to perturbative expansions whereas results valid in the intermediate interacting regime can only be obtained numerically [70, 71]. For example, **Eq**. (6.47) and **Eq**. (6.48), as well as **Eq**. (5.26) in Chapter **5**., are obtained in such a way and provide estimates of the Luttinger parameter of the dilute anyon-Hubbard model that complement the weak-coupling result of **Eq**. (6.67), with respect to their respective premises. The cut-off q_c, restricting the momentum support of the excitations in the harmonic-fluid treatment, is analogous to the maximally allowed momenta $|Q|$ in such Bethe solvable models, see **Eq**. (6.52). Hence we can conclude, as long as the anyon-Hubbard model is faithfully represented by one of the Bethe integrable models, that also their momentum cut-off can be used for the correlation functions, i.e. $q_c = Q$. This quantity can be analytically estimated in analogy to the healing length ξ of the Bogoliubov chapter [61], by setting the energy of the excitations equal to their chemical potential μ

$$\hbar u q_c = \mu. \tag{6.98}$$

Eq. (6.98) yields then the critical momenta q_c via the identification of μ with the healing length characteristic for Lieb-Liniger type of models, i.e. $\mu \propto \xi^{-2}$, ranging from weak couplings $q_c = (\gamma/\cos(\theta/2)^{1/2}\rho_0$ to the Tonks regime $q_c = k_F$ [61]. Nevertheless this equivalence is very restricted to low-densities as well as small statistical parameters, so what to do outside of that parameter range?

Numerically this does not pose any problems as very strong and accurate techniques are available as the *DMRG* algorithm [173], but analytically no routine exists to obtain them and results are very rare [61, 131, 132]. The perturbative strong-coupling result of Cazalilla for the Bose-Hubbard model [130, 131], was applied in Chapter **5**. to the anyon-Hubbard model, yielding the estimates of the Luttinger parameters for half-filling and strong onsite interactions of **Eq**. (5.50), where the momentum cut-off should be chosen sufficiently close to $k_F = \pi/2$. The one-dimensional scattering length of the Bose-Hubbard was used by Affleck to estimate the Luttinger parameters in the strong-coupling regime [132], where the same technique was pursued in chapter (**5**.) by means of an anyonic scattering ansatz. In analogy to the results of Affleck, **Eq**. (5.26) and **Eq**. (5.27) provide the Luttinger parameters for all values of the statistical parameter but valid only for very small densities. Also here the implied restriction to the strong coupling regime suggests that a momentum cut-off should be chosen close to the Tonks limit.

Leaving again the range of validity of these two approaches, one could at least estimate the momentum cut-off by the inverse healing length obtained in chapter (**4**.) by the Bogoliubov approximation for weak statistical interactions, i.e. $q_c \propto \xi^{-1}$ in **Eq**. (4.31).

Quite remarkably the Bogoliubov result for small condensate densities n_0 corresponds to the choice $q_c \propto \sqrt{V_2(\theta)}$, if the condensate density n_0 is identified with an inverse length scale a^{-1}. The raison d'être of this statement is conjectured in analogy to the Lieb-Liniger gas, where a short-distance cut-off in terms of the Bogoliubov healing length, i.e. $b \propto \xi$, can be used to recover almost exactly the Bethe results of Popov for the one-particle density matrix in weak-coupling regime [61, 184].

6.6 Conclusion

In order to conclude this chapter of the thesis, it is helpful to remind ourselves that in the realm of one-dimensional anyons there existed various partially disjoint definitions of the fundamental entities. Three prevalent ones that are used in the physicist community are those directly defined in the continuum *à* la Leinaas-Myrheim or Kundu [4, 7], and more or less recently anyons defined on a lattice *à* la anyon-Hubbard [13]. All three concepts have some features in common, characteristic to one dimension, as for example the necessity of disorder operators of the Jordan-Wigner type to represent such particles via canonical bosons [8, 175]. The formal exchange of these $1d$ anyons is incorporated into effective interactions of their canonical parent particles, as can be seen from **Eq**. (6.27) for the dilute anyon-Hubbard model, from **Eq**. (6.41) for Kundu anyons and via the second quantized form of the Leinaas-Myrheim anyons the Lieb-Liniger model [5]. A further important similarity is the seemingly improper transmutation between canonical bosons and fermions, as can be seen on hand of the deformed commutation relations in **Eq**. (6.7), which can only algebraically transmute to pseudo-fermions for the Kundu or anyon-Hubbard type models, as well as the Tonks-Girardeau limit of the Lieb-Liniger model in terms of Leinaas-Myrheim anyons [5]. Nevertheless a clear connection between the three types was never deeply investigated, except for a side remark in the original work of Kundu that shows that his anyons are actually Leinaas-Myrheim anyons obeying special boundary conditions and a reparametrization of the statistical parameter [7]. In subsequent investigations of the lattice anyons, a straight-forward lattice continuum correspondence of the anyon-Hubbard model and the Kundu anyons was conjectured, potentially prematurely concluded by a naive notion of anyonic continuum limits [21, 88]. The refined continuum procedure of the anyon-Hubbard model pursued in this chapter, is capable of resolving such technical issues on a more rigorous footing and thus classifies the three seemingly disjoint concepts of one-dimensional anyons.

Thereby we find that the lattice version **Eq**. (6.2) or its effective model **Eq**. (6.27) are by far more versatile in phenomenology compared to their continuum pendants, being themselves statistical parameter dependent deformation of the original Kundu model and its variants and thus also to Leinaas-Myrheim. The original Kundu model suffered from ill-defined interactions, when expressed in terms of bosons, that were harshly criticized by various authors [12, 115]. Kundu elegantly bypassed this subtle issue by

the application of the Jordan-Wigner gauge transformation, but from an experimental point of view this is rather unsatisfactory as one has to implement the actual bosons with highly singular interactions. By the detour over the optical lattice such issues do not appear as the lattice spacing a serves as an ultraviolet cut-off that naturally regularizes highly singular interactions, whereby we can physically prove that assumption by comparing two kinds of continuum limits starting from **Eq**. (6.14) and **Eq**. (6.21) whose only difference relies in normal ordering in the lattice or in the continuum. The renormalization of effective interaction while approaching the continuum is furthermore illustrated by increasing Friedel oscillations of the anyon-Hubbard model, see **Fig**. (6.2). Furthermore, we can relate the dilute anyon-Hubbard model explicitly to the integrable Kundu model and its variants for small statistical angles. Therefore we can explain some characteristic properties microscopically on hand of the Bethe solutions, as we can estimate non-universal parameters, groundstate energies and the effect of the current-density coupling on the Bethe roots. As the low-density effective field theory is not solvable for arbitrary θ, we employ the harmonic fluid approach to obtain a special form of a parity-breaking Luttinger liquid. One of its main characteristics is the velocity imbalance of left/right-moving species caused by the current density coupling, which is relevant for the temporal as well as finite temperature behavior of correlation functions [66]. Further features of such parity breaking Luttinger liquids are revealed for twisted (periodic) boundary conditions, namely the non-separability of zero-modes for arbitrary parameters that are deeply related to the properties of conformal field theories, as well as the dependence of the persistent current on the relative particle number fluctuation. For this geometry we calculate the temporal density-density correlation function that contains additional phase shifts by the current zero modes, as well as inhomogeneous decay of correlations dependent on the chirality.

Chapter 7

Bosonization of the extended Anyon-Hubbard Model

Statistical transmutation in one spatial dimension can lead to interesting physical effects, not observable in higher dimension [4, 7, 13, 33]. The change of statistics is thereby mediated by effective interactions that are not achievable by ordinary, local inter-particle potentials, due to their intrinsic momentum dependence that breaks parity as well as temporal inversion. Nevertheless, anyons *à* la Jordan-Wigner are not the only possibility to engineer particle species beyond the canonical choices [8]. The maximal local occupancy of the Jordan-Wigner anyons is a priori set by the choice of their parent particles, as exchange statistics and exclusion principles are disjoint concepts in this case without referring to a specific Hamiltonian that may restrict the occupancy by effective statistical repulsion [8]. Haldane realized that instead of manipulating the non-local commutators of some parent particles, one can change the local ones into a form, such that the allowed single-particle orbitals of the particles are restricted without touching their mutual exchange statistics [8, 14]. In opposition to the former approach this is explicit at the level of the particles algebra, by projecting out higher powers of creation/annihilation operators, and thus does not need to be referred to a specific Hamiltonian. The goal of this chapter is to combine those two approaches to one-dimensional anyons and study the interplay of the induced statistical interactions with ordinary ones [185] [1], on the low-energy phase diagram. This specific choice is especially motivated by the appearance of topologically non-trivial effects for such constrained bosonic systems [186–188], in analogy to the valence-bond solids that appear in integer spin chains [189–191]. These phases may express hidden non-local orders beyond the Landau paradigm, that are not detectable by local order parameters, but are nevertheless protected by certain symmetries [192–194]. Conversely, the question arises in which sense such symmetry-protected topological phases exist also for one-dimensional anyons,

[1] The ordinary inter-particle interactions contain a repulsive/attractive two-body potential and a nearest-neighbor repulsion.

and if they exist, are they stable under statistical transmutation that inherently breaks certain symmetries [185]? The focus here is on an advanced field theoretical treatment of the low-energy properties of the model [51, 187, 195], supporting the phase diagram characteristics obtained by large-scale numerical investigation with physical vividness. The complexity of the problem forces us to use different low-energy representation of the field theory for different statistical parameters, which is numerically confirmed and allows for an optimal choice of a naive field theory prior to any renormalization-group considerations. Thereby, we derive explicitly the symmetry breaking low-energy contributions whose appearance determines the fate of the topological phases [187, 196]. This allows for a detailed comparison of the differences between bosonic/anyonic or spin SPT phases in terms of bare coupling values of the underlying low-energy field theory. Furthermore, by the interplay of large statistical repulsion and strong attractive two-body interactions a so called Dimer phase is formed [33]. Besides classifying this phase theoretically, we find yet another Landau forbidden transition, not related to phenomenology of SPT orders.

7.1 The Extended and Constrained Anyon Hubbard Model

The model that we investigate is the so-called extended anyon-Hubbard model at unit filling [185], in analogy to the bosonic model studied in the literature [186, 187, 197, 198][2] , i.e.

$$\hat{H} = -\sum_{j=1}^{L} \left(\hat{a}_j^\dagger \hat{a}_{j+1} + \text{h.c.} \right) + \frac{U}{2} \sum_{j=1}^{L} \hat{n}_j \left(\hat{n}_j - 1 \right) + V \sum_{j=1}^{L} \hat{n}_j \hat{n}_{j+1}. \tag{7.1}$$

𝔼ıı. (7.1) describes the hopping of anyons on a one-dimensional lattice under the influence of a two-particle interaction scaled by U and a nearest-neighbor potential scaled by V The connectivity of a finite lattice is either open or twisted according to the Jordan-Wigner duality discussed in the introduction [24]. In this part of the thesis, we are mostly interested in the thermodynamic behavior, and thus usually consider an infinite lattice, i.e. $j \in \mathbb{Z}$, which leads additionally to a translationally invariant Hamiltonian. **Eq**. (7.1) breaks bosonic time reversal and inversion symmetry, due to the anyonic statistics, but is invariant with respect to the generalized inversion symmetry found in **Ref**. [185]. Priorly, we have seen that this symmetry corresponds to a parity transformation for the anyonic operators, equipped with a θ-dependent gauge phase for particle-number conserving Hamiltonians [26].

We consider always a positive sign of V, as the sign of experimentally achievable bosonic dipole interaction is necessarily positive [199], but allow for repulsive as well as attractive

[2]The wording "extended" originates from the presence of an additional nearest-neighbor repulsion, with respect to the ordinary Bose-Hubbard model. "Constrained", thereby names the circumstance that we do not consider canonical bosons. but a particular realization of Haldane's exclusion statistics [14].

two-particle interactions. The attentive reader should be immediately concerned about the possible absence of a ground-state for strong attractive interactions, that is known to appear in Bose-Hubbard type models [96]. Nevertheless this scenario is explicitly ruled out as we consider constrained anyons, whose local parent particles are represented by soft-core bosons with only up to two-particles per orbital, i.e. $\hat{b}_j^3 = 0$. This circumstance can be formalized by a second-quantized version of Haldane's approach to fractional exclusion statistics [8, 14], i.e.

$$\begin{aligned} &\left[\hat{b}_i, \hat{b}_j\right] = 0 = \left[\hat{b}_i^\dagger, \hat{b}_j^\dagger\right], \\ &\left[\hat{b}_i, \hat{b}_j^\dagger\right] = \delta_{i,j}\left[1 - \hat{F}_j\right], \quad \hat{F}_j = \frac{3}{2}\hat{n}_j\left(\hat{n}_j - 1\right), \\ &\left[\hat{b}_j^\dagger \hat{b}_j, \hat{b}_i^\dagger\right] = \delta_{i,j}\hat{b}_j^\dagger, \quad \hat{b}_j^\dagger \hat{F}_j = 0, \end{aligned} \tag{7.2}$$

deforming the local canonical commutation relations of the bosons with the projector $\hat{F}_j$. The entities in **Eq**. (7.2) build the set of parent particles that represents the anyons that we consider in **Eq**. (7.1), after the attachment of the Jordan-Wigner string according to the conventions used throughout this thesis. In contrast to the literature, which considers a priori a scenario with canonical bosons and large U such that the constraint $\hat{b}_j^3 = 0$ is effectively obeyed [187, 197], the algebra in **Eq**. (7.2) allows to study different regions of parameter space. This especially allows to study gapless phases of the constrained anyons, expected for small positive or negative U and a vanishing nearest neighbor interactions V, as well as the limit of strong local on-site attraction due to the absence of a wave-function collapse. Furthermore, for comparable energy scales U and V the bosonic version of **Eq**. (7.1) is known to inherit topologically non-trivial phases [185], whose presence and stability is one of the guiding question of this chapter.

7.2 The Relation to the $S = 1$ Heisenberg chain

Similar to the consideration in chapter 1 about the absence of single-particle properties for one-dimensional anyons due to their non-trivial commutators [22], the constrained bosons in **Eq**. (7.2) are also intrinsically interacting and induce a non-linear time evolution on its creation and annihilation operators. On the other hand these particles have therefore the advantage that their Hilbert-space dimension is finite, in contrast to canonical bosons, which generally simplifies numerical implementations, and allows for far-reaching analytical predictions by analogy to well-known spin $S = 1$ Heisenberg-type models and various perturbations of it. Thus in the following subsection the emphasis is on the non-linear representation of our constrained bosons in terms of spin 1 operators [200], and their transformation behavior with respect to the dihedral group [194, 196]. This internal spin symmetry group is crucial for the protection of

topological phases later on, and thus their action on the constrained bosonic operators has to be investigated.

The explicit form of the constrained bosons in terms of spin-1 operators is necessarily non-linear and is given by the following expressions [200]

$$\begin{aligned}\hat{b} &= \frac{1}{\sqrt{2}}\hat{S}^{+}\left(1+(1-\sqrt{2})\hat{S}^{z}\right) = \begin{pmatrix} 0 & 1 & 0 \\ 0 & 0 & \sqrt{2} \\ 0 & 0 & 0 \end{pmatrix}, \\ \hat{n} &= 1-\hat{S}^{z} = \begin{pmatrix} 0 & 0 & 0 \\ 0 & 1 & 0 \\ 0 & 0 & 2 \end{pmatrix},\end{aligned} \tag{7.3}$$

whereas $\left[\hat{S}^{\pm},\hat{S}^{z}\right]$ denotes the $su(2)$ spins in its three-dimensional representation. A major difference between canonical bosons and fermions is the presence of the Pauli principle for the latter, formalized by the local fermionic anti-commutation relations. The consequence is a hardcore condition for the fermions allowing only a single occupied mode, which furthermore allows for canonical particle-hole transformation that relate particles to their own anti-particles, i.e. creation to annihilation operators[3]. Even if the local occupancy of these bosons in **Eq**. (7.2) is a priori restricted, they still do not possess a canonical particle-hole transformation as can be defined for fermions. Nevertheless from **Eq**. (7.3) one can conclude that x,y-rotations around the angle π, i.e.

$$\begin{aligned}&\hat{U}_{x,y}(\pi) = e^{i\pi\hat{S}^{x,y}}, \\ &\hat{U}^{\dagger}_{x,y}(\pi)\hat{S}^{\pm}\hat{U}_{x,y}(\pi) = \pm\hat{S}^{\mp} \\ &\hat{U}^{\dagger}_{x,y}(\pi)\hat{S}^{z}\hat{U}_{x,y}(\pi) = -\hat{S}^{z},\end{aligned} \tag{7.4}$$

[3]In canonical boson systems the mapping $\hat{b}^{\dagger} \leftrightarrow \hat{b}$ is a non-canonical transformation, that does not preserve the algebraic structure and thus does not feature a particle interpretation nor a unitary realization, i.e. $\left[\hat{b},\hat{b}^{\dagger}\right] \rightarrow -\left[\hat{b},\hat{b}^{\dagger}\right]$.

lead to something similar, together with a permutation of the internal states $|0\rangle \leftrightarrow |2\rangle$ in the matrix representation of the constrained bosonic operators, e.g.

$$\hat{U}^{\dagger}_{x,y}(\pi)\hat{b}\hat{U}_{x,y}(\pi) = \pm\sqrt{2}\left[\hat{b}^{\dagger} - \hat{b}^{\dagger}\hat{n}/2\right] = \pm\begin{pmatrix} 0 & 0 & 0 \\ \sqrt{2} & 0 & 0 \\ 0 & 1 & 0 \end{pmatrix},$$
$$\hat{U}^{\dagger}_{x,y}(\pi)\hat{n}\hat{U}_{x,y}(\pi) = 2 - \hat{n} = \begin{pmatrix} 2 & 0 & 0 \\ 0 & 1 & 0 \\ 0 & 0 & 0 \end{pmatrix}. \tag{7.5}$$

Eq. (7.5) can then be understood as a kind of particle-hole transformation that may become an explicit one whenever the spin non-linearity in **Eq**. (7.3) is negligible and the bosons obey an $su(2)$ algebra asymptotically [186, 187][4]. Interestingly, the π-rotations in **Eq**. (7.4) express not only the quasi particle-hole transformation of the constrained bosons, they additionally possess a group structure when applied to the spin operators, i.e.

$$\hat{U}_i(\pi)\hat{U}_j(\pi) = \hat{U}_k(\pi), \quad i \neq j \neq k \in [x, y, z]\,,$$
$$\hat{U}_i(\pi)^2 = 1, \tag{7.6}$$

that is known as the dihedral group D_2. **Eq**. (7.6) is furthermore a natural symmetry of $su(2)$-invariant spin chains in the absence of magnetic fields, irrespective of their representation, that among other symmetries is important for the discussion of bosonic or spin SPT phases later on [187, 196]. In the next section we will review some facts about the so called λ-D-model [190, 191, 195], which corresponds in lowest-order to our model in **Eq**. (7.1), once the spin non-linearity in **Eq**. (7.3) can be neglected, and thus serves as a good starting point to learn about some of the phases in our anyonic model. Later on we will investigate the difference of constrained bosons and spins, by comparing their effective low-energy field theories, which are the relevant forms for discussing the phase-diagram as well as ground-states symmetries [187, 196].

7.3 The λ-D-Model

The properties of spin chains in one dimension with larger spin quantum number, i.e. $S > 1/2$, have been of large interest in the past [201–204]. One of the reason for that is the absence of an exact solution for such XXZ-type of models and their variants, which may lead to rich many-body effects that are not two-body reducible, as well as thermalization

[4]The wording asymptotically is used here in the sense of the low-energy regimes of the models [187].

properties that are otherwise hindered by integrability [205]. Despite the absence of exact solutions for most of such genuine physical spin systems, there exists plenty of strong analytic results as for example the famous Haldane conjecture [201, 206], or the Lieb-Schulz-Mattis theorem [25, 206]. While the latter has the status of a mathematical theorem, stating that the ground-state of half-odd integer spin chains with $U(1)$ and translational invariance, is either gapless or spontaneously breaks translation symmetry in the thermodynamic limit [25]. Haldane used a field-theoretical approach in his seminal work instead [201], showing, in accordance to Lieb, Schulz and Mattis, that the presence of an energy gap in the spectrum of translationally invariant and $U(1)$-symmetric anti-ferromagnets, depends solely on S being integral or half-integral. More precisely, in the integer case there is a parameter range such that the ground-state is unique and gapped, whereas no such range exist in the half-integral case. These results and various generalizations [207, 208] form the backbone of our understanding of the low-energy physics of such models today and will serve us well also for the discussion of our constrained bosonic system later on.
Yet another milestone in this field of research was motivated by the properties of an exactly solvable model proposed by Affleck, Kennedy, Lieb and Tasaki [189], i.e.

$$\hat{H}_{AKLT} = \sum_j \vec{S}_j \cdot \vec{S}_{j+1} + \frac{1}{3}\left(\vec{S}_j \cdot \vec{S}_{j+1}\right)^2, \tag{7.7}$$

the bi-linear, bi-quadratic $S = 1$ chain. The ground-state of **Eq**. (7.7) is the prototype of a valence-bond solid and symmetry-protected topological spin phases in the following sense [189, 192, 194]. Each onsite spin 1 operator can be imagined as being composed of two spin 1/2 operators in triplet configuration, i.e. while the singlet state with $S = 0$ is projected out. These half-integer spins now may bind to a singlet state in between adjacent sites, a so called valence bond, together with characteristically degenerate edge modes appearing due to an unpaired bond for finite open chains and non-vanishing string-orders beyond the Landau paradigm [209]. The artificiality of the model should not bother us at all, as these characteristic features are universally present in the context of symmetry protected topological phases, as for example the Haldane phase which is a possible ground-state of the $S = 1$ Heisenberg chain and its variants [193, 194]. Also for the case of such non-Landau phases, the analogy to spin chains will guide us the way of how to investigate the ground-sates of our constrained boson Hamiltonian.

Having discussed some generalities about one-dimensional spin chains, we proceed with the discussion of the λ-D model. A model which is not only a historically prominent example, hosting Landau as well as SPT phases, but also corresponds to the extended anyon-Hubbard model in **Eq**. (7.1) once the spin non-linearity is asymptotically

irrelevant [186, 187]. The model is given by the following Hamiltonian [190, 191, 195],

$$\hat{H}_{\lambda,D} = \sum_j \left(\hat{S}^x_j \hat{S}^x_{j+1} + \hat{S}^y_j \hat{S}^y_{j+1} + \lambda \hat{S}^z_j \hat{S}^z_{j+1} \right) + D \sum_j \left(\hat{S}^z_j \right)^2 . \tag{7.8}$$

Eq. (7.8) expresses an anti-ferromagnetic, i.e. $\lambda > 0$, anisotropic $su(2)$ spin chain in $S = 1$ dimensional representation with a single ion anisotropy scaled by D [190, 195]. The $su(2)$ symmetry is broken for general values of $|\lambda| \neq 1$ and for any finite D, whereas the model is invariant under the dihedral group in **Eq**. (7.6) and general S^z rotations indicating a $U^z(1)$ symmetry. Besides that, the chain is also invariant under spatial $\hat{P}$ and temporal parity transformations $\hat{K}_S$, as well as with respect to translations $\hat{T}$ if periodic boundary conditions are assumed[5], yielding the following symmetry group of the λ-D model,

$$G_{\hat{H}_{\lambda,D}} = \left[\hat{U}^{x,y}(\pi), \hat{U}^z(1), \hat{K}_S, \hat{P}, \hat{T} \right] . \tag{7.9}$$

Whenever the system size L is odd(even), spatial inversion $\hat{P}$ corresponds to site (bond)-centered parity $\hat{P}_{S,L}$, whereas for infinite system sizes we consider both transformations simultaneously [196]. Some of the phases of the model can be already inferred by simple perturbative considerations, where only the un-perturbed part of the Hamiltonian may be used for the discussion. Later on we will see that such a simple minded approach is insufficient to describe non-trivial hidden orders that are found in such models, that cannot be described by ordinary product states [190, 191].

7.3.1 The large D Phase

For very small λ and large D the ground-state can be understood as a small perturbation on a 0 spin state on each site with zero total magnetization [190], i.e.

$$\begin{aligned} \lim_{D\to\infty} \hat{H}_{\lambda,D} &\approx D \sum_j \left(\hat{S}^z_j \right)^2 , \\ |D\rangle &= \prod_j |0\rangle_j , \end{aligned} \tag{7.10}$$

which is called the large D-phase in the literature. Clearly, the ground-state in **Eq**. (7.10) is gapped and unique with zero variance in the transverse direction. Furthermore the state $|D\rangle$ does not break any symmetry of the Hamiltonian, neither of **Eq**. (7.9) nor its large D limit in **Eq**. (7.10), and thus there is no local order parameter that is specific for this phase [190]. Furthermore quantum-mechanical locality implies for $|D\rangle$,

[5] Note that the time reversal transformation for spin systems is defined as $\hat{K}_S = \hat{K} e^{i\pi \hat{S}^y}$, with $\hat{K}$ being complex conjugation, and is thus anti-unitary. For bosonic systems without internal degrees of freedom time reversal is only given by complex conjugation $\hat{T} = \hat{K}$, on the other hand.

that any two arbitrary local observables $\hat{A}_i, \hat{B}_j$ are un-correlated if they are sufficiently separated in space [210, 211], i.e.,

$$\lim_{|i-j|\to\infty} \mathrm{cov}(\hat{A}_i \hat{B}_j) = 0, \tag{7.11}$$

which is always obeyed for classical states that do not possess any entanglement. Nevertheless states like $|D\rangle$, that obey the cluster decomposition theorem as in **Eq**. (7.11), have the remarkable property that they are thermodynamically stable in the sense that extensive observables have a sub-dominant variance compared to their expectation values and are thus robust against local measurements [211]. This is in contrast to "cat" states for example, that appear as symmetry compatible eigenstates, which are spontaneously broken into one of their stable components as we exemplary discuss now for the anti-ferromagnetic *Néel* state. Later on we will meet the large D phase again, discussing its difference to the topologically non-trivial Haldane phase, which also has the full symmetry of the Hamiltonian but the two are distinguishable by different hidden string orders beyond the Landau paradigm.

7.3.2 The Anti-Ferromagnetic Phase

Reversing the role of the parameters U and λ, an Ising anti-ferromagnetic order is formed instead, with an alternation of spin values of ± 1 across the lattice or a (anti)-symmetric linear combination of them [190], i.e.

$$\begin{aligned}
&\lim_{\lambda\to\infty} \hat{H}_{\lambda,D} \approx V \sum_j \hat{S}^z_j \hat{S}^z_{j+1}, \\
&|\mathrm{Ising}, \pm\rangle = \Big(\prod_{j \ \mathrm{odd}} |+1\rangle_j |-1\rangle_{j+1} \pm \prod_{j \ \mathrm{even}} |-1\rangle_j |+1\rangle_{j+1} \Big)/\sqrt{2}, \\
&|\mathrm{Ising}, 1\rangle = \prod_{j \ \mathrm{odd}} |+1\rangle_j |-1\rangle_{j+1}\,, \\
&|\mathrm{Ising}, 2\rangle = \prod_{j \ \mathrm{even}} |-1\rangle_j |+1\rangle_{j+1}\,,
\end{aligned} \tag{7.12}$$

leaving the possibility of a symmetric ground-state or spontaneous symmetry breaking in the thermodynamic limit [211]. The linear combinations in **Eq**. (7.12) have a definite action with respect to translational, bond-centered inversion for even L, and time transformations, as well as π-rotations around the $x, y-$axis with eigenvalue ± 1, while the remaining states are transformed into each other[6]. Nevertheless, one should note that the only symmetries of the Hamiltonian that can be represented by locally uniform unitary operators are the π-rotations in x, y-direction and the $U(1)$ symmetry of arbitrary transverse rotations, and hence only those can be used to rigorously classify

[6] Of course all states have a definite action with respect to $U(1)$-rotations. Parity can only be broken for a bi-partite lattice, as all states in **Eq**. (7.12) are parity symmetric for odd L.

the symmetry breaking pattern in terms of a local Landau order parameter [211]. As the $U(1)$ symmetry of transverse rotations cannot be broken due to the Mermin-Wagner theorem and the continuity of the group [74, 75, 129], the discrete $\mathbb{Z}_2$ symmetry of x, y-rotations is the only remaining potential candidate to admit a Landau symmetry breaking pattern [211], i.e.

$$G_{\hat{H}_{eff}} = \left[\hat{U}^z(1), \hat{U}^{x,y}(\pi), \hat{T}, \hat{P}_{S,L}, \hat{K}_S\right], \tag{7.13}$$

$$G_{\text{Residual}} = \left[\hat{U}^z(1), \hat{T}^2, \hat{P}_S, \hat{P}_L\hat{T}, \hat{K}_S\hat{T}\right], \tag{7.14}$$

$$G_{\text{Broken}} = G_{\hat{H}_{eff}}/G_{\text{Residual}} = \left[\hat{U}^{x,y}(\pi), \hat{T}, \hat{P}_L, \hat{K}_S\right], \tag{7.15}$$

whereas of course also symmetries that do not allow to define a local order parameter are broken. Whether these symmetries are then actually broken in the thermodynamic limit, can be inferred from such an order parameter, if it is not invariant with respect to the eventually broken symmetries G_{Broken} in **Eq**. (7.15) but to the residual ones G_{Residual} in **Eq**. (7.14). A suitable local order parameter fulfilling these requirements can be deduced from the generators $\hat{S}^{x,y}_j$ of the broken elements of the dihedral symmetry group, according to **Eq**. (7.6), by commuting them with a so called interpolating field $\hat{\Phi}$ [211], i.e.

$$\hat{O}_V(j) = \left[\hat{S}^{x,y}_j, \hat{\Phi}_i\right] \propto \delta_{i,j}(-1)^j \hat{S}^z_j, \quad \Phi_i = (-1)^i \hat{S}^{x,y}_i. \tag{7.16}$$

The interpolating field in **Eq**. (7.16) can be chosen as either a staggered magnetization in x, y-direction, depending on the generator, where both choices lead to the same local order parameter that distinguishes between different symmetry broken states[7]. From **Eq**. (7.16) one can then consistently define an extensive global order parameter, i.e.

$$\hat{O}_V = \sum_j \hat{O}_V(j), \tag{7.17}$$

which has a definite action with respect to all broken symmetries G_{Broken} while being symmetric with respect to the residual ones G_{Residual}. The rather unexpected scenario that the ground-state of a system has a smaller symmetry group than its Hamiltonian, i.e. $G_{\text{Residual}} \subset G_{\hat{H}_{eff}}$ in **Eq**. (7.13) and (7.14), can then be formalized by the non-commutativity of the following two limits [211],

$$\lim_{\gamma\to 0}\lim_{L\to\infty}\left(\hat{H}_{\lambda;D} + \gamma\sum_j \hat{O}_V(j)\right) \neq \lim_{L\to\infty}\lim_{\gamma\to 0}\left(\hat{H}_{\lambda;D} + \gamma\sum_j \hat{O}_V(j)\right). \tag{7.18}$$

[7] The alternating factor in **Eq**. (7.16) is used to obtain a unique limit point, when $|i-j| \to \infty$ as it ensures translational invariance of the order parameter. Furthermore the broken symmetry states are exact eigenstates of the staggered magnetization and are thus a natural choice for an order parameter [211].

Eq. (7.18) can be understood as the inequality of a Hamiltonian in the thermodynamic limit coupled to an infinitesimally small perturbation (RHS), with a Hamiltonian that approaches the thermodynamic regime but is coupled to a small symmetry breaking perturbation for all finite sizes (LHS). If **Eq**. (7.18) holds the $\mathbb{Z}_2$ symmetry is spontaneously broken into one of the non-invariant states in **Eq**. (7.12), and a real long-range order in transversal direction emerges that correlates points in the lattice even if they are infinitely far away from each other [190], i.e.

$$\lim_{|i-j|\to\infty}(-1)^{i-j}\langle\hat{S}_i^z\hat{S}_j^z\rangle \neq 0. \tag{7.19}$$

Thereby the diagonal long-range order in **Eq**. (7.19) is quite different from disordered phases where correlations decay exponentially or Luttinger type models with algebraically decreasing ones below certain temperatures [43]. The reason why the Hamiltonian chooses a ground-state that is not compatible with its symmetries, can then be explained finally, by the thermodynamic instability of those macroscopic superpositions violating **Eq**. (7.11), which leads to large fluctuations of extensive observables [211]. Hence, experimentally the broken symmetry states are always observed instead of the symmetric ones, as according to **Eq**. (7.18) even infinitesimal perturbations on a thermodynamic system may lead to huge qualitative differences compared to perturbing a finite system of any size. Thereby this singular thermodynamic limit needs to be understood to hold for system sizes that are sufficiently larger than any intrinsic length scale of the system such that finite-size effects become unimportant [211]. Conversely a, strictly speaking finite, experimental setup does not necessarily contradict to those requirements, whereas sometimes even incredibly small samples are well described as being thermodynamic.

7.3.3 The XY Phases

Even if we have argued before, that the sign of bosonic dipolar interactions is necessarily positive in one dimension [199], we still want to consider the case of small negative λ, which helps us to understand the differences between our model in **Eq**. (7.1) and the spin chain discussed here. Namely, for not too large $\lambda < 0$ there exist two gapless phases known as the $XY1$ and $XY2$ phase [195], whereas the ferromagnetic order that is formed for large negative λ is not of our interest. These names indicate already, that for the gapless phases the x, y-part of the Hamiltonian is the most relevant one, i.e.

$$\lim_{\lambda,U\to 0}\hat{H}_{\lambda,D} \approx \sum_j \hat{S}_j^x\hat{S}_{j+1}^x + \hat{S}_j^y\hat{S}_{j+1}^y, \tag{7.20}$$

whereas the interpretation of **Eq**. (7.20) is more complicated as for the spin $S = 1/2$ case, due to the absence of a single-particle description in terms of Jordan-Wigner fermions. Anyhow, in analogy to fluid-like states of canonical particles, the gapless

phases have a dominantly decaying correlation function of a spin 1 or 2 excitations, i.e.

$$\begin{aligned} \hat{O}_{XY1}(j) &= \hat{S}^{+}_{j}, \\ \hat{O}_{XY2}(j) &= (\hat{S}^{+}_{j})^{2}, \end{aligned} \tag{7.21}$$

respectively, as described within Luttinger liquid theory [195]. The order parameters in **Eq**. (7.21) would correspond in higher dimensions to phases that break the $U(1)$ symmetry of the total magnetization, while the latter is in addition invariant with respect to dihedral rotations in z-direction and spin time reversal symmetry. As true long-range order arising through spontaneous breaking of continuous symmetry groups is destroyed by strong quantum fluctuations in one dimension [74, 75, 129], two states are formed instead that can be illustrated as the quasi-condensation of magnons $\hat{S}^{+} \approx \hat{b}^{\dagger}$ or magnon pairs $(\hat{S}^{+})^{2} \approx (\hat{b}^{\dagger})^{2}$ according to the lowest order Holstein-Primakoff expansion [212]. Here quasi-condensation means that the large-distance limit of correlators of the XY order parameters in **Eq**. (7.21) has the slowest, and thus dominant, algebraic decay in their respective phases

$$\begin{aligned} \langle \hat{O}^{\dagger}_{XY1}(i)\hat{O}_{XY1}(j)\rangle &\approx \langle \hat{b}^{\dagger}_{i}\hat{b}_{j}\rangle \approx \frac{1}{|i-j|^{\alpha}}, \\ \langle \hat{O}^{\dagger}_{XY2}(i)\hat{O}_{XY2}(j)\rangle &\approx \langle (\hat{b}^{\dagger}_{i})^{2}(\hat{b}_{j})^{2}\rangle \approx \frac{1}{|i-j|^{\beta}}, \end{aligned} \tag{7.22}$$

instead of attaining constant values at infinity. Going beyond this simple spin-wave picture one finds a specialty of the $XY2$ phase, namely the presence of a relatively slow decay of transversal fluctuations $\hat{O}_{V}(j)$, and the exponential decay of the $XY1$ order parameter instead of just a quicker algebraic decay as expected from a single Luttinger liquid [195]. Anyhow these details concerning the gapless phases will be recapitulated and clarified later on by means of an effective field-theory following the seminal work of Schulz on the bosonization of spin chains for arbitrary S.

7.3.4 The Haldane Phase

For intermediate values of $\lambda > 0$ and D both gapped phases are separated by the so called Haldane insulator phase, that cannot be understood by simple perturbative considerations anymore [189–191]. This gapped phase has the full symmetry of the Hamiltonian, i.e. $G_{\text{Residual}} = G_{\hat{H}_{\lambda,D}}$, and thus cannot be a locally ordered phase in the sense of Landau. Furthermore, all local correlation functions vanish exponentially in this phase. Nevertheless, a hidden order can be revealed by a duality transformation [190],

i.e.

$$\hat{U}_{KT} = \prod_{j<k} e^{i\pi \hat{S}^z_j \hat{S}^x_k}, \tag{7.23}$$

$$\begin{aligned}
\hat{U}_{KT}\hat{S}^x_j\hat{U}^{-1}_{KT} &= \hat{S}^x_{j,d} = \hat{S}^x_j e^{i\pi\sum_{l>j}\hat{S}^x_l}, \\
\hat{U}_{KT}\hat{S}^y_j\hat{U}^{-1}_{KT} &= \hat{S}^y_{j,d} = e^{i\pi\sum_{l<j}\hat{S}^z_l}\hat{S}^y_j e^{i\pi\sum_{l>j}\hat{S}^x_l}, \\
\hat{U}_{KT}\hat{S}^z_j\hat{U}^{-1}_{KT} &= \hat{S}^z_{j,d} = e^{i\pi\sum_{l<j}\hat{S}^z_l}\hat{S}^z_j,
\end{aligned} \tag{7.24}$$

that changes the spin operators in a non-local manner. The transformation in **Eq**. (7.24) leads to a Hamiltonian that looks quite complicated

$$\begin{aligned}
\hat{H}^{\text{dual}}_{\lambda,D} =& \sum_j \left(\hat{S}^x_{j,d}\hat{S}^x_{j+1,d} + \hat{S}^y_{j,d}\hat{S}^y_{j+1,d} + \lambda\hat{S}^z_{j,d}\hat{S}^z_{j+1,d}\right) + D\sum_j\left(\hat{S}^z_{j,d}\right)^2, \\
&- \sum_j \left(\hat{S}^x_j\hat{S}^x_{j+1} - \hat{S}^y_j e^{i\pi(\hat{S}^z_j+\hat{S}^x_{j+1})}\hat{S}^y_{j+1} + \lambda\hat{S}^z_j\hat{S}^z_{j+1}\right) + D\sum_j\left(\hat{S}^z_j\right)^2,
\end{aligned} \tag{7.25}$$

but is nevertheless local. The symmetries of the dual Hamiltonian in **Eq**. (7.24) and those of the λ-D model in **Eq**. (7.9) are related by the duality transformation $\hat{U}_{KT}$, whereas again only the dihedral group symmetry, is locally generated by the dual operators in **Eq**. (7.24). In the dual Haldane phase this symmetry is now spontaneously broken with a four-fold degenerate groundstate and thus the dual operators form a long-range order in the sense of **Eq**. (7.19) [190, 191], i.e.

$$\lim_{|i-j|\to\infty}\langle\hat{S}^{x,y,z}_{i,d}\hat{S}^{x,y,z}_{j,d}\rangle \neq 0. \tag{7.26}$$

Reversing the duality transformation in **Eq**. (7.24), **Eq**. (7.26) corresponds to a non-local order for the original spins, that remains in-detectable by any local observable. Hence we could rephrase the Haldane phase as a hidden order that becomes an ordinary Landau order by a suitable necessarily non-local transformation of the order parameters and symmetry operations. But it turns out that not every aspect of this phase can be explained by spontaneous symmetry breaking, according to Landau.

In opposition to the ordinary anti-ferromagnetic order in **Eq**. (7.19), quantum-mechanical locality is not really broken in **Eq**. (7.26), as the dual spin operators represents quantities whose support is not of finite range in the thermodynamic limit. Hence not all non-local orders are necessarily non-trivial, as in the case of the Haldane phase. For example from **Eq**. (7.25) we may immediately conclude that also the Ising anti-ferromagnetic phase arising for large λ has a hidden-string order in transversal direction, by the same reasoning used before for the local Landau order parameter [190, 191]. Nevertheless, a wisely chosen non-local order parameter may reveal hidden structures for phases that are not classifiable via a symmetry breaking pattern, as for example for

non-zero λ in the large D-phase [186–188], i.e.

$$\hat{O}_P(j) = e^{i\pi \sum_{l<j} \hat{S}^z_l}. \tag{7.27}$$

The parity order parameter in **Eq**. (7.27) becomes finite in the large D-phase but vanishes in the Haldane phase, for ground-states that deviate form the simple product form of **Eq**. (7.10), due to the impact of nearest-neighbor interactions λ and spin-flips along the bond $(j, j+1)$. Pictorially, such an order corresponds to a formation of dilute pairs of spin ± 1 around the product state in **Eq**. (7.10) [187, 188].

So in view of the duality relation, what is the difference between the hidden orders in the large D and the Haldane phase? While the large D phase is not related to symmetry breaking in none of the dual pictures, the dual Haldane phase breaks spontaneously the dihedral symmetry, leading to a four-fold degenerate ground-state for sufficiently long open chains [190, 191]. Reversing the duality transformation in **Eq**. (7.24), which is only defined un-ambiguously for open chains, this degeneracy corresponds to spin 1/2 edge-modes at both ends of the chain, as they also occur in the $AKLT$ state [193, 194]. These spin 1/2 degrees of freedom are projective representations of the dihedral group [192], instead of the linear ones in terms of spin 1 operators in **Eq**. (7.6). [8] Hence, both phases can be distinguished by the presence of these edge states, while they are indistinguishable by any local order in the bulk[9]. Conversely, once these edge modes are destroyed by a perturbation that breaks all their symmetries, both the large D and the Haldane phase can be adiabatically connected, without a phase transition between them. Thereby the presence of time reversal $\hat{K}_S$, or link-parity $\hat{P}_L$, symmetry alone is sufficient to protect the distinction of both phases, which is not related to any symmetry breaking as for the dihedral group [193, 194]. If some of these symmetries remain intact on the other hand, then both phases are separated and correspond to topologically different entities. As the distinction of both entities is protected by symmetry, the Haldane phase is called a symmetry-protected topological phase, while the large D phase corresponds to a topologically trivial one [192].

7.4 Modified Gutzwiller Mean-Field

As a poor man approach, to get some insights into the phase-diagram of our model, we apply a slightly generalized Gutzwiller mean-field ansatz [18, 27, 213]. The basic idea of the Gutzwiller approach is to minimize the Hamiltonians energy with respect to a general trial wave-function in product form that is adapted to the spatial resolution of the underlying phases and the local Hilbert space dimension of the problem [110]. In

[8] Projective means here that the commutation of group elements are defined up to a phase factor $e^{i\phi}$, whereas the linear representations correspond to the trivial choice $\phi = 0$.

[9] Similar arguments apply also for periodic systems protected by link-parity, as can be shown in the language of matrix product states, and thus the discussion here is not restricted to open chains [193, 194].

order to reduce numerical effort, the Gutzwiller basis is usually chosen to be site-local and thus translationally invariant, which has the obvious disadvantage that longer-range spatial structures cannot be resolved [18,27], as for example the Ising anti-ferromagnetic order which needs at least two sub-lattices. In this sense especially the Haldane phase is not expected to be detectable by such an approach in our case, as it cannot be deformed into a product state once all its protecting symmetries remain intact and furthermore features non-local hidden orders that cannot be explained by a site-local Hamiltonian [187][10]. In addition, such product states do not inherit any quantum entanglement and treat all Hamiltonians equally, irrespective of the spatial dimension they are defined in. Hence one should be cautious when the method is applied to low-dimensional systems, where strong quantum fluctuation may destroy any continuous long-range order that is otherwise captured well by mean-field approaches in higher dimensions. Besides all this criticism, whenever the actual, possibly strongly correlated, ground-state of the system is in some limit close to a product state, a look through the eyes of mean-field theory may still be rewarding and its simplicity is thereby strongly appreciated [110]. In this sense we can already obtain some qualitative information about the phase diagram at the mean-field level and its fate with respect to statistical transmutations. Later on the method has to be complemented with a more adequate numerical or analytical treatment, that is perfectly suited for the phenomenology of one-dimensional many-body systems and quantitative predictions.

7.4.1 Derivation and Order Parameters

The generalization with respect to the ordinary approach consists first of allowing for a two-site Gutzwiller basis, instead of the usually assumed translational invariant one [18, 27, 88, 110], i.e.

$$|G\rangle_A |G\rangle_B = \prod_{i\in A} \left(\sum_{n_A=0}^{n_{A,\max}} A^i_{n_A} |n_A\rangle_i \right) \prod_{j\in B} \left(\sum_{n_B=0}^{n_{B,\max}} B^j_{n_B} |n_B\rangle_j \right), \tag{7.28}$$

where we choose here $n_{A,B,\max} = 2$ to fulfill the bosonic onsite constraint $\hat{b}^3 = 0$. Second, we assume that the Gutzwiller coefficients in **Eq**. (7.28) carry a spatial dependence, besides the bi-partition, which is expressed via an additional linear spatial-dependent

[10] In the case of the dual λ-D model in **Eq**. (7.25), the Haldane phase corresponds just to a local order and thus can be detected by local mean-field approaches [187]. Nevertheless due to the difference of spins and anyons, the duality transformed extended anyon-Hubbard model according to **Eq**. (7.24) would be manifestly non-local, reflecting the fact that some of the protecting symmetries of the Haldane phase are destroyed. Hence a local mean-field approach would be inapplicable again in this case.

phase factor [18], i.e.

$$A_{n_A}^{2j} = |A_{n_A}| e^{i\gamma_{n_A}^A} e^{2ij\beta_{n_A}^A},$$
$$B_{n_B}^{2j+1} = |B_{n_B}| e^{i\gamma_{n_B}^B} e^{i(2j+1)\beta_{n_B}^B}, \tag{7.29}$$

which corresponds then to a set of 18 different variational parameters in total. Nevertheless, as the Gutzwiller wave-function in **Eq**. (7.28) needs to be normalized and an average lattice filling of one is required, two additional constraints for all the coefficients arise [26, 27]

$$\left(\sum_{n_A=0}^{n_{A,\max}} |A_{n_A}^i|^2\right) = 1 \wedge \left(\sum_{n_B=0}^{n_{B,\max}} |B_{n_B}^j|^2\right) = 1,$$
$$|A_1|^2 + 2|A_2|^2 + |B_1|^2 + 2|B_2|^2 = 2, \tag{7.30}$$

reducing the number of parameters by three to 15. The reduction of complexity is already enormous at this point, as we only have to solve a, still numerically costly, variational problem instead of performing a computationally infeasible matrix diagonalization in the full 3^L-dimensional Hilbert space.

The local self-consistency relations that are relevant for the discussion of the extended anyon-Hubbard model in **Eq**. (7.1) can then expressed in terms of these variational parameters of **Eq**. (7.29), i.e.

$$\begin{aligned}
\Psi_A^{2j} &= \langle \hat{b}_{2j} \rangle = A_0^* A_1 e^{-2ij(\beta_0^A - \beta_1^A)} + \sqrt{2} A_1^* A_2 e^{-2ij(\beta_1^A - \beta_2^A)}, \\
\phi_A^{2j} &= \langle e^{-i\theta \hat{n}_{2j}} \hat{b}_{2j} \rangle = A_0^* A_1 e^{-2ij(\beta_0^A - \beta_1^A)} + \sqrt{2} A_1^* A_2 e^{-2ij(\beta_1^A - \beta_2^A)} e^{-i\theta}, \\
\langle \hat{n}_{2j} \rangle &= |A_1|^2 + 2|A_2|^2,
\end{aligned} \tag{7.31}$$

and analogously for the B sub-lattice, by the replacement $[(A_{n_A}^{2j}, 2j) \leftrightarrow (B_{n_B}^{2j+1}, 2j+1))]$. In **Eq**. (7.31) we can identify the local density on the A sub-lattice $\langle \hat{n}_{2j} \rangle$ with the order parameter of the Ising anti-ferromagnet (charge-density wave) from **Eq**. (7.16), which can distinguish between the large D (Mott) phase by a density alternation of double occupation and a hole instead of a single particle on both sub-lattices. Immediately it should be clear that in the current mean-field framework string orders as in **Eq**. (7.26) cannot be resolved, thus we do not expect any signature of the Haldane phase in this investigation. Ψ_A^{2j} on the other hand, clearly corresponds to the order parameter of the $XY1$ phase in **Eq**. (7.21), as in the λ-D-model, whereas its algebraic decay is changed into real long-range order as a mean-field artifact. The role of ϕ_A^{2j} is less clear on the other hand, as it is not independent of Ψ_A^{2j}, thus its ability to distinguish between

phases independently of Ψ_A^{2j} has to be investigated numerically and we cannot identify it with the $XY2$ order parameter in **Eq**. (7.21), or a novel phase yet [88]. Nevertheless the bi-partition of the superfluid order parameters may indicate a difference between the two gapless phases, as homogeneity is expected for the $XY1$ phase but is a priori unclear for $XY2$ case.

In the next step we postulate as a physically motivated requirement, that the mean-field energy of the extended anyon-Hubbard model should be extensive in the thermodynamic limit. The linear spatial dependence of the Gutzwiller coefficients leads to the presence of multiple geometric sums in the global mean-field energy [18], i.e.

$$\sum_{j=1}^{L} q^j = \frac{q(1-q^L)}{1-q}, \tag{7.32}$$

that can be made extensive in L by choosing $q = 1$ with the following values of artificial phase parameters $\beta_{n_A,n_B}^{A,B}$, i.e.

$$\begin{aligned}
\Delta\beta_0^A - \Delta\beta_0^B &= (\beta_0^A - \beta_1^A) - (\beta_0^B - \beta_1^B) = l_1\pi, \\
\Delta\beta_1^A - \Delta\beta_1^B &= (\beta_1^A - \beta_2^A) - (\beta_1^B - \beta_2^B) = l_2\pi, \\
\Delta\beta_0^A - \Delta\beta_1^B &= (\beta_0^A - \beta_1^A) - (\beta_1^B - \beta_2^B) = l_3\pi, \\
\Delta\beta_1^A - \Delta\beta_0^B &= (\beta_1^A - \beta_2^A) - (\beta_0^B - \beta_1^B) = l_4\pi, \quad l_{1,2,3,4} \in \mathbb{Z}.
\end{aligned} \tag{7.33}$$

The choice in **Eq**. (7.33) implies that one can consider the differences $\Delta\beta_{0,1}^{A,B}$ to be equal on the sub-lattices, which reduces the number of degrees of freedom from 15 to 11, and furthermore that they mutually differ only by a phase δ taking either the value 0 or π, i.e.

$$\Delta\beta_1^B = \Delta\beta_0^B + \delta. \tag{7.34}$$

Consequently, **Eq**. (7.33) leads to the following local mean-field energy

$$\begin{aligned}
\langle\hat{H}\rangle/L = \frac{E_{MF}}{L} = &- J[\Big[4|A_0||A_1||B_1||B_0|\cos(\Delta\beta_0^B)\cos(\Delta\gamma_0^A - \Delta\gamma_0^B)\Big] \\
&+ 8\Big[|A_1||A_2||B_1||B_2|\cos(\Delta\beta_0^B + \delta - \theta)\cos(\Delta\gamma_1^A - \Delta\gamma_1^B)\Big] \\
&+ 4\sqrt{2}\left[|A_0||A_1||B_1||B_2|\cos(\Delta\gamma_0^A - \Delta\gamma_1^B - \frac{\theta}{2})\cos(\Delta\beta_0^B + \delta - \frac{\theta}{2})\right] \\
&+ 4\sqrt{2}\left[|A_1||A_2||B_0||B_1|\cos(\Delta\gamma_1^A - \Delta\gamma_0^B + \frac{\theta}{2})\cos(\Delta\beta_0^B - \frac{\theta}{2})\right]] \\
&+ U(|A_2|^2 + |B_2|^2) + V(|A_1|^2 + 2|A_2|^2))(|B_1|^2 + 2|B_2|^2)),
\end{aligned} \tag{7.35}$$

whereas the classical Gutzwiller result can be recovered by setting the artificial phase parameter to zero. **Eq**. (7.35) depends only on the difference of the ordinary Gutzwiller

phases, i.e.

$$\begin{aligned}\Delta\gamma_0^{A,B} &= \gamma_0^{A,B} - \gamma_1^{A,B},\\ \Delta\gamma_1^{A,B} &= \gamma_1^{A,B} - \gamma_2^{A,B},\end{aligned} \tag{7.36}$$

reducing the effective degrees of freedom further from 11 to 9. As 9 variational parameters still correspond to a numerically demanding extremalization procedure we further simplify **Eq**. (7.35), by observing that the cosine terms, which only contain the phase differences of the ordinary Gutzwiller coefficients, from **Eq**. (7.36) are necessarily bounded by ± 1, in order to extremize E_{MF}. This consideration implies the following conditions for the ordinary Gutzwiller phases,

$$\begin{aligned}\Delta\gamma_0^A &= \Delta\gamma_0^B + \pi l_5,\\ \Delta\gamma_1^A &= \Delta\gamma_1^B + \pi l_6,\\ \Delta\gamma_0^A &= \Delta\gamma_1^B + \frac{\theta}{2} + \pi l_7,\\ \Delta\gamma_1^A &= \Delta\gamma_0^B - \frac{\theta}{2} + \pi l_8, \quad l_{5,6,7,8} \in \mathbb{Z},\end{aligned} \tag{7.37}$$

leading to the final form of the mean-field energy,

$$\begin{aligned}\frac{\tilde{E}_{MF}}{L} =& - J[\Big[4|A_0||A_1||B_1||B_0|\mathrm{sgn}_1\cos(\Delta\beta_0^B)\Big]\\ &+ 8\left[|A_1||A_2||B_1||B_2|\mathrm{sgn}_2\cos(\Delta\beta_0^B + \delta - \theta)\right]\\ &+ 4\sqrt{2}\left[|A_0||A_1||B_1||B_2|\mathrm{sgn}_3\cos(\Delta\beta_0^B + \delta - \frac{\theta}{2})\right]\\ &+ 4\sqrt{2}\left[|A_1||A_2||B_0||B_1|\mathrm{sgn}_4\cos(\Delta\beta_0^B - \frac{\theta}{2})\right]]\\ &+ U(|A_2|^2 + |B_2|^2) + V(|A_1|^2 + 2|A_2|^2))(|B_1|^2 + 2|B_2|^2)).\end{aligned} \tag{7.38}$$

From **Eq**. (7.38) we can furthermore conclude that the choice of δ corresponds just to changing the sign functions to a different value and can thus be set to zero without the loss of generality. So we end up with 8 effective variational parameters which have to be adjusted such that **Eq**. (7.38) is minimized, whereas four of them are luckily constrained to the values ± 1.

7.4.2 Superfluid Phases

Before we discuss the mean-field phase diagram, we should comment on the benefits of the modified approach over its classical counterpart. Especially the phenomenology of superfluid phases of such one-dimensional anyons is more faithfully described in

the following sense. The classical, local, Gutzwiller ansatz does not inherit any spatial modulation, which corresponds necessarily to a condensation of bosons at zero momentum in the superfluid phase, or alternatively a phase incoherent Mott insulator [18, 110]. For our one-dimensional anyons such an assumption is definitely incorrect as they are known to condense at finite momentum [13, 18, 27, 33], and may feature in addition other gapped phases beyond the spatially uniform Mott insulator. These obstacles can be partially circumvented by the additional phase degrees of freedom used here, in the spirit of **Ref**. [18], as well as the bi-partition of order parameters. The effect of the first is to spatially modulate the superfluid order parameters for extensive mean-field energies besides the bi-partition, i.e.

$$\begin{aligned} \Psi^j_{A,B} &= O^{\mathrm{SF}}_{a,\mathrm{A/B}} e^{-ij\Delta\beta_0}, \quad \phi^j_{A,B} = O^{\mathrm{SF}}_{b,\mathrm{A/B}} e^{-ij\Delta\beta_0}, \\ O^{\mathrm{SF}}_{a,b\mathrm{A/B}} &= |O^{\mathrm{SF}}_{a,b\mathrm{A/B}}| e^{i\arg(O^{\mathrm{SF}}_{a,b\mathrm{A/B}})}, \end{aligned} \tag{7.39}$$

where $O^{\mathrm{SF}}_{a,b\mathrm{A/B}}$ denotes the order parameters according to the classical Gutzwiller ansatz in a two-site basis [110]. The choice of classical Gutzwiller phases in **Eq**. (7.37) shows furthermore that the order parameters $O^{\mathrm{SF}}_{a,b\mathrm{A/B}}$ have an equivalent amplitude but a different phase on each of their sub-lattices, whereas they are exactly the same for zero θ. Hence it suffices to consider only one of them on each sub-lattice to distinguish between gapless and insulating phases, as they are not independent and only differ by a phase. As $O^{\mathrm{SF}}_{a\mathrm{A/B}}$ corresponds to the ordinary superfluid order parameter in bosonic systems we choose it as the fundamental quantity for the upcoming discussion of the superfluid phases in the mean-field framework.

The bi-partition of order parameters itself can reproduce a condensation at two different points in momentum space, namely at $k = 0$ or π [214], depending on whether both order parameters are equal or not [88]. Thus one can conclude that according to our mean-field theory, the bosons condense in form of the following quasi-momentum distribution in the thermodynamic limit,

$$\begin{aligned} \langle \hat{n}_k \rangle \propto & \left[|O^{\mathrm{SF}}_{a,\mathrm{A}}|^2 + |O^{\mathrm{SF}}_{a,\mathrm{B}}|^2 + 2|O^{\mathrm{SF}}_{a,\mathrm{A}}||O^{\mathrm{SF}}_{a,\mathrm{B}}| \cos\left(\arg(O^{\mathrm{SF}}_{a,\mathrm{A}}) - \arg(O^{\mathrm{SF}}_{a,\mathrm{B}})\right) \right] \delta(k + \Delta\beta_0) \\ & + \left[|O^{\mathrm{SF}}_{a,\mathrm{A}}|^2 + |O^{\mathrm{SF}}_{a,\mathrm{B}}|^2 - 2|O^{\mathrm{SF}}_{a,\mathrm{A}}||O^{\mathrm{SF}}_{a,\mathrm{B}}| \cos\left(\arg(O^{\mathrm{SF}}_{a,\mathrm{A}}) - \arg(O^{\mathrm{SF}}_{a,\mathrm{B}})\right) \right] \delta(k + \Delta\beta_0 + \pi). \end{aligned} \tag{7.40}$$

Eq. (7.40) features a double peak structure unless $O^{\mathrm{SF}}_{a,\mathrm{B}} = \pm O^{\mathrm{SF}}_{a,\mathrm{A}}$, with condensation points shifted by the artificial phase $\Delta\beta_0$ [18], whereas the phase difference of the order parameters changes the weight of the respective peaks. Furthermore, the weights of the peaks are in general interrelated by a π phase shift of only one of the order parameters. The superfluid order parameters are only fully translationally and $k \leftrightarrow -k$ invariant for

θ being exactly zero, see **Fig**. (7.1). For increasing θ the amplitudes remain the same at first while the phases begin to deviate from zero *mod* 2π, which implies a small but finite signal around $k \approx -\Delta\beta_0 - \pi$, and a dominant one at $k \approx -\Delta\beta_0$, even in the case of the ordinary superdfluid ($SF1$). At around $\theta = 0.5\pi$ also the amplitudes start to become different for negative U, which we identify with the emergence of a new superfluid phase ($SF2$). In this case the dominance of the $k \approx -\Delta\beta_0$ peak is eventually reduced, which is known in this context as a staggered superfluid that breaks the $k \leftrightarrow -k$ symmetry irrespective of $\Delta\beta_0$ [214]. In analogy to the λ-D model we should assign the $XY1$ and the $XY2$ phases to those regimes, even if their features are only incorrectly captured by the mean-field approach, and actually only appear for $\lambda < 0$ in the spin-1 case [195].

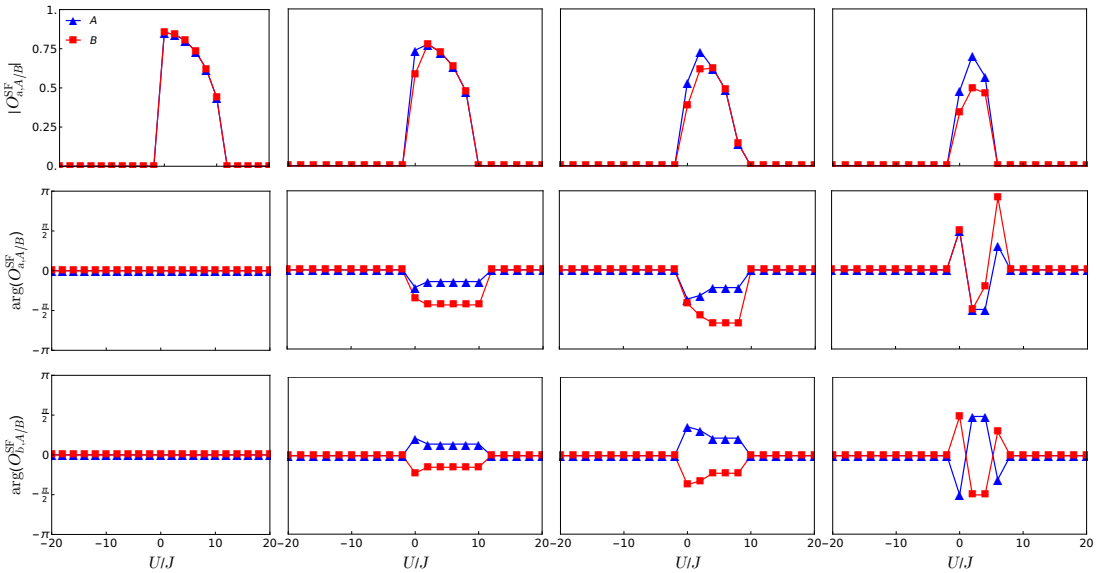

Figure 7.1: *Absolute value* $|O^{SF}_{a,A/B}|$ *and argument* $\arg(O^{SF}_{a,A/B})$ *of the classical Gutzwiller order parameters, as functions of* U *for fixed* $V/J = 1.2$ *and various statistical parameters, i.e.* $\theta/\pi = 0,\ 0.5,\ 0.75$ *and* 1 *respectively. In the last row only the argument* $\arg(O^{SF}_{b,A/B})$ *of the dependent order parameter is shown for the same set of parameters, as the amplitudes are equivalent as it is discussed in the main text [17].*

7.4.3 Mean-Field Phase Diagram

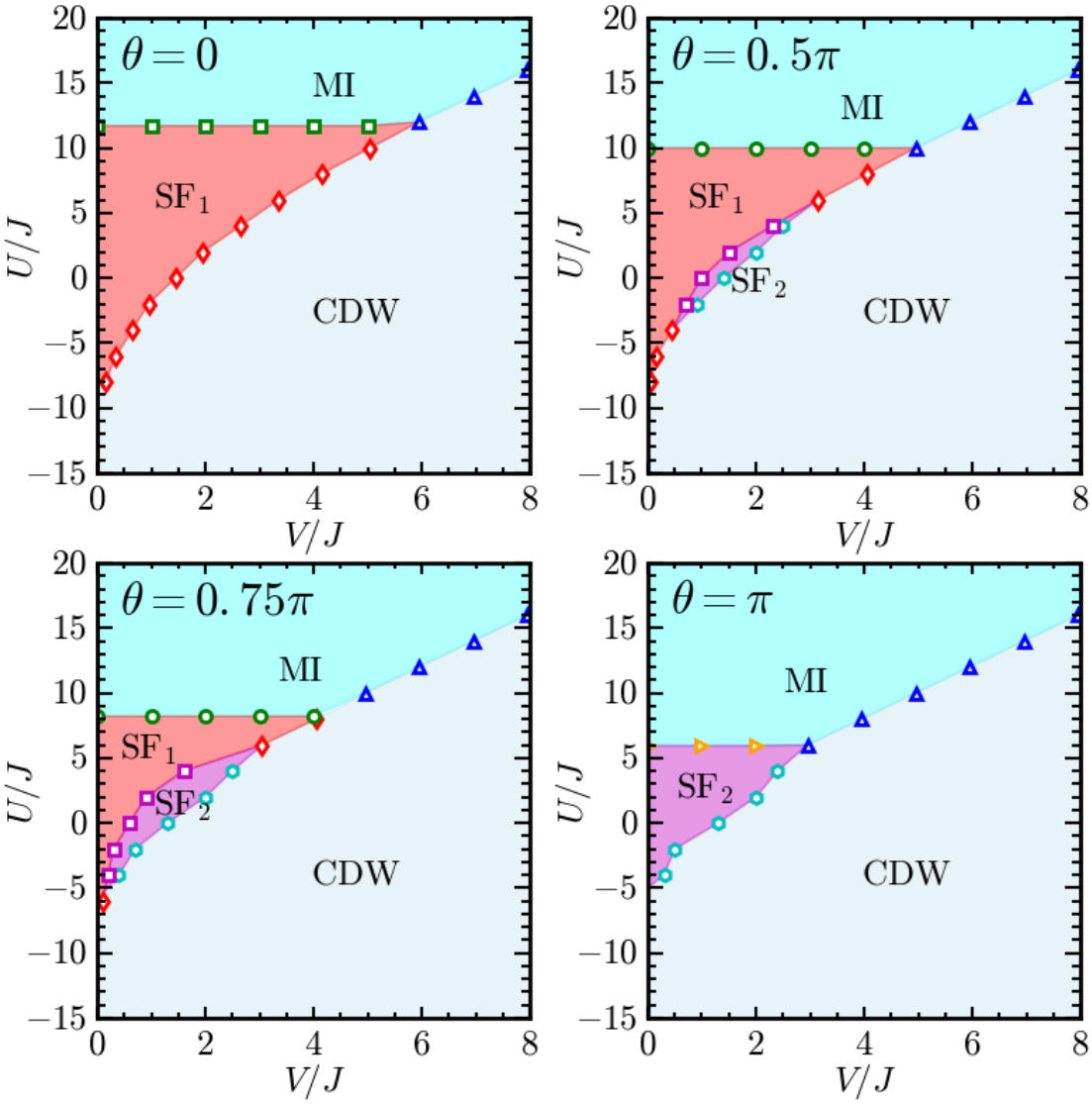

Figure 7.2: *Phase diagram for different values of the statistical parameter θ obtained by the Gutzwiller approach. For a vanishing θ there exist only three phases in the diagram, namely the Mott, the Charge-Density (CDW) wave and the superfluid $XY1(SF1)$ phase. For increasing statistical transmutation another superfluid $XY2(SF2)$ phase appears at the boundary to the CDW phase, repressing the $SF1$ phase completely until the pseudo-fermionic limit is approached. The plot was taken out of* **Ref**. *[17]*

In order to compute the phase diagram in **Fig**. (7.2), we choose the lattice site ($j = 0$) for the superfluid order parameters, as by construction their absolute value is only dependent on the sub-lattice. Hence, considering only a single site j is sufficient to determine the phase diagram topography completely as long as E_{MF} is extensive. Whenever the superfluid order parameters are zero, we identify the region as gapped,

whereas the density structure on the sub-lattice distinguishes then further between the Mott phase and the Charge-Density-Wave.

The major disadvantage of the Gutwiller phase diagram is the absence of a gapped phase residing between the Mott and the CDW phase, see **Fig**. (7.2), which follows from its incapability of resolving longer-range correlations, as explained in the derivation. Instead, the gapless region is in general massively over-estimated. Conversely, we would expect to find gapped phases in this region of the phase diagram instead, in analogy to the λ-D model. So we should identify the two superfluid phases in the Gutzwiller approach actually with the Haldane and a second unknown gapped phase that appears for relatively large θ. In this sense, the Gutzwiller approach may not be the best method to reveal non-trivial gapped phases of the model, but qualitative insight into them can still be obtained. For example, the emergence of statistically induced phase transitions for varying θ can be resolved clearly in **Fig**. (7.2) [13], by the destruction of the $SF1$ phase in favor of the $SF2$ order. Although the $SF1$ phase cannot be strictly identified with the Haldane insulator in this framework, its disappearance with increasing statistical transmutation allows for similar predictions for the actual SPT phase. Furthermore, the circumstance that the $SF2$ phase is characterized by an imbalanced condensate density between the two sub-lattices, implies a further symmetry breaking with respect to the ordinary superfluid which is homogeneous on the other hand. Hence one could argue that the new gapped phase that is actually conjectured behind the $SF2$ phase should correspond to a symmetry-breaking order, as the CDW phase, with a minimal spatial structure that is necessary larger than two lattice sites.

In general, the area that is surrounded by the insulating phases decreases in size with increasing θ, which can be interpreted as the destruction of phase coherence due to statistical interactions. Interestingly this reduction seems to be rather small for $\theta \leq \frac{\pi}{2}$, whereas it shrinks more drastically for higher values of the statistical parameter. This could indicate that also such statistical interactions are in some sense perturbative, even if no small parameter exist as the Peierls phase is always of the order of one. Additionally the narrowing seems to be slightly inhomogeneous with respect to positive or negative values of U which is less pronounced in the latter case. This circumstance could be interpreted such that the attractive interaction $U < 0$ can be compensated by the, necessarily repulsive, statistical interaction to some degree, whereas the repulsion is effectively amplified for $U > 0$. As a final word to the mean-field phase diagram, we would like to mention that the transition between the Mott/CDW phase is quite trivially reproduced i.e. $U \approx 2V$, which is only asymptotically correct in lowest order in J [187].

7.5 Numerical Investigation of The Phase Diagram

As we have seen in the last section the Gutzwiller mean-field approach is insufficient to explain the non-trivial gapped phases of the extended anyon-Hubbard model, while some generalities about there emergence or fate with respect to statistical transmutation can already be understood at this level. In this upcoming section these issues are addressed via a full numerical investigation by means of a large-scale Density-Matrix Renormalization Group ($DMRG$) analysis [170,171,173]. The various available $DMRG$ algorithms are the methods of choice for the investigation of ground-state properties of one-dimensional non-integrable and gapped quantum many-body Hamiltonians, for system sizes L that make exact diagonalization numerically unfeasible. The inapplicability of exact methods arises through the fact that the total Hilbert space dimension of a given problem $\dim\mathcal{H}_{\text{tot}}$ is multiplicative in the local Hilbert space dimension $\dim\mathcal{H}_{\text{loc}}$, i.e.

$$\dim\mathcal{H}_{\text{tot}} = (\dim\mathcal{H}_{\text{loc}})^{L}, \tag{7.41}$$

meaning that the quantity grows exponentially with the system size L [215, 216]. Even if the dimension in **Eq**. (7.41) may be effectively reduced by the application of matrix sparsity patterns or block-diagonalization via symmetries, a generic Hamiltonian remains numerically intractable for large system sizes [170,171,173,216]. This inevitable problem has to be approached by approximate methods, as for example the mean-field approach in the last section, or quasi-exact methods whose precision is only limited by the available computational power. The guiding principle of the success of the $DMRG$ method in one spatial dimension, is that the actual ground-state of the system resides in an extremely small subspace of **Eq**. (7.41), that distinguishes oneself by the exclusively small entanglement and the relatively quick decay of correlations [215, 217]. Instead of introducing the numerical method and its variants itself, as this thesis partially concerns only the analytical part complementary to the corresponding numerical investigations in the PhD thesis of Kevin Jägering [17], we would rather like to discuss the reasons of its supremacy in describing especially gapped phases in one dimension. Thereby the focus is on the theoretical foundations which make the $DMRG$ algorithm the method of choice in one dimension and the quantities that are used to describe the phases and their transitions.

7.5.1 Correlations for Gapped Phases

As already highlighted in the discussion of phases in the λ-D model, unique and gapped phases have the remarkable feature that the covariance of any correlation, of an operator

$\hat{O}_j$ with itself at a different place $\hat{O}_i$, quickly decays in distance [216, 218, 219], i.e.

$$|\mathrm{cov}\left(\hat{O}_i\hat{O}_j\right)| \leq Ce^{-|i-j|/\xi}||\hat{O}_j||||\hat{O}_i||; \quad \xi = 2v/\Delta E, \quad C = \text{const.}, \tag{7.42}$$

a fact that is not only restricted to simple, symmetry-compatible, product states, as in **Eq**. (7.11). In **Eq**. (7.42) ξ denotes the correlation length which is composed of the energy gap ΔE and the Lieb-Robinson velocity v. The group velocity v itself, is a measure how quickly perturbations can spread temporally across the system [220], i.e.

$$|||[\hat{O}_i(t), \hat{\tilde{O}}_j]||| \leq ce^{-a(|i-j|-vt)}; \quad c, a = \text{const.}, \tag{7.43}$$

where $[\hat{O}_i(t), \hat{\tilde{O}}_j]$ denoted a commutator of two arbitrary operators, and $\hat{O}_i(t)$ is a temporally evolved operator[11]. Interestingly the Lieb-Robinson bound in **Eq**. (7.43) is unrelated to a particular state of the system but solely on the Hamiltonian governing the dynamics.

From **Eq**. (7.42) one sees that ξ is a measure of how quickly correlations decay in a given system, whereas the quantity is diverging with a vanishing energy gap. Thus, numerically gapped phases are easier to resolve as gapless ones, in the sense that they need in general smaller system sizes to show the full decay of correlations [173]. For example, the gapless Luttinger liquid shows an algebraic decay of dominant correlations [43], which falls of much slower than **Eq**. (7.42). In addition, ξ is also useful to detect phase transitions, as by definition both phases have the same energy there and the transition line is gapless. Furthermore, even the asymptotic divergence of ξ can be characteristic for particular transitions [221, 222], and thus can be used as a tool to classify them.

7.5.2 Entanglement Entropy and the Area Law Conjecture

A special property of one-dimensional, gapped Hamiltonians can be conveniently formalized by means of the entanglement entropy [215, 223]. The quantity is defined as the Von Neumann entropy [216, 223], i.e.

$$S(\hat{\rho}) = -\mathrm{tr}\hat{\rho}\ln(\hat{\rho}) \tag{7.44}$$

of the so-called reduced density matrix $\hat{\rho} \equiv \hat{\rho}_{R,L}$, obtainable by partially tracing out a sub-system from the pure density matrix,

$$\hat{\rho}_{R,L} = \mathrm{tr}_{L,R}\hat{\rho}. \tag{7.45}$$

The entanglement entropy in **Eq**. (7.44) is thereby equivalent for each L, R following from the Schmidt decomposition of an arbitrary pure state into two orthonormal

[11] In both **Eq**. (7.42) and **Eq**. (7.43) the symbol $||\cdot||$ denotes the operator norm, or loosely speaking the strength of an operator.

bases [223, 224], but what can we learn from it? Well, if the groundstate is assumed to be pure, its Von Neumann entropy has to vanish by definition, but this is not necessarily the case for the entanglement entropy. Namely, if both sub-systems are in product form, and fully un-entangled, they are mutually independent implying that $S(\rho_{L,R}) = 0$. If they depend on each other, on the other hand, than it follows that $S(\rho_{L,R}) > 0$, and the two compartments are entangled.

The measure $\mathrm{S}(\rho_{L,R})$ is furthermore the object of interest in the famous area law conjecture [215]. This conjecture basically states, that the entanglement entropy of the ground-state of a d dimensional quantum system scales with its $(d-1)$-dimensional surface [216], i.e.

$$S(\rho_{L,R}) \approx \mathcal{O}\left(L^{d-1}\right) + ..., \tag{7.46}$$

where "..." indicates potential, sub-dominant corrections. **Eq**. (7.46) is actually a mathematical theorem for local and gapped one-dimensional Hamiltonians, whereas generic results for higher dimensional systems are relatively scarce [215]. Gapless phases on the other hand, that arise as superfluids or critical phases on a phase boundary, scale logarithmically in the correlation length ξ, i.e.

$$S(\rho_{L,R}) \propto c \ln(\xi), \tag{7.47}$$

with c being the central charge of the underlying two-dimensional conformal field theory [225][12]. The results in **Eqs**. (7.46) and (7.47) are crucial for the numerical evaluation of the phases of one-dimensional systems in the following sense. While **Eq**. (7.46) implies that such gapped ground-state phases can be efficiently approximated by matrix-product states with small local dimension and a comparably small set of variational parameters, **Eq**. (7.47) can be used to classify phase transitions or gapless phases by the characteristic central charge c of their conformal field theory [221, 222, 225]. Besides of that one can obtain additional information about the order of a phase transition, see for example in **Fig**. (7.3), by the smoothness of $S(\rho_{L,R})$, and its derivative across the transition, in analogy to the classical thermodynamical entropy [221, 222].

[12]The central charge c is defined as the scaling factor, of the lowest order contribution, of the operator product expansion of the Stress-Energy tensor $T(u)$ with itself, i.e. $T(z)T(u) \approx \frac{c/2}{(z-u)^4} + ...$ The Stress-Energy tensor $T(u)$ is thereby a characteristic property of the two-dimensional conformal field theory and so is its central charge c [225].

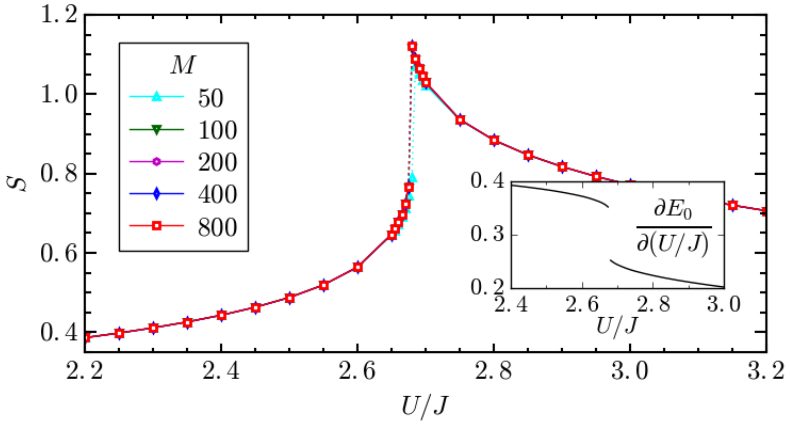

Figure 7.3: *Entanglement entropy S, following from* **Eqs**. *(7.44) and (7.45), and the partial derivative of the ground state energy E_0 of* **Eq**. *(7.1) with the parameter U (inset) plotted over U/J at $V = 3.0, \theta = \pi$ across the CDW to MI transition line. While the entropy shows a characteristic cusp, the first derivative of E_0 is discontinuous, indicating a 1st order transition. Data from iDMRG, $M = 50$ to $M = 800$. The numerical preparation and documentation of the results was performed in the PhD thesis of Kevin Jägering [17].*

7.5.3 Fidelity and it's Susceptibility

Another useful quantity to observe the occurrence of phase transitions in the framework of $DMRG$ is the fidelity of quantum states F and especially its susceptibility χ [223,226]. The fidelity is defined as the absolute value of the overlap between a quantum state $|\Psi(\lambda)\rangle$ depending on a parameter λ with a state with a slightly shifted parameter$|\Psi(\lambda + \delta\lambda)\rangle$ [223, 226],i.e.

$$F = |\langle\Psi(\lambda)|\,|\Psi(\lambda + \delta\lambda)\rangle\,|. \tag{7.48}$$

As the quantity in **Eq**. (7.48) may change too smoothly for small $\delta\lambda$ inside a phase, or too rapidly in the vicinity of a phase transition to be a useful detection tool[13], it is convenient to define its logarithmic derivative [226],

$$\chi_F = -\frac{\partial^2 \ln(F)}{\partial\delta\lambda^2}|_{\delta\lambda=0}. \tag{7.49}$$

The susceptibility in **Eq**. (7.49) is in general an extensive function inside a phase, but is maximal or even divergent in the vicinity of a phase transition. Thus one can additionally relate χ to a thermodynamic quantity, in analogy to the entanglement entropy.

In general, the fidelity susceptibility χ and the entanglement entropy $S(\rho_{R,L})$ are

[13] In general the quantum fidelity of a many-body system vanishes exponentially with the system size [226].

formidable tools in the study of quantum phase transitions in one dimension, e.g. see **Fig**. (7.4). Especially important is thereby the fact that they are solely dependent on the states of the Hilbert space itself, and thus do not require any a priori knowledge about the occurring phases and transitions. Nevertheless one is usually aware of some information concerning the phases of a Hamiltonian. This is achieved either by analogy to similar models, as in our case to the λ-D model, or educated guesses based on a symmetry breaking pattern, as we have used for the Ising anti-ferromagnet. In the next subsection we discuss the order parameters for the investigation of the phase-diagram of the extended anyon-Hubbard model.

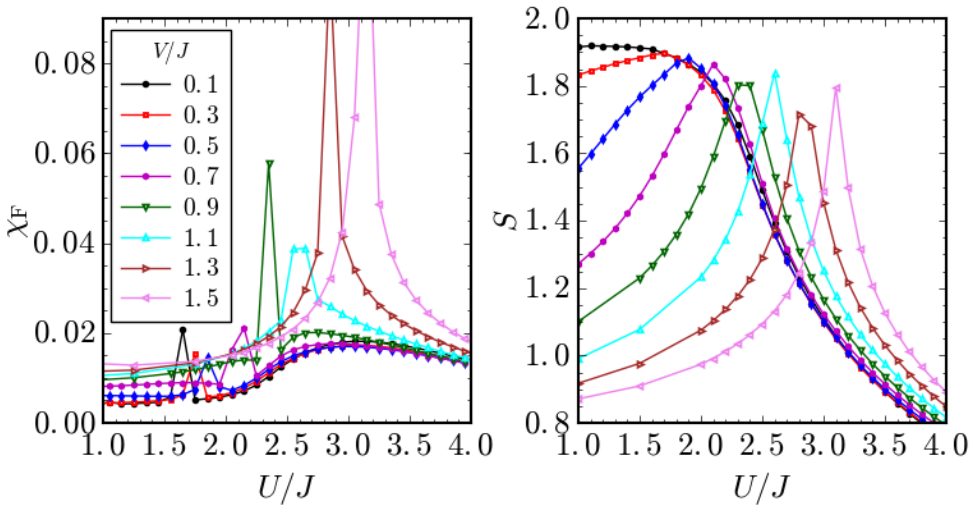

Figure 7.4: *Fidelity susceptibility χ_F (left) and entanglement entropy S (right), as in* **Eqs**. *(7.49), (7.44) and (7.45) respectively, plotted over U/J across the Haldane to Mott transition for various fixed values of V. The change of a rather smooth behavior to sharp function for both quantities in U and V, indicates the evolution from an adiabatic passage to a second-order transition. Data shown from iDMRG, $M = 400$ in the PhD thesis of Kevin Jägering [17].*

7.5.4 Order Parameters and their Scaling

As explained before, our extended anyon-Hubbard model in **Eq**. (7.1) can be viewed as a particular deformation of the λ-D model in **Eq**. (7.8) [187,195], and so we may use its order parameters to draw the phase diagram. This deformation, which precisely inherits the difference between a spin-1 and a constrained bosons in **Eq**. (7.3), is furthermore of higher-order operator content as the ordinary interactions in the λ-D model [187]. Hence one could be tempted to conclude that such corrections might be completely irrelevant for low enough energies, as long as they obey the same symmetries as the spin model. Conversely, we have seen in **Eq**. (7.5) that even the constrained bosons at $\theta = 0$, transform non-linearly with respect to the x, y parts of the dihedral group in **Eq**. (7.6), and so the extended anyon-Hubbard model may break those symmetries

in the low-energy sector. A finite statistical parameter may additionally break parity and bosonic time-reversal symmetries, due to the density-dependent Peierls phase [185]. Hence we conclude that whenever such symmetry incompatible terms become relevant for low energies, the Haldane and the Mott phase are adiabatically connected, as all the protecting symmetries are broken [187, 196], see **Fig**. (7.4). From comparison to the dual λ-D model in **Eq**. (7.25) it is furthermore indicated that a possible symmetry breaking pattern in the dual Haldane phase of the extended anyon-Hubbard model is, strictly speaking, only possible for the longitudinal π-rotation in spin space. As, the remaining directions are explicitly broken and these perturbations are non-locally extended over the hole lattice and thus not understandable by Landau theory. So the hidden order, as in **Eq**. (7.26), is in our case restricted to, or at least dominant in, the z-direction implying either a very small value or exponential decay of the others [187], as shown in **Fig**. (7.5).

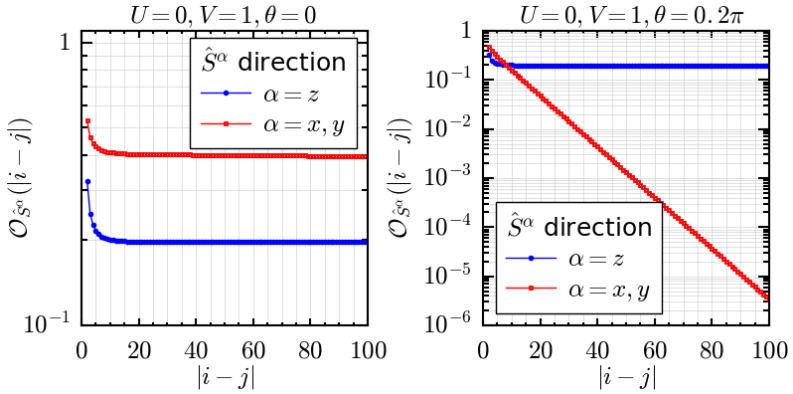

Figure 7.5: *Measurement of the string-order parameters $\mathcal{O}_{\hat{S}^\alpha}$ defined in* **Eq**. *(7.24) and translated to bosonic operators via* **Eq**. *(7.3), deep in the Haldane phase. Measured via DMRG with open boundary conditions with $L = 200$ and $M = 500$ with $i = 50$ and $j = 51..150$ to minimize boundary errors. These results indicate a clear difference between the Haldane phase in spin or bosonic systems, as anticipated by symmetry arguments. The numerical preparation and documentation of the results was performed in the PhD thesis of Kevin Jägering [17].*

Before we show the table of order parameters in **Tab**. (7.7), that have been used for the numerical evaluation of the phase diagram, we have to comment on the single phase that we cannot relate to any of the λ-D model [190, 191, 195]. The so-called Dimer phase, first encountered in **Ref**. [33], appears for large statistical parameters and is identified in our case with the $SF2$ phase of the Gutzwiller approach in **Fig**. (7.2). Sadly, there does not exist a microscopic description of the phase yet, but in analogy to dimerized phases in spin chains one could use the fact that $\langle \hat{H}_{\text{even}} \rangle \neq \langle \hat{H}_{\text{odd}} \rangle$, as a possible indication for the new phase [227]. From a numerical point of view this is indeed sufficient to fully classify this phase but does not provide a microscopic picture, nor a symmetry breaking pattern [211]. A reason for this is that the measure $\langle \hat{H}_{\text{even}} \rangle \neq \langle \hat{H}_{\text{odd}} \rangle$

is explicitly parameter dependent, instead of being only implicitly dependent via the expectation value. Thus, it does not feature a simple interpretation as the usual local order parameter of dimerized spin chains [227], i.e.

$$\hat{O}_{\mathrm{DIMER}}(j) = (-1)^j \vec{S}_j \cdot \vec{S}_{j+1}, \tag{7.50}$$

nor does the Hamiltonian in **Eq**. (7.1) has an explicit dimerization or two-site hopping. Later on this issue will be addressed by deriving a microscopic order parameter from the set of all possible local order parameters and further field-theoretical considerations based on spin-charge separation [8].

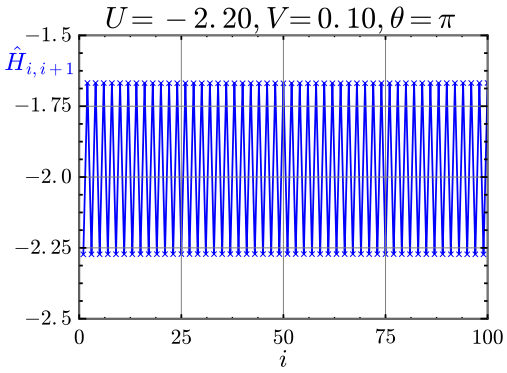

Figure 7.6: *Bond energy $\hat{H}_{i,i+1}$ of* **Eq**. *(7.1), as a function of i in the dimerized phase. $\hat{H}_{i,i+1}$ is thereby measured in the center 100 sites of a DMRG simulation of $L = 200$ sites with open boundary conditions and a cutoff dimension $M = 400$. The numerical preparation and documentation of the results was performed in the PhD thesis of Kevin Jägering [17].*

Phases	ΔE	Density	Order parameter
Mott Insulator (MI)	> 0	$\langle n \rangle = 1$	$\hat{O}_{\mathrm{P}}(j) = e^{i\pi \sum_{l<j} (\hat{n}_l - 1)}$
Charge Density Wave (CDW)	> 0	$\langle n \rangle \neq 1$	$\hat{O}_{\mathrm{CDW}}(j) = (-)^j (\hat{n}_j - 1)$
Haldane Insulator (HI)	> 0	$\langle n \rangle = 1$	$\hat{O}_{\mathrm{HI}}(j) = (\hat{n}_j - 1) e^{i\pi \sum_{l<j} (\hat{n}_l - 1)}$
Superfluid (SF)	$= 0$	$\langle n \rangle = 1$	$\hat{O}_{\mathrm{Sf}}(j) = \hat{b}_j$ power-law decay
Paired Superfluid (PSF)	$= 0$	$\langle n \rangle = 1$	$\hat{O}_{\mathrm{PSf}}(j) = \hat{b}_j^2$ power-law decay
Dimerized Phase (DIMER)	> 0	$\langle n \rangle = 1$	$\langle \hat{H}_{\mathrm{even}} \rangle \neq \langle \hat{H}_{\mathrm{odd}} \rangle$

Figure 7.7: *Overview over the phases of* **Eq**. *(7.1) with arbitrary $\theta \in [0, \pi]$ at integer filling, showing in order the abbreviation, energy gap ΔE, local density $\langle n \rangle$ and the numerically used order parameters in [17].*

For second order phase transitions, the order parameter concept provides a tool to detect phase transitions and furthermore helps to classify them in terms of universality classes, which is a collection of models approaching the same scaling limit in a

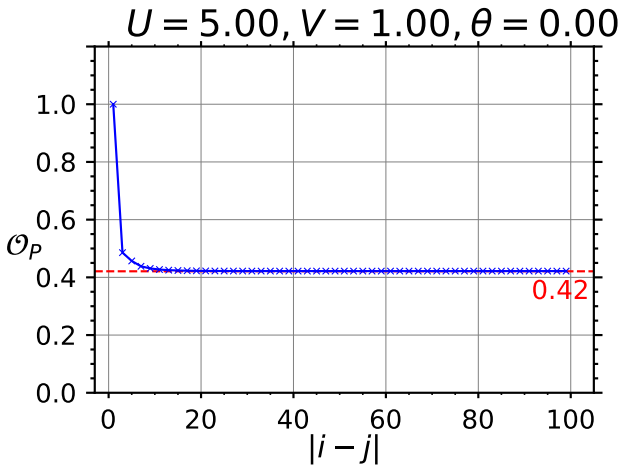

Figure 7.8: *$\mathcal{O}_P$ defined in* **Eq.** *(7.27) as a function of the distance $|i-j|$, indicating hidden long-range order in the Mott (large D) phase. Measured with DMRG using $L = 200$ with (twisted) periodic boundary conditions and a cutoff dimension $M = 400$. The numerical preparation and documentation of the results was performed in the PhD thesis of Kevin Jägering [17].*

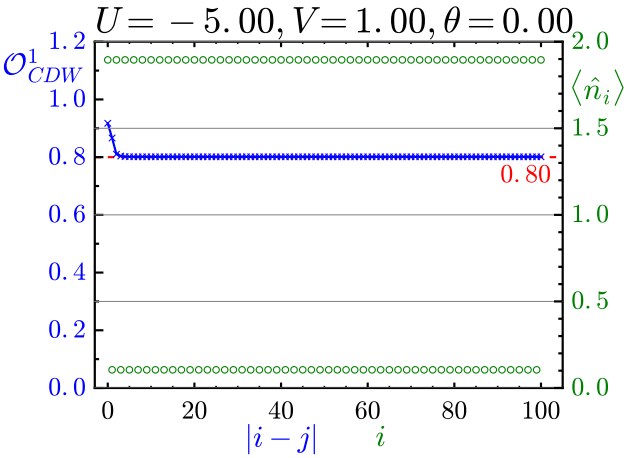

Figure 7.9: *$\mathcal{O}^1_{\mathrm{CDW}}$ from* **Eq.** *(7.19) and the local densities $\langle \hat{n}_i \rangle$ on even and odd sub-lattices plotted over the site distance $|i-j|$ and the site i respectively, in order to show the presence of long-range order and the inhomogeneous density profile. Measured with DMRG using $L = 200$ with (twisted) periodic boundary conditions and a cutoff dimension $M = 400$. The numerical preparation and documentation of the results was performed in the PhD thesis of Kevin Jägering [17].*

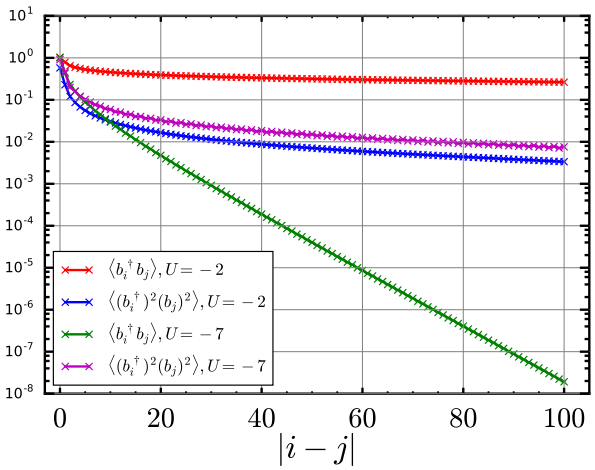

Figure 7.10: *Logarithmic plot of the single-particle or pair correlation function inside the gapless phases. The plot shows either characteristic algebraic decay (red, purple and blue data) or exponential decay (green data) clearly distinguishing the superfluid ($XY1$) and pair-superfluid ($XY2$) phases, measured via DMRG with open boundary conditions with $L = 200$ and $M = 500$. The numerical preparation and documentation of the results was performed in the PhD thesis of Kevin Jägering [17].*

renormalization group sense [211, 221, 222]. A consequence of that common scaling limit is for example that order parameters have an equivalent critical scaling around the phase separation in a reduced parameter $\tilde{\lambda}$, i.e.

$$\lim_{\tilde{\lambda}\to 0^{\pm}} \hat{O}(\tilde{\lambda}) \propto \tilde{\lambda}^{k}, \quad \tilde{\lambda} = (\lambda - \lambda_{\text{crit}})/\lambda_{\text{crit}}. \tag{7.51}$$

The proportionality sign in the thermodynamic relation **Eq**. (7.51) , indicates that the amplitudes may differ depending on the site from which the transition is approached, whereas their ratio is again universal [221, 222]. The critical exponent k, denoting the degree of homogeneity, surely depends on the specific choice of the order parameter, whereas the requirements of analytic and numerical investigators may differ in the following sense. Numerically, any observable that is characteristic in the sense of an order parameter is a valid tool to distinguish between two phases, whereas this choice is consequently non-unique. On the other hand this is rather unsatisfactory in view of **Eq**. (7.51), as different choices hinder the unique classification of universality. Therefore, it is advisable to consider an order parameter that is adapted to the symmetry but cannot be reduced into smaller constituents anymore, and so different models can be uniquely compared [228][14].

[14] As an example for this circumstance one can think of an order parameter $\hat{O}$, deduced by symmetry, and a symmetry compatible function of it $\hat{f}(\hat{O})$. While both choices can be used to mark the transitions, there critical exponents differ in general [228].

Another issue of the numerical investigation is that relations as in **Eq**. (7.51) refer to a thermodynamic systems, which clearly cannot be computed by standard methods, instead a finite size scaling has to be performed for all quantities. In the case of **Eq**. (7.51) this can be cured by assuming that the order parameter is a homogeneous function of the reduced parameter $\tilde{\lambda}$ and the length L [229],

$$\hat{O}(\tilde{\lambda}) \equiv L^{-\beta/\nu}\hat{O}(\tilde{\lambda}L^{1/\nu}), \tag{7.52}$$

where $\hat{O}(\tilde{\lambda}L^{1/\nu})$ denotes a characteristic scaling function. The exponent β in **Eq**. (7.52) corresponds thereby to the thermodynamic one in **Eq**. (7.51), whereas ν quantifies the length scaling behavior of the order parameter by approaching this limit. These exponents can then be obtained by varying them such that the different scaling functions $\hat{O}(\tilde{\lambda}L^{1/\nu})$ converge to a common point, for different L. Also in this case it cannot be excluded that different choices of order parameters correspond to different length scaling coefficients ν, thus one should be careful about the definition of it in order to avoid ambiguities in the classification of universality classes.

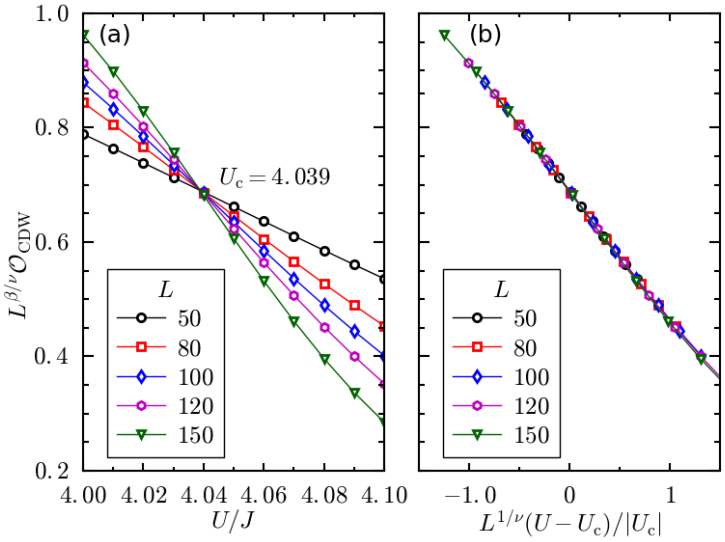

Figure 7.11: *Data collapse of $\mathcal{O}_{CDW}$ order parameter defined in* **Eq**. *(7.52) along the HI to CDW transition line. The plot is shown for $V = 3.0, \theta = 0$ as a function of U/J for different lengths, i.e. $L = 50$ to $L = 150$. Best fitting points for a transition at critical coupling $U_c = 4.039(2)$ and exponents $\beta = 0.247(4)$ and $\nu = 1.03(3)$. The numerical preparation and documentation of the results was performed in the PhD thesis of Kevin Jägering [17].*

7.5.5 BKT Transitions and Level Spectroscopy

So far we were mostly concerned about quantities to describe second-order phase transitions, according to the Ehrenfest classification [221, 222]. Thereby a kth order

transition is defined such that the first discontinuity in a thermodynamic potential appears in its $k-$th derivative, making it a non-analytic function at the phase boundary, i.e. at $\tilde{\lambda} = 0$. Exaggerating this concept one could ask the question, if there are phase transitions of $k = \infty$ order, which we mean in the sense that the thermodynamic potentials are infinitely differentiable but non-analytic? This is indeed the case for the famous Berezinski-Kosterlitz-Thouless (BKT) transition [230–232], whose defining relation can be expressed by an essential singularity of the correlation length ξ near the critical point separating a gapped and a gapless phase [233], i.e.

$$\begin{gathered} \xi \propto e^{c/\sqrt{\tilde{\lambda}}}; \quad c > 0, \\ F_{\text{singular}} = \begin{cases} \xi^{-2}, & \tilde{\lambda} > 0, \\ 0, & \text{else}, \end{cases} \end{gathered} \tag{7.53}$$

and its connection to the singular part of the free energy F_{singular}. The thermodynamic potential in **Eq**. (7.53) is indeed differentiable to all orders but is non-analytic at the critical point, a fact that can be checked for example from the non-existence of a corresponding Taylor series of F_{singular} around $\tilde{\lambda} = 0$.

We can see from **Eq**. (7.42), that the energy gap ΔE is proportional to the inverse correlation length ξ^{-1}, thus such transitions are generally difficult to investigate numerically, as the gap vanishes exponentially in the thermodynamic limit. For finite systems on the other hand, the gap in the vicinity of the transition can be found by a scaling ansatz [234],

$$L\Delta E(L)\left(1 + \frac{1}{2\ln(L) + C}\right) = X(\xi/L); \quad C = \text{const}, \tag{7.54}$$

with the corresponding scaling function $X(\xi/L)$. **Eq**. (7.54) accounts thereby to the logarithmic correction of $\Delta E(L)$, that are characteristic for such transitions and finally the reason why they are also challenging for finite L. This issue can be addressed more elegantly by the method of level crossing spectroscopy [235]. Namely, investigating the energy differences of some wisely chosen representative, excited states of the involved phases, let's call them phase α and β, might cancel those corrections exactly, e.g.

$$\Delta E(L) \equiv \Delta E_\alpha(L) - \Delta E_\beta(L). \tag{7.55}$$

The transition can then be found from **Eq**. (7.55), with the help of exact diagonalization, by varying the physical parameters until the gap vanishes and a subsequent finite size scaling of that quantity. The representative states in our investigation are chosen in analogy to previous works on spin chains, which are for the gapped phases just the first

excited state at unit filling [236], i.e.

$$|\Psi_{\text{rep.}}(\text{MI, HI, CDW})\rangle = |\Psi_{1,\text{N=L}}(\text{MI, HI, CDW})\rangle\,. \tag{7.56}$$

For the representative state of the superfluids we slightly symmetrize the expression for the XY phases in spin chains for 4 particles more or less in the groundstate [236] , i.e.

$$|\Psi_{\text{rep.}}(\text{SF})\rangle = \frac{1}{2}\Big(\,|\Psi_{\Delta N=4}(\text{SF})\rangle + |\Psi_{\Delta N=-4}(\text{SF})\rangle\,\Big), \tag{7.57}$$

due to the expected absence of particle-hole symmetry in our intrinsically bosonic system [187].

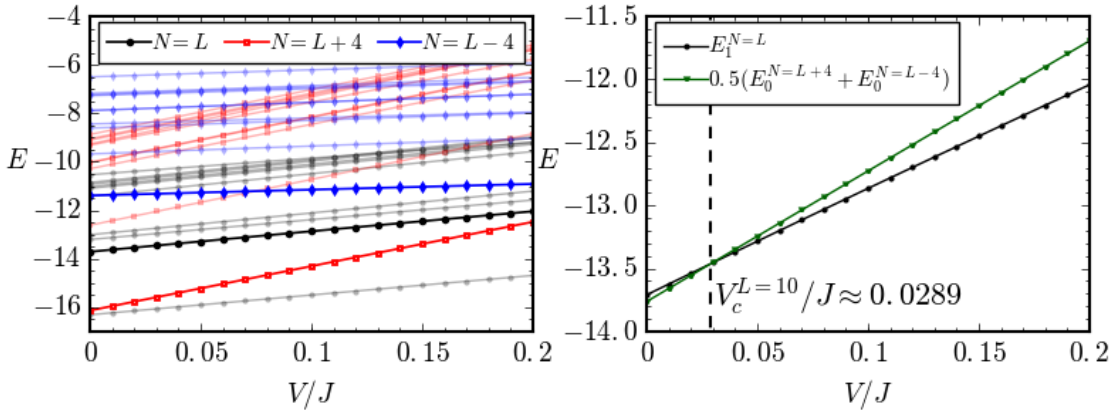

Figure 7.12: *Left: Energy spectra for $k = 0$ at integer filling $N = L$ and with $N = L \pm 4$ particles at fixed $U/J = 0$ and $\theta = 0$ across the SF to HI transition calculated by exact diagonalization for $L = 10$ sites from* **Ref**. *[17]. Non-representative levels of the phases are drawn transparently here, while representative ones are in-transparent. Right: Crossing of the 'representative levels that correspond to $|\Psi_{\text{rep}}(SF)\rangle$ in* **Eq**. *7.57 green (average of bold red and blue level in left plot) and $|\Psi_{\text{rep}(HI)}\rangle$ in* **Eq**. *(7.56) black (bold black level in left plot) gives phase transition point $V_c^{L=10}/J \approx 0.0289$. E_n^N denotes the energy of the n-th particle excitation of the N-particle sector.*

7.5.6 Phase Diagram for $\theta \approx 0, \pi$

As the full information about the phases in the extended anyon-Hubbard, and their fate with respect to statistical transmutation, are difficult to obtain in its full glory, we focus mostly on the cases $\theta = 0, \pi$, see **Figs**. (7.13) and (7.15). We find in general that for very small θ or large statistical parameters starting from $\theta \approx 0.9\pi$, the phase topography is qualitatively the same as in the $\theta = 0, \pi$ cases. In **Fig**. (7.13) the $\theta = 0$ case is shown with a phase diagram almost identical to the λ-D-model [190, 191, 195], except slight differences [185]. In the parameter regime that is considered here, the gapped phases are dominating, where the large V, D orders are separated by a Haldane phase at intermediate values. The Haldane phase itself shows thereby an anisotropy, or even

exponential decay in x, y-direction, in its non-local hidden orders contrary to the spin chain [187], as shown in **Fig**. (7.5). Interestingly, around $V \approx 0$ there exist relatively small superfluid shells corresponding to the $XY1$ and $XY2$ phases respectively [195], see **Fig**. (7.14), that only appear for negative anisotropies in the spin model. Conversely, this means that the correlated spin flips, arising through the bosonic nature of the particles, can have an attractive effect on neighboring lattice points and induce an effectively negative V. One sees in addition, that superfluid behavior is more stable for attractive onsite interaction [187], whereas for large values above $U = -6J$ it is energetically favorable to quasi-condense in pairs. In general, superfluidity seems to be less robust with respect to nearest neighbor interactions than with respect to onsite ones.

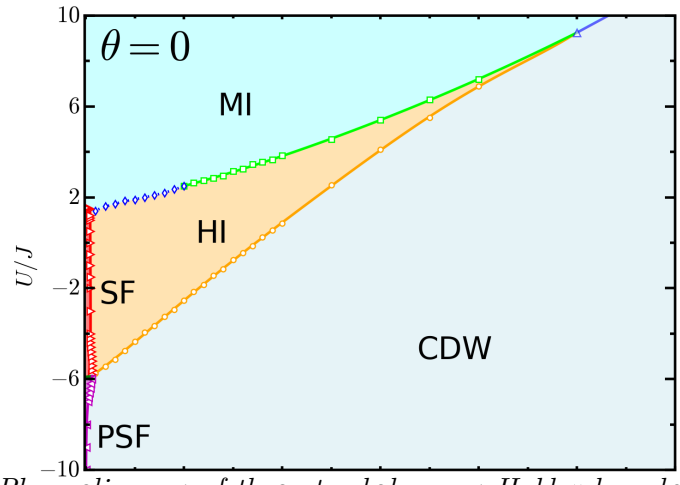

Figure 7.13: *Phase diagram of the extended anyon-Hubbard model in* **Eq**. *(7.1) in the bosonic limit at $\theta = 0$. Phase transitions between gapped phases are determined by peaks in fidelity susceptibility χ_F, correlation length ξ and entanglement entropy S from DMRG ($M = 400$), e.g.* **Fig**. *(7.21) [17]. It should be noted again, that the correlation length is obtained via the transfer-matrix, instead of calculating the decay of correlators, see* **Ref**. *([17]) for the details. Gapless to gapped BKT transitions are calculated via level crossing spectroscopy with exact diagonalization, as shown for example in* **Fig**. *7.12, for $L = 8$ to $L = 18$ sites and further supported by DMRG calculations with up to $L = 32$ sites, extrapolated to $L = \infty$ [17].*

For $\theta \approx \pi$ the phase diagram is displayed in **Fig**. (7.15), where the intermediate Haldane insulator is now completely exchanged with the Dimer phase. Thereby the occupied area in the phase diagram is much smaller and strongly shifted towards negative U and smaller V, implying that the Dimer phase is relatively unstable to perturbations. Furthermore we can conclude that the statistically mediated interaction is quite strong and mostly repulsive in nature, as observed already multiple times in this thesis and in the literature [13, 26, 27, 33]. In analogy to the Haldane insulator, the Dimer phase appears only for intermediate interactions and thus cannot be explained by simple perturbative arguments, a problem that we solve later on by proposing a

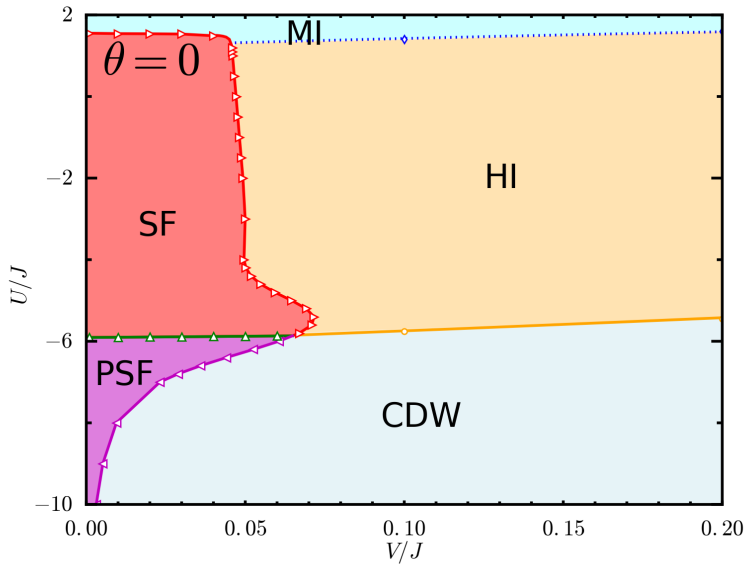

Figure 7.14: *Zoom into small V/J region of phase diagram at $\theta = 0$ shown in* **Ref**. *[17]. All gapped/gapless BKT transitions were determined by level crossing spectroscopy, according to* **Eq**. *(7.55), with exact diagonalization for $L = 8$ to $L = 18$ sites. The results were supported further by DMRG up to $L = 32$ sites, and extrapolated to infinite sizes [17].*

minimal local order parameter. Up to now the new dimerized phase is classified as being a gapped, symmetry breaking phase, as indicated by the mean-field treatment and numerically observed groundstate degeneracy, with uniform density and imbalanced bond Hamiltonians $\langle \hat{H}_{\text{even}} \rangle \neq \langle \hat{H}_{\text{odd}} \rangle$, see **Fig**. (7.6). Indeed this phase seems to be pretty interesting, as it emerges from the interplay of algebraic occupation constraints, statistically induced interactions, and relatively large onsite attraction [33]. In addition we find that besides the non-trivial topological phase, also no ordinary superfluid order can exist for strong statistical interactions at this filling fraction [187].

7.5.7 The Fate of the Haldane Insulator

One of the major questions of this investigation is the stability of the Haldane insulator with respect to statistical transmutation [185]. The mean-field treatment already indicated its stability over a wide range of statistical parameters, whereas it was necessary to identify the two gapless phases with the Haldane and Dimer phase respectively. The circumstance that the non-trivial SPT phase does not vanish instantly for finite but small θ, incorporates in addition the fact that symmetry breaking perturbations need to be sufficiently strong, or relevant in a renormalizations sense, in order to destroy the coherence of the Haldane phase [15] [196, 237]. This means that there exists a critical

[15] In our case we can conclude that this is indeed a renormalization group argument as shown later on by bosonization, but is already implied by the non-perturbative nature of our statistical interactions, i.e. the absolute value of the correlated hopping in **Eq**. (7.1) cannot be much smaller or larger than J itself.

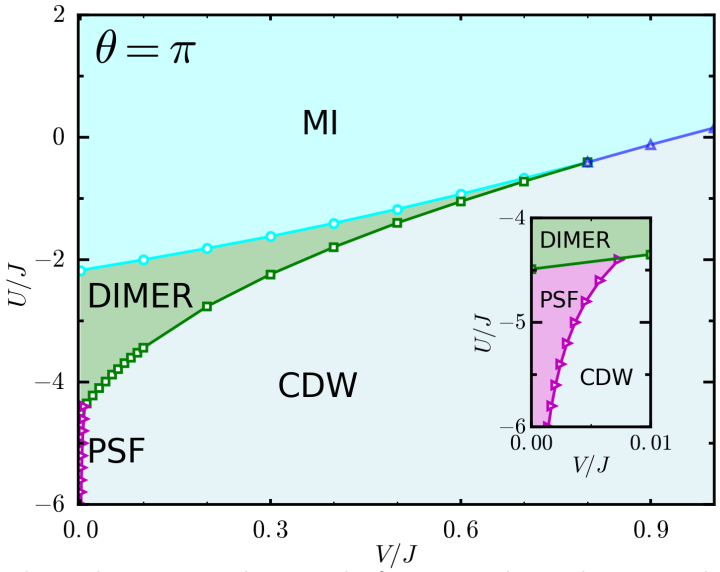

Figure 7.15: *Phase diagram in the pseudo-fermionic limit determined in* **Ref**. *([17]). All phase transitions between gapped phases are obtained by DMRG (M=800) from fidelity susceptibility, entanglement entropy and correlation length, as in* **Fig**. *(7.9). PSF to CDW transition determined by level crossing spectroscopy analogous to* **Fig**. *(7.14).*

value of the statistical parameter up to which the Haldane phase can exist, which we determine by measuring the extent of the Haldane phase in the U direction for different values of V and as a function of θ , see **Figs**. (7.16) and (7.17). From **Fig**. (7.16) we can see that the shrinking of the Haldane phase is rather slow until $\theta \approx 0.3\pi$ and then almost linear up to $\theta \approx 0.7\pi$. Of course, the decay still depends on the nearest neighbor interaction V, whereas the Haldane insulator seems to be more stable for larger values. In **Fig**. (7.17) a more detailed plot is shown with a zoom into the relevant parameter region. One can conclude that there is a set of statistical parameters ranging from $\theta \approx 0.8\pi - 0.9\pi$, where both the Haldane and Dimer phase can coexist, whereas the topological phase eventually fully disappears beyond that. Interestingly, for the value of the statistical parameter where the Dimer and the Haldane phase have the same energy, a 4-critical point is implied where all gapped phases coincide.

7.5.8 Phase Transitions close to the Bosonic Limit

Having discussed the topography of phases in the (U, V) plane for two representative values of θ, we come now to their transitions. Starting with the $\theta \approx 0$ case, we find that all gapless to gapped transitions are of BKT type, as signaled numerically by the smooth behavior of thermodynamic quantities and critical points determined by level spectroscopy, as can be seen for example in **Figs**. (7.18) and (7.14). The transition between the two gapless phases is predicted to be of Ising universality [221, 222], i.e. $c = 1/2, \nu = 1$ and related to a $\mathcal{Z}_2$ symmetry breaking, in analogy to the λ-D

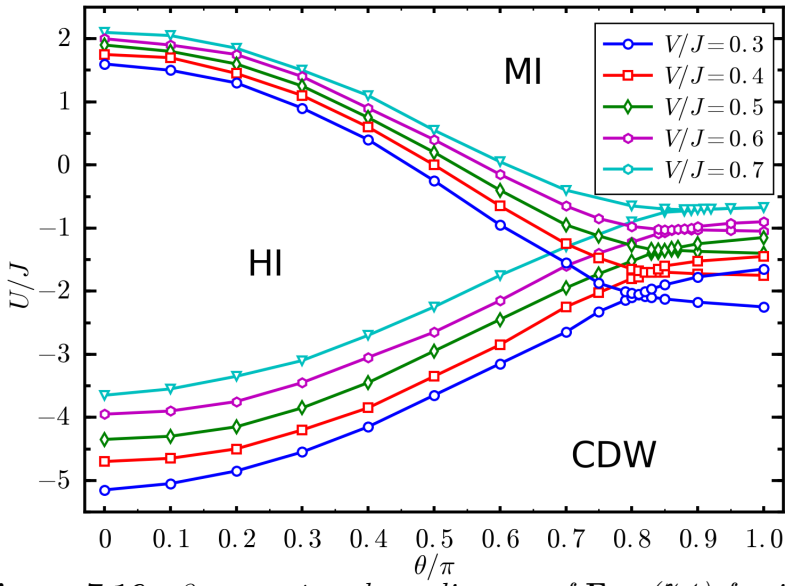

Figure 7.16: *3-parameter phase diagram of* **Eq**. *(7.1) for intermediate* $\theta \in [0, \pi]$ *obtained by DMRG (M=400) in* **Ref**. *[17]. The x-axis corresponds to the normalized statistical phase* θ/π *with the on-site interaction* U/J *displayed on the y-axis. The symbols show the phase transition points and extent of the Haldane and Dimer phases respectively, for fixed* V/J *values according to the plot legend [17].*

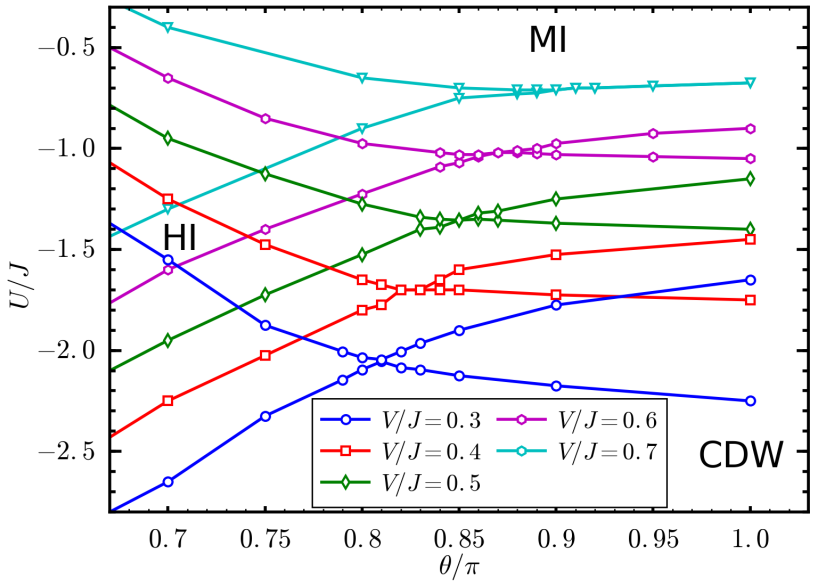

Figure 7.17: *Zoom into the phase diagram in* **Fig** *(7.16) for statistical parameter* $0.7\pi \leq \theta \leq \pi$ *close to the 4-critical points obtained by DMRG calculations, with* $M = 400$, *in* **Ref**. *[17]. The different symbols indicate analogously to* **Fig** *(7.16) the phase boundaries at a two-dimensional slice of the phase diagram for fixed values of* V/J.

model [33, 195]. Unluckily, due to the limited amount of data accuracy obtainable by the level spectroscopy, we can only confirm the order of the phase transitions but not its

specific class, see **Fig**. (7.18). The determination of the transitions between the gapped phases is much more precise on the other hand. Starting from the CDW phase we can clearly find an Ising transition to the Haldane insulator, and a first order one to the Mott phase [187, 196]. The transition of the Mott insulator and the Haldane phase is much more subtle on the other hand. Namely, for relatively small V we find indeed an adiabatic passage between the phases with no signatures of a phase transitions, e.g. indicated by the blue oval points in **Figs**. (7.13), (7.14) and (7.19). This is in agreement with the definition of SPT phases and the breaking of all its protecting symmetries [187, 196]. Furthermore this is a feature not observable in the λ-D model and thus is a purely bosonic/anyonic characteristic [195]. But, this finding seems to be contradictory for $\theta = 0$, as not all the symmetries that protect the Haldane phase are broken, and thus an adiabatic passage should be impossible by definition. For $\theta \neq 0$ on the other hand, all the protecting symmetries are broken and the two phases should be topologically equal, whenever these terms are relevant. This problem can be resolved by means of a field theoretical treatment, which shows that the protecting symmetries have all the same representation in the low-energy degrees of freedom and thus are indistinguishable [187, 196][16]. Conversely, also in the bosonic limit all the protecting symmetries can be broken whenever one of them is. Indeed, this depends on whether these perturbations are relevant, which can be numerically confirmed in a region where the hopping is still comparable to other energy scales. Roughly starting at $V/J \approx 1$, we find a clear evidence of a second-order phase transition between the two phases, i.e. green squares in **Figs**. (7.13), (7.14) and (7.19), and thus the Mott and Haldane insulator are topologically different as the protecting symmetries are all intact [187, 196]. The universality class is called Gaussian, from the unit central charge representing a Gaussian field theory at the transition, and a length scaling coefficient ν that varies along the transition line [238].

7.5.9 Phase Transitions close to the Pseudo-Fermionic Limit

For the pseudo-fermionic limit in **Fig**. (7.20) some features of the phase diagram remain the same, i.e. the transition type between gapless and gapped phases and the first-order transition from the Mott to the CDW phase. A remarkable difference on the other hand between the two limits is the universality class of the transitions to the intermediate phase. Namely we find the Ising-type transition now between the Mott and the Dimer phase, see **Fig**. (7.21), and the Gaussian transition between the two symmetry breaking phases. Interestingly the latter scenario seems not to be captured by the Landau theory, which either predicts a crossover or a first-order transitions between phases with the same symmetry [196, 227]. Nevertheless such an argumentation is up to now spurious in the sense that we have the exact symmetry breaking scheme in the CDW phase

[16] More precisely, some of them are only equivalent up to the compactification radii of chiral fields.

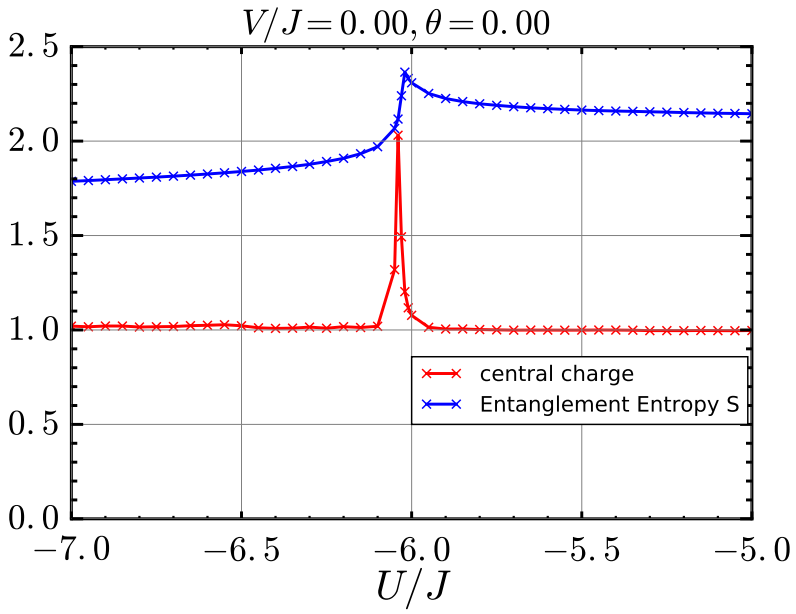

Figure 7.18: *Central charge c and entanglement entropy S measured across the superfluid (right side) to pair-superfluid (left side) transition obtained by DMRG in* **Ref**. *[17],. for $M = 400$ and $M = 800$.*

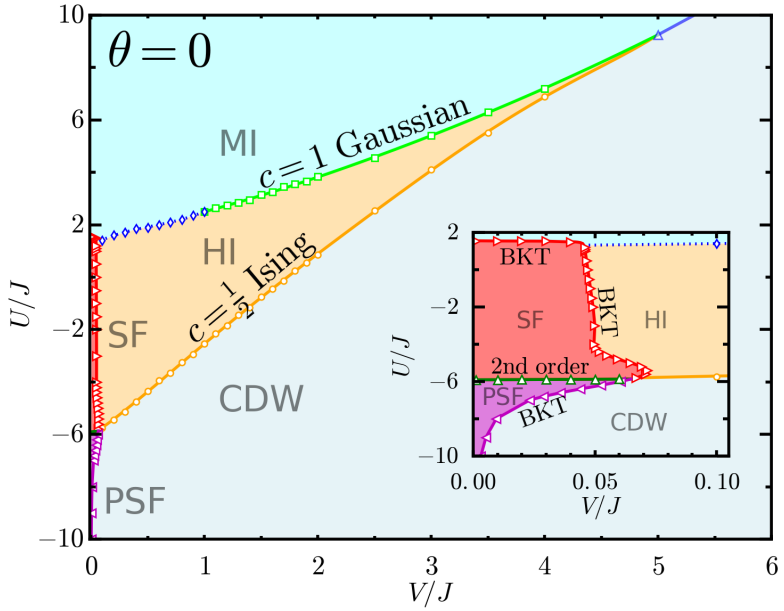

Figure 7.19: *Overview of the determined universality classes and transition orders, obtained numerically in* **Ref**. *[17], for $\theta = 0$ embedded into the phase diagram*

but not for the Dimer yet. Nevertheless, we have strong numerical evidence for this Gaussian transition in form of peaks in thermodynamical quantities, the entanglement entropy scaling of the central charge, as well as the correct critical coefficients obtained

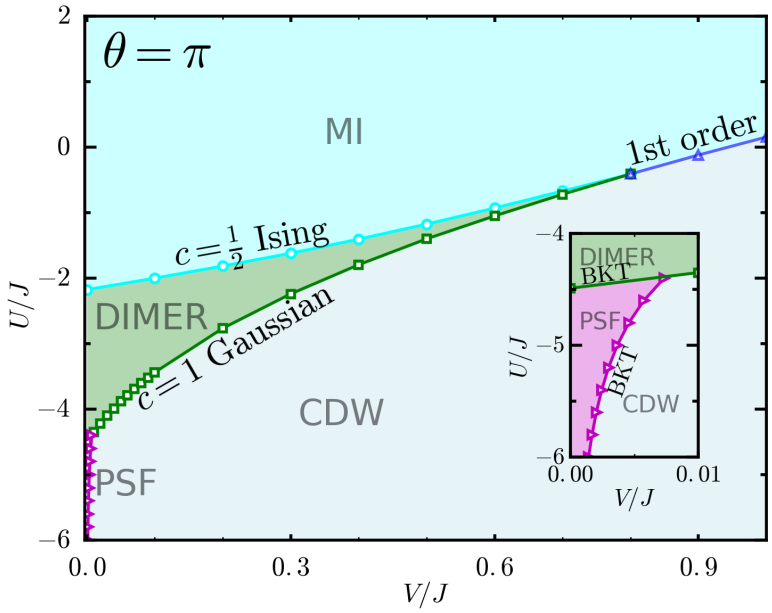

Figure 7.20: *Overview of the determined universality classes and transition orders, obtained numerically in* **Ref**. *[17], for $\theta = \pi$ embedded into the phase diagram.*

by length scaling of the two respective order parameters, see **Fig**. (7.22).

7.6 Bosonization close to the bosonic Limit

We start our field-theoretical investigation by studying the extended anyon-Hubbard model for small statistical deformations. In order to properly bosonize the Hamiltonian we at first map the constrained boson exactly to spin-1 operators according to **Eq**. (7.3) [200], i.e.

$$\hat{b}_l = \frac{1}{\sqrt{2}} \hat{S}_l^+ \left(1 + (1 - \sqrt{2}) \hat{S}_l^z\right), \tag{7.58}$$

and then we use the Schulz decomposition [195], i.e.

$$\hat{\mathbf{S}}_l = \hat{\mathbf{S}}_{l,1} + \hat{\mathbf{S}}_{l,2}. \tag{7.59}$$

In **Eq**. (7.59) a spin-1 operator is represented as a symmetric combination of two spin-1/2 degrees of freedom, which implies an additional permutation symmetry among the two. By choosing a mapping of matrix dimension 4×4, the $S = 1$ representation of the $su(2)$ algebra is clearly not fulfilled on the level of Spin-1 generators. Nevertheless it turns out that the fourth unphysical, or mathematically obsolete, state that is represented by

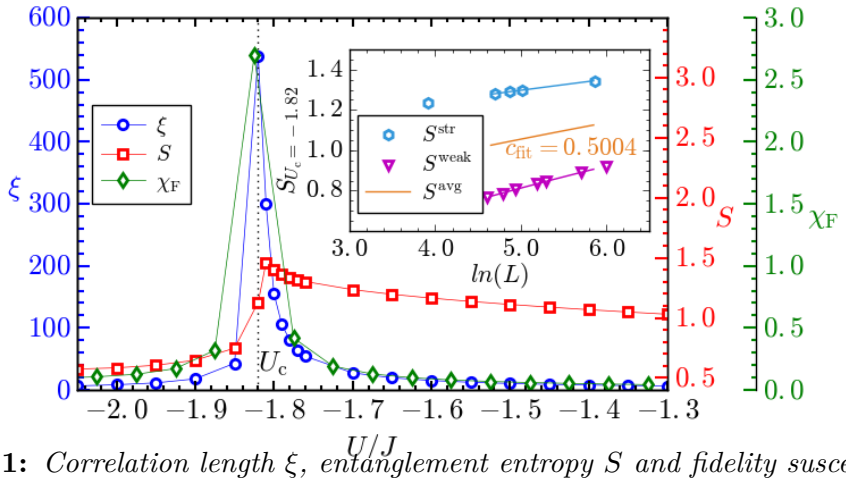

Figure 7.21: *Correlation length ξ, entanglement entropy S and fidelity susceptibility χ_F as a function of U/J along the MI to Dimer transition line at $V = 0.2, \theta = \pi$, showing a 2nd order transition at $U_c = -1.82$. Data obtained from iDMRG, $M = 800$, in the PhD thesis of Kevin Jägering [17]. It should be noted that the correlation length is obtained via the transfer-matrix, instead of calculating the decay of correlators, see* **Ref**. *[17] for the details. Inset shows the entanglement entropy at the transition point $V = 0.2, U_c = -1.82$ plotted over $\ln(L)$. Depending on whether the sub-system division is performed on a strong or weak bond, one obtains central charges corresponding to the slope of S^{str} or S^{weak}. For infinite sizes the average S^{avg} of the two fitting lines is considered instead. The slope of S^{avg} corresponds to a central charge $c = 0.5004$.*

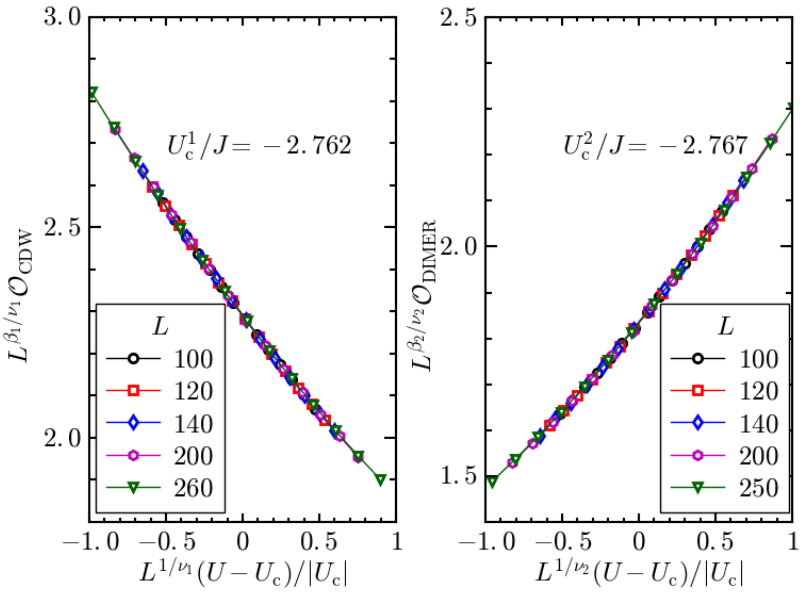

Figure 7.22: *Data collapse of both $\mathcal{O}_{CDW}$ and $\mathcal{O}_{DIMER}$, according to* **Tab**. *(7.7), determined in* **Ref**. *[17]. The observables are measured along the Dimer to CDW transition line at fixed $V = 0.2, \Theta = \pi$ varying U/J. Fitting suggests $U_C^1/J = -2.762(3), \beta_1 = 0.55(2), \nu_1 = 1.50(2)$ for the $\mathcal{O}_{CDW}$ collapse in agreement to $U_c^2 = -2.767(2)/J, \beta_2 = 0.54(1)$, $\nu_2 = 1.48(3)$ for $\mathcal{O}_{DIMER}$. Data from DMRG with $M = 400$ [17].*

the singlet, i.e.

$$|A\rangle =\propto (\hat{S}^{+}_{l,1} - \hat{S}^{+}_{l,2})\,|0\rangle\,, \tag{7.60}$$

cannot be reached in the ground-state manifold of the Hamiltonian of the λ-D-model and its variants [8, 43, 195]. Thus, the mapping of **Eq**. (7.59) becomes exact at the level of the Hamiltonian, as long as only the ground-state is considered, a fact that we will reconsider soon in more detail, following the construction in **Ref**. [8]. Nevertheless, before we can discuss this detail we need to deduce first the form of the spin ladder Hamiltonian that corresponds to the extended anyon-Hubbard model.

The Schulz decomposition leads to the following form of bosonic annihilation operator

$$\hat{b}_l = \frac{1}{\sqrt{2}}(\hat{S}^{+}_{l,1} + \hat{S}^{+}_{l,2})\left(1 + (1-\sqrt{2})(\hat{S}^{z}_{l,1} + \hat{S}^{z}_{l,2})\right). \tag{7.61}$$

where then the kinetic energy of **Eq**. (7.1) can be written as

$$\hat{\mathcal{K}} = -\frac{J}{4}\sum_{l}\left(\hat{\mathcal{K}}^{\mathrm{intra}}_{l,l+1} + \hat{\mathcal{K}}^{\mathrm{inter}}_{l,l+1}\right), \tag{7.62}$$

with the intra- and inter-chain contributions that are each interrelated by permutation of the internal species, i.e.

$$\begin{aligned}
\hat{\mathcal{K}}^{\mathrm{intra}}_{l,l+1} &= \hat{\mathcal{K}}^{\mathrm{intra},1}_{l,l+1} + \hat{\mathcal{K}}^{\mathrm{intra},2}_{l,l+1} = \frac{1}{2}\sum_{q_1\neq q_2}\hat{S}^{+}_{l,q_1}\hat{S}^{-}_{l+1,q_1}\hat{F}^{l*}_{q_2,q_2} + \mathrm{h.c.},\\
\hat{\mathcal{K}}^{\mathrm{inter}}_{l,l+1} &= \hat{\mathcal{K}}^{\mathrm{inter},1,2}_{l,l+1} + \hat{\mathcal{K}}^{\mathrm{inter},2,1}_{l,l+1} = \frac{1}{2}\sum_{q_1\neq q_2}\hat{S}^{+}_{l,q_1}\hat{S}^{-}_{l+1,q_2}\hat{F}^{l*}_{q_1,q_2} + \mathrm{h.c.}.
\end{aligned} \tag{7.63}$$

The lattice gauge functions in **Eq**. (7.63), that lead to correlated spin-flips, dependent on the other chain, are defined as

$$\hat{F}^{l}_{q_1,q_2} = z_1 + z_2\hat{S}^{z}_{l+1,q_1} + z_3\hat{S}^{z}_{l,q_2} + z_4\hat{S}^{z}_{l,q_2}\hat{S}^{z}_{l+1,q_1} \tag{7.64}$$

with complex coefficients depending on θ, i.e.

$$\begin{aligned}
z_1 &= (1+\sqrt{2})(1+\sqrt{2}e^{i\theta})/4,\\
z_2 &= (1-\sqrt{2})(1+\sqrt{2}e^{i\theta})/2,\\
z_3 &= (1+\sqrt{2})(1-\sqrt{2}e^{i\theta})/2,\\
z_4 &= (1-\sqrt{2})(1-\sqrt{2}e^{i\theta}).
\end{aligned} \tag{7.65}$$

On the other hand the interacting part of the bond Hamiltonian representing an attractive/repulsive single-ion anisotropy as well as a nearest-neighbor coupling, is given

by the following form

$$\hat{H}^{\text{int}}_{l,l+1} = \frac{U}{2}\sum_{q_1,q_2}(1-\delta_{q_1,q_2})\hat{S}^z_{l,q_1}\hat{S}^z_{l,q_2} + V\sum_{q_1,q_2}\hat{S}^z_{l,q_1}\hat{S}^z_{l+1,q_2}. \tag{7.66}$$

7.6.1 The Elegance of the Schulz Mapping

Before we start the actual bosonization procedure of our ladder compound, we formalize the former statement about the appearance of the singlet state on the level of the Hamiltonian composed of **Eqs**. (7.62) and (7.66) [8], i.e.

$$\hat{H} = \hat{\mathcal{K}} + \sum_l \hat{H}^{\text{int}}_{l,l+1}. \tag{7.67}$$

Thereby we neglect the lattice gauge functions $\hat{F}^l_{q_1,q_2}$ in the kinetic energy for simplicity, yielding

$$\hat{H} \approx -\frac{J}{4}\sum_l \left[\hat{S}^+_{l,1}\hat{S}^-_{l+1,1} + \hat{S}^+_{l,1}\hat{S}^-_{l+1,2} + \hat{S}^+_{l,2}\hat{S}^-_{l+1,1} + \hat{S}^+_{l,2}\hat{S}^-_{l+1,2} + \text{h.c.}\right] + \sum_l \hat{H}^{\text{int}}_{l,l+1}. \tag{7.68}$$

The four-dimensional local Hilbert space of the two spin 1/2s can be alternatively represented in a different basis, namely as triplet and singlet operators [8], i.e. $\left[|0\rangle, \hat{b}^\dagger_S|0\rangle, \hat{b}^\dagger_S\hat{b}^\dagger_S|0\rangle, \hat{b}^\dagger_A|0\rangle\right]$, i.e.

$$\begin{aligned}\hat{b}^\dagger_S|0\rangle &= \frac{1}{\sqrt{2}}\left(\hat{b}^\dagger_1 + \hat{b}^\dagger_2\right)|0\rangle, \\ \hat{b}^\dagger_A|0\rangle &= \frac{1}{\sqrt{2}}\left(\hat{b}^\dagger_1 - \hat{b}^\dagger_2\right)|0\rangle,\end{aligned} \tag{7.69}$$

which have a definite action with respect to a permutation of the internal species. By insertion of the transformation in **Eq**. (7.69) into **Eq**. (7.68) the following effective Hamiltonian can be derived [8],

$$\hat{H} \approx -\frac{J}{4}\sum_{\tilde{l}\in\mathcal{N}_A}\hat{b}^\dagger_{S,\tilde{l}}\hat{b}_{S,\tilde{l}+1} + \text{h.c.} + \frac{U}{2}\sum_{\tilde{l}\in\mathcal{N}_A}\hat{n}_{S,\tilde{l}}(\hat{n}_{S,\tilde{l}}-1) + V\sum_{\tilde{l}\in\mathcal{N}_A}(\hat{n}_{S,\tilde{l}}-1)(\hat{n}_{S,\tilde{l}+1}-1), \tag{7.70}$$

with

$$\hat{n}_{S,\tilde{l}} = 1 - \left[\hat{b}_{S,\tilde{l}}, \hat{b}^\dagger_{S,\tilde{l}}\right]. \tag{7.71}$$

The sum $\tilde{l} \in \mathcal{N}_A$ in **Eq**. (7.70) consists of all lattice points which do not include any site containing a singlet operator, i.e. $\hat{b}_{A,l}$ with $l \notin \mathcal{N}_A$, as the Hamiltonian in **Eq**. (7.68) features a local $U(1)$ symmetry with respect to those, i.e. leaves the singlet state locally invariant. Any singlet state appearing at $l \notin \mathcal{N}_A$ would be frozen out of the original lattice via Pauli repulsion, i.e.

$$\hat{b}^{\dagger}_{S,l}\hat{b}^{\dagger}_{A,l} = \hat{b}^{\dagger}_{A,l}\hat{b}^{\dagger}_{S,l} = 0, \tag{7.72}$$

thus the Hilbert space of the Hamiltonian in **Eq**. (7.70) can be subdived into disjoint parts labeled by the numbers of singlets they contain. By variational arguments one can conclude that the number of singlets in the ground-state of **Eq**. (7.70) vanishes, and thus $\tilde{l} \in \mathcal{N}_A$ coincides with the whole lattice. Following this logic and remembering that the triplet operators satisfy the $SU(2)$ algebra in $S = 1$ representation, i.e.

$$\begin{aligned} \hat{S}^{+}_{l} &= \frac{\hat{b}^{\dagger}_{S,l}}{\sqrt{2}} \\ \hat{S}^{-}_{l} &= \frac{\hat{b}_{S,l}}{\sqrt{2}} \\ \hat{S}^{z}_{l} &= \hat{n}_{S,l} - 1, \end{aligned} \tag{7.73}$$

the Hamiltonian in **Eq**. (7.70) can be recast into its original in **Eq**. (7.68) [8], i.e.

$$\hat{H} \approx -\frac{J}{2}\sum_{\tilde{l}\in\mathcal{N}_A}\left[\hat{S}^{+}_{\tilde{l}}\hat{S}^{-}_{\tilde{l}+1} + \text{h.c.}\right] + \frac{U}{2}\sum_{\tilde{l}\in\mathcal{N}_A}\hat{S}^{z}_{\tilde{l}}(\hat{S}^{z}_{\tilde{l}}+1) + V\sum_{\tilde{l}\in\mathcal{N}_A}\hat{S}^{z}_{\tilde{l}}\hat{S}^{z}_{\tilde{l}+1}, \quad l \in \emptyset. \tag{7.74}$$

Thus we conclude that the mapping is exact on the level of the ground-state manifold of the Hamiltonian, even it does not preserve the correct $S = 1$ representation algebraically. Furthermore the relation between our model, neglecting the lattice gauge, and the λ-D model are evident.

7.6.2 Some Facts about the Bosonization of Spin Ladders

As we have now ensured ourselves about the validity of the Schulz mapping and highlighted its elegance by projecting out unnecessary degrees of freedom straight from the beginning, a few remarks on the bosonization of spin ladders are necessary. Let us start the discussion with recapitulating some facts about the bosonization of a single spin 1/2 chain of the XXZ type [43], i.e.

$$\hat{H}_{\text{XXZ}} = J\sum_{l}\left[\hat{S}^{+}_{l}\hat{S}^{-}_{l+1} + \text{h.c.}\right] + J_z\sum_{l}\hat{S}^{z}_{l}\hat{S}^{z}_{l+1}. \tag{7.75}$$

Eq. (7.75) can be bosonized by standard methods [43], with numerically reliable universal low-energy parameters in the naive continuum limit, provided that $J_z \ll J$. But, also

beyond this interaction regime the Luttinger liquid can describe the correct low-energy physics of **Eq**. (7.75), if renormalized constants u, K are used, instead of the bare ones and one is not inside the (anti)-ferromagnetic phase. Let us now assume that we isotropically couple two one-dimensional chains to a quasi one-dimensional ladder [43], i.e.

$$\hat{H}_{\text{Ladder}} = \sum_{\alpha=1,2} \hat{H}^{\alpha}_{\text{XXZ}} + \sum_{j,\beta} J_{\perp} \hat{S}^{\beta}_{j,1} \hat{S}^{\beta}_{j,2}, \quad \beta = x, y, z. \tag{7.76}$$

One can apply perturbative bosonization to each chain, yielding two coupled and interacting Luttinger liquids in spin-charge basis [43, 195].

$$\hat{H}_c = \hat{H}^0_c + \int dx \frac{g_1}{(\pi a)^2} \cos(2\Phi_c)\Big], \tag{7.77}$$

$$\hat{H}_s = \hat{H}^0_s + \int dx \frac{g_2}{(\pi a)^2} \cos(2\Phi_s) + \frac{g_3}{(\pi a)^2} \cos(2\Theta_s)\Big], \tag{7.78}$$

$$\hat{H}_{c,s} = \frac{g_4}{(\pi a)^2} \int dx \;\; \cos(2\Phi_c)\cos(2\Phi_s). \tag{7.79}$$

In **Eq**. (7.77) and (7.78), $\hat{H}^0_{c/s}$ denotes the non-interacting Luttinger liquid with universal parameters u and $K_{c/s}$,

$$\begin{aligned} u_{c/s} &= u\left[1 \pm \frac{K J_{\perp} a}{2\pi u}\right], \\ K_{c/s} &= K\left[1 \mp \frac{K J_{\perp} a}{2\pi u}\right], \end{aligned} \tag{7.80}$$

that are directly related to the universal parameters of the single chain bosonization of **Eq**. (7.75) and are valid expressions whenever the transversal coupling of the chains in **Eq**. (7.76) is reasonably small compared to the single chain density stiffness, i.e. $aJ_{\perp} \ll \frac{u}{K}$. Whenever the transversal coupling becomes the dominant energy scale on the other hand, we may encounter two different scenarios, depending on its sign. Namely for large ferromagnetic $J_{\perp}$, the two spin 1/2s on the rung will be aligned forming an effective spin 1 according to the Schulz decomposition **Eq**. (7.59). By the intra-chain couplings those integer spins on a site become then finally an effective chain in analogy to **Eq**. (7.74). If the transversal coupling is large and positive on the other hand each rung forms a singlet instead, irrespective of the other couplings, and thus yields a gapped ground-state [43] [17].

The Sine-Gordon like terms, that perturb the free Luttinger liquids are scaled by the coupling constants g, and are all proportional to the transversal coupling $J_{\perp}$ [43].

[17] Nevertheless the current formalism can also be used to describe positive couplings, if they are not too large.

Comparing now the two Hamiltonians in **Eq**. (7.76) and **Eq**. (7.68) one can conclude that they essentially correspond to equivalent low-energy representations according to **Eq**. (7.77) and (7.78) with different coupling values. Thereby, it is crucial to assume the existence of a continuous renormalization group connection between the weak and strong-coupling limit, in order to justify the perturbative treatment in a parameter region where the transversal coupling is as large as the other energy scales [195]. Luckily, renormalization effects are indeed rather weak and also isotropic couplings can be described by the same theory in **Eq**. (7.77) and (7.78) with different numerical values of the coupling constants [43]. It was Heinz Schulz himself that applied the decomposition in **Eq**. (7.59) to the λ-D model in **Eq**. (7.8) [195], and used the bosonization solution of the corresponding spin ladder, in the sense of **Eqs**. (7.77) to (7.79), to determine roughly the transition lines and describe the low-energy phases. These considerations imply that there is no essential difference in the low-energy description of a ladder system as in **Eq**. (7.76) and the λ-D model, provided one uses the correct, i.e. potentially renormalized, coupling constants [43]. This finally indicates that the described procedure can also be for the extended anyon-Hubbard Hamiltonian, even if the form in is more complicated due to the presence of the correlated spin-flips $\hat{F}^{l}_{q_1,q_2}$ [187].

7.6.3 Numerical Tests of the Schulz Mapping in the Pseudo-Fermionic Limit

As the Schulz decomposition implies for our model too, that the intra-chain hopping contributions have the same energy as the inter-chain processes, including the lattice gauge functions, we have to assume a similar weak-strong coupling correspondence relating the ladder compound to the single chain. Accepting this, we should be worried in addition about the validity a Luttinger liquid descriptions for the single chains in the following sense. The reference state with respect to whom the normal ordering procedure of bosonization is defined corresponds to the two independent intra-chain Fermi vacuua. The relevant object of such Hamiltonians is thus necessarily the XY part of the single chains, in order to be able to use perturbative bosonization in analogy to the XXZ model in **Eq**. (7.75). The intra-chain XY part of our constrained model are far more complicated on the other hand, due to the presence of the lattice gauge function in **Eq**. (7.64). The function $\hat{F}^{l}_{q_1,q_2}$ is first of all complex, which couples additionally x and y operators on neighboring lattices sites. Furthermore, it is operator-valued, containing the longitudinal operators of the other chain, which corresponds to correlated spin-flips involving unusual three or four-spin interactions in the spin-1 picture. Once these contributions become dominant instead of the linearly dispersing contribution, a breakdown of the Luttinger liquid or at least strong renormalization effects on the coupling constants cannot be excluded, a scenario which we would clearly like to avoid. Numerically, we can estimate the relevance of the exactly solvable term of each

intra-chain contribution, i.e.

$$\hat{\mathcal{K}}_{l,l+1}^{\text{intra},m,0} = \frac{z_1}{2}\hat{S}_{l,m}^{+}\hat{S}_{l+1,m}^{-} + \text{h.c.} \tag{7.81}$$

by simulating and comparing the bond energies of **Eq**. (7.81) to the total amount of each intra-chain hopping processes, given by

$$\hat{\mathcal{K}}_{l,l+1}^{\text{intra},m} = \frac{1}{2}\left[\hat{S}_{l,m}^{+}\hat{S}_{l+1,m}^{-}\hat{F}_{m}^{l,*} + \text{h.c.}\right]. \tag{7.82}$$

We know a priori that the Luttinger liquid can faithfully describe either gapless phases as the superfluid and pair-superfluid phases, or critical lines between gapped phases. As we are especially interested in the latter scenario we evaluate and compare **Eqs**. (7.81) and (7.82) on representative transition lines. For $\theta = 0$ the quantities in **Eqs**. (7.81) and (7.82) are evaluated on the middle bond $(l, l+1)$ and for parameter values on the transition lines between the Mott and the Haldane phase, see **Tab**. (7.1) [172].

	MI-HI a) $(U = 5.4,\, V = 3)$,	MI-HI b) $(U = 1.85,\, V = 0.3)$
$\hat{\mathcal{K}}_{l,l+1}^{\text{intra},1,0}$	0.502601	0.547766
$\hat{\mathcal{K}}_{l,l+1}^{\text{intra},1}$	0.372447	0.400156
$\hat{\mathcal{K}}_{l,l+1}^{\text{intra},2,0}$	0.502601	0.547766
$\hat{\mathcal{K}}_{l,l+1}^{\text{intra},2}$	0.372447	0.400156

Table 7.1: *Energy contributions of intra-chain hopping processes according to* **Eqs**. *(7.81) and (7.82) at criticality, evaluated at the middle bond $(L/2, L/2+1)$ via exact diagonalization, for $L = 20$ and $\theta = 0$ [172]. The a) column is measured at the transition while b) is measured at the crossover between the two phases. The dominance of $\hat{\mathcal{K}}_{l,l+1}^{\text{intra},m,0}$ shows that the Schulz mapping suits well for this parameter set, and the single chains $m = 1, 2$ can be safely bosonized. The symmetry of the Schulz mapping implies on the other hand that the inter-chain processes have the same energy, which is not explicitly shown here.*

For $\theta = \pi$ on the other hand, we evaluate the energies on the middle bond, and on its left neighbor, for studying the Dimer to CDW transition, see **Tab**. (7.2). In the bosonic limit we find that the Schulz decomposition fits very perfectly well, as the exactly solvable part $\hat{\mathcal{K}}_{l,l+1}^{\text{intra},m,0}$ has a larger energy as the sum of all intra-chain hopping processes $\hat{\mathcal{K}}_{l,l+1}^{\text{intra},m}$. This implies that the remaining contributions, perturbing the groundstate of $\hat{\mathcal{K}}_{l,l+1}^{\text{intra},m,0}$, are small in this case and of negative sign. Thereby we don't find large differences between the crossover region or on the real transition line, yielding an exactly solvable part of $\hat{\mathcal{K}}_{l,l+1}^{\text{intra},m,0}$ weighting around 135 percent of the total intra-chain hopping $\hat{\mathcal{K}}_{l,l+1}^{\text{intra,m}}$. Therefore we can conclude that each intra-chain Hamiltonian $\hat{\mathcal{K}}_{l,l+1}^{\text{intra},m}$can be bosonized safely for $\theta \approx 0$, without worrying about strong renormalization effects on the weak-coupling values of the resulting field theory.

	a) ($U=-2.25$, $V=3$),	b) ($U=-2.25$, $V=3$)
$\hat{\mathcal{K}}^{\text{intra},1,0}_{l,l+1}$	0.050710	-0.018058
$\hat{\mathcal{K}}^{\text{intra},1}_{l,l+1}$	0.185040	0.313993
$\hat{\mathcal{K}}^{\text{intra},2.0}_{l,l+1}$	0.050710	-0.018058
$\hat{\mathcal{K}}^{\text{intra},2}_{l,l+1}$	0.185040	0.313993

Table 7.2: *Exact diagonalization results of intra-chain hopping processes according to* **Eqs**. *(7.81) and (7.82) at the CDW to Dimer transition [172]. The energies are evaluated at the middle bond (a) ($L/2, L/2+1$) and its left-neighboring bond (b), for $L=20$ and $\theta=\pi$. The dominance of $\hat{\mathcal{K}}^{\text{intra},m,0}_{l,l+1}$ is lost for this parameter set, and shows that the Schulz mapping may not be the optimal choice to keep renormalization effects minimal for the single-chain bosonization.*

For $\theta \approx \pi$ the situation is quite different, where we find that the weight of $\hat{\mathcal{K}}^{\text{intra},m,0}_{l,l+1}$is only around 27 percent on the middle bond. So we can conclude that the correlated hopping terms change their sign and become dominant, which at least indicates strong renormalization effects on the single-chain Luttinger liquid. For the neighboring bond the situation is even worse as the contribution of $\hat{\mathcal{K}}^{\text{intra},m,0}_{l,l+1}$changes its sign to negative, whereas it represents only around 6 percent of $\hat{\mathcal{K}}^{\text{intra},m}_{l,l+1}$in absolute values. This is indeed a true manifestation of the dimerization along the bonds, and an indication that the Schulz mapping may not be the optimal choice to resolve this part of the phase diagram. As the lattice gauge functions arise only through the bosonic/anyonic nature of the particles, they are not dependent on external parameters instead of θ. Thus their relevance strongly depends on the way the spin 1 operator is expressed in terms of spin 1/2's, whereas the Schulz decomposition is clearly not the only possibility to achieve this. As we are finally aiming for a field-theory that gives us trustworthy universal parameters prior to any renormalization group analysis, this finding leads us to the decision to use yet another mapping to describe the phases and their transitions in the pseudo-fermionic limit.

7.6.4 Derivation of the Field Theory

As we have ensured ourselves about the applicability of the Schulz decomposition for small statistical parameters, see **Tab**. (7.1), we will discuss the differences of the bosonization procedure of the λ-D and the extended anyon-Hubbard model, see **Eqs**. (7.8) and (7.1) [187]. We begin with applying the Jordan-Wigner transformation on each spin degree of freedom in the ladder [43], i.e.

$$\hat{S}^{+}_{l,q} = \hat{c}^{\dagger}_{l,q} \exp\left(i\pi \sum_{k<l} \hat{n}_{k,q} \right), \quad \hat{n}_{l,q} = \hat{c}^{\dagger}_{l,q}\hat{c}_{l,q}. \tag{7.83}$$

Furthermore, each of the, now fermionic, intra-chain dispersions are linearized around $k_{F,q} = \pi/2$, corresponding to the required unit filling for the actual constrained bosonic degrees of freedom. This decomposes each fermion into a left and right-moving species relative to the Fermi-surface [43], i.e.

$$\hat{\Psi}^q(x) \propto \hat{\Psi}^q_R(x) e^{ik_{F,q}x} + \hat{\Psi}^q_L(x) e^{-ik_{F,q}x}, \tag{7.84}$$

that can then be finally represented as exponentials of inherently bosonic fields,

$$\psi^q_{R/L} \propto \frac{1}{\sqrt{2\pi\alpha}} e^{i(\Theta_q \pm \Phi_q)}. \tag{7.85}$$

In **Eqs**. (7.85) the dual fields Θ_q and Φ_q, representing the fluctuations of phase and density in the Luttinger paradigm, are defined as usual in this thesis, with an ultra-violet cut-off α much smaller than the lattice spacing a. With the help of **Eqs**. (7.84) and (7.85) one can derive the bosonized expressions for the spin degrees of freedom [18] [187] , i.e.

$$\begin{aligned} \hat{S}^+_{l,q} &= e^{i\hat{\Theta}_q(x)} \left(1 + c_1 \frac{(-1)^x}{\pi a} \sin(2\hat{\phi}_q(x))\right), \\ \hat{S}^z_{l,q} &= \frac{1}{\pi} \partial_x \hat{\phi}_q(x) + c_2 \frac{(-1)^x}{\pi a} \sin(2\hat{\phi}_q(x)), \end{aligned} \tag{7.86}$$

where $c_{1,2}$ denotes non-universal constants.

One of the extensions we assume with respect to the usual bosonization of spin 1 chains, as the λ-D model, is that we explicitly take the lattice gauge functions of each chain process into account [187], as sketched in **appendix** (7.11.1), as their importance was highlighted in the former subsection. This technique developed in **Ref**. [140, 141] basically amounts to perform a point-splitting operation on all the constituents of the lattice gauge functions, as well as on the kinetic parts individually and subsequently calculate the operator product expansion between the fluctuating contributions, indicated by the normal ordering symbol :: , e.g.

$$\begin{aligned} &\hat{S}^z_{l,q} \Longrightarrow \langle \hat{S}^z_{l,q} \rangle + : \hat{S}^l_{l,q} : \\ &\hat{S}^+_{l,\bar{q}\neq q} \hat{S}^-_{l+1,\bar{q}\neq q} \Longrightarrow \langle \hat{S}^+_{l,\bar{q}\neq q} \hat{S}^-_{l+1,\bar{q}\neq q} \rangle + : \hat{S}^+_{l,\bar{q}\neq q} \hat{S}^-_{l+1,\bar{q}\neq q} :, \\ &\hat{S}^+_{l,\bar{q}\neq q} \hat{S}^-_{l+1,\bar{q}\neq q} \hat{S}^z_{l,q} \Longrightarrow \left(\langle \hat{S}^+_{l,\bar{q}\neq q} \hat{S}^-_{l+1,\bar{q}\neq q} \rangle + : \hat{S}^+_{l,\bar{q}\neq q} \hat{S}^-_{l+1,\bar{q}\neq q} :\right) \left(\langle \hat{S}^z_{l,q} \rangle + : \hat{S}^l_{l,q} :\right). \end{aligned} \tag{7.87}$$

Thereby we approximately neglect any operator product expansions between the inter-chain hopping and its lattice gauge. This assumption is based on the expected weak

[18] Note that the current definitions of bosonized spin operators include the staggered rotations that flips the sign of the x, y terms, i.e. $\hat{S}^{x,y}_{j,q} = (-1)^j \hat{S}^{x,y}_{j,q}$, such that they have the same signs in **Eq**. (7.8) and the spin representation of **Eq**. (7.1)

to strong-coupling continuity of transversal couplings in the bosonization of such spin ladder models. In the procedure of **Eq**. (7.87) we subsequently keep only the lowest order contributions compatible with free Luttinger liquid Hamiltonians and Sine-Gordon like perturbation of minimal order. As usual we neglect highly oscillatory terms with a prefactor of $e^{\pm 2ik_{F,q}x} \equiv (-1)^x$ [43], arising from the half-filling condition for each species.

Physically, the approach in **Eq**. (7.87) allows for a renormalization of the density stiffness of each individual chain by the other one's lattice gauge, as well as the current stiffness. This procedure leads furthermore to an amplification of sinusoidal vertex operators by the lattice gauge, that tend to localize the fields, besides the generation of symmetry breaking terms that inherit the anyonic nature of the problem. For the operator product expansions the following formulas turn out to be quite useful [140, 141],

$$\sin(2\sqrt{\pi}\phi_\alpha(x))\sin(2\sqrt{\pi}\phi_\alpha(x+a)) \approx \frac{1}{2} - \frac{1}{2}\cos(4\sqrt{\pi}\phi_\alpha(x)) - \pi a^2 \left(\frac{\delta\phi_\alpha(x)}{\delta x}\right)^2 ,$$

$$\frac{\delta\phi_d(x)}{\delta x}\sin(2\sqrt{\pi}\phi_d(x+a)) = -\sin(2\sqrt{\pi}\phi_d(x))\frac{\delta\phi_d(x+a)}{\delta x} = -\frac{1}{\sqrt{\pi}a}\cos(2\sqrt{\pi}\phi_d(x)), \tag{7.88}$$

whereas the normal ordering procedure and expectation values are performed with respect to each single intra-chain Luttinger liquid, according to **Eq**. (7.81).

One of the rather special features of one-dimensional electronic systems is the potential appearance of spin-charge separation [42, 43]. This effect basically amounts to the fact that both spin and charge correspond to degrees of freedom that can evolve independently, even if they originate from symmetric or anti-symmetric combinations of a spin up and a spin down fermion. The analog of this circumstance in our inherently bosonic system is the separation of linear combinations of particle and hole fluctuations above the unit filling, as it is expressed in bosonization via a further transformation of the dual fields into (anti-)symmetric variables [43, 187, 195],

$$\begin{aligned} \Phi_c &= \Phi_1 + \Phi_2, \quad \Theta_c = (\Theta_1 + \Theta_2)/2, \\ \Phi_s &= \Phi_1 - \Phi_2, \quad \Theta_s = (\Theta_1 - \Theta_2)/2. \end{aligned} \tag{7.89}$$

The charge (c) degrees of freedom in **Eqs**. (7.89) can be identified with the total number operator of the bosons via **Eqs**. (7.3), whereas the spin (s) sector does not feature a simple interpretation as in the case of spinfull fermions. In a later section the identification of bosonic lattice operators and low-energy continuum fields are re-investigated by means of the fundamental $su(3)$ language of locally 3 dimensional Hilbert spaces [8], whereas currently there interpretation is somewhat blurred due to

the Schulz representations of spin 1 operators.

Keeping only the lowest order operator contributions, see **Tab**. (7.3), we obtain finally the following coupled field theory,

$$\hat{H}_c = \hat{H}_c^0 \int dx \Big[A(\partial_x \Theta_c) + B(\partial_x \Phi_c) + C_c(\partial_x \Theta_c)(\partial_x \Phi_c) + \frac{g_1}{(\pi a)^2} \cos(2\Phi_c) \Big], \tag{7.90}$$

$$\hat{H}_s = \hat{H}_s^0 + \int dx \Big[C_s(\partial_x \Theta_s)(\partial_x \Phi_s) + \frac{g_2}{(\pi a)^2} \cos(2\Phi_s) + \frac{g_3}{(\pi a)^2} \cos(2\Theta_s) \Big], \tag{7.91}$$

$$\hat{H}_{c,s} = \frac{g_4}{(\pi a)^2} \int dx \ \ \cos(2\Phi_c) \cos(2\Phi_s), \tag{7.92}$$

where $\hat{H}_{c,s}$ corresponds to the coupling between both sectors and $\hat{H}_{c/s}^0$ denotes the ordinary Hamiltonians of Tomonaga-Luttinger liquids[19] [43], i.e.

$$\hat{H}_{c/s}^0 = \frac{u_{c/s}}{2\pi} \int dx \Big[K_{c/s} (\partial_x \Theta_{c/s})^2 + \frac{1}{K_{c/s}} (\partial_x \Phi_{c/s})^2 \Big] \tag{7.93}$$

Operators	Scaling Dimension Δ,
$\cos(2\Phi_c)$	K_c
$\cos(2\Phi_s)$	K_s
$\cos(2\Theta_s)$	$1/K_s$
$\cos(2\Phi_c)\cos(2\Phi_s)$	$K_c + K_s$

Table 7.3: *Scaling dimensions of the non-explicitly marginal, Sine-Gordon type, perturbations of the free Luttinger liquid in* **Eqs**. *(7.90) to (7.92) [196]. The scaling dimension Δ determines the relevance of an operator in a renormalization group sense, i.e. whenever $\Delta < 2$ the term is relevant in the long wave-length limit [43]. If the scaling dimension is larger than 2 on the other hand, then the term is irrelevant and the corresponding coupling constant flows to zero. Whenever Δ equals the space-time dimension 2 a term is called marginal, and those can be relevant or not depending on higher orders in the renormalization-group flow [50, 225]. Thereby we distinguish here explicitly marginal terms, as for example the bi-linear contributions of the field gradients $(\partial_x \Theta_{c/s})$ $(\partial_x \Phi_{c/s})$, from those which depend on the values of the universal parameters $K_{c/s}$.*

The Luttinger parameters that determines the decay of correlation function, as well as the scaling dimension of operators that perturb the free Luttinger liquid, are given

[19]The spin-charge coupling $\hat{H}_{c,s}$ in **Eqs**. (7.92) can be safely neglected unless some fine tuning of paramaters is considered, due to the larger scaling dimension compared to other terms in the field theory, see **Tab**. (7.3). If we assume furthermore that either $\hat{\phi}_c$ or $\hat{\phi}_s$ is pinned the spin-charge coupling only renormalizes g_2 or g_1 respectively.

by the following expressions,

$$K_c = 2\left(1 + \frac{4}{\pi}\frac{U + 6V + J\mathrm{Re}(z_4)}{J\mathrm{Re}(z_1 - z_4/2\pi^3)}\right)^{-1/2}, \tag{7.94}$$

$$K_s = 2\left(1 - \frac{4}{\pi}\frac{U - 2V - J\mathrm{Re}(z_4)}{J\mathrm{Re}(z_1 - z_4/2\pi^3)}\right)^{-1/2}, \tag{7.95}$$

whereas for the sound velocities for each channel we obtain,

$$\begin{aligned} u_c &= Ja\pi\mathrm{Re}(z_1 - z_4/2\pi^3)/K_c, \\ u_s &= Ja\pi\mathrm{Re}(z_1 - z_4/2\pi^3)/K_s. \end{aligned} \tag{7.96}$$

Both sound velocities $u_{c/s}$ can change their sign depending on θ, which potentially indicates a break-down of the bosonization approach, similar to **Eq**. (7.80), due to the worsening of the linearization of the spectrum. In comparison to bosonization of the λ-D model, the Luttinger parameters $K_{c/s}$ in **Eqs**. (7.95) and (7.94) are non-trivially altered by the lattice gauge. Namely, it changes the value of the number stiffness as well as the phase stiffness in each sector, where the latter is generally only expected for systems without Galilean invariance [43]. This finally affects whether a given vertex operator is relevant or not, according to **Tab**. (7.3).

The original, constrained bosonic operators take the following form in terms of the spin and charge fields to lowest order [187],

$$\hat{b}_j \propto e^{i\hat{\Theta}_c(x)}\cos\left(\hat{\Theta}_s(x)\right) + ..., \tag{7.97}$$

$$\hat{n}_j \propto \partial_x\hat{\phi}_c(x) + \mathrm{const.}(-1)^x \sin\left(\hat{\phi}_c(x)\right)\cos\left(\hat{\phi}_s(x)\right) + ..., \tag{7.98}$$

which corresponds exactly to the expressions obtained if one would bosonize the spin 1 operators directly. This circumstance should be clear already from the definition in **Eq**. (7.61), which inherits the fact that both entities differ only by higher-order contributions in a field theoretical sense [187]. From **Eqs**. (7.97) and (7.98) we can additionally deduce the symmetry correspondences between lattice operators and low energy fields, shown in **Tabs**. (7.4) and (7.6) for bosons and in **Tabs**. (7.5) and (7.7) for spins [196]. Thereby we demand for consistency with the transformation behavior of the individual spin 1/2 operators in **Eq**. (7.86) and consider an infinite system size from here on. As the system now does not contain any boundary we additionally consider parity transformations centered on a bond instead of only site-centered inversion [196]. This distinguishes if the parity operation is changing the sub-lattice index or not. A discrete change of the sub-lattice index is thereby not equivalent to translations in the continuum, which are continuous and are usually neglected as shifting a continuum field essentially produces less relevant terms containing gradients [176, 196].

Symmetries	Lattice	$\hat{H}_c$
Index permutation $\hat{I}$	$\hat{b}_j \to \hat{b}_j$	$\hat{\phi}_c \to \hat{\phi}_c,\ \hat{\Theta}_c \to \hat{\Theta}_c$
Sub-lattice translation $\hat{T}$	$\hat{b}_j \to \hat{b}_{j+1}$	$\hat{\phi}_c \to \hat{\phi}_c + \pi,\ \hat{\Theta}_c \to \hat{\Theta}_c$
Bosonic time reversal $\hat{K}$	$\hat{b}_j \to \hat{b}_j$	$\hat{\phi}_c \to \hat{\phi}_c,\ \hat{\Theta}_c \to -\hat{\Theta}_c$
$U(1)$ gauge $\hat{U}(\alpha)$	$\hat{b}_j \to \hat{b}_j e^{i\alpha}$	$\hat{\phi}_c \to \hat{\phi}_c,\ \hat{\Theta}_c \to \hat{\Theta}_c + \alpha$
Site Parity $\hat{P}_S$	$\hat{b}_j \to \hat{b}_{-j}$	$\hat{\phi}_c(x) \to -\hat{\phi}_c(-x) + \pi,$ $\hat{\Theta}_c(x) \to \hat{\Theta}_c(-x)$
Link Parity $\hat{P}_L$	$\hat{b}_j \to \hat{b}_{1-j}$	$\hat{\phi}_c(x) \to -\hat{\phi}_c(-x),$ $\hat{\Theta}_c(x) \to \hat{\Theta}_c(-x)$
$\hat{U}(\theta/2(\hat{n}_j - 1))\hat{K}\hat{P}_S$	$\hat{b}_j \to e^{i\theta\hat{n}_{-j}}\hat{b}_{-j}$	$\hat{\phi}_c(x) \to -\hat{\phi}_c(-x) + \pi\ ,$ $\hat{\Theta}_c \to -\hat{\Theta}_c(-x) + \frac{\theta}{\pi}\partial_x\hat{\phi}_c(-x)$
$\hat{U}(\theta/2(\hat{n}_j - 1))\hat{K}\hat{P}_L$	$\hat{b}_j \to e^{i\theta\hat{n}_{1-j}}\hat{b}_{1-j}$	$\hat{\phi}_c(x) \to -\hat{\phi}_c(-x)\ ,$ $\hat{\Theta}_c \to -\hat{\Theta}_c(-x) + \frac{\theta}{\pi}\partial_x\hat{\phi}_c(-x)$

Table 7.4: *The relations between lattice symmetry transformations and continuum operators of the charge field, based on* **Eqs**. *(7.97) and (7.98), and the lattice operations of* **Eqs**. *(7.1), for infinite system sizes. Additionally, the transformations are chosen such that the two spin 1/2 degrees of freedom in the Schulz decomposition transform uniformly [196]. The one-site translation in the lattice corresponds to the interchange of the sub-lattice index in the continuum, whereas real continuum translations are assumed to be irrelevant due to their higher-order operator content [176, 196]. The symmetry of interchanging the leg index in the spin-ladder is internal, i.e. has no impact on the lattice bosons nor spin 1 operators, and does not change the signs of the charge fields in the long wave-length limit. For an infinite system size we additionally consider the inversion around a bond $\hat{P}_L$, that itself is composed of the sub-lattice interchange and $\hat{P}_S$. The generalized inversion symmetry of the extended anyon-Hubbard model found in* **Ref**. *[185] corresponds to a non-linear gauge transformation for the phase field, as well as temporal and parity inversion, and does not lead to a low-energy symmetry in an obvious manner.*

Spin 1 symmetries	Lattice	$\hat{H}_c$
Spin time reversal $\hat{K}_S$	$\vec{\hat{S}}_j \to -\vec{\hat{S}}_j$	$\hat{\phi}_c \to -\hat{\phi}_c,\ \hat{\Theta}_c \to \hat{\Theta}_c + \pi$
$\hat{U}_x(\pi) = e^{i\pi\hat{S}^x}$	$\hat{S}^{\pm}_j \to \hat{S}^{\mp}_j,\ \hat{S}^z_j \to -\hat{S}^z_j$	$\hat{\phi}_c \to -\hat{\phi}_c,\ \hat{\Theta}_c \to -\hat{\Theta}_c$
$\hat{U}_y(\pi) = e^{i\pi\hat{S}^y}$	$\hat{S}^{\pm}_j \to -\hat{S}^{\mp}_j,\ \hat{S}^z_j \to -\hat{S}^z_j$	$\hat{\phi}_c \to -\hat{\phi}_c,\ \hat{\Theta}_c \to -\hat{\Theta}_c + \pi$

Table 7.5: *Relevant symmetry relations between spin* 1 *operators defined in* **Eq**. *(7.59), and the low-energy charge fields. While interchanging the ladder index is also an internal symmetry of the spin* 1 *operators, time reversal is differently defined compared to the bosonic case. Other lattice dependent symmetries are equivalent for both entities, and are thus not shown here. The elements of the dihedral group in* **Eq**. *(7.6), that could be interpreted as a kind of particle-hole transformation for constrained lattice bosons in* **Eq**. *(7.5) [187], lead to additionally symmetry transformations, that might become asymptotically exact due to the low-energy equivalence of bosons and spins.*

Symmetries	Lattice	$\hat{H}_s$
Index permutation $\hat{I}$	$\hat{b}_j \to \hat{b}_j$	$\hat{\phi}_s \to -\hat{\phi}_s,\ \hat{\Theta}_s \to -\hat{\Theta}_s$
Sub-lattice translation $\hat{T}$	$\hat{b}_j \to \hat{b}_{j+1}$	$\hat{\phi}_s \to \hat{\phi}_s,\ \hat{\Theta}_s \to \hat{\Theta}_s$
Bosonic time reversal $\hat{K}$	$\hat{b}_j \to \hat{b}_j$	$\hat{\phi}_s \to \hat{\phi}_s,\ \hat{\Theta}_s \to -\hat{\Theta}_s$
$U(1)$ gauge $\hat{U}(\alpha)$	$\hat{b}_j \to \hat{b}_j e^{i\alpha}$	$\hat{\phi}_s \to \hat{\phi}_s,\ \hat{\Theta}_s \to \hat{\Theta}_s$
Site Parity $\hat{P}_S$	$\hat{b}_j \to \hat{b}_{-j}$	$\hat{\phi}_s(x) \to -\hat{\phi}_s(-x),\ \hat{\Theta}_s(x) \to \hat{\Theta}_s(-x)$
Link Parity $\hat{P}_L$	$\hat{b}_j \to \hat{b}_{1-j}$	$\hat{\phi}_s(x) \to -\hat{\phi}_s(-x),\ \hat{\Theta}_s(x) \to \hat{\Theta}_s(-x)$
$\hat{U}(\theta/2(\hat{n}_j - 1))\hat{K}\hat{P}_S$	$\hat{b}_j \to e^{i\theta\hat{n}_{-j}}\hat{b}_{-j}$	$\hat{\phi}_s(x) \to -\hat{\phi}_s(-x)\ ,\hat{\Theta}_s \to -\hat{\Theta}_s(-x)$
$\hat{U}(\theta/2(\hat{n}_j - 1))\hat{K}\hat{P}_L$	$\hat{b}_j \to e^{i\theta\hat{n}_{1-j}}\hat{b}_{1-j}$	$\hat{\phi}_s(x) \to -\hat{\phi}_s(-x)\ ,\hat{\Theta}_s \to -\hat{\Theta}_s(-x)$

Table 7.6: *By demanding consistency of the transformations in* **Tab**. *(7.4) with both half-integer spins in the ladder, the transformation behavior of the spin sector can be obtained analogously. The internal transformation that interchanges the spin index of the ladder, flips the sign of the dual fields in the spin-sector. Thereby the spin sector generally transforms in a more simple way than the charge fields do.*

Spin 1 symmetries	Lattice	$\hat{H}_s$
Spin time reversal $\hat{K}_S$	$\vec{\hat{S}}_j \to -\vec{\hat{S}}_j$	$\hat{\phi}_s \to -\hat{\phi}_s,\ \hat{\Theta}_s \to \hat{\Theta}_s$
$\hat{U}_x(\pi) = e^{i\pi\hat{S}^x}$	$\hat{S}^{\pm}_j \to \hat{S}^{\mp}_j,\ \hat{S}^z_j \to -\hat{S}^z_j$	$\hat{\phi}_s \to -\hat{\phi}_s,\ \hat{\Theta}_s \to -\hat{\Theta}_s$
$\hat{U}_y(\pi) = e^{i\pi\hat{S}^y}$	$\hat{S}^{\pm}_j \to -\hat{S}^{\mp}_j,\ \hat{S}^z_j \to -\hat{S}^z_j$	$\hat{\phi}_s \to -\hat{\phi}_s,\ \hat{\Theta}_s \to -\hat{\Theta}_s$

Table 7.7: *Relevant symmetry relations between spin* 1 *operators defined in* **Eq**. *(7.59), and the anti-symmetric fields in the continuum. Also in this case, the spin sector fields reverse their sign under an interchange of the ladder index.*

The interchanging of the spin index is on the other hand an internal symmetry of the bosons and spins, mapping the lattice operators onto themselves, and thus has no physical interpretation. We find additionally in **Tabs**. (7.4) and (7.6), similarly to the continuum limit of the ordinary anyon-Hubbard model of the former section, that the generalized inversion symmetry of the lattice model is probably reduced in the long-wavelength limit [185], to contain only temporal and parity inversion. This can be seen from the fact that the non-linear gauge transformation of the phase field are of higher order in the density gradient and would therefore renormalize the density stiffness, which clearly cannot be a symmetry in general.

Whether our low-energy theory in **Eqs**. (7.97) and (7.98) is finally symmetric with respect to any transformation in **Tabs**. (7.4) to (7.7), has to be decided once the relevant terms of the field theory are known for the respective phases. Furthermore, the relevance of any of the sinusoidal vertex operators in **Eqs**. (7.95) implies that the well known $U(1)_{\phi_{c/s}} \bigotimes U(1)_{\Theta_{c/s}}$ symmetry of the Luttinger liquid, manifest by the invariance with respect to $\phi_{c,s} \to \phi_{c/s} + \alpha_{c/s}$ and $\Theta_{c/s} \to \Theta_{c/s} + \beta_{c/s}$, is reduced to a discrete shift invariance in both fields [50, 227], see **Tab**. (7.8). We find in general, that the potential asymmetry with respect to parity and temporal inversion, as well as the dihedral group

Relevant Operators	Reduced symmetry
$\cos(2\Phi_c)$	$\mathbb{Z}_{2,\phi_c} \bigotimes U(1)_{\Theta_c}$
$\cos(2\Phi_s)$	$\mathbb{Z}_{2,\phi_s} \bigotimes U(1)_{\Theta_s}$
$\cos(2\Theta_s)$	$\mathbb{Z}_{2,\Theta_s} \bigotimes U(1)_{\phi_s}$
$\cos(2\Phi_c)\cos(2\Phi_s)$	$\mathbb{Z}_{2,\phi_c} \bigotimes \mathbb{Z}_{2,\phi_s}$

Table 7.8: *Reduction of the different $U(1)$ symmetries of the Luttinger model by the respective sinusoidal vertex operators [50, 227], whose minima describe the gapped phases of* **Eqs**. *(7.1). All the remaining, intact, $U(1)$ symmetries are not explicitly shown here, as the sinusoidals act exclusively on the respective fields.*

in **Eqs**. (7.6), is manifest in the free Luttinger liquid, while all terms are permutation symmetric as they should. Those asymmetries are caused by the linear or bilinear couplings in the field gradients, i.e.

$$A = \frac{J}{\sqrt{\pi}}\mathrm{Im}(z_1 - z_4/2\pi^3) = \frac{J}{4\sqrt{\pi}}\left[2 + \sqrt{2} + (\sqrt{2} - 4)\pi^3\right]\sin(\theta), \tag{7.99}$$

$$B = \frac{J}{2\sqrt{\pi}}\mathrm{Re}(z_2 + z_3) = \frac{J}{8\sqrt{\pi}}\left[2 - \sqrt{2} - (\sqrt{2} + 8)\cos(\theta)\right], \tag{7.100}$$

$$C_c = -C_s = \frac{J}{4\pi}\mathrm{Im}(z_2 + z_3) = -\frac{J}{16\pi}\left[\sqrt{2} + 8\right]\sin(\theta), \tag{7.101}$$

that purely depend on the lattice gauge and the statistical parameter. As we have seen already in a former chapter, the linear gradient terms lead to local gauge transformation of the dual fields, which is affecting the respective correlation functions. The bilinear terms on the other hand, induce an asymmetry between left and right moving species that is observable in time-dependent correlation functions and in the zero-mode structure for finite sizes. We have seen, that the consideration of this explicitly marginal interaction does not alter correlation functions with respect to dilatations, but changes their behavior under rotations in the language of conformal field theory [26]. Such terms have zero conformal spin, which generically renormalizes the Luttinger parameters and sound velocities but does not change the scaling dimensions of operators of the form of **Tab**. (7.3) [50]. For an infinite system size those bilinears can be diagonalized by a rotation to a new set of dual fields,

$$\begin{pmatrix} \hat{\phi}_{c/s} \\ \hat{\Theta}_{c/s} \end{pmatrix} = R(\eta_{c/s}) \begin{pmatrix} \hat{\tilde{\phi}}_{c/s} \\ \hat{\tilde{\Theta}}_{c/s}, \end{pmatrix} \tag{7.102}$$

with an orthogonal rotation matrix, $R(\eta_{c/s})$

$$R(\eta_{c/s}) = \begin{pmatrix} \cos(\eta_{c/s}) & -\sin(\eta_{c/s}) \\ \sin(\eta_{c/s}) & \cos(\eta_{c/s}) \end{pmatrix}$$
$$\eta_{c/s} = \frac{1}{2}\left[\tan^{-1}\Big(\frac{C_{c/s}K_{c/s}}{u_{c/s}(1-K_{c/s}^2)}\Big) + \pi n\right], \quad n \in \mathbb{Z}. \tag{7.103}$$

The application of **Eq**. (7.102) yields then a diagonal Luttinger liquid, if all g_is are zero, with symmetrically dispersing left and right movers. Nevertheless, it forbids the semi-classical evaluation of sinusoidal vertex operator of a single field as an effective potential that pins the field into one of its minima [196].
For example, a term of the form $\cos(\alpha\hat{\tilde{\phi}}_{c/s} \pm \beta\hat{\tilde{\Theta}}_{c/s})$ produces a combination of sinusoidals in the dual fields by the addition theorem. If one assumes that one of the fields is pinned at a mean value, the dual one strongly fluctuates, due to their Heisenberg uncertainty, and thus cannot be pinned as an in-complementary operator [187, 196]. This circumstance further leads to an exponential decay of any correlation functions containing the strongly fluctuating field [43].

For the discussion of gapped phases we follow **Refs**. [187, 196], by assuming that neither the bilinear terms, nor the linear gradients, do have an impact on which coupling constant g_i, in **Eqs**. (7.104) to (7.106), reaches the strong coupling first. Thus we neglect any of the four terms explicitly whenever we discuss the vertex operators in **Tab**. (7.3) semi-classically. Nevertheless, their existence manifests the violation of symmetry, caused by the bosonic/anyonic nature of the particles relative to a spin 1 chain [185], see **Eqs**. (7.77) and (7.78), and is thus in some sense indispensable. We see from **Eqs**. (7.100) to (7.101) that those couplings only depend on the hopping parameter J, and the dependence on the statistical parameter for A and $C_{c/s}$ is perturbative in small θ. This indicates that there is a symmetry difference between the anyonic and the $\theta = 0, \pi$ case. Namely, the density gradient scaled by B, is also present in the non-anyonic case and inherits the difference in symmetry between the λ-D model and the constrained bosons, by breaking explicitly the spin symmetries in the charge field according to **Tab**. (7.5) [187, 196]. For non-zero θ additional space-time asymmetries, according to **Tabs**. (7.4) and (7.6), arise on the other hand, as present in the lattice model. We can conclude that those symmetries should be broken when the interactions U, V are sufficiently small and the free Luttinger part is relevant. In order to re-include such symmetry breaking patterns from scratch we follow the arguments of **Refs**. [187, 196] , and add symmetry-incompatible vertex operators of relevant scaling dimension to the theory, whenever the symmetry is expected to be broken. The logical argument is that such terms should be generated during the renormalization group flow anyway, once the symmetries are

effectively broken. A crucial observation is thereby that a lot of symmetry operations in **Tabs**. (7.4) to (7.7), that are inherently different in the lattice, transform equally on the level of the low-energy degrees of freedom. Thus if one of these symmetries is broken by a sinusoidal vertex operator, all of them are simultaneously broken. For example, in the $\theta = 0$ case there is still a difference in symmetry between a bosonic and a spin system, deducible from **Tab**. (7.5), while parity and bosonic time reversal remain intact. Nevertheless if we assume that this symmetry breaking is relevant we have to add for example a vertex operator of the form $\sin(2\phi_{c/s})$ to our field theory. Such an operator breaks the dihedral symmetry as well as spin time reversal, as it should, but also site- and bond-centered inversion are inherently broken [187, 196]. Thus the distinction of different symmetries is blurred for low-energies, whenever they act similarly on the low-energy degrees of freedom.

The pinning terms that appear in our bosonized theory from the beginning, are scaled by the following coupling constants

$$\frac{g_1}{a} = \frac{1}{2}(2V - U) + \frac{J}{2\pi}\mathrm{Re}(z_4), \tag{7.104}$$

$$\frac{g_2}{a} = \frac{1}{2}(U - 2V) + \frac{J}{2\pi}\mathrm{Re}(z_4), \tag{7.105}$$

$$\frac{g_3}{a} = -J\pi\mathrm{Re}(z_1), \tag{7.106}$$

$$\frac{g_4}{a} = V - \frac{2J\mathrm{Re}[z_4]}{a\pi}, \tag{7.107}$$

where one observes that an asymmetry, i.e. $g_1 \neq -g_2$, arises through the bosonic/anyonic nature of the particles, as well as a possible sign change of g_3, which do not appear in the bosoization of the λ-D, or the Bose-Hubbard model [187, 196]. Concerning a, potentially valid, semi-classical evaluation of the pinning fields while neglecting gradient terms, such asymmetries in the coupling constants imply the emergence of new gapped phases. Thereby different sign combinations of the relevant coupling constants in **Eqs**. (7.104) to (7.106), are later on identified with the various gapped phases of our model. Furthermore we may judge if the occurring gapped phases are symmetry breaking ones or not, depending on whether the minimum of the classical potential is unique inside the fields compactification radius [196].

As we are now equipped with a low-energy field theory, and are aware of its symmetries correspondences, we can now tackle the low-energy signatures of the different phases of **Eq**. (7.1), as well as their transitions, close to the bosonic limit. Furthermore we have numerical evidence that the bosonization approach pursued here may be subject to strong renormalization effects close to the pseudo-fermionic limit, hence we derive first another field-theory in the next section, that is suitable in the $\theta \approx \pi$ regime. To ensure ourselves about the validity of the new mapping, analogous numerical considerations as for the Schulz transformation in **Tabs**. (7.1) and (7.9) are pursued. Later on the

field theoretical predictions are compared to the numerical results, concerning order parameters and types of transitions.

7.7 Bosonization close to the pseudo-fermionic Limit

In the vicinity of the pseudo-fermionic limit we try a different mapping to a spin ladder, which preserves the $S = 1$ representation of the $su(2)$ algebra in each step. In opposition to the Schulz approach in **Eq**. (7.59), this leads then to exact transformations between the different entities that do not depend on the specific form of the Hamiltonian. More explicitly, we use the same mapping in **Eqs**. (7.3) from the constrained boson to spin-1, and then transform the later exactly to spin-$\frac{1}{2}$'s by projecting out the unphysical state explicitly. A possible transformation for doing this is the following [8],

$$\begin{aligned}
\hat{S}^+ &= \sqrt{2}\left[\hat{S}_1^+\left(\frac{1}{2}-\hat{S}_2^z\right)+\hat{S}_2^+\left(\frac{1}{2}+\hat{S}_1^z\right)\right],\\
\hat{S}^- &= \sqrt{2}\left[\hat{S}_1^-\left(\frac{1}{2}-\hat{S}_2^z\right)+\hat{S}_2^-\left(\frac{1}{2}+\hat{S}_1^z\right)\right],\\
\hat{S}^z &= \hat{S}_1^z+\hat{S}_2^z,
\end{aligned} \tag{7.108}$$

where we have neglected the lattice index in **Eq**. (7.108) for simplicity.

This transformation is not symmetric with respect to an interchange of the spin index, in opposition to **Eq**. (7.59), which would lead to a more complicated field theory embodying this asymmetry. In analogy to the former section we can test the usefulness of the transformation as a starting point for the perturbative single-chain bosonization, by numerically comparing the energies of the inter-chain and intra-chain processes, see **Fig**. (7.23). We find that the inter-chain hopping contributions are indeed dominant in energy, which suggests that we have to symmetrize **Eq**. (7.108). We do so by using **Eq**. (7.108) on even lattice sites whereas we permute the internal species for the odd ones

Figure 7.23: *Profile of the bond strengths* $\langle\hat{\mathcal{K}}^{\text{intra},1}_{j,j+1}\rangle$, $\langle\hat{\mathcal{K}}^{\text{inter},1,2}_{j,j+1}\rangle$, $\langle\hat{\mathcal{K}}^{\text{inter},2,1}_{j,j+1}\rangle$ *and* $\langle\hat{\mathcal{K}}^{\text{intra},2}_{j,j+1}\rangle$ *of a spin-*$1/2$ *two-leg ladder as in* **Eq**. *(7.63), but with with species defined according to* **Eq**. *(7.108). This profile was obtained via DMRG calculations in the Dimer phase with Hamiltonian parameters* $\theta = \pi$, $U/J = -2.3$ *and* $V/J = 0.0$ *[17]. Red and blue colors correspond to a negative or positive sign of the bond strengths, while the thickness illustrate their absolute value. The asymmetry between the two species leads to dominant inter-chain contributions, which is not an optimal choice to start the bosonization process on two independent Fermi-vacua. This profile suggests to use a symmetrized mapping, that is different on both lattice partitions, by permuting every second site.*

respectively. This leads to the following form of constrained bosonic operators in terms of a two-leg spin-ladder,

$$\hat{b}_l = \eta_{l+1}\hat{S}^+_{l,1}\left(\frac{1}{2}+(-1)^{l+1}\hat{S}^z_{l,2}\right)+\eta_l\hat{S}^+_{l,2}\left(\frac{1}{2}+(-1)^{l}\hat{S}^z_{l,1}\right) \tag{7.109}$$

with

$$\eta_l = [(1+\sqrt{2})+(-1)^l(1-\sqrt{2})]/2. \tag{7.110}$$

The mapping in **Eq**. (7.109) has the property that it is symmetric with respect to a combined permutation of the ladder and the sub-lattice index, whereas the Schulz mapping in **Eq**. (7.61) is permutation symmetric on each lattice site.

Insertion of the new transformation of **Eq**. (7.109) into **Eq**. (7.1) yields the following inter- and intra-chain spin-flip contributions

$$\hat{\mathcal{K}}_{l,l+1} = \hat{\mathcal{K}}^{\text{intra},1}_{l,l+1}+\hat{\mathcal{K}}^{\text{intra},2}_{l,l+1}+\hat{\mathcal{K}}^{\text{inter},1,2}_{l,l+1}+\hat{\mathcal{K}}^{\text{inter}2,1}_{l,l+1} \tag{7.111}$$

with

$$\hat{\mathcal{K}}^{\text{intra}}_{q,q} = -\frac{J}{\sqrt{2}}\sum_l \epsilon^l_q \hat{S}^+_{l+1,1}\hat{S}^-_{l,1}\hat{G}^l_{q,q}+\text{h.c.}, \tag{7.112}$$

$$\hat{\mathcal{K}}^{\text{inter}}_{q_1,q_2} = -\frac{J}{2}\sum_l \zeta^l_{q_2}\hat{S}^+_{l+1,q_2}\hat{S}^-_{l,q_1}\hat{G}^l_{q_1,q_2}+\text{h.c.}, \tag{7.113}$$

whereas the external interactions transform identically to **Eq**. (7.66). In contrast to the former approach, each process possess a complex-valued dimerization, i.e.

$$\epsilon^l_q = (1+e^{i\theta})+(-1)^{l+q}(1-e^{i\theta}), \tag{7.114}$$

$$\zeta^l_q = (1+2e^{i\theta})+(-1)^{l+q}(1-2e^{i\theta}), \tag{7.115}$$

with an also dimerized but real-valued lattice gauge function

$$\hat{G}^l_{q_1,q_2} = \left(\frac{1}{2}+(-1)^{l+1+q_1}\hat{S}^z_{l+1,q_1}\right)\left(\frac{1}{2}+(-1)^{l+q_2}\hat{S}^z_{l,q_2}\right). \tag{7.116}$$

7.7.1 Numerical Test of the Symmetrized Mapping

In analogy to the former section we test our new mapping numerically by comparing the energy of each full intra-chain processes with the exactly solvable part that describes the unperturped single chain Luttinger liquid. So we use **Eq**. (7.109) to define the

full intra-chain contribution $\hat{\mathcal{K}}^{\text{intra},m}_{l,l+1}$, similar to **Eq**. (7.82), and compare it with its lowest-order contribution $\hat{\mathcal{K}}^{\text{intra},m,0}_{l,l+1}$, as defined in **Eq**. (7.81). As our new mapping is asymmetric with respect to the interchanging of the legs, we furthermore measure the lowest order of each inter-chain contributions individually $\hat{\mathcal{K}}^{\text{inter},m,0}_{l,l+1}$, i.e.

$$\hat{\mathcal{K}}^{\text{intra},m,n,0}_{l,l+1} = -\frac{1}{4}\left(\frac{1}{2}\zeta^{l}_{m}\hat{S}^{+}_{l+1,m}\hat{S}^{-}_{l,n} + \text{h.c.}\right), \tag{7.117}$$

and compare it with the full part in **Eq**. (7.113). From this we have access to the strength of the x, y-part of the transversal coupling, and can investigate the impact of the correlated hopping on these processes. Nevertheless, whether their total strength is really important for our perturbative treatment of the individual chains, or there exists a weak to strong coupling continuity in the spirit of Schulz, can only be judged later on by consistency of the resulting field theory with the numerical predictions of the critical behavior.

	MI-HI a) ($U = 5.4$, $V = 3$),	MI-HI b) ($U = 1.85$, $V = 0.3$)
$\hat{\mathcal{K}}^{\text{intra},1,0}_{l,l+1}$	0.129936	0.121174
$\mathcal{K}^{\text{intra},1}_{l,l+1}$	0.519745	0.484697
$\hat{\mathcal{K}}^{\text{intra},2,0}_{l,l+1}$	0.129936	0.121174
$\mathcal{K}^{\text{intra},2}_{l,l+1}$	0.519745	0.484697

Table 7.9: *Energy contributions of intra-chain hopping processes defined analogously to* **Eqs**. *(7.81) and (7.82), but with the new symmetric mapping from* **Eq**. *(7.109) [172]. The quantities are measured along the transition (a), or crossover (b), between the Mott and Haldane phase with the same parameters as in* **Tab**. *(7.1). We find that the exactly solvable part is equal among the chains, containing each one quarter of the total intra-chain bond energy. In comparison to* **Tab**. *(7.1), we see that the new mapping is not as good as the Schulz decomposition, for choosing the exactly solvable part of the intra-chain processes as the dominant contribution around $\theta \approx 0$.*

Even this approach was not intended for this parameter region, we investigate first the new mapping on the Mott to Haldane transition line and crossover for small statistical parameters, see **Tab**. (7.9). By comparison to **Tab**. (7.1) one sees that the Schulz mapping indeed works far better in the sense that most of the bond energies are concentrated in the exactly solvable part that describes the unperturbed single chain Luttinger liquid. In the new mapping this exactly solvable part weights only one fourth of the total intra-chain processes instead, whereas the two chains have equivalent values. The inter-chain contributions displayed in **Tab**. (7.10) now differ in value compared to the intra-chain ones, with much smaller values in the transversal direction. We find that the coupling between the chains is asymmetric, where the process of flipping a spin at the bond $(j, j+1)$ from the lower to the upper leg is always larger in energy, whereas in the crossover region, the stronger one becomes almost equal in size compared to the

	MI-HI a) ($U = 5.4$, $V = 3$),	MI-HI b) ($U = 1.85$, $V = 0.3$)
$\hat{\mathcal{K}}^{\text{inter},1,2,0}_{l,l+1}$	0.052015	0.102837
$\mathcal{K}^{\text{inter},1,2}_{l,l+1}$	0.208058	0.411347
$\hat{\mathcal{K}}^{\text{inter},2,1,0}_{l,l+1}$	0.040676	0.051448
$\mathcal{K}^{\text{inter},2,1}_{l,l+1}$	0.162703	0.205794

Table 7.10: *Energy contributions of inter-chain hopping processes according to* **Eqs**. *(7.113) and (7.117) evaluated at Mott to Haldane criticality [172]. In opposition to the Schulz mapping in* **Tab**. *(7.1) the inter- and intra-chain processes are different, whereas the inter-chain processes are generally weaker as the intra-chain ones in* **Tab**. *(7.9). Interestingly the transversal processes become much larger in the crossover region as compared to the values attained at the transition line. There is also an asymmetry between the process of going from leg 1 to leg 2 at the bond $(j, j+1)$ or vice versa, whereas each lowest order process weights again one fourth of the total amount.*

intra-chain processes. Also here, the lowest order contributions defined in **Eq**. (7.117) weights one quarter of the sum of the full bond process.

	a) ($U = -2.25$, $V = 3$),	b) ($U = -2.25$, $V = 3$)
$\hat{\mathcal{K}}^{\text{intra},1,0}_{l,l+1}$	0.070256	0.160844
$\mathcal{K}^{\text{intra},1}_{l,l+1}$	0.281025	0.643377
$\hat{\mathcal{K}}^{\text{intra},2,0}_{l,l+1}$	0.070256	0.167266
$\mathcal{K}^{\text{intra},2}_{l,l+1}$	0.281025	0.669066

Table 7.11: *Exact diagonalization results of intra-chain hopping processes analogously defined to* **Eqs**. *(7.81) and (7.82), but with the new symmetric mapping from* **Eq**. *(7.109) [172]. The energies are evaluated again at the middle bond a) $(L/2, L/2+1)$ and its left-neighboring bond b) at the CDW to Dimer transition line, for $L = 20$ and $\theta = \pi$. On the middle bond the new mapping works roughly equal to the Schulz decomposition, with equally dominating, lowest order, intra-chain contributions, weighting one fourth of the total amount. On the left neighboring bond a slight imbalance between the two chains is developed, whereas the leading order remains positive and is by far more dominant as for the Schulz mapping, see* **Tab**. *(7.2). Again, the large difference between the bond energies is characteristic for the Dimer phase.*

In the pseudo-fermionic limit we have seen in **Tab**. (7.2) that the Schulz mapping seems not to be suitable in the sense that the lowest order intra-chain contributions are small compared to all processes and even changes sign, alternating between the different bonds. While our new mapping works about equally well on the middle bond, see **Tab**. (7.11), it seems to be much better on the neighboring one. Namely, also here the lowest order weights one fourth of all the individual intra-chain processes and is always positive. Again we find that there is a big energy difference between the two bonds, wheres the processes on the left-neighboring ones become slightly asymmetric. The inter-leg energy contributions displayed in **Tab**. (7.12) are comparably small and asymmetric, whereas

	a) $(U=-2.25,\, V=3)$,	b) $(U=-2.25,\, V=3)$
$\hat{\mathcal{K}}^{\text{inter},1,2,0}_{l,l+1}$	0.027124	-0.004407
$\mathcal{K}^{\text{inter},1,2}_{l,l+1}$	0.108497	-0.017626
$\hat{\mathcal{K}}^{\text{inter},2,1,0}_{l,l+1}$	0.003518	-0.009269
$\mathcal{K}^{\text{inter},2,1}_{l,l+1}$	0.014074	-0.037075

Table 7.12: *Exact diagonalization results of inter-chain hopping processes according to* **Eqs**. *(7.113) and (7.117) at the CDW to Dimer transition line [172]. Thereby, the same parameter set as in* **Tab**. *(7.2) or* **Tab**. *(7.11) is used. Again we find that the inter-chain processes are smaller in size than those inside a chain, whereas there is again an imbalance between the former on both bonds. On the left neighboring bond all contributions change their sign and are different in value, yet another manifestation dimerized phase.*

they become negative on the left-neighboring bonds. Especially the circumstance of positive lowest-order intra-chain contributions throughout the bonds, tempted us to conclude the supremacy of our new mapping in the pseudo-fermionic limit. Thereby we understand the supremacy in the sense of the avoiding of a, potentially appearing breakdown of the bosonization treatment caused by negative sound velocities, prior to a renormalization group analysis. Additionally we hope for weak renormalization effects on the coupling, and universal, constants of the theory, such that we can use bare values to discuss our phase transitions and gapless phases later on. As both mappings are exact at the level of Hamiltonians and can simulate the extended anyon-Hubbard model perfectly [172], the current discussion is really about choosing an optimal mapping for the bosonization treatment prior to any renormalization group considerations.

7.7.2 The effective Field Theory

Following exactly the same routine as in the $\theta \approx 0$ case, we can derive a two-channel field theory in effective spin and charge degrees of freedom, i.e.

$$\hat{H}_c = \hat{H}_c^0 + \int dx \Big[A(\partial_x \Theta_c) + \frac{g_1}{(\pi a)^2} \cos(2\Phi_c) + \frac{\tilde{g}_1}{(\pi a)^2} \sin(2\Phi_c) \Big], \quad (7.118)$$

$$\hat{H}_s = \hat{H}_s^0 + \int dx \Big[\frac{g_2}{(\pi a)^2} \cos(2\Phi_s) + \frac{g_3}{(\pi a)^2} \cos(2\Theta_s) \Big], \quad (7.119)$$

$$\hat{H}_{cs} = \int dx \Big[\frac{g_4}{(\pi a)^2} \cos(2\Phi_c)\cos(2\Phi_s) + \frac{g_5}{(\pi a)^2} \sin(2\Phi_c)\sin(2\Phi_s) \Big], \quad (7.120)$$

whereas the correlated hopping bosonization following **Ref**. [140] is sketched in **appendix** (7.11.2). **Eqs**. (7.118) to (7.120) are similar to the former field theory in **Eqs**. (7.90) to (7.91), but is indeed more symmetric with respect to the free Luttinger liquid basis, despite a more complicated transformation in the lattice. Instead of linear and bilinear field gradients in both channels, the new field theory only contains a

chemical potential of phase excitation in the charge sector, i.e.

$$A = -\sqrt{\frac{2}{\pi}} J(1/2 + 1/\pi^2)\sin(\theta). \tag{7.121}$$

The Luttinger parameters of the two sectors are given by the following expressions

$$K_c = 2\left(1 + \frac{\pi(U+6V) + 8\sqrt{2}J\cos(\theta/2)}{\sqrt{2}J(\pi^2/2+1)(1+\cos\theta)}\right)^{-1/2}, \tag{7.122}$$

$$K_s = 2\left(1 - \frac{\pi(U-2V) - 8\sqrt{2}J\cos(\theta/2)}{\sqrt{2}J(\pi^2/2+1)(1+\cos\theta)}\right)^{-1/2}, \tag{7.123}$$

where we observe a similar rescaling of the current and density stiffness as in **Eqs**. (7.94) and (7.95). The sound velocities for each channel are given by the equations,

$$u_c = \sqrt{2}Ja(\pi/2 + 1/\pi)(1+\cos\theta)/K_c, \tag{7.124}$$

$$u_s = \sqrt{2}Ja(\pi/2 + 1/\pi)(1+\cos\theta)/K_s, \tag{7.125}$$

where again a breakdown of Luttinger physics is possible, as a function of θ. The bosonized form of the constrained bosonic operators are deduced from **Eq**. (7.109), i.e.

$$\hat{b}_j \propto e^{i\hat{\Theta}_c(x)}\left(\cos\left(\hat{\Theta}_s(x)\right) + i(-1)^j\frac{1-\sqrt{2}}{1+\sqrt{2}}\sin\left(\hat{\Theta}_s(x)\right)\right) + ..., \tag{7.126}$$

$$\hat{n}_j \propto \partial_x\hat{\phi}_c(x) + \text{const.}(-1)^x\sin\left(\hat{\phi}_c(x)\right)\cos\left(\hat{\phi}_s(x)\right) + ..., \tag{7.127}$$

where of course we obtain the same form of the density operator, but a slightly modified annihilation operator compared to the Schulz mapping in **Eq**. (7.97) [187]. Analogous to the former section, **Eq**. (7.97) and (7.98), as well as **Eq**. (7.86) and (7.109) allow us to deduce the symmetry correspondences between all lattice and continuum entities shown in **Tabs**. (7.13) to (7.16). A crucial difference between the two approaches resides in the fact that the interchanging of the spin index of the ladder is not an internal symmetry of the lattice mapping anymore, but has to be complemented with a sub-lattice interchange, manifest in **Eqs**. (7.126). Therefore the definitions of link-parity and sub-lattice translations have to incorporate this interchange, in order to be consistent with the transformation behavior of **Eq**. (7.109). The same holds true for the respective spin 1 operators, formed by symmetrizing **Eq**. (7.108), where additionally the dihedral and time-reversal operation have to be defined modulo leg permutations. So we can conclude that the internal symmetry is still granted if a larger unit-cell is assumed in the lattice.

We find that the potential symmetry breaking is now encoded explicitly in the odd sinusoidal vertex operators, that can break various symmetries in spin or bosonic degrees of freedom. Those new operators have the same scaling dimensions as the $\cos(2\hat{\phi}_c)$ or

$\cos(2\hat{\phi}_c)\cos(2\hat{\phi}_s)$ terms in **Tab**. (7.3) respectively and thus are relevant whenever the others are. Additionally they act analogously to **Tab**. (7.8), in reducing the different $U(1)$ symmetries in each channel to discrete translation [50, 227].

Symmetries	Lattice	$\hat{H}_c$
$\hat{T}^* = \hat{T}\hat{I}$	$\hat{b}_j \to \hat{b}_{j+1}$	$\hat{\phi}_c \to \hat{\phi}_c + \pi,\ \hat{\Theta}_c \to \hat{\Theta}_c$
Bosonic time reversal $\hat{K}$	$\hat{b}_j \to \hat{b}_j$	$\hat{\phi}_c \to \hat{\phi}_c,\ \hat{\Theta}_c \to -\hat{\Theta}_c$
$U(1)$ gauge $\hat{U}(\alpha)$	$\hat{b}_j \to \hat{b}_j e^{i\alpha}$	$\hat{\phi}_c \to \hat{\phi}_c,\ \hat{\Theta}_c \to \hat{\Theta}_c + \alpha$
Site Parity $\hat{P}_S$	$\hat{b}_j \to \hat{b}_{-j}$	$\hat{\phi}_c(x) \to -\hat{\phi}_c(-x) + \pi,$ $\hat{\Theta}_c(x) \to \hat{\Theta}_c(-x)$
Link Parity* $\hat{P}^*_L = \hat{P}_L\hat{I}$	$\hat{b}_j \to \hat{b}_{1-j}$	$\hat{\phi}_c(x) \to -\hat{\phi}_c(-x),$ $\hat{\Theta}_c(x) \to \hat{\Theta}_c(-x)$
$\hat{U}(\theta/2(\hat{n}_j - 1))\hat{K}\hat{P}_S$	$\hat{b}_j \to e^{i\theta\hat{n}_{-j}}\hat{b}_{-j}$	$\hat{\phi}_c(x) \to -\hat{\phi}_c(-x) + \pi$, $\hat{\Theta}_c \to -\hat{\Theta}_c(-x) + \frac{\theta}{\pi}\partial_x\hat{\phi}_c(-x)$
$\hat{U}(\theta/2(\hat{n}_j - 1))\hat{K}\hat{P}^*_L$	$\hat{b}_j \to e^{i\theta\hat{n}_{1-j}}\hat{b}_{1-j}$	$\hat{\phi}_c(x) \to -\hat{\phi}_c(-x)$, $\hat{\Theta}_c \to -\hat{\Theta}_c(-x) + \frac{\theta}{\pi}\partial_x\hat{\phi}_c(-x)$

Table 7.13: *For the low-energy field theory in* **Eqs**. *(7.118) to (7.119), the symmetry transformations on the dual fields can be found analogously to* **Tabs**. *(7.4) to (7.6). One has to slightly change the definitions of the link parity $\hat{P}_L$ and the sub-lattice translations to include also the interchange of the ladder index. Thus for the new mapping the internal symmetry of the Schulz approach is still valid if a larger unit cell is considered.*

The coupling constants perturbing the free Luttinger Hamiltonians are scaled by the following coupling constants,

$$\frac{g_1}{a} = \frac{1}{2}(2V - U) + \frac{2\sqrt{2}J}{\pi}(1 + \cos\theta), \tag{7.128}$$

$$\frac{g_2}{a} = \frac{1}{2}(U - 2V) + \frac{2\sqrt{2}J}{\pi}(1 + \cos\theta), \tag{7.129}$$

$$\frac{\tilde{g}_1}{a} = \frac{J}{\sqrt{2}}(\cos\theta - 1), \tag{7.130}$$

$$\frac{g_3}{a} = -\frac{\pi J}{2}(1 + 2\cos\theta), \tag{7.131}$$

$$\frac{g_4}{a} = V, \tag{7.132}$$

$$g_5 = -\frac{4J}{\sqrt{2}}\cos(\theta/2), \tag{7.133}$$

where we find again an asymmetry in $g_{1/2}$ [187, 196] and a potential sign change in g_3, that is purely caused by the lattice gauge. In analogy to the gradient terms of the field theory near the bosonic limit, the symmetry breaking terms $\tilde{g}_1$ and g_5 are due to the bosonic/ anyonic nature of the particles. Thereby, the spin-charge coupling g_5 corresponds to the symmetry breaking term that remains if we would consider the bosonic limit again. We find in opposition to the former field theory that this coupling

breaks link parity and sub-lattice translations, also in the $\theta = 0$ case, caused by the sub-lattice dependence of the mapping **Eqs**. (7.109). Additionally, the spin symmetries that are defined modulo the index permutation are also broken in the bosonic limit, in agreement with the symmetries deduced for the Schulz approach.

7.8 Phase Transitions in the bosonic Limit

For sufficiently small statistical parameters we have ensured ourselves that the Schulz approach to the bosonization of a spin 1 operator is indeed a suitable for our needs. So we use **Eqs**. (7.90) and (7.91) to describe the occurring phases and transitions in our model. In this parameter regime we mostly follow the literature concerning the bosonization of the extended Bose-Hubbard or the λ-D model [43, 187, 195, 196], where we assume that the gradient contributions in **Eqs**. (7.90) and (7.91), do not change which coupling constants flows to strong coupling in the respective phases, see **Tab**. (7.17). This is supported numerically, as for $\theta \approx 0$ there are no huge changes in the phase diagram except a slightly decimated Haldane phase, see e.g. **Figs**. (7.16) and (7.17). Nevertheless we may re-include those contributions whenever we discuss the superfluid phases or the emergence of symmetry breaking contributions, as explained in the derivation. In contrast to the bosonizatioon of the λ-D or the extended Bose-Hubbard model [43,187,195,196], we have on the other hand a set of coupling constants that are altered by the lattice gauge, and thus can lead to new phases.

The order parameters for all phases, as well as the relevant contributions of **Eqs**. (7.90) and (7.91), are shown in **Tab**. (7.17) and correspond exactly to those of the λ-D or the extended Bose-Hubbard model [43, 187, 195, 196]. The bosonization of all order parameter follows from **Tab**. (7.7) and **Eq**. (7.61) and can computed straight-forwardly. The parity and the string order parameter in z-direction are more difficult on the other hand [55,187], whereas we can neglect the y, z components as they decay exponentially for

Symmetries	Lattice	$\hat{H}_s$
$\hat{T}^* = \hat{T}\hat{I}$	$\hat{b}_j \to \hat{b}_{j+1}$	$\hat{\phi}_s \to -\hat{\phi}_s,\ \hat{\Theta}_s \to -\hat{\Theta}_s$
Bosonic time reversal $\hat{K}$	$\hat{b}_j \to \hat{b}_j$	$\hat{\phi}_s \to \hat{\phi}_s,\ \hat{\Theta}_s \to -\hat{\Theta}_s$
$U(1)$ gauge $\hat{U}(\alpha)$	$\hat{b}_j \to \hat{b}_j e^{i\alpha}$	$\hat{\phi}_s \to \hat{\phi}_s,\ \hat{\Theta}_s \to \hat{\Theta}_s$
Site Parity $\hat{P}_S$	$\hat{b}_j \to \hat{b}_{-j}$	$\hat{\phi}_s(x) \to -\hat{\phi}_s(-x),\ \hat{\Theta}_s(x) \to \hat{\Theta}_s(-x)$
Link Parity $\hat{P}_L^* = \hat{P}_L\hat{I}$	$\hat{b}_j \to \hat{b}_{1-j}$	$\hat{\phi}_s(x) \to \hat{\phi}_s(-x),\ \hat{\Theta}_s(x) \to -\hat{\Theta}_s(-x)$
$\hat{U}(\theta/2(\hat{n}_j - 1))\hat{K}\hat{P}_S$	$\hat{b}_j \to e^{i\theta\hat{n}_{-j}}\hat{b}_{-j}$	$\hat{\phi}_s(x) \to -\hat{\phi}_s(-x)\ ,\hat{\Theta}_s \to -\hat{\Theta}_s(-x)$
$\hat{U}(\theta/2(\hat{n}_j - 1))\hat{K}\hat{P}_L^*$	$\hat{b}_j \to e^{i\theta\hat{n}_{1-j}}\hat{b}_{1-j}$	$\hat{\phi}_s(x) \to \hat{\phi}_s(-x)\ ,\hat{\Theta}_s \to \hat{\Theta}_s(-x)$

Table 7.14: *Symmetry relations for the spin sector of the field theory in* **Eq**. *(7.119). Analogously to* **Tab**. *(7.6) the symmetry operations in terms of the spin sector can be found by demanding consistency for the transformations on the individual spin 1/2 degrees of freedom in* **Eq**. *(7.86) [196].*

Spin 1 symmetries	Lattice	$\hat{H}_c$
$\hat{K}_S^* = \hat{K}_S\hat{I}$	$\vec{\hat{S}}_j \to -\vec{\hat{S}}_j$	$\hat{\phi}_c \to -\hat{\phi}_c$, $\hat{\Theta}_c \to \hat{\Theta}_c + \pi$
$\hat{U}_x^*(\pi) = \hat{U}_x(\pi)\hat{I}$	$\hat{S}_j^{\pm} \to \hat{S}_j^{\mp}$, $\hat{S}_j^z \to -\hat{S}_j^z$	$\hat{\phi}_c \to -\hat{\phi}_c$, $\hat{\Theta}_c \to \hat{\Theta}_c$
$\hat{U}_y^*(\pi) = \hat{U}_y(\pi)\hat{I}$	$\hat{S}_j^{\pm} \to \hat{S}_j^{\mp}$, $\hat{S}_j^z \to -\hat{S}_j^z$	$\hat{\phi}_c \to -\hat{\phi}_c$, $\hat{\Theta}_c \to -\hat{\Theta}_c + \pi$

Table 7.15: *Correspondences between the symmetries for spin 1 operators defined via symmetrizing* **Eqs**. *(7.108) and the low-energy charge fields in* **Eq**. *(7.118). Also for these transformations, bosonic and spin symmetries have a similar action on the low-energy degrees of freedom and are thus in some sense indistinguishable when they act on the pinning fields [196].*

Spin 1 symmetries	Lattice	$\hat{H}_s$
$\hat{K}_S^* = \hat{K}_S\hat{I}$	$\vec{\hat{S}}_j \to -\vec{\hat{S}}_j$	$\hat{\phi}_s \to \hat{\phi}_s$, $\hat{\Theta}_s \to \hat{\Theta}_s$
$\hat{U}_x^*(\pi) = \hat{U}_x(\pi)\hat{I}$	$\hat{S}_j^{\pm} \to \hat{S}_j^{\mp}$, $\hat{S}_j^z \to -\hat{S}_j^z$	$\hat{\phi}_s \to \hat{\phi}_s$, $\hat{\Theta}_s \to -\hat{\Theta}_s$
$\hat{U}_y^*(\pi) = \hat{U}_y(\pi)\hat{I}$	$\hat{S}_j^{\pm} \to \hat{S}_j^{\mp}$, $\hat{S}_j^z \to -\hat{S}_j^z$	$\hat{\phi}_s \to \hat{\phi}_s$, $\hat{\Theta}_s \to \hat{\Theta}_s$

Table 7.16: *Symmetry transformation from spin 1 operators to the anti-symmetric sector.*

finite θ, see **Fig**. (7.5). Those two order parameters are so tricky to handle because they are non-local and contain also higher order contributions beyond the long-wavelength density fluctuations in the exponent. Their exact expressions were derived exactly in **Ref**. [55], but can also be obtained by symmetrizing the long-wave-length contributions of the naive continuum limit [187], i.e.

$$\begin{aligned} e^{i\pi\sum_{i<j}\hat{n}_i} &\approx e^{i\hat{\phi}_c(x)} \\ \hat{O}_P(j) &\approx \cos\left(\hat{\phi}_c(x)\right) \\ \hat{O}_{HI}(j) &\approx \sin\left(\hat{\phi}_c(x)\right). \end{aligned} \tag{7.134}$$

While the parity order parameter in **Eq**. (7.134) is odd only for site-centered inversions P_S and sub-lattice translations, the Haldane order parameter is even with respect to P_S but breaks sub-lattice translations, bond-centered inversion P_L and all spin symmetries except z-rotations, see **Tabs**. (7.4) and (7.5)[20]. Conversely, if one of those order parameters attains a finite expectation value, see **Tab**. (7.17) then the dual symmetry breaking is encoded in the ground-state phases too. Thereby the bosonization procedure remarkably incorporates the symmetry breaking pattern only visible in the dual λ-D model in **Eq**. (7.25), in terms of local observables [239]. Thereby a crucial point is that the symmetry breaking is intrinsically non-local and so does not lead to a degenerate groundstate in the case of the Mott or Haldane insulator, as can be inferred

[20]The next leading order of the Haldane order parameter was shown in **Ref**. [187] to be of the form, $\partial_x\hat{\phi}_c(x)\cos(\hat{\phi}_c(x)))$, which breaks also site-centered inversion $\hat{P}_s$.

from **Tab**. (7.17) [196]. For example in the Mott phase we have to require that $g_1 < 0$ and $g_3 < 0$ are relevant. Pinning one of the field inside a minimum, let's say $\hat{\phi}_S$, the compactification radius of the other field is fixed by the transformation in **Eq**. (7.89), i.e. $\hat{\phi}_c \equiv \hat{\phi}_c + 2\pi$. Hence it follows that two possible minima of both fields are not contained inside the compactification and thus should be viewed as unique, whereas the same argument also applies to the Haldane phase [196]. For an ordinary, gapped, symmetry breaking phase, this is not true and one of the fields develops two minima inside its compactification radius, and so the groundstate is degenerate. This duality is manifest in the equivalent symmetry breaking pattern of the Haldane and the CDW order parameter in **Tab**. (7.17), whose lattice versions are interrelated by the non-local Kennedy-Tasaki-Lieb transformation, see **Eq**. (7.24) [190, 191].

Phases	Bosonized Order parameter	Relevant Coupling	Broken Symmetries
(MI)	$\cos\left(\hat{\phi}_c(x)\right)$	$g_1 < 0,\ g_3 < 0$	$\hat{T}, \hat{P}_S$
(CDW)	$\sin\left(\hat{\phi}_c(x)\right)\cos\left(\hat{\phi}_s(x)\right)$	$g_1 > 0,\ g_2 < 0$	$\hat{P}_L, \hat{T}, \hat{U}_{x,y}(\pi), \hat{K}_S$
(HI)	$\sin\left(\hat{\phi}_c(x)\right)$	$g_1 > 0,\ g_3 < 0$	$\hat{P}_L, \hat{T}, \hat{U}_{x,y}(\pi), \hat{K}_S$
(SF)	$e^{i\hat{\Theta}_c(x)}\cos\left(\hat{\Theta}_s(x)\right)$	$\hat{H}_c^0,\ g_3 < 0$	$\hat{K}, \hat{K}_S, \hat{P}_{S,L}, \hat{U}_{x,y,z}(\pi)$
(PSF)	$e^{2i\hat{\Theta}_c(x)}$	$\hat{H}_c^0$,, $g_2 < 0$	$\hat{K}, \hat{K}_S, \hat{P}_{S,L}, \hat{U}_{x,y}(\pi)$

Table 7.17: *Bosonized form of operators used to describe the phases in the bosonic limit, as well as the relevant couplings of the respective phase, and their symmetry implications. Thereby it is crucial to understand that the symmetries are only broken in the dual space and the ground-state is unique for the SPT phases. The order parameters shown here are exactly the same as for the λ-D or the extended Bose-Hubbard model [187, 195, 196], where the distinction between spins and constrained bosons resides in higher order irrelevant operators, that are not shown here. This allows us to use the same scheme of relevant coupling constants as for the spin model, where we assume that the gradient terms do not change the renormalization group flow of the couplings drastically, and symmetry breaking vertex operators are up to now neglected. For the gapless phases we include the symmetry breaking terms on the other hand, where we neglect the global bosonic $U(1)$ symmetry, due to the Mermin-Wagner theorem [74, 75, 129]. In addition, all the phases can further be classified in terms of $U(1)_{\phi/\Theta}$ symmetries of the Luttinger liquid or their reduction depending on the relevant operators, see* **Tab**. *(7.18) [227].*

Furthermore, we can additionally classify phases by their different reduction patterns of the $U(1)$ symmetries of the dual fields, see **Tab**. (7.18). Here we find of course, that the two SPT share the same reduction scheme as they have the same set of relevant couplings.

7.8.1 Mott to Haldane Insulator Transition

The transition between the two SPT phases, or its crossover, was confirmed numerically by sharp or smooth information theoretic measures, see **Fig**. (7.4), non-vanishing

Phases	Reduced $U(1)$ symmetries
MI	$\mathbb{Z}_{2,\phi_c} \bigotimes U(1)_{\Theta_c} \bigotimes U(1)_{\phi_s} \bigotimes \mathbb{Z}_{2,\Theta_s}$
HI	$\mathbb{Z}_{2,\phi_c} \bigotimes U(1)_{\Theta_c} \bigotimes U(1)_{\phi_s} \bigotimes \mathbb{Z}_{2,\Theta_s}$
CDW	$\mathbb{Z}_{2,\phi_c} \bigotimes U(1)_{\Theta_c} \bigotimes \mathbb{Z}_{2,\phi_s} \bigotimes U(1)_{\Theta_s}$
SF	$U(1)_{\phi_c} \bigotimes U(1)_{\Theta_c} \bigotimes U(1)_{\phi_s} \bigotimes \mathbb{Z}_{2,\Theta_s}$
PSF	$U(1)_{\phi_c} \bigotimes U(1)_{\Theta_c} \bigotimes \mathbb{Z}_{2,\phi_s} \bigotimes U(1)_{\Theta_s}$

Table 7.18: *Reduction of Luttinger liquid $U(1)$ symmetries for the respective phases, according to the relevant coupling constants in* **Tab**. *(7.17). It should be noted, that the Haldane and the Mott insulator show exactly the same patterns, as they should as being complementary SPT phases.*

characteristic string orders in **Figs**. (7.5) and 7.8, as well as parameter-dependent universal coefficients along the Gaussian transition line. Analytically, the ordinary form of the λ-D model or its extensions, do not allow for a continuous transition between the two phases according to Landau theory, as both are invariant with respect to the same local onsite symmetries. In this case, Landau theory would predict either a first order transition or a crossover between the phases [196, 227], where the latter would actually fit to the adiabatic passage numerically observed for a comparably large hopping. On the other hand, in the dual λ-D model in **Eq**. (7.25) the Haldane phase is related to a symmetry breaking pattern, while the large D phase is still symmetric with respect to all onsite symmetries [190, 191]. Hence one could argue that Landau theory would predict correctly a continuous transition between the two in this dual picture. Despite this partial success, the unification of both transition, and especially the interchange mechanism, seems to be beyond the Landau paradigm.

From a field theoretical perspective we conclude, in analogy to the phases in the λ-D model shown in **Tab**. (7.17) [187, 195, 196], that the charge sector is the relevant one and the Gaussian transition occurs at $g_1 = 0$. **Eq**. (7.104) shows that the critical line obtained for the λ-D model, that can also be obtained by a simple mean-field consideration, is altered by the presence of the lattice gauge. The transition is described by the free charge sector in **Eq**. (7.90), with a compactified boson of unit central charge [187, 196]. In this case the two non-Landau order parameters $\sin(\phi_c), \cos(\phi_c)$ are only non-zero in their respective phases, and the two phases are topologically distinct as all the protecting symmetries are still intact [187, 196], see the green squares in **Fig**. (7.19). This is consistent with the irrelevance of such symmetry breaking terms for comparably suppressed hopping. As we have seen in the derivation of the field theory, the bosonic nature of the particles leads to breaking of the spin-space symmetries of the λ-D chain, whereas a non-zero statistical parameter leads to the additional breaking of parity symmetries, as well as bosonic time reversal, see **Tabs**. (7.4) to (7.7). Nevertheless, the distinction between the symmetries are partially blurred for low-energies and so for example parity is effectively broken also in the bosonic case whenever we follow

Ref. [187,196] and add the vertex operator $\sin(2\phi_c)$ to take the broken spin symmetries into account. Furthermore, theses effects are only dependent on the lattice gauge and are thus expected to be especially relevant when the hopping is, which is indeed the case in this region of the Haldane phase. In accordance with **Tab**. (7.17), we conclude then, that the relevant part of the charge sector should be written in the following form [187, 196],

$$\begin{aligned}\hat{H}^{\mathrm{rel}}_{\mathrm{HI},c} &= \int dx \left[\frac{g_1}{(\pi a)^2}\cos\left(2\hat{\phi}_c(x)\right) + \frac{\bar{g}_1}{(\pi a)^2}\sin\left(2\hat{\phi}_c(x)\right)\right] \\ &= \mathrm{sgn}(g_1+\bar{g}_1)\frac{\sqrt{g_1^2+\bar{g}_1^2}}{(\pi a)^2}\int dx \cos\left(2\hat{\phi}_c(x) + \arctan(-\bar{g}_1/g_1)\right),\end{aligned} \tag{7.135}$$

whereas the g_3 term of the spin sector is additionally pinned. **Eq**. (7.135) implies that there exists an adiabatic passage between the two SPT phases, by smoothly going from one minima to the other without a phase transition [187, 196], see the blue ovals in **Fig**. (7.19). Thereby the hidden string order parameters $\sin(\phi_c), \cos(\phi_c)$ acquire each a finite expectation value in both phases, which implies a symmetry breaking according to the Kennedy-Tassaki-Lieb duality but still non-degenerate groundstates [187, 196]. The symmetry breaking vertex operator $\sin(2\phi_c)$ is on the other hand forbidden if the spin-symmetries or parity symmetries in **Tabs**. (7.4) to (7.7) are still intact, hence one says that those symmetries are protecting the distinction of SPT phases. Up to now the discussion is completely equivalent to the Bose-Hubbard case, as the additional anyonic symmetry breaking beyond the asymmetry of $\hat{\phi}_c(x) \to -\hat{\phi}_c(x)$ is encoded in the charge phase field $\hat{\Theta}_c(x)$. The $U(1)$ symmetry of bosonic particle number conservation forbids any vertex operator of this field, and such effects are thus not visible in our case. This can also be seen from the non-linear parity transformation of the extended anyon-Hubbard model in **Tabs**. (7.4) and (7.6), which trivially reduces to ordinary parity transformations in **Eq**. (7.135). Therefore we prefer to contradict the wording of **Ref**. [185], to call the Haldane phase in our model anyonic, as at least for our Hamiltonian the protecting symmetries are equivalent to the bosonic case [187]. Anyonic models that do not have a $U(1)$ symmetry could be used to investigate the potential appearance of such an anyonic Haldane phases, but are explicitly non-local in the lattice and thus not very physical. Also the derived string order parameter of **Ref**. [185], corresponding to the anyonic Haldane phase, should trivially reduce for our model to the one valid for the purely bosonic model.

7.8.2 Gapless Phases and their Transitions

The two gapless phases of our model can be related to the XY orders of the λ-D models with bosonized order parameters of the form [195],

$$\hat{O}_{SF}(j) = \hat{b}_j \propto e^{i\hat{\Theta}_c(x)} \cos\left(\hat{\Theta}_s(x)\right), \tag{7.136}$$

$$\hat{O}_{PSF}(j) = \hat{b}_j^2 \propto e^{2i\hat{\Theta}_c(x)}, \tag{7.137}$$

see **Tab**. (7.17). The gapless charge sector in **Eq**. (7.90) is the one that governs both superfluid orders, as it should. The reasoning behind that is its relation to the total number of bosons, as can be inferred from the zero-modes for finite system sizes, and so to the corresponding $U(1)$ symmetry and its forbidden breaking in low dimensions according to the Mermin-Wagner theorem [74, 75, 129, 240]. The statement of the theorem is thereby perfectly contained in the Luttinger framework by an algebraic decay of the order parameters instead of real long-range order [52].

According to **Tab**. (7.17), have to demand that g_1 is irrelevant, such that the sector is gapless, which implies that $K_c > 2$, as can be inferred from **Tab**. (7.3). In contrast to **Ref**. [187] we see that attaining this value of the universal parameter is simplified by attractive on-site interactions U that can effectively balance out the nearest neighbor interaction V and the repulsive effect of the lattice gauge for small θ, i.e. for $U < -6V - J\mathrm{Re}(z_4)$ according to **Eq**. (7.94). This is in accordance with the numerical predictions, as for example shown in **Fig**. (7.14), that indeed show a stabilization of superfluid coherence for attractive onsite interactions U. The spin sector in **Eq**. (7.91) on the other hand determines if the superfluid or pair-superfluid order emerges in the following sense [195]. For $K_s < 1$, i.e. for $U < 2V + J\mathrm{Re}(z_1) - 3J\pi\mathrm{Re}(z_1 - z_4/2\pi^3)/4$ according to **Eq**. (7.95), the g_2 term is more relevant as g_3, and we can treat it semi-classically, implying that the $\hat{\phi}_s$ is pinned into a minimum that depends on the sign of g_2. Thereby the sign change of g_2 is altered by the lattice gauge, in contrast to the ordinary bosonic or spin 1 case [187, 195], see **Eq**. (7.105).

This implies furthermore, that the dual field $\hat{\Theta}_s$ is strongly fluctuating by the Heisenberg uncertainty, meaning that every expectation value containing the field is exponentially decaying [43, 55]. In this case, the ordinary superfluid order parameter in **Eq**. (7.136) is indeed exponentially decaying, while the pair-superfluid order parameter of **Eq**. (7.137) decays algebraically, see **Fig**. (7.10) [195]. So in this case we have a pair-superfluid order, where we have additionally staggered, transversal contributions arising from the density operator in **Eq**. (7.98) [195]. For $K_s > 1$, the g_3 term dominates and the Θ_s field is pinned on the other hand. As g_3 is always negative for small θ, i.e. changes sign at $\theta = 3\pi/4$ according to **Eq**. (7.106), the minimum is attained at $\Theta_s = 0$ and the superfluid order in **Eq**. (7.136) is naturally dominant over its square in **Eq**. (7.137). Thus in this case we have an ordinary superfluid order, with the slowest

decay of **Eq**. (7.136). The staggered contribution of the density operator then decays exponentially, as it contain a strongly fluctuating field ϕ_s [195].

Up to now the two superfluids have exactly the same properties as the XY orders in the λ-D model, but what is the impact of the anyonic statistics ? To answer this question we have to re-include the gradient terms into the discussion, that are responsible for the anyonic symmetry breaking, as can be seen in **Tabs**. (7.4), (7.6) and (7.17). The properties of both superfluids are severely affected by the bilinear coupling C_c and the attached phase gradient A, as we have seen in the former chapter. Their presence explains the shifted quasi-momentum distribution of anyon-Hubbard type models [13, 18, 27, 33], by a trivial gauge shift of the $\hat{\Theta}_c$ field, as well as the asymmetry between left and right-movers that becomes relevant for finite times or temperatures [26, 241]. Thus we can conclude that the superfluid orders in the anyonic system have the same relevant order parameters as the λ-D model, but inherit the characteristic symmetry breaking of their correlation functions via a parity-time asymmetric Luttinger liquid, **Tab**. (7.17). Comparing **Eq**. (7.136) and (7.137) without the gradient terms, we see that the two transform differently with respect to spin time-reversal, see **Tab**. (7.5), and to $U(1)$ rotations with an angle $\alpha = \pi$, see **Tab**. (7.4), that correspond to z-rotations of the dihedral group. While the ordinary superfluid order parameter is odd under those transformations the pair-superfluid one is invariant, implying a symmetry difference between the two phases in the λ-D model. The gradient terms break also the remaining spin time reversal symmetry, among other bosonic symmetries, in the pair-superfluid phase, while π-rotations around the z-axis are still intact, see **Tab**. (7.17). Furthermore, the two phases can be distinguished by their different $\mathbb{Z}_2$ symmetries in the spin sector, see **Tab**. (7.18).

Especially the pair-superfluid is interesting for us, as it does not appear in un-constrained bosonic systems, and occurs purely due to the interplay of intrinsic particle number restrictions and attractive onsite interactions, that would otherwise lead to a wavefunction collapse for un-constrained bosons. As noted by Schulz himself for the λ-D model [195], the description of this phase in terms of the two field theories as in **Eq**. (7.90) and (7.91), is physically rewarding but can be understood more easily from perturbative arguments derived in **appendix** (7.11). Namely, by considering first order perturbation theory for strongly attractive U, the following effective model can be derived from **Eq**. (7.1) [242],

$$\hat{H}_{\text{eff}} \approx -\bar{J}\sum_j \left(e^{i\theta}\hat{s}_j^+\hat{s}_{j+1}^- + \text{h.c.}\right) + \bar{\Delta}\sum_j \hat{s}_j^z\hat{s}_{j+1}^z, \quad \bar{J} = \frac{2}{|U|}, \bar{\Delta} = \frac{(2|U|V+1)}{|U|}, J = 1 \tag{7.138}$$

The effective spin 1/2 operators in **Eq**. (7.138) correspond to bosonic two-particle excitations in the sub-space of having only a hole or a double occupation locally. In

comparison to the results derived for the λ-D model [242], our pair-superfluid in **Eq**. (7.138), has an additional phase in the kinetic energy that depends on the statistical parameter. **Eq**. (7.138) is thus a generalization of the XXZ chain, that features the following Luttinger liquid description at half-filling [43], i.e.

$$\hat{H}_{\text{eff}} \approx \hat{H}_0 + \frac{2}{\pi}\sin(\theta)\int dx\ \ \partial_x\Theta(x). \tag{7.139}$$

In **Eq**. (7.139) $\hat{H}_0$ denotes the ordinary Luttinger liquid Hamiltonian with parameters u and K corresponding to a XXZ chain in weak-coupling, with a Fermi-velocity rescaled by the statistical parameter, i.e. $v_F = \bar{J}a\cos(\theta)$, and a linear phase field gradient that inherits the symmetry breaking. The Hamiltonian straightforwardly leads to the algebraic decay of pair-correlations as the dominant order via the following equation,

$$\langle(\hat{b}_i^\dagger)^2(\hat{b}_j)^2\rangle \approx \langle\hat{s}_i^+\hat{s}_j^-\rangle \propto \frac{e^{i\sin(\theta)(x-y)/(\pi v_J)}}{|x-y|^{\frac{1}{2K}}}. \tag{7.140}$$

Eq. (7.140) manifests the difference between the $XY2$ phase and the pair-superfluid phase of our constrained anyonic system, by a complex phase that leads to a quasi-condensation point shifted away from $k \approx 0$.

The transitions of the gapped to gapless phases, have been numerically proven to be of BKT like [230–232], see **Fig**. (7.19). This implies that the relevant field theory should be of Sine-Gordon type, which indicates that the marginal interactions can be safely neglected in **Eq**. (7.90). Starting from the Mott, the Haldane, or the Charge-Density-Wave, the transition to the superfluid phases occur if g_1 becomes irrelevant, expressible by a BKT scaling of g_1 and the scaling dimension Δ_1[21] [243] , i.e.

$$\frac{dg_1(l)}{dl} = (2-\Delta_1)g_1(l), \qquad \frac{d\Delta_1(l)}{dl} = -bg_1^2(l)\Delta_1^3(l), \tag{7.141}$$

where b denotes a non-universal numerical constant. The different BKT transitions can then be distinguished by the relevance of the $g_{2,3}$ term of the spin sector, implying either an ordinary superfluid to gapped, or pair-superfluid to gapped transition. Thereby the transitions of the superfluid to the Haldane and Mott phase have the same $U(1)$ reducing pattern and are distinguished only by the sign of g_1, see **Tabs**. (7.18) and (7.17) respectively. To be more precise, whenever the distinction between the two SPT phase is repealed, we should rather speak of a single transition from the superfluid to a SPT phase which has either more Mott or Haldane character along the transition line. Finally the generalization the BKT scaling relations in **Eq**. (7.141), to include all gradient couplings of the charge sector in **Eq**. (7.90), would be a formidable task to support our assumption of their irrelevance analytically.

[21] The following formula is a priori only valid if all linear and bi-linear gradient terms are neglected.

Going from the CDW phase all the way through the superfluid phases to the Mott insulator, for some small V, the negative sector is pinned by either the g_2 or g_3 term. At the phase boundary between the superfluid and the pair-superfluid both terms have to become equally relevant, i.e. at $K_s = 1$ for $U = 2V + J\mathrm{Re}(z_1) - 3J\pi\mathrm{Re}(z_1 - z_4/2\pi^3)/4$ according to **Eq**. (7.95). The sub-group inclusion of the residual symmetries of the two gapless phases, deduced from **Tab**. (7.17), indicates a second-order transition of Ising type, as predicted by Schulz for the λ-D model [195]. Sadly only the correct transition order but not a central charge of $c = 1/2$ was confirmed numerically, see **Fig**. (7.18), whereas we relate this issue to the poor numerical precision used in here, as this transition was actually not of our main interest. Analytically the universality class can be derived from a refermionization of the left and right-movers of the spin-sector in **Eq**. (7.91), at the self-dual point [43, 187, 196, 244], i.e. $g_3 = g_2 =: g_{2,3}$ implying that $U = -2\pi\mathrm{Re}(z_1) - J\mathrm{Re}(z_4)/\pi + V$ according to **Eqs**. (7.105) and (7.106), as well as $K_s = 1$. Refermionization amounts to inverting the bosonization procedure,

$$\begin{aligned} e^{-i(\Theta_s+\Phi_s)} &\propto \hat{\psi}^\dagger_{R,s}, \\ e^{-i(\Theta_s-\Phi_s)} &\propto \hat{\psi}^\dagger_{L,s}, \end{aligned} \tag{7.142}$$

whereas the new left and right movers are not those of the single-chains anymore, but correspond to an anti-symmetric combination of them. At $K_s = 1$ this leads to a pairing term for the g_3-coupling and a left-to-right interchange for g_2 [43, 196, 244], i.e.

$$\begin{aligned} \cos(2\hat{\Theta}_s) &\overbrace{\propto}^{K_s=1} \left(\psi^\dagger_{R,s}\psi^\dagger_{L,s} + \mathrm{h.c.}\right), \\ \cos(2\hat{\phi}_s) &\overbrace{\propto}^{K_s=1} \left(\psi^\dagger_{R,s}\psi_{L,s} + \mathrm{h.c.}\right), \end{aligned} \tag{7.143}$$

yielding finally a Bogoliubov type model with a linear dispersion of both species. Such Bogoliubov Hamiltonians can be diagonalized straight-forwardly [125, 126], but exactly at the self-dual point we have additionally that $g_2 = g_3$ which allows for an elegant solution in terms of Majorana fermions, i.e.

$$\begin{aligned} \hat{\psi}^\dagger_{R,s} &= \frac{\hat{c}_1 + i\hat{c}_2}{\sqrt{2}}, \\ \hat{\psi}^\dagger_{L,s} &= \frac{\hat{\tilde{c}}_1 + i\hat{\tilde{c}}_2}{\sqrt{2}}. \end{aligned} \tag{7.144}$$

The transformation in **Eq**. (7.144) can also be applied to the bilinear gradient term C_s of the spin sector, that we re-include now, yielding two Majorana theories at the critical line $g_3 = g_2 =: g_{2,3}$ and $K_s = 1$ [196, 244], i.e.

$$\hat{H}_s = -\frac{i}{2}\sum_{j=1,2}\int dx\,\left[(u_s - C_s/2)\hat{\tilde{c}}_j\partial_x\hat{\tilde{c}}_j - (u_s + C_s/2)\hat{c}_j\partial_x\hat{c}_j\right] - \frac{2ig_{2,3}}{\pi a}\int dx\;\hat{c}_1\hat{\tilde{c}}_1. \tag{7.145}$$

From **Eq**. (7.145) one can conclude that the first field is massive, whereas the second one is free, corresponding to an Ising model at criticality with a central charge of $c = 1/2$ [187, 196, 244][22]. Thereby the sound velocity should always be larger than the current-density coupling, i.e. $u_s > |C_s|$, to ensure thermodynamic stability of the left and right-movers. According to **Tab**. (7.8), an equally relevant g_2 and g_3 at the critical line corresponds to a complete reduction of all continuous $U(1)$ symmetries of the spin sector to the $\mathbb{Z}_2$ symmetries. For this $c = 1/2$ transition, the $U(1)$ symmetries of the charge sector are intact, as the Hamiltonian is gapless.

7.8.3 Charge-Density-Wave to Haldane insulator transition

The transition of the CDW to the Haldane insulator was numerically confirmed to be of second order with a central charge of $c = 1/2$, and a characteristic scaling of the CDW order parameter shown in **Fig** (7.11). From a field theoretical point of view the transition can explained analogously to the former subsection by refermionization of the left and right movers [43, 187, 196, 244], see **Eq**. (7.144). Namely, the transition happens whenever the g_3-term becomes less relevant than g_2, i.e. for $K_s < 1$. In contrast to the transition between the gapless phases, the charge sector is gapped and thus g_1 is relevant, whereas the spin sector describes the Ising transition exactly at $g_2 = g_3$ and $K_s = 1$. Thus we can in principle distinguish the two Ising transitions with respect to their $U(1)$ reduction pattern according to **Tab**. (7.18), whereas the $U(1)$ symmetry of the density field ϕ_c is reduced to $\mathbb{Z}_2$. Also in this case, the transition order is consistent with Landau theory and the sub-group inclusion of the residual symmetry groups of the Haldane and the CDW phase, i.e. $G_{CDW}^{\text{residual}} \subset G_{HI}^{\text{residual}}$. Namely, in the Haldane case the ground-state is unique with all local symmetries being intact, and thus the residual symmetry group is equal to that of the full Hamiltonian. In the CDW phase on the other hand some symmetries are broken, which implies that the residual group is contained in the full symmetry group of the Hamiltonian. This circumstance is reflected in the groundstate degeneracies of both phases in **Tab**. (7.17), that follows

[22] It should be noted that when both g_2 and g_3 become zero the theory in **Eq**. (7.145) corresponds to a central charge of $c = 1/2 + 1/2 = 1$. This can only happen for statistical parameters of $\theta = 3/4\pi$ according to **Eq**. (7.106), which is not the aimed regime of our theory, and cannot be identified with this transition anymore, as indicated by the numerical phase diagram that only shows pair-superfluid order for large statistical parameters.

from a semi-classical evaluation of vertex operators [196]. The fact that both bosonized order parameter break the same symmetries, underlines the pictorial representation of the non-trivial Haldane phase as a CDW order with an unknown amount of single occupation separating the alternations [186,187]. While both order parameters are finite in the CDW phase, indicating an ordinary order and thus also a trivial, hidden order, the CDW order parameter decays exponentially in the Haldane phase and only the now non-trivial hidden order remains intact.

7.9 The Dimer Phase and its Transitions at $\theta \approx \pi$

In the pseudo-fermionic limit, we have seen that our symmetrized mapping works better than the Schulz decomposition in keeping the most dominant energy contributions inside the intra-chain processes. So we expect rather weak renormalization effects of the x, y inter-chain couplings, such that the new theory describes the occurring phases and their transitions more accurately in terms of bare coupling constants. From the numerical phase diagram in **Fig**. (7.15) we see that the parameter region of interest is for strongly attractive U, whereas especially the hopping energy J is always small compared to U. This generally suppresses ordinary superfluid order and portends that the symmetry breaking terms inheriting the anyonic/bosonic nature of our model are not very pronounced. Nevertheless, for comparably small ratios of the attractive onsite interactions and the kinetic energy, the dimerized phase arises [33]. From the bare Luttinger parameter of the charge sector in **Eq**. (7.122), we can conclude that this channel is gapped in this region, i.e. for $U \geq -(8\sqrt{2}\cos(\theta/2)/\pi + 6V)$ it follows that $K_c \leq 2$, and thus the sinusoidal vertex operators in **Eq**. (7.118) are relevant. Analogously to **Eq**. (7.135), the charge density field ϕ_c is pinned in its minimum according to the new coupling constant $\bar{g}_1$ [187, 196], i.e.

$$\begin{aligned} \langle \phi_c \rangle &= \min_{\phi_c} \bar{g}_1 \cos(2\phi_c + \xi_c), \\ \bar{g}_1 &= \mathrm{sgn}(g_1 + \tilde{g}_1)\sqrt{g_1^2 + \tilde{g}_1^2}, \\ \xi_c &= \arctan\left(-\tilde{g}_1/g_1\right), \end{aligned} \tag{7.146}$$

that depends on the symmetry breaking vertex operator $\tilde{g}_1$. It follows that the spin-charge coupling in **Eq**. (7.120) effectively renormalizes the spin sector to the following

form,

$$\hat{H}_s = \hat{H}_s^0 + \int dx \Big[\frac{\tilde{g}_2}{(\pi a)^2} \cos(2\phi_s + \xi_s) + \frac{g_3}{(\pi a)^2} \cos(2\Theta_s) \Big], \tag{7.147}$$

$$\tilde{g}_2 = \mathrm{sgn}(g_2 - \mathrm{sgn}(\bar{g}_1) g_4 \cos(\xi_c)) \sqrt{(g_2 - \mathrm{sgn}(\bar{g}_1) g_4 \cos(\xi_c))^2 + (g_5 \sin(\xi_c))^2}, \tag{7.148}$$

$$\xi_s = \arctan\left(\frac{\mathrm{sgn}(\bar{g}_1) g_5 \sin(\xi_c)}{g_2 - \mathrm{sgn}(\bar{g}_1) g_4 \cos(\xi_c)} \right), \tag{7.149}$$

whereas the single field theory parametrically depends on the minimum of the charge sector. **Eq**. (7.147) describes then all relevant gapped to gapped transitions in the pseudo-fermionic limit, whereas the pair-superfluid order can only emerge for $K_c > 2$ and is excluded here. Before we describe those transitions in analogy to the bosonic limit, we develop a microscopic theory for the dimerized phase, derive its order parameter and discuss its low-energy signatures. Thereby the discussion is in principle valid for both low-energy theories derived in this chapter, but is later on only examined for **Eq**. (7.147), due to its numerically anticipated supremacy in the pseudo-fermionic limit.

7.9.1 A Microscopic Theory of the Dimer Phase

So far we have numerically used an order parameter for the Dimer phase, that was sufficient to detect the phase, but too general to allow for a microscopic picture of the phase or its symmetries. In the following subsection such a local Landau order parameter is proposed based on the on-site $su(3)$ algebra [8], forming all possible local operators of the local Hilbert space dimension 3, and its extension considering a bond instead of a site as the fundamental unit. We define $su(2)$ sub-algebras on a bond that have a definite action with respect to an interchange of the internal species of the particle description of $su(3)$. These internal species are then related to the two leg degrees of freedom in the spin-ladder description of the extended anyon-Hubbard model. The bosonization of these currents reproduces all known symmetry breaking phases of such two-leg spin ladders, whereas two of the four can be identified with dimerized phases [196]. As a non-vanishing order parameter corresponds to a specific set of relevant coupling constants, we can identify our dimerized phase with a staggered Dimer, at the hand of their allowed bare coupling values. This finally allows to draw a microscopic picture of the Dimer phase in terms of bosonic lattice operators and to formalize the in-applicability of conventional Landau theory for the Dimer to CDW transition.

The basis of this approach is that the local Hilbert space dimension 3 determines all local operators and thus also all possible local order parameters in terms of an $su(3)$ algebra [8]. The generators $S^{\mu\nu}$ in the fundamental representation can be compactly

written in matrix notation [8],

$$S_j = \begin{pmatrix} \frac{2}{3} - \tilde{n}_j & \tilde{b}_{j,1} & \tilde{b}_{j,2} \\ \tilde{b}^\dagger_{j,1} & \tilde{n}_{j,1} - \frac{1}{3} & \tilde{b}^\dagger_{j,1}\tilde{b}_{j,2} \\ \tilde{b}^\dagger_{j,2} & \tilde{b}^\dagger_{j,2}\tilde{b}_{j,1} & \tilde{n}_{j,2} - \frac{1}{3} \end{pmatrix} = \begin{pmatrix} \frac{2}{3} - (1-\hat{n}_j)^2 & \hat{b}^\dagger_j(1-\hat{n}_j) & \frac{\hat{n}_j\hat{b}_j}{\sqrt{2}} \\ (1-\hat{n}_j)\hat{b}_j & \frac{(1-\hat{n}_j)(2-\hat{n}_j)}{2} - \frac{1}{3} & \frac{(\hat{b}_j)^2}{\sqrt{2}} \\ \frac{\hat{b}^\dagger_j\hat{n}_j}{\sqrt{2}} & \frac{(\hat{b}^\dagger_j)^2}{\sqrt{2}} & \frac{\hat{n}_j(1-\hat{n}_j)}{2} - \frac{1}{3} \end{pmatrix}, \tag{7.150}$$

fulfilling the site-local commutation relations,

$$\left[S^{\mu\bar{\mu}}, S^{\nu\bar{\nu}}\right] = \delta_{\bar{\mu}\nu} S^{\mu\bar{\nu}} - \delta_{\bar{\nu}\mu} S^{\nu\bar{\mu}}. \tag{7.151}$$

The first matrix in **Eq**. (7.150) consists of operators of constrained hard-core bosons, i.e. $\tilde{b}^\dagger_1 = \hat{b}^\dagger_1(1-\hat{n}_2)$, which only allow for single occupance, whereas the second matrix contains our constrained bosons defined in **Eq**. (7.2). Spin 1 operators can then be expressed in terms of this fundamental language [8], i.e.

$$\begin{aligned} \hat{S}^+ &= \sqrt{2}\left[\tilde{b}^\dagger_1 + \tilde{b}_2\right], \\ \hat{S}^z &= \left[\tilde{n}_1 - \tilde{n}_2\right], \end{aligned} \tag{7.152}$$

that can be identified with the non-symmetric mapping in **Eq**. (7.108), together with a π-rotation around the x-axis for the second species, see **Eq**. (7.6). This means that we can relate a permutation symmetric version of **Eq**. (7.152), modulo a sub-lattice translation, to our symmetrized version of **Eq**. (7.108), by an x-rotation of both species plus an index permutation, which flips the sign of all dual charge and spin fields according to **Tabs**. (7.15) and (7.16).

This internal transformation leads to an interchange of the identification of the long-wavelength fluctuations of the charge and spin density field with the spin 1 operators in the lattice. This means that in this framework the spin field is identified with the total number of constrained bosons, relative to the unit filling, while the charge field does not feature a simple interpretation, i.e.

$$\begin{aligned} \hat{S}^z &= (1-\hat{n}) \propto \partial_x \hat{\phi}_s(x) + ..., \\ (\hat{S}^z)^2 &\propto \partial_x \hat{\phi}_c(x) + ..., \end{aligned} \tag{7.153}$$

but can be related to a spin-nematic order parameter in spin 1 chains [8]. Conversely, this corresponds to the, so far lacking, interpretation of the spin field for our constrained bosons, that is otherwise hard to see from the Schulz mapping or transformations of the form of **Eq**. (7.108).

Exemplifying this rather abstract framework further, we may immediately recognize the local CDW order parameter as the diagonal element of the $su(2)$ sub-algebra of **Eq**. (7.150) in a Jordan-Schwinger like representation [91], i.e.

$$\begin{aligned} (\hat{S}^{+})^2 &\propto \hat{s}^{+} = \tilde{b}_1^{\dagger}\tilde{b}_2, \\ \hat{S}^{z} &\propto \hat{s}^{z} = \frac{1}{2}\left[\tilde{n}_1 - \tilde{n}_2\right]. \end{aligned} \tag{7.154}$$

The $S = 1$ dimensional representation of the original spin operators in **Eq**. (7.152) is thereby reduced to the $S = 1/2$ dimensional representation in **Eq**. (7.154) in the subspace of having only holes or double occupations per site. Including also the staggered contributions in **Eq**. (7.153) one obtains,

$$\begin{aligned} \hat{S}^{z} &\propto \partial_x \hat{\phi}_s(x) + \text{const.}(-1)^x \sin\left(\hat{\phi}_s(x)\right)\cos\left(\hat{\phi}_c(x)\right) + ..., \\ (\hat{S}^{z})^2 &\propto \partial_x \hat{\phi}_c(x) + \text{const.}(-1)^x \sin\left(\hat{\phi}_c(x)\right)\cos\left(\hat{\phi}_s(x)\right) + ..., \end{aligned} \tag{7.155}$$

showing that the $\hat{S}^z$ operator in **Eq**. (7.154) yields the same expression as in **Eq**. (7.98), with exchanged roles of spin and charge, whereas the bosonization of its square yields exactly **Eq**. (7.98) [187]. We see that the two, site-local, symmetry breaking order parameters have a definite transformation behavior with respect to a permutation of the internal species, which is the case of all order local order parameters defined in the following. Additionally, the staggered parts of **Eq**. (7.155) are known as the Ising anti-ferromagnetic and stripe anti-ferromagnetic orders in two-leg spin 1/2 ladders [196], modulo an interchange of spin and charge degrees of freedom. Whereas the $(\hat{S}^z)^2$ order is not observed in the spin-ladder bosonization of the ordinary λ-D model [187], as the requirement on the coupling constants $g_1 < 0$ and $g_2 > 0$ is not fulfilled in its parameter space. Analogously, we do not expect such an order for our field theory in **Eq**. (7.118) to (7.120) either, as the condition $g_1 < 0$ seems not to be fulfilled for strong attractive U in **Eq**. (7.128), even if the renormalization due to $\tilde{g}_1$ in **Eq**. (7.146) is included.

A local Landau order parameter is not necessarily site local, but is restricted to have a finite support in the thermodynamic limit. Thus the easiest extension of a site local order parameter should be defined on a bond instead. Of course this extends the local Hilbert space dimension from 3 to 9, meaning that the fundamental language is given by a $su(3)_j \bigotimes su(3)_{j+1}$ algebra instead [8]. As there are now a lot of different possibilities to choose of, we demand additionally that our order parameters should be even or odd with respect to an internal index permutation, that flips the sign of the spin fields but leaves the charge ones unchanged. A more or less obvious possibility is

to define two $su(2)$ sub-algebras for each species $\sigma = 1, 2$ on the bond $(j, j+1)$, i.e.

$$\begin{aligned}\hat{J}^{\sigma,x}_{j,j+1} &= \frac{1}{2}[\tilde{b}^{\dagger}_{j,\sigma}\tilde{b}_{j+1,\sigma} + \text{h.c.}],\\ \hat{J}^{\sigma,y}_{j,j+1} &= \frac{1}{2i}[\tilde{b}^{\dagger}_{j,\sigma}\tilde{b}_{j+1,\sigma} - \text{h.c.}],\\ \hat{J}^{\sigma,z}_{j,j+1} &= \frac{1}{2}[\tilde{n}_{j,\sigma} - \tilde{n}_{j+1,\sigma}],\end{aligned} \tag{7.156}$$

and subsequently build their even/odd linear combination,

$$\Delta\hat{J}^{\pm,\alpha}_{j,j+1} = \hat{J}^{1,\alpha}_{j,j+1} \pm \hat{J}^{2,\alpha}_{j,j+1}; \quad \alpha \in [x, y, z]\,. \tag{7.157}$$

The two $su(2)$ algebras defined in **Eq**. (7.156) correspond physically to the current algebras of a particle or a hole on top of the unit filled bond, see **Eq**. (7.151), whereas both only correspond to $S = 1/2$ dimensional representations in this respective sub-spaces [91]. Furthermore, the two sub-algebras are generally non-commuting, and thus one can show that the anti-symmetric linear combinations in **Eq**. (7.157) does not fulfill an $su(2)$ algebra in the full Hilbert space of the bond but only for certain particle numbers. The bosonized expressions of the constituents of **Eq**. (7.157) can be used now to infer the correct Dimer order parameter. For example the longitudinal part $\Delta\hat{J}^{\pm,z}_{j,j+1}$ gives exactly the staggered contributions in **Eq**. (7.155), whereas the y-components do not contain sinusoidal vertex operators but are related to the long-wavelength fluctuations of the phase field for each sector,

$$\Delta\hat{J}^{\pm,y}_{j,j+1} \propto \partial_x\hat{\Theta}_{c,s}(x). \tag{7.158}$$

It should be noted that the definition in **Eq**. (7.158) has an equivalent identification of lattice and continuum entities as for our field theory, in contrast to density fields in **Eq**. (7.153), up to a sign change of the charge phase field.

Hence we conclude that the x-operators in **Eq**. (7.156) are the only valid candidates for a Dimer order parameter, with staggered contributions, i.e.

$$(-1)^j\Delta\hat{J}^{-,x}_{j} \approx \sin\left(\hat{\phi}_c(x)\right)\sin\left(\hat{\phi}_s(x)\right), \tag{7.159}$$

$$(-1)^j\Delta\hat{J}^{+,x}_{j} \approx \cos\left(\hat{\phi}_c(x)\right)\cos\left(\hat{\phi}_s(x)\right), \tag{7.160}$$

that correspond to a staggered or columnar Dimer order parameters found in two-leg spin 1/2 ladders [196]. We can immediately conclude from **Eqs**. (7.159) and (7.160) that the couplings $g_{1,2}$ of our effective field theories in **Eqs**. (7.90) and (7.91) or **Eqs**. (7.118) and (7.119) should be relevant. For our two different field theories we have to check again if the residual symmetry groups of the bosonized CDW and Dimer order obey a sub-group inclusion, see **Tabs**. (7.19) and (7.20), whereas we briefly discuss the

symmetry behavior of both theories for completeness, while we only use the symmetrized one to discuss the Dimer phase later on.

Phases	Order parameter	Relevant Coupling	G_{Residual}
Dimer	$\sin\left(\hat{\phi}_c(x)\right)\sin\left(\hat{\phi}_s(x)\right)$	$g_1 > 0,\, g_2 > 0$	$\hat{U}^{y,x}(\pi), \hat{U}^z(1), \hat{K}_S, \hat{K}, \hat{P}_L$
Dimer*	$\cos\left(\hat{\phi}_c(x)\right)\cos\left(\hat{\phi}_s(x)\right)$	$g_1 < 0,\, g_2 < 0$	$\hat{U}^{y,x}(\pi), \hat{U}^z(1), \hat{K}_S, \hat{K}, \hat{P}_L$
CDW	$\sin\left(\hat{\phi}_c(x)\right)\cos\left(\hat{\phi}_s(x)\right)$	$g_1 > 0,\, g_2 < 0$	$\hat{P}_S, \hat{U}_z(1), \hat{K}$

Table 7.19: *Comparison of relevant coupling constants, as well as residual symmetries, for the potential Dimer operators, i.e. staggered and $(*)$ columnar, and the CDW one, for the field theory near the bosonic limit. We obtain the residual symmetries from* **Tabs**. *(7.4) to (7.7) and the order parameters in* **Eqs**. *(7.98) and* **Eqs**. *(7.159) and (7.160). We find that both Dimer candidates have the same residual symmetries, that do not obey a sub-group inclusion with respect to those of the CDW. The sign of the relevant coupling constants are exactly the same as for the spin-ladder bosonization of spin* 1 *chains, found in* **Ref**. *[196]. For the field theory in the bosonic limit, an enhancement of the coupling constants by symmetry breaking perturbations can be inserted by hand if needed, analogously to* **Eq**. *(7.146).*

hases	Order parameter	Relevant Coupling	G_{Residual}
Dimer	$\sin\left(\hat{\phi}_c(x)\right)\sin\left(\hat{\phi}_s(x)\right)$	$\bar{g}_1 > 0,\, \bar{g}_2 > 0$	$\hat{T}^*, \hat{U}^z(1), \hat{K}$
Dimer*	$\cos\left(\hat{\phi}_c(x)\right)\cos\left(\hat{\phi}_s(x)\right)$	$\bar{g}_1 < 0,\, \bar{g}_2 < 0$	$\hat{U}^{y,x,*}(\pi), \hat{U}^z(1), \hat{K}^*_S, \hat{K}, \hat{P}_L$
CDW	$\sin\left(\hat{\phi}_c(x)\right)\cos\left(\hat{\phi}_s(x)\right)$	$\bar{g}_1 > 0,\, \bar{g}_2 < 0$	$\hat{P}_S, \hat{U}_z(1), \hat{K}$

Table 7.20: *Comparison of relevant coupling constants, as well as residual symmetries, for the potential Dimer operators and the CDW one, for the field theory near the pseudo-fermionic limit. We obtain the residual symmetries from* **Tabs**. *(7.13) to (7.16) and the same order parameters as in* **Tab**. *(7.19), where we find now that both Dimer candidates have different residual symmetries, that also do not obey a sub-group inclusion with respect those of the CDW. For the field theory in the pseudo-fermionic limit, the renormalization of the coupling constants is according to* **Eqs**. *(7.146) and (7.147).*

In **Tabs**. (7.19) and (7.20) we find that for none of the Dimer orders exists a sub-group relation to the residual symmetries of the CDW, hence both choices would be consistent with a Landau forbidden transition. It is known, that the dimer orders in **Eqs**. (7.159) and (7.160) appear in the spin ladder bosonization of the λ-D model only by the inclusion of four spin interactions or the careful consideration of higher-order irrelevant operators, renormalizing the coupling constants g_1 and g_2 to attain different signs [196]. In our effective field theory in the pseudo-fermionic limit this is provided by the lattice gauge, where we can already conclude form **Eqs**. (7.128) and (7.105) that only the staggered Dimer phase in **Eqs**. (7.159) can be realized for our model, if the lattice gauge and V balance out the attractive onsite interactions U. The values of the two

coupling constants g_1 and g_2 are further altered according to **Eqs**. (7.146) and (7.147), where the effect of including the symmetry breaking perturbations is not expected to change the constants drastically in this parameter region. Due to the same reasoning the values of the order parameter are changed by the new minima in **Eqs**. (7.146) and (7.147), but still indicate an alternating value in the dimerized phase. Analogously to the CDW phase the ground-state according to **Eq**. (7.159) is then doubly degenerate due to two independent solutions inside the compactification radii of the fields [196].

As a clear microscopic picture of our dimer phase is blurred by the low-energy continuum description, we re-investigate the newly found Dimer order parameter $\Delta\hat{J}_j^{-,x}$ in the lattice instead. Such a perfectly bond-dimerized state would arise from the following effective Hamiltonian,

$$\hat{H}^{\text{eff.}}_{\text{Dimer}} \equiv \sum_{j\in\text{Bonds}} \Delta\hat{J}_j^{-,x}\Delta\hat{J}_{j+1}^{-,x}. \tag{7.161}$$

The two low-energy, symmetry-breaking eigenstates of **Eq**. (7.161) are then given by alternations of singlet states having a hole or an additional particle delocalized on the bond, i.e.

$$|-1\rangle_j = \frac{1}{\sqrt{2}}\left[|1_j, 0_{j+1}\rangle - |0_j, 1_{j+1}\rangle\right], \tag{7.162}$$

$$|+1\rangle_j = \frac{1}{\sqrt{2}}\left[|1_j, 2_{j+1}\rangle - |2_j, 1_{j+1}\rangle\right], \tag{7.163}$$

$$|\text{Dimer}, 1\rangle = \prod_{j\in\text{Bonds}} |-1\rangle_j |+1\rangle_{j+1}, \tag{7.164}$$

$$|\text{Dimer}, 2\rangle = \prod_{j\in\text{Bonds}} |+1\rangle_j |-1\rangle_{j+1}, \tag{7.165}$$

where analogously to the CDW phase the symmetry compatible linear combinations are spontaneously broken in the thermodynamic limit. **Eqs**. (7.164) and 7.165 can be viewed as anti-ferromagnetic orders in the x-direction, that is defined on a bond instead of the longitudinal one, that is defined on-site for the CDW phase. Analogously to the symmetries of the anti-ferromagnetic phase in the λ-D model, we would like to discuss the lattice symmetries of the Dimer states in **Eqs**. (7.164) and (7.165) in a similar fashion. So we obtain the following symmetry breaking pattern,

$$G_{\hat{H}_{eff}} = \left[\hat{U}^x(1), \hat{U}^{y,z}(\pi), \hat{T}, \hat{P}_{S,L}, \hat{K}\hat{U}^z(\pi)\right] \tag{7.166}$$

$$G_{\text{Residual}} = \left[\hat{U}^x(1), \hat{T}^2, \hat{P}_S, \hat{P}_L\hat{T}, \hat{K}\hat{U}^z(\pi)\hat{T}\right] \tag{7.167}$$

$$G_{\text{Broken}} = G_{\hat{H}_{eff}}/G_{\text{Residual}} = \left[\hat{U}^{y,z}(\pi), \hat{T}, \hat{P}_L, \hat{K}\hat{U}^z(\pi)\right], \tag{7.168}$$

which has the same form as for the CDW phase in **Eqs**. (7.13) to (7.15). The only differences lie in the fact that all Dimer symmetry operations are defined on a single

bond index instead of on-site, with the x-direction being considered as diagonal. This leads for example to a redefinition of spin time reversal, and a different geometrical meaning for the spatial lattice transformations. Analogously to the procedure for the CDW phase in **Eq**. (7.16) the bond local order parameter $\hat{O}_{\text{Dimer}}(j)$ for the dimer can be derived, as the $su(2)$ algebra of $\Delta\hat{J}_j^{-,\alpha}$ holds for the respective states, yielding

$$\hat{O}_{\text{Dimer}}(j) = (-1)^j \Delta\hat{J}_j^{-,x}. \tag{7.169}$$

In contrast to **Eq**. (7.16), the bond-staggered y,z-rotations can be used as the interpolating field for deriving **Eq**. (7.169) by the application of the $su(2)$ commutation relations [211]. Also in this case we can define a global version of $\hat{O}_{\text{Dimer}}(j)$,

$$\hat{O}_{\text{Dimer}} = \sum_{j\in\text{Bonds}} \hat{O}_{\text{Dimer}}(j), \tag{7.170}$$

that can be used to formalize the spontaneous symmetry breaking as in **Eq**. (7.18), as it is invariant with respect to the residual symmetries but has a definite action under the application of the broken ones, see **Eqs**. (7.167) and (7.168).

The comparison of **Eqs**. (7.14) and (7.167) formalizes the reason why Landau theory predicts the wrong transition, between the CDW and the Dimer phase, in terms of lattice symmetries. Namely, the residual symmetry groups have a similar appearance, meaning they have an identical action on their fundamental spin operators, but they are represented differently and thus no sub-group inclusion between the two exists [227]. This is in agreement with the residual groups of the low-energy order parameter in **Tabs**. (7.19) and (7.20), that also show no sub-group inclusion, even if they appear in a different form. Landau theory predicts a first-order transition between the phases or a crossover, whereas we have clear numerical evidence that the transition is continuous [227], see **Fig**. (7.22). Later on we see that bosonization resolves that contradiction analogously to the Landau forbidden transition in **Eq**. (7.135).

7.9.2 The Dimer to Mott Transition

In contrast to the transition from the Haldane to the Mott phase for $\theta \approx 0$, the transition to the Dimer phase is now numerically found to be in the Ising universality class, i.e. a continuous transition with central charge $c = 1/2$, see **Fig**. (7.21) and a length scaling coefficient ν equal to one, see **Fig**. (7.22). The second-order transition is thereby in accordance to the predictions of Landau theory, as there is a sub-group inclusion between the unique Mott and the degenerate Dimer phase with residual low-energy symmetries according to **Tab**. (7.20).

To explain this transition at the hand of the single field theory in **Eq**. (7.147) we have to require again self-duality at criticality [43, 187, 195, 196], meaning the Hamiltonian

should be invariant for $\phi_s \leftrightarrow \Theta_s$ which is only achievable for $K_s = 1$ and $\xi_s = 0$. The first requirement $K_s = 1$ is identical to the discussion of the refermionization in **Eq**. (7.145) and is fulfilled for $U = -3\sqrt{2}(\pi^2/2+1)(1+\cos(\theta))/\pi + 2V - 8\sqrt{2}\cos(\theta/2)/\pi$, according to the bare coupling values in **Eq**. (7.123). The second premise $\xi_s = 0$ implies that the $g_{2,4}$ terms in **Eq**. (7.147) should be much larger than g_5, which should also be effectively fulfilled for large $|U|$ and V, according to their bare coupling values in **Eqs**. (7.129), (7.132) and (7.133). Hence we conclude that the minimum of the spin density field ϕ_s in **Eq**. (7.147) is not strongly affected by the symmetry breaking perturbation g_5.

Nevertheless, symmetry breaking contributions of the charge sector in **Eq**. (7.146) are very important in the following sense. Namely, we have found from the derived Dimer order parameter in **Eq**. (7.159) that g_1 has to be positive in the Dimer phase and thus it has to change its sign if the phase is approached from the Mott side, where it holds that $g_1 < 0$, see **Eq**. (7.128). Without the consideration of the symmetry breaking perturbation $\tilde{g}_1$ in **Eq**. (7.146) this would imply that the charge sector becomes gapless at criticality, whereas its presence implies the absence of a gap closing in **Eq**. (7.146) when g_1 flows from $-\infty$ to ∞ [187,196]. Thus we have to consider the relevance of $\tilde{g}_1$ for the charge sector, whereas we expect that the overall sign of the renormalized coupling constant $\bar{g}_1$ in **Eq**. (7.146) is not affected by $\tilde{g}_1$ for comparably strong interactions.

Under theses premises, the mechanism of explaining the transition is then similar to the Haldane to CDW transition in the $\theta \approx 0$ case. In the Mott phase it holds for the charge sector that $\bar{g}_1 < 0$, whereas for the spin sector the g_3 term is more relevant than $\bar{g}_2$, provided that $1 < K_s < 2$, which is indeed the case for strong repulsive U. The Luttinger parameter K_s in **Eq**. (7.123) is monotonically decreasing for increasing attractive interactions U and thus it holds that $K_s < 1$ in the Dimer phase and the renormalized coupling $\bar{g}_2$ becomes more relevant than g_3. Thereby, a positive value of $\bar{g}_2$ is ensured whenever the lattice gauge can balance out the effect of U and V in the Dimer phase. Exactly at criticality it holds that $K_s = 1$ and $\bar{g}_2 = g_3$ [187, 196], whereas in contrast to **Eq**. (7.145) the Majorana theories at criticality have exactly the same velocity due to the absence of bilinear field gradients in the free Luttinger liquid. As explained above the sign change of $\bar{g}_1$ does not induce a phase transition of the charge sector due to the presence of the symmetry breaking contribution $\tilde{g}_1$, and thus the physical mechanisms behind the transition here are indeed different from the Haldane to CDW transition.. Additionally, this $c = 1/2$ transition has exactly the same $U(1)$ reduction patterns as the one between the Haldane and CDW phase, due to the same involved coupling constants with different signs, see **Tab**. (7.8).

7.9.3 The Dimer to CDW Transition

The Dimer to CDW transition was intensively investigated numerically to prove the unexpected Gaussian universality by means of peaks in information theoretical measures, variable scaling of both order parameters. As it was shown before that neither in the lattice, see **Eq**. (7.14), nor in the continuum, see **Tab**. (7.20), there exists s sub-group inclusion between the two phases, the transition is beyond the Landau paradigm [227]. From a field theoretical perspective, we can deduce from the former section that especially the renormalized spin sector in **Eq**. (7.147) is relevant for the transition, that nevertheless depends parametrically on the minimum of the gapped charge sector in **Eq**. (7.146). From the CDW order parameter in **Eq**. (7.127) we see that $\bar{g}_{1,2}$ are relevant [187, 195, 196], whereas the latter has to change its sign to negative values. The coupling g_3 on the other hand is irrelevant for this transition as $K_s < 1$. The sign change of $\bar{g}_2$ in **Eq**. (7.147) seems to be impossible, unless we demand that the symmetry breaking phase ξ_c of the charge sector in **Eq**. (7.146) vanishes. This implies that $\tilde{g}_1$ becomes zero, or conversely that g_1 is much stronger than the symmetry breaking perturbation. If this is indeed the case the minimum of the charge density field ϕ_c is dictated solely by g_1, and the spin sector reduces to the following form,

$$\hat{H}_s^{\text{Dimer}\leftrightarrow\text{CDW}} = \hat{H}_s^0 + \frac{g_2 - \text{sgn}(g_1)g_4}{(\pi a)^2} \int dx \cos(2\phi_s(x)). \tag{7.171}$$

From **Eq**. (7.171) we can conclude that the spin sector becomes gapless exactly at $g_2 = g_4$ which happens in the weak-coupling limit for, $V = \frac{U}{4} + \frac{\sqrt{2}J}{\pi}(1 + \cos(\theta))$. As the the nearest neighbor interaction is necessarily positive, and U negative in this region, we conclude that the lattice gauge has to overpower the attractive onsite interaction, where we have to neglect the case $\theta = \pi$ explicitly. Contrary to the transitions in the bosonic limit, the spin sector describes the occurring Gaussian transition with an emergent $U(1)_{\phi_s} \bigotimes U(1)_{\Theta_s}$ symmetry at criticality. Due to the relation of the Dimer order parameter in **Eq**. (7.159), to the fundamental $su(3)$ language in **Eq**. (7.151) [8], we can physically identify those emergent symmetries with the conservation of the spin-nematic operator $(\hat{S}^z)^2$ in **Eq**. (7.154), that measures holes or double occupations with respect to integer filling, as well as the relative current of those holes or double occupations according to **Eq**. (7.158).

7.10 Conclusion

In this chapter the low-energy properties of the constrained and extended anyon-Hubbard model have been investigated analytically, with emphasis on the differences to related bosonic or spin models [187,195,196]. A guiding question was the stability of the bosonic Haldane insulator with respect to statistical transmutation, or even more the existence

of an anyonic Haldane insulator as predicted in **Ref**. [185]. Thereby the motivation of the work was to support the large-scale numerical investigations, performed by Kevin Jägering in his *PhD* thesis [17], with additional physical insight from mean-field or field-theoretical considerations. The low-energy phases of the generalized Gutzwiller mean-field theory in **Fig**. (7.2), qualitatively resembles the topography of the quasi-exact results in **Figs**. (7.13) and (7.15), whereas especially the interchange between Haldane and Dimer orders can be nicely illustrated if both are identified with the gapless phases as a mean-field artifact. The unanimity of both approaches is quite surprising, in view of the generic weakness of mean-field theories in low dimensions [74, 75, 129, 240]. The gapless phases inherit the expected asymmetry with respect to spatial and temporal inversion according to **Eq**. (7.40), caused by the deformed anyonic commutation relations, in contrast to previous mean-field approaches [18, 27, 88] We find furthermore that the critical statistical parameter for which the Haldane order is completely destroyed is quite large and indeed close to the *DMRG* predictions, see **Figs**. (7.13) (7.16) and (7.17). So we can conclude that some aspects of the observed statistically induced phase transition can already be resolved at the mean-field level.

Beyond a simple mean field picture, we have used two different effective field theories to describe the model's low-energy sector near the bosonic or pseudo-fermionic limit. For small statistical parameters we follow earlier works on spin chains [195, 196] or on Bose-Hubbard type models [187], which we extent to explicitly include the correlated hopping processes that inherit the anyonic behavior [140, 141]. The low-energy theory reflects the additional symmetry breaking of constrained bosons with respect to spin 1 operators, and of anyons with respect to the bosons, in terms of new operator content in comparison to **Refs**. [187, 195, 196]. These contributions are especially relevant in the weak-coupling sector and cause finally the shifted quasi-momentum distributions that appear for such anyonic fluids microscopically [13, 26, 27, 33]. In the strong coupling limit these terms are not so important, as they depend purely on the hopping and we follow **Refs**. [187, 195, 196], to discuss the phases and their transitions, whereas coupling constants and universal parameters are generally altered by the statistical interactions. Thereby we find that all numerically predicted transition types are matching the field-theoretical results. By deriving the low-energy form of the non-linear inversion symmetry of such anyonic hopping operators, we find that the so called anyonic Haldane insulator in **Ref**. [185] is actually protected by the same symmetry as its bosonic pendant [187, 196]. This can be concluded from the fact, that both protecting symmetries have the same action on particle-number preserving Hamiltonians, that forbid the presence of sinusoidal vertex operators in the charge phase field Θ_c in the semi-classical evaluation of gapped phases. Conversely, we would prefer to consider both the anyonic and the bosonic Haldane phase as being equal, whereas a proof of this statement based on full renormalization group calculations would be a formidable task. For increasing statistical parameters the Haldane order is slowly replaced by a dimerized

phase [33], for which we provide the first microscopic picture as an anti-ferromagnetic x-order that is defined on the bond, instead of on-site. In terms of bosons, this phase corresponds to the alternation of singlet bonds that localize an additional particle or hole therein, whereas it is called staggered Dimer in the field of spin-ladders [196]. The quite rigorous construction of the Dimer phase formalizes the in-applicability of Landau theory, to describe the numerically predicted Gaussian phase transition to the CDW phase that is z-polarized on-site instead [227]. Furthermore the construction reveals the microscopic interpretation of the fundamental low-energy variables of the spin-sector, as a component of the spin-nematic order parameter in the case of ϕ_c, and as the relative current of particles and holes above unit filling for Θ_c.
In the pseudo-fermioniuc limit, where the Dimer order is the dominant one, we do not rely on the bosonization schemes of **Refs**. [187, 195, 196]. Instead we use a numerically supported transformation to the spin-ladder, which is perfectly suited for the application of perturbative bosonization in this parameter regime. Form relevant couplings in the naive continuum limit, we can infer that the Dimer phase is indeed stabilized by the balance of attractive on-site interactions and statistical repulsion, in agreement with its occupied region in the numerical phase diagram. The transition classes of the intermediate Dimer phase to the Mott and CDW phase are exactly interchanged in comparison to those of the Haldane insulator. Field-theoretically we can explain the numerical results solely by a semi-classically evaluation of the spin-sector, that governs both the unexpected Gaussian and the Ising transition. The interchanging of the transition types is then related to different possible minima of the charge sector. Namely, whenever the minimum of the charge sector is affected by symmetry breaking perturbations we have an Ising transition. If on the other hand the minimum of $\hat{H}_c$ is not influenced by such perturbations, the transition described by the spin-sector is Gaussian instead.

Despite their success in describing the phase diagram near the two limits $\theta \approx 0, \pi$, intermediate regions of θ and the interchange of Haldane to Dimer orders are difficult to describe by a semi-classical evaluation of the two field theories. Therefore a full renormalization group analysis of both effective field theories, and a mutual identification of their flow diagrams, would definitely be enlightening. Furthermore the investigation of finite size properties of both effective theories, that have been defined so far in an infinite setup, is inevitable to relate the theoretical results to actual experiments [52, 61, 241].
Drifting away from the scope of the extended anyon-Hubbard model, an interesting task would be the definition of a truly anyonic SPT phase. A promising approach could potentially be found in the realm of q-deformed Lie algebras and their corresponding SPT phases [245–247]. Such constructions could be potentially related to one-dimensional anyons by Jordan-Schwinger like representations of a quantum group at $q = e^{i\theta}$ [16, 91].

7.11 Appendix: Strong Coupling Perturbation Theory

In the following appendix we derive the effective strong coupling Hamiltonian of **Eq**. (7.138) from the extended anyon-Hubbard model in **Eq**. (7.1). The method was suggested first by Heinz Schulz in **Ref**. [195], and later in **Ref**. [242], to investigate the $XY2$ phase of the λ-D model from a simpler perspective.
The starting point is the highly degenerate classical groundstate that is effectively obtained from **Eq**. (7.1) for strongly attractive U, i.e.

$$\begin{gathered}\lim_{-|U|\to-\infty}\hat{H}\approx\hat{H}^0\\ \hat{H}^0=-\frac{|\mathrm{U}|}{2}\sum_j\left(\hat{S}^{\mathrm{z}}_j\right)^2+\frac{|\mathrm{U}|}{2}\mathrm{L}\end{gathered}\tag{7.172}$$

In **Eq**. (7.172) a constant, that corresponds to the energy of a given configuration, is subtracted for convenience [242]. As the perturbation operator we consider the rest of the Hamiltonian in **Eq**. (7.1), including the correlated hopping as well as the nearest neighbor interactions [242], i.e.

$$\begin{gathered}\hat{H}^1=-\frac{1}{2}\sum_j\left(\hat{A}^\dagger_j(\theta)\hat{A}_{j+1}(0)+\mathrm{h.c.}\right)+V\sum_j\hat{S}^{\mathrm{z}}_j\hat{S}^{\mathrm{z}}_{j+1}\\ \hat{A}^\dagger_k(\theta)=\left[1+(1-\sqrt{2}\exp(i\theta))\hat{S}^{\mathrm{z}}_k\right]\hat{S}^-_k\end{gathered}\tag{7.173}$$

Now we can perturbatively derive an effective Hamiltonian by projecting the resolvent operator onto the subspace of only doubly occupied or empty sites, denoted by $\hat{P}_0$ [139, 242],

$$\hat{P}_0G(E)\hat{P}_0=\hat{P}_0\frac{1}{(E-\hat{H})}\hat{P}_0\equiv\frac{1}{(E-\hat{H}_{\mathrm{eff}})},\tag{7.174}$$

whereas we can invert **Eq**. (7.1), while assuming $\mathrm{E}=0$ according to **Eq**. (7.172), and expand to second order in $\hat{H}^1$,

$$\hat{H}_{\mathrm{eff}}\approx\hat{P}_0\hat{H}^1\hat{P}_0-\frac{1}{|U|}\hat{P}_0\hat{H}^1\hat{H}^1\hat{P}_0\approx\sum_j V\hat{S}^{\mathrm{z}}_j\hat{S}^{\mathrm{z}}_{j+1}-\frac{1}{4|U|}\left(\hat{A}^\dagger_j(\theta)\hat{A}_{j+1}(0)+\mathrm{h.c.}\right)^2.\tag{7.175}$$

Following **Ref**. [242], we replace the spin-1 operators by spin-1/2 ones in this subspace i.e. $(\hat{S}^+)^2\to2\hat{s}^+;\hat{s}^{\mathrm{z}}\to2\hat{s}^{\mathrm{z}}$ and obtain then finally the spin-1/2 effective Hamiltonian

shown in **Eq**. (7.138),

$$\hat{H}_{\text{eff}} \approx -\bar{J}\sum_j \left(e^{i\theta}\hat{s}_j^+\hat{s}_{j+1}^- + \text{h.c.}\right) + \bar{\Delta}\sum_j \hat{s}_j^z\hat{s}_{j+1}^z, \quad \bar{J} = \frac{2}{|U|}, \bar{\Delta} = \frac{(2|U|V+1)}{|U|}, J = 1. \tag{7.176}$$

The effective Hamiltonian yields an XXZ-type model similar to the one derived in **Ref**. [242] for the λ-D, see **Eq**. (7.8). The difference relies in the complex hopping of holes or double occupations that is dependent on the statistical parameter θ.

7.11.1 Appendix: Bosonization of correlated Hopping at $\theta \approx 0$

The lattice gauge functions of the correlated intra-chain processes of the extended anyon-Hubbard model that follows from the Schulz mapping in **Eq**. (7.59), are complex valued. Thus we cannot follow the same strategy as in **Ref**. [140, 141] and decompose the correlated hopping as the expectation values and fluctuations of the respective kinetic energies $\hat{Q}_{j,j+1}^{q_{1,2}} = \hat{c}_{q,j}^\dagger \hat{c}_{q,j+1} + \text{h.c.}$, and lattice gauges $\hat{F}_{q_1,q_2}^j$,

$$\begin{aligned} \hat{Q}_{j,j+1}^{q_{1,2}} &\Longrightarrow \langle \hat{Q}_{j,j+1}^{q_{1,2}} \rangle + : \hat{Q}_{j,j+1}^{q_{1,2}} :, \\ \hat{F}_{q_1,q_2}^j = \hat{F}_{q_1,q_2}^j(\hat{n}_{q_{1,2}}) &\Longrightarrow \hat{F}_{q_1,q_2}^j(: \hat{n}_{q_{1,2}} : + \langle \hat{n}_{q_{1,2}} \rangle). \end{aligned} \tag{7.177}$$

Instead we have to calculate the operator product expansions between the hermitian conjugated pairs of the hopping and the lattice gauge explicitly. In order to do so we have to cancel out fluctuations in every product of vertex operators of the same species, for example,

$$\lim_{a\to 0} \hat{\Psi}_{\eta,l}^\dagger(x)\hat{\Psi}_{\eta,l}(x+a) \approx : \hat{\Psi}_{\eta,l}^\dagger(x)\hat{\Psi}_{\eta,l}(x) : + a : \hat{\Psi}_{\eta,l}^\dagger(x)\frac{\delta\Psi_{\eta,l}}{\delta x}(x) : + c_{\eta,l}; \tag{7.178}$$
$$\eta = L, R, \;\; l = 1, 2.$$

In **Eq**. (7.178), $c_{\eta,l}$ is a numerical constant that diverges characteristically as the limit $a \to 0$ is approached [43]. Thus the intra-chain processes are, after a Jordan-Wigner transformation [9], given exemplary by expressions of the form

$$: \hat{\mathcal{K}}_{i,i+1}^{\text{intra},\alpha} := (z_1^* + z_2^* : \hat{n}_{i+1,\tilde{\alpha}} : + z_3^* : \hat{n}_{i,\tilde{\alpha}} : + z_4^* : \hat{n}_{i,\tilde{\alpha}} : \hat{n}_{i+1,\tilde{\alpha}} :) : \hat{c}_{i,\alpha}^\dagger \hat{c}_{i+1,\alpha} : + \text{h.c.}. \tag{7.179}$$

The fermionic bilinears are bosonized as usual

$$\begin{aligned}\frac{:\hat{c}^{\dagger}_{i,\alpha}\hat{c}_{i+1,\alpha}:}{a} =& -\left(i\left[\frac{1}{\sqrt{\pi}}\frac{\delta\Theta_{\alpha}(x)}{\delta x}\right]-\frac{a}{2}\left[\left(\frac{\delta\Theta_{\alpha}(x)}{\delta x}\right)^{2}+\left(\frac{\delta\phi_{\alpha}(x)}{\delta x}\right)^{2}\right]\right) \\ &+i(-1)^{x}\left[\frac{1}{\pi\alpha}\cos(2\sqrt{\pi}\phi_{\alpha}(x))\right]-\tilde{c}_{\alpha}.\end{aligned} \tag{7.180}$$

Here we have defined $\tilde{c}_{\alpha}=c_{R,\alpha}+c_{L,\alpha}$ additionally. Now we can proceed with the bosonization of the lattice gauge function by replacing the normal ordered density operators with [43],

$$:\hat{n}_{j,\tilde{\alpha}}:=\left[\frac{1}{\sqrt{\pi}}\frac{\delta\phi_{\tilde{\alpha}}(x)}{\delta x}-\frac{(-1)^{j}}{\pi\alpha}\sin(2\sqrt{\pi}\phi_{\tilde{\alpha}}(x))\right], \tag{7.181}$$

yielding the following form with the aid of the operator product expansions in **Eq**. (7.88),

$$\begin{aligned}\hat{F}^{j}_{\alpha,\tilde{\alpha}}(:\hat{n}_{\tilde{\alpha},i}:,:\hat{n}_{\tilde{\alpha},i+1}:) &= [z_1^{*}-\frac{z_4^{*}}{2\pi^2}]+\frac{a}{\sqrt{\pi}}(z_2^{*}+z_3^{*})\frac{\delta\phi_{\tilde{\alpha}}(x)}{\delta x}+2z_4^{*}(\frac{\delta\phi_{\tilde{\alpha}}(x)}{\delta x})^{2} \\ &+\frac{z_4^{*}}{2\pi^2}\cos(4\sqrt{\pi}\phi_{\tilde{\alpha}}(x)) \\ &+\frac{(-1)^{x}}{\pi}(z_2^{*}-z_3^{*})\sin(2\sqrt{\pi}\phi_{\tilde{\alpha}}(x)+\frac{2(-1)^{x}}{\pi^2}z_4^{*}\cos(2\sqrt{\pi}\phi_{\tilde{\alpha}}(x)).\end{aligned} \tag{7.182}$$

Now we have to multiply both equations **Eqs**. (7.180) and (7.182), leading to the single intra-chain Hamiltonians

$$\begin{aligned}:\hat{\mathcal{K}}^{\mathrm{intra},\alpha}_{i,i+1}:=& a\frac{2}{\sqrt{\pi}}\mathrm{Im}[z_1-\frac{z_4}{2\pi^2}]\frac{\delta\Theta_{\alpha}(x)}{\delta x}+a^2\mathrm{Re}[z_1-\frac{z_4}{2\pi^2}]\left[(\frac{\delta\Theta_{\alpha}(x)}{\delta x})^2+(\frac{\delta\phi_{\alpha}(x)}{\delta x})^2\right] \\ &+\frac{2a^2}{\pi}\mathrm{Im}[z_2+z_3]\frac{\delta\phi_{\tilde{\alpha}}(x)}{\delta x}\frac{\delta\Theta_{\alpha}(x)}{\delta x}+\frac{4\tilde{c}_{\alpha}}{\pi}\mathrm{Re}[z_4][(\frac{\delta\phi_{\tilde{\alpha}}(x)}{\delta x})^2 \\ &+a\ \cos(4\sqrt{\pi}\phi_{\tilde{\alpha}}(x))]+\frac{2a^2\tilde{c}_{\alpha}}{\sqrt{\pi}}\mathrm{Re}[z_2+z_3]\frac{\delta\phi_{\tilde{\alpha}}(x)}{\delta x} \\ &-\frac{2}{a\pi^3}\mathrm{Re}[z_4]\cos(2\sqrt{\pi}\phi_{\tilde{\alpha}}(x))\cos(2\sqrt{\pi}\phi_{\alpha}(x)).\end{aligned} \tag{7.183}$$

As the lattice kinetic energy in **Eq**. (7.62) is manifestly permutation symmetric, we can simply obtain the second intra-chain contribution by a transposition of the indices, i.e.

$$\begin{aligned}\hat{P}^{\dagger}_{\alpha\tilde{\alpha}}f(\alpha)\hat{P}_{\alpha\tilde{\alpha}} &= f(\tilde{\alpha}) \\ \hat{P}^{\dagger}_{\alpha\tilde{\alpha}}\hat{\mathcal{K}}^{\mathrm{intra},\alpha}_{j,j+1}\hat{P}_{\alpha\tilde{\alpha}} &= \hat{\mathcal{K}}^{\mathrm{intra},\tilde{\alpha}}_{j,j+1}.\end{aligned} \tag{7.184}$$

For the inter-chain processes on the other hand we neglect any operator product expansion between the inter-species bilinears and the corresponding lattice gauge functions. Furthermore, as both species are independent, they do not have to be regularized according **Eq**. (7.178), and thus the lattice gauge function do not renormalize the density or phase stiffness. The bosonization of the interaction part of the Hamiltonian in **Eq**. (7.66), and the inter-chain coupling $\hat{\mathcal{K}}^{\text{inter}}$, is on the other hand rather trivial and coincides with the procedure in **Refs**. [187, 195, 196]

7.11.2 Appendix: Bosonization of correlated Hopping at $\theta \approx \pi$

The symmetrized version of the mapping **Eq**. (7.108), that we have used for the pseudo-fermionic limit, results in real-valued lattice gauge functions, as in **Eq**. (7.116). Therefore, we can rely on the techniques used in **Refs**. [140, 141] to cancel out fluctuations by point-splitting the different ingredients in the lattice gauge,

$$\begin{aligned} &\hat{Q}^{q_{1,2}}_{j,j+1} \Longrightarrow \langle \hat{Q}^{q_{1,2}}_{j,j+1} \rangle + : \hat{Q}^{q_{1,2}}_{j,j+1} : \\ &\hat{G}^{j}_{q_1,q_2} = \hat{G}^{j}_{q_1,q_2}(\hat{n}_{q_{1,2}}) \Longrightarrow \hat{G}^{j}_{q_1,q_2}(: \hat{n}_{q_{1,2}} : + \langle \hat{n}_{q_{1,2}} \rangle). \end{aligned} \tag{7.185}$$

The expectation values of the intra-chain kinetic energies $\langle \hat{Q}^{q_{1,2}}_{j,j+1} \rangle$ are evaluated by diagonalizing them in the lattice and integrating the corresponding dispersion over the Fermi-sphere. So we perform the procedure on the intra-chain contribution of the first leg exemplarily,

$$: \hat{K}^{\text{intra},1} := -\frac{J}{\sqrt{2}} \sum_i (\langle \hat{Q}_{j,j+1}(1) \rangle + : \hat{Q}_{j,j+1}(1) :) \hat{F}_1(: \hat{n}_{2,i} :, : \hat{n}_{2,i+1} :). \tag{7.186}$$

The single contributions are given by

$$\begin{aligned} &\langle \hat{Q}_{j,j+1}(1) \rangle \hat{F}_1(: \hat{n}_{2,i} :, : \hat{n}_{2,i+1} :) \longrightarrow \langle \hat{Q}_{j,j+1}(1) \rangle \Big(-\frac{a}{\pi\alpha} \sin(2\sqrt{\pi}\phi_2(x)) \\ &- a^2 \frac{1}{\pi} (\frac{\delta\phi_2(x)}{\delta x})^2 + \frac{1}{(\pi)^2} \left[\frac{1}{2} - \frac{1}{2} \cos(4\sqrt{\pi}\phi_2(x)) - \pi a^2 \left(\frac{\delta\phi_2(x)}{\delta x} \right)^2 \right] \Big), \end{aligned} \tag{7.187}$$

and

$$
\begin{aligned}
&: \hat{Q}_{j,j+1}(1) : \hat{F}_1(: \hat{n}_{d,i} :, : \hat{n}_{d,i+1} :) \longrightarrow \qquad (7.188)\\
&\Big(a\Big[[2(1-(-1)^j)\sin(\theta)\frac{1}{\sqrt{\pi}}\frac{\delta\Theta_1(x)}{\delta x}\\
&- a(1+\cos(\theta)+(-1)^j(1-\cos(\theta)))\left[(\frac{\delta\Theta_1(x)}{\delta x})^2+(\frac{\delta\phi_1(x)}{\delta x})^2\right]\Big]\\
&- a(-1)^x\left[\frac{2(1+\cos(\theta)+(-1)^j(1-\cos(\theta)))}{\pi\alpha}\cos(2\sqrt{\pi}\phi_1(x))\right]\Big)\\
&\Big(\frac{1}{4}+a\frac{(-1)^{j+1}}{2}\left(\frac{1}{\sqrt{\pi}}\frac{\delta\phi_2(x+a)}{\delta x}-\frac{(-1)^{j+1}}{\pi\alpha}\sin(2\sqrt{\pi}\phi_2(x+a))\right)\\
&+a\frac{(-1)^j}{2}\left(\frac{1}{\sqrt{\pi}}\frac{\delta\phi_2(x)}{\delta x}-\frac{(-1)^j}{\pi\alpha}\sin(2\sqrt{\pi}\phi_2(x))\right)\\
&a^2(-\frac{1}{\pi}(\frac{\delta\phi_2(x+a)}{\delta x})^2-\frac{1}{\sqrt{\pi}}\frac{(-1)^{j+1}}{\pi\alpha}\frac{1}{\sqrt{\pi}a}\cos(2\sqrt{\pi}\phi_2(x))+\frac{1}{\sqrt{\pi}}\frac{(-1)^j}{\pi\alpha}\frac{1}{\sqrt{\pi}a}\cos(2\sqrt{\pi}\phi_2(x)))\\
&+\frac{1}{(\pi)^2}\left[\frac{1}{2}-\frac{1}{2}\cos(4\sqrt{\pi}\phi_2(x))-\pi a^2\left(\frac{\delta\phi_2(x)}{\delta x}\right)^2\right]\Big).
\end{aligned}
$$

Thus we finally obtain for the first leg,

$$
\begin{aligned}
&: \hat{K}^{\text{intra},1} := \qquad (7.189)\\
&-\frac{J}{\sqrt{2}}\int dx(\frac{1}{2}+\frac{1}{\pi^2})\sin(\theta)\frac{1}{\sqrt{\pi}}\frac{\delta\Theta_1(x)}{\delta x}\\
&-a(\frac{1}{2}+\frac{1}{\pi^2})(\frac{(1+\cos(\theta))}{2})\left[(\frac{\delta\Theta_1(x)}{\delta x})^2+(\frac{\delta\phi_1(x)}{\delta x})^2\right]\\
&-\frac{(1-\cos(\theta))}{\pi a^2}(1+\frac{2}{\pi^2})\cos(2\sqrt{\pi}\phi_1)+\frac{2(1-\cos(\theta))}{(\pi a)^2}\cos(2\sqrt{\pi}\phi_1)\sin(2\sqrt{\pi}\phi_2)\\
&+\frac{1}{\pi}\frac{4(1+\cos(\theta))}{(\pi a)^2}\cos(2\sqrt{\pi}\phi_1)\cos(2\sqrt{\pi}\phi_2)\\
&+\langle\hat{Q}_{j,j+1}(1)\rangle(-\frac{1}{\pi}\sin(2\sqrt{\pi}\phi_2(x)) \qquad (7.190)\\
&+\frac{1}{(\pi)^2}\left[\frac{1}{2}-\frac{1}{2(\pi a)^2}\cos(4\sqrt{\pi}\phi_2(x))-2\pi a^2\left(\frac{\delta\phi_2(x)}{\delta x}\right)^2\right]),
\end{aligned}
$$

where we have neglected fast oscillating terms and higher order couplings. The contributions for the second leg can be calculated analogously, where we additionally deduce the following form,

$$\langle\hat{Q}_{j,j+1}(1/2)\rangle=\frac{2}{\pi}\cos(\theta/2) \qquad (7.191)$$

for the expectation values of the intra-chain kinetic energies [140]. Also for this field theory the interaction part, also given by **Eq**. (7.66) and the inter-chain coupling are bosonized straightforwardly, see **Refs**. [187, 195, 196].

Chapter 8

Spin Correlations in the Finite XXZ-Chain

A huge advantage of the bosonization treatment is the renormalization group irrelevance of band curvature contributions [57–59], that would lead to deviations from a purely relativistic dispersion, at the critical point of quantum phase transitions or in general for one-dimensional gap-less quantum fluids [48]. This purely linear dispersion is the gift and the curse of the approach, in the sense that the form of arbitrary correlation functions is always pre-determined by its conformal invariance. Hence the same mechanism that makes the calculation of arbitrary static correlators so favorable, leads to several inconsistencies in the computation of dynamical quantities, as the RG-exact Lorentzian invariance of the low-energy sector is incorrectly imposed to hold also in the high-energy regime. An example for such relativistic artifacts in dynamical quantities calculated by ordinary abelian bosonization is the infinitely sharp line shape in the dynamical structure factor for small momenta, caused by the assumed degeneracies, that should correspond indeed to a finite width, related to decay mechanisms of the excitations near the Fermi surface [248–250]. Further artifacts of this type are the incorrect prediction of the form of the particle-hole continuum, caused by the CPT-symmetry of the Luttinger liquid that only holds for Lorentz invariant local quantum field theories [1, 250]. Further complications might appear for integrable models whose high-energy structure, as well as thermalization properties and thus long-range temporal behavior, is inextricably intertwined with the presence of higher-order conserved currents that have no known clear signature in the ordinary Luttinger liquid [97], as that is also a fixed point of non-integrable models in general [47].

In the following subpart of this thesis, the spin-1/2 XXZ chain with applied magnetic field, in one spatial dimension is investigated, with focus on the advanced field theoretical treatment of correlation functions. The previously mentioned issues result in deviations of the analytical predictions of the ordinary bosonization with numerical data on the dynamical structure factor, showing a systematic asymmetry between the two approaches,

that is the fundamental quantity in structuring scattering experiments [67, 168, 251] whether probed in inelastic neutron-scattering in the realm of condensed matter or Bragg-scattering in the haze of cold atoms. The finite-size non-linear bosonization in the spirit of **Refs**. [57–59, 252, 253] is therefore applied to the longitudinal part of the spin-spin correlation function for periodic as well as for open chains, in order to fix the occurring mismatch.
Finite size correlation functions are explicitly calculated and their limiting behavior in the bulk or near the boundaries is investigated, complementing the results of the literature for infinite or semi-infinite geometries [254, 255] while including also spatially modulated correlations we further extend them by providing estimates on the impurity diffusivities and time scales. Thereby a special variant of the Lehmann representation is found via a generalized Jacobi-Anger representation of the correlation function [256–258], that is universally applicable to general correlation functions expressed by vertex operators. This might severely simplify future numerical investigations or further analytic approximations, that are beyond the scope of this thesis. Thus this chapter should be viewed to be under construction and merely paving the way to a more quantitative numerical investigation beyond the bare coupling values derived by the field theoretical treatment. Especially interesting would be a detailed investigation of these coupling constants for various boundary conditions and magnetic fields, by means of the exact Bethe ansatz [97, 163, 250]. As there exist no analytical results so far, for finite systems and magnetic fields, we pursue only the phenomenological treatment here [252].

8.1 Preliminaries

8.1.1 The Model

The drosophila in the realm of Bethe integrable spin chains with non-trivial boundaries is the one-dimensional spin-1/2 XXZ chain [67, 259, 260], with broad applications ranging from the magnetic properties of real world materials like $SrCuO_2$ or $SrCuO_3$ [261, 262] to pure academic interest concerning the physical and mathematical properties of its exact solution [163, 263–265]

$$\hat{H} = \sum_{j=0}^{L} \left(\frac{1}{2} \left[\hat{S}_j^+ \hat{S}_{j+1}^- + \text{h.c.} \right] + \Delta \hat{S}_j^z \hat{S}_{j+1}^z - h \hat{S}_j^z \right). \tag{8.1}$$

The $\hat{S}_j^{\pm,z}$ operators in **Eq**. (8.1) denote $su(2)$ spins in their $2S+1=2$ dimensional representation, i.e.

$$\begin{aligned}
&\left[\hat{S}_i^+, \hat{S}_j^-\right] = 2\delta_{i,j}\hat{S}_j^z \\
&\left[\hat{S}_i^\pm, \hat{S}_j^z\right] = \pm\delta_{i,j}\hat{S}_j^\pm, \\
&\left(S_j^x\right)^2 + \left(S_j^y\right)^2 + \left(S_j^z\right)^2 = S(S+1)\hat{1}_{2S+1\times 2S+1}, \quad \forall j \in [1, L],
\end{aligned} \tag{8.2}$$

where realistic boundary conditions are typically chosen to be of Dirichlet type, implying the following constraint on the virtual lattice sites $(0, L+1)$ respectively, i.e.

$$\hat{\vec{S}}_{0,L+1}\left|\Psi\right\rangle \equiv \vec{0}\left|\Psi\right\rangle, \qquad \forall\left|\Psi\right\rangle, \qquad \hat{\vec{S}}_j = \left(\hat{S}^x, \hat{S}^y, \hat{S}^z\right)_j^T. \tag{8.3}$$

Alternatively to **Eq**. (8.3) we can impose cyclic boundary conditions on the spin chain in **Eq**. (8.1), by demanding

$$\hat{\vec{S}}_{j+L}\left|\Psi\right\rangle \equiv \hat{\vec{S}}_j\left|\Psi\right\rangle, \qquad \forall\left|\Psi\right\rangle. \tag{8.4}$$

Spatial symmetries that depend on the connectivity of the underlying lattice are obviously affected by the choice of boundary conditions in **Eq**. (8.3) or **Eq**. (8.4). The Hamiltonian in **Eq**. (8.1) is invariant under parity that interchanges the lattice sites $\hat{S}_j^{\pm,z} \leftrightarrow \hat{S}_{L-j+1}^{\pm,z}$, hence the eigenstates of **Eq**. (8.1) can be labeled according to their even or odd parity for both type of boundary conditions discussed here. Translational invariance on the other hand is explicitly broken through the presence of finite boundaries in **Eq**. (8.3), which leads to a non-conservation of quasi-momentum and characteristic oscillations near the edges, among other effects [145,146,148,169]. This lack of translational invariance make periodic boundaries more feasible for theoretical calculations, whereas experimentalists usually prefer open boundary due to the lack of periodic probes or conceptual difficulties in creating tight toroidal traps in one dimension [180]. Effective open boundaries often arise via impurity scattering that effectively cuts larger chains into mesoscopic sub-compartments with impenetrable boundaries [67]. Thus in practical applications open boundaries are closer to reality whereas the requirement of translational invariance is mathematically more convenient. Conversely the mathematical inconvenience of non-translational invariant systems leads in the current context to interesting effects usually only slightly touched in text-book literature of statistical mechanics, surface-critical phenomena [262]. To be more precise the paradigm of Luttinger physics that one-dimensional phases of matter can be distinguished by their dominantly decaying correlations, becomes dependent on whether the support of that correlation function contains the boundary or not. Besides such lattice dependent symmetries, the spins in **Eq**. (8.1) are assumed to be under the influence of a weak magnetic field in z-direction, such that π-rotations of about the x, y-axis are not conserved anymore,

reducing the dihedral $\mathbb{Z}_2 \otimes \mathbb{Z}_2$ symmetry to $\mathbb{Z}_2$ and thus inducing an alignment in z-direction. Furthermore the global $SU(2)$ symmetry in **Eq**. (8.1) is explicitly broken down to $U(1) \subset SU(2)$, unless $\Delta = 1$, which leads to a preferential direction of the spin operators and a conservation of the quantity $\hat{\mathcal{S}}^z = \sum_{j=1}^{L} \hat{S}_j^z$ instead of $\hat{\vec{\mathcal{S}}} = \sum_{j=1}^{L} \hat{\vec{S}}_j$.

8.1.2 Phases in the XXZ Chain

In order to obtain a more intuitive picture of the different contributions in the spin Hamiltonian **Eq**. (8.1), that is hindered by the rather abstract meaning of the $su(2)$ algebra in **Eq**. (8.2), the Jordan-Wigner duality is used to represent the $su(2)$ algebra in **Eq**. (8.2) locally in terms of fermions which furthermore transforms the spin bonds $\hat{S}_j^+ \hat{S}_{j+1}^-, \hat{S}_j^z \hat{S}_{j+1}^z$ in **Eq**. (8.1) to fermionic bonds $\hat{c}_j^\dagger \hat{c}_{j+1}, \hat{n}_j \hat{n}_{j+1}$ [9,24], i.e.

$$\hat{H} \approx -\sum_{j=0}^{L} \left(\frac{1}{2} \left[\hat{c}_j^\dagger \hat{c}_{j+1} + \text{h.c.} \right] - \Delta \hat{n}_j \hat{n}_{j+1} + h \hat{n}_j \right). \tag{8.5}$$

Eq. (8.5) describes basically hopping fermions on a line that interact between the lattice sites j and $j+1$ with a strength of Δ, and a chemical potential given by h. In **Eq**. (8.5) we neglect a discussion about potential boundary phases of the Jordan-Wigner string for cyclic boundary conditions. It should be noted on the other hand that the sign in front of the kinetic energy is shifted by a local gauge transformation $\hat{c}_j \to (-1)^j \hat{c}_j$, such that the total energy is minimized by increasing the hopping. The approximation sign in **Eq**. (8.5) indicates constant shifts of energy in the Hamiltonian, as well as potential off-sets at the boundary that scale as $\mathcal{O}(L^{-1})$.

Forgetting about the integrability of the models **Eq**. (8.1) and **Eq**. (8.5) one can already infer some of the underlying physics by treating the particle Hamiltonian perturbatively. For a very small anisotropy $|\Delta| \ll 1$, the fermions in **Eq**. (8.5) are essentially non-interacting with a dispersion shifted by the magnetic field $h \ll 1$, i.e. ϵ_{k-h}. Including also relatively small interactions up to $|\Delta| < 1$ this phase corresponds to the so-called XY-phase, as the x, y-directions of the spins are dominating over the z-direction. To be more precise, the X, Y-ground-state has a vanishing magnetization and is a paramagnet characterized by a spinon vacuum for no external magnetic field [266]. For finite magnetic fields h the XY groundstate acquires a non-zero magnetization, but remains gapless up to a critical field strength of $h_c = \frac{J}{2}(1+\Delta)$ [267,268]. For strong anisotropies $|\Delta| \gg 1$ and weak magnetic fields $h \ll 1$ the hopping of fermions is supposed to be suppressed and some kind of crystalline order should take place. The form of that order depends on whether the fermions are interacting attractively, $\text{sign}(\Delta) = -1$, or repulsively, $\text{sign}(\Delta) = +1$ [43]. In the strongly attractive case $\Delta \ll 0$, this phase can be identified further with a ferromagnetic one, where the spins are all aligned in z-direction and a ground-state magnetization of $S^{z,tot} = \sum_j \langle \hat{S}_j^z \rangle \in [-L, L]$. The crystalline order that appears for strongly repulsive interactions $\Delta \gg 1$ is called a Néel phase, distributing

exactly one particle on the bond in the case of half-filling, i.e. $h \approx 0$. This corresponds then to an antiferromagnetic order with no total magnetization and spontaneously breaking of the $\hat{S}^z \to -\hat{S}^z$ symmetry, whereas the exact form of the localization will be adjusted by a finite chemical potential h.

8.1.3 Finite-Size Bosonization of the Dynamical Structure Factor

This rough trend of the phases is indeed much more complicated, whereas the details are hidden in the opaque Bethe-solutions of **Eq**. (8.1) that represent a mathematically firm but sometimes physically impracticable approach to the calculation of observables [259, 269–274]. Hence it would be desirable to use an approximate method that grasps most of the features in the parameter regime one is aiming for, but remains versatilily applicable. In the realm of gapless one-dimensional quantum fluids like **Eq**. (8.5) for small to intermediate Δ, the paradigm are the Luttinger liquids. The Bethe ansatz and the Luttinger liquids are deeply connected with each other, whereas the latter incorporates a more course-grained approach to the long-wavelength limit of correlation functions in the vicinity of a linear dispersion that can be obtained rigorously by means of the Bethe ansatz and conformal field theory. In the following we shortly recapitulate some results concerning the bosonization of the XXZ chain. As the amount of literature surrounding the topic is rather large [42, 43, 50], we focus especially on the longitudinal dynamical structure factor and the impact of finite magnetic fields or boundary conditions. The consequences of using a low-energy theory like the bosonization to describe energy-resolved quantities are discussed on hand of the dynamical structure factor.

The Hamiltonian **Eq**. (8.5) can be bosonized by the standard techniques, leading to the familiar form of the Tomonaga-Luttinger liquid

$$\hat{H} = u \int_0^L dx \left[\frac{1}{K} \left(\partial_x \phi(x) \right)^2 + K \left(\partial_x \Theta(x) \right)^2 \right], \tag{8.6}$$

as described in the Chapter 2. The Luttinger parameters u and K can be obtained exactly by means of the corresponding Bethe solutions, i.e.

$$\begin{aligned} K &= \frac{\pi}{2(\pi - \arccos(\Delta))}, \\ u &= J\pi \frac{\sin(\arccos(\Delta))}{\arccos(\Delta)}, \end{aligned} \tag{8.7}$$

and so are valid also beyond the weak-coupling regime. It should be clear that other contributions appear in principle in **Eq**. (8.6), that can reduce the $U(1)_\phi \bigotimes U(1)_\Theta$

symmetry of the Hamiltonian, i.e.

$$\hat{H}^n_{pert.} \propto \int_0^L dx \;\; \cos(n\sqrt{2\pi K}\phi(x)), \tag{8.8}$$

to $\mathbb{Z}_2(\phi) \bigotimes U(1)_\Theta$, but are Giamarchi2004aside the Luttinger liquid phase. From a practical point of view the inclusion of a perturbation of the form **Eq**. (8.8) changes the simple structure of correlators in the Luttinger liquid meaning that in general observables have to be calculated perturbativly or are hidden in exact but complicated quasi-particle states as the solitons in the sine-Gordon model.

As the form in **Eq**. (8.6) is universal, the implications of Luttinger liquid behavior for a given model are rather generic for gap-less one-dimensional quantum states. Thus physically the critical information resides in how the collective bosonic fields are related to the original spin degrees of freedom in **Eq**. (8.2), as choosing the dominant correlations of interest is heavily model dependent. The longitudinal component is easy to express in terms of fermions, as there are no peculiarities arising through the Jordan-Wigner string, and is essentially equal to the normal ordered fermionic density operator [42, 43, 67, 176], i.e.

$$\hat{S}^z(x,t) = \sqrt{\frac{K}{\pi}}\partial_x\hat{\phi}(x,t) + A\sin(\sqrt{4\pi K}\hat{\phi}(x,t) + 2k_F x). \tag{8.9}$$

Due to the Bethe-integrability of the XXZ-chain the non-universal quantity A can be obtained exactly by the asymptotic form of Bethe correlators in the thermodynamic limit, which have to be computed numerically in general [69, 259, 275]. The explicit spatial dependence in **Eq**. (8.9) leads to the decomposition of the longitudinal spin operator in a slowly varying part given by the derivative of the bosonic density field and a fast oscillating one given by the sinusoidal vertex operator. Fast oscillating means in that context that the term $\sin(\sqrt{4\pi K}\hat{\phi}(x,t) + 2k_F x)$ does not turn into a smooth expression in the continuum limit and thus averages out under the integral depending on the Fermi momentum. In the free field case the ground-state filling fraction is given by **Eq**. (8.5) is $k_F = \frac{\pi}{2a}$, hence the sinusoidal oscillates quickly. Conversely, a finite magnetic field changes k_F and thus may change if a term is relevant in **Eq**. (8.9) or not, with respect to fast spatial oscillations.

Additionally we have to demand that the bosonized spin operators obey the correct boundary conditions, which leads in the case of the experimentally more relevant Dirichlet conditions to the following mode expansion for the density field [66, 67, 176],

$$\hat{\phi}(x,t) = \frac{2x}{L}\hat{Q} + \underbrace{\sum_{l=1}^{\infty} \frac{\sin(\frac{\pi l x}{L})}{\sqrt{\pi l}} \left(e^{-i\frac{\pi l v t}{L}}\hat{b}_l + e^{i\frac{\pi l v t}{L}}\hat{b}_l^\dagger\right)}_{\hat{\phi}_{osc}(x,t)}. \tag{8.10}$$

The density zero mode in **Eq**. (8.10), is finally related to the magnetization $S^{z,tot}$ of the spin chain in **Eq**. (8.1), i.e.

$$S^{z,tot} = \int_0^L dx \sqrt{\frac{K}{\pi}} \partial_x \hat{\phi}(x). \tag{8.11}$$

In the following we will quickly recapitulate the analytical bosonization results concerning the longitudinal part of the structure factor, and furthermore discuss the deviation from the numerics and thus the reasoning of why to extend the method to non-linear dispersions. So the correlation of interest is the following longitudinal spin-spin correlation function [67]

$$\langle \hat{S}^z(x,t)\hat{S}^z(y,0)\rangle \approx A^2(-1)^{x+y}\langle \sin(\sqrt{4\pi K}\hat{\phi}(x,t))\sin(\sqrt{4\pi K}\hat{\phi}(y,0))\rangle, \tag{8.12}$$

where only the oscillatory contribution of the bosonized spin operator in **Eq**. (8.9) is taken into account. The reasoning for neglecting non-oscillatory contributions in **Eq**. (8.12) is that numerical experiments reveal that the low-energy support of the dynamical structure factor is in a narrow region around the anti-ferromagnetic wave vector, which originates from the commensurability of the spatial Fourier transformation with the oscillating factor. On the other hand, the non-oscillatory, or long-wavelength, contribution of the dynamical structure factor is probed by momenta close to zero and is predicted to be of delta function form [61, 251, 276], exactly resonant at the energy of the low-lying excitations. As stated in the introduction, this delta-shape of the dynamical structure factor for small momenta is nonphysical and may be broaded by including high-energy impurities to describe decay mechanisms of the low-lying excitations [276]. Nevertheless we neglect this as an unimportant detail due to its limited experimental relevance, yet a complete description for finite systems would still be of academic interest.

Insertion of the mode decomposition in **Eq**. (8.10) into the correlation function in **Eq**. (8.12) leads first into a separation of the expectation value into a zero mode part and the parts containing the finite momentum components, where we use the following short-hand notation for convenience

$$\begin{aligned}
&\langle \sin(\sqrt{4\pi K}\hat{\phi}(x,t))\sin(\sqrt{4\pi K}\hat{\phi}(y,0))\rangle \equiv \frac{1}{2}\left(G^+(x,y,t) + G^-(x,y,t)\right), \\
&G^{\pm}(x,y,t) = \langle e^{2i\pi(x\mp y)S^z_{tot}/L}\rangle \langle e^{i\sqrt{4\pi K}\hat{\phi}_{osc}(x,t)} e^{\mp i\sqrt{4\pi K}\hat{\phi}_{osc}(x,t)}\rangle.
\end{aligned} \tag{8.13}$$

The zero mode contribution gives a spatially dependent phase factor which depends explicitly on the total magnetization of the system and just corresponds to momentum shifts in the spatial Fourier transformation later on. Application of the Baker-Campbell-

Haussdorf formula to normal order the expectation values in $G^{\pm}(x,y,t)$ leads essentially to two equivalent forms of the correlation function, whereas a more detailed treatment of the calculation is shown in the part concerning the non-linear bosonization. Relevant for now is only that those contributions corresponds to the well-known form manifesting the algebraic decay in the thermodynamic limit [67], i.e.

$$G^{\pm}(x,y,t) = \left[\frac{2L}{\pi}\sin(\frac{\pi x}{L})\right]^{-K}\left[\frac{2L}{\pi}\sin(\frac{\pi y}{L})\right]^{-K}\left[\frac{\sin(\frac{\pi(x+y-vt)}{2L})\sin(\frac{\pi(x+y+vt)}{2L})}{\sin(\frac{\pi(x-y-vt)}{2L})\sin(\frac{\pi(x-y+vt)}{2L})}\right]^{\pm K}, \tag{8.14}$$

or to a form that is suitable for the determination of the dynamical structure factor as **Eq**. (8.14) cannot be easily Fourier transformed in terms of elementary functions. The second form of $G^{\pm}(x,y,t)$ is best understood in the (ω,k) plane, where the excitation structure of the low-energy theory is manifest [67, 258]. Thus we perform first an integration in the time domain

$$\int_{-\infty}^{\infty} dt e^{i\omega t} G^{\pm}(x,y,t) = 2\pi \sum_{m=0}^{\infty} S_m^{\pm}(x,y)\delta(\omega-\omega_m), \tag{8.15}$$

where the generic form of the periodic function with period $T = 2L/v$ is obtained with the Fourier coefficient

$$S_m^{\pm}(x,y) = \frac{1}{T}\int_{-T/2}^{T/2} G^{\pm}(x,y,t)e^{-i\frac{m\pi v}{L}t}dt. \tag{8.16}$$

The Fourier coefficient can then be partially integrated in time, revealing a recurrence relation among the coefficients [67, 258], i.e.

$$S_m^{\pm}(x,y) = \frac{\pm 1}{m}\sum_{l=1}^{m} S_{m-l}^{\pm}(x,y)4K\sin(\frac{\pi x}{L}l)\sin(\frac{\pi y}{L}l). \tag{8.17}$$

The Fourier coefficients have to be also Fourier transformed in space, which in general cannot be done in closed form, i.e.

$$S_m^{\pm}(k) = \frac{1}{L}\int_0^L dx \int_0^L dy \;\; e^{i(\pi-k)(x-y)} S_m^{\pm}(x,y), \tag{8.18}$$

yielding finally the dynamical structure factor

$$S(\omega,k) = A^2\pi \sum_{m=0}^{\infty}\left[S_m^{+}(k) - S_m^{-}(k)\right]\delta(\omega - \frac{\pi v}{L}m). \tag{8.19}$$

In **Eq**. (8.18) we have introduced an additional shift in the Fourier transformation, to take the alternating factors of the $2k_F$ oscillations into account. The result in **Eq**. (8.19) is quite remarkable as it allows for the calculation of the dynamical structure factor of

the open XXZ chain just by solving a comparably easy recurrence relation instead of the non-trivial integration of $G^{\pm}(x,y,t)$.

In the bulk limit, i.e. $xy \ll (x-y)^2 - (vt)^2$, all correlation functions are generally believed to be independent of the boundary conditions, which can be exemplary shown for the case of $G^{\pm}(x,y,t)$ in **Eq**. (8.14) and is discussed in detail for the non-linear bosonization later on. Thus one might as well use the form of the Fourier coefficient for periodic boundary conditions to obtain the $L \to \infty$ result for open boundary conditions, i.e

$$S_L^{per.}(\tilde{\omega}_m, \tilde{k}_l) = \frac{(\frac{2\pi}{L})^{2K} 2A^2L^2}{\Gamma^2(K)} \frac{\Gamma(\frac{m+l}{2}+K)}{\Gamma(\frac{m+l}{2}+1)} \frac{\Gamma(\frac{m-l}{2}+K)}{\Gamma(\frac{m-l}{2}+1)}, \tag{8.20}$$

keeping in mind the slightly different quantizations of energy $\tilde{\omega}_m = \frac{2\pi v}{L} m$ and momentum $\tilde{k}_l = \frac{2\pi}{L} l$, that become irrelevant for relatively large system sizes L. By using Stirling's formula for the Γ functions the expression **Eq**. (8.20) for the thermodynamic limit reads finally

$$S_\infty(\omega, \underbrace{q+\pi}_{k}) = 2(A\pi)^2 \frac{(2v)^{1-2K}}{\Gamma^2(K)} \left[(\omega+vq)\left[(\omega-vq)\right]^{K-1}\right. \left.\left[\Theta\Big(q+|\frac{\omega}{L}|\Big) - \Theta\Big(q-|\frac{\omega}{L}|\Big)\right]\right., \tag{8.21}$$

with no support outside the region $q \in \mathbb{B} \equiv (-\frac{\omega}{v}, \frac{\omega}{v})$ and a characteristic divergence at its surface $q \in \partial B$, if the Luttinger parameter is below one. **Eq**. (8.21) contains an important information concerning the motivation to go beyond the standard bosonization treatment, namely the occurring divergences of the dynamical structure factor in the thermodynamic limit, that also appear in the case of non-interacting fermions but are not clearly related to the ordinary algebraic decay of correlators in the Luttinger theory [253] . The presence of arbitrary magnetic fields, and interactions, alters the singularities in **Eq**. (8.21) to the more general, numerically deduced, form of a lower/middle/upper threshold singularity with different exponents and characteristic limiting behavior,

$$S_\infty^{h\neq 0}(\omega = \omega_{L,M,U}(q), q) \propto \Theta(\omega - \omega_{L,M,U}(q)) \left[\omega - \omega_{L,M,U}(q)\right]^{-\mu_{L,M,U}} . \tag{8.22}$$

The momentum dependence of the upper, middle or lower thresholds in **Eq**. (8.22) imply already that one has to go beyond standard bosonization with linearly dispersing modes to include band curvature effects and interactions simultaneously. In the current context a more general theory is achieved by projecting the elementary degrees of freedom onto the low-energy contributions around k_F as well as on one or several high-energy impurities $k_i \neq k_F$. The momenta k_i that the high-energy impurities are supposed to be projected on can then be modeled such that they phenomenologically describe the wanted processes which are not captured by a purely linear dispersion. The

threshold energies in **Eq**. (8.22) are then identified to be the energy difference between the Fermi-surface and a hole $k_i < k_F$ or a high energy excitation $k_i > k_F$.

But before we discuss the technique of non-linear bosonization, we want to address another issue concerning the finite-size bosonization for the dynamical structure factor in the XXZ-chain where the divergence is replaced by a sharply peaked spike instead. In several undergraduate and graduate theses realized in the research group of Prof. Sebastian Eggert under the co-supervision of Dr. Imke Schneider, the topic was to investigate the impact of a small magnetic field on the dynamical structure factor of the open XXZ chain [17]. It was revealed by a comparison of the standard bosonization approach with the quasi-exact $DMRG$ method, that the ordinary bosonization fails to describe the line shape of the Fourier coefficient of the dynamical structure factor in **Eq**. (8.19) for different excitations m, see **Fig**. (8.1). Thereby, the deviation from the numerics becomes stronger approaching the isotropic point, i.e. $\Delta = 1$, which is additionally related to the occurrence of logarithmic corrections arising through the $SU(2)$ invariance that is also not faithfully captured by abelian bosonization. Nevertheless, we will not focus on such effects as the combination of non-linear bosonization and non-abelian groups is far beyond that chapter. Thus from here on we consider a situation where the anisotropy is large enough such that there is a clear mismatch expected between abelian bosonization and the non-linear one, but Δ is small enough that we do not have to worry about an emergent $SU(2)$ symmetry.

In order to understand the mismatch from an analytical side we should first investigate the relation between the Fermi momentum and the magnetization i.e.

$$h\sum_{j=1}^{L}\hat{S}_j^z = h\left[\hat{N} - L/2\right] \equiv h\left[L/2 - \hat{N}\right]. \tag{8.23}$$

From **Eq**. (8.23) one can conclude that the effective Fermi momentum of the spin chain is given by its value which minimizes the energy of the field free case, i.e. $k_F^{h=0} = \pm\frac{\pi}{2}$, relative to the total magnetization that is caused by the magnetic field, i.e.

$$k_F^{h\neq 0} = \frac{\pi}{2} \pm \frac{\pi\sum_j S_j^z}{L}. \tag{8.24}$$

The sign ambiguity in **Eq**. (8.24) originates from the choice of the lowest or the highest spin weight state as the vacuum of the Jordan-Wigner fermions. The traditional approach to bosonization linearizes a fermionic dispersion at the Fermi-momentum, which is a good approximation as long as the curvature can be neglected. The procedure is optimal in the case of half-filling $k_F = \pm\frac{\pi}{2}$ where the curvature of the dispersion is minimized. It follows then from **Eq**. (8.24) that the linearization is not optimal anymore for increasing magnetization, which depends of course on the magnetic field as being the corresponding Lagrange multiplier. Thus already at the level of standard Taylor

series analysis we can conclude that curvature effects will become important for finite magnetic fields. **Fig**. (8.1) now shows some kind of asymmetry between the heights of the peaks in the numerical data and the standard bosonization, whereas a global re-scaling of the latter is always possible due to the non-universality of the pre-factors in the bosonization approach [48, 276]. Hence the strategy that is pursued in the following, is to reverse the higher and lower peak heights of the standard bosonization approach by adding a mobile impurity at the momentum surrounding the maximum of the lower peak. Thereby the momentum in **Fig**. (8.1) that the mobile impurity should possess has to be understood of course relative to the Fermi momentum and the corresponding magnetization niveau. This leads consequently to the rapprochement to the numerical data, that eventually needs to be finalized by a re-scaling of the pre-factors.

In the following the procedure of obtaining an effective field theory that includes such high-energy contributions non-perturbatively is briefly described, following the PhD thesis of Pereira [276]. Later on we use different mode decompositions to account for the finite size properties of the longitudinal spin correlation function, which is nothing but the inverse Fourier transform of the dynamical structure factor.

8.1.4 Non-linear Bosonization

A crucial limitation of the bosonization approach is the necessity of a linear dispersion of the particles, which implies that an infinite number of terms would have to be added if this prerequisite is not fulfilled. The Bethe ansatz is universally applicable instead, by implicitly re-summing all those contributions of the band curvature and higher order derivatives [276]. In the following we will study **Eq**. (8.1) by means of the non-linear bosonization technique, that aims to take those high-energy contributions into account heuristically, by attaching additional fermionic degrees of freedom $\hat{d}_n(x)$ to the standard left/right-decomposition with respect to the Fermi momenta, i.e.

$$\hat{\Psi}^\dagger(x) \approx \mathrm{e}^{-ik_\mathrm{F}x}\hat{\Psi}^\dagger_R(x) + \mathrm{e}^{ik_\mathrm{F}x}\hat{\Psi}^\dagger_L(x) + \sum_n \mathrm{e}^{ik_\mathrm{n}x}\hat{d}^\dagger_n(x). \tag{8.25}$$

The amount of additional creation/annihilation operators $\hat{d}_n(x)$ in **Eq**. (8.1), denoting the high-energy excitations, are in principle model/application dependent and are taken up to $n = 2$ in the context of the XXZ chain [250, 252, 253, 277] whereas in the case of low-magnetic fields only a single impurity is necessary. Most importantly the decomposition of Fermi operators in **Eq**. (8.25) should be understood in the sense of projection operators that artificially separate the Hilbert space into the low-energy subspaces and its complement $\hat{P}_\mathrm{low} + \hat{P}_\mathrm{high} = 1$, meaning that the low-energy projections of the real Fermi operators is given by the ordinary bosonization $\hat{P}^\dagger_\mathrm{low}\hat{\Psi}^\dagger(x)\hat{P}_\mathrm{low} = \mathrm{e}^{-ik_\mathrm{F}x}\hat{\Psi}^\dagger_R(x) + \mathrm{e}^{ik_\mathrm{F}x}\hat{\Psi}^\dagger_L(x)$ whereas the mobile impurity corresponds to the complement $\hat{P}^\dagger_\mathrm{high}\hat{\Psi}(x)\hat{P}_\mathrm{high} = \sum_n \mathrm{e}^{ik_\mathrm{n}x}\hat{d}_n(x)$. As a word of caution one should remark that the clean

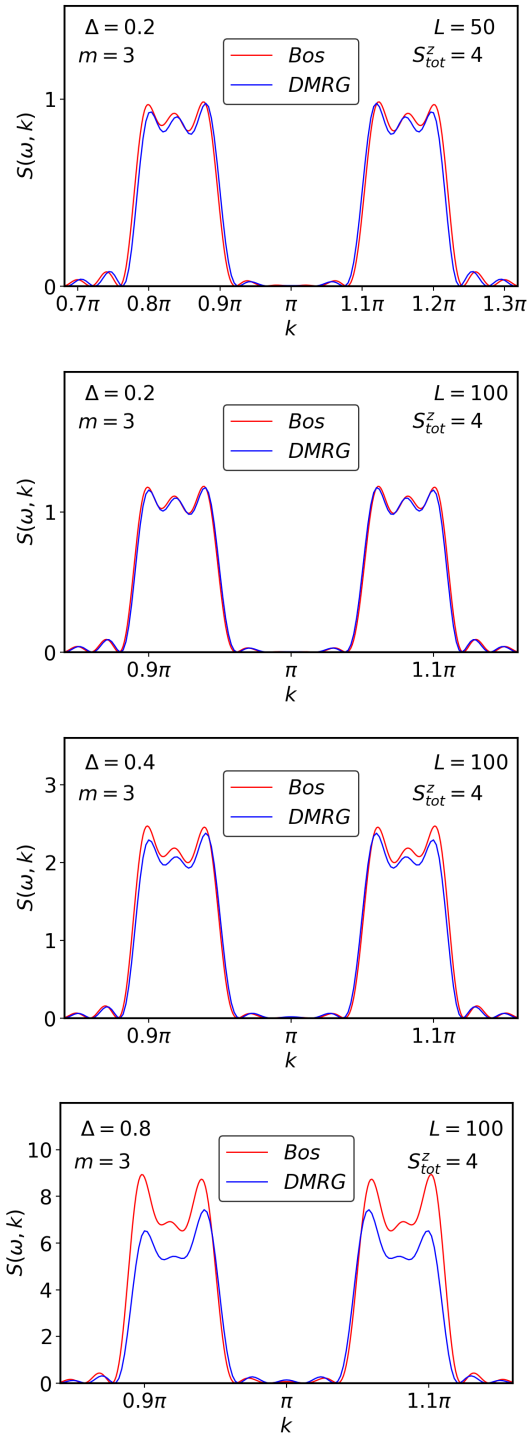

Figure 8.1: *Comparison of the dynamical structure factor from standard bosonization (red) and DMRG (blue, cutoff $M = 500$) with $J = 1$ and $\Delta = 0.2$ (top row), $\Delta = 0.4$ (bottom left) and $\Delta = 0.8$ (bottom right) at finite magnetic field corresponding to $S^z_{\text{total}} = 4$. The figure is from the PhD thesis of Kevin Jägering [17].*

separation in **Eq**. (8.25) into high and low-energy scales is physically far from trivial, as can be seen in momentum space where the distances between the impurity momenta and the Fermi-momentum decides what corresponds to which regime, i.e. $|k_F - k_n|$, even if these distances could be arbitrarily small in principle depending on the Hamiltonians parameters. Furthermore one expects, exclusively for integrable models, that there is a parametric continuity between the non-interacting/low-energy projection and its interacting/high-energy complement, meaning that they are adiabatically connected as can be explicitly shown by exact methods [255, 276].

Insertion of the decomposition **Eq**. (8.25) for $n = 1$ into the fermionized XXZ-chain **Eq**. (8.5), leads approximately to the following Hamiltonian, coupling a single high-energy degree of freedom $\hat{d}(x)$ to the low-energy ones $\partial_x \phi_{L,R}(x)$ [250]. The corresponding Hamiltonian density reads then

$$\begin{aligned}\hat{\mathcal{H}}_{\text{imp.}} \approx \frac{v}{2}\left[K\left(\partial_x\Theta(x)\right)^2 + \frac{1}{K}\left(\partial_x\Phi(x)\right)^2\right] + \hat{d}^\dagger(x)\left[-\epsilon - iu\partial_x - \frac{(\partial_x)^2}{2m}\right]\hat{d}(x) \\ + \frac{1}{\sqrt{\pi}}\left[\frac{\tilde{\kappa}_L - \tilde{\kappa}_R}{2}\partial_x\Theta(x) + \frac{\tilde{\kappa}_L + \tilde{\kappa}_R}{2}\partial_x\phi(x)\right]\hat{d}^\dagger(x)\hat{d}(x),\end{aligned} \tag{8.26}$$

where the bare coupling constants are defined in **Eq**. (8.135) at the end of the chapter. In terms of the chiral fields **Eq**. (8.26) can be alternatively expressed as

$$\begin{aligned}\hat{\mathcal{H}}_{\text{imp.}} \approx \frac{v}{2}\left[\left(\partial_x\phi_R(x)\right)^2 + \left(\partial_x\phi_L(x)\right)^2\right] + \hat{d}^\dagger(x)\left[-\epsilon - iu\partial_x - \frac{(\partial_x)^2}{2m}\right]\hat{d}(x) \\ + \frac{1}{\sqrt{2\pi K}}\left[\kappa_L\partial_x\phi_L(x) - \kappa_R\partial_x\phi_R(x)\right]\hat{d}^\dagger(x)\hat{d}(x),\end{aligned} \tag{8.27}$$

together with $\kappa_{L,R} = (\frac{1+K}{2})\tilde{\kappa}_{L,R} - (\frac{1-K}{2})\tilde{\kappa}_{R,L}$, which may be used to model the lower threshold singularity of the dynamical structure factor asymptotically exact if the systems parameters are taken to their re-normalized values. Especially the coupling constants of the mobile impurity and the chiral fields $\kappa_{R,L}$, as well as the impurity parameters ϵ, u and m, are understood to implicitly depend on the impurity momentum relative to k_F. The high-energy modes have to be decoupled from the left/right moving fields in **Eq**. (8.26) which can be achieved by the following non-local unitary transformation [255]

$$\hat{U}([x]_0^L) = \exp\left(i\int_0^L \frac{dx}{\sqrt{2\pi K}}\left[\gamma_R\phi_R(x) - \gamma_L\phi_L(x)\right]\hat{d}^\dagger(x)\hat{d}(x)\right), \tag{8.28}$$

as the Hamiltonian with respect to whom all correlation functions are calculated needs to be diagonal in order to use the toolbox of conformal field theory sense-fully. The coefficients in **Eq**. (8.28) have to be chosen like

$$\gamma_{L,R} = \kappa_{L,R}/(v \pm u), \tag{8.29}$$

such that the fields in **Eq**. (8.26) are decoupled. The unitary $\hat{U}([x]_0^L)$ transforms the left/right moving field operators according to

$$\hat{U}^\dagger([x]_0^L)\hat{\Psi}_{L,R}(x)\hat{U}([x]_0^L) = \hat{\tilde{\Psi}}_{L,R}(x) = \hat{\Psi}_{L,R}(x)\mathrm{e}^{\pm\frac{i}{\sqrt{K}}\int_0^x dx'\hat{d}^\dagger(x')\hat{d}(x')}, \tag{8.30}$$

which can be interpreted as the old operators with an attached Jordan-Wigner like string that induces a phase shift on the mobile impurities in the interval $x' \in [0, x]$. The transformed impurity operators on the other hand are given by

$$\hat{U}^\dagger([x]_0^L)\hat{d}(x)\hat{U}([x]_0^L) = \hat{\tilde{d}}(x) = \hat{d}(x)\mathrm{e}^{\frac{i}{\sqrt{2\pi K}}\left[\gamma_R\tilde{\phi}_R(x)-\gamma_L\tilde{\phi}_L(x)\right]} \tag{8.31}$$

with $\tilde{\phi}_{L,R}(x) = \hat{U}^\dagger([x]_0^L)\phi_{L,R}(x)\hat{U}([x]_0^L)$, enjoying a modification via a gauge phase that is dependent on the transformed bosonic fields $\tilde{\phi}_{L,R}(x)$. Application of the **Eq**. (8.28) leads finally to the desired diagonal form of **Eq**. (8.26)

$$\hat{\mathcal{H}}_{\text{imp.}} \approx \frac{v}{2}\left[\left(\partial_x\tilde{\phi}_L(x)\right)^2 + \left(\partial_x\tilde{\phi}_R(x)\right)^2\right] + \hat{\tilde{d}}^\dagger(x)\left[-\epsilon - iu\partial_x - \frac{(\partial_x)^2}{2m}\right]\hat{\tilde{d}}(x) + ..., \tag{8.32}$$

that implies that the effective ground-state of **Eq**. (8.32) is in product form with respect to ordinary and high-energy degrees of freedom, as both entities mutually commute. The symbol "..." in **Eq**. (8.32) stands for renormalization group irrelevant couplings between the impurity and the long-wavelength fields that are neglected.

8.2 Longitudinal Spin Correlation

The central point of this part of the thesis is the investigation of the following spin-spin correlation function

$$G(x, y, t) := \langle\hat{S}^z(x, t)\hat{S}^z(y, 0)\rangle, \tag{8.33}$$

by means of the non-linear bosonization approach. We choose the longitudinal part for simplicity, as the treatment of ladder operators is more complicated due to the presence of a Jordan-Wigner string between the constituents at (x, t) and $(0, 0)$. **Eq**. (8.33) corresponds to correlations between local density fluctuations relative to half-filling in the particle picture, i.e

$$\hat{S}_j^z \to \hat{n}_j - \frac{1}{2} \to :\hat{n}_j: + \delta_j \approx :\hat{n}_j:, \tag{8.34}$$

where the S^z operator is approximately equivalent to the normal ordered fermionic density under the assumption that the local magnetization is negligible $|\delta_j| = |\langle\hat{n}_j\rangle - \frac{1}{2}| \ll 1$. This normal ordered density operator can now be projected onto the chiral/impurity

fields of **Eq**. (8.25), leading to

$$
\begin{aligned}
:\hat{n}_l := \hat{\Psi}_R^\dagger(x)\hat{\Psi}_R(x) + \hat{\Psi}_L^\dagger(x)\hat{\Psi}_L(x) + \sum_{\alpha=1,\bar{1}} \hat{d}_\alpha^\dagger(x)\hat{d}_\alpha(x) \qquad (8.35)\\
+ \left[e^{i2k_F x}\hat{\Psi}_L^\dagger(x)\hat{\Psi}_R(x) + \sum_{\alpha=1,\bar{1}} e^{i(k_F-k_\alpha)x}\hat{\Psi}_R^\dagger(x)\hat{d}_\alpha(x) + e^{i(k_\alpha+k_F)x}\hat{\Psi}_L^\dagger(x)\hat{d}_\alpha(x) + \text{h.c.} \right]\\
+ e^{-i(k_1-k_{\bar{1}})x}\hat{d}_1^\dagger(x)\hat{d}_{\bar{1}}(x) + \text{h.c.}
\end{aligned}
$$

Up to now **Eq**. (8.35) contains up to two impurities for the sake of generality, where we restrict ourselves to a single impurity with momentum $k_1 = k_F - q$ as sufficiently weak magnetic fields are considered [250, 252, 253, 277]. Meaning that the Fermi-momentum k_F is only slightly adjusted and thus most of the signal of the dynamical structure factor is expected to come from the contributions surrounding $k \approx \pi$, see for example **Fig**. (8.1). In the thermodynamic limit this corresponds to the lower threshold of the dynamical structure factor as in **Eq**. (8.21), with the relevant excitation in **Eq**. (8.35), being a particle right at the Fermi surface and a deep hole, i.e. $e^{iq}\hat{\Psi}_R^\dagger(x)\hat{d}(x)$. For the sake of generality we nevertheless include also the ordinary part of the density-density correlator, as well as the corresponding left-moving contribution, by insertion of **Eq**. (8.35) into **Eq**. (8.33)

$$
\begin{aligned}
G(x,y,t) = \sum_{\eta,\bar{\eta}} e^{-i2k_F(x+\sigma y)}\langle \hat{\Psi}_\eta^\dagger(x,t)\hat{\Psi}_{\bar{\eta}}(x,t)\hat{\Psi}_{\sigma(\eta)}^\dagger(y,0)\hat{\Psi}_{\sigma(\bar{\eta})}(y,0)\rangle \qquad (8.36)\\
+ \sum_{\alpha} e^{i(k_F \mp k_\alpha)(x-y)}\langle \hat{\Psi}_{R,L}^\dagger(x,t)\hat{d}_\alpha(x,t)\hat{d}_\alpha^\dagger(y,0)\hat{\Psi}_{R,L}(y,0)\rangle + \text{h.c.},
\end{aligned}
$$

where $\eta, \bar{\eta} \in [R, L]$ and $\sigma = 1$ if $\sigma(\eta) = \eta$ or $\sigma = -1$ if $\sigma(\eta) = \bar{\eta}$. In **Eq**. (8.36) only the lowest-order contribution is considered, meaning that for example interactions between multiple impurities are neglected as they are assumed to be only relevant for very high energies and large magnetic fields. In order to proceed we need to express the occurring operators in **Eq**. (8.36) by the transformed ones in **Eq**. (8.30) and **Eq**. (8.31), as the expectation values can only be calculated non-perturbatively with the help of conformal field theory if the underlying field theory is non-interacting. After the transformations are inserted, the expectation values decompose into product form for impurity and bosonic fields respectively, as indicated by the additive structure of the Hamiltonian

Eq. (8.32), i.e.

$$
\begin{aligned}
G(x,y,t) = &\sum_{\eta,\bar{\eta}} e^{-i2k_F(x+\sigma y)} \langle \hat{\tilde{\Psi}}^{\dagger}_{\eta}(x,t) \hat{\tilde{\Psi}}_{\bar{\eta}}(x,t) \hat{\tilde{\Psi}}^{\dagger}_{\sigma(\eta)}(y,0) \hat{\tilde{\Psi}}_{\sigma(\bar{\eta})}(y,0) \rangle \\
&+ \sum_{\alpha} e^{i(k_F \mp k_\alpha)(x-y)} \Bigg[\\
&\langle \hat{\tilde{\Psi}}^{\dagger}_{R,L}(x,t) \hat{\tilde{\Psi}}_{R,L}(y,0) e^{\frac{-i}{\sqrt{2\pi K}}(\gamma^{\alpha}_{R}\tilde{\phi}_R(x,t) - \gamma^{\alpha}_{L}\tilde{\phi}_L(x,t))} e^{\frac{i}{\sqrt{2\pi K}}(\gamma^{\alpha}_{R}\tilde{\phi}_R(y,0) - \gamma^{\alpha}_{L}\tilde{\phi}_L(y,0))} \rangle \\
&\langle \hat{\tilde{d}}_{\alpha}(x,t) e^{\frac{\pm i}{\sqrt{2\pi K}} \int_x^y dz \hat{\tilde{d}}^{\dagger}_{\alpha}(z,0)\hat{\tilde{d}}_{\alpha}(z,0)} \hat{\tilde{d}}^{\dagger}_{\alpha}(y,0) \rangle \langle e^{\frac{i}{\sqrt{2\pi K}}(\pm 1 - [\gamma^{\alpha}_{R} - \gamma^{\alpha}_{L}]) \int_x^y dz \hat{\tilde{d}}^{\dagger}_{\bar{\alpha}}(z,0)\hat{\tilde{d}}_{\bar{\alpha}}(z,0)} \rangle + \text{h.c.} \Bigg]
\end{aligned}
\tag{8.37}
$$

In the following we are only interested in the impurity part of the correlation function in **Eq**. (8.37) as the non-impurity part is trivially invariant under the decoupling transformation **Eq**. (8.30) and **Eq**. (8.31). For simplicity we investigate the case of a single mobile impurity, i.e. $\alpha = 1$, and additionally assume that in the ground state there does not exist such an impurity, i.e. $\hat{d}^{\dagger}_{\alpha}\hat{d}_{\alpha}\,|GS\rangle = 0\,|GS\rangle$, leading to the simplified form in **Eq**. (8.38)

$$
\begin{aligned}
G(x,y,t)^{\text{imp}}_{R,L} = &e^{i(k_F \mp k_1)(x-y)} \langle \hat{\tilde{\Psi}}^{\dagger}_{R,L}(x,t) \hat{\tilde{\Psi}}_{R,L}(y,0) e^{\frac{-i}{\sqrt{2\pi K}}(\gamma_R \tilde{\phi}_R(x,t) - \gamma_L \tilde{\phi}_L(x,t))} \\
&e^{\frac{i}{\sqrt{2\pi K}}(\gamma_R \tilde{\phi}_R(y,0) - \gamma_L \tilde{\phi}_L(y,0))} \rangle \langle \hat{\tilde{d}}(x,t) \hat{\tilde{d}}^{\dagger}(y,0) \rangle + \text{h.c.}.
\end{aligned}
\tag{8.38}
$$

Up to now we have assumed that the derivation of the mobile impurity Hamiltonian, as well as the non-local unitary that decouples it from the rest, is independent on the given boundary conditions for the bosonic fields. Thus in the next step we need to choose a finite geometry and the corresponding mode decompositions for the chiral fields according to **Eqs**. (8.143) and (8.146) in **appendix** (8.13) and in **appendix** (8.14), respectively. Furthermore, we have to deduce the eigenfunctions of the mobile impurity, to be able to calculate the impurity correlation function **Eq**. (8.38).

8.3 Single-Particle Impurity

The longitudinal spin correlation in **Eq**. (8.38), contains the spatio-temporal auto-correlation function $\langle \hat{\tilde{d}}(x,t) \hat{\tilde{d}}^{\dagger}(y,0) \rangle$, which we assume to be well described by a single mobile impurity. The solutions to the Hamiltonian in **Eq**. (8.39) serve as tools to engineer the correct form of the correlation functions for the respective boundaries. So the focus in the following is not on a rigorous derivation, nor justification, of the impurity Hamiltonian, but more on adjusting its dispersion such that they suit to the numerically predicted form of correlation functions, according to **Fig**. (8.1). In that spirit, and due the fact that **Eq**. (8.39) has no solution that fulfills the Dirichlet boundary conditions

for linear dispersions exactly, i.e.

$$\hat{H}_{imp} = \int_0^L dx \;\; \hat{d}^\dagger \left[-\epsilon_0 - iu\partial_x + ... \right] \hat{d}, \tag{8.39}$$

we approximate the impurity contribution by a particle in a box with the corresponding eigenfunctions. Analogously for periodic boundary conditions, the impurity is formally replaced by a single particle on a circle. Thus we use the following single-particle Hamiltonian instead of **Eq**. (8.39)

$$\hat{\tilde{H}}_{imp} = \int_0^L dx \;\; \hat{d}^\dagger \left[-\epsilon_0 - \frac{1}{2}(\partial_x)^2 \right] \hat{d}, \tag{8.40}$$

meaning that we consider the impurity as described by an ordinary Schrödinger operator, instead of a first-order differential equation. Even if a terminology *à* la "effective mass" and "linearization of a dispersion" only makes sense in the many-body context, we still may relate the, in some sense massive, particles in **Eq**. (8.40) approximately to the massless case later on, by linearizing the quadratic energy dependence of the Schrödinger operator. This procedure might seem rather contradictory, as it implies taking some kind of low-energy limit of the high-energy impurity. Thus to be logically consistent one needs to keep in mind that even a low-energy impurity needs to be sufficiently larger in energy compared to the ordinary chiral fields. Furthermore both entities need to be so low in energy with respect to some particular scale, such that the low-energy sector of the XXZ-chain is addressed and the theory remains at least partially scale invariant.

8.3.1 Open Boundary Conditions

The eigenfunctions for a single particle obeying Dirichlet boundary conditions in **Eq**. (8.40) are given by the following expression for each mode p,

$$\psi_p(x) = \sqrt{\frac{2}{L}} \sin(q_p x). \tag{8.41}$$

The momentum quantization of the impurity, ensuring those boundary condition for the wave-function in **Eq**. (8.41), reads

$$q_p = \frac{\pi p}{L}. \tag{8.42}$$

The corresponding energies are quadratically dependent on the quantum number p and read

$$\omega_p = \frac{\hbar^2 \pi^2}{2m(L)^2} p^2, \tag{8.43}$$

where the mass of the impurity is understood as being dependent on the momentum of the high-energy projection of the field operator according to **Eq**. (8.25). Together with the previous definitions, the pair-correlation function takes the simple form

$$\langle \hat{\tilde{d}}(x,t)\hat{\tilde{d}}^{\dagger}(y,0)\rangle \approx \frac{2}{L}\sum_{p=1}^{\infty}\sin(q_p x)\sin(q_p y)e^{i\omega_p t}. \tag{8.44}$$

8.3.2 Periodic Boundary Conditions

For a single free particle confined on a circle, the eigenfunctions consist of plane waves in analogy to the Fourier decomposition of periodic signals, i.e. $\psi_p(x) = \sum_{p\in\mathbb{Z}} \alpha_p(t)e^{iq_p x}$. Hence the impurity correlator is given by the following expression

$$\langle \hat{\tilde{d}}(x,t)\hat{\tilde{d}}^{\dagger}(y,0)\rangle \approx \frac{1}{2\pi}\sum_{p=-\infty}^{\infty} e^{iq_p(x-y)}e^{i\omega_p t}, \tag{8.45}$$

with the impurity momenta

$$q_p = \frac{2\pi p}{L} \tag{8.46}$$

and the corresponding eigenenergies

$$\omega_p = \frac{\hbar^2}{2mR^2}p^2, \tag{8.47}$$

whereas R denoting the radius of the circle in **Eq**. (8.47). In contrast to **Eq**. (8.42), **Eq**. (8.46) embodies translational invariance, as the correlator depends only on the relative coordinate and not on their individual values.
The correlators in **Eqs**. (8.44) and (8.45) can be elegantly expressed as sums of, or as a single, Jacobi θ-functions

$$\theta(\tau,z) = \sum_{p=-\infty}^{\infty} e^{i\pi p^2\tau + 2\pi i p z}, \tag{8.48}$$

containing linear combinations of the spatio-temporal coordinates as its arguments. This representation will be important later on for the calculation of bulk or boundary limits of **Eq**. (8.38) as **Eq**. (8.48) is related to the fundamental solution of the diffusion equation on the circle or for Dirichlet boundaries. This suggests already the specific regularization scheme used in the next subsection, to determine the long-time limit of the impurity correlator in the relativistic/low-energy regime.

As a side remark, we have neglected a trivial energy shift of the impurities that correspond to the constant factors in the impurity Hamiltonians [255], in both impurity correlators for open or periodic boundaries respectively. They can be simply re-introduced by attaching an exponential factor $e^{\pm i\epsilon t}$ to the impurity correlation functions

Eq. (8.44) and **Eq**. (8.45) if needed, that will lead to a trivial energy shift in the dynamical structure factor later on. These factors are nevertheless conceptually of importance, as they are ultimately responsible for one or several singularities in the dynamical structure factor in **Eq**. (8.22), depending on the number of mobile impurities.

8.3.3 Relativistic Impurities and the Heat Kernel Regularization of the Delta Function

Up to now we have assumed that the high-energy impurity is described by an ordinary Schrödinger equation, due to the absence of non-trivial solutions of the linearized first-order equation in **Eq**. (8.39) for open boundary conditions. This assumption might be a wise choice for fitting, analytically analyzing, the dynamical structure factor or not, and perhaps re-normalized coupling constants and approximate eigenfunctions work better in some cases. The solutions to the respective Schrödinger equations are indeed a practicable starting point to analytically investigate the impact of the high-energy impurity on the otherwise conformal correlators from ordinary bosonization. We want to deduce especially the long-time and spatial bulk or boundary asymptotics of the impurity correlators, derived by different methods in [255]. The approach pursued here consists of linearizing the quadratic energy dependence of the single-particle Schrödinger operators, yielding effectively a δ-correlated impurity/ impurities. A successive heat-kernel regularization of these correlation functions, incorporates the diffusive nature of the mobile impurity in the bulk/boundary regime straight from the beginning. The regularization scheme is further motivated in detail by the relation between the Schrödinger and heat equation on the respective spatial domains.

The massive impurity correlator for each type of boundary conditions can be written as

$$\langle \hat{\tilde{d}}(x,t)\hat{\tilde{d}}^{\dagger}(y,0)\rangle^{OBC/PBC} \propto \sum_{p=-\infty}^{\infty} D(q_p,x,y)^{OBC/PBC} e^{i\omega_p t}, \tag{8.49}$$

together with the coefficient $D(q_p,x,y)$

$$\begin{aligned} D(q_p,x,y)^{OBC} &= \frac{1}{4(L)}\left[(e^{iq_p[x-y]}+e^{-iq_p[x-y]})-(e^{iq_p[x+y]}+e^{-iq_p[x+y]})\right], \\ D(q_p,x,y)^{PBC} &= \frac{1}{2\pi}e^{iq_p(x-y)}. \end{aligned} \tag{8.50}$$

Remarkably upon substituting $t=i\tau$, **Eq**. (8.49) corresponds exactly to the heat kernel on the circle or for Dirichlet boundary conditions respectively [108]. This means that in imaginary time τ, the impurity correlators expressed as the Jacobi θ functions, or linear combinations of it, are the fundamental solutions to the heat equation for the given type of boundary conditions. Thus the convolution of the impurity correlators in **Eq**. (8.49) with some function $f(x)$ induces the solution of the heat equation, on the given domain,

for the initial value $f(x)$. This relation between the Schrödinger and heat equation is rather well know, but suggests in the current context a specific regularization scheme for the occurring delta functions in the mesoscopic L /relativistic limit of **Eq**. (8.49).

For the investigation of the singularity structure of $S(q,\omega)$, as well as its boundary and bulk limits, it is convenient to perform a low-energy limit in **Eq**. (8.49), by assuming a linear dependence on the quantum number p in **Eqs**. (8.43) and (8.47), i.e. relatively low energies for the high-energy impurity

$$\partial_p \omega_p \approx q_p u. \tag{8.51}$$

In this way one can approximately define a low-energy limit for the correlators of the single-particle Hamiltonians in **Eq**. (8.49), lacking even non-trivial solutions in the Dirichlet case, which is understood as being an engineering tool rather than a fundamental quantity. Nevertheless despite its convenience at the moment, taking the wrong eigenvalues to some eigenfunctions according to **Eq**. (8.51) may result in uncontrollable physical behavior for large impurity momenta p and care should be taken if the formulas that are derived under this assumption are used for numerical evaluations of $S(q,\omega)$ later on. In addition, the numerical values of u should be considered as being re-normalized instead of those derived from **Eq**. (8.51).

Taking **Eq**. (8.51) seriously, we have to choose if the momentum of the impurity should stay discrete, i.e. $p \in \mathbb{Z}$, meaning that the energy/momentum quantization of the impurity is in some sense naturally represented. On the other hand one may choose the impurity momentum approximately as continuous , i.e. $p \in \mathbb{R}$, which would make the linearization of the spectrum more meaningful. If the momenta p are assumed to be still discrete, then the derivative in **Eq**. (8.51) has to be formally replaced with the corresponding difference quotient which yields furthermore a factor of the order L^{-1} that is unimportant for the following discussion. Due to the phononic dispersion, and discrete momenta p, the impurity correlators in **Eq**. (8.49) can then be written as a single Dirac comb for periodic boundary conditions,

$$\langle \hat{\hat{d}}(x,t)\hat{\hat{d}}^{\dagger}(y,0)\rangle^{PBC} \underbrace{\approx}_{\omega_p \approx q_p u} \langle \hat{\hat{d}}(x,t)\hat{\hat{d}}^{\dagger}(y,0)\rangle^{PBC}_{\omega_p \approx q_p u} \equiv L \sum_{k\in\mathbb{Z}} \delta(x-y-ut-kL), \tag{8.52}$$

or as multiple Dirac combs for the Dirichlet case, i.e.

$$\langle \hat{\tilde{d}}(x,t)\hat{\tilde{d}}^{\dagger}(y,0)\rangle^{OBC} \underbrace{\approx}_{\omega_p \approx q_p u} \langle \hat{\tilde{d}}(x,t)\hat{\tilde{d}}^{\dagger}(y,0)\rangle^{OBC}_{\omega_p \approx q_p u} \tag{8.53}$$
$$\equiv L\left[\sum_{k\in\mathbb{Z}} \delta(x-y+ut-kL) + \sum_{l\in\mathbb{Z}} \delta(x-y-ut-lL)\right]$$
$$- L\left[(\sum_{m\in\mathbb{Z}} \delta(x+y+ut-mL) + \sum_{n\in\mathbb{Z}} \delta(x+y-ut)-nL)\right].$$

For larger but still mesoscopic system sizes, each Dirac comb in **Eqs**. (8.52) and (8.53) has a very long period L, and further multiples of the fundamental period may be neglected. Hence one can conclude that the combs can be replaced by single δ functions for mesoscopic L, i.e.

$$\langle \hat{\tilde{d}}(x,t)\hat{\tilde{d}}^{\dagger}(y,0)\rangle^{PBC}_{\omega_p \approx q_p u} \underbrace{\propto}_{1 \ll L} \delta(x-y-ut), \tag{8.54}$$

and **Eqs**. (8.54) and (8.55) can be interpreted quasi-classically in the sense that the quantization of quantum numbers becomes effectively continuous,

$$\langle \hat{\tilde{d}}(x,t)\hat{\tilde{d}}^{\dagger}(y,0)\rangle^{OBC}_{\omega_p \approx q_p u} \underbrace{\propto}_{1 \ll L} [\delta(x-y+ut) + \delta(x-y-ut)] \tag{8.55}$$
$$- [(\delta(x+y+ut) + \delta(x+y-ut))]\,.$$

The linear approximation for large enough L implies then that the impurity is essentially uncorrelated, except at a single light cone $x-y-ut$, for periodic boundary conditions. For the open boundary case in Eq. (8.55) $\hat{d}(x)$ is correlated at different spatio-temporal points, expressing the loss of translational invariance. **Eqs**. (8.54) and (8.55) can also be obtained from **Eq**. (8.49) directly, by considering continuous momenta p and a linear dispersion from the beginning. This means that if p is chosen to be discrete then the approximate low-energy eigenfunctions remain periodic as expressed by their Dirac cone structure, whereas the correlators loose this periodicity for approximately continuous p. Even if both approaches should coincide for mesoscopic L and are thus assumed to be equivalent if we seek further analytical approximations, it is a priori unclear if the discretely indexed correlators in **Eqs**. (8.52) and (8.53) or the continuous ones in **Eqs**. (8.54) and (8.55) are more favorable as the ordinary eigenfunctions for engineering the correct form of the dynamical structure factor $S(q,\omega)$ beyond standard bosonization.

To calculate the boundary and bulk limits of the impurity correlation function in **Eqs**. (8.54) and (8.55), and in the latter case show their equivalence, it is inevitable to re-regularize the occurring delta functions. Furthermore **Eqs**. (8.54) and (8.55) should be equal for infinite, not mesoscopic, system sizes, a fact that is also not straightforward

to show without a proper re-normalization. Thus one is facing the delicate issue of regularizing distributions in a physical sense, such that the close-range or far-range limits of the impurity correlators can be performed in terms of analytic functions instead of formal distributions and furthermore match the asymptotics of the underlying physical problem. A physically motivated, but of course mathematically non-unique, choice is obviously the heat kernel as a nascent delta function, i.e.

$$\delta(z) = \lim_{\tilde{t}\to 0} \frac{1}{\sqrt{2\pi\tilde{t}}} e^{-\frac{z^2}{\tilde{t}}}, \qquad \tilde{t} = \epsilon t, \quad z \in \mathbb{R} \tag{8.56}$$

due to the relation of **Eq**. (8.49) to the fundamental solution of the diffusion equation for the respective boundary condition. In order to motivate this assumption even more, we show exemplarily for the case of periodic boundary conditions that **Eq**. (8.56) is connected to **Eq**. (8.49) by a suitable periodic continuation, whereas the same can be shown also for Dirichlet boundary conditions. So we consider some periodic initial data $f(x+2\pi) = f(x)$ and its convolution with the heat kernel in **Eq**. (8.56), meaning we calculate the heat flow for the periodic initial condition $f(x)$ on the circle [108], i.e.

$$\begin{aligned} &\int_{-\infty}^{\infty} f(y+\phi) \frac{1}{\sqrt{2\pi\tilde{t}}} e^{-\frac{y^2}{\tilde{t}}} dy = \sum_{k\in\mathbb{Z}} \int_{2\pi k}^{2\pi k+2\pi} f(y-2\pi k+\phi) \frac{1}{\sqrt{2\pi\tilde{t}}} e^{-\frac{(y-2\pi k)^2}{\tilde{t}}} dy \quad (8.57) \\ &= \int_0^{2\pi} f(y+\phi) \sum_{k\in\mathbb{Z}} e^{-k^2\tilde{t}} e^{iky} dy, \end{aligned}$$

where the second line in **Eq**. (8.57) can be shown by Poisson summation. **Eq**. (8.57) now means that heat kernel in **Eq**. (8.56) defined on the real numbers can be constrained to the case of cyclic, or Dirichlet boundary conditions, whereas most importantly the impurity correlators in **Eqs**. (8.54) and (8.55) can be recovered by switching again to imaginary times, i.e. $\tilde{\tau} = -i\tilde{t}$. Hence one may conclude that the chosen regularization in **Eq**. (8.56) is the "physically correct" one, as the procedure is in some sense invertable and logically connected to the problem at hand, with the additional benefit of relating the impurity energy to the smallness parameter ϵ of the regularization. **Eq**. (8.56) enjoys the probabilistic interpretation as inducing the Brownian motion of a particle starting at the origin at time $\tilde{t}$, normally distributed with variance $\tilde{t}$ and zero mean [278,279]. Thus the conjectured regularization perfectly fits to the diffusive form of temporal correlators predicted by non-linear bosonization [205].

The regularized/classical impurity correlators can then be written as

$$\begin{aligned} \langle \hat{\tilde{d}}(x,t) \hat{\tilde{d}}^\dagger(y,0) \rangle_\epsilon^{PBC} &\propto \sqrt{\frac{1}{2\pi\epsilon t}} e^{-\frac{(x-y+ut)^2}{\epsilon t}}, \qquad (8.58) \\ \langle \hat{\tilde{d}}(x,t) \hat{\tilde{d}}^\dagger(y,0) \rangle_\epsilon^{OBC} &\propto \sqrt{\frac{1}{2\pi\epsilon t}} \left[e^{-\frac{(x-y+ut)^2}{\epsilon t}} + e^{-\frac{(x-y-ut)^2}{\epsilon t}} - e^{-\frac{(x+y+ut)^2}{\epsilon t}} - e^{-\frac{(x+y-ut)^2}{\epsilon t}} \right], \end{aligned}$$

where the regulator ϵ has the physical dimension of a diffusion constant, i.e. $[Length^2/Time]$. Hence ϵ quantifies how easy the high-energy impurity is diffusing through the "medium" which is given by the normal excitations surrounding the Fermi-sphere. In this spirit **Eq**. (8.56) can be understood as the limit of a negligible impurity diffusion/low energies, as the effective diffusion constant approaches zero.

In order to investigate the limiting behavior of the impurity correlators near the boundaries, deep in the bulk or as auto-correlations, one considers the spatial points of interest to be sufficiently close to each other, i.e. $x \approx y$, such that both points belong to the same region in space or are in fact approximately equal. This leads then to the following form of the impurity correlators for the respective boundary condition

$$\begin{aligned}\langle \hat{\tilde{d}}(x,t)\hat{\tilde{d}}^\dagger(x\approx y,0)\rangle_\epsilon^{OBC} &\approx \sqrt{\frac{1}{2\pi\epsilon t}}\left[2-2\cosh(\frac{4xu}{\epsilon})e^{-\frac{(2x)^2}{\epsilon t}}\right]e^{-\frac{u^2t}{\epsilon}}, \\ \langle \hat{\tilde{d}}(x,t)\hat{\tilde{d}}^\dagger(x\approx y,0)\rangle_\epsilon^{PBC} &\approx \sqrt{\frac{1}{2\pi\epsilon t}}e^{-\frac{u^2t}{\epsilon}}.\end{aligned} \tag{8.59}$$

Following the work of Pereira in **Ref**. [255] the "auto-correlation" limit is most easily obtained for periodic boundary conditions, by expanding the exponential factor in **Eq**. (8.59) for $u^2t \ll \epsilon$, i.e.

$$\langle \hat{\tilde{d}}(x,t)\hat{\tilde{d}}^\dagger(y\approx x,0)\rangle_\epsilon^{\text{Bulk,OBC}} = \langle \hat{\tilde{d}}(x,t)\hat{\tilde{d}}^\dagger(y\approx x,0)\rangle_\epsilon^{\text{PBC}} \propto t^{-\frac{1}{2}}, \tag{8.60}$$

meaning that one considers effective diffusion constants ϵ of the impurity to be much larger than u^2t. Hence in order to have a meaningful limiting behavior in **Eq**. (8.56), the impurity velocity u should be sufficiently small, i.e. $u^2t \approx 0 \ll \epsilon$, such that we can still consider $\epsilon t \approx 0$ effectively for large enough times t. Very small impurity velocities u would imply, at least in the many-body case, that the linearization of the dispersion vanishes and $\hat{d}(x)$ represents a particle in the vicinity of strong band curvature. In the terminology of Brownian motion **Eq**. (8.60) corresponds exactly to a one-dimensional diffusion process, due to an algebraic temporal decay of the form $t^{-d/2}$, with d being the spatial dimensionality [279].

Furthermore one would expect that the correlator for open boundaries should be equal to the periodic case deep in the bulk [66, 67], i.e. $x \approx L/2 \approx y$. Thus the asymptotic values of the open boundary correlator in the bulk with L large enough, is given by the following expression

$$\begin{aligned}\langle \hat{\tilde{d}}(x\approx L/2,t)\hat{\tilde{d}}^\dagger(x\approx y\approx L/2,0)\rangle_\epsilon^{OBC} &\overbrace{\approx}^{L\gg 1} \sqrt{\frac{1}{2\pi\epsilon t}}\left[2-e^{\frac{4xu}{\epsilon}}e^{-\frac{(2x)^2}{\epsilon t}}\right]e^{-\frac{u^2t}{\epsilon}}, \\ &\overbrace{\propto}^{\epsilon t<\mathcal{O}(L^2)} \langle \hat{\tilde{d}}(x\approx y\approx L/2,t)\hat{\tilde{d}}^\dagger(x\approx y\approx L/2,0)\rangle_\epsilon^{PBC}\end{aligned} \tag{8.61}$$

From **Eq**. (8.61) we can conclude then that the two correlators are indeed proportional to each other in the bulk and for large enough system sizes, provided that the effective length scale $\sqrt{\epsilon t}$ is smaller than L. Re-referring to Brownian motion this requirement should always be fulfilled, as this corresponds exactly to half the mean squared displacement of the mobile impurity that needs to be smaller than the square of the system size L^2 [279]. Conversely, by performing again the limit of $\tilde{t} = \epsilon t \to 0$ in **Eq**. (8.61) one may show that both impurity correlators coincide in the infinite size limit, as expected on general grounds.

A fundamental question is whether the diffusive temporal decay of the auto-correlation limit, predicted by **Eq**. (8.59), is somehow amplified to an anomalous diffusion process near the systems boundaries or not [255]. The boundary limit applies of course only to the open boundary case in **Eq**. (8.59) and is achieved by assuming the following inequalities for the diffusivities at $a, L-a$, $\epsilon \gg u^2 t$, $\epsilon \gg \frac{(2a)^2}{t} \equiv \frac{4(L-a)^2}{t}$, as well as $\epsilon \gg 4au \equiv 4(L-a)u$. In order to connect to the results of **Ref**. [255] for semi-infinite boundaries, we further have to assume that the two inequalities $\epsilon \gg 2au \equiv 2(L-a)u$ and $\epsilon \gg u^2 t$ are dominant with respect to the remaining one, meaning that we expand the corresponding functions to zeroth/first order respectively. Additionally we demand that the inequalities should be asymptotically equal at both boundaries. Then, $\epsilon \gg 4au \equiv 4(L-a)u$ only makes sense if $u \propto \mathcal{O}(L^{-2})$ or smaller for large L, as this ensures asymptotically that $\epsilon \gg \mathcal{O}(L^{-2})$ is small and equal on both boundaries. This implies according to $\epsilon \gg u^2 t$ that the considered time scales t for the upper bound of the impurity velocity $u \propto \mathcal{O}(L^{-2})$ should be at least smaller than $t < \mathcal{O}(L^4)$. This condition ensures that the regularization $\epsilon \gg \mathcal{O}(L^{-n}),\ \ n \in \mathbb{N}^+$ remains a small quantity for these times, whereas even smaller impurity velocities $u < \mathcal{O}(L^{-2})$ lead to larger achievable and logically consistent time scales $t < \mathcal{O}(u^{-2})$. In order that the inequality $\epsilon \gg \frac{(2a)^2}{t} \equiv \frac{4(L-a)^2}{t}$ is asymptotically valid at both boundaries, we need to assume on the other hand, that the time scale is at least of the order $t \propto \mathcal{O}(L^3)$, with $\epsilon \gg \mathcal{O}(L^{-3})$. So we can finally conclude that we can fulfill the boundary limit and a suitably small ϵ regularization, if very small impurity velocities $u \leq \mathcal{O}(L^{-2})$ are considered and time scales in the range $\mathcal{O}(L^3) \leq t < \mathcal{O}(u^{-2})$. To guarantee additionally the validity of the limit $\epsilon t \to 0$ asymptotically in L, the regularization should always be understood as being necessarily of lower order in L as the time scale one would like to describe.

The explicit form of the boundary limit is then given by

$$\langle \hat{\tilde{d}}(x,t) \hat{\tilde{d}}^{\dagger}(y,0) \rangle_{\epsilon}^{\text{Boundary,OBC}} \propto t^{-\frac{3}{2}} xy. \tag{8.62}$$

Eq. (8.62) can now be interpreted such that at the boundary the impurity-driven temporal diffusion becomes anomalous with the coefficient $t^{-1/2-1}$. Meaning that the impurity correlators decay quicker in time when they reside in the vicinity of the

boundary. Physically one may interpret this suppressed diffusion, as being caused by the vanishing of the wave function near the boundary [255,276]. Alternatively one could rephrase this in the context of Brownian motion, by saying that the equal probability of moving either to the left or right becomes imbalanced due to the presence of a boundary. The natural question that arises now is how this sub-diffusive behavior of the impurity correlator near the boundary is amplified by the corresponding chiral correlators and their scaling dimension.

Remarkably the same temporal decay as in **Eqs**. (8.60), (8.61) and (8.62) can be obtained by assuming a continuous spectrum and a finite momentum cut-off for the impurity correlation function in **Eq**. (8.44) [255]. This comparison implies that we can relate the finite momentum cut-off used in **Ref**. [255] to the choice of an impurity diffusivity/regulator ϵ in the δ regularization in **Eq**. (8.56). Furthermore we can conclude that we need to neglect the momentum quantization of impurity correlators in order to compute their asymptotic values near the boundary or bulk, in accordance with the procedure used for chiral correlators [176]. Further information deduced here are the estimates that relate the impurity velocity u and the time scale t where the boundary limit is asymptotically well defined to orders of the system size L. Furthermore the results in **Ref**. [255] are somehow extended to include also spatial modulations near both boundaries, instead of setting $x = a = y$. If one is not just interested in the asymptotic form of impurity correlators near the boundary/bulk, but more in a numerical investigation of the dynamical structure factor for finite sizes, the corresponding single or linear combination of Jacobi functions in **Eq**. (8.49) should be considered as a starting point instead of the approximations deduced in this subsection. But, as approximate eigenfunctions may work better in some cases, the linearization of the spectrum according to **Eq**. (8.51) can always be re-introduced if needed. Ultimately, which choice of effective impurity description, i.e. mass-less or massive, suits better to the quasi-exact data according to **Fig**. (8.1) remains an open problem until a direct numerical comparison is performed. Nevertheless, we could show in this subsection that simple manipulations of the single-impurity correlators in **Eq**. (8.49) may be used to analytically investigate the asymptotic behavior of the high-energy impurity, where we can explicitly show some kind of white-noise/ Brownian regime for the low-energy approximations in **Eqs**. (8.54) and (8.55) and **Eq**. (8.58) respectively. The δ-correlations in **Eq**. (8.54) can be used later on to re-investigate the singularity of the dynamical structure factor in the thermodynamic limit, whereas the diffusive behavior of the full density-density correlation function in the bulk or near the boundary can only be addressed by the regularization to Brownian motion in **Eq**. (8.58).

8.4 Chiral Field Correlation Function for Open Boundaries

The chiral part of the full impurity correlation function for open boundary conditions can be obtained by inserting the mode decomposition of **Eq**. (8.143) into **Eq**. (8.38), and subsequently apply the normal ordering. Before we proceed, we write the chiral part of the impurity correlation function of **Eq**. (8.38) in compact notation,

$$\begin{aligned} G(x,y,t)^{\text{chiral}}_{R,L} &= \langle \hat{\tilde{\Psi}}^{\dagger}_{R,L}(x,t)\hat{\tilde{\Psi}}_{R,L}(y,0) \\ &\quad * e^{\frac{-i}{\sqrt{2\pi K}}(\gamma_R\tilde{\phi}_R(x,t)-\gamma_L\tilde{\phi}_L(x,t))} e^{\frac{i}{\sqrt{2\pi K}}(\gamma_R\tilde{\phi}_R(y,0)-\gamma_L\tilde{\phi}_L(y,0))}\rangle \\ &\equiv \langle * e^{A_{R,L}(x,t)} e^{B(y,0)_{R,L}} e^{C(x,t)_{R,L}} e^{D(y,0)_{R,L}}\rangle, \end{aligned} \tag{8.63}$$

where we use in the following that for open boundary conditions only one of the chiral fields exist according to the folding trick [66, 67],

$$A_{R,L}(x,t) = i\frac{\alpha}{2}\left[\alpha_{R,L}\tilde{\phi}_R(x,t) - \alpha_{L,R}\tilde{\phi}_R(-x,t) + \alpha_{L,R}\hat{\phi}_0\right], \tag{8.64}$$

$$B_{R,L}(y,0) = -i\frac{\alpha}{2}\left[\alpha_{R,L}\tilde{\phi}_R(y,0) - \alpha_{L,R}\tilde{\phi}_R(-y,0) + \alpha_{L,R}\hat{\phi}_0\right],$$

$$C_{R,L}(x,t) = \frac{-i}{\sqrt{2\pi K}}\left(\gamma_R\tilde{\phi}_R(x,t) + \gamma_L\tilde{\phi}_R(-x,t) - \gamma_L\hat{\phi}_0\right),$$

$$D_{R,L}(y,0) = \frac{i}{\sqrt{2\pi K}}\left(\gamma_R\tilde{\phi}_R(y,0) + \gamma_L\tilde{\phi}_R(-y,0) - \gamma_L\hat{\phi}_0\right),$$

with $\alpha_{R,L} = (\frac{1}{\sqrt{K}} \pm \sqrt{K})$ and $\alpha = \sqrt{2\pi}$. The expectation value with respect to the Luttinger liquid state can now be calculated straight-forwardly by observing that each factor consists of exponential functions of linear combinations of bosonic creation and annihilation operators [42, 43]. At first we use the reduced Baker-Campbell-Haussdorf theorem to obtain a single exponential function of the bosonic operators inside the expectation value, i.e.

$$\begin{aligned} G(x,y,t)^{\text{chiral}}_{R,L} &= \langle e^{A_{R,L}(x,t)} e^{B(y,0)_{R,L}} e^{C(x,t)_{R,L}} e^{D(y,0)_{R,L}}\rangle \\ &= \tilde{C}^{R,L}(x,y,t)\langle e^{A_{R,L}(x,t)+B(y,0)_{R,L}+C(x,t)_{R,L}+D(y,0)_{R,L}}\rangle, \end{aligned} \tag{8.65}$$

where the pre-factor in **Eq**. (8.65) is given by all possible commutators appearing in the vertex operators

$$\begin{aligned}\tilde{C}^{R,L}(x,y,t) =& e^{\frac{1}{2}\left(\left[A_{R,L}(x,t),B_{R,L}(y,0)\right]+\left[A_{R,L}(x,t),C_{R,L}(x,t)\right]+\left[A_{R,L}(x,t),D_{R,L}(y,0)\right]\right)} \\ & * e^{\frac{1}{2}\left(\left[C_{R,L}(x,t),D_{R,L}(y,0)\right]+\left[B_{R,L}(y,0),C_{R,L}(x,t)\right]+\left[B_{R,L}(y,0),D_{R,L}(y,0)\right]\right)},\end{aligned} \tag{8.66}$$

that are listed at the end of the chapter. Collecting all terms in **Eq**. (8.66) according to the characteristic linear combination of spatio-temporal coordinates, we obtain the following form that will be convenient later on,

$$\begin{aligned}\tilde{C}^{R,L}(x,y,t) &= e^{(\frac{\alpha^2}{4}\alpha_{R,L}^2+\frac{\gamma_R^2}{2\pi K})f(x-y-vt)/2+(\frac{\alpha^2}{4}\alpha_{L,R}^2-\frac{\gamma_L^2}{2\pi K})f(x-y+vt)/2} \\ &* e^{-(\frac{\alpha^2}{4}\alpha_{R,L}\alpha_{L,R}+\frac{\alpha(\alpha_{L,R}\gamma_R+\alpha_{R,L}\gamma_L)}{2\sqrt{2\pi K}}-\frac{\gamma_R\gamma_L}{2\pi K})f(x+y-vt)/2} \\ &* e^{(\frac{\alpha^2}{4}\alpha_{R,L}\alpha_{L,R}-\frac{\alpha(\alpha_{L,R}\gamma_R+\alpha_{R,L}\gamma_L)}{2\sqrt{2\pi K}}-\frac{\gamma_R\gamma_L}{2\pi K})f(x+y+vt)/2} e^{\frac{\alpha}{2\sqrt{2\pi K}}(\alpha_{R,L}\gamma_L+\alpha_{L,R}\gamma_R)(f(2x)+f(2y))/2} \\ &* e^{-\frac{\alpha}{2\sqrt{2\pi K}}\left[(\alpha_{R,L}\gamma_L+\alpha_{L,R}\gamma_R)\frac{x+y-vt}{4L}-\alpha_{L,R}\gamma_R\frac{x-y-vt}{4L}-\gamma_L(\alpha_{R,L}-\alpha_{L,R})\frac{x+y-vt}{4L}+\alpha_{L,R}\gamma_L\frac{x-y+vt}{4L}\right]\left[\hat{Q},\hat{\phi}_0\right]/2} \\ &* e^{(\frac{\alpha^2}{4}(\alpha_{L,R}^2\frac{x-y+vt}{4L}+\alpha_{R,L}\alpha_{L,R}\frac{x-y-vt}{4L})+\frac{1}{2\pi K}(\gamma_R\gamma_L\frac{x-y-vt}{4L}-\gamma_L^2\frac{x-y+vt}{4L}))\left[\hat{Q},\hat{\phi}_0\right]/2},\end{aligned} \tag{8.67}$$

where we have defined the following short-hand notation for the c-number of the central field commutators in **Eq**. (8.66).

$$f(x+y+vt) = \frac{i}{2}\left[\frac{x+y+vt}{4L}+\frac{1}{2\pi}\sum_{l=1}^{\infty}\frac{1}{l}\sin(k_l[x+y+vt])\right]. \tag{8.68}$$

In the next step we have to normal order the vertex operators explicitly to finally obtain the remaining expectation value of

$$\langle e^{A_{R,L}(x,t)+B(y,0)_{R,L}+C(x,t)_{R,L}+D(y,0)_{R,L}}\rangle = \bar{C}^0_{R,L}(x-y,t)e^{\frac{1}{2}\sum_{l=1}^{\infty}|A_l^{R,L}(x,y,t)|^2\left[\hat{b}_l,\hat{b}_l^\dagger\right]}. \tag{8.69}$$

In **Eq**. (8.69) the zero mode contribution $\bar{C}^0_{R,L}(x-y,t)$, corresponding to an L-dependent momentum and energy shift in the structure factor later on, is given by

$$\bar{C}^0_{R,L}(x-y,t) = \langle e^{i\left[\epsilon^+_{R,L}(x-y)+\epsilon^-_{R,L}vt\right]\frac{\hat{Q}}{2L}}\rangle = e^{i\left[\epsilon^+_{R,L}(x-y)+\epsilon^-_{R,L}vt\right]\frac{\langle\hat{Q}\rangle}{2L}}, \tag{8.70}$$

with the left/right inhomogeneous factors

$$\begin{aligned}\epsilon^+_{R,L} &= \frac{\alpha}{2}(\alpha_{R,L}+\alpha_{L,R})+\frac{\gamma_L-\gamma_R}{\sqrt{2\pi K}} \\ \epsilon^-_{R,L} &= -\left[\frac{\alpha}{2}(\alpha_{R,L}-\alpha_{L,R})-\frac{\gamma_L+\gamma_R}{\sqrt{2\pi K}}\right].\end{aligned} \tag{8.71}$$

The absolute value of the finite momentum components in **Eq**. (8.69) determines the characteristic oscillation behavior of the final correlation function, where again

$$|A_l^{R,L}(x,y,t)|^2 = \frac{1}{4\pi l}\left[A^2(2-2\cos(k_l(x-y-vt))) + B^2(2-2\cos(k_l(x-y+vt)))\right] \tag{8.72}$$
$$-\frac{1}{4\pi l}\left[2AB(\cos(2k_l x)+\cos(2k_l y)) - \cos(k_l(x+y-vt)) - \cos(k_l(x+y+vt))\right],$$

$$A = \frac{\alpha\alpha_{R,L}}{2} - \frac{\gamma_R}{\sqrt{2\pi K}},$$
$$B = \frac{\alpha\alpha_{L,R}}{2} + \frac{\gamma_L}{\sqrt{2\pi K}}. \tag{8.73}$$

The dependence on different linear combinations of spatio-temporal coordinates instead of $x-y\pm vt$ indicates the lack of translational invariance [66,67,176]. **Eq**. (8.73) denotes notational short-cuts that builds the exponents of different factors in the correlation function later on. These factors A, B consist of the scaling dimensions of the chiral fields shifted by the coupling to the high-energy impurity according to **Eq**. (8.28). The cut-off dependent pre-factor of the correlation function can be calculated from the following expression

$$\tilde{C}_{R,L}(x,y) = e^{\sum_{l=1}^{\infty}\frac{1}{4\pi l}\left[A^2+B^2-AB(\cos(2k_l x)+\cos(2k_l y))\right]}, \tag{8.74}$$

after an appropriate regularization. The remaining part of the correlation function can be written as

$$\langle e^{A_{R,L}(x,t)+B(y,0)_{R,L}+C(x,t)_{R,L}+D(y,0)_{R,L}}\rangle = \bar{C}^0_{R,L}(x-y,t)\tilde{C}_{R,L}(x,y) \tag{8.75}$$
$$e^{-\sum_{l=1}^{\infty}\frac{1}{4\pi l}\left[(A^2-B^2)\sin(k_l(x-y))\sin(k_l vt)+(A^2+B^2)\cos(k_l(x-y))\cos(k_l vt)-2AB\cos(k_l(x+y))\cos(k_l vt)\right]},$$

leading to the final form of the chiral correlation function before choosing an appropriate cut-off

$$\begin{aligned} G(x,y,t)^{\text{chiral},OBC}_{R,L} =& \tilde{C}^{R,L}(x,y,t)\bar{C}^0_{R,L}(x-y,t)\tilde{C}_{R,L}(x,y) \\ &* e^{-\sum_{l=1}^{\infty}\frac{1}{4\pi l}\left[(A^2-B^2)\sin(k_l(x-y))\sin(k_l vt)+(A^2+B^2)\cos(k_l(x-y))\cos(k_l vt)\right]} \\ &* e^{\sum_{l=1}^{\infty}\frac{1}{4\pi l}\left[2AB\cos(k_l(x+y))\cos(k_l vt)\right]}. \end{aligned} \tag{8.76}$$

8.5 Chiral Field Correlation Function for Periodic Boundaries

For periodic boundary conditions, the calculation of the chiral part of the impurity correlation function can be done analogously to the previous section, except that the

mode decomposition **Eq**. (8.146) has to be inserted of course. Furthermore, translational invariance allows us to consider only the relative coordinate $x \equiv x_1 - x_2$ instead of both individually,

$$G(x,t)^{\text{chiral},PBC}_{R,L} = \langle \hat{\tilde{\Psi}}^{\dagger}_{R,L}(x,t)\hat{\tilde{\Psi}}_{R,L}(0,0) * e^{\frac{-i}{\sqrt{2\pi K}}(\gamma_R\tilde{\phi}_R(x,t)-\gamma_L\tilde{\phi}_L(x,t))} e^{\frac{i}{\sqrt{2\pi K}}(\gamma_R\tilde{\phi}_R(0,0)-\gamma_L\tilde{\phi}_L(0,0))}\rangle. \tag{8.77}$$

This translational invariance leads also to a drastic reduction in the pre-factors that factorizes for the two chiralities

$$\tilde{C}^{R,L}(x,t) = e^{\left((\frac{\alpha\alpha_{R,L}}{2})^2+\frac{\gamma_R^2}{2\pi K}\right)f(x-vt)} e^{-\left((\frac{\alpha\alpha_{L,R}}{2})^2+\frac{\gamma_L^2}{2\pi K}\right)f(x+vt)}, \tag{8.78}$$

$$\bar{C}^0_{R,L}(x,t) = e^{i\left[A\langle\hat{Q}_R\rangle\frac{x-vt}{L}+B\langle\hat{Q}_L\rangle\frac{x+vt}{L}\right]}, \tag{8.79}$$

that now coexist, in contrast to the open chain. This perfect left/right separation is of course also manifest in the essential part of the correlation function, i.e.

$$G(x,t)^{\text{chiral},PBC}_{R,L} = \tilde{C}^{R,L}(x,t)\bar{C}^0_{R,L}(x,t) e^{-\left[\frac{(A)^2}{4\pi}+\frac{(B)^2}{4\pi}\right]\sum_{l=1}^{\infty}\frac{1}{l}} * e^{-\left[\frac{(A)^2}{2\pi}\sum_{l=1}^{\infty}\frac{(1-\cos(k_l(x-vt)))}{l}-\frac{(B)^2}{4\pi}\sum_{l=1}^{\infty}\frac{(1-\cos(k_l(x+vt)))}{l}\right]}, \tag{8.80}$$

whereas also **Eq**. (8.80) has to be explicitly regularized to obtain the divergence-free characteristic decay of the Luttinger liquid. The constants A, B, that build the decay exponents, are defined as before in **Eq**. (8.73) for open boundary conditions.

8.6 Regularization

One of the drawbacks of the bosonization approach is the presence of intrinsic infinities in any correlation function one wishes to calculate. Their occurrence can be viewed as an artifact of the linear dispersion that is unbounded in the momenta. Conversely it does not make sense to consider arbitrary large momenta for the excitations surrounding the Fermi-momenta, as can be already understood pictorially from the slope approximating an actual dispersion around k_F that diverges from it for too large momenta. In order to regularize the correlation function, we can assume a cut-off of the form $a(l) = e^{-\frac{b}{2}l}$ for the mode decompositions **Eq**. (8.143) and **Eq**. (8.146), where $b > 0$ to ensure convergence summing over all modes in series of the form of **Eq**. (8.81) and ensure boundedness from above for the mode Hamiltonian. Conversely, dimensional analysis reveals that b plays the role of a minimal length scale that limits the Luttinger liquid's spatial resolution. In the following we will calculate all cut-off dependent quantities for

both types of boundaries and explicitly regularize them, starting with the pre-factor for open boundaries in **Eq**. (8.74). The following identity is essential for the calculation of various correlation functions in bosonization

$$\sum_{l=1}^{\infty} \frac{q^l}{l} = -\ln(1-q), \tag{8.81}$$

valid provided that $|q| < 1$, which is clearly fulfilled with a suitably small cut-off b. So we obtain for **Eq**. (8.74)

$$\begin{aligned}
\tilde{C}_{R,L}(x,y) &= \left(e^{\ln(1-e^{-b})}\right)^{-\frac{(A^2+B^2)}{2\pi}} \left(e^{\ln(1-2e^{-b}\cos(\frac{2\pi}{L}x)+e^{-2b}+x\leftrightarrow y)}\right)^{\frac{(AB)}{4\pi}} \\
&= \left(1-e^{-b}\right)^{-\frac{(A^2+B^2)}{2\pi}} \left(1-2e^{-b}\cos(\frac{2\pi}{L}x)+e^{-2b}\right)^{\frac{(AB)}{4\pi}} \\
&\quad * \left(1-2e^{-b}\cos(\frac{2\pi}{L}y)+e^{-2b}\right)^{\frac{(AB)}{4\pi}} \\
&\approx (b)^{-\frac{(A^2+B^2)}{2\pi}} \left(4\sin(\frac{\pi}{L}x)^2\sin(\frac{\pi}{L}y)^2\right)^{\frac{(AB)}{4\pi}},
\end{aligned} \tag{8.82}$$

where in the last step we expanded to lowest order in the regularization b, which shows the characteristic infinity mentioned earlier and is consistent with the convergence of **Eq**. (8.81). In full analogy to open boundary conditions this pre-factor can be calculated for periodic ones

$$e^{-\left[\frac{(A)^2}{4\pi}+\frac{(B)^2}{4\pi}\right]\sum_{l=1}^{\infty}\frac{e^{-bl}}{l}} \approx (b)^{-\left[\frac{(A)^2}{4\pi}+\frac{(B)^2}{4\pi}\right]}, \tag{8.83}$$

which is exactly the same as in **Eq**. (8.82) except for the spatially dependent factors that are needed to cancel out the non-translational invariant part in **Eq**. (8.84) deep in the bulk. The essential part that predicts the spatio-temporal modulation of the density-density correlation can be calculated in the same manner. Thus we obtain the final form for open boundary conditions

$$\begin{aligned}
&G(x,y,t)^{\text{chiral},OBC}_{R,L} = \tilde{C}^{R,L}(x,y,t)\bar{C}^{0}_{R,L}(x-y,t)\,(b)^{-\frac{(A^2+B^2)}{4\pi}} \left(4\sin(\frac{\pi}{L}x)^2\sin(\frac{\pi}{L}y)^2\right)^{\frac{(AB)}{4\pi}} \\
&* \left(\frac{\sin(k_l(x-y-vt))^2}{\sin(k_l(x-y+vt))^2}\right)^{\frac{A^2-B^2}{8\pi}} \left(4\sin(k_l(x+y+vt))^2\sin(k_l(x+y-vt))^2\right)^{-\frac{AB}{4\pi}} \\
&* \left(4\sin(k_l(x-y-vt))^2\sin(k_l(x-y+vt))^2\right)^{\frac{A^2+B^2}{8\pi}},
\end{aligned} \tag{8.84}$$

that has to be multiplied with its corresponding mobile impurity correlator **Eq**. (8.49) to build the wanted composite correlator. For periodic boundary conditions the functional

form of the correlation is given by the much simpler expression

$$G(x,t)^{\text{chiral},PBC}_{R,L} = \bar{C}^{0}_{R,L}(x,t)\tilde{C}^{R,L}(x,t)\,(b)^{\frac{1}{4\pi}\left[(A)^2+(B)^2\right]} \left(\frac{1}{2\sin(k_l(x-vt))^2}\right)^{\frac{1}{4\pi}(A)^2} \left(\frac{1}{2\sin(k_l(x+vt))^2}\right)^{\frac{1}{4\pi}(B)^2}, \tag{8.85}$$

due to translational invariance.

8.7 Bulk and Boundary Limits of Chiral Correlators

As mentioned already in the introduction, we are especially interested in boundary critical phenomena [64], that determine the paradigmatic decay of the longitudinal spin-spin correlation function in the vicinity of a boundary [66, 176]. Additionally, one can check the validity of the finite size calculations by the consistence of the bulk limit of the open boundary correlator in **Eq**. (8.84) with the periodic system in **Eq**. (8.85). This manifests that correlators far away from boundaries are asymptotically equal to cyclic systems, if the system size L is so large that the quantization due to the boundaries can be safely neglected. Furthermore, as the bulk behavior is also identified with the spatio-temporal decay of an infinite system, due to the effective loss of momentum quantization, the role of the mobile impurity in describing the singularity exponent of the dynamical structure factor is shortly revisited. These singularity exponents are furthermore related to the algebraic decay of the correlation function near the boundary or bulk.

The characteristic behavior of correlation functions far away from the boundaries can be obtained by considering the following inequality for the spatially separated points x, y [66, 176]

$$xy \gg (x-y)^2 - (vt)^2. \tag{8.86}$$

The sinusoidal dependences on the spatial points have to be eliminated before, by considering the limit $L \to \infty$ and performing the respective Taylor expansion to lowest order. Additionally we have neglected here any oscillating pre-factors in **Eq**. (8.66) as

they do not modify the algebraic decay in absolute value. So we obtain

$$
\begin{aligned}
G(x,y,t)^{\text{chiral,bulk}}_{R,L} &\approx \left(4\sin(\frac{\pi}{L}x)^2\sin(\frac{\pi}{L}y)^2\right)^{\frac{(AB)}{4\pi}} \qquad (8.87)\\
&* \left(\frac{\sin(k_l(x-y-vt))^2}{\sin(k_l(x-y+vt))^2}\right)^{\frac{A^2-B^2}{8\pi}} \left(4\sin(k_l(x+y+vt))^2\sin(k_l(x+y-vt))^2\right)^{-\frac{AB}{4\pi}}\\
&* \left(4\sin(k_l(x-y-vt))^2\sin(k_l(x-y+vt))^2\right)^{\frac{A^2+B^2}{8\pi}}\\
&\approx (xy)^{\frac{AB}{2\pi}}\left(\frac{x-y-vt}{x-y+vt}\right)^{\frac{A^2-B^2}{4\pi}} (x+y+vt)^{-\frac{AB}{2\pi}}\,(x+y-vt)^{-\frac{AB}{2\pi}}\\
&* \qquad (x-y-vt)^{\frac{A^2+B^2}{4\pi}}\,(x-y+vt)^{\frac{A^2+B^2}{4\pi}}\\
&\approx (x-y-vt)^{-\frac{A^2}{2\pi}}\,(x-y+vt)^{-\frac{B^2}{2\pi}}\,.
\end{aligned}
$$

Eq. (8.87) obeys the same characteristic decay as for periodic boundary conditions and sufficiently large system sizes. This has the rather trivial interpretation that far away from the boundary there is no dependence on it left, as supposed for volume-dependent phenomena. The boundary limit on the other hand can only be applied to finite systems with open boundaries **Eq**. (8.84), as the periodic system is of course finite but does not possess a boundary as every point in the system could be labeled as such.

In order to reconnect to the dynamical structure factor and especially its lower threshold singularity as in **Eq**. (8.22) we use the bulk limit of **Eq**. (8.87), corresponding to the infinitely large L, and convolve it with the impurity correlator for an infinite system in **Eq**. (8.54). Re-introducing additionally the previously neglected energy off-set ϵ of the mobile impurity, one can show that

$$
\begin{aligned}
S^{zz}(q,\epsilon) &\propto \int_{-\infty}^{\infty} e^{i(\omega-\epsilon)t}\left((u-v)t+i\eta\right)^{-\frac{A^2}{2\pi}}\left((u+v)t-i\eta\right)^{-\frac{B^2}{2\pi}}dt \qquad (8.88)\\
&\propto \int_{-\infty}^{\infty}\left(\frac{e^{i(\omega-\epsilon)t}}{t-i\eta}\right)^{1-\frac{1}{2\pi}(A^2+B^2)}\\
&\propto \underbrace{\Theta(\omega-\epsilon)/(\omega-\epsilon)^{\frac{1}{2\pi}(A^2+B^2)}}_{\frac{1}{2\pi}(A^2+B^2)<1},
\end{aligned}
$$

where an additional short-distance cut-off η is used and the off-set is understood to be dependent on the momentum q, i.e. $\epsilon \equiv \epsilon(q)$. **Eq**. (8.88) shows now that we can address exactly the point of singularity of the dynamical structure factor in **Eq**. (8.22), as well as its exponents, by engineering the properties of the mobile impurity. Here the point of divergence is given by the energy off-set of the impurity $\epsilon(q)$, whereas its exponent is

related to the coupling of the impurity to the chiral fields according to **Eq**. (8.28), i.e.

$$\frac{1}{2\pi}(A^2+B^2) = 1 - \frac{1}{4}\left[\sqrt{K} + \frac{1}{\sqrt{K}}\left(1-\gamma_R/\pi\right)^2\right] - \frac{1}{4}\left[\sqrt{K} - \frac{1}{\sqrt{K}}\left(1-\gamma_L/\pi\right)^2\right]. \tag{8.89}$$

The boundary limit on the other hand can be calculated by employing the following inequality

$$vt \gg x, y \tag{8.90}$$

and considering the spatially separated points so close to each other that we can approximate $x - y \approx 0$. Then we obtain finally for sufficiently large system sizes L from **Eq**. (8.84),

$$\begin{aligned} G(x,y,t)^{\text{chiral,boundray}}_{R,L} &\approx (xy)^{\frac{AB}{2\pi}} \left(\frac{x-y-vt}{x-y+vt}\right)^{\frac{A^2-B^2}{4\pi}} (x+y+vt)^{-\frac{AB}{2\pi}} (x+y-vt)^{-\frac{AB}{2\pi}} \\ &* (x-y-vt)^{\frac{A^2+B^2}{4\pi}} (x-y+vt)^{\frac{A^2+B^2}{4\pi}} \\ &= (xy)^{\frac{AB}{2\pi}} (vt)^{-\frac{A^2+B^2-2AB}{2\pi}}. \end{aligned} \tag{8.91}$$

Finally **Eqs**. (8.87) and (8.91) have to be combined with the respective limiting values of the correlation function of the mobile impurity. So we obtain the following limits of the longitudinal spin-spin correlation functions in non-linear bosonization for the bulk

$$\begin{aligned} G(x,y,t)^{imp,Bulk}_{R,L} &= \langle \hat{\tilde{d}}(x,t)\hat{\tilde{d}}^\dagger(y,0)\rangle^{\text{Bulk}}_{\epsilon} A(x,y,t)^{\text{chiral,bulk}}_{R,L} \\ &\approx t^{-1/2}\,(x-y-vt)^{-\frac{A^2}{2\pi}} (x-y+vt)^{-\frac{B^2}{2\pi}}, \end{aligned} \tag{8.92}$$

and the boundary respectively

$$\begin{aligned} G(x,y,t)^{imp,Boundary}_{R,L} &= \langle \hat{\tilde{d}}(x,t)\hat{\tilde{d}}^\dagger(y,0)\rangle^{\text{Boundary}}_{\epsilon} A(x,y,t)^{\text{chiral,Boundary}}_{R,L} \\ &\approx t^{-\frac{3}{2}} (xy)^{\frac{AB}{2\pi}+1} (vt)^{-\frac{A^2+B^2-2AB}{2\pi}}. \end{aligned} \tag{8.93}$$

In **Eq**. (8.92) and **Eq**. (8.93) we have again neglected the oscillatory factors incorporating the energy of the deep hole below the Fermi level [253, 255] and representing the energy at which the dynamical structure factor diverges in **Eq**. (8.88), as they do not contribute functionally to the algebraic decay. As explained before, the same expression for the bulk limit in **Eq**. (8.92) could be obtained starting immediately with periodic boundary conditions, where the only difference would reside in the different spatially dependent phase factors in **Eq**. (8.66), that do not alter the absolute value anyway. From **Eq**. (8.92) and **Eq**. (8.93) we can reconnect to the auto-correlation results of **Ref**. [255], by setting the relative coordinate $x - y$ to zero in the bulk and considering $x = a = y$ for

the boundary case, yielding

$$G(x,x,t)_{R,L}^{imp,Bulk} \propto \; t^{-1/2-\frac{A^2+B^2}{2\pi}} \equiv t^{-\alpha_{Bulk}} \tag{8.94}$$
$$G(a,a,t)_{R,L}^{imp,Boundary} \propto t^{-\frac{3}{2}-\frac{A^2+B^2-2AB}{2\pi}} = t^{-\alpha_{Bulk}} t^{-1+\frac{AB}{\pi}}.$$

In the limit of **Eq**. (8.94), the anomalous, and intrinsically different, diffusion behavior in the bulk or near the boundaries is manifest. Thereby the already anomalous diffusion of the impurity correlators is further amplified by the coupling to the chiral fields expressed via the shifted scaling dimensions A, B in **Eq**. (8.73).

Here, especially **Eq**. (8.92) and **Eq**. (8.93) represent crucial results of the current chapter, by describing the universal decay inside the two fundamental spatial regimes of the longitudinal spin correlation function for the open XXZ spin 1/2 chain. The novum with respect to the results of **Ref**. [255], concerning the auto-correlation limit near the boundary, consists especially in the inclusion of spatial dependencies in **Eq**. (8.93). Nevertheless, as it was argued already in **Ref**. [255], the local correlation limit in **Eq**. (8.94) shows a clearer bulk/ boundary contrast than the spatially dependent correlators.

Furthermore explicit estimates on the achievability of the boundary limits, depending on the impurity velocity, i.e. $u < \mathcal{O}(L^{-2})$, and time scales, i.e. $\mathcal{O}(L^3) \leq t < \mathcal{O}(u^{-2})$, have been derived in a previous section by demanding consistency requirements at both boundaries. Finally, the functional forms of the decay coefficients in **Eq**. (8.92) and **Eq**. (8.93) originating from a field-theoretical treatment are only reliable in the weak-coupling limit, but the Luttinger parameter K and the coupling $\gamma_{R,L}$ can be computed by the corresponding Bethe ansatz equation. The anomalous diffusion coefficients in the bulk or near the boundary could then be investigated exactly, depending on the applied magnetic field.

8.8 Generalized Jacobi-Anger Expansion

The dynamical structure factor can be alternatively represented in the Lehmann decomposition [256], an equivalent representation of correlation functions known from quantum field theory. In our case this essentially corresponds to a Fourier series decomposition of correlation functions according to the periodicity of their momentum quantization, $k_l^{OBC} = \frac{\pi l}{L}$ or $k_l^{PBC} = \frac{2\pi l}{L}$ respectively. In the ordinary bosonization approach to the XXZ model, the Lehmann representation of correlation functions allows for a recursive evaluation of the dynamical structure factor in **Eq**. (8.19), as well as other selected quantities, in closed analytic form [67, 258]. In the following, a similar decomposition is pursued for the chiral part of the finite size correlation functions in **Eqs**. (8.76) and (8.80). Thereby we obtain the exact Fourier coefficients of the correlation function in terms of products of infinite-variable Bessel functions [257], for

each occurring combination of spatio-temporal coordinates, that each can be expressed via an integral relation. Consequently, the subsequent Fourier transformation to the dynamical structure factor becomes trivial. In lowest order in the cut-off b we find that these integral equations can be expressed in closed form, which might pave the way for further analytical treatment of the asymptotics of the dynamical structure factor later on. In the same spirit we find that the signum functions, contained in the pre-factors of correlation functions and indicating phase shifts for different space-time regions can be related to certain Hilbert transforms acting on functions in those regions [280] . Furthermore the procedure is not related to the details of the correlation function used in this chapter and is thus universally applicable to arbitrary correlation functions in bosonization and allows for closed form expressions of energy- and momentum-resolved observables. Even if this section is rather inconclusive at the end, due to its unfinished status, it nevertheless paves the way for the semi-analytical evaluation and further analytical treatment of the finite-size dynamical structure factor in non-linear /ordinary bosonization.

8.8.1 Infinite-variable Bessel function

In order to prepare the derivation of the series representation of the correlation functions, two kinds of infinite-variable Bessel functions are introduced [257]. The first function $J_n([\beta_l]_{l=1}^{\infty})$ denotes a generalized Jacobi-Anger function, defined like

$$J_n([\beta_m]_{m=1}^{\infty}) = \frac{1}{\pi}\int_0^{\pi} \cos\left(n\theta - \sum_{m=1}^{\infty}\beta_m \sin(m\theta)\right)d\theta, \tag{8.95}$$

together with the infinite set of variables β_m, corresponding to the summation over the modes in the respective vertex operators. The following Jacobi-Anger representation is then essential for the derivation of the Lehmann representation

$$e^{\sum_{l=1}^{\infty}\beta_l \sin(l\tau)} = \sum_{n=-\infty}^{\infty} e^{in\tau} J_n([\beta_l]_{l=1}^{\infty}), \tag{8.96}$$

that can be understood in analogy to a Fourier decomposition of the periodic function $e^{\sum_{l=1}^{\infty}\beta_l \sin(l\tau)}$. The functions $J_n([\beta_m]_{m=1}^{\infty})$ enjoy the following two recurrence relation, i.e.

$$\begin{aligned} nJ_n([\beta_m]_{m=1}^{\infty}) &= \frac{1}{2}\sum_{m=1}^{\infty} m\beta_m \left[J_{n-m}([\beta_m]_{m=1}^{\infty}) + (J_{n+m}([\beta_m]_{m=1}^{\infty})\right], \\ \partial_{\alpha_m} J_n([\beta_m]_{m=1}^{\infty}) &= 1/2\left[J_{n-m}([\beta_m]_{m=1}^{\infty}) - J_{n+m}([\beta_m]_{m=1}^{\infty})\right], \end{aligned} \tag{8.97}$$

that allows to express a given mode $J_n([\beta_m]_{m=1}^{\infty})$ by all those above and below. Additionally the function also obeys the reflection property [257]

$$J_n([\beta_m]_{m=1}^{\infty}) = J_n([-\beta_m]_{m=1}^{\infty}), \tag{8.98}$$

as well as a sum rule, i.e.

$$\sum_{n\in\mathbb{Z}} \left[J_n([\beta_m]_{m=1}^{\infty})\right]^2 = 1, \tag{8.99}$$

and an addition formula

$$J_n([\beta_{1,m}+\beta_{2,m}]_{m=1}^{\infty}) = \sum_{k\in\mathbb{Z}} J_{n-k}([\beta_{1,m}]_{m=1}^{\infty}) J_k([\beta_{2,m}]_{m=1}^{\infty}). \tag{8.100}$$

The second function $I_n([\beta_l]_{l=1}^{\infty})$ denotes a generalization of the modified Bessel functions which are defined in close analogy to **Eq**. (8.95) as

$$I_n([\beta_m]_{m=1}^{\infty}) = \frac{1}{\pi}\int_0^{\pi} \cos\left(n\theta - \sum_{m=1}^{\infty}\beta_m \cos(m\theta)\right) d\theta, \tag{8.101}$$

together with their Fourier like decomposition

$$e^{\sum_{l=1}^{\infty}\beta_l\cos(l\tau)} = \sum_{n=-\infty}^{\infty} e^{in\tau} I_n([\beta_l]_{l=1}^{\infty}). \tag{8.102}$$

In comparison to **Eq**. (8.103), the signs in the recurrence relation is interchanged, i.e.

$$\begin{aligned} nI_n([\beta_m]_{m=1}^{\infty}) &= \frac{1}{2}\sum_{m=1}^{\infty} m\beta_m \left[I_{n-m}([\beta_m]_{m=1}^{\infty}) - (I_{n+m}([\beta_m]_{m=1}^{\infty})\right], \\ \partial_{\alpha_m} I_n([\beta_m]_{m=1}^{\infty}) &= 1/2\left[I_{n-m}([\beta_m]_{m=1}^{\infty}) + I_{n+m}([\beta_m]_{m=1}^{\infty})\right]. \end{aligned} \tag{8.103}$$

Also the reflection property is different, whereas the addition formula remains the same

$$\begin{aligned} I_n([\beta_m]_{m=1}^{\infty}) &= I_{-n}([\beta_m]_{m=1}^{\infty}), \\ I_n([\beta_{1,m}+\beta_{2,m}]_{m=1}^{\infty}) &= \sum_{k\in\mathbb{Z}} I_{n-k}([\beta_{1,m}]_{m=1}^{\infty}) I_k([\beta_{1,m}]_{m=1}^{\infty}). \end{aligned} \tag{8.104}$$

At this point it should be mentioned that for the prerequisite of the convergence of $\sum_{m=1}^{\infty} m|\beta_m|$, such that the special functions are well defined, a suitable cut-off for the mode decomposition should be used as usual. The identities in **Eqs**. (8.97) and (8.103) pave the way to deduce similar recurrence relations as have been found for the

dynamical structure factor in the usual bosonization [67, 258]. Anyhow the success of the former approaches pursued in **Refs**. [67, 258] relies on the circumstance that a given excitation level in the Lehmann representation can be solely expressed in terms of lower level excitations. In contrast to that, **Eqs**. (8.97) and (8.103) involve all lower as well as higher orders of excitations and thus a computational profit is probably not guaranteed. Nevertheless, the function identities presented here might be useful to conduct similar procedures in future investigations, or at least simplify the final correlation function in non-linear bosonization. Despite these problems, the use of such generalized Fourier decompositions of correlations functions have the huge advantage that they allow for trivial transformations to Fourier space using their fundamental periodicity, and are thus predestined to study the dynamical structure factor.

8.8.2 Correlation Function for arbitrary Cut-off

If we keep the necessity of the regularization procedure in mind, the chiral correlation function for both types of boundary conditions in **Eq**. (8.84) and **Eq**. (8.85) can then be re-written with the help of the generalized Jacobi-Anger decomposition in **Eq**. (8.102),

$$
\begin{aligned}
&G(x,y,t)^{\text{chiral,OBC}}_{R,L} = \tilde{C}^{R,L}(x,y,t)\bar{C}^{0}_{R,L}(x-y,t)\tilde{C}_{R,L}(x,y) \qquad (8.105)\\
&*\prod_{i=1}^{4}\sum_{n_i\in\mathbb{Z}}\Bigg[e^{i\frac{\pi n_1(x-y-vt)}{L}}e^{i\frac{\pi n_2(x-y+vt)}{L}}e^{i\frac{\pi n_3(x+y-vt)}{L}}e^{i\frac{\pi n_4(x+y+vt)}{L}}I_{n_1}\Big(\Big[\frac{A^2}{4\pi l}\Big]_{l=1}^{\infty}\Big)I_{n_2}\Big(\Big[\frac{B^2}{4\pi l}\Big]_{l=1}^{\infty}\Big)\\
&*I_{n_3}\Big(\Big[\frac{-2AB}{4\pi l}\Big]_{l=1}^{\infty}\Big)I_{n_4}\Big(\Big[\frac{-2AB}{4\pi l}\Big]_{l=1}^{\infty}\Big)\Bigg],
\end{aligned}
$$

$$
\begin{aligned}
&G(x,t)^{\text{chiral,PBC}}_{R,L} = \tilde{C}^{R,L}(x,t)\bar{C}^{0}_{R,L}(x,t) \qquad (8.106)\\
&\prod_{i=1}^{2}\sum_{n_i\in\mathbb{Z}}\Bigg[e^{i\frac{2\pi n_1(x-y-vt)}{L}}e^{i\frac{2\pi n_2(x-y+vt)}{L}}I_{n_1}\Big(\Big[\frac{A^2}{4\pi l}\Big]_{l=1}^{\infty}\Big)I_{n_2}\Big(\Big[\frac{B^2}{4\pi l}\Big]_{l=1}^{\infty}\Big)\Bigg].
\end{aligned}
$$

The non zero-mode pre-factors $\tilde{C}^{R,L}(x,y,t)$ and $\tilde{C}^{R,L}(x,t)$ decompose exactly into exponentials containing each combination of spatio-temporal coordinates, as well as the exponentials containing the sum of sinusoidals, corresponding to the respective signum functions later on. These signum functions hinder the calculation of the dynamical structure factor in closed form, which can be circumvented by expressing them partially in Jacobi-Anger form via **Eq**. (8.96), e.g.

$$
\begin{aligned}
e^{\alpha f(x+y+vt)} =& e^{\alpha\frac{i}{2}\left[\frac{x+y+vt}{4L}+\frac{1}{2\pi}\sum_{l=1}^{\infty}\frac{1}{l}\sin(k_l[x+y+vt])\right]} \qquad (8.107)\\
=& e^{i\alpha\frac{x+y+vt}{8L}}\sum_{n\in\mathbb{Z}}e^{\frac{in\pi}{L}(x+y+vt)}J_n\Big(\big[\frac{\alpha}{4\pi l}\big]_{l=1}^{\infty}\Big).
\end{aligned}
$$

So we find a full series representation for the correlators including all pre-factors and without specifying a cut-off yet. For open boundary conditions we obtain the rather lengthy formula,

$$
\begin{aligned}
G(x,y,t)^{\text{chiral,OBC}}_{R,L} &= \underbrace{\bar{C}^0_{R,L}(x-y,t)}_{\text{zero-mode}}\underbrace{e^{\sum_{l=1}^{\infty}\frac{e^{-bl}}{4\pi l}\left[A^2+B^2\right]}}_{\text{cut-off}} \\
&* \underbrace{e^{(\frac{i\beta_1}{8L}+\alpha_1)(x-y-vt)}e^{(\frac{i\beta_2}{8L}+\alpha_2)(x-y+vt)}e^{(\frac{i\beta_3}{8L}+\alpha_3)(x+y+vt)}e^{(\frac{i\beta_4}{8L}+\alpha_4)(x+y-vt)}e^{\frac{i\beta_5}{8L}(2x)}e^{\frac{i\beta_5}{8L}(2y)}}_{L-\text{dependent gauge-phases}} \\
&* \prod_{i=1}^{4}\sum_{n_i\in\mathbb{Z}}\sum_{\tilde{n}_i\in\mathbb{Z}}\Bigg[\underbrace{e^{i\frac{\pi(n_1+\tilde{n}_1)(x-y-vt)}{L}}e^{i\frac{\pi(n_2+\tilde{n}_2)(x-y+vt)}{L}}e^{i\frac{\pi(n_3+\tilde{n}_3)(x+y-vt)}{L}}e^{i\frac{\pi(n_4+\tilde{n}_4)(x+y+vt)}{L}}}_{\text{Fourier harmonics of }(x,y,vt)-\text{combinations}} \\
&* \prod_{i=4}^{6}\sum_{n_i\in\mathbb{Z}}\sum_{\tilde{n}_i\in\mathbb{Z}}\Bigg[\underbrace{e^{i\frac{\pi(n_4+\tilde{n}_4)(x+y+vt)}{L}}e^{i\frac{\pi(n_5+\tilde{n}_5)(2x)}{L}}e^{i\frac{\pi(n_6+\tilde{n}_6)(2y)}{L}}}_{\text{Fourier harmonics of }(x,y,vt)-\text{combinations}} \\
&* \underbrace{I_{n_1}\Big(\Big[\frac{A^2}{4\pi l}\Big]_{l=1}^{\infty}\Big)I_{n_2}\Big(\Big[\frac{B^2}{4\pi l}\Big]_{l=1}^{\infty}\Big)I_{n_3}\Big(\Big[\frac{-2AB}{4\pi l}\Big]_{l=1}^{\infty}\Big)}_{\textit{decay}\text{ exponents of }(x,y,vt)-\text{combinations}} \\
&* \underbrace{I_{n_4}\Big(\Big[\frac{-2AB}{4\pi l}\Big]_{l=1}^{\infty}\Big))I_{n_5}\Big(\Big[\frac{2AB}{4\pi l}\Big]_{l=1}^{\infty}\Big)I_{n_6}\Big(\Big[\frac{2AB}{4\pi l}\Big]_{l=1}^{\infty}\Big)}_{\textit{decay}\text{ exponents of }(x,y,vt)-\text{combinations}} \\
&* \underbrace{J_{\tilde{n}_1}\Big(\Big[\frac{\beta_1}{4\pi l}\Big]_{l=1}^{\infty}\Big)J_{\tilde{n}_2}\Big(\Big[\frac{\beta_2}{4\pi l}\Big]_{l=1}^{\infty}\Big)J_{\tilde{n}_3}\Big(\Big[\frac{\beta_3}{4\pi l}\Big]_{l=1}^{\infty}\Big)}_{\text{Signum functions of }(x,y,vt)-\text{combinations}} \\
&* \underbrace{J_{\tilde{n}_4}\Big(\Big[\frac{\beta_4}{4\pi l}\Big]_{l=1}^{\infty}\Big)J_{\tilde{n}_5}\Big(\Big[\frac{\beta_5}{4\pi l}\Big]_{l=1}^{\infty}\Big)J_{\tilde{n}_6}\Big(\Big[\frac{\beta_6}{4\pi l}\Big]_{l=1}^{\infty}\Big)}_{\text{Signum functions of }(x,y,vt)-\text{combinations}}\Bigg]\Bigg]
\end{aligned}
\tag{8.108}
$$

where a list of the occurring constants is given in **Eq**. (8.110) at the end of the chapter. The representation in **Eq**. (8.108) can be Fourier transformed straight-forwardly, in contrast to the equivalent formulation leading to the algebraic decay for very large system sizes, but contains 12 sums representing the 6 linear combination of spatio-temporal coordinates together with their corresponding signum function. For the case of periodic boundary conditions we obtain analogously a much simpler expression due to translational invariance, i.e.

$$
\begin{aligned}
G(x,t)^{\text{chiral,PBC}}_{R,L} &= \bar{C}^0_{R,L}(x,t)e^{\sum_{l=1}^{\infty}\frac{e^{-bl}}{4\pi l}\left[A^2+B^2\right]}e^{(\frac{i\tilde{\beta}_1}{8L}+\tilde{\alpha}_1)(x-y-vt)}e^{(\frac{i\tilde{\beta}_2}{8L}+\tilde{\alpha}_2)(x-y+vt)} \\
&* \prod_{i=1}^{2}\sum_{n_i\in\mathbb{Z}}\sum_{\tilde{n}_i\in\mathbb{Z}}\left[e^{i\frac{2\pi(n_1+\tilde{n}_1)(x-y-vt)}{L}}e^{i\frac{2\pi(n_2+\tilde{n}_2)(x-y+vt)}{L}}I_{n_1}\Big(\Big[\frac{A^2}{4\pi l}\Big]_{l=1}^{\infty}\Big)J_{\tilde{n}_1}\Big(\Big[\frac{\tilde{\beta}_1}{4\pi l}\Big]_{l=1}^{\infty}\Big)\right] \\
&* \left[I_{n_2}\Big(\Big[\frac{B^2}{4\pi l}\Big]_{l=1}^{\infty}\Big)J_{\tilde{n}_2}\Big(\Big[\frac{\tilde{\beta}_2}{4\pi l}\Big]_{l=1}^{\infty}\Big)\right],
\end{aligned}
\tag{8.109}
$$

with the same interpretation of the individual contributions as before. So we have finally decomposed the full correlation function according to the generalized Jacobi-Anger decomposition including all pre-factors, except the zero-modes that are already in exponential form and thus do not need to be processed further. A list of the appearing constants for the open boundary case in **Eq**. (8.117) is shown below,

$$\begin{aligned}
\alpha_1 &= \left[\frac{\alpha}{2\sqrt{2\pi K}}\left[\alpha_{L,R}\gamma_R\right] + \frac{\alpha^2}{4}\alpha_{L,R}\alpha_{R,L} + \frac{\gamma_R\gamma_L}{2\pi K}\right]\left[\hat{Q},\hat{\phi}_0\right]/(8L),\\
\beta_1 &= (\frac{\alpha^2}{4}\alpha_{R,L}^2 + \frac{\gamma_R^2}{2\pi K})/2,\\
\alpha_2 &= \left[-\frac{\alpha}{2\sqrt{2\pi K}}\left[\alpha_{L,R}\gamma_L\right] + \frac{\alpha^2}{4}\alpha_{L,R}^2 - \frac{\gamma_L^2}{2\pi K}\right]\left[\hat{Q},\hat{\phi}_0\right]/(8L),\\
\beta_2 &= -(\frac{\alpha^2}{4}\alpha_{L,R}^2 + \frac{\gamma_L^2}{2\pi K})/2,\\
\alpha_3 &= 0,\\
\beta_3 &= (\frac{\alpha^2}{4}\alpha_{R,L}\alpha_{L,R} - \frac{\alpha(\alpha_{L,R}\gamma_R + \alpha_{R,L}\gamma_L)}{2\sqrt{2\pi K}} - \frac{\gamma_R\gamma_L}{2\pi K})/2,\\
\alpha_4 &= -\frac{\alpha}{2\sqrt{2\pi K}}\left[(\alpha_{R,L}\gamma_L + \alpha_{L,R}\gamma_R) - \gamma_L(\alpha_{R,L} - \alpha_{L,R})\right]\left[\hat{Q},\hat{\phi}_0\right]/(8L),\\
\beta_4 &= -(\frac{\alpha^2}{4}\alpha_{R,L}\alpha_{L,R} + \frac{\alpha(\alpha_{L,R}\gamma_R + \alpha_{R,L}\gamma_L)}{2\sqrt{2\pi K}} - \frac{\gamma_R\gamma_L}{2\pi K})/2,\\
\beta_5 &= \frac{\alpha}{2\sqrt{2\pi K}}(\alpha_{R,L}\gamma_L + \alpha_{L,R}\gamma_R)/2\\
\beta_6 &= \frac{\alpha}{2\sqrt{2\pi K}}(\alpha_{R,L}\gamma_L + \alpha_{L,R}\gamma_R)/2,
\end{aligned} \tag{8.110}$$

whereas both α_i, β_i represent L-dependent constants. For the case of periodic boundary conditions in **Eq**. (8.109), the constants of the gauge phases are given by

$$\begin{aligned}
\tilde{\alpha}_1 &= 0,\\
\tilde{\beta}_1 &= \beta_1,\\
\tilde{\alpha}_2 &= 0,\\
\tilde{\beta}_2 &= \beta_2.
\end{aligned} \tag{8.111}$$

8.8.3 Correlation Function Asymptotics for a vanishing Cut-off

Interestingly, the pre-factors of the Jacobi-Anger expanded correlation function **Eq**. (8.105) and **Eq**. (8.106) can be obtained analytically according to **Eq**. (8.101), if the

lowest order in the cut-off b is considered, i.e.

$$
\begin{aligned}
I_n([\alpha_n]_{m=1}^{\infty}) &= \frac{1}{\pi}\int_0^{\pi}\cos\left(n\theta-\alpha_n\sum_{m=1}^{\infty}e^{-bm}\cos(m\theta)/m\right)d\theta \qquad (8.112)\\
&\overbrace{=}^{b\ll 1}\frac{e^{-\alpha_n/8}}{2}\Big[-\frac{i\beta[-1,n-\frac{i\alpha_n}{8\pi},1+\frac{i\alpha_n}{4\pi}]}{\pi}\\
&+e^{\alpha_n/4}\Big(-\frac{i\beta[-1,-n+\frac{i\alpha_n}{8\pi},1-\frac{i\alpha_n}{4\pi}]}{\pi}+\frac{\mathrm{csch}(\alpha_{\mathrm{n}}/4)\Gamma[-n+\frac{i\alpha_n}{8\pi}]}{\Gamma[\frac{i\alpha_n}{4\pi}]\Gamma[1-n-\frac{i\alpha_n}{8\pi}]}\Big]\\
&+e^{\alpha_n/4}\Big(+\frac{2\Gamma[n-\frac{i\alpha_n}{8\pi}]}{(-1+e^{\alpha_n/2})\Gamma[-\frac{i\alpha_n}{4\pi}]\Gamma[1+n+\frac{i\alpha_n}{8\pi}]}\Big)\Big]\\
&\equiv I_n([\alpha_n]).
\end{aligned}
$$

In **Eq**. (8.112) $\beta[a,b,c]$ and $\Gamma[x]$ denote the incomplete Beta function and the ordinary Gamma function respectively, that do not depend on any spatio-temporal coordinate and so the chiral correlation function can be easily Fourier transformed later on.

Analogously to **Eq**. (8.112), the Jacobi-Anger coefficient $J_n\Big([\frac{\alpha}{4\pi l}]_{l=1}^{\infty}\Big)$ can also be integrated analytically for a vanishing cut-off, i.e.

$$
\begin{aligned}
J_n([\alpha_n]_{m=1}^{\infty}) &= \frac{1}{\pi}\int_0^{\pi}\sin\left(n\theta-\alpha_n\sum_{m=1}^{\infty}\sin(m\theta)/m\right)d\theta \qquad (8.113)\\
&\overbrace{=}^{b\ll 1}\frac{8\sin(\alpha_n/8)}{8\pi n+\alpha}\equiv J_n(\alpha_n),
\end{aligned}
$$

that we can furthermore use to simplify the final correlation function drastically, as it is exemplarily shown in the following

$$
\begin{aligned}
&e^{\alpha f(x+y+vt)}\sum_{n_x}I_{n_x}e^{\frac{in_x\pi}{L}(x+y+vt)}\overbrace{=}^{b\ll 1}e^{\alpha\frac{i}{2}[\frac{x+y+vt}{4L}]}\sum_{n_x}\sum_{n_y}I_{n_x}\frac{8\sin(\alpha/8)}{8\pi n_y+\alpha}e^{\frac{i(n_x+n_y)\pi}{L}(x+y+vt)} \qquad (8.114)\\
&=2\sin(\alpha/8)e^{\alpha\frac{i}{2}[\frac{x+y+vt}{4L}]}\sum_{n_+}\sum_{n_-}I_{\frac{n_++n_-}{2}}\frac{1}{\pi}\frac{1}{n_-+n_++\frac{\alpha}{\pi}}e^{\frac{i(n_+)\pi}{L}(x+y+vt)}\\
&*\overbrace{\propto}^{\sum_{n_-}\to\int_{-\infty}^{\infty}dn_-}2\sin(\alpha/8)e^{\alpha\frac{i}{2}[\frac{x+y+vt}{4L}]}\sum_{n_+}e^{\frac{i(n_+)\pi}{L}(x+y+vt)}\int dn_-I_{\frac{n_+-n_-}{2}}\frac{1}{\pi}\frac{1}{n_-+n_++\frac{\alpha}{\pi}}\\
&*\overbrace{\propto}^{\int_{-\infty}^{\infty}dn_-\equiv\mathrm{p.v.}\int_{-\infty}^{\infty}dn_-}2\sin(\alpha/8)e^{\alpha\frac{i}{2}[\frac{x+y+vt}{4L}]}\sum_{n_+}e^{\frac{i(n_+)\pi}{L}(x+y+vt)}\hat{H}\left[I_{\frac{n_+-n_-}{2}}\right]\Big(n_++\frac{\alpha}{\pi}\Big).
\end{aligned}
$$

In **Eq**. (8.114) we have approximated one of the sums over the integers by a continuous integration, such that we obtain the defining relation of the Hilbert transform [280], i.e.

$$\hat{H}[f](t) = \frac{1}{\pi}\text{p.v.}\int_{-\infty}^{\infty} f(\tau)/(t-\tau)d\tau, \tag{8.115}$$

where we neglect potential issues arising for the principal value and existence of the Hilbert transform. The constant in **Eq**. (8.114) arises through the integral measure that approximates the n_- sum and only corresponds to a global re-scaling that can be fixed by comparison to numerical methods. If we assume the validity of the approximation in **Eq**. (8.114), the pre-factors of the correlation function can be reduced to exponential functions of the spatio-temporal arguments, that finally makes the Fourier transformation for the longitudinal structure factor feasible in closed form without further approximations. Hence, in the following, each part of the correlation function is collected according to its spatio-temporal argument and is united with the factors of $\tilde{C}^{R,L}(x,y,t)$ and $\tilde{C}^{R,L}(x,t)$ respectively. We obtain exemplary for the spatio-temoral combination $x-y-vt$ in open boundary conditions

$$\begin{aligned}
&e^{\alpha_1(x-y-vt)}e^{\beta_1 f(x-y-vt)}\sum_{n_1} I_{n_1} e^{\frac{i\pi n_1(x-y-vt)}{L}} \\
\propto& 2e^{\alpha_1(x-y-vt)}\sin(\beta_1/8)e^{\frac{i\beta_1(x-y-vt)}{8L}}\sum_{n_{+,1}} e^{\frac{i(n_{+,1})\pi}{L}(x-y-vt)}\hat{H}\left[I_{\frac{n_{+,1}-n_{-,1}}{2}}\right]\left(n_{+,1}+\frac{\beta_1}{\pi}\right), \\
\alpha_1 =& \left[\frac{\alpha}{2\sqrt{2\pi K}}\left[\alpha_{L,R}\gamma_R\right]+\frac{\alpha^2}{4}\alpha_{L,R}\alpha_{R,L}+\frac{\gamma_R\gamma_L}{2\pi K}\right]\left[\hat{Q},\hat{\phi}_0\right]/(8L), \\
\beta_1 =& (\frac{\alpha^2}{4}\alpha_{R,L}^2+\frac{\gamma_R^2}{2\pi K})/2,
\end{aligned} \tag{8.116}$$

where a list of the other constants α_i, β_i arising from different linear combinations is displayed afterwards in the corresponding **appendix**. Hence the final form of the correlation function before Fourier transformation is approximated by

$$\begin{aligned}
G(x,y,t)^{\text{chiral},OBC}_{R,L} \approx& (b)^{-\frac{(A^2+B^2)}{2\pi}}\bar{C}^0_{R,L}(x-y,t)\Big[\prod_{i=1}^{6}\sin(\beta_i/8)\Big]e^{(\frac{i\beta_1}{8L}+\alpha_1)(x-y-vt)} \\
*& e^{(\frac{i\beta_2}{8L}+\alpha_2)(x-y+vt)}e^{(\frac{i\beta_3}{8L}+\alpha_3)(x+y+vt)}e^{(\frac{i\beta_4}{8L}+\alpha_4)(x+y-vt)}e^{\frac{i\beta_5(2x)}{8L}}e^{\frac{i\beta_6(2y)}{8L}}\Big[\prod_{i=1}^{6}\sum_{n_{i,+}}\Big]\Big[e^{\frac{i\pi n_{+,1}(x-y-vt)}{L}} \\
*& e^{\frac{i\pi n_{+,2}(x-y+vt)}{L}}e^{\frac{i\pi n_{+,3}(x+y+vt)}{L}}e^{\frac{i\pi n_{+,4}(x+y-vt)}{L}}e^{\frac{2i\pi n_{+,5}(x)}{L}}e^{\frac{2i\pi n_{+,6}(y)}{L}}\Big] \\
*& \prod_{i=1}^{6}\hat{H}\left[I_{\frac{n_{+,i}-n_{-,i}}{2}}\right]\left(n_{+,i}+\frac{\beta_i}{\pi}\right),
\end{aligned} \tag{8.117}$$

where one needs to pay attention that the arguments of the Hilbert transformed Jacobi-Anger coefficient are different according to **Eq**. (8.112). The abbreviations

$\hat{H}\left[I_{\frac{n_{+,i}-n_{-,i}}{2}}\right]\left(n_{+,i}+\frac{\beta_i}{\pi}\right)$ stand for the Hilbert transform of the modified Bessel function in **Eq**. (8.112) with index $\frac{n_{+,i}}{2}$, whereas the Hilbert transform is then performed integrating **Eq**. (8.112) over $n_{i,-}$ around $\left(n_{+,i}+\frac{\beta_i}{\pi}\right)$ in the Hilbert kernel, see **Eq**. (8.115).

Analogously to **Eq**. (8.117), the same procedure can be applied to the case of cyclic boundary conditions, yielding a much simpler expression containing the left and right moving linear combination of spatio-temporal coordinates,

$$
\begin{aligned}
G(x,y,t)^{\text{chiral},PBC}_{R,L} \approx (b)^{-\frac{(A^2+B^2)}{2\pi}}\, \bar{C}^0_{R,L}(x,t)\Big[\prod_{i=1}^{2}\sin(\beta_i/8)\Big] e^{(\frac{i\tilde{\beta}_1}{8L}+\tilde{\alpha}_1)(x-y-vt)} \qquad (8.118)\\
* e^{(\frac{i\tilde{\beta}_2}{8L}+\tilde{\alpha}_2)(x-y+vt)}\Big[\prod_{i=1}^{2}\sum_{n_{i,+}}\Big]\left[e^{\frac{i2\pi n_{+,1}(x-y-vt)}{L}} e^{\frac{i2\pi n_{+,2}(x-y+vt)}{L}}\right]\\
* \prod_{i=1}^{2}\hat{H}\left[I_{\frac{n_{+,i}-n_{-,i}}{2}}\right]\left(n_{+,i}+\frac{\tilde{\beta}_i}{\pi}\right).
\end{aligned}
$$

Nevertheless, it is advised to treat **Eqs**. (8.117) and (8.118) carefully, as they come from a lowest-order cut-off expansion that is definitely not valid for all physical regimes of the XXZ model and might diverge as can be seen from the pre-factor $(b)^{-\frac{(A^2+B^2)}{2\pi}}$ that occurs in both equations. Additionally the arguments of the infinite-variable Bessel functions do not converge anymore in this case, thus the validity of the Jacobi-Anger expansion is questionable. Thus for arbitrary parameters it would be more coherent to use the full expressions in **Eqs**. (8.108) and (8.109) together with a suitable cut-off scheme for the individual summations, to calculate the dynamical structure factor which is basically reduced now to perform simple exponential integrals.

8.9 Dynamical Structure Factor for finite Systems

In the previous sections we have already discussed the characteristic bulk and boundary behavior of the longitudinal spin correlation function. Nevertheless what is experimentally easily probed is not the spatial decay of dominant correlation function, but the system's linear response to a scattering particle with momentum k and energy ω, the dynamical structure factor $S(k,\omega)$ [67,168,251]. Especially in the last section the emphasis was on finding the Fourier series expansion of the chiral correlation function in terms of generalized Bessel functions, with the advantage that the result in **Eqs**. (8.117) and (8.118) are inherently periodic in spatial and temporal coordinates such that Fourier transformation becomes trivial. The impurity part of the density-density correlator in **Eq**. (8.38) consists of the product of the impurity correlator and a chiral field part, which means that the dynamical structure factor corresponds to a convolution of the two correlators in Fourier space. To calculate the boundary and bulk limits in

Eq. (8.92) and **Eq**. (8.93) it was convenient to use the approximate/low-energy δ form of the impurity correlator in **Eqs**. (8.54) and (8.55). Taking these expressions for the calculation of $S(k,\omega)$ has the huge advantage that the convolution with the impurity correlator becomes trivial, due to the screening properties of the Dirac delta. In the following the emphasis is more on finding an analytical expression for the dynamical structure factor that can probably be evaluated purely numerically. Thus it is preferable to treat the impurity correlators first in the exact form of Jacobi theta functions. Due to the series representation of those functions the impurity part can then still be Fourier transformed in closed form, as will be shown below. Nevertheless the same approximations, as for example in **Eq**. (8.51), can be re-introduced to the final form of the dynamical structure factor $S(k,\omega)$, as ultimately it can not be precluded that approximate eigenfunctions for the impurity may work better in some cases, at least for the Dirichlet case where a linearization of the Schrödinger equation is not well defined.

The impurity part of the dynamical structure factor is then defined as,

$$S(k,\omega)^{imp}_{R,L} = \frac{1}{L}\int_{-\infty}^{\infty} dt \int_0^L dx \int_0^L dy \;\; A(x,y,t)^{\mathrm{imp}}_{R,L} e^{i\omega t} e^{-ik(x-y)}, \tag{8.119}$$

where the integration in **Eq**. (8.119) can be further simplified in the translationally invariant case of periodic boundary conditions. The full real-space and time resolved impurity part of the correlation function is given by

$$G(x,y,t)^{\mathrm{imp}}_{R,L} = e^{i(k_F \mp k_1)(x-y)} G(x,y,t)^{\mathrm{chiral}}_{R,L} \langle \hat{\tilde{d}}(x,t) \hat{\tilde{d}}^{\dagger}(y,0)\rangle + \mathrm{h.c.}, \tag{8.120}$$

where one should use **Eqs**. (8.44) and (8.45) for the impurity correlators and **Eqs**. (8.108) and (8.109) for the chiral part, for open or periodic boundary conditions, respectively. The integral limits in **Eq**. (8.119) are either finite as the system size is or infinite as the direction of time. The implication of that is, that the exponential factors in $G(x,y,t)^{\mathrm{imp}}_{R,L}$ integrate either to $\mathrm{sinc}(x) = \sin(\pi x)/(\pi x)$ like functions, i.e.

$$\int_0^L e^{i\pi a z/L} dz = \frac{2L}{\pi a} e^{i\pi a/2} \sin(\pi a/2), \tag{8.121}$$

evaluating to the respective Kronecker δ for even integer a and further converging to delta functions in the thermodynamic limit. Or, in the latter case they can be straightforwardly evaluated to a delta function in the time domain

$$\int_{-\infty}^{\infty} dt \;\; e^{iat} e^{i\omega t} = \delta(a-\omega), \tag{8.122}$$

that is physically the energy resonance condition of the dynamical structure factor, or mathematically the Dirac comb for the Fourier series representation of $S(k,\omega)$. In the case of periodic boundary conditions theses exponential factors have the interpretation

of momenta or energy shifts according to the definition of the Fourier transform

$$\begin{aligned} F(k-b,\omega-a) =& \frac{1}{L}\int_{-\infty}^{\infty} dt \int_0^L dx \int_0^L dy \;\; f(x-y,t) e^{i(\omega+a)t} e^{i(k+b)(x-y)} \\ =& \int_{-\infty}^{\infty} dt \int_0^L dr \;\; f(r,t) e^{i(\omega+a)t} e^{i(k+b)r}, \end{aligned} \tag{8.123}$$

whereas for open boundary conditions only global energy shifts can be absorbed as the exponential factors do not only group according to the difference of spatial coordinates, i.e. $r = x - y$. Thus the overall form of the dynamical structure factor reads for periodic boundary conditions

$$S(k,\omega)_{R,L}^{imp,PBC} = \sum_{p\in\mathbb{Z}} S(k,\omega,p)_{R,L}^{imp,PBC}, \tag{8.124}$$

$$\begin{aligned} S(k,\omega,p)_{R,L}^{imp,PBC} =& \prod_{i=1}^{2} \sum_{n_i\in\mathbb{Z}} \sum_{\tilde{n}_i\in\mathbb{Z}} \Gamma^{PBC} \int_{-\infty}^{\infty} dt \\ & \int_0^L dr \;\; e^{i\omega t} e^{-ik(r)} (e^{ik_0^{PBC} r} e^{i\omega_0^{PBC} t} + \text{c.c.}) \end{aligned}$$

$$\begin{aligned} =& \prod_{i=1}^{2} \sum_{n_i\in\mathbb{Z}} \sum_{\tilde{n}_i\in\mathbb{Z}} \Gamma^{PBC} \frac{1}{\pi} \frac{e^{-i\left(k-k_0^{PBC}\right)L/2} \sin\left[\left(k-k_0^{PBC}\right)L/2\right]}{k-k_0^{PBC}} \delta\left(\omega+\omega_0^{PBC}\right) \\ &+ \prod_{i=1}^{2} \sum_{n_i\in\mathbb{Z}} \sum_{\tilde{n}_i\in\mathbb{Z}} \Gamma^{PBC} \frac{1}{\pi} \frac{e^{-i\left(k+k_0^{PBC}\right)L/2} \sin\left[\left(k+k_0^{PBC}\right)L/2\right]}{k+k_0^{PBC}} \delta\left(\omega-\omega_0^{PBC}\right) \end{aligned} \tag{8.125}$$

Here the pre-factor Γ^{PBC} is implicitly indexed with respect to the 4 integers $n_{1,2}, \tilde{n}_{1,2}$, which is notationally suppressed in **Eq**. (8.124), additionally the momenta and energy

shifts are indexed by the impurity mode p

$$\begin{aligned}\Gamma^{PBC} \equiv&\Gamma^{PBC}(n_1,\tilde{n}_1,n_2,\tilde{n}_2) \qquad (8.126)\\ =&e^{\sum_{l=1}^{\infty}\frac{e^{-bl}}{4\pi l}[A^2+B^2]}I_{n_1}\Big(\Big[\frac{A^2}{4\pi l}\Big]_{l=1}^{\infty}\Big)J_{\tilde{n}_1}\Big(\Big[\frac{\tilde{\beta}_1}{4\pi l}\Big]_{l=1}^{\infty}\Big)I_{n_2}\Big(\Big[\frac{B^2}{4\pi l}\Big]_{l=1}^{\infty}\Big)J_{\tilde{n}_2}\Big(\Big[\frac{\tilde{\beta}_2}{4\pi l}\Big]_{l=1}^{\infty}\Big),\\ \omega_0^{PBC} \equiv&\omega_0^{PBC}(n_1,\tilde{n}_1,n_2,\tilde{n}_2,p)\\ =&\underbrace{\epsilon_0}_{\text{singularity}-\text{energy}}+\underbrace{\omega_p^{PBC}}_{\text{impurity}-\text{dispersion}}\underbrace{-A\langle\hat{Q}_R\rangle/L+B\langle\hat{Q}_L\rangle/L}_{zero-mode} \qquad (8.127)\\ &\underbrace{-\beta_1/(8L)+\beta_2/(8L)}_{\text{L}-\text{dependend phases}}\underbrace{-\frac{2\pi}{L}(n_1+\tilde{n}_1)+\frac{2\pi}{L}(n_2+\tilde{n}_2)}_{\text{Fourier}-\text{harmonics of light}-\text{cones}+\text{corresponding sign}-\text{functions}},\\ k_0^{PBC} \equiv&k_0^{PBC}(n_1,\tilde{n}_1,n_2,\tilde{n}_2,p)\\ =&\underbrace{k_F\mp k_1}_{\text{Lattice}-\text{harmonics impurity}+\text{chiral}}+\underbrace{k_p^{PBC}}_{\text{impurity}-\text{momentum}}+\underbrace{A\langle\hat{Q}_R\rangle/L+B\langle\hat{Q}_L\rangle/L}_{\text{zero}-\text{mode}} \qquad (8.128)\\ &+\underbrace{\beta_1/(8L)+\beta_2/(8L)}_{\text{L}-\text{dependend phases}}+\underbrace{\frac{2\pi}{L}(n_1+\tilde{n}_1)+\frac{2\pi}{L}(n_2+\tilde{n}_2)}_{\text{Fourier}-\text{harmonics of light}-\text{cones}+\text{corresponding sign}-\text{functions}}.\end{aligned}$$

The dynamical structure factor in **Eq**. (8.124) sums up all possible contributions of impurity momenta or energies, compatible with the respective quantizations according to the boundary conditions, whereas a single mode p has to be chosen in order to adjust the semi-analytics to the numerical data. Due to the same reasoning, the lattice harmonics of the impurity relative to the Fermi momentum $q = k_F - k_1$ in **Eq**. (8.128) should acquire the respective quantization $q \equiv k_p^{PBC}$ for now, as well as other re-normalized constants that implicitly depend on q. Nevertheless it might be more suitable to approximate the impurity modes as being continuous, i.e. $p \in \mathbb{R}$, with the obvious advantage of no minimal momentum resolution in q. As stated before, also performing a low-energy limit of the impurity energy, i.e. $\omega_p \approx q_p u$, should be reconsidered as an engineering tool for the final numerical evaluation of $S(k,\omega)$.

Eq. (8.124) looks misleadingly simple, as multiple sums over the ordinary and modified infinite-variable Bessel functions of **Eqs**. (8.95) and (8.101) still have to be evaluated. Further simplifications of **Eq**. (8.124) are probably possible, based on the identities of those generalized functions, for example the reflection property of the modified function $I_n([\beta_m]_{m=1}^{\infty})$ in **Eq**. (8.104) that simplifies the summations over n_1, n_2 from $\mathbb{Z}$ to $\mathbb{N}$. Nevertheless a fully recursive solution to the Fourier coefficients of the dynamical structure factor in **Eq**. (8.124), as found in **Ref**. [67, 258], seems to be unlikely as the respective recurrence relations in **Eqs**. (8.103) and (8.97) of the generalized functions are two-sided. A drastic simplification would be achieved by considering **Eq**. (8.118) for the Fourier transformation of the dynamical structure factor

instead. This would have the advantage that the Fourier coefficients of the dynamical structure factor would consist of Hilbert transforms, see **Eq**. (8.115), of the analytic functions in **Eq**. (8.112) that can be easily implemented numerically. Furthermore the number of sums would reduce from four to two. Nevertheless, care is advised in this case as the cut-off is considered in lowest order, such that the Jacobi-Anger expansion is not convergent anymore and thus mathematically uncontrolled behaviour may spoil the physical interpretation.

Physically, **Eq**. (8.124) shows some kind of resonance condition of the incoming scattering object with momentum k and energy ω. This resonance is infinitely narrow in energy, at $\pm\omega_0^{PBC}$, but extended in a narrow region around the momentum $\pm k_0^{PBC}$ as indicated by the sinc functions that go over to the respective Kronecker δ functions, if $\pm k_0^{PBC}$ is quantized according to the fundamental period of the bosonic modes, i.e. $\pm k_0^{PBC} \equiv \frac{2\pi n}{L}$. In the infinite size/ thermodynamic limit this leads then to the corresponding Dirac δ functions, describing the momentum resonance between probe and scattering particle. If the scattering particle is then resonant with the probe the intensity of the signal is given by the sums of the pre-factor in **Eq**. (8.126), that do not allow for further obvious interpretations at this point. On the other hand the resonances in **Eqs**. (8.127) and (8.128) allow for a clear interpretation as graphically supported.

Switching to open boundary conditions the impurity part of the dynamical structure factor is more complicated, as expected for the translationally non-invariant case, but functionally similar. In this case, the dynamical structure factor can be decomposed according to the four different linear combinations of spatio-temporal arguments of the Jacobi Theta functions in the impurity correlator in **Eq**. (8.44), i.e. $x - y \pm vt$ and $x + y \pm vt$

$$S(k,\omega)_{R,L}^{imp,OBC} = S(k,\omega)_{R,L,1}^{imp,OBC} + S(k,\omega)_{R,L,2}^{imp,OBC} - S(k,\omega)_{R,L,3}^{imp,OBC} - S(k,\omega)_{R,L,4}^{imp,OBC}. \tag{8.129}$$

The factors in **Eq**. (8.129) can be labeled again according to the impurity momentum p

$$S(k,\omega)_{R,L,j}^{imp,OBC} = \sum_{p\in\mathbb{Z}} S(k,\omega,p)_{R,L,j}^{imp,OBC}, \tag{8.130}$$

that individually represent a particular high-energy correction to the dynamical structure factor for a given set of parameters in the Hamiltonian. A single contribution is given

by

$$S(k,\omega,p)^{imp,OBC}_{R,L,j} = \prod_{i=1}^{6}\sum_{n_i,\tilde{n}_i\in\mathbb{Z}} \frac{\Gamma^{OBC}}{L}\int_{-\infty}^{\infty} dt \int_0^L dx \int_0^L dy \; e^{i\omega t}e^{-ik(x-y)}(e^{ik_{0,j}^{OBC}x}e^{i\bar{k}_{0,j}^{OBC}y}e^{i\omega_0^{OBC}t} + \text{c.c.}) \tag{8.131}$$

$$= \prod_{i=1}^{6}\sum_{n_i,\tilde{n}_i\in\mathbb{Z}} \Bigg[\frac{\Gamma^{OBC}e^{-i\left(k_{0,j}^{OBC}+\bar{k}_{0,j}^{OBC}\right)L/2}\sin\left[\left(k-k_{0,j}^{OBC}\right)L/2\right]\sin\left[\left(k+\bar{k}_{0,j}^{OBC}\right)L/2\right]}{2L^2(k-k_{0,j}^{OBC})(k+\bar{k}_{0,j}^{OBC})}\delta\left(\omega+\omega_0^{OBC}\right)$$

$$+ \frac{\Gamma^{OBC}e^{-i\left(k_{0,j}^{OBC}+\bar{k}_{0,j}^{OBC}\right)L/2}\sin\left[\left(k+k_{0,j}^{OBC}\right)L/2\right]\sin\left[\left(k-\bar{k}_{0,j}^{OBC}\right)L/2\right]}{2L^2(k+k_{0,j}^{OBC})(k-\bar{k}_{0,j}^{OBC})}\delta\left(\omega-\omega_0^{OBC}\right)\Bigg].$$

The Fourier coefficients in **Eq**. (8.129) contain additional sinc-like functions in comparison to the periodic case in **Eq**. (8.124), reflecting another resonance condition for the second spatial dependence and for each linear combinations of coordinates. The different contributions for open boundary conditions have the same physical interpretation as in the periodic case but are slightly more complex. The pre-factor Γ^{OBC} contains more generalized Bessel functions, i.e.

$$\begin{aligned}\Gamma^{OBC} \equiv \Gamma^{OBC}([n_i]_{i=1}^{i=6},[\tilde{n}_i]_{i=1}^{i=6}) &= e^{\sum_{l=1}^{\infty}\frac{e^{-bl}}{4\pi l}\left[A^2+B^2\right]} \\ &* J_{\tilde{n}_1}\Big(\Big[\frac{\beta_1}{4\pi l}\Big]_{l=1}^{\infty}\Big)J_{\tilde{n}_2}\Big(\Big[\frac{\beta_2}{4\pi l}\Big]_{l=1}^{\infty}\Big)J_{\tilde{n}_3}\Big(\Big[\frac{\beta_3}{4\pi l}\Big]_{l=1}^{\infty}\Big) \\ &* J_{\tilde{n}_4}\Big(\Big[\frac{\beta_4}{4\pi l}\Big]_{l=1}^{\infty}\Big)J_{\tilde{n}_5}\Big(\Big[\frac{\beta_5}{4\pi l}\Big]_{l=1}^{\infty}\Big)J_{\tilde{n}_6}\Big(\Big[\frac{\beta_6}{4\pi l}\Big]_{l=1}^{\infty}\Big)I_{n_1}\Big(\Big[\frac{A^2}{4\pi l}\Big]_{l=1}^{\infty}\Big)I_{n_2}\Big(\Big[\frac{B^2}{4\pi l}\Big]_{l=1}^{\infty}\Big) \\ &* I_{n_3}\Big(\Big[\frac{-2AB}{4\pi l}\Big]_{l=1}^{\infty}\Big)I_{n_4}\Big(\Big[\frac{-2AB}{4\pi l}\Big]_{l=1}^{\infty}\Big))I_{n_5}\Big(\Big[\frac{2AB}{4\pi l}\Big]_{l=1}^{\infty}\Big)I_{n_6}\Big(\Big[\frac{2AB}{4\pi l}\Big]_{l=1}^{\infty}\Big),\end{aligned} \tag{8.132}$$

one for each combination of (x,y,vt) appearing in **Eq**. (8.84). The resonance like conditions for the momenta in (x,y) coordinates, as well as for the energy of the

scatterer are given by

$$k_{0,j} \equiv k_{0,j}([n_i]_{i\neq 6},[\tilde{n}_i]_{i\neq 6},p) = \sum_{j=1}^{4}\left(\frac{i\beta_j}{8L}+\alpha_j\right)+\frac{i\beta_5}{4L}+\frac{\pi}{L}\sum_{j=1}^{4}(n_j+\tilde{n}_j)+\frac{2\pi}{L}(n_5+\tilde{n}_5) \tag{8.133}$$

$$+\epsilon^{+}_{R,L}\frac{\langle\hat{Q}\rangle}{2L}+(-1)^{j+1}q_p^{OBC}+k_F\mp k_1,$$

$$\bar{k}_{0,j} \equiv \bar{k}_{0,j}([n_i]_{i\neq 5},[\tilde{n}_i]_{i\neq 5},p) = -\sum_{j=1}^{2}\left(\frac{i\beta_j}{8L}+\alpha_j\right)+\sum_{j=2}^{4}\left(\frac{i\beta_j}{8L}+\alpha_j\right)+\frac{i\beta_6}{4L},$$

$$-\frac{\pi}{L}\sum_{j=1}^{2}(n_j+\tilde{n}_j)+\frac{\pi}{L}\sum_{j=2}^{4}(n_j+\tilde{n}_j)+\frac{2\pi}{L}(n_6+\tilde{n}_6)-\epsilon^{+}_{R,L}\frac{\langle\hat{Q}\rangle}{2L}+(-1)^{j}q_p^{OBC}-k_F\pm k_1,$$

$$\omega_0^{OBC} \equiv \omega_0^{OBC}([n_i]_{i\neq 5,6},[\tilde{n}_i]_{i\neq 5,6},p) = -\left(\frac{i\beta_1}{8L}+\alpha_1\right)+\left(\frac{i\beta_2}{8L}+\alpha_2\right)+\left(\frac{i\beta_3}{8L}+\alpha_3\right) \tag{8.134}$$

$$-\left(\frac{i\beta_4}{8L}+\alpha_4\right)+\frac{\pi}{L}\sum_{j=1}^{4}(-1)^{j}(n_j+\tilde{n}_j)+\epsilon^{-}_{R,L}\frac{\langle\hat{Q}\rangle}{2L}+\epsilon_0+\omega_p^{OBC},$$

with the same requirements of re-quantizing the remaining constants as in the periodic case. Concerning potential simplifications of the dynamical structure factor for open boundaries, nothing more than what has been discussed for the periodic case can be added here. So the fate of computing the impurity part of the dynamical structure factor depends on the numerical skills of the successor of this work, in handling the high-dimensional problem in a clever way.

8.10 Conclusion

This chapter could not be finished during the time of the doctoral education, and a numerical evaluation of the finite-size dynamical structure factor in **Eqs**. (8.124) and (8.129) is still missing. Nevertheless, as even the tiniest advances deserve attention they are valued too in the following sense. We have calculated the longitudinal spin correlation function for the finite XXZ spin 1/2 chain including weak magnetic field by means of the non-linear bosonization approach with a single mobile impurity. The geometries that we have considered are either open chains with two-fold impenetrable boundaries or cyclic ones that posses translational invariance. Through the decoupling of low and high energy degrees of freedom in **Eq**. (8.32) the eigenstates are necessarily separable, and the functional behavior of the longitudinal correlation is obtained by just combining the impurity correlators in **Eq**. (8.49) with the associated chiral part in **Eq**.

(8.84) and **Eq**. (8.85) respectively, while we keep full track of the boundary dependent zero-mode contributions and finite-size effects thereby. For the open chains, we calculate the bulk as well as the boundary limit of the correlator in **Eq**. (8.92) and **Eq**. 8.93), complementing the spin auto-correlations derived in **Ref**. [255] for the semi-infinite chain to describe also their spatial dependence. We find the same algebraic temporal decay attached to the mobile impurity correlation function as in **Ref**. [255], but via a heat kernel regularization that allows for a more physical interpretation of the impurity momentum cut-off as the choice of diffusivity for the high-energy particle. By including also a second boundary condition, in contrast to a semi-infinite system, we find estimates for the impurity velocity u, its diffusivity ϵ and the time scales t for which the bulk or boundary limits are valid in non-linear bosonization. We find a Fourier decomposition of chiral correlation functions in terms of products of ordinary and modified infinite-variable Bessel functions [257] that allow to study arbitrary energy and momentum resolved observables in the bosonization approach. This technique is then used to calculate the dynamical structure factor of the mobile impurity in the XXZ chain for finite geometries and for arbitrary parameters of the Hamiltonian, see **Eqs**. (8.124) and (8.129). Attempts to Fourier transform chiral correlation functions directly in algebraic form are restricted to special values of the Luttinger parameter K, due to the necessity of performing complicated contour integration [67, 251]. Nevertheless a clear interpretation of the Fourier coefficients of the dynamical structure factor is still hindered by the complexity of multiple sums of the generalized functions and further simplifications are needed. For the special case of a vanishing cut-off those generalized functions can be integrated in closed form. For the modified infinite-variable Bessel functions, this yields on the one hand combinations of Γ and β functions that pave the way to study further approximations or asymptotics analytically, see **Eq**. (8.112). The ordinary pendants on the other hand, that correspond to the Fourier series of exponentials of the signum function, correspond in that limit to certain Hilbert transforms of those modified Bessel functions, operating on domains given by all possible linear combinations of spatio-temporal coordinates, see **Eq**. (8.114). The properties of the Hilbert transform are not only consistent with the $\pi/2$ phase shifts that vertex operators acquire while passing different regions of their spatio-temporal coordinates, but may also simplify future numerical investigations drastically. Nevertheless one should be cautious while working in the limit of a vanishing cut-off, as physical divergences might appear in this case and a mathematically sound treatment is impossible due to the non-convergence of the Jacobi-Anger expansions in **Eqs**. (8.96) and (8.102). Sadly, only the derivation of the dynamical structure factor for the respective boundary conditions could be shown here, hence the chapter should be viewed as the starting point for a more detailed investigation as well as the comparison to quasi-exact numerical data. Problematic here is the reversed role of boundary conditions for the analytics or numerics, in the sense that periodic ones are suitable analytically but difficult to compute numerically and

for open ones the reversed relation holds. Nevertheless, the motivation of the project is more polarized towards the correctness of the analytics and not of the nonetheless quasi-exact numerics that is "just" slower in convergence and harder to implement [172]. Therefore it is suggested to re-perform the numerical computations of **Fig**. (8.1) for the periodic boundary case, which allows then to use the much simpler expression for the dynamical structure factor in **Eq**. (8.124) and to fix the appearing constants of the mobile impurity by means of the Bethe ansatz that up to date do not exist in closed form for the open boundary case.

8.11 Appendix: Bare Coupling Constants

As the last part of this chapter, we would like to present a list of the constants appearing in the bare coupling limit [252, 253], as well as a list of the appearing commutators that build the pre-factors for open boundary conditions in **Eq**. (8.66), as they are too lengthy to present in the main text. In principle, microscopic expressions for the universal parameters as well as those of the mobile impurity can be obtained by the respective Bethe ansatz solution of the XXZ chain, also for finite magnetic fields. As closed form expressions for the high-energy impurity are not obtainable, for finite magnetic fields, the naive continuum values serve as a good starting point for a deeper numerical investigation of the dynamical structure factor. Therefore a list of the appearing constants in lowest order in the anisotropy Δ is given below, where we additionally assume that $0 < q < k_F \leq \pi/2 - \frac{\pi \sum_j \hat{S}^z_j}{L}$ to ensure positivity and finitness for some of

the parameters,

$$v_F = J\sin(k_F), \tag{8.135}$$

$$\epsilon \approx J\cos(k_F - q),$$

$$u \approx J\sin(k_F - q),$$

$$m \approx \left[J\cos(k_F - q)\right]^{-1},$$

$$\tilde{\kappa}_{R,L} \approx 2\Delta\left[1 - \cos(k_F \mp q)\right],$$

$$K \approx 1 - \frac{2\Delta}{\pi}\sin k_F,$$

$$v \approx v_F\left(1 + \frac{2\Delta}{\pi}\sin k_F\right),$$

$$\gamma_R \approx \frac{2\Delta(1-\cos(q))}{\sin(k_F) - \sin(k_F - q)},$$

In **Eq**. (8.135), the numerical variable $q \equiv k^{OBC/PBC}$ denotes the momentum of the high-energy impurity that needs to be adjusted for different parameters (h, Δ) to fix the mismatch between the analytics and the numerical data, as shown in **Fig**. (8.1). The Fermi momentum is thereby understood to be shifted by the total magnetization as in **Eq**. (8.24), adjusted by the applied magnetic field h. For the case of periodic boundary conditions, and a vanishing magnetic field, various exponents have been calculated in closed form in **Ref**. [252], whereas different cases have to be treated purely numerically.

8.12 Appendix: List of the Field Commutators

The elementary field commutators in the pre-factor in **Eq**. (8.66) can be calculated via the mode decomposition in **Eq**. (8.143), leading to the following expressions

$$[A_{R,L}(x,t), B_{R,L}(y,0)] = (\frac{\alpha}{2})^2 \left(\alpha_{R,L}\alpha_{L,R}\frac{x-y-vt}{4L} + \alpha_{L,R}^2\frac{x-y+vt}{4L}\right)[\hat{Q},\hat{\phi}_0] \tag{8.136}$$
$$+ (\frac{\alpha}{2})^2 \left(\alpha_{R,L}^2 f(x-y-vt) - \alpha_{R,L}\alpha_{L,R} f(x+y-vt)\right)$$
$$+ (\frac{\alpha}{2})^2 \left(\alpha_{L,R}^2 f^*(x-y+vt) - \alpha_{R,L}\alpha_{L,R} f^*(x+y+vt)\right),$$

$$[A_{R,L}(x,t), C_{R,L}(x,t)] = \frac{\alpha}{2}\frac{1}{\sqrt{2\pi K}}\left[(\alpha_{R,L}\gamma_L + \alpha_{L,R}\gamma_R) f(2x)\right] \tag{8.137}$$
$$- \frac{\alpha}{2}\frac{1}{\sqrt{2\pi K}}\left[(\alpha_{R,L}\gamma_L + \alpha_{L,R}\gamma_R)\frac{x-vt}{4L}[\hat{Q},\hat{\phi}_0]\right],$$
$$[A_{R,L}(x,t), D_{R,L}(y,0)] = -\frac{\alpha}{2}\frac{1}{\sqrt{2\pi K}}\left[\alpha_{R,L}\gamma_R f(x-y-vt) + \alpha_{R,L}\gamma_L f(x+y-vt)\right]$$
$$+ \frac{\alpha}{2}\frac{1}{\sqrt{2\pi K}}\left[\alpha_{L,R}\gamma_R f^*(x+y+vt) + \alpha_{L,R}\gamma_L f^*(x-y+vt)\right]$$
$$+ \frac{\alpha}{2}\frac{1}{\sqrt{2\pi K}}\left[\gamma_L(\alpha_{R,L} - \alpha_{L,R})\frac{x-vt}{4L} - \alpha_{L,R}(\gamma_R - \gamma_L)\frac{y}{4L}\right][\hat{Q},\hat{\phi}_0], \tag{8.138}$$

$$[B_{R,L}(y,0), C_{R,L}(x,t)] = -\frac{\alpha}{2}\frac{1}{\sqrt{2\pi K}}\left[\alpha_{R,L}\gamma_R f(x+y-vt) + \alpha_{L,R}\gamma_L f^*(x-y+vt)\right]$$
$$+ \frac{\alpha}{2}\frac{1}{\sqrt{2\pi K}}\left[\alpha_{R,L}\gamma_R f(x-y-vt) + \alpha_{R,L}\gamma_L f^*(x+y+vt)\right]$$
$$+ \frac{\alpha}{2}\frac{1}{\sqrt{2\pi K}}\left[\gamma_L(\alpha_{R,L} - \alpha_{L,R})\frac{y}{4L} - \alpha_{L,R}\gamma_R\frac{x-vt}{4L} + \alpha_{L,R}\gamma_L\frac{x+vt}{4L}\right][\hat{Q},\hat{\phi}_0], \tag{8.139}$$

$$[B_{R,L}(y,0), D_{R,L}(y,0)] = \frac{\alpha}{2}\frac{1}{\sqrt{2\pi K}}\left[(\alpha_{R,L}\gamma_L + \alpha_{L,R}\gamma_R) f(2y)\right] \tag{8.140}$$
$$- \frac{\alpha}{2}\frac{1}{\sqrt{2\pi K}}\left[(\alpha_{R,L}\gamma_L + \alpha_{L,R}\gamma_R)\frac{y}{4L}[\hat{Q},\hat{\phi}_0]\right],$$

$$[C_{R,L}(x,t), D_{R,L}(y,0)] = \frac{1}{2\pi K}\left[\gamma_R^2 f(x-y-vt) + \gamma_L^2 f^*(x-y+vt)\right] \tag{8.141}$$
$$+ \frac{\gamma_L\gamma_R}{2\pi K}\left[f(x+y-vt) + f^*(x+y+vt)\right]$$
$$- \frac{1}{2\pi K}\left[\gamma_R\gamma_L\frac{x-y-vt}{4L} - \gamma_L^2\frac{x-y+vt}{4L}\right][\hat{Q},\hat{\phi}_0],$$

where we have defined the following short-hand notation for the c-number of the central field commutators

$$f(x+y+vt) = \frac{i}{2}\left[\frac{x+y+vt}{4L} + \frac{1}{2\pi}\sum_{l=1}^{\infty}\frac{1}{l}\sin(k_l[x+y+vt])\right]. \tag{8.142}$$

8.13 Appendix: Mode decomposition for Open Boundaries

The mode decomposition of the bosonic density $\phi(x)$ and phase field $\Theta(x)$ that diagonalizes the non-impurity part in **Eq**. (8.32) and furthermore satisfies the correct boundary conditions for the spin operators, i.e. $\hat{\vec{\mathcal{S}}}_{L,0} = 0$, can be obtained from the following expressions for the right-movers [66, 67]

$$\phi_R(x,t) = \frac{\hat{\phi}_0}{2} + \hat{Q}\frac{x-vt}{2L} + \sum_{l=1}^{\infty}\frac{1}{\sqrt{4\pi l}}\left[-ie^{ik_l(x-vt)}\hat{b}_l + \text{h.c.}\right], \tag{8.143}$$

where $\left[\hat{b}_l, \hat{b}_{\bar{l}}^{\dagger}\right] = \delta_{l,\bar{l}}$ denotes the bosonic excitations above the Fermi-sea with momenta $k_l = \frac{\pi l}{L}$. For Dirichlet boundaries only one of the counter-propagating fields is relevant by analytic continuation of the other, called the folding trick,

$$\phi_R(x) = -\phi_L(-x) + \hat{\phi}_0, \tag{8.144}$$

where the expression in **Eq**. (8.144) incorporates more general results of Cardy concerning the properties of boundary conformal field theory [64]. A straight-forward application of the mode decomposition in **Eq**. (8.143), leads to the commutation relations for the bosonic right-movers, i.e.

$$\begin{aligned}[\phi_R(x,t), \phi_R(y,t_0)] =& \frac{i}{4L}\left[(x-y-v(t-t_0))\right] + \frac{i}{2\pi}\sum_{l=1}^{\infty}\frac{1}{l}\sin(k_l[x-y-v(t-t_0)]), \\ =& \frac{i}{4}\text{sign}\left(x-y-v(t-t_0)\right), \quad \forall\ x-y-v(t-t_0) \in (0,2L)\end{aligned} \tag{8.145}$$

Due to the existence of only one of the chiral fields also only a single zero-mode exists, that is related to the total magnetization in terms of spin degrees of freedom or corresponds to the particle number conservation of Jordan-Wigner fermions [67]. Nevertheless there is no current zero mode in this case that exactly vanishes as the center of mass position of the fluid corresponds to a constant [51]. The spin operators generally do not obey simple expressions in terms of the impurities and chiral fields and depend on the specific projection in **Eq**. (8.25), in contrast to the ordinary bosonization [67]. It is a priori unclear what the entity $\hat{d}^{\dagger}(x)$ should represent, meaning loosely speaking what order of derivatives is assumed to be relevant in **Eq**. (8.32) in the case that only a single impurity

is considered. Or, if multiple impurities are present, if a regular, or a chiral/irregular representation of the impurities should be chosen. This choice finally dictates if the final correlation function in non-linear bosonization shows rather a diffusive or ballistic behavior. These issues also hinder the allocation of a physical interpretation to the zero modes in terms of spin degrees of freedom as this depends crucially on the expansion **Eq**. (8.25) and the meaning of the mobile impurity. Nevertheless the relation between the magnetization and the number of Jordan-Wigner fermions is independent of the actual low-energy projection and is given by **Eq**. (8.24).

8.14 Appendix: Mode decomposition for Cyclic Boundaries

In the case of cyclic boundary conditions, two counter propagating fields exist with a momentum quantization according to $k_l = \frac{2\pi l}{L}$,

$$\begin{aligned}\phi_R(z,t) &= \phi_R^0 + Q_R\frac{z-vt}{L} + \sum_{l=1}^{\infty}\frac{1}{\sqrt{4\pi l}}e^{ik_l(z-vt)}\hat{b}_{l,R} + \text{h.c.},\\ \phi_L(z,t) &= \phi_L^0 + Q_L\frac{z+vt}{L} + \sum_{l=1}^{\infty}\frac{1}{\sqrt{4\pi l}}e^{-ik_l(z+vt)}\hat{b}_{l,L} + \text{h.c.}.\end{aligned} \tag{8.146}$$

The bosonic species in **Eq**. (8.146) satisfy the usual bosonic canonical commutation relations among themselves, i.e. $\left[\hat{b}_{i,\alpha}, \hat{b}^{\dagger}_{j,\beta}\right] = \delta_{i,j}\delta_{\alpha,\beta}$, expressing the independence of the non-zero mode parts of $\phi_{R,L}(z,t)$ at the operator level, whereas globally the two entities are still coupled via their zero modes

$$\begin{aligned}\left[\phi^0_{R,L}, Q_{R,L}\right] &= \mp\frac{i}{2},\\ \left[\phi_R(z,t), \phi_L(\bar{z},\bar{t})\right] &= \left[\phi^0_R, \phi^0_L\right] = \frac{i}{4},\\ \left[\phi_{R,L}(z,t), \phi_{R,L}(\bar{z},\bar{t})\right] &= \pm\frac{i}{2L}\left[z-\bar{z}\mp v(t-\bar{t})\right] \pm \frac{i}{2\pi}\sum_{l=1}^{\infty}\frac{1}{l}\sin(k_l(z-\bar{z}\mp v(t-\bar{t}))),\\ &= \pm\frac{i}{4}\text{sign}\left(z-\bar{z}\mp v(t-\bar{t})\right), \quad \forall\ z-\bar{z}\mp v(t-\bar{t}) \in (0,L).\end{aligned} \tag{8.147}$$

In contrast to the case of open boundary conditions the particle number of each species is conserved individually, which is usually rephrased in terms of the dual fields corresponding then to number and current zero mode being the symmetric or anti-symmetric linear combination of them. In order to calculate arbitrary expectation values for the respective boundary conditions in terms of the chiral fields, the mode decomposition in **Eq**. (8.143) or **Eq**. (8.146) have to be inserted with an extensive use of the Baker-Campbell-Haussdorf formula for centrally commuting operators, i.e.

$[A, B] = c\hat{I}$, $c \in \mathbb{C}$

$$e^{A+B} = e^A e^B e^{\frac{[A,B]}{2}}. \tag{8.148}$$

Normal ordering of the bosonic modes inside the expectation values explicitly allows to simplify the calculation of correlation functions drastically by the application of the following identity

$$\langle e^{f(\hat{b}^\dagger)} e^{f(\hat{b})} \rangle = 1, \tag{8.149}$$

for some analytic operator-valued functions $f(\hat{b}^\dagger), f(\hat{b})$ [42] and $\langle \cdot \rangle$ representing the expectation value with respect to a quasi-free state, as for example the Luttinger liquid.

Chapter 9

Conclusion and Outlook

The last part of this PhD thesis presents the recapitulation of individual results and their integration into our general understanding of strongly correlated one-dimensional systems. Beyond that, potential interesting extensions, generalizations and new directions of the research field are briefly outlined. Notable progress in the description of Luttinger liquids, and their variants, could be achieved in two ways. The largest parts of this thesis are chapters (**6**) and (**7**), which are concerned with the field-theoretical treatment of one-dimensional lattice anyons and the difference to ordinary, single-component, Luttinger liquids. From a broader perspective, both theories differ only by an exactly marginal interaction and linear gradient terms in the dual fields, that are responsible for the breaking of spatial and temporal inversion symmetry that is inherent to anyonic physics. The effect of those contributions is at first to equip the chiral species with different velocities, as well as shifted ordinates with respect to their linearization around the Fermi momenta. Such manipulations of the backbone of single-component Luttinger liquids have far reaching consequences, especially the induced left/right asymmetry of temporal, or finite-temperature correlation functions. Furthermore we have shown in chapter (**6**), that the zero-modes of the liquid couple for twisted boundary conditions and are in general not additive. This leads generally to different selection rules, compared to the ordinary Luttinger liquid, which inherit the topological properties of those one-dimensional anyons. So we conclude that the model describes a new class of relativistic quantum fluids with a plethora of potential applications or generalizations, where all the Luttinger-specific properties, as for example the fragmenting effect of impurities or other surface-critical or dynamical phenomena, have to be re-investigated for the new model [43, 176, 281]. Beyond such general statements, about the universal description of parity/time asymmetric field theories, we have studied the dilute anyon-Hubbard model and it's low-energy properties in quite some detail in chapter (**6**). A rigorous continuum limit provide not only the classification of the model as a generalization of the seemingly disjoint, and prevalent, approaches to one-dimensional anyons of Kundu or of Leinaas and Myrheim [4, 5, 19, 282]. Furthermore, we could relate the theory's

universal parameters to 2,3-particle interactions, as well as current-density couplings, microscopically. This does not only elevate Kundu anyons out of the realm of purely academical models, by regularizing the harshly criticized, singular interaction by a finite lattice spacing, but conversely provides analytical insight into the fundamental properties of such Hubbard anyons via the rigorous results of the Bethe solutions of their integrable limits. Beyond the low-density limit, we cannot rely on exact results anymore, but provide analytical estimates of the strong-coupling universal parameters of these Hubbard anyons, in the spirit of similar investigations pursued for the Bose-Hubbard model [130, 136]. Going beyond the fundamental properties of such anyonic liquids, their behavior as critical theories at quantum phase boundaries is investigated in chapter (**7**), on hand of the constrained and extended anyon-Hubbard model. By using different, numerically supported, low-energy projections that are suitable near the bosonic or pseudo-fermionic limits respectively, we characterize all different phases and their transitions in perfect agreement with the previous predictions of large-scale numerical investigations. Thereby we find for relatively small statistical parameters that the universality class of the transitions remains unaffected, and only the gapless phases, that play a sub-dominant role due to strong-interactions and integer filling, are altered analogously to the single-component case. For large statistical parameters the topography of the phase diagram changes drastically, whereas superfluid coherence, as well the topological protection of the bosonic Haldane phase, is lost due to strong statistical interactions and pronounced statistically-induced symmetry breaking. Instead, only two-particle excitations remain gapless in that parameter region, which leads in addition to a stabilization of a dimerized phase for a balanced interplay of attractive onsite, as well as nearest-neighbor, interactions and statistical repulsion. For this dimerized phase a microscopic picture is rigorously derived by group-theoretical methods, as bond-centered, alternating singlet states with an additional particle or hole delocalized. It would be interesting to generalize such anyonic Luttinger liquids to internal degrees of freedom, and include further bi-linear, exactly marginal, interactions that couple density and phase degrees of freedom of different channels in all possible combinations. Of special importance would be here the impact of such couplings on one of the paradigms of one-dimensional physics, the spin-charge separation and the eventual extension of the bosonization from abelian currents to more general, non-abelian, groups [42, 50]. The second major focus of this thesis was the investigation and computation of finite-size correlation functions, in the framework of non-linear bosonization, in chapter (**8**) and their energy/momentum-resolved representation [58]. A novum with respect to previous approaches is the closed-form calculation of the dynamical structure factor for hard wall and periodic boundary conditions, whose actual numerical evaluation, and it's comparison to experimental data, is a formidable task for future investigations by itself. Apart from this particular application, the general decomposition of chiral correlation functions into Jacobi-Anger series potentially paves

the way to study arbitrary correlators in energy/momentum representation, and thus provides an alternative approach compared to complicated contour integration. Known critical exponents of the dynamical density-density correlator near the bulk or near a semi-infinite boundary are generalized to an actual finite system. The inclusion of the second boundary allows then to find additional estimates on the range of validity of those exponents for comparably long time scales. Conversely, it would be of great importance to test the method of non-linear bosonization per se, by comparing those predictions to actual experimental data.

Bibliography

[1] W. Pauli. Über den Zusammenhang des Abschlusses der Elektronengruppen im Atom mit der Komplexstruktur der Spektren. *Zeitschrift fur Physik*, 31(1):765–783, February 1925.

[2] F. Wilczek. *Fractional Statistics and Anyon Superconductivity*, volume 10 of *Series on Directions in Condensed Matter Physics*. World Scientific, 1990.

[3] E. Artin. Theory of braids. *Ann. Math.*, 48:101, 1947.

[4] J. M. Leinaas and J. Myrheim. On the theory of identical particles. *Il Nuovo Cimento B*, 37(1):1–23, 1977.

[5] Thore Posske, Björn Trauzettel, and Michael Thorwart. Second quantization of Leinaas-Myrheim anyons in one dimension and their relation to the Lieb-Liniger model. *Phys. Rev. B*, 96:195422, Nov 2017.

[6] Elliott H. Lieb and Werner Liniger. Exact analysis of an interacting Bose gas. 1 the general solution and the ground state. *Phys. Rev.*, 130:1605–1616, May 1963.

[7] Anjan Kundu. Exact solution of double δ function Bose gas through an interacting anyon gas. *Phys. Rev. Lett.*, 83:1275–1278, Aug 1999.

[8] C. D. Batista and G. Ortiz. Algebraic approach to interacting quantum systems. *Adv.Phys.*, 53:1–82, 2004.

[9] P. Jordan and E. Wigner. Über das Paulische Äquivalenzverbot. *Zeitschrift für Physik*, 47(9):631–651, 1928.

[10] Lewi Tonks. The complete equation of state of one, two and three-dimensional gases of hard elastic spheres. *Physical Review*, 50:955–963, Nov 1936.

[11] M. Girardeau. Relationship between systems of impenetrable Bosons and Fermions in one dimension. *Journal of Mathematical Physics*, 1(6):516–523, 1960.

[12] M. D. Girardeau. Anyon-fermion mapping and applications to ultracold gases in tight waveguides. *Phys. Rev. Lett.*, 97:100402, Sep 2006.

[13] Tassilo Keilmann, Simon Lanzmich, Ian McCulloch, and Marco Roncaglia. Statistically induced phase transitions and anyons in 1d optical lattices. *Nat. Commun.*, 2:361, 2011.

[14] F. D. M. Haldane. "Fractional statistics" in arbitrary dimensions: A generalization of the Pauli principle. *Phys. Rev. Lett.*, 67:937–940, 1991.

[15] F. H. L. Essler, H. Frahm, F. Göhmann, A. Klümper, and V. E. Korepin. *The one-dimensional Hubbard model*. Cambridge University Press, 2003.

[16] A. Lerda and S. Sciuto. Anyons and quantum groups. *Nuclear Physics B*, 401(3):613 – 643, 1993.

[17] Kevin Jägering. *DMRG Simulations of Dynamics and Phase Transitions of One Dimensional Quantum Systems*. PhD thesis, University of Kaiserslautern, 2020.

[18] Martin Bonkhoff. Interacting anyons in a one-dimensional optical lattice. Master's thesis, University of Kaiserslautern, 2016.

[19] Anjan Kundu. Generation of integrable quantum nonultralocal model through braided Yang-Baxter equation. *invited talk at the Int. Conf. on Problems in QFT (Alushta, May 13-18, 1996)*, 08 1996.

[20] M. Batchelor, Angela Foerster, Xi-Wen Guan, J. Links, and H. Zhou. The quantum inverse scattering method with anyonic grading. *Journal of Physics A: Mathematical and Theoretical*, 41, 11 2008.

[21] Anjan Kundu. Quantum integrable 1d anyonic models: Construction through braided Yang-Baxter equation. *Symmetry, Integrability and Geometry : Methods and Applications*, 6, 05 2010.

[22] Allan D. C. Tosta, Ernesto F. Galvão, and Daniel J. Brod. Gaussian optical networks for one-dimensional anyons. *Phys. Rev. A*, 104:022604, Aug 2021.

[23] N. N. Bogoljubov. On a new method in the theory of superconductivity. *Il Nuovo Cimento (1955-1965)*, 7(6):794–805, 1958.

[24] Emilio Cobanera, Gerardo Ortiz, and Zohar Nussinov. The bond-algebraic approach to dualities. *Advances in Physics - ADVAN PHYS*, 60, 03 2011.

[25] Elliott Lieb, Theodore Schultz, and Daniel Mattis. Two soluble models of an antiferromagnetic chain. *Annals of Physics*, 16(3):407 – 466, 1961.

[26] Martin Bonkhoff, Kevin Jägering, Sebastian Eggert, Axel Pelster, Michael Thorwart, and Thore Posske. Bosonic continuum theory of one-dimensional lattice anyons. *Phys. Rev. Lett.*, 126:163201, Apr 2021.

[27] Guixin Tang, Sebastian Eggert, and Axel Pelster. Ground-state properties of anyons in a one-dimensional lattice. *New J. Phys.*, 17(12):123016, 2015.

[28] Adhip Agarwala, Gaurav Kumar Gupta, Vijay B. Shenoy, and Subhro Bhattacharjee. Statistics-tuned phases of pseudofermions in one dimension. *Phys. Rev. B*, 99:165125, Apr 2019.

[29] Florian Lange, Satoshi Ejima, and Holger Fehske. Strongly repulsive anyons in one dimension. *Phys. Rev. A*, 95:063621, Jun 2017.

[30] Christoph Sträter, Shashi C. L. Srivastava, and André Eckardt. Floquet realization and signatures of one-dimensional anyons in an optical lattice. *Phys. Rev. Lett.*, 117:205303, Nov 2016.

[31] Stefano Longhi and Giuseppe Della Valle. Anyons in one-dimensional lattices: a photonic realization. *Optics letters*, 37:2160–2, Jun 2012.

[32] Vincent Lienhard, Pascal Scholl, Sebastian Weber, Daniel Barredo, Sylvain de Léséleuc, Rukmani Bai, Nicolai Lang, Michael Fleischhauer, Hans Peter Büchler, Thierry Lahaye, and Antoine Browaeys. Realization of a density-dependent Peierls phase in a synthetic, spin-orbit coupled Rydberg system. *Phys. Rev. X*, 10:021031, May 2020.

[33] Sebastian Greschner and Luis Santos. Anyon Hubbard model in one-dimensional optical lattices. *Phys. Rev. Lett.*, 115:053002, 2015.

[34] Christian Schweizer, Fabian Grusdt, Moritz Berngruber, Luca Barbiero, Eugene Demler, Nathan Goldman, Immanuel Bloch, and Monika Aidelsburger. Floquet approach to Z2 lattice gauge theories with ultracold atoms in optical lattices. *Nature Physics*, 15(11):1168–1173, 2019.

[35] Frederik Görg, Kilian Sandholzer, Joaquín Minguzzi, Rémi Desbuquois, Michael Messer, and Tilman Esslinger. Realization of density-dependent Peierls phases to engineer quantized gauge fields coupled to ultracold matter. *Nat. Phys.*, 15(11):1161–1167, 2019.

[36] André Eckardt and Egidijus Anisimovas. High-frequency approximation for periodically driven quantum systems from a Floquet-space perspective. *New Journal of Physics*, 17(9):093039, sep 2015.

[37] André Eckardt. Colloquium: Atomic quantum gases in periodically driven optical lattices. *Rev. Mod. Phys.*, 89:011004, Mar 2017.

[38] Peter Hänggi. *Driven quantum systems.* Lecture Notes: University of Augsburg, 10 2018.

[39] Dallin S. Durfee and Wolfgang Ketterle. Experimental studies of Bose-Einstein condensation. *Opt. Express*, 2(8):299–313, Apr 1998.

[40] L.P. Pítajevskíj and S. Stringari. *Bose-Einstein Condensation*. International Series of Monographs on Physics. Clarendon Press, 2003.

[41] Tao Wang, Shijie Hu, Sebastian Eggert, Michael Fleischhauer, Axel Pelster, and Xue-Feng Zhang. Floquet-induced superfluidity with periodically modulated interactions of two-species hardcore bosons in a one-dimensional optical lattice. *Phys. Rev. Research*, 2:013275, Mar 2020.

[42] Sebastian Eggert. One-dimensional quantum wires: A pedestrian approach to bosonization. *Lecture notes Foresight Summer School Korea*, August 2007.

[43] Thierry Giamarchi. Quantum physics in one dimension. 01 Oxford University Press 2004.

[44] S.H. Strogatz. *Nonlinear Dynamics and Chaos with Student Solutions Manual: With Applications to Physics, Biology, Chemistry, and Engineering, Second Edition*. CRC Press, 2018.

[45] Sin-itiro Tomonaga. Remarks on Bloch's Method of Sound Waves applied to Many-Fermion Problems. *Progress of Theoretical Physics*, 5(4):544–569, 07 1950.

[46] Daniel C. Mattis and Elliott H. Lieb. Exact solution of a many-fermion system and its associated boson field. *Journal of Mathematical Physics*, 6(2):304–312, 1965.

[47] F. D. M. Haldane. Luttinger liquid theory of one-dimensional quantum fluids. i. properties of the Luttinger model and their extension to the general 1d interacting spinless fermi gas. *Journal of Physics C: Solid State Physics*, 14(19):2585–2609, jul 1981.

[48] F. D. M. Haldane. Effective harmonic-fluid approach to low-energy properties of one-dimensional quantum fluids. *Physical Review Letters*, 47:1840–1843, Dec 1981.

[49] H.J. Schulz. Interacting electrons in one dimension: Luttinger liquids. *Physica C: Superconductivity*, 235-240:217–220, 1994.

[50] D. Sénéchal. An introduction to bosonization. *arXiv e-prints*, pages cond–mat/9908262, August 1999.

[51] Thierry Giamarchi. Quantum physics in one dimension. *Oxford University Press 2004*, 01 2004.

[52] M. A. Cazalilla, R. Citro, T. Giamarchi, E. Orignac, and M. Rigol. One dimensional bosons: From condensed matter systems to ultracold gases. *Rev. Mod. Phys.*, 83:1405–1466, Dec 2011.

[53] Jan von Delft and Herbert Schoeller. Bosonization for beginners — refermionization for experts. *Ann. Phys. (Berlin)*, 7(4):225–305, 1998.

[54] A. M. Chang. Chiral luttinger liquids at the fractional quantum hall edge. *Rev. Mod. Phys.*, 75:1449–1505, Nov 2003.

[55] E. Orignac and T. Giamarchi. Weakly disordered spin ladders. *Phys. Rev. B*, 57:5812–5829, Mar 1998.

[56] Serena Fazzini and Arianna Montorsi. Hidden charge orders in low-dimensional Mott insulators. *Applied Sciences*, 9:784, 02 2019.

[57] Adilet Imambekov, Thomas L. Schmidt, and Leonid I. Glazman. One-dimensional quantum liquids: Beyond the luttinger liquid paradigm. *Rev. Mod. Phys.*, 84:1253–1306, Sep 2012.

[58] Adilet Imambekov and Leonid I. Glazman. Universal theory of nonlinear luttinger liquids. *Science*, 323(5911):228–231, 2009.

[59] F. H. L. Essler, R. G. Pereira, and I. Schneider. Spin-charge-separated quasiparticles in one-dimensional quantum fluids. *Phys. Rev. B*, 91:245150, Jun 2015.

[60] J. M. Luttinger. An exactly soluble model of a many-fermion system. *Journal of Mathematical Physics*, 4(9):1154–1162, 1963.

[61] M A Cazalilla. Bosonizing one-dimensional cold atomic gases. *Journal of Physics B: Atomic, Molecular and Optical Physics*, 37(7):1–47, mar 2004.

[62] D. Schmeltzer. Persistent current for a luttinger liquid. *Phys. Rev. B*, 47:7591–7593, Mar 1993.

[63] F. Acerbi, G. Morchio, and F. Strocchi. Nonregular representations of ccr algebras and algebraic fermion bosonization. *Reports on Mathematical Physics*, 33(1):7–19, 1993.

[64] John L. Cardy. Conformal invariance and surface critical behavior. *Nuclear Physics B*, 240(4):514–532, 1984.

[65] Sebastian Eggert and Ian Affleck. Magnetic impurities in half-integer-spin heisenberg antiferromagnetic chains. *Phys. Rev. B*, 46:10866–10883, Nov 1992.

[66] Ann E. Mattsson, Sebastian Eggert, and Henrik Johannesson. Properties of a luttinger liquid with boundaries at finite temperature and size. *Phys. Rev. B*, 56:15615–15628, Dec 1997.

[67] Annabelle Bohrdt, Kevin Jägering, Sebastian Eggert, and Imke Schneider. Dynamic structure factor in impurity-doped spin chains. *Phys. Rev. B*, 98:020402, Jul 2018.

[68] Anton Deitmar and Siegfried Echterhoff. *Principles of Harmonic Analysis*. Springer International Publishing, 2014.

[69] J. Sirker. The luttinger liquid and integrable models. *International Journal of Modern Physics B*, 26, 07 2012.

[70] Guillaume Lang, Frank Hekking, and Anna Minguzzi. Ground-state energy and excitation spectrum of the Lieb-Liniger model : accurate analytical results and conjectures about the exact solution. *SciPost Phys.*, 3:003, 2017.

[71] Yu-Zhu Jiang, Yang-Yang Chen, and Xi-Wen Guan. Understanding many-body physics in one dimension from the lieb–liniger model. *Chinese Physics B*, 24(5):050311, apr 2015.

[72] Robert Lynch. The quantum phase problem: a critical review. *Physics Reports*, 256(6):367–436, 1995.

[73] N. Didier, A. Minguzzi, and F. W. J. Hekking. Complete series for the off-diagonal correlations of a one-dimensional interacting bose gas. *Phys. Rev. A*, 80:033608, Sep 2009.

[74] N. D. Mermin and H. Wagner. Absence of ferromagnetism or antiferromagnetism in one- or two-dimensional isotropic heisenberg models. *Phys. Rev. Lett.*, 17:1133–1136, Nov 1966.

[75] P. C. Hohenberg. Existence of long-range order in one and two dimensions. *Phys. Rev.*, 158:383–386, Jun 1967.

[76] Huan-Qiang Zhou, Jon Links, Mark D. Gould, and Ross H. McKenzie. Solvable models of bose–einstein condensates: A new algebraic bethe ansatz scheme. *Journal of Mathematical Physics*, 44(10):4690–4701, 2003.

[77] Huan-Qiang Zhou, Jon Links, Ross H McKenzie, and Xi-Wen Guan. Exact results for a tunnel-coupled pair of trapped bose einstein condensates. *Journal of Physics A: Mathematical and General*, 36(7):L113–L119, feb 2003.

[78] Jon Links, Huan-Qiang Zhou, Ross H McKenzie, and Mark D Gould. Algebraic bethe ansatz method for the exact calculation of energy spectra and form factors: applications to models of Bose Einstein condensates and metallic nanograins. *Journal of Physics A: Mathematical and General*, 36(19):R63–R104, apr 2003.

[79] Gilberto N. Santos Filho. Current algebra for a generalized two-sites bose-hubbard model. In Sergio Duarte, Jean-Pierre Gazeau, Sofiane Faci, Tobias Micklitz, Ricardo Scherer, and Francesco Toppan, editors, *Physical and Mathematical Aspects of Symmetries*, pages 299–304, Cham, 2017. Springer International Publishing.

[80] G. J. Milburn, J. Corney, E. M. Wright, and D. F. Walls. Quantum dynamics of an atomic Bose-Einstein condensate in a double-well potential. *Phys. Rev. A*, 55:4318–4324, Jun 1997.

[81] R Gati and M K Oberthaler. A bosonic josephson junction. *Journal of Physics B: Atomic, Molecular and Optical Physics*, 40(10):R61–R89, may 2007.

[82] F. Trimborn. Phasenraumdynamik des Bose Hubbard Modells. Master's thesis, University of Kaiserslautern, 2007.

[83] Eva-Maria Graefe and Chiara Liverani. Mean-field approximation for a bose–hubbard dimer with complex interaction strength. *Journal of Physics A: Mathematical and Theoretical*, 46(45):455201, oct 2013.

[84] G. Mazzarella, L. Salasnich, A. Parola, and F. Toigo. Coherence and entanglement in the ground state of a bosonic josephson junction: From macroscopic schrödinger cat states to separable fock states. *Phys. Rev. A*, 83:053607, May 2011.

[85] A. M. Perelomov. Coherent states for arbitrary lie group. *Communications in Mathematical Physics*, 26(3):222–236, 1972.

[86] Wei-Min Zhang, Da Hsuan Feng, and Robert Gilmore. Coherent states: Theory and some applications. *Rev. Mod. Phys.*, 62:867–927, Oct 1990.

[87] Wanzhou Zhang, Ernv Fan, Tony Scott, and Yunbo Zhang. Beats, broken-symmetry superfluid on a one dimensional anyon hubbard model. 11 2015.

[88] Wanzhou Zhang, Sebastian Greschner, Ernv Fan, Tony Scott, and Yunbo Zhang. Ground state properties of the one-dimensional unconstrained pseudo-anyon hubbard model. *Phys. Rev. A*, 95:053614, 05 2017.

[89] V.Z. Enol'skii, V.B. Kuznetsov, and M. Salerno. On the quantum inverse scattering method for the dst dimer. *Physica D: Nonlinear Phenomena*, 68(1):138 – 152, 1993.

[90] Links Jon and Katrina Hibberd. Bethe ansatz solutions of the bose-hubbard dimer. *Symmetry, Integrability and Geometry: Methods and Applications*, 2, 12 2006.

[91] P. Jordan. Der zusammenhang der symmetrischen und linearen gruppen und das mehrkörperproblem. *Zeitschrift für Physik*, 94(7):531–535, 1935.

[92] R. Peierls. Zur theorie des diamagnetismus von leitungselektronen. *Zeitschrift für Physik*, 80(11):763–791, 1933.

[93] Natig Atakishiyev, Maurice Kibler, and Kurt Wolf. Su(2) and su(1,1) approaches to phase operators and temporally stable phase states: Applications to mutually unbiased bases and discrete fourier transforms. *Symmetry*, 2, 09 2010.

[94] Emilio Cobanera and Gerardo Ortiz. Equivalence of topological insulators and superconductors. *Phys. Rev. B*, 92:155125, Oct 2015.

[95] P. H. Seagraves. *Representation of Permutation Operators in Quantum Mechanics*. PhD thesis, University of British Columbia, 1964.

[96] Norman Oelkers and Jon Links. Ground-state properties of the attractive one-dimensional bose-hubbard model. *Phys. Rev. B*, 75:115119, Mar 2007.

[97] V. Korepin, A. Izergin, and N. Bogoliubov. Quantum inverse scattering method and correlation functions. *Journal of Soviet Mathematics*, 31, 02 1993.

[98] Michio Jimbo. Introduction to the yang-baxter equation. *International Journal of Modern Physics A*, 04(15):3759–3777, 1989.

[99] Peter D. Lax. Integrals of nonlinear equations of evolution and solitary waves. *Communications on Pure and Applied Mathematics*, 21(5):467–490, 1968.

[100] A. G. Izergin and V. E. Korepin. Pauli principle for one-dimensional bosons and the algebraic bethe ansatz. *Letters in Mathematical Physics*, 6(4):283–288, 1982.

[101] Xiaoguang Wang, Barry Sanders, and Pan. Entangled coherent states for systems with su(2) and su(1,1) symmetries. *J. Phys. A: Math. Gen.*, 33:7451, 10 2000.

[102] R. Aldrovandi and P. Ferreira. Quantum pendulum. *American Journal of Physics - AMER J PHYS*, 48:660–664, 08 1980.

[103] Gerhard Wolf. On the asymptotic behavior of the fourier coefficients of mathieu functions. *Journal of research of the National Institute of Standards and Technology*, 113(27096109):11–15, February 2008.

[104] Roberto Coïsson, Graziano Vernizzi, and Xiaoke Yang. *Mathieu functions and numerical solutions of the Mathieu equation*. September 2009.

[105] Wolfgang Schweizer. *Mathieu Functions*, pages 165–179. Springer International Publishing, Cham, 2021.

[106] P. Caruthers and M. Nieto. Phase and angle variables in quantum mechanics. *Rev. Mod. Phys.*, 40:411–440, Apr 1968.

[107] Guy Bonneau, Jacques Faraut, and Galliano Valent. Self-adjoint extensions of operators and the teaching of quantum mechanics. *American Journal of Physics*, 69(3):322–331, 2001.

[108] A. Grigoryan. *Heat Kernel and Analysis on Manifolds.* AMS/IP studies in advanced mathematics. American Mathematical Soc.

[109] Fabrice Baudoin. *Diffusion processes and stochastic calculus.* Zürich: European Mathematical Society (EMS), 2014.

[110] Eugene Demler. Strongly correlated systems in atomic and condensed matter physics. `http://cmt.harvard.edu/demler/TEACHING/Physics284/physics284.html`, 2011. lecture notes.

[111] C.J. Foot and D.P. Foot. *Atomic Physics.* Oxford Master Series in Physics. OUP Oxford, 2005.

[112] Franco Dalfovo, Lev Pitaevskii, and Sandro Stringari. Bose einstein condensates. *Uspekhi Fizicheskikh Nauk - USP FIZ NAUK*, 167, 12 2005.

[113] Robert Seiringer. The excitation spectrum for weakly interacting bosons. *Communications in Mathematical Physics*, 306(2):565–578, 2011.

[114] E.H. Lieb, R. Seiringer, J.P. Solovej, and J. Yngvason. *The Mathematics of the Bose Gas and its Condensation.* Oberwolfach Seminars. Birkhäuser Basel, 2005.

[115] Ovidiu I Pâtu, Vladimir E Korepin, and Dmitri V Averin. Correlation functions of one-dimensional lieb–liniger anyons. *J. Phys. A*, 40(50):14963, 2007.

[116] Ovidiu I Pâţu, Vladimir E Korepin, and Dmitri V Averin. One-dimensional impenetrable anyons in thermal equilibrium: Ii. determinant representation for the dynamic correlation functions. *J. Phys. A*, 41(25):255205, 2008.

[117] M T Batchelor, X-W Guan, and J-S He. The bethe ansatz for 1d interacting anyons. *J. Stat. Mech.*, 2007(03):P03007, 2007.

[118] M. T. Batchelor, X.-W. Guan, and N. Oelkers. One-dimensional interacting anyon gas: Low-energy properties and haldane exclusion statistics. *Phys. Rev. Lett.*, 96:210402, Jun 2006.

[119] Pawel Blasiak, Andrzej Horzela, Karol Penson, Allan Solomon, and Gérard Duchamp. Combinatorics and boson normal ordering: A gentle introduction. *Am. J. Phys*, 75, April 2007.

[120] Peng Zhang, Koichiro Yaji, Takahiro Hashimoto, Yuichi Ota, Takeshi Kondo, Kozo Okazaki, Zhijun Wang, Jinsheng Wen, G. D. Gu, Hong Ding, and Shik Shin. Observation of topological superconductivity on the surface of an iron-based superconductor. *Science*, 360(6385):182–186, 2018.

[121] B.C. Rennie and A.J. Dobson. On stirling numbers of the second kind. *Journal of Combinatorial Theory*, 7(2):116 – 121, 1969.

[122] D. van Oosten, P. van der Straten, and H. T. C. Stoof. Quantum phases in an optical lattice. *Phys. Rev. A*, 63:053601, Apr 2001.

[123] Marin Bukov. Bose-fermi mixtures: A mean-field study. Master's thesis, LMU Munich, 2013.

[124] M. A. Cazalilla, R. Citro, T. Giamarchi, E. Orignac, and M. Rigol. One dimensional bosons: From condensed matter systems to ultracold gases. *Rev. Mod. Phys.*, 83:1405–1466, 2011.

[125] Vincent Flynn, Emilio Cobanera, and Lorenza Viola. Deconstructing effective non-hermitian dynamics in quadratic bosonic hamiltonians. *New Journal of Physics*, 03 2020.

[126] Flynn, Vincent P., Cobanera, Emilio, and Viola, Lorenza. Restoring number conservation in quadratic bosonic hamiltonians with dualities. *EPL*, 131(4):40006, 2020.

[127] R. Rossignoli and A. M. Kowalski. Complex modes in unstable quadratic bosonic forms. *Phys. Rev. A*, 72:032101, Sep 2005.

[128] S. Greschner, G. Sun, D. Poletti, and L. Santos. Density-dependent synthetic gauge fields using periodically modulated interactions. *Phys. Rev. Lett.*, 113:215303, Nov 2014.

[129] Herbert Wagner. Long-wavelength excitations and the goldstone theorem in many-particle systems with "broken symmetries". *Zeitschrift für Physik*, 195(3):273–299, 1966.

[130] M. A. Cazalilla. Differences between the Tonks regimes in the continuum and on the lattice. *Phys. Rev. A*, 70:041604, Oct 2004.

[131] M. Cazalilla. One-dimensional optical lattices and impenetrable bosons. *Physical Review A*, 67, 01 2003.

[132] Ian Affleck, Walter Hofstetter, David R Nelson, and Ulrich Schollwöck. Non-hermitian luttinger liquids and flux line pinning in planar superconductors. *Journal of Statistical Mechanics: Theory and Experiment*, 2004(10):P10003, oct 2004.

[133] A. K. Kolezhuk, F. Heidrich-Meisner, S. Greschner, and T. Vekua. Frustrated spin chains in strong magnetic field: Dilute two-component bose gas regime. *Phys. Rev. B*, 85:064420, Feb 2012.

[134] M. Olshanii. Atomic scattering in the presence of an external confinement and a gas of impenetrable bosons. *Phys. Rev. Lett.*, 81:938–941, Aug 1998.

[135] M Valiente and D Petrosyan. Two-particle states in the hubbard model. *Journal of Physics B: Atomic, Molecular and Optical Physics*, 41(16):161002, aug 2008.

[136] W Hofstetter, I Affleck, D Nelson, and U Schollwöck. Non-hermitian luttinger liquids and vortex physics. *Europhysics Letters (EPL)*, 66(2):178–184, apr 2004.

[137] M. Cazalilla and AF Ho. Instabilities in binary mixtures of one-dimensional quantum degenerate gases. *Phys. Rev. Lett.*, 91:150403, 11 2003.

[138] T.C. Choy and F.D.M. Haldane. Failure of Bethe-ansatz solutions of generalisations of the hubbard chain to arbitrary permutation symmetry. *Physics Letters A*, 90(1):83 – 84, 1982.

[139] D F James and J Jerke. Effective hamiltonian theory and its applications in quantum information. *Canadian Journal of Physics*, 85(6):625–632, 2007.

[140] G. I. Japaridze and A. P. Kampf. Weak-coupling phase diagram of the extended Hubbard model with correlated-hopping interaction. *Phys. Rev. B*, 59:12822–12829, May 1999.

[141] S Fazzini, L Barbiero, and A Montorsi. Low energy quantum regimes of 1d dipolar hubbard model with correlated hopping. *Journal of Physics: Conference Series*, 841:012016, may 2017.

[142] Zhu Ren-Gui and Wang An-Min. Limiting case of 1d delta anyon model. *Communications in Theoretical Physics*, 50(6):1265–1268, dec 2008.

[143] Pasquale Calabrese and Mihail Mintchev. Correlation functions of one-dimensional anyonic fluids. *Phys. Rev. B*, 75:233104, Jun 2007.

[144] M T Batchelor, X-W Guan, and A Kundu. One-dimensional anyons with competing delta-function and derivative delta-function potentials. *Journal of Physics A: Mathematical and Theoretical*, 41(35):352002, jul 2008.

[145] Fabrizio Anfuso and Sebastian Eggert. Luttinger liquid in a finite one-dimensional wire with box-like boundary conditions. *Phys. Rev. B*, 68:241301, Dec 2003.

[146] Reinhold Egger and Hermann Grabert. Friedel oscillations for interacting fermions in one dimension. *Phys. Rev. Lett.*, 75:3505–3508, Nov 1995.

[147] Stefan Rommer and Sebastian Eggert. Spin- and charge-density oscillations in spin chains and quantum wires. *Phys. Rev. B*, 62:4370–4382, Aug 2000.

[148] J. Friedel. Metallic alloys. *Il Nuovo Cimento (1955-1965)*, 7(2):287–311, 1958.

[149] Frank Wilczek. Quantum mechanics of fractional-spin particles. *Phys. Rev. Lett.*, 49:957–959, 1982.

[150] Fabian Essler, Holger Frahm, Frank Göhmann, Andreas Klümper, and Vladimir Korepin. The one-dimensional Hubbard model. *The One-Dimensional Hubbard Model, Cambridge, UK: Cambridge University Press*, 08 2010.

[151] Dominik Muth, Michael Fleischhauer, and Bernd Schmidt. Discretized versus continuous models of p-wave interacting fermions in one dimension. *Physical Review A*, 82:013602, Jul 2010.

[152] Sebastian Greschner, Daniel Huerga, Gaoyong Sun, Dario Poletti, and Luis Santos. Density-dependent synthetic magnetism for ultracold atoms in optical lattices. *Phys. Rev. B*, 92:115120, Sep 2015.

[153] Yu. M. Shirokov. Algebra of one-dimensional generalized functions. *Theoretical and Mathematical Physics*, 39(3):471–477, 1979.

[154] Manuel Valiente. Bose-fermi dualities for arbitrary one-dimensional quantum systems in the universal low-energy regime. *Phys. Rev. A*, 102:053304, Nov 2020.

[155] Manuel Valiente. Universal duality transformations in interacting one-dimensional quantum systems. *Phys. Rev. A*, 103:L021302, Feb 2021.

[156] Alan Sexton. Abramowitz and stegun a resource for mathematical document analysis. In *Abramowitz and Stegun A Resource for Mathematical Document Analysis*, volume 7362, 07 2012.

[157] L. Accardi and A. Boukas. Powers of the delta function. *Quantum Probability and Infinite Dimensional Analysis, WORLD SCIENTIFIC*, July 2007.

[158] Jens Fischer and Rudolf Stens. On inverses of the dirac comb. *Mathematics, Multidisciplinary Digital Publishing Institute*, 7:1196, 12 2019.

[159] U. Aglietti, L. Griguolo, R. Jackiw, S.-Y. Pi, and D. Seminara. Anyons and chiral solitons on a line. *Phys. Rev. Lett.*, 77:4406–4409, Nov 1996.

[160] Silvio J. Rabello. A gauge theory of one-dimensional anyons. *Phys. Lett. B*, 363(3):180 – 183, 1995.

[161] H. Kleinert. Path integrals over fluctuating non-relativistic fermion orbits. *Physics Letters B*, 225(4):381 – 384, 1989.

[162] Daniel Ferrante. Lattice quantum field theory — a constructive approach. *Lecture Notes: Brown university*, May 2002.

[163] H. Bethe. Zur theorie der metalle. *Zeitschrift für Physik*, 71(3):205–226, 1931.

[164] Bireswar Basu-Mallick, Tanaya Bhattacharyya, Diptiman Sen Sinp, Kolkata, IISc., and Bangalore. Quantum bound states for a derivative nonlinear schrödinger model and number theory. *Modern Physics Letters A*, 19:2697–2706, 2004.

[165] Ovidiu Patu, Vladimir Korepin, and Dmitri Averin. Correlation functions of one-dimensional lieb-liniger anyons. *Journal of Physics A Mathematical and Theoretical*, 40, 07 2007.

[166] H. Kleinert. Path integrals over fluctuating non-relativistic fermion orbits. *Phys. Lett. B*, 225(4):381 – 384, 1989.

[167] M. T. Batchelor and X.-W. Guan. Generalized exclusion statistics and degenerate signature of strongly interacting anyons. *Phys Rev B*, 74:195121, Nov 2006.

[168] R Citro, S De Palo, E Orignac, P Pedri, and M-L Chiofalo. Luttinger hydrodynamics of confined one-dimensional bose gases with dipolar interactions. *New Journal of Physics*, 10(4):045011, apr 2008.

[169] Stefan A. Söffing, Michael Bortz, Imke Schneider, Alexander Struck, Michael Fleischhauer, and Sebastian Eggert. Wigner crystal versus friedel oscillations in the one-dimensional hubbard model. *Phys. Rev. B*, 79:195114, May 2009.

[170] Steven R. White. Density matrix formulation for quantum renormalization groups. *Phys. Rev. Lett.*, 69:2863–2866, Nov 1992.

[171] Steven R. White. Density-matrix algorithms for quantum renormalization groups. *Phys. Rev. B*, 48:10345–10356, Oct 1993.

[172] Kevin Jägering and Shijie Hu. Private communications. University of Kaiserslautern, AG Eggert.

[173] U. Schollwöck. The density-matrix renormalization group. *Rev. Mod. Phys.*, 77:259–315, Apr 2005.

[174] Riccardo Fantoni. How should we choose the boundary conditions in a simulation which could detect anyons in one and two dimensions? *Journal of Low Temperature Physics*, 202(1):247–262, 2021.

[175] Matthias Plaschke. Local anyonic quantum fields on the circle leading to cone-local anyons in two dimensions. *Letters in Mathematical Physics*, 105(8):1033–1055, 2015.

[176] Sebastian Eggert and Ian Affleck. Magnetic impurities in half-integer-spin heisenberg antiferromagnetic chains. *Phys. Rev. B*, 46:10866–10883, Nov 1992.

[177] Jari M. Kinaret, Mats Jonson, Robert I. Shekhter, and Sebastian Eggert. Interplay of coulomb blockade and aharonov-bohm resonances in a luttinger liquid. *Phys. Rev. B*, 57:3777–3780, Feb 1998.

[178] A. A Odintsov, W Smit, and H Yoshioka. Persistent current and correlation effects in carbon nanotubes. *Europhysics Letters (EPL)*, 45(5):598–604, mar 1999.

[179] V. Meden and U. Schollwöck. Persistent currents in mesoscopic rings: A numerical and renormalization group study. *Phys. Rev. B*, 67:035106, Jan 2003.

[180] Marco Cominotti, Davide Rossini, Matteo Rizzi, Frank Hekking, and Anna Minguzzi. Optimal persistent currents for interacting bosons on a ring with a gauge field. *Phys. Rev. Lett.*, 113:025301, Jul 2014.

[181] Geva Arwas, Doron Cohen, Frank Hekking, and Anna Minguzzi. Resonant persistent currents for ultracold bosons on a lattice ring. *Phys. Rev. A*, 96:063616, Dec 2017.

[182] M. Pletyukhov and V. Gritsev. Persistent currents in a multicomponent tomonaga-luttinger liquid: Application to a mesoscopic semiconductor ring with spin-orbit interaction. *Phys. Rev. B*, 70:165316, Oct 2004.

[183] Daniel C. Mattis and Elliot H. Lieb. *Exact Solution of a Many-Fermion System and Its Associated Boson Field*, pages 98–106.

[184] Christophe Mora and Yvan Castin. Extension of Bogoliubov theory to quasicondensates. *Phys. Rev. A*, 67:053615, May 2003.

[185] Florian Lange, Satoshi Ejima, and Holger Fehske. Anyonic haldane insulator in one dimension. *Phys. Rev. Lett.*, 118:120401, Mar 2017.

[186] Emanuele G. Dalla Torre, Erez Berg, and Ehud Altman. Hidden order in 1d Bose insulators. *Phys. Rev. Lett.*, 97:260401, Dec 2006.

[187] Erez Berg, Emanuele G. Dalla Torre, Thierry Giamarchi, and Ehud Altman. Rise and fall of hidden string order of lattice bosons. *Phys. Rev. B*, 77:245119, Jun 2008.

[188] Steffen Patrick Rath, Wolfgang Simeth, Manuel Endres, and Wilhelm Zwerger. Non-local order in Mott insulators, duality and Wilson loops. *Annals of Physics*, 334:256–271, 2013.

[189] Ian Affleck, Tom Kennedy, Elliott H. Lieb, and Hal Tasaki. Rigorous results on valence-bond ground states in antiferromagnets. *Phys. Rev. Lett.*, 59:799–802, Aug 1987.

[190] Tom Kennedy and Hal Tasaki. Hidden $z_2 \times z_2$ symmetry breaking in Haldane-gap antiferromagnets. *Phys. Rev. B*, 45:304–307, Jan 1992.

[191] Tom Kennedy and Hal Tasaki. Hidden symmetry breaking and the Haldane phase in S=1 quantum spin chains. *Communications in Mathematical Physics*, 147(3):431–484, 1992.

[192] Xie Chen, Zheng-Cheng Gu, and Xiao-Gang Wen. Classification of gapped symmetric phases in one-dimensional spin systems. *Phys. Rev. B*, 83:035107, Jan 2011.

[193] Frank Pollmann and Ari M. Turner. Detection of symmetry-protected topological phases in one dimension. *Phys. Rev. B*, 86:125441, Sep 2012.

[194] Frank Pollmann, Erez Berg, Ari M. Turner, and Masaki Oshikawa. Symmetry protection of topological phases in one-dimensional quantum spin systems. *Phys. Rev. B*, 85:075125, Feb 2012.

[195] H. J. Schulz. Phase diagrams and correlation exponents for quantum spin chains of arbitrary spin quantum number. *Phys. Rev. B*, 34:6372–6385, Nov 1986.

[196] Yohei Fuji. Effective field theory for one-dimensional valence-bond-solid phases and their symmetry protection. *Phys. Rev. B*, 93:104425, Mar 2016.

[197] Xiaolong Deng, Roberta Citro, Edmond Orignac, Anna Minguzzi, and Luis Santos. Polar bosons in one-dimensional disordered optical lattices. *Phys. Rev. B*, 87:195101, May 2013.

[198] Satoshi Ejima and H. Fehske. Entanglement properties of the nontrivial haldane insulator in the 1d extended bose-hubbard model. *Journal of Physics: Conference Series*, 592:012134, March 2015.

[199] S. Baier, J. Mark M., D. Petter, K. Aikawa, L. Chomaz, Z. Cai, M. Baranov, P. Zoller, and F. Ferlaino. Extended Bose-hubbard models with ultracold magnetic atoms. *Science*, 352(6282):201–205, April 2016.

[200] M. Dalmonte, M. Di Dio, L. Barbiero, and F. Ortolani. Homogeneous and inhomogeneous magnetic phases of constrained dipolar bosons. *Phys. Rev. B*, 83:155110, Apr 2011.

[201] F. D. M. Haldane. Nonlinear field theory of large-spin Heisenberg antiferromagnets: Semiclassically quantized solitons of the one-dimensional easy-axis néel state. *Phys. Rev. Lett.*, 50:1153–1156, Apr 1983.

[202] F.D.M. Haldane. Continuum dynamics of the 1-d Heisenberg antiferromagnet: Identification with the o(3) nonlinear sigma model. *Physics Letters A*, 93(9):464–468, 1983.

[203] Ian Affleck and F. D. M. Haldane. Critical theory of quantum spin chains. *Phys. Rev. B*, 36:5291–5300, Oct 1987.

[204] I Affleck. Quantum spin chains and the haldane gap. *IOP Publishing„ 3047-3072*, 1(19):3047–3072, may 1989.

[205] J. Sirker, R. G. Pereira, and I. Affleck. Diffusion and ballistic transport in one-dimensional quantum systems. *Phys. Rev. Lett.*, 103:216602, Nov 2009.

[206] Ian Affleck and Elliott H. Lieb. A proof of part of Haldane's conjecture on spin chains. *Letters in Mathematical Physics*, 12(1):57–69, 1986.

[207] Yoshiko Ogata, Yuji Tachikawa, and Hal Tasaki. General Lieb-Schultz-Mattis type theorems for quantum spin chains. *Communications in Mathematical Physics*, 385(1):79–99, 2021.

[208] Kyle Wamer, Miklós Lajkó, Frédéric Mila, and Ian Affleck. Generalization of the Haldane conjecture to su(n) chains. *Nuclear Physics B*, 952:114932, 2020.

[209] Marcel den Nijs and Koos Rommelse. Preroughening transitions in crystal surfaces and valence-bond phases in quantum spin chains. *Phys. Rev. B*, 40:4709–4734, Sep 1989.

[210] P. Lowdon. Confinement and the cluster decomposition property in QCD. *Nuclear and Particle Physics Proceedings*, 282-284:168–172, 2017. 19th International Conference in Quantum Chromodynamics.

[211] Aron Beekman, Louk Rademaker, and Jasper van Wezel. An introduction to spontaneous symmetry breaking. *SciPost Physics*, dec 2019.

[212] T. Holstein and H. Primakoff. Field dependence of the intrinsic domain magnetization of a ferromagnet. *Phys. Rev.*, 58:1098–1113, Dec 1940.

[213] D. Jaksch, C. Bruder, J. I. Cirac, C. W. Gardiner, and P. Zoller. Cold bosonic atoms in optical lattices. *Phys. Rev. Lett.*, 81:3108–3111, Oct 1998.

[214] Kuldeep Suthar, Rebecca Kraus, Hrushikesh Sable, Dilip Angom, Giovanna Morigi, and Jakub Zakrzewski. Staggered superfluid phases of dipolar bosons in two-dimensional square lattices. *Phys. Rev. B*, 102:214503, Dec 2020.

[215] J. Eisert, M. Cramer, and M. B. Plenio. Colloquium: Area laws for the entanglement entropy. *Rev. Mod. Phys.*, 82:277–306, Feb 2010.

[216] J. Eisert. Entanglement and tensor network states. *Modeling and Simulation 3, 520*, 2013.

[217] Yimin Ge and Jens Eisert. Area laws and efficient descriptions of quantum many-body states. *New Journal of Physics*, 18(8):083026, aug 2016.

[218] Matthew B. Hastings and Tohru Koma. Spectral gap and exponential decay of correlations. *Communications in Mathematical Physics*, 265(3):781–804, 2006.

[219] Bruno Nachtergaele and Robert Sims. Lieb-Robinson bounds and the exponential clustering theorem. *Communications in Mathematical Physics*, 265(1):119–130, 2006.

[220] Elliott H. Lieb and Derek W. Robinson. The finite group velocity of quantum spin systems. *Communications in Mathematical Physics*, 28(3):251–257, 1972.

[221] Jean Zinn-Justin. *Quantum Field Theory and Critical Phenomena.* Oxford University Press, jun 2002.

[222] Jean Zinn-Justin. *Phase Transitions and Renormalization Group.* Oxford University Press, jul 2007.

[223] Michael A. Nielsen and Isaac L. Chuang. *Quantum Computation and Quantum Information: 10th Anniversary Edition.* Cambridge University Press, 2010.

[224] Dominik Janzing. *Entropy of Entanglement*, pages 205–209. Springer Berlin Heidelberg, Berlin, Heidelberg, 2009.

[225] Paul H. Ginsparg. Applied conformal field theory. In *Lecture notes: Fields, Strings and Critical Phenomena, (Les Houches, Session XLIX, 1988)*, 1988.

[226] Lei Wang, Ye-Hua Liu, Jakub Imriška, Ping Nang Ma, and Matthias Troyer. Fidelity susceptibility made simple: A unified quantum monte carlo approach. *Phys. Rev. X*, 5:031007, Jul 2015.

[227] Christopher Mudry, Akira Furusaki, Takahiro Morimoto, and Toshiya Hikihara. Quantum phase transitions beyond Landau-Ginzburg theory in one-dimensional space revisited. *Phys. Rev. B*, 99:205153, May 2019.

[228] Steven Weinberg. *The Quantum Theory of Fields*, volume 2. Cambridge University Press, 1996.

[229] Qiang Luo, Shijie Hu, Bin Xi, Jize Zhao, and Xiaoqun Wang. Ground-state phase diagram of an anisotropic spin-$\frac{1}{2}$ model on the triangular lattice. *Phys. Rev. B*, 95:165110, Apr 2017.

[230] V. L. Berezinskiĭ. Destruction of Long-range Order in One-dimensional and Two-dimensional Systems having a Continuous Symmetry Group I. Classical Systems. *Soviet Journal of Experimental and Theoretical Physics*, 32:493, January 1971.

[231] V. L. Berezinskiĭ. Destruction of Long-range Order in One-dimensional and Two-dimensional Systems Possessing a Continuous Symmetry Group. II. Quantum Systems. *Soviet Journal of Experimental and Theoretical Physics*, 34:610, January 1972.

[232] J M Kosterlitz and D J Thouless. Ordering, metastability and phase transitions in two-dimensional systems. *Journal of Physics C: Solid State Physics*, 6(7):1181–1203, apr 1973.

[233] Kenji Harada and Naoki Kawashima. Kosterlitz-Thouless transition of quantum XY model in two dimensions. *Journal of the Physical Society of Japan*, 67, 03 1998.

[234] M. Dalmonte, J. Carrasquilla, L. Taddia, E. Ercolessi, and M. Rigol. Gap scaling at Berezinskii-Kosterlitz-Thouless quantum critical points in one-dimensional Hubbard and Heisenberg models. *Phys. Rev. B*, 91:165136, Apr 2015.

[235] Ling Wang and Anders W. Sandvik. Critical level crossings and gapless spin liquid in the square-lattice spin-1/2 $J_1 - J_2$ Heisenberg antiferromagnet. *Phys. Rev. Lett.*, 121:107202, Sep 2018.

[236] Shohei Miyakoshi, Satoshi Nishimoto, and Yukinori Ohta. Entanglement properties of the Haldane phases: A finite system-size approach. *Phys. Rev. B*, 94:235155, Dec 2016.

[237] Michael Berry. Quantal phase factors accompanying adiabatic changes. *Proc. R Soc. A*, 392(1802):45–57, 1984.

[238] Shijie Hu, B. Normand, Xiaoqun Wang, and Lu Yu. Accurate determination of the gaussian transition in spin-1 chains with single-ion anisotropy. *Phys. Rev. B*, 84:220402, Dec 2011.

[239] H. V. Kruis, I. P. McCulloch, Z. Nussinov, and J. Zaanen. Geometry and the hidden order of Luttinger liquids: The universality of squeezed space. *Phys. Rev. B*, 70:075109, Aug 2004.

[240] J. K. Freericks and H. Monien. Strong-coupling expansions for the pure and disordered Bose-Hubbard model. *Phys. Rev. B*, 53:2691–2700, Feb 1996.

[241] Ann E. Mattsson, Sebastian Eggert, and Henrik Johannesson. Properties of a Luttinger liquid with boundaries at finite temperature and size. *Phys. Rev. B*, 56:15615–15628, Dec 1997.

[242] C. Degli Esposti Boschi, E. Ercolessi, F. Ortolani, and M. Roncaglia. On $\mathsf{c} = 1$ critical phases in anisotropic spin-1 chains. *The European Physical Journal B - Condensed Matter and Complex Systems*, 35(4):465–473, 2003.

[243] Mariana Malard. Sine-Gordon model: Renormalization group solution and applications. *Brazilian Journal of Physics*, 43(3):182–198, 2013.

[244] D. G. Shelton, A. A. Nersesyan, and A. M. Tsvelik. Antiferromagnetic spin ladders: Crossover between spin s=1/2 and s=1 chains. *Phys. Rev. B*, 53:8521–8532, Apr 1996.

[245] R. A. Santos, F. N. C. Paraan, V. E. Korepin, and A. Klümper. Entanglement spectra of the q-deformed Affleck-Kennedy-Lieb-Tasaki model and matrix product states. *EPL (Europhysics Letters)*, 98(3):37005, may 2012.

[246] Raul A Santos, Francis N C Paraan, Vladimir E Korepin, and Andreas Klümper. Entanglement spectra ofq-deformed higher spin VBS states. *Journal of Physics A: Mathematical and Theoretical*, 45(17):175303, apr 2012.

[247] Thomas Quella. Symmetry-protected topological phases beyond groups: The q-deformed bilinear-biquadratic spin chain. *Phys. Rev. B*, 103:054404, Feb 2021.

[248] A. Luther and I. Peschel. Calculation of critical exponents in two dimensions from quantum field theory in one dimension. *Phys. Rev. B*, 12:3908–3917, Nov 1975.

[249] Gerhard Müller, Hans Beck, and Jill C. Bonner. Zero-temperature dynamics of the $s = \frac{1}{2}$ linear Heisenberg antiferromagnet. *Phys. Rev. Lett.*, 43:75–78, Jul 1979.

[250] R G Pereira, J Sirker, J-S Caux, R Hagemans, J M Maillet, S R White, and I Affleck. Dynamical structure factor at small q for the XXZ spin-1/2 chain. *Journal of Statistical Mechanics: Theory and Experiment*, 2007(08):P08022–P08022, aug 2007.

[251] Guillaume Roux, A. Minguzzi, and Tommaso Roscilde. Dynamic structure factor of one-dimensional lattice bosons in a disordered potential: A spectral fingerprint of the bose-glass phase. *New Journal of Physics*, 15:055003, 05 2013.

[252] Rodrigo G. Pereira, Steven R. White, and Ian Affleck. Exact edge singularities and dynamical correlations in spin-1/2 chains. *Phys. Rev. Lett.*, 100:027206, Jan 2008.

[253] Rodrigo G. Pereira, Steven R. White, and Ian Affleck. Spectral function of spinless fermions on a one-dimensional lattice. *Phys. Rev. B*, 79:165113, Apr 2009.

[254] Hamed Karimi and Ian Affleck. Transverse spectral functions and dzyaloshinskii-moriya interactions in xxz spin chains. *Phys. Rev. B*, 84:174420, Nov 2011.

[255] I. S. Eliëns, F. B. Ramos, J. C. Xavier, and R. G. Pereira. Boundary versus bulk behavior of time-dependent correlation functions in one-dimensional quantum systems. *Phys. Rev. B*, 93:195129, May 2016.

[256] H. Lehmann. Über eigenschaften von ausbreitungsfunktionen und renormierungskonstanten quantisierter felder. *Il Nuovo Cimento (1943-1954)*, 11(4):342–357, 1954.

[257] S. Lorenzutta, Giuseppe Maino, Giuseppe Dattoli, Amalia Torre, and Cesare Chiccoli. Infinite-variable bessel functions of the anger type and the fourier expansions. *Reports on Mathematical Physics*, 39:163–176, 04 1997.

[258] Imke Schneider and Sebastian Eggert. Recursive method for the density of states in one dimension. *Phys. Rev. Lett.*, 104:036402, Jan 2010.

[259] Jesko Sirker and Michael Bortz. The openXXZ-chain: bosonization, the bethe ansatz and logarithmic corrections. *Journal of Statistical Mechanics: Theory and Experiment*, 2006(01):P01007–P01007, jan 2006.

[260] Michael Bortz and Jesko Sirker. Boundary susceptibility in the openXXZ-chain. *Journal of Physics A: Mathematical and General*, 38(26):5957–5977, jun 2005.

[261] N. Motoyama, H. Eisaki, and S. Uchida. Magnetic susceptibility of ideal spin 1 /2 heisenberg antiferromagnetic chain systems, sr_2cuo_3 and $srcuo_2$. *Phys. Rev. Lett.*, 76:3212–3215, Apr 1996.

[262] Sebastian Eggert, Ian Affleck, and Minoru Takahashi. Susceptibility of the spin 1/2 heisenberg antiferromagnetic chain. *Phys. Rev. Lett.*, 73:332–335, Jul 1994.

[263] C. N. Yang and C. P. Yang. One-dimensional chain of anisotropic spin-spin interactions. ii. properties of the ground-state energy per lattice site for an infinite system. *Phys. Rev.*, 150:327–339, Oct 1966.

[264] C. N. Yang and C. P. Yang. One-dimensional chain of anisotropic spin-spin interactions. i. proof of bethe's hypothesis for ground state in a finite system. *Phys. Rev.*, 150:321–327, Oct 1966.

[265] F C Alcaraz, M N Barber, M T Batchelor, R J Baxter, and G R W Quispel. Surface exponents of the quantum XXZ, Ashkin-Teller and Potts models. *Journal of Physics A: Mathematical and General*, 20(18):6397–6409, dec 1987.

[266] Hans Mikeska and Alexei Kolezhuk. One-dimensional magnetism. In *Lect. Notes Phys.*, volume 645, pages 1–83. June 2004.

[267] Fabio Franchini. The XXZ chain. In *An Introduction to Integrable Techniques for One-Dimensional Quantum Systems*, pages 71–92. Springer International Publishing, Cham, 2017.

[268] Mykhailo Rakov and Michael Weyrauch. Spin- 1/2 XXZ Heisenberg chain in a longitudinal magnetic field. *Physical Review B*, 100, October 2019.

[269] A. H. Bougourzi, M. Couture, and M. Kacir. Exact two-spinon dynamical correlation function of the one-dimensional Heisenberg model. *Phys. Rev. B*, 54:R12669–R12672, Nov 1996.

[270] Michael Karbach, Gerhard Müller, A. Hamid Bougourzi, Andreas Fledderjohann, and Karl-Heinz Mütter. Two-spinon dynamic structure factor of the one-dimensional s= Heisenberg antiferromagnet. *Phys. Rev. B*, 55:12510–12517, May 1997.

[271] Sergei Lukyanov and Véronique Terras. Long-distance asymptotics of spin–spin correlation functions for the XXZ spin chain. *Nuclear Physics B*, 654(3):323–356, 2003.

[272] Jean-Sébastien Caux, Rob Hagemans, and Jean Michel Maillet. Computation of dynamical correlation functions of Heisenberg chains: the gapless anisotropic regime. *Journal of Statistical Mechanics: Theory and Experiment*, 2005(09):P09003–P09003, sep 2005.

[273] N Kitanine, K K Kozlowski, J M Maillet, G Niccoli, N A Slavnov, and V Terras. Correlation functions of the open XXZ chain: II. *Journal of Statistical Mechanics: Theory and Experiment*, 2008(07):P07010, jul 2008.

[274] Jean-Sébastien Caux, Hitoshi Konno, Mark Sorrell, and Robert Weston. Exact form-factor results for the longitudinal structure factor of the massless XXZ model in zero field. *Journal of Statistical Mechanics: Theory and Experiment*, 2012(01):P01007, jan 2012.

[275] J. Sirker, R. G. Pereira, and I. Affleck. Conservation laws, integrability, and transport in one-dimensional quantum systems. *Phys. Rev. B*, 83:035115, Jan 2011.

[276] Rodrigo Pereirea. *Dynamical Correlations of S=1/2 Quantum Spin Chains*. PhD thesis, University of British Columbia, 2008.

[277] R. G. Pereira, J. Sirker, J.-S. Caux, R. Hagemans, J. M. Maillet, S. R. White, and I. Affleck. Dynamical spin structure factor for the anisotropic spin-1/2 Heisenberg chain. *Phys. Rev. Lett.*, 96:257202, Jun 2006.

[278] M. von Smoluchowski. Zur kinetischen Theorie der Brownschen Molekularbewegung und der Suspensionen. *Annalen der Physik*, 326(14):756–780, January 1906.

[279] Rüdiger Bessenrodt. Brownsche bewegung: Hundert Jahre Theorie der wichtigsten Brücke zwischen Mikro- und Makrophysik. *Physikalische Blätter*, 33(1):7–16, 1977.

[280] Frederick W. King. *Hilbert Transforms*, volume 2 of *Encyclopedia of Mathematics and its Applications*. Cambridge University Press, 2009.

[281] Inès Safi and H. J. Schulz. Interacting electrons with spin in a one-dimensional dirty wire connected to leads. *Phys. Rev. B*, 59:3040–3059, Jan 1999.

[282] T. H. Hansson, J. M. Leinaas, and J Myrheim. Dimensional reduction in anyon systems. *Nucl. Phys. B.*, 384(3):559–580, 1992.

Chapter 10

Acknowledgment

As the path to the completion of a *PhD* thesis can be arduous and rocky, I am thankful for everyone who accompanied me on my way. First of all I have to thank Prof. Sebastian Eggert for guiding me all the way from a diploma student until the end of my *PhD* career. I am grateful for all your support and for sharing your knowledge, where I especially enjoyed the discussions on the more subtle details of the bosonization method. I have to express my deepest gratitude to Priv.-Doz. Dr. Axel Pelster for the endless help through all these years and the opening of doors that were believed to remain locked ultimately. With this I proudly enqueue myself in the line of young scientists, who owe you years of support and patience. Furthermore I would like to thank Dr. Imke Schneider for her assistance during my *PhD* time and teaching me the fascinating topic of non-linear bosonization.

All these years at the university of Kaiserslautern would have not been the same without my colleagues from and surrounding the *AG* Eggert, including: Denis Morath, Dominik Strassel, Javed Akram, Bernhard Irsigler, "Pouya" Kazemi, Polina Matveeva, Milan Radonjic, Serena Fazzini, Aslam Parvej and many more. Thank you all for the good times and the team atmosphere. Thereby, I feel especially in debt to my two partners in crime Shijie Hu and Kevin Jägering, without you the completion of this thesis would not have been possible and I am deeply sorry for any inconvenience. I also want to thank Martin Kübler, Merten Grupe and Kai Kuthan for all the relaxing coffee breaks and the good times outside of the university.

Many thanks is also dedicated to the Hamburg connection, Thore Posske and Prof. Michael Thorwart. I truly appreciate your support and the nice time in Hamburg, as well the joint work and fruitful discussions. Additionally, I want to thank Prof. Michael Thorwart also for being the second appraiser of this thesis, and Thore for all your advice concerning good scientific practice and writing.

Last but not least I want to thank all my friends at home and my family for supporting me through all these years. Especially, I want to express my deepest gratitude to Liselotte and Magda, without you my life would not be the same. You have been always

there for me whether the times were good or bad, debts that I can never pay off.

Chapter 11

Curriculum Vitae

Personal Information

name	Martin Bonkhoff
university address	Department of Physics, University of Kaiserslautern, 67663 Kaiserlautern, Germany
electronic address	bonkhoff@physik.uni-kl.de
date and place of birth	April 1, 1989 in 66482 Zweibrücken, Germany
nationality	German/ Belgian

Education

02/2017 – 12/2021	PhD studies at University of Kaiserslautern Supervisor: Prof. Dr. Sebastian Eggert
2010 – 2016	Diploma in Biophysics *Diploma Thesis: Interacting Anyons in a* 1*d Optical Lattice* Supervisor: Prof. Dr. Sebastian Eggert
2009	Abitur, Berufs-Oberschule 2 in 66482 Zweibrücken, Germany

Chapter 12

Selected Conferences and Schools

Kaiserslautern (Germany), 12/2018	International School and Workshop on Anyon Physics of Ultracold Atomic Gases (talk): *Statistically induced quantum phase transition in the extended Anyon-Hubbard model - a Bosonization approach*
Los Angeles (USA), 03/2018	APS March Meeting (talk): *Statistically induced quantum phase transition in the extended Anyon-Hubbard model*
Virtual (USA), 03/2021	APS March Meeting (talk): *Bosonic Continuum Theory of* 1*d Lattice Anyons*
Virtual (Germany), 09/2021	DPG Herbsttagung (poster): *Bosonic Continuum Theory of* 1*d Lattice Anyons*

Chapter 13

Publications

Bosonic Continuum Theory of One-Dimensional Lattice Anyons,
Martin, Kevin Jägering, Sebastian Eggert, Axel Pelster, Michael Thorwart, and Thore Posske
Physical Review Letters 126, 163201 , (2021)